Author:
Johnson, Charlie L

Title:
Implementing the Ten Altland-Zirnbauer Classes on the Dirac Graph Through Symmetry

UNIVERSITY OF BRISTOL

DOCTORAL THESIS

IMPLEMENTING THE TEN ALTLAND-ZIRNBAUER CLASSES ON THE DIRAC GRAPH THROUGH SYMMETRY

CHARLIE JOHNSON

School of Mathematics

A dissertation submitted to the University of Bristol in accordance with the requirements for award of the degree of Doctor of Philosophy in the Faculty of Science

September 2020

Declaration

I declare that the work in this dissertation was carried out in accordance with the requirements of the University's Regulations and Code of Practice for Research Degree Programmes and that it has not been submitted for any other academic award. Except where indicated by specific reference in the text, the work is the candidate's own work. Work done in collaboration with, or with the assistance of, others, is indicated as such. Any views expressed in the dissertation are those of the author.

SIGNED: DATE:

Abstract

The generalised Bohigas-Giannoni-Schmit Conjecture (BGS-Conjecture) states that the spectral statistics of classically chaotic Hermitian systems without unitary symmetries match the statistics of one of ten random matrix ensembles, chosen according to the symmetry class of the system under the Altland-Zirnbauer Tenfold Way. This is the classification of the forms of the time-reversal, charge-conjugation and chiral operators on the system, and whether it is symmetric under them. The BGS-Conjecture is unproven but well supported, including by testing individual systems for consistency with it. Systems for all ten ensembles have been tested numerically, but experimental verification has been managed for only six classes, leaving four needing lab confirmation. This is due to them requiring experimentally hard to realise forms of time-reversal and charge-conjugation operators. Here we show all ten ensembles are realisable on a system with a single chosen form of time-reversal and charge-conjugation by the application of unitary symmetries, giving a lab-realisable example system for each ensemble. Allowing unitary symmetries causes the system to decompose into subsystems, which have new, independent, local forms of the time-reversal, charge-conjugation and chiral operators. When the BGS-Conjecture is applied to the individual subsystems, the ensemble measured can then differ from that predicted by the global operator forms. We show this allows symmetries to be killed, or converted into the form for any desired Altland-Zirnbauer class for a subsystem. As our system, we choose the Dirac graph. We study the action of time-reversal, charge-conjugation and the chiral operator on the Dirac graph, and define the most general version of symmetry on a Dirac graph. With an algorithm to find a graph with any chosen set of symmetries, a graph in each Altland-Zirnbauer class is constructed. Numerical simulations confirm that all ten ensembles are found, opening up full testing of the generalised BGS-Conjecture in the lab.

v

There are different kinds of rules. From the simple comes the complex, and from the complex comes a different kind of simplicity. Chaos is order in a mask. . .

    -Terry Pratchett, Thief of Time

Acknowledgements

There are many people who should be thanked for their help while I was researching and writing this. Firstly, my supervisors, Martin Sieber and Sebastian Müller, who have pointed me at interesting problems and supported me as I searched for a solution. Their rigorous feedback has greatly improved the following work, even if I would have liked to do fewer rewrites.

Next, the Algebra and Geometry group for letting a physicist tag along and answering my many questions. The seminars were excellent, and the company and after seminar biscuits even better.

My fellow PhDs have made the last four years incredible fun. Mingle, postgrad seminars and board games nights has meant this has been an incredibly enjoyable experience, so my thanks go to everyone who has helped organise these, and all the other social events I have attended. Everyone who has offered advise or an ear in the common room and over lunch. Further thanks go to my office mates in 2A.14 who have been excellent company and offered excellent discussion.

To all of you, I give my thanks.

Contents

List of Tables

List of Figures

1. *Introduction*

The calculation of the energy levels of a quantum system is a common problem, but a hard one - it requires not only knowing the Hamiltonian of the system, but having a Hamiltonian that is sufficiently simple to work with, and find eigenvalues for. Unfortunately in a lot of systems, one or both of these conditions fail, the energy levels cannot be calculated analytically and it might be assumed that all information about the energy spectrum is lost.

However, there is a subset of quantum problems where this is not true, as under certain circumstances it is possible to identify statistical information about the distribution of the energy levels.

Out of work in the 1950s on the initial data from neutron resonances in heavy nuclei experiments, the question was raised over what form the distribution of the spacings between consecutive resonance levels took, [57, 82, 174]. Wigner, [172, 173, 174], argued that the nuclei were sufficiently large and complex that statistical methods could be applied to them. This would mean that instead of calculating an exact Hamiltonian for them and deriving the energy levels, statistically, it was sufficient to model the required Hamiltonian as a series of random draws out of the set of real symmetric matrices of the appropriate size. The spacing distribution of the resonances then had to match the statistics of the eigenvalue spacing statistics of the matrices in the group of real symmetric matrices. This formed the ensemble of random matrices known as the Gaussian Orthogonal Ensemble or the GOE ensemble, with experimental agreement of this conjecture of the level spacings following the GOE statistics being seen over the following years, [131].

The systems considered by Wigner were always symmetric under an involutive time-reversal, $\hat{\mathcal{T}} : t \to -t$ so that $\hat{\mathcal{T}}^2 = \mathbb{I}$, and only symmetric under the involutive time-reversal. As Dyson, [50], began considering a broader range of complex systems, he found that it was necessary to introduce an additional two ensembles to cover the situations Wigner didn't - first the ensemble of complex Hermitian matrices which forms the Gaussian Unitary ensemble, or the GUE ensemble, and the set of quaternionic Hermitian matrices which forms the Gaussian Symplectic Ensemble, or the GSE ensemble - forming his Threefold Way, [51]. Remaining in the simplest setup where systems are at most symmetric under time-reversal, Dyson expanded the definition of $\hat{\mathcal{T}}$ to be a more general operator, chosen so that it is anti-linear, $\hat{\mathcal{T}} z = z^* \hat{\mathcal{T}}$, to match the fact that $\psi(x, -t)$ is a solution of the complex conjugated Schrödinger equation, anti-unitary so $\langle \hat{\mathcal{T}}\psi | \hat{\mathcal{T}}\phi \rangle = \langle \psi | \phi \rangle^*$, and allowing $\hat{\mathcal{T}} = \pm\mathbb{I}$ so that it is now allowed that $\hat{\mathcal{T}}^2 = -\mathbb{I}$. The additional types of statistics then appear when the system isn't symmetric under $\hat{\mathcal{T}}$ for the GUE ensemble; and when the system is symmetric under $\hat{\mathcal{T}}$ but $\hat{\mathcal{T}}^2 = -\mathbb{I}$ for the GSE ensemble. The threefold classification

	Ensemble
$\hat{\mathcal{T}}$ is a symmetry, $\hat{\mathcal{T}}^2 = \mathbb{I}$	GOE
$\hat{\mathcal{T}}$ is a symmetry, $\hat{\mathcal{T}}^2 = -\mathbb{I}$	GSE
$\hat{\mathcal{T}}$ is not a symmetry	GUE

Table 1.1: The Dyson Threefold Way when the unitary subgroup U of the symmetry group G of the system is trivial. The classes only depend on whether $\hat{\mathcal{T}}$ is a symmetry, and its square.

this creates of the system under the action of $\hat{\mathcal{T}}$, and the ensemble its statistics correspond to is presented in Table 1.1.

However, Dyson's seminal work, [51], went further and also described the cases where a system was symmetric under other operators in addition to $\hat{\mathcal{T}}$, including general linear, unitary transformations; or it wasn't symmetric under $\hat{\mathcal{T}}$ but was symmetric under a sort of 'generalised' time-reversal operator $\hat{\alpha} = \tilde{\alpha}\hat{\mathcal{T}}$ which combined a unitary transformation $\tilde{\alpha}$ with the time-reversal operator, giving a general anti-unitary operator. He showed that in this case, random matrix predictions could still be made, but there would not be a single ensemble corresponding to the statistics of the entirety of the energy spectrum, rather there would be several ensembles corresponding to separate sub-spectra in the full spectrum.

Dyson furthermore showed that these sub-spectra could be isolated and their statistics predicted entirely by studying the group of transformations of the Hilbert space which leave the system invariant, and their representations. In more detail, the transformations which commute with the Hamiltonian and which preserve the transition probabilities between different states can be collated to form the symmetry group of the system, $G = \left\{\hat{O} \in \text{Hom}(\mathcal{H}) \mid \hat{O}\hat{H} = \hat{H}\hat{O},\right.$ $\left.\left|\left\langle\hat{O}\psi\middle|\hat{O}\phi\right\rangle\right|^2 = |\langle\psi|\phi\rangle|^2 \,\forall\, |\phi\rangle, |\psi\rangle \in \mathcal{H}\right\}$. Isolating then the subgroup of operators in G that are linear and unitary forms the normal subgroup $U = \left\{\hat{O} \in G \mid \left\langle\hat{O}\psi\middle|\hat{O}\phi\right\rangle = \langle\psi|\phi\rangle \,\forall\, |\phi\rangle, |\psi\rangle \in \mathcal{H}\right\}$ of G, which has representation R on the Hilbert space $\mathcal{H}$. Dyson then states that all that is needed to fully predict the statistical behaviour of the energy level spectrum is to know the forms of G, U and R.

Firstly, when U contains more than scalar multiplication, then the full energy spectrum $\{E_i\}$ splits into a number of independent sub-spectra, $\{E_i\}_a$ so that $\{E_i\} = \bigcup_a \{E_i\}_a$ and $\{E_i\}_a \cap \{E_i\}_{a'} = \emptyset$ if $a \neq a'$. This corresponds to the full Hilbert space splitting into a series of subspaces, $\mathcal{H} = \bigoplus_a \mathcal{H}_a$, each with their own sub-Hamiltonian $\hat{H}_a$ so that $\hat{H} = \bigoplus_a \hat{H}_a$, with $\{E_i\}_a$ being the eigenvalues of $\hat{H}_a$. These decompositions correspond to the representation R of U on $\mathcal{H}$ splitting into irreducible representations, so there exists one sub-spectrum in the full spectrum for every unique irreducible representation in the decomposition of R.

Having a subspace $\mathcal{H}_a$ and sub-Hamiltonian $\hat{H}_a$, then a subspace symmetry group can be defined, $G_a = \left\{\hat{O} \in \text{Hom}(\mathcal{H}_a) \mid \hat{O}\hat{H}_a = \hat{H}_a\hat{O}, \left|\left\langle\hat{O}\psi\middle|\hat{O}\phi\right\rangle\right|^2 = |\langle\psi|\phi\rangle|^2 \,\forall\, |\phi\rangle, |\psi\rangle \in \mathcal{H}_a\right\}$, which can include only scalar multiplication and potentially the operation of time-reversal, $\hat{\mathcal{T}}_a : t \to -t$, $\hat{\mathcal{T}}_a z = z^* \hat{\mathcal{T}}_a$, on the subspace. This then causes the general case to shift back to the specific case where at most time-reversal symmetry was possible, so the ensemble statistics for the sub-space can be read off from Table 1.1 by applying it to the square of $\hat{\mathcal{T}}_a$ in the same manner as was done for $\hat{\mathcal{T}}$.

That is, if $\hat{\mathcal{T}}_a \in G_a$ and $\hat{\mathcal{T}}_a^2 = \mathbb{I}$, then the sub-spectrum displays statistics matching the GOE ensemble; if $\hat{\mathcal{T}}_a \in G_a$ and $\hat{\mathcal{T}}_a^2 = -\mathbb{I}$ then the sub-spectrum statistics match the GSE ensemble; and finally if $\hat{\mathcal{T}}_a \notin G_a$ then the sub-spectrum statistics match the GUE ensemble. These are the only three possibilities for $\hat{\mathcal{T}}_a$.

Note how Dyson's methodology is entirely independent of any details of the system that is being considered - all that is needed to predict the statistics of the spectrum are the forms of $\hat{\mathcal{T}}$, G, U and R. An important corollary of this is that the statistics predicted by Dyson's method rely not on the implementation of the system, so that the properties predicted are universal to any system sharing the same $\hat{\mathcal{T}}$, G, U and R when the conditions for the random matrix correspondence are met.

Of course it was necessary to experimentally test these predictions, but the number of sufficiently complex systems that could be realised outside of the GOE class was limited. However, the requirement on a system to be 'sufficiently large and complex' that Wigner and Dyson had based their assumptions on is now widely believed to be overly restrictive. Initial evidence of the properties of possible random matrix statistics occurring in simple, classically non-integrable systems, [20, 34, 114], led to the study of the statistics of the Sinai billiard - a system with a mere two degrees of freedom - by Bohigas, Giannoni and Schmit, where they found excellent agreement between the level spacing statistics of the billiard and the GOE ensemble, [25]. With the Sinai billiard system being too small and simple to fulfil the conditions posed by Wigner and Dyson, they instead conjectured that it was sufficient that the classical analogue of the quantum system under consideration was chaotic. In doing so, and posing what is now known as the BGS-conjecture - that a generic quantum system that is sufficiently classically chaotic in the large system limit has statistics matching a canonical random matrix ensemble identified by having the same symmetries as the relevant system, [170] - they inextricably tied the fields of 'quantum chaos', or the study of quantum equivalents of classically chaotic systems, [35, 71, 73, 157], to the study of random matrices, [70, 115], that was developing out of the work of Wigner and Dyson. There have been many arguments over exactly what the exact requirements of 'sufficiently chaotic' are on the classical system, [25, 154], but the conjecture is generally believed to hold, and while it has no general proof, it has been supported by some semi-classical work, [21, 120, 121, 122, 147, 148], and has been analytically proven in the case of the quantum graph, [62, 63, 130, 159].

The BGS-conjecture then both opens up the number of systems which can be tested against random matrix predictions, and increases the importance of doing so as a key method of testing its validity by checking for either individual systems to be consistent with the conjecture, or identifying counter examples. These tests can be numeric simulations, or experiments, however it is important to have a mixture, and we will focus primarily on the experimental side as one of the aims of the thesis is to improve the methods of constructing experimental setups to test some of the more complicated random matrix ensembles that are introduced later. We note several works applying numerics to the BGS problem here though. For confirming the GOE ensemble there has been numerical studies of the Feingold-Peres model, [56]; billiards, [25]; and the quantum graph, [101]; along with various systems constructed to have GOE statistics in [24, 64, 94, 125]. The GUE ensemble has been tested against billiard models, [109]; and quantum graphs, [101]; along with various systems constructed to have GUE statistics in [24, 64, 94, 125]. The GSE ensemble statistics have been confirmed numerically in the cases of Hamiltonians with quartic potentials,

[36]; the kicked top for a particle with half-integer spin, [141, 142, 160]; and quantum cat-maps, [97]; along with various systems constructed to have GSE statistics in [24, 64, 94, 125].

Experimental work on systems to confirm the BGS-conjecture has largely focussed on the GOE ensemble, with examples including nuclear resonance data, [131], and in particular [132] within it, along with [26, 76, 178]; microwave cavity resonances, [4, 45]; microwave networks, [107, 152]; acoustic resonances, [128, 140]; and the hydrogen atom in a strong magnetic field, [80]; along with many other examples. There is also a reasonable amount of study of the GUE statistics, with them having been experimentally observed in microwave cavity experiments, [44, 46, 153, 158]; and microwave networks, [107, 152].

However despite the numerous systems shown numerically to have GSE statistics, experimental tests against the GSE random matrix predictions were not managed until recently. This is because of the sort of system needed to implement a time-reversal operator of the form $\hat{\mathcal{T}}^2 = -\mathbb{I}$, which is the form required to show GSE statistics if no other symmetries are present in the system - a $\hat{\mathcal{T}}^2 = -\mathbb{I}$ operator implies that the system comprises of an odd number of fermions, which is significantly harder to realise in the lab than the bosons associated to the GOE $\hat{\mathcal{T}}^2 = \mathbb{I}$ time-reversal, and which leads to quantum systems that can be mimicked by classical setups. There have been various prior attempts at seeing the GSE statistics experimentally, of course. An early one applied tangential methods, using the fact that a GOE spectrum with every second level removed from the spectra is statistically the same as a GSE ensemble, [115], to convert the experimental spectra of GOE microwave billiards into a GSE spectrum, [4]; and there has been work on condensed matter systems which have behaviour linked to the GSE ensemble which have been experimentally tested according to their condensed matter properties, [98, 116], but not the standard random matrix measures such as the level spacing distribution. Thus, it is only within recent years that a system has been realised experimentally and shown to hold to the standard measures of random matrix theory associated to quantum chaos. The first, [133], of these was the study of Au nanoparticles, [105]; while the slightly later quantum graph method, suggested in [92] and experimentally verified in [113, 133, 134, 135], is better known and uses methods that will be easier to extend here, and thus will have more of our focus.

The difficulty in realising GSE statistics in the lab outside of the example in [105] came entirely from the artificial limit of working with systems with a trivial unitary subgroup - Dyson's work already covered non-trivial examples of U and how the behaviour of the local time-reversal operator $\hat{\mathcal{T}}_a$ on $\mathcal{H}_a$ could be very different to the behaviour of the global time-reversal $\hat{\mathcal{T}}$ operator on $\mathcal{H}$, but there was little work done on systems taking advantage of this fact until recently. The first study to really deal with the divergence in the sub-spectra statistics from the form that would have been predicted by considering the global $\hat{\mathcal{T}}$ was the billiard of Leyvraz, Schmit and Seligman, [109]. Their billiard included a threefold rotation symmetry which splits the spectra into three sub-spectra, and while the billiard itself is symmetric under a $\hat{\mathcal{T}}^2 = \mathbb{I}$ time-reversal operator which would predict GOE statistics in the case of no unitary symmetries, two of the three sub-spectra show GUE statistics, the rotation symmetry having killed the time-reversal symmetry in these sub-spaces. Works studying this phenomena in other systems however remained limited and none turned the technique to the issue of realising GSE statistics in the lab prior to [92].

Considering this methodology of starting in a system which would have GOE statistics, then creating a subspace with the desired statistics through the use of symmetry, Joyner, Müller and

Sieber, [92], identified the group $U = Q_8$, $G = U \times Z_2$ as a symmetry group such that there was a representation R of U on $\mathcal{H}$ where despite the global time-reversal having the bosonic form of $\hat{\mathcal{T}}^2 = \mathbb{I}$, there exists a subspace with GSE statistics. This system can be constructed as a quantum graph - and with the equations describing a generic quantum graph being identical to those describing a microwave graph, [83], implemented in the lab as a microwave wire network, which is a simple classical system to build. This has allowed the typical identifiers associated with a random matrix ensemble to be compared against a lab system displaying GSE statistics, [113, 134, 135], through microwave wire experiments.

In addition to this, a second quantum graph has been recently identified, [3], based on a billiard system identified in [176] which has been numerically shown to hold GSE statistics and is compliant with the methodology of microwave wire experiments laid out by [83], and as such which could be physically realised. This would bring the number of systems tested experimentally for the GSE statistics up to three if done.

Thus, all three ensembles identified by Wigner and Dyson have been tested for on chaotic systems in the lab, and been seen to comply with the BGS-conjecture. However, the systems displaying the statistics described by Wigner and Dyson form only a small subset of Hermitian chaotic quantum systems - to cover the full set and describe their statistical behaviour it is necessary to work with what is known as the Altland-Zirnbauer Tenfold Way instead.

The limitation of the systems Wigner and Dyson considered is that they consider systems where either negative energy levels are not allowed, or the negative energy part of the level spectrum is independent of the positive energy part, and when this ceases to hold it has been necessary to add seven additional ensembles to the original three to describe how the positive energy solutions can relate to the negative energy solutions. The first three of these seven ensembles were described by Verbaarschot, Shuryak and Zahed based on work on the Dirac operator in QCD, [146, 166, 167], while Altland and Zirnbauer introduced the final four ensembles from work on superconductors, [5, 6]. It has since been proven that the classification of Altland and Zirnbauer is complete for Hermitian systems, and these ten ensembles are the only ensembles a Hermitian chaotic quantum system's statistics can match, [79]; there are of course other ensembles outside the Altland-Zirnbauer Tenfold Way possible when the system isn't Hermitian, [95].

Altland and Zirnbauer showed that in order to identify the statistics of a spectrum in the expanded classification it was necessary not only to consider symmetries in the dynamics of the system, but also symmetries in the energy level spectrum of the system - it is possible to have a mirror symmetry about zero so that whenever the level E_n, $n \geq 1$, is present in the system, so too is the level $E_{-n} = -E_n$. This means that two new operators on the system become relevant in addition to the time-reversal operator - the anti-linear particle-hole reversal or charge-conjugation operator $\hat{\mathcal{C}}$ which exchanges particles with holes or anti-particles, and the linear chiral operator $\hat{\mathcal{P}}$, combining the action of $\hat{\mathcal{T}}$ and $\hat{\mathcal{C}}$, $\hat{\mathcal{P}} = \hat{\mathcal{C}}\hat{\mathcal{T}}$ - with both of these operators potentially anti-commuting with the Hamiltonian. The relation between these operators and the spectral mirror symmetries is that in the simplest setup where there are no unitary symmetry operators that commute with the Hamiltonian, then $\hat{\mathcal{C}}$ can be shown to provide a potential spectral mirror symmetry, as the anti-commutation relation $\hat{\mathcal{C}}\hat{H} = -\hat{H}\hat{\mathcal{C}}$ implies that if $\hat{H} |\psi\rangle = E |\psi\rangle$ is an energy eigenstate with eigenvalue E, then $\hat{H}\hat{\mathcal{C}} |\psi\rangle = -\hat{\mathcal{C}}\hat{H} |\psi\rangle = -E\hat{\mathcal{C}} |\psi\rangle$ and $\hat{\mathcal{C}} |\psi\rangle$ is an existing

	$\hat{\mathcal{C}}$ is a symmetry, $\hat{\mathcal{C}}^2 = \mathbb{I}$	$\hat{\mathcal{C}}$ is a symmetry, $\hat{\mathcal{C}}^2 = -\mathbb{I}$	$\hat{\mathcal{C}}$ is not a symmetry	
$\hat{\mathcal{T}}$ is a symmetry, $\hat{\mathcal{T}}^2 = \mathbb{I}$	BDI	CI	AI	
$\hat{\mathcal{T}}$ is a symmetry, $\hat{\mathcal{T}}^2 = -\mathbb{I}$	DIII	CII	AII	
$\hat{\mathcal{T}}$ is not a symmetry	D	C	AIII, $\hat{\mathcal{P}}$ is a symmetry	A, $\hat{\mathcal{P}}$ is not a symmetry

Table 1.2: The Altland-Zirnbauer Tenfold Way when the unitary-commuting subgroup U of G is trivial. The classes depend only on which of $\hat{\mathcal{T}}, \hat{\mathcal{C}}$ and $\hat{\mathcal{P}}$ are symmetries of the system, and the squares of $\hat{\mathcal{T}}, \hat{\mathcal{C}}$ when they are symmetries.

energy eigenstate with energy $-E$. The equivalent relation $\hat{\mathcal{P}}\hat{H} = -\hat{H}\hat{\mathcal{P}}$ can cause $\hat{\mathcal{P}}$ to also produce a spectral mirror symmetry, with the same effect on the energy levels.

The ten different classes in the Altland-Zirnbauer Tenfold Way in this simple case then come from applying the threefold classification of an operator - as either a symmetry that squares to the identity; a symmetry that squares to minus the identity; or not a symmetry - to each of the operators $\hat{\mathcal{T}}$ and $\hat{\mathcal{C}}$ individually. This would define nine classes, but the case where neither are a symmetry splits into two based on whether or not $\hat{\mathcal{P}}$ is a symmetry or not. This defines the Tenfold Way seen in Table 1.2, labelling the system with one of the descriptors A, AI, AII, AIII, BDI, CII, C, D, CI and DIII, with each corresponding to a different random matrix ensemble classified by Altland and Zirnbauer and described in [70, 156]. Only the first six of these ensembles have commonly used names - being the GUE, GOE, GSE, chiral-GUE, chiral-GOE and chiral-GSE ensembles respectively - so the class labels for the systems will be used instead throughout the thesis, referring to the class of the system, the class of the symmetry group and the random matrix ensemble interchangeably. When it is absolutely necessary for the ensembles for the classes C, D, CI, and DIII to be refereed to specifically though, we will use the abbreviations AZ-C, AZ-D, AZ-CI and AZ-DIII for them respectively.

As with the Wigner-Dyson classification, the situation for the Altland-Zirnbauer classification is more complicated when additional unitary-commuting symmetries are allowed in the system, or the system is not symmetric under charge-conjugation or the chiral operation but is symmetric under a generalised charge-conjugation operation $\hat{\gamma} = \tilde{\gamma}\hat{\mathcal{C}}$ or generalised chiral operator, $\hat{\pi} = \tilde{\pi}\hat{\mathcal{P}}$ combining a unitary transform $\tilde{\gamma}$ or $\tilde{\pi}$ with either charge-conjugation or the chiral operator. Once again, random matrix statistics are possible, but only once the independent sub-spectra have been identified and isolated, and the method to do this involves identifying the symmetry group G of the system, its normal subgroup U and U's representation R on $\mathcal{H}$.

In this more general case, the symmetry group is now considered to include operators that anti-commute with the Hamiltonian. This makes the updated symmetry group $G = \left\{ \hat{O} \in \mathrm{Hom}(\mathcal{H}) \mid \hat{O}\hat{H} = \pm\hat{H}\hat{O}, \left| \langle \hat{O}\psi | \hat{O}\phi \rangle \right|^2 = |\langle \psi | \phi \rangle|^2 \ \forall |\phi\rangle, |\psi\rangle \in \mathcal{H} \right\}$. The relevant normal sub-group U of G, becomes the set of unitary transforms which *do* commute with the Hamiltonian $U = \left\{ \hat{O} \in G \mid \hat{O}\hat{H} = \hat{H}\hat{O}, \langle \hat{O}\psi | \hat{O}\phi \rangle = \langle \psi | \phi \rangle \ \forall |\phi\rangle, |\psi\rangle \in \mathcal{H} \right\}$ and from here Dyson's method of isolating sub-spectra and identifying their statistics remains unchanged.

Once again, U containing more than scalar multiplication causes the full spectra to split into independent sub-spectra $\{E_n\} = \bigcup_a \{E_n\}_a$ to match the Hilbert space splitting into sub-spaces

Class	Ensemble	$\hat{\mathcal{T}}_a$	$\hat{\mathcal{C}}_a$	$\hat{\mathcal{P}}_a$	Class	Ensemble	$\hat{\mathcal{T}}_a$	$\hat{\mathcal{C}}_a$	$\hat{\mathcal{P}}_a$
A	GUE	$\notin G_a$	$\notin G_a$	$\notin G_a$	AIII	chGUE	$\notin G_a$	$\notin G_a$	$\in G_a$
AI	GOE	$\in G_a$ $\hat{\mathcal{T}}_a^2 = \mathbb{I}$	$\notin G_a$	$\notin G_a$	BDI	chGOE	$\in G_a$ $\hat{\mathcal{T}}_a^2 = \mathbb{I}$	$\in G_a$ $\hat{\mathcal{C}}_a^2 = \mathbb{I}$	$\in G_a$
AII	GSE	$\in G_a$ $\hat{\mathcal{T}}_a^2 = -\mathbb{I}$	$\notin G_a$	$\notin G_a$	CII	chGSE	$\in G_a$ $\hat{\mathcal{T}}_a^2 = -\mathbb{I}$	$\in G_a$ $\hat{\mathcal{C}}_a^2 = -\mathbb{I}$	$\in G_a$
D		$\notin G_a$	$\in G_a$ $\hat{\mathcal{C}}_a^2 = \mathbb{I}$	$\notin G_a$	CI		$\in G_a$ $\hat{\mathcal{T}}_a^2 = \mathbb{I}$	$\in G_a$ $\hat{\mathcal{C}}_a^2 = -\mathbb{I}$	$\in G_a$
C		$\notin G_a$	$\in G_a$ $\hat{\mathcal{C}}_a^2 = -\mathbb{I}$	$\notin G_a$	DIII		$\in G_a$ $\hat{\mathcal{T}}_a^2 = -\mathbb{I}$	$\in G_a$ $\hat{\mathcal{C}}_a^2 = \mathbb{I}$	$\in G_a$

Table 1.3: The Altland-Zirnbauer class of the sub-space for each form of the local symmetry group G_a, with the common name of the corresponding ensemble for the spectral statistics where a common name for the ensemble exists.

$\mathcal{H} = \bigoplus_a \mathcal{H}_a$ with their own sub-Hamiltonians, $\hat{H} = \bigoplus_a \hat{H}_a$, and R splitting into irreducible representations. This allows the definition of the local symmetry group
$G_a = \left\{ \hat{O} \in \mathrm{Hom}(\mathcal{H}_a) \mid \hat{O}\hat{H}_a = \pm\hat{H}_a\hat{O}, \, \left|\langle \hat{O}\psi | \hat{O}\phi \rangle\right|^2 = |\langle \psi | \phi \rangle|^2 \, \forall \, |\phi\rangle, |\psi\rangle \in \mathcal{H}_a \right\}$ which includes at most scalar multiplication and the local time-reversal, charge-conjugation and chiral operators, $\hat{\mathcal{T}}_a, \hat{\mathcal{C}}_a$ and $\hat{\mathcal{P}}_a$ respectively. The sub-spectrum can then be given an Altland-Zirnbauer class based on which of $\hat{\mathcal{T}}_a, \hat{\mathcal{C}}_a$ and $\hat{\mathcal{P}}_a$ are included in G_a and the form of their squares as seen in Table 1.3, this class then corresponds to matching one of the ten random matrix ensembles described in [70, 156].

The BGS-conjecture is assumed to be extendible to the new systems covered by Altland and Zirnbauer, thus there are a new set of classes for which experiments need to be carried out for to test the conjecture. There is however, a similar problem to the GSE case in finding examples that can be created in the lab for several of the new classes. This is despite a plethora of numerical examples existing for each of the clsses - the Feingold-Peres model can display AI, BDI or CI statistics, [56]; the Dirac operator on an $SU(2)$ lattice under QCD can show one of the classes A, AI, AII, AIII, BDI and CII, [15, 125]; and by taking different values of $\mathcal{N}$ in supersymmetric SYK models each of the ten classes can be simulated, [94]; numerous other examples are discussed in [14] - and experimental examples in condensed matter that haven't applied the traditional random matrix checks to the system, see the systems discussed in [14, 39, 55, 143]. Experimental verification of the standard measures of the random matrix predictions on the other hand, have so far been limited to the classes AIII, BDI and CII, [136]. This obviously leaves examples of the classes C, CI, D and DIII outstanding.

There is a necessity then to identify a set of systems which cover each of the seven new classes and which could be potentially be realised in the lab. Given a lot of the difficulty can arise from implementing specific forms of $\hat{\mathcal{T}}, \hat{\mathcal{C}}$ and $\hat{\mathcal{P}}$, this would optimally take a system with a specific easy to implement pair of $\hat{\mathcal{T}}$ and $\hat{\mathcal{C}}$ and then use techniques like that of Leyvraz, Schmit and Seligman, and Joyner, Müller and Sieber in using symmetry to create subspaces in the system and selectively kill or convert the local $\hat{\mathcal{T}}_a$ and $\hat{\mathcal{C}}_a$ into the appropriate forms for each ensemble.

It is important to note two prior works that have had similar goals or techniques. The first is by Gnutzmann and Seif, [64, 144], which defines the Andreev star graph, a series of

superconducting wires that are linked in the center, so that a particle can travel up and down the wires and experience Andreev reflection at the loose ends, becoming a hole with an added phase, or scattering between different wires at the center point according to a chosen scattering matrix. An Andreev graph without additional symmetry naturally sits in the Altland-Zirnbauer class CI, [67], however by using different manipulations of the Andreev reflection parameters and the scattering matrix at the center, Gnutzmann and Seif shifted the ensemble statistics to be in each of the ten different classes. Essentially, the matrices describing the reflections and scatterings were drawn from those allowed under the desired class, and the ensemble was used to generate itself. Like Gnutzmann and Seif, we will use a generalisation of the quantum graph, and we will use a simple manipulation of the vertex scattering matrices to place the system into one class before symmetry is added; however, our method of manipulating the vertex scattering conditions shall not change between the different classes, moving between classes will be done entirely through symmetry in the graph's geometry, so that each ensemble is created by drawing from the unitary ensemble. This means that only one rule on the scattering matrices need be imposed, instead of a different one for each class, and thus the number of different vertex conditions to have to be able to implement in the lab is significantly reduced.

The second work of note is by Blatzios, [24], which takes a system with trivial unitary-commuting subgroup, U, from each Altland-Zirnbauer class - so a collection of ten systems where each is symmetric under a different one of the ten possible forms of G with U the trivial group - and then adds a threefold rotation as a unitary commuting symmetry to each system, now setting $U = Z_3$ and studying what classes appear in each of the new sub-spaces created by the symmetry. This did return a sub-space showing the statistics of each of the ten classes, but it required iterating over the different initial systems to achieve it, keeping the chosen form of U fixed. We wish to choose a single system, and then apply different symmetry groups G and unitary commuting subgroup U to find the different classes in contrast.

At this point we restate our aim - identify a single system with fixed forms of $\hat{\mathcal{T}}$ and $\hat{\mathcal{C}}$ as operators, and by initialising it with different symmetry groups, produce ten examples of subspaces, each showing the statistics of a different random matrix ensemble from Altland and Zirnbauer's classification. Furthermore, demonstrate that these subspaces can be constructed as stand-alone systems. We then hope that this produces a set of systems which can be realised in the lab to show each of the ten ensembles described under Altland and Zirnbauer's classification.

To do this, we first discuss the abstract representation and corepresentation theory of the groups with the structure of a symmetry group in Chapter 2. We introduce both the Dyson Threefold and Altland-Zirnbauer Tenfold classifications of corepresentations, and how they are linked to the structure of the corepresentations and their commutators. The modifications to these theories needed to allow for non-involutive global forms of $\hat{\mathcal{T}}$ and $\hat{\mathcal{C}}$ are also discussed.

In Chapter 3 we then qualitatively discuss the meaning of quantum symmetries and the physical interpretations of different types of symmetry operator. The theory of Chapter 2 is applied, showing how corepresentations describe the action of symmetry groups on the system, and how the reduction into subspaces is possible and how it affects symmetry groups described. How knowing the Altland-Zirnbuer class of a subspace can be used to identify the structure of the corresponding sub-Hamiltonian is introduced prior to being expanded upon in Chapter 4.

Quantum chaos is finally introduced, with a discussion on the universal behaviours seen in the Gaussian systems considered here.

Chapter 4 then details the random matrix theory behind the ten ensembles involved in the Altland-Zirnbauer classification, along with a set of characteristic distributions of properties of the system that can be used to identify each ensemble when given the spectral data of a system. At this point, knowing the symmetry group G, we can identify what statistics should appear in its spectra, as well as test for these statistics, meaning we can move onto looking for the desired example systems.

The first part of identifying the example systems is identifying suitable symmetry groups. The methodology behind searching for these groups is described in Chapter 5, with suitable examples for producing each Altland-Zirnbauer class located.

Chapters 6 and 7 then move onto discussing the models which can be used to represent these symmetry groups. Chapter 6 starts with the quantum graph, giving the most general definition of symmetry on a quantum graph and then using this to generalise the algorithm used by Joyner, Müller and Sieber to find models symmetric under $G = U \times Z_2$ symmetry groups, extending it to cover all possible forms of symmetry groups described by Dyson, the first stage of defining the algorithm which will be necessary to build the Altland-Zirnbauer example systems. This allows the first three systems from Chapter 5 to be modelled and tested numerically. While the GOE, GUE and GSE ensembles tested here have already been covered in the literature, the work here fills the final gaps in the description of symmetric quantum graphs, discussing implementing generalised time-reversal symmetries on the graph and testing ensemble-generation methods and identifying ensembles through measuring spectral statistics other than the spacing distribution as practise for dealing with the Altland-Zirnbauer ensembles.

In Chapter 7 we then turn to the models that will allow us to fulfil the task of finding ten systems showing the ten ensemble statistics of the Altland-Zirnbauer classification. We turn to the Dirac graph, introduced by Bulla and Trenkler, [31], as a variant of the quantum graph which allows both particle and anti-particle solutions by supplanting the Schrödinger equation on the wires with the Dirac equation; the Dirac graph having already had application to the study of quantum chaos and random matrix theory, [27].

The Dirac equation is introduced, its one-dimensional form and solutions discussed and its action under $\hat{\mathcal{T}}$ and $\hat{\mathcal{C}}$ described. The Dirac graph can then be described, and a definition of symmetry on it given, including the restrictions on its form to be symmetric under $\hat{\mathcal{T}}$, $\hat{\mathcal{C}}$ and $\hat{\mathcal{P}}$. The algorithm of Joyner, Müller and Sieber then receives its final extension, now covering all of the symmetry groups considered by Altland and Zirnbauer, so that a graph symmetric under any form of applicable symmetry group G can be generated. Systems for each of the ten Altland-Zirnbauer ensembles are constructed, and simulated numerically, showing agreement with the predictions and fulfilling the aim of the thesis. Finally, there is discussion of how Dirac graphs can be converted into equivalent quantum graphs for potential microwave implementations.

In addition to this, there are primers on group theory, super-algebra and quantum systems in Appendices A, B and C, along with a discussion on how the graphs considered here have structure that can be taken advantage of for doing periodic orbit expansions for semiclassical approximation of statistical measures in Appendix D. The results of the algorithmic classification

of symmetry groups according to the Dyson and Altland-Zirnbauer methodologies are given for small groups in Appendix E.

2. *Representation Theory*

We begin by covering the pure representation theory that will be necessary to understand how geometric, time-reversal, charge-conjugation and chiral operators act on quantum states. First, having given a primer on group theory in Appendix A we consider the standard unitary representations of finite groups. These will be used for describing geometric and other unitary symmetries in Section 2.1. In Section 2.2 we study the modifications to unitary representations that are allowable when a Z_2-grading is imposed; Section 2.3 covers the case when a $Z_2 \times Z_2$-grading is used. Z_2-gradings will allow for time-reversal symmetries; $Z_2 \times Z_2$-gradings for charge-conjugation and the chiral operation when we come to work with their application as the method of switching between symmetry transforms of a quantum system, and quantum operators. Finally, we cover projective representations, which will be necessary for dealing with spin particles.

2.1 Representation of Finite Groups

The study of unitary representations of finite groups is the subject of many books, and lecture courses. We will draw primarily from [99, 149] here, with additions from [52, 53, 86, 96], and while aiming to keep language consistent with [117] for comparison with the later sections.

It is often the case that group theory is introduced by the study of two abstract sets and their multiplication rules, say the nth roots of unity under multiplication, and $\mathbb{Z}/n\mathbb{Z}$ under addition. Comparing how these two act, it is realised that they are at an abstract level the 'same', and both are implementations of the group Z_n. Group theory has its power in recognising abstract rules and structure, and using these to prove things for all its implementations rather than do each individually.

However, in its abstractness, group theory loses all information about how groups interact with other objects. In order to recover this, representation theory gives methods to calculate and classify different implementations of a group acting in a vector space, while identifying 'fundamental' representations of a group and studying their structure. Representation theory can be a powerful tool for understanding groups in its own right, for example Burnside's Theorem for groups was first proved with representation theory, and it would take another 70 years for a solely group theoretic proof to be generated, [32, 86]. It is though, primarily the information on how groups transform vector spaces that we will care about here.

We begin with the formal definition of a representation, linking group elements to the invertible maps $GL(V)$ of a vector space, [96].

Definition 2.1.1. *Let G be a finite group, V a finite dimensional vector space and $\mathrm{GL}(V) \subset$* **Hom**(V) *be the set of invertible linear maps from V to itself. Then, a representation R of G is a homomorphism*

$$R : G \to GL(V), \qquad R : g \to R(g).$$

In our case, it will only be necessary to consider those linear representations that can be written with matrices, [86, 96]:

Definition 2.1.2. *Let G be a finite group, K a field and $\mathrm{GL}(n, K)$ be the group of invertible $n \times n$ matrices with entries in K. Then a matrix representation M of G is a homomorphism*

$$M : G \to GL(n, K), \qquad M : g \to M(g).$$

It has dimension $\dim(M) = n$.

There is no conflict between the two definitions of a representation when both exist; when $V = K^n$, with a basis $\{e_i\}$ and a bilinear form $(\cdot, \cdot)$, a linear representation $R : G \to \mathrm{GL}(V)$ can be converted to a matrix representation $M : G \to \mathrm{GL}(n, K)$ by defining the matrices with elements, [53],

$$M_{ij}(g) = (e_i, R(g)e_j).$$

In these cases $\mathrm{GL}(V) = \mathrm{GL}(n, K)$ and it is permissible to write $R : G \to \mathrm{GL}(V)$ is a matrix representation.

We also restrict ourselves to fields of characteristic 0, that is the fields where if 1 is the multiplicative identity there is no sum $1 + 1 + \cdots + 1 = 0$. We will see later that is is sufficient to consider the fields $\mathbb{R}$ and $\mathbb{C}$.

Given a representation of a group G, it is natural to ask what representations of groups G' related to G we can construct. Four primary methods exist - first are the direct sums and tensor products that come naturally from their existence on matrices:

Definition 2.1.3. *Let G be a finite group, V_1, V_2 vector spaces and R_1, R_2 matrix representations of G on V_1, V_2 respectively. Then, two further representations of G can be formed:*

- *The direct sum representation $R_1 \oplus R_2 : G \to GL(V_1 \oplus V_2)$ is defined as*

$$(R_1 \oplus R_2)(g)(v_1 \oplus v_2) = R_1(g)v_1 \oplus R_2(g)v_2$$

  It has dimension $\dim(R_1) + \dim(R_2)$.

- *The tensor product representation $R_1 \otimes R_2 : G \to GL(V_1 \otimes V_2)$ is defined as*

$$(R_1 \otimes R_2)(g)(v_1 \otimes v_2) = R_1(g)v_1 \otimes R_2(g)v_2$$

  It has dimension $\dim(R_1) \times \dim(R_2)$.

The second pair are the induced and restricted representations which relate a representation R_H on the vector space V_H for a subgroup $H < G$ to the representation R_G of its supergroup G on the vector space V_G, [96]:

Definition 2.1.4. *Let G be a group with representation R_G on $V_G = K^n$, and H a subgroup of G of index $[H : G]$ with transversal $T = \{s_a\}$ in G, and representation R_H on $V_H = K^m$. Then:*

- *The restriction of R_G onto H, $R_G{\downarrow}_H$ is the representation of H on V_G such that $R_G{\downarrow}_H(h) = R_G(h)$.*

- *The matrix representation $R_H{\uparrow}^G$ of G induced by R_H of H is defined on $V' = K^{[G:H]} \otimes K^m$ as the block matrix,*

$$\mathbb{R}_H{\uparrow}^G(g)_{(a,i),(b,j)} = \begin{cases} R_H(s_a^{-1}gs_b)_{ij} & s_a^{-1}gs_b \in H \\ \\ 0 & otherwise \end{cases}$$

The restricted representation of G to H essentially constructs a representation of H by taking a representation of G and forgetting the additional information about the elements of G not in H. The induced representation takes a known representation R_H of H and then uses the coset structure of H in G to extend the representation by identifying how the representation R_H acts within each of the coset copies of H, and how elements in G but not H permute the cosets around. This gives the block structure given above.

Induced representations from normal subgroups will be of great use, in particular the case where $G/H = Z_2$ with transversal $T = \{e, a\}$, which by substituting into the definition of the induced representation is seen to give a representation with the structure,

$$R_H{\uparrow}^G(g \in H) = \begin{pmatrix} R_H(g) & 0 \\ 0 & R_H(a^{-1}ga) \end{pmatrix}, \qquad R_H{\uparrow}^G(g \in aH) = \begin{pmatrix} 0 & R_H(ga) \\ R_H(a^{-1}g) & \end{pmatrix}, \qquad (2.1)$$

while the case where $G/H = K_4$ with the transversal $T = \{e, a, b, c = ab\}$ gives the induced representation

$$R_H{\uparrow}^G(g \in H) = \begin{pmatrix} R_H(g) & 0 & 0 & 0 \\ 0 & R_H(a^{-1}ga) & 0 & 0 \\ 0 & 0 & R_H(b^{-1}gb) & 0 \\ 0 & 0 & 0 & R_H(c^{-1}gc) \end{pmatrix}$$

$$R_H{\uparrow}^G(g \in aH) = \begin{pmatrix} 0 & R_H(ga) & 0 & 0 \\ R_H(a^{-1}g) & 0 & 0 & \\ 0 & 0 & 0 & R_H(b^{-1}gc) \\ 0 & 0 & R_H(c^{-1}gb) & 0 \end{pmatrix}$$

$$R_H{\uparrow}^G(g \in bH) = \begin{pmatrix} 0 & 0 & R_H(gb) & 0 \\ 0 & 0 & 0 & R_H(a^{-1}gc) \\ R_H(b^{-1}g) & 0 & 0 & 0 \\ 0 & R_H(c^{-1}ga) & 0 & 0 \end{pmatrix} \qquad (2.2)$$

$$R_H{\uparrow}^G(g \in cH) = \begin{pmatrix} 0 & 0 & 0 & R_H(gc) \\ 0 & 0 & R_H(a^{-1}gb) & 0 \\ 0 & R_H(b^{-1}ga) & 0 & 0 \\ R_H(gc^{-1}) & 0 & 0 & 0 \end{pmatrix}.$$

These two induced representations will see application in describing the Dyson Threefold Way, [30], and the Altland-Zirnbauer Tenfold Way respectively.

Identification of equivalent objects R, R' always involves finding if there are bijective homomorphisms between the two. The representation version of the bijective homomorphisms, which in context are also called intertwiners, will also have further roles to play in classifying representations, [149].

Definition 2.1.5. *Let G be a finite group, V_1, V_2 be vector spaces and R_1, R_2 be matrix representations of G on V_1, V_2 respectively. Then an intertwiner $T \in \mathrm{Hom}(V_1, V_2)$ is a function such that*

$$TR_1(g) = R_2(g)T$$

If T is a bijection, then R_1, R_2 are equivalent representations, $R_1 \cong R_2$.

Equivalence of representations, and direct sums of representations give the foundation to begin classifying representations.

Firstly, we recognise that we can restrict consideration of matrix representations to unitary matrices without loss of generality, $\mathrm{GL}(n, K) \to \mathcal{U}(n, K)$, [99].

Theorem 2.1.6. *Let G be a finite group, V a vector space with inner product $\langle \cdot, \cdot \rangle$ and $R : G \to \mathrm{GL}(V)$ a representation. Then there exists an inner product $\langle \cdot, \cdot \rangle'$ which R is unitary in respect to,*

$$\langle R(g)u, R(g)v \rangle' = \langle u, v \rangle', \qquad \forall u, v \in V, \ g \in G$$

Proof. We prove this by construction of an appropriate inner product as

$$\langle u, v \rangle' = \frac{1}{|G|} \sum_{g \in G} \langle R(g)u, R(g)v \rangle$$

which satisfies the requirements of an inner product and is invariant under $\langle u, v \rangle' \to \langle R(g)u, R(g)v \rangle'$ by Theorem A.0.7. □

Corollary 2.1.7. *Let G be a finite group, and $R : G \to \mathrm{GL}(n, K)$ be a matrix representation. Then there exists a matrix T such that*

$$TR(g)T^{-1} \in \mathcal{U}(n, K) \qquad \forall g \in G$$

and $U(g) = TR(g)T^{-1} \cong R(g)$ provides a unitary matrix representation of G that is equivalent to R.

Next we can identify whether or not a representation is a direct sum of representations, [99].

Proposition 2.1.8. *Let G be a finite group and $R : G \to GL(V)$ a matrix representation. If there exists a proper subspace $W \subset V$, $W \neq \emptyset$, such that W is invariant under R,*

$$R(g)w \in W, \qquad \forall g \in G, \ w \in W$$

then R is the direct sum of the two representations $R_W : G \to \mathrm{GL}(W)$ and $R_{W^\perp} : G \to \mathrm{GL}(W^\perp)$.

If no such proper subspace exists, then R is an irreducible representation of G, and will be labelled ρ.

Irreducible representations of groups form the building blocks of all of representation theory; from them every representation of a group can be constructed, [33, 99]:

Theorem 2.1.9 (Maschke)**.** *Let G be a finite group with irreducible representations $\{\rho_i\}$ and representation R all over a field of characteristic 0. Then either $R = \rho_i$ is irreducible, or R is completely decomposable as a direct sum of irreducible representations with multiplicities s_i,*

$$R = \bigoplus_i \bigoplus_{n=1}^{s_i} \rho_i$$

Proof. We use proof by induction on the dimension of the representation. A dimension 1 representation is trivially irreducible. Assume that all representations of dimension n or less are either irreducible or a direct sum of irreducible representations. Take a representation of dimension $n+1$, either it is irreducible, or by Proposition 2.1.8 we can find $R_W, R_{W^\perp}$ such that $R = R_W \oplus R_{W^\perp}$. As $\dim(R_W), \dim(R_{W^\perp}) \leq n$, then they are either irreducible or completely reducible, and the direct sum of their decompositions into irreducible components gives the decomposition for R. $\square$

This seems trivial, however the full version for a field of any characteristic only holds for groups where the character of the field doesn't divide the order of the group, [33]. Thus, our choice to consider only characteristic 0 fields is essential here in guaranteeing Maschke's theorem holds for all groups. Complete reducibility is essential though, as the most important classification methods will hold *only* for irreducible representations.

Classification of a potentially infinite set of irreducible representations seems impossible, however we are guaranteed that finite groups only have a finite number of irreducible representations.

Theorem 2.1.10. *Let G be a finite group, then the number of unique irreducible representations of G, is the number of unique conjugacy classes of G,*

$$|\{\rho_i\}| = |\{C_g\}|$$

Proof. See [149] for a proof using class functions and character theory. $\square$

Though not irreducible, the representation known as the regular representation will be of great use, [99]:

Definition 2.1.11. *Let G be a finite group of order n and $V = \mathbb{R}^n$. We identify the basis elements e_i of V with the group elements g_i of G, $e_i \leftrightarrow g_i$ and define the regular representation $R_{reg.}$ as the matrices*

$$(R_{reg.})_{jk}(g_i) = \begin{cases} 1 & g_j g_k^{-1} = g_i \\ 0 & otherwise \end{cases}$$

Essentially, $R_{\text{reg.}}$ describes how the elements of G permute under multiplication. It will appear later as the representation of a group acting on its Cayley Graph, and will be the reason every possible sub-spectrum appears on a quantum Cayley Graph, underpinning the algorithms used to

generate the desired spectral statistics for a given group. The reason for this is that the regular representation of G includes *exactly* one copy of every irreducible representation of G.

Theorem 2.1.12. *Let G be a finite group with n irreducible representations $\{\rho_i\}$ then the regular representation decomposes into irreducible components as*

$$R_{reg.} = \bigoplus_{\rho_i \in \{\rho_i\}} \rho_i$$

Proof. See [99] for a particularly elegant proof of this using character theory. □

Finally, irreducibility of representations will have an impact on the existence and form of intertwiners between representations, [53]:

Theorem 2.1.13 (Schur). *Let ρ_1, ρ_2 be two irreducible representations of G on V. Let T be an intertwiner for ρ_1, ρ_2 so that $T\rho_1 = \rho_2 T$. Then, either,*

- $T = z\mathbb{I}$, *is a scalar multiple of the identity on V and $\rho_1 \cong \rho_2$.*

- $T = 0$, *the intertwiner is trivial and the two irreducible representations are inequivalent.*

Proof. See [53] for a proof. □

2.1.1 Classification of Finite Irreducible Representations

We now consider what fields matrix representations can be taken over, by applying Artin-Wedderburn's Theorem to restrict them to elements of a division ring. The method followed is from [51, 171].

Artin-Wedderburn's theorem in its general form states that all semi-simple algebras A over a field K can be written as a direct product of matrix algebras M_i with entries from division rings D_i over K, [54]. To apply it to the matrix representations then requires the definition of a suitable algebra out of the representation, the obvious one being the group algebra, and its commutator algebra, [51].

Definition 2.1.14. *Let G be a finite group, with matrix representation R over K. Then the group algebra $A = \langle R(g) \rangle$ is the algebra generated by the elements of $R(g)$ over K.*

The commutator algebra $\overline{A}$ of A is defined as the algebra generated by the set of matrices $\overline{A}$ that commute with all elements of A.

In this case, $\overline{A}$ is also the algebra generated by the set of self-intertwiners of the representation R, $\overline{A} = Z = \langle T \in \mathrm{Hom}(V, V) | R(g)T = TR(g) \ \forall g \in G \rangle$. These algebras are guaranteed to be semi-simple when K is chosen to be a characteristic 0 field, [33].

Defining the two forms of algebra tA, A_t that can be constructed from the algebra A, [51],

$$A_t = \begin{pmatrix} a_{11} & a_{12} & \dots \\ a_{21} & \ddots & \\ \vdots & & \end{pmatrix} \quad a_{ij} \in A, \qquad tA = \{\mathbb{I}_t \otimes a \mid a \in A\}$$

then Artin-Wedderburn's theorem can be given in Dyson's notation as:

Theorem 2.1.15. *Let A be a matrix algebra over a characteristic 0 field K, decomposable into n components. Then $\overline{A}$ is also decomposable into n components and the pair have structure*

$$A = \sum_{i=1}^{n} s_i(E_i)_{t_i}, \qquad \overline{A} = \sum_{i=1}^{n} t_i(E_i)_{s_i}$$

where E_i is an associative division algebra over K.

In order to apply this to unitary matrix representations over $\mathbb{C}^n$ it is useful to note that a representation over $\mathbb{C}^n$ can always be converted into a representation over $\mathbb{R}^{2n}$ by applying the map, [51],

$$\mathfrak{R}(a + ib) = \begin{pmatrix} a & -b \\ b & a \end{pmatrix}, \qquad \mathfrak{R}\left(\begin{pmatrix} a_{11} & \cdots \\ \vdots & \ddots \end{pmatrix}\right) = \begin{pmatrix} \mathfrak{R}(a_{11}) & \cdots \\ \vdots & \ddots \end{pmatrix} \tag{2.3}$$

The algebra over $\mathbb{C}^n$ with basis $\{e_i\}$ can then be written as an algebra over $\mathbb{R}^{2n}$ with basis $\{\mathfrak{R}(e_i)\} \cup \left\{ i = \mathbb{I}_n \otimes \begin{pmatrix} 0 & -1 \\ 1 & 0 \end{pmatrix} \right\}$, giving the map

$$\mathfrak{R} : A = \langle\{e_i\}\rangle \to A_{\mathfrak{R}} = \left\langle \{\mathfrak{R}(e_i)\} \cup \left\{ i = \mathbb{I}_n \otimes \begin{pmatrix} 0 & -1 \\ 1 & 0 \end{pmatrix} \right\} \right\rangle \tag{2.4}$$

between a complex algebra and its real version.

Using this map on the algebras $A, \overline{A}$ before the Artin-Wedderburn Theorem is applied to them, then Frobenius' Theorem, [51], applies to the decomposition elements E_i, restricting them to one of three forms:

Theorem 2.1.16 (Frobenius)**.** *The only associative division algebras over $\mathbb{R}$ are $\mathbb{R}, \mathbb{C}$ and $\mathbb{H}$.*

This identifies the possible division algebras for Theorem 2.1.15:

Corollary 2.1.17. *Let R be a unitary matrix representation of G over $\mathbb{C}^n$, generating the group algebra A and its commutator algebra $\overline{A}$. Then $A_{\mathfrak{R}}, \overline{A}_{\mathfrak{R}}$ decompose into irreducible components*

$$A_{\mathfrak{R}} = \sum_{i=1}^{n} s_i(E_i)_{t_i}, \qquad \overline{A}_{\mathfrak{R}} = \sum_{i=1}^{n} t_i(E_i)_{s_i}$$

for some s_i, t_i, where $E_i \cong \mathbb{R}, \mathbb{C}$ or $\mathbb{H}$ for each i.

For irreducible representations, the result is generally paraphrased as, [149]:

Theorem 2.1.18. *Let G be a finite group, and ρ an irreducible unitary matrix representation, then ρ is isomorphic to a matrix representation over one of $\mathbb{R}, \mathbb{C}$ or $\mathbb{C}$ with quaternionic structure, $\mathbb{H}$. It will be termed a real, complex or quaternionic (pseudo-real) representation respectively.*

Another approach to classifying the field K the representation is taken over, is to consider how the representation acts under complex conjugation, $\mathcal{K} : x \to x^*$, [149]. Formally on a vector space X, a complex conjugate map $\mathcal{K} : X \to X$ is a map so that

- $\mathcal{K}(ax + by) = a^*\mathcal{K}(x) + b^*\mathcal{K}(y) \; \forall a, b \in \mathbb{C}, \; x, y \in X$.

- $\langle \mathcal{K}x, \mathcal{K}y \rangle = \langle y, x \rangle = \langle x, y \rangle^*$

- $\mathcal{K}^2 = \mathbb{I}$.

These requirements can be summarized as requiring that $\mathcal{K}$ is involutive (requirement 3) and anti-linear, anti-unitary (requirements 1 and 2). The anti-linear, anti-unitary requirements will appear again in defining graded representations and the definition of complex conjugtion as the operator $\mathcal{K}$ will persist throughout this thesis.

Given ρ and $\mathcal{K}$, the complex conjugation representation is defined as

$$\rho^*(g) = \mathcal{K}\rho(g)\mathcal{K}$$

and it must either be equivalent or inequivalent to ρ, which in turn classifies the field ρ is defined over, [149]:

Theorem 2.1.19. *Let G be a finite group, and ρ an irreducible representation with complex conjugate representation ρ^*. Then, either there exists an intertwiner S such that*

$$\rho^* = S\rho S^{-1}, \qquad \begin{cases} SS^* = \mathbb{I} & \text{and } \rho \text{ is real} \\ SS^* = -\mathbb{I} & \text{and } \rho \text{ is quaternionic} \end{cases}$$

or

$$\rho^* \ncong \rho, \qquad \text{and } \rho \text{ is complex}$$

Both of the above approaches of classifying K as real, complex or quaternionic are useful, and will see application in defining structure on graded groups.

2.1.2 Character Theory

Irreducible representations are the idealised objects of study of representation theory, however they are difficult to construct. The regular representation does encode a copy of every one, but finding the correct transformation to separate them is a complicated task. However, for most purposes, the matrix form of an irreducible representation is unnecessary - all the relevant information is encoded in the representation's character, [99, 149]:

Definition 2.1.20. *Let G be a finite group with matrix representation R. Then the character χ_R of R is defined as*

$$\chi_R(g) = \text{Tr}(R(g)).$$

The fact that the easiest proofs of Theorems 2.1.10 and 2.1.12 require character theory is a hint towards their power. They obey a number of incredibly useful rules, [52, 99]:

Proposition 2.1.21. *Let G be a finite group, with the set of conjugacy classes $\{C_g\}$, the set of irreducible representations $\{\rho_i\}$, and the representation R. Then:*

1. For a given representation R, $\chi_R(g)$ is dependent only on the conjugacy class of g. That is $\chi_R(g_1) = \chi_R(g_2) \; \forall g_2 \in C_{g_1}$. Thus, the characters of the conjugacy class $c \in \{C_g\}$ can be referred to as $\chi_R(c)$.

2. The character of an element's inverse is the complex conjugate of the character, $\chi_R(g^{-1}) = \chi_R^*(g)$.

3. The characters of inequivalent irreducible representations are orthogonal, with respect to the inner product on characters,

$$\langle \chi_{\rho_i}, \chi_{\rho_j} \rangle = \frac{1}{|G|} \sum_{c \in \{C_g\}} |c| \chi_{\rho_i}(c) \chi_{\rho_j}^*(c) = \delta_{ij} \tag{2.5}$$

4. The characters of two conjugacy classes C_j, C_k of elements j, k inequivalent under conjugation, $i \sim j \Leftrightarrow \exists g \in G : i = gjg^{-1}$, are orthogonal when averaged over the irreducible representations,

$$\frac{|C_i|}{|G|} \sum_{r \in \{\rho_i\}} \chi_r(C_j) \chi_r^*(C_k) = \delta_{j \sim k}$$

5. Given a reducible representation R, then its decomposition into irreducible components $R = \bigoplus_i \bigoplus_{n=1}^{s_i} \rho_i$ can be calculated by finding the multiplicities of each of the irreducible representations ρ_i in R. These are given by

$$s_i = \langle \chi_R, \chi_{\rho_i} \rangle$$

for each irreducible representation ρ_i of G.

6. If a representation R has dimension d, then $\chi_R(e) = d$.

Characters have the advantage over matrix representations in that they are algorithmically computable having been given a group without it representation, with examples of such algorithms including Burnside's Method appearing in [52]. They are therefore more suitable for any work with representations done on computers, and will provide an essential tool for designing the algorithms described in Chapter 5.

The standard way of presenting the information about the characters of a group is in the character table.

Definition 2.1.22. *Let G be a finite group, $\{\rho_i\}$ the set of unique irreducible representations and $\{C_g\}$ the set of unique conjugacy classes of G. Then the character table Γ of G is the $|\{\rho_i\}| \times |\{\rho_i\}|$ table with entries given by*

$$\Gamma_{ij} = \chi_{\rho_i}(C_j)$$

Characters can also be applied to the problem of classifying the fields of irreducible representations by combining the classification of irreducible representations ρ by their equivalence to ρ^* according to Theorem 2.1.19 with the character orthogonality relation 2.5 to form the Frobenius-Schur Indicator, [52]:

Theorem 2.1.23. *Let G be a finite group with irreducible matrix representation ρ over K. Then, ρ is real, complex or quaternionic according to the indicator*

$$FSI_U(\rho) = \frac{1}{|G|} \sum_{g \in G} \chi_\rho(g^2) = \begin{cases} 1 & \rho \text{ real} \\ 0 & \rho \text{ complex} \\ -1 & \rho \text{ quaternionic} \end{cases}$$

2.2 Representation of Z_2-Graded Groups

The reason for the study of representations is that the symmetry group G of a quantum system can often be inferred from the geometry of the system more easily than it can be found through the testing of combinations of operators. When this geometric analysis is done, an abstract group is found, and it is then necessary to reconstruct the appropriate operators on the Hilbert space. Furthermore, as previously mentioned, the representations of the symmetry group and its subgroup U predict the statistical behaviour of the energy levels of the system. However, the representations discussed in the last section produce purely unitary operators, and it has already been discussed how time-reversal and charge-conjugation type operators require anti-unitary operators. This issue can however be circumvented, by the application of *graded groups*. These are groups where additional structure is identified in the elements, which allows representations of them to include the necessary anti-unitary elements.

We begin with the grading structure needed to describe systems with generalised time-reversal but not generalised charge-conjugation or generalised chiral symmetries. These groups were first studied in the context of physics by Wigner, [175], and developed by [30, 47, 48] as the magnetic groups; their special representations are most commonly known as corepresentations. We note that Moore, [59, 117], on the other hand calls them ϕ-representations to avoid the fact the term corepresentation is already used for representations of co-algebras. In keeping with the majority of the physics literature, we will continue to discuss them as 'corepresentations' rather than adopting Moore's language despite the issue of the name overlap. This will also allow a degree of useful name overloading when dealing with situations where either Z_2-graded or the $Z_2 \times Z_2$-graded groups discussed in Section 2.3 could be present, as we can refer to the representations of both as corepresentations.

From here on, we treat the subject abstractly, laying the foundation to apply these groups in Chapter 3. This will allow the theory to be discussed more rigorously, however we do ensure that naming conventions are kept consistent with physically motivated labels and interpretations. There is only one thing of importance to note before doing this - the symmetry group G described in the introduction is not the symmetry group normally considered, but is the extension of the true symmetry group, which acts on the *projective* Hilbert space, not the full Hilbert space, with the true symmetry group being found by taking $G \to G/\mathcal{U}(1)$. The link between the true symmetry group and the extended symmetry group and how one can move between them is discussed in Chapter 3. The important change however, is that scalar multiplication is removed as a member of G - which sets all phase shifts in the operators to 1 - and in all cases to be considered turns the extended symmetry group - which was infinite - into a finite group. These

are necessary measures when working with an abstract group, in order to find the correct finite number of corepresentations, which will act on the projective Hilbert space. It should be noted however, that phrasing around whether a subset of scalars is included in the symmetry group can be fairly fluid in the physics community. None are included here initially, and the abstract techniques of re-including scalar multiplication in the corepresentations of the true symmetry groups to find their representation on the full Hilbert space are discussed in Section 2.4.

Reiterating, we now call the true symmetry group G, and drop the prefix of 'true' from its description.

With this motivation, we now start with the most general definition of a graded group:

Definition 2.2.1. *Let G, G' be finite groups. (G, R) is a G'-graded group if $R : G \to G'$ is a homomorphism. If $U = \ker(R)$ and T is the transversal of U in G, then $G = \bigcup_{t \in T} tU$.*

G is then divided into subsets that interact with each other according to G'.

The first relevant grading here is the Z_2 grading, [30, 117]:

Definition 2.2.2. *A Z_2-graded group (G, ϕ) is the finite group G with the group homomorphism $\phi : G \to Z_2$. Labelling $\ker(\phi) = U$ and $A = \{g \in G \mid \phi(g) = -1\}$ then $G = U \cup A$. Choosing an element $\alpha \in G - \ker(\phi)$, then $G = U \cup \alpha U$.*

This either splits G into two halves - a normal subgroup U of index 2 and its coset, αU, or else $U = G$ as the map ϕ is trivial.

Lemma 2.2.3. *If $A \neq \emptyset$ then $|A| = |U| = |G|/2$.*

Proof. If A is non-empty, then it is a coset of U in G and $G = U \cup A$. Therefore $|U| = |A|$ and $|U| + |A| = |G|$ which implies $|A| = |U| = |G|/2$. If $A = \emptyset$ then $\ker \phi = G$ and $\phi = 1$ is the trivial map. $\square$

In almost all cases of interest though, A will be non-empty, as this is the case when the new structure of the corepresentations of Z_2-graded groups becomes relevant. This is the ability for corepresentation elements to be anti-linear, that is to apply the complex conjugation operator to all elements to their right. Due to this non-linearity, these elements are no longer homomorphisms when taken over a vector space that allows multiplication of its vectors by complex numbers. This would be an issue, as the standard representation definition requires the originating vector space V to be complex, however, by taking the same basis elements $\{e_i\}$ and then allowing multiplication by only scalars in $\mathbb{R}$, a subspace $V_\mathbb{R} \subset V$ is created, and the anti-linear corepresentation elements are homomorphisms on this subspace of V. The space $GL(V_\mathbb{R})$ can then be taken as the space to define the representation elements, with the domain of the functions in it then extended to all of V. As the domain is being extended, there is no requirement that the functions remain linear on the new parts of the domain - allowing the necessary anti-linear elements.

We note that where the previous section used $GL(V)$ as the name of the group of invertible, linear maps, when V is finite dimensional it is more common to call the space $\mathrm{Aut}(V)$ in the physics literature, which we do from here out. This is allowable, as all the vector spaces under consideration in our applications will be finite so $GL(V) = \mathrm{Aut}(V)$.

The formal definition of a corepresentation is given as, [59, 117, 176]:

Definition 2.2.4. *Let (G, ϕ) be a Z_2-graded group. Let V be a vector space over $\mathbb{C}$ with subspace $V_{\mathbb{R}}$ where scalar multiplication is restricted to $\mathbb{R}$. Then the corepresentation $\mathcal{R}$ of (G, ϕ) is defined as*

$$\mathcal{R} : G \to \mathrm{Aut}(V_{\mathbb{R}}), \qquad \mathcal{R}(g)z = \begin{cases} z\mathcal{R}(g) & \phi(g) = 1 \\ z^*\mathcal{R}(g) & \phi(g) = -1 \end{cases} \quad \forall z \in \mathbb{C}.$$

Given that U is a normal subgroup of G of index 2, a matrix representation R of U induces a matrix corepresentation of G by a modification of the induced representation formulae for Z_2 in Equation 2.1, as, [30],

$$\mathcal{R}(g \in U) = \begin{pmatrix} R(g) & 0 \\ 0 & R^*(\alpha^{-1}g\alpha) \end{pmatrix}, \qquad \mathcal{R}(g \in \alpha U) = \begin{pmatrix} 0 & R(g\alpha) \\ R^*(\alpha^{-1}g) & 0 \end{pmatrix} \mathcal{K} \qquad (2.6)$$

so that the complex conjugate representation is taken whenever α^{-1} appears, and the complex conjugation map is added for elements of αU. As $\mathcal{K}$ is anti-unitary, corepresentation elements can no longer all be unitary, but are instead are unitary/anti-unitary based on whether g is in U or αU, [176]:

Theorem 2.2.5. *Let (G, ϕ) be a Z_2 graded group, V a vector space with inner product $\langle \cdot, \cdot \rangle$ and $\mathcal{R} : G \to \mathrm{Aut}(V_{\mathbb{R}})$ a corepresentation. Then there exists and inner product $\langle \cdot, \cdot \rangle'$ which $\mathcal{R}(u \in U)$ is unitary with respect to and $\mathcal{R}(a \in \alpha U)$ is anti-unitary with respect to,*

$$\langle \mathcal{R}(u)v, \mathcal{R}(u)w \rangle' = \langle v, w \rangle', \quad \langle \mathcal{R}(a)v, \mathcal{R}(a)w \rangle' = \langle v, w \rangle'^*, \quad \forall v, w \in W, \ u \in U, a \in \alpha U.$$

Group elements of U will be termed unitary, and elements of αU, anti-unitary.

Proof. We prove this by construction of a suitable inner product. Assuming that the inner product $\langle \cdot, \cdot \rangle'$ on V already exists, then

$$\langle v, w \rangle' = \frac{1}{|G|} \sum_{u \in U} \langle \mathcal{R}(u)v, \mathcal{R}(u)w \rangle + \langle \mathcal{R}(u\alpha)v, \mathcal{R}(u\alpha)w \rangle^*$$

is an inner product and satisfies the unitary/anti-unitary requirement. $\qquad \square$

This is also where the labels for the two subsets U, A of G come from - U stands for the unitary elements, and A stands for the anti-unitary elements.

While an anti-unitary element can no longer be written solely as a unitary matrix, it is still possible to standardise the form of their corepresentations, so it is not required to look for many different forms of anti-unitary operator - looking at the matrix forms for a corepresentation, the anti-unitary elements can always be represented by a unitary matrix right-multiplied by an anti-unitary operation $\mathcal{K}$. The unitary-matrix part of a corepresentation will be defined as $\tilde{\mathcal{R}}$, so that for a unitary element, $\mathcal{R} = \tilde{\mathcal{R}}$, while for an anti-unitary element, $\mathcal{R} = \tilde{\mathcal{R}}\mathcal{K}$.

Equivalence of corepresentations is again through the existence of intertwiners between the corepresentations, [176]:

Definition 2.2.6. *Let (G, ϕ) be a Z_2-graded group, V_1, V_2 vector spaces, and $\mathcal{R}_1, \mathcal{R}_2$ be corepresentations of (G, ϕ) on V_1, V_2 respectively. Then an intertwiner $T \in \mathrm{Hom}(V_1, V_2)$ is a morphism*

such that

$$T\mathcal{R}_1(g) = \mathcal{R}_2(g)T \qquad \forall g \in G.$$

If T is a bijection, then $\mathcal{R}_1, \mathcal{R}_2$ are equivalent corepresentations, $\mathcal{R}_1 \cong \mathcal{R}_2$.

Looking only at the unitary matrix parts of the corepresentations, two corepresentations $\mathcal{R}_1, \mathcal{R}_2$ will then be equivalent if

$$\exists T \in \mathcal{U}(n), \qquad \begin{aligned} \tilde{\mathcal{R}}_1(u \in U)T &= T\tilde{\mathcal{R}}_2(u \in U) \\ \tilde{\mathcal{R}}_1(a \in \alpha U)T^* &= T\tilde{\mathcal{R}}_2(a \in \alpha U). \end{aligned}$$

Irreducible corepresentations can also be defined the same way as irreducible representations, [30]:

Definition 2.2.7. *Let $\mathcal{R}$ be a corepresentation on V of $G = U \cup \alpha U$, a Z_2-graded group. If there exists a proper subspace $W \subsetneq V$, $W \neq \emptyset$ such that W is invariant under $\mathcal{R}$,*

$$\mathcal{R}(g)w \in W, \qquad \forall g \in G, \ w \in W$$

then $\mathcal{R}$ is the direct sum of two corepresentations $\mathcal{R}_W : G \to \mathrm{Aut}(W_{\mathbb{R}})$ and $\mathcal{R}_{W^\perp} : G \to \mathrm{Aut}(W_{\mathbb{R}}^\perp)$.

If no such proper subspace exists then $\mathcal{R}$ is an irreducible corepresentation of G, and will be labelled ϱ.

This means Maschke's Theorem of complete reducibility further holds for corepresentations, and can be proved in exactly the same way as for unitary representations, [176].

Theorem 2.2.8. *Let (G, ϕ) be a finite Z_2-graded group with irreducible corepresentations $\{\varrho_i\}$ and corepresentation $\mathcal{R}$ all over a field of characteristic 0. Then either $\mathcal{R} = \varrho_i$ is irreducible, or $\mathcal{R}$ is completely decomposable as a direct sum of irreducible corepresentations with multiplicities s_i,*

$$\mathcal{R} \cong \bigoplus_i \bigoplus_{n=1}^{s_i} \varrho_i.$$

2.2.1 Classification of Finite Irreducible Corepresentations

We now come to the problem of attempting to classify the irreducible corepresentations of a Z_2-graded group in a manner similar to that which was done for the unitary representations of an ungraded group. This lead to the classification of corepresentations under another threefold way, this time introduced by Dyson, [51]. The methodology here will be nearly the same as in Section 2.1.1, applying Artin-Wedderburn's Theorem to a group algebra, and then applying Fronbenius' Theorem to restrict the number of allowable division algebras.

We begin by defining the applicable group algebra. In this case, where the corepresentation contains complex-conjugation as an element, it is necessary to work immediately over the real vector space found by applying the map from Equation 2.3 to the vector space V. In this basis $\mathcal{K}$ has a matrix representation, $K = \mathbb{I}_n \otimes \left(\begin{smallmatrix} 1 & 0 \\ 0 & -1 \end{smallmatrix} \right)$, allowing it to appear in the matrix algebra. Dyson's construction of the group algebra and its commutator algebra, [51], is thus:

Definition 2.2.9. *Let $\mathcal{R}$ on V over $\mathbb{C}$ be a corepresentation of the Z_2-graded group $G = U \cup \alpha U$. Let $\mathfrak{R} : \mathbb{C}^n \to \mathbb{R}^{2n}$ be the map defined by Equation 2.3 and let $K = \mathbb{I}_n \otimes \left(\begin{smallmatrix} 1 & 0 \\ 0 & -1 \end{smallmatrix} \right)$ be the matrix representation of complex conjugation in this basis.*

Then the group algebra X over $\mathbb{R}$ is the algebra defined with the basis

$$\left\{ \mathfrak{R}(\tilde{\mathcal{R}}(g \in U)) \right\} \cup \left\{ \mathfrak{R}(\tilde{\mathcal{R}}(g \in \alpha U))K \right\} \cup \left\{ i = \mathbb{I}_n \otimes \begin{pmatrix} 0 & -1 \\ 1 & 0 \end{pmatrix} \right\}.$$

The commutator algebra $\overline{X}$ of X is defined as the algebra generated by the matrices over $\mathbb{R}^{2n}$ such that they commute with all the elements of X.

The form of Artin-Wedderburn's Theorem given in Theorem 2.1.15 applied to this group algebra, with the division algebras over $\mathbb{R}$ already identified by Frobenius' Theorem, then gives, [51]:

Theorem 2.2.10. *Let $\mathcal{R}$ be a corepresentation of the Z_2-graded group (G, ϕ) generating the group algebra X and its commutator algebra $\overline{X}$ over $\mathbb{R}^{2n}$. Then $X, \overline{X}$ decompose into irreducible components*

$$X \cong \sum_{i=1}^{n} s_i(E_i)_{t_i}, \qquad \overline{X} \cong \sum_{i=1}^{n} t_i(E_i)_{s_i}$$

for some s_i, t_i, where $E_i \cong \mathbb{R}, \mathbb{C}$ or $\mathbb{H}$ for each i.

Looking at the irreducible representations in particular gives what is known as Dyson's Threefold Way, [51]:

Theorem 2.2.11. *Let $G = U \cup \alpha U$ be a Z_2-graded group and ϱ an irreducible matrix corepresentation. Then the group algebra X over $\mathbb{R}$ generated by ϱ is isomorphic to a matrix algebra over one of the division rings $\mathbb{R}, \mathbb{H}, \mathbb{C}$. It will be termed a Wigner Type I, II or III corepresentation respectively.*

In the same way real, complex and quaternionic representations could be identified by whether they were equivalent to their complex conjugate representation, comparison of the irreducible representation ρ generating $\mathcal{R}$ and its copy under the action of α allows the Wigner type of $\mathcal{R}$ to be identified, [30].

Theorem 2.2.12. *Let $G = U \cup \alpha U$ a Z_2-graded group, ρ an irreducible representation of U and $\mathcal{R}$ the corepresentation of G generated by ρ. Then, the action of α on ρ is given by*

$$\alpha : \rho \to \overline{\rho}(u) = \rho^*(\alpha^{-1} u \alpha).$$

and either there exists an intertwiner W such that

$$\overline{\rho} = W \rho W^{-1}, \qquad \begin{cases} WW^* = \mathbb{I} & \mathcal{R} \text{ is of Type I} \\ WW^* = -\mathbb{I} & \mathcal{R} \text{ is of Type II} \end{cases}$$

or

$$\overline{\rho} \not\cong \rho, \qquad \mathcal{R} \text{ is of Type III.}$$

The Frobenius-Schur Indicator can also be modified to tell apart the different corepresentation classes, [30, 48]:

Theorem 2.2.13. *Let $G = U \cup \alpha U$ be a Z_2-graded group with irreducible representation ρ of U generating the corepresentation $\mathcal{R}$ of G. Then $\mathcal{R}$ is of Wigner Type I, II, III according to the Frobenius-Schur Indicator*

$$FSI_A(\mathcal{R}) = \frac{1}{|U|} \sum_{u \in U} \chi_\rho((u\alpha)^2) = \begin{cases} 1 & \mathcal{R} \text{ Type I} \\ 0 & \mathcal{R} \text{ Type III} \\ -1 & \mathcal{R} \text{ Type II} \end{cases}$$

Proof. The proof is very similar to that of the Frobenius-Schur indicator, but only applying the sum to the subset A of elements. See [30] for the standard proof. $\square$

Taking a corepresentation derived using Equation 2.6, its Wigner Type also gives its reducibility, [30]:

Theorem 2.2.14. *Let $G = U \cup \alpha U$ be a Z_2-graded group, ρ an irreducible representation of U and $\mathcal{R}$ the matrix corepresentation generated by ρ according to Equation 2.6.*

Then, if $\mathcal{R}$ is of Wigner Type II or III, $\mathcal{R}$ is irreducible. If $\mathcal{R}$ is of Type I with $\overline{\rho} = W\rho W^{-1}$, it reduces as

$$\mathcal{R}(g \in U) \cong \begin{pmatrix} \rho(g) & 0 \\ 0 & \rho(g) \end{pmatrix}, \qquad \mathcal{R}(g \in \alpha U) \cong \begin{pmatrix} \rho(g\alpha^{-1})W & 0 \\ 0 & -\rho(g\alpha^{-1})W \end{pmatrix}.$$

Dyson's Tenfold Way

Occasional reference is made to a 'Tenfold Way' of Dyson. This is is due to the fact that given a corepresentation $\mathcal{R}$ generated by the irreducible representation ρ, the pair can be classified according to both Theorem 2.1.18 and Theorem 2.2.11; alternatively by Theorem 2.1.19 and Theorem 2.2.11 or alternatively Theorem 2.1.23 and Theorem 2.2.13, [51]:

Theorem 2.2.15. *Let $G = U \cup \alpha U$ be a finite Z_2-graded group. Let ρ be an irreducible unitary representation of U and $\mathcal{R}$ the corepresentation of G generated by ρ.*

Then the classification of ρ as real, complex or quaternionic and the classification of $\mathcal{R}$ as Wigner Type I, II and III are independent and form a nine-fold classification.

Furthermore, the case when ρ is complex and $\mathcal{R}$ is of Wigner Type III can be split into two - if $\overline{\rho}(u) = \rho^*(\alpha^{-1}u\alpha)$ and $\overline{\rho}(u) = \rho^*(u)$, then the class $\mathbb{C}III$ implies that $\rho \not\cong \rho^*$ and $\rho \not\cong \overline{\rho}$. However it is still possible that $\rho \cong \overline{\rho}^*$, creating two subclasses within the class $\mathbb{C}III$ - the class $\mathbb{C}III1$ when the equivalence breaks, and the class $\mathbb{C}III2$ when the equivalence holds.

This forms Dyson's Tenfold Way, the combination of the Frobenius class of the representation ρ and the Wigner Type of the corepresentation $\mathcal{R}$ that it generates:

	$\rho \cong \rho^*,\ SS^* = \mathbb{I}$	$\rho \cong \rho^*,\ SS^* = -\mathbb{I}$	$\rho \not\cong \rho^*$	
$\rho \cong \overline{\rho},\ WW^* = \mathbb{I}$	$\mathbb{R}I$	$\mathbb{H}I$	$\mathbb{C}I$	
$\rho \cong \overline{\rho},\ WW^* = -\mathbb{I}$	$\mathbb{R}II$	$\mathbb{H}II$	$\mathbb{C}II$	
$\rho \not\cong \overline{\rho}$	$\mathbb{R}III$	$\mathbb{H}III$	$\rho \not\cong \overline{\rho}^* \ \mathbb{C}III1$	$\rho \cong \overline{\rho}^* \ \mathbb{C}III2$

In order to tell the ten classes apart, the indicators FSI_U and FSI_A can be used, along with the additional indicator Ind_{CIII} which is used when $FSI_U(\rho) = FSI_A(\rho) = 0$ and tells apart the $\mathbb{C}III1$ and $\mathbb{C}III2$ classes:

Theorem 2.2.16. *Let G be a Z_2-graded group with unitary sub-group U. Let ρ be an irreducible representation of U generating the corepresentation $\mathcal{R}$ of G. If $FSI_U(\rho) = FSI_A(\rho) = 0$, then the class of the pair $\rho, \mathcal{R}$ according to Dyson's tenfold-way can be found by applying the indicator,*

$$Ind_{\mathbb{C}III}(\rho) = \frac{1}{|U|} \sum_{u \in U} \chi_\rho(u) \chi_\rho^*(\alpha^{-1}u\alpha) = \begin{cases} 0 & \mathbb{C}III1 \\ 1 & \mathbb{C}III2 \end{cases} \tag{2.7}$$

Proof. The classes $\mathbb{C}III1$ and $\mathbb{C}III2$ are differentiated depending on whether $\rho(u) = \rho(\alpha^{-1}u\alpha) = \tilde{\rho}(u)\ \forall u \in U$. This is the requirement that $\rho \cong \tilde{\rho}$. Equivalence of two irreducible representations ρ_1, ρ_2 can be checked by using the character orthogonality relation,

$$\frac{1}{|U|} \sum_{u \in U} \chi_{\rho_1}(u) \chi_{\rho_2}^*(u) = \begin{cases} 0 & \rho_1 \not\cong \rho_2 \\ 1 & \rho_1 \cong \rho_2 \end{cases}$$

so substituting $\rho_1 = \rho$ and $\rho_2 = \tilde{\rho}$ gives the above indicator. $\qquad\square$

The Dyson Tenfold Way is useful as it gives significantly more information about the structure of the algebras X and $\overline{X}$, as can be seen in in Table 2.1, [51]. The structure given to $\overline{X}$ by the combination of studying combinations of indicators will continue to be important, as it will allow structure to be imposed on the Hamiltonian of the system, once the applications of graded symmetry groups are applied to quantum systems. In Appendix E, the corepresentations of the groups of order up to $G \leq 30$ will be classified according to Dyson's Tenfold Way by using the indicators given above and the search algorithms for Z_2-graded groups from Chapter 5.

2.3 Representation of $Z_2 \times Z_2$-Graded Groups

Corepresentations of Z_2-graded groups were introduced to cover systems with time-reversal symmetry. Here the additional Z_2 grading that needs to be added to describe systems with chiral and particle-hole or charge-conjugation symmetry, where operators anti-commute with the Hamiltonian, such as in certain types of superconductors, [64], is discussed. Again we stick to a more abstract definition before expanding on their applications in Chapter 3.

	X	$\overline{X}$
$\mathbb{R}I$	$2\mathbb{R}_n$	$n\mathbb{R}_2$
$\mathbb{R}II$	$\mathbb{H}_n$	$n\overline{\mathbb{H}}$
$\mathbb{R}III$	$\mathbb{C}_n$	$n\mathbb{C}$
$\mathbb{H}I$	$4\mathbb{R}_n$	$n\mathbb{R}_4$
$\mathbb{H}II$	$2\mathbb{H}_n$	$n\overline{\mathbb{H}}_2$
$\mathbb{H}III$	$2\mathbb{C}_n$	$n\mathbb{C}_2$
$\mathbb{C}I$	$2\mathbb{R}_n \oplus 2\mathbb{R}_n$	$n\mathbb{R}_2 \oplus n\mathbb{R}_2$
$\mathbb{C}II$	$\mathbb{H}_n \oplus \mathbb{H}_n$	$n\overline{\mathbb{H}} \oplus n\overline{\mathbb{H}}$
$\mathbb{C}III1$	$\mathbb{C}_n \oplus \mathbb{C}_n$	$n\mathbb{C} \oplus n\mathbb{C}$
$\mathbb{C}III2$	$2\mathbb{C}_n$	$n\mathbb{C}_2$

Table 2.1: The structure imposed on X and $\overline{X}$ by the Dyson Tenfold Way class of the irreducible representation ρ generating them, [51]. This also makes clear the importance of separating the classes $\mathbb{C}III1$ and $\mathbb{C}III2$, as the forms of $X, \overline{X}$ for $\mathbb{C}III2$ are significantly more restricted than in the case of $\mathbb{C}III1$.

We consider the $Z_2 \times Z_2$-graded groups:

Definition 2.3.1. *A $Z_2 \times Z_2$-graded group (G, ϕ, ξ) is the finite group with the group homomorphism $\phi \times \xi : G \to Z_2 \times Z_2$. Choosing the sets and elements*

$$U \quad = \quad \{g \in G \mid \phi(g) = 1 = \xi(g)\} \quad \alpha \in A \quad = \quad \{g \in G \mid \phi(g) = -1, \xi(g) = 1\}$$
$$\gamma \in C \quad = \quad \{g \in G \mid \phi(g) = -1 = \xi(g)\} \quad \pi \in P \quad = \quad \{g \in G \mid \phi(g) = 1, \xi(g) = -1\}$$

then

$$G = U \cup A \cup C \cup P, \qquad G = U \cup \alpha U \cup \gamma U \cup \pi U.$$

Lemma 2.3.2. *Let (G, ϕ, ξ) be a $Z_2 \times Z_2$-graded group. Then either $G = U$; $G = U \cup A$, $|A| = |G|/2$; $G = U \cup C$, $|C| = |G|/2$; $G = U \cup P$, $|P| = |G|/2$; or $G = U \cup A \cup C \cup P$, $|A| = |C| = |P| = |G|/4$.*

Proof. In the case that only one of A, C, P is non-empty, the proof of Lemma 2.2.3 holds.

To show that if at least two of A, C, P are non-empty, then the third is also non empty, consider that $\forall a \in A, c \in C$ then $ac, ca \in P$, similarly $\forall a \in A, p \in P$ then $ap, pa \in C$ and $\forall p \in P, c \in C$ then $pc, cp \in A$. There are then the multiplication rules on the sets $AC = P$, $AP = C$, $CP = A$ and two non-empty sets construct a third non-empty set.

If all three of A, C, P are non-empty, then they are co-sets of U in G and must be of the same size and sum to $|G|$, $|U| = |A| = |C| = |P| = |G|/4$. $\qquad\square$

Effectively, to form a $Z_2 \times Z_2$-graded group, a Z_2-graded group has been taken, then an additional structure added on top of the original grading. This means that when considering their representations, they must be consistent with the corepresentations of a Z_2-graded group, but with an additional structure added. These representations of $Z_2 \times Z_2$-graded groups, which we again call corepresentations, are studied by [24, 59, 117], and add the necessary additional structure by being defined over not a vector space, but a super-vector space, $V = V^0 + V^1$,

as described in Appendix B and [117, 165]. This means that the automorphism group $\text{Aut}(V_\mathbb{R})$ also requires grading, and becomes $\mathbf{Aut}(V_\mathbb{R})$, and the representation elements can now be either even or odd transformations of V, depending on where in $\mathbf{Aut}(V_\mathbb{R})$ they sit. We note that the corepresentation elements are always homogeneous.

Formally, the corepresentation of a $Z_2 \times Z_2$-graded group is given by, [59, 117]:

Definition 2.3.3. *Let (G, ϕ, ξ) be a $Z_2 \times Z_2$-graded group, V a super-vector space over $\mathbb{C}$ and $V_\mathbb{R}$ its restriction of scalar multiplication to $\mathbb{R}$. Then the corepresentation $\mathcal{R}$ is the super-homomorphism*

$$\mathcal{R} : G \to \mathbf{Aut}(V_\mathbb{R}), \qquad \mathcal{R}(g)z = \begin{cases} z\mathcal{R}(g) & \phi(g) = 1 \\ z^*\mathcal{R}(g) & \phi(g) = -1 \end{cases}, \qquad \mathcal{R}(g) \in \begin{cases} \mathbf{Aut}(V_\mathbb{R})^0 & \xi(g) = 1 \\ \mathbf{Aut}(V_\mathbb{R})^1 & \xi(g) = -1 \end{cases}.$$

Given that when all of $A, \mathbb{C}$ and P are non-empty U is a normal subgroup of G of index 4, with Klein-4 quotient group $G/U = K_4$, the induced representation in Equation 2.2 can be modified to take a matrix representation R of U and generate the matrix corepresentation $\mathcal{R}$ of G by the formulae,

$$
\begin{aligned}
\mathcal{R}(g \in U) &= \begin{pmatrix} R(g) & 0 & 0 & 0 \\ 0 & R^*(\alpha^{-1}g\alpha) & 0 & 0 \\ 0 & 0 & R(\pi^{-1}g\delta) & 0 \\ 0 & 0 & 0 & R^*(\gamma^{-1}g\gamma) \end{pmatrix} \\[2mm]
\mathcal{R}(g \in \alpha U) &= \begin{pmatrix} 0 & R(g\alpha) & 0 & 0 \\ R^*(\alpha^{-1}g) & 0 & 0 & 0 \\ 0 & 0 & 0 & R(\pi^{-1}g\gamma) \\ 0 & 0 & R^*(\gamma^{-1}g\pi) & 0 \end{pmatrix} \mathcal{K} \\[2mm]
\mathcal{R}(g \in \delta U) &= \begin{pmatrix} 0 & 0 & R(g\pi) & 0 \\ 0 & 0 & 0 & R^*(\alpha^{-1}g\gamma) \\ R(\pi^{-1}g) & 0 & 0 & 0 \\ 0 & R^*(\gamma^{-1}g\alpha) & 0 & 0 \end{pmatrix} \\[2mm]
\mathcal{R}(g \in \gamma U) &= \begin{pmatrix} 0 & 0 & 0 & R(g\gamma) \\ 0 & 0 & R^*(\alpha^{-1}g\pi) & 0 \\ 0 & R(\pi^{-1}g\alpha) & 0 & 0 \\ R^*(\gamma^{-1}g) & 0 & 0 & 0 \end{pmatrix} \mathcal{K}
\end{aligned}
\tag{2.8}
$$

having swapped the ordering of P, C for better symmetry under $U, A \leftrightarrow P, C$. These matrices very clearly show the super-vector space structure of the corepresentation - the space is split into two subspaces $V = V^0 \oplus V^1$ and elements of $U \cup \alpha U$ preserve the subspaces, while elements of $\gamma U \cup \pi U$ invert the subspaces, the exact definition of even and odd operators on super-vector spaces.

Equivalence of the corepresentations now require super-intertwiners to take into account that the concept of commutation is extended to super-commutation, as per Equation B.1.7, on super-vector spaces, [117]:

Definition 2.3.4. *Let (G, ϕ, ξ) be a $Z_2 \times Z_2$-graded group, V_1, V_2 super-vector spaces and $\mathcal{R}_1, \mathcal{R}_2$ corepresentations of (G, ϕ, ξ) on V_1, V_2 respectively. Then the super-intertwiner $T \in \mathbf{Hom}(V_1, V_2)$ is the graded $\mathbb{C}$-linear transformation between V_1, V_2 such that*

$$T^0 \mathcal{R}_1(g) = \mathcal{R}_2(g)T^0, \qquad T^1 \mathcal{R}_1(g) = \xi(g)\mathcal{R}_2(g)T^1 \qquad \forall g \in G.$$

If T is bijective, then $\mathcal{R}_1, \mathcal{R}_2$ are equivalent (ϕ, ξ)-representations, $\mathcal{R}_1 \cong \mathcal{R}_2$.

Irreducibility of the corepresentations continues to maintain its standard definition, [117].

Definition 2.3.5. *Let $\mathcal{R}$ be a corepresentation on V of the $Z_2 \times Z_2$ graded group (G, ϕ, ξ). If there exists a proper super-vector sub-space $W \subsetneq V$, $W \neq \emptyset$ such that W is G-invariant,*

$$\mathcal{R}(g)w \in W \qquad \forall g \in G, w \in W$$

then $\mathcal{R}$ is the direct sum of two corepresentations, $\mathcal{R}_W : G \to \mathbf{Aut}(W_{\mathbb{R}})$ and $\mathcal{R}_{W^\perp} : G \to \mathbf{Aut}(W_{\mathbb{R}}^\perp)$ and is reducible.

If no such proper subspace exists then $\mathcal{R}$ is an irreducible corepresentation of G and will be labelled ς.

Maschke's Theorem of complete reducibility then still applies for the same reasons as before:

Theorem 2.3.6. *Let (G, ϕ, ξ) be a finite $Z_2 \times Z_2$-graded group with irreducible corepresentations $\{\varsigma_i\}$ and corepresentation $\mathcal{R}$, all over a field of characteristic 0. then either $\mathcal{R} = \varsigma_i$ is irreducible, or $\mathcal{R}$ is completely decomposable as a direct sum of irreducible corepresentations with multiplicities s_i,*

$$\mathcal{R} = \bigoplus_i \bigoplus_{n=1}^{s_i} \varsigma_i.$$

2.3.1 Classification of Finite Irreducible Corepresentations

Having defined Dyson's Threefold Way on the corepresentations of the Z_2-graded groups, we move onto classifying the corepresentations of the $Z_2 \times Z_2$ graded groups. Again, this is done by studying the decomposition of the algebra generated by the group according to a version of the Artin-Wedderburn theorem. However, there are modifications required to deal with the fact that the group algebra must now be graded, being a super-algebra. This firstly requires a slightly different version of the group algebra to be taken [93]:

Lemma 2.3.7. *Let (G, ϕ, ξ) be a $Z_2 \times Z_2$-graded group, then the group algebra $K[G]$ over the field K of characteristic 0 is the algebra defined by*

$$u = \sum_{g \in G} \lambda_g g, \qquad \lambda_g \in K$$

with

$$\sum_{g \in G} \lambda_g g + \sum_{g \in G} \mu_g g = \sum_{g \in G} (\lambda_g + \mu_g) g$$

$$\sum_{g \in G} \lambda_g g \times \sum_{h \in G} \mu_h h = \sum_{g,h \in G} (\lambda_h \mu_{h^{-1}g}) g$$

Taking the grading where homogeneous algebra elements are built of sums of elements entirely from U or entirely from αU, with degree based on which set is used to build u,

$$\left| \sum_{g \in G} \lambda_g g \right| = \begin{cases} 0 & \lambda_g = 0 \; \forall g : \xi(g) = -1 \\ 1 & \lambda_g = 0 \; \forall g : \xi(g) = 1 \end{cases}$$

then $K[G]$ is a semi-simple super-algebra.

The inverse of the group element h appearing in the subscript of the sum is the standard form for group actions to be homomorphic.

Next, instead of being able to consider the super-algebra $K[G]$ itself, it must be reconsidered as its own super-module, in the way described in Appendix B. Due to $K[G]$ being semi-simple, then all of its super-modules are also semi-simple, [165], and as a super-module, $K[G]$ can be expressed as

$$K[G] = \bigoplus_i M_i$$

where the super-modules M_i are simple. Given that modules take the same role for algebras that representations did for groups, constructing the simple super-module decomposition of $K[G]$ is equivalent to taking the irreducible representation decomposition of a representation of a group. Furthermore, as taking $K[G]$ as its own super-module is equivalent to starting with the regular representation, this produces all simple modules of $K[G]$.

With the simple modules - equivalent to the irreducible representations - identified, it is now possible to look at applying a form of Artin-Wedderburn's theorem to each of the modules. When not needing super-algebras, this theorem stated that the algebra $K[G]$ and its commutant decomposed into direct sums of division algebras. The super-Artin-Wedderburn theorem isn't able to guarantee that the module $K[G]$ decomposes into division algebras, but it is able to guarantee that the super-commutants for each of the simple modules is isomorphic to a super-division algebra when considered individually, [165]:

Lemma 2.3.8. *If A is a super-algebra over K and M a simple super-module for A, then the super-commutant A_M of M is isomorphic to a super division algebra over K.*

While this is less strong in not determining the form of $K[G]$ but only the super-commutants of its simple components, the theorem covers exactly what is needed for the Altland-Zirnbauer Tenfold Way and its applications to quantum chaos - one of the key factors in defining random matrix ensembles is that they are the super-commutant of a suitable symmetry group, as will be discussed at the end of Section 3.1 and in Chapter 4.

As was done for the regular and Z_2-graded groups, using the map $\mathfrak{R}$ from Equation 2.3 with $\mathcal{K} \to \mathbb{I} \otimes \left(\begin{smallmatrix} 1 & 0 \\ 0 & -1 \end{smallmatrix} \right)$ and $i \to \mathbb{I} \otimes \left(\begin{smallmatrix} 0 & -1 \\ 1 & 0 \end{smallmatrix} \right)$, then $K[G]$ can be defined over $\mathbb{R}$ instead of $\mathbb{C}$, having the

knock on effect of the super-module $K[G]$ also being defined over $\mathbb{R}$. Rephrasing and paraphrasing the super-Artin-Wedderburn theorem, this allows for a 'super-Schur' theorem, [117]:

Theorem 2.3.9. *Let (G, ϕ, ξ) be a $Z_2 \times Z_2$ graded group with irreducible corepresentation ς. Let*

$$\mathcal{Z}(\varsigma) = \left\{ T \in \mathbf{Hom}(V, V) \mid T^0 \varsigma(g) = \varsigma(g) T^0 \ T^1 \varsigma(g) = \xi(g) \varsigma(g) T^1 \right\}$$

be the super-commutant of ς as a representation and let $Z = \langle \mathcal{Z}(\varsigma) \rangle$ be the associated super-algebra over $\mathbb{R}$ generated by its elements. Then Z is isomorphic to a real associative super-division algebra.

Like the number of real associative division algebras are limited to three by Frobenius's Theorem, Wall's Theorem describes the ten possible real associative super division algebras, [117, 168]:

Theorem 2.3.10 (Wall)**.** *The only associative super-division algebras over $\mathbb{R}$ are $\mathbb{R}^{1|0}$, $\mathbb{C}^{1|0}$, $\mathbb{H}^{1|0}$ as purely even super algebras, and $Cl_1^{\mathbb{C}}$, $Cl_{\pm 1}^{\mathbb{R}}$, $Cl_{\pm 2}^{\mathbb{R}}$ and $Cl_{\pm 3}^{\mathbb{R}}$.*

The Clifford algebras $Cl_{\pm i}^K$ are described in Appendix B.2, along with a demonstration that they are super-division algebras.

It is hard to prove that there are only ten real associative division algebras, but given the ten above, it is easy to verify that they are the required ten. This provides a tenfold classification of the irreducible corepresentations, which are labelled by the Cartan classes of symmetric spaces, [117],

Class	A	$AIII$	AI	BDI	D	$DIII$	AII	CII	C	CI
$Z \cong$	$\mathbb{C}$	$Cl_1^{\mathbb{C}}$	$\mathbb{R}$	$Cl_1^{\mathbb{R}}$	$Cl_2^{\mathbb{R}}$	$Cl_3^{\mathbb{R}}$	$\mathbb{H}$	$Cl_{-1}^{\mathbb{R}}$	$Cl_{-2}^{\mathbb{R}}$	$Cl_{-3}^{\mathbb{R}}$

Due to the classification being equivalent to the one introduced by Altland and Zirnbauer in [6] to describe the connection between $Z_2 \times Z_2$-graded groups, random matrices and the Cartan symmetric spaces, this classification is known as the Altland-Zirnbauer Tenfold Way, and in physics is considered an extension of the Dyson Threefold Way, adding the allowance of particle-hole and chiral symmetries to Dyson's time-reversal when calculating the associated random matrix statistics of the quantum system. These applications are discussed in Chapter 4.

As with the Z_2-graded corepresentation, the classification of an irreducible corepresentation of a $Z_2 \times Z_2$-graded group can be found by considering if the underlying unitary representation is equivalent to its copies under the action of conjugation by α, γ, π, [24]:

Theorem 2.3.11. *Let (G, ϕ, ξ) be a $Z_2 \times Z_2$-graded group with irreducible corepresentation ς induced by the irreducible unitary representation ρ of $U \triangleleft G$. Consider the representations of U given by*

$$\bar{\rho}(u) = \rho^*(\alpha^{-1} u \alpha), \qquad \hat{\rho}(u) = \rho^*(\gamma^{-1} u \gamma), \qquad \tilde{\rho}(u) = \rho(\pi^{-1} u \pi)$$

then ten cases exist according to whether $\rho \cong \bar{\rho}$, $\rho \cong \hat{\rho}$ and $\rho \cong \tilde{\rho}$,

	$\hat{\rho} = S\rho S^{-1}$ $SS^* = \mathbb{I}$	$\hat{\rho} = S\rho S^{-1}$ $SS^* = -\mathbb{I}$	$\hat{\rho} \not\cong \rho$	
$\overline{\rho} = W\rho W^{-1}$ $WW^* = \mathbb{I}$	BDI	CI	AI	
$\overline{\rho} = W\rho W^{-1}$ $WW^* = -\mathbb{I}$	$DIII$	CII	AII	
$\overline{\rho} \not\cong \rho$	D	C	$\tilde{\rho} \not\cong \rho$ A	$\tilde{\rho} \cong \rho$ $AIII$

and this classification is equivalent to that given in Theorem 2.3.9.

Also again, generalised Frobenius-Schur Indicators can then be defined to identify the groups, [24]:

Theorem 2.3.12. *Let (G, ϕ, ξ) be a $Z_2 \times Z_2$-graded group and ς an irreducible corepresentation of (G, ϕ, ξ) induced by ρ of U. Then*

$$FSI_A = \frac{1}{|U|} \sum_{u \in U} \chi_\rho\big((u\alpha)^2\big), \qquad FSI_C = \frac{1}{|U|} \sum_{u \in U} \chi_\rho\big((u\gamma)^2\big)$$

$$Ind_P = \frac{1}{|U|} \sum_{u \in U} \chi_\rho(u)\chi_\rho^*(\pi^{-1}u\pi)$$

give the Altland-Zirnbauer class of ς according to Table 2.2.

Class	FSI_A	FSI_C	Ind_P	$Z \cong$
A	0	0	0	$\mathbb{C}$
$AIII$	0	0	1	$Cl_1^{\mathbb{C}}$
AI	1	0	0	$\mathbb{R}$
BDI	1	1	1	$Cl_1^{\mathbb{R}}$
D	0	1	0	$Cl_2^{\mathbb{R}}$
$DIII$	-1	1	1	$Cl_3^{\mathbb{R}}$
AII	-1	0	0	$\mathbb{H}$
CII	-1	-1	1	$Cl_{-1}^{\mathbb{R}}$
C	0	-1	0	$Cl_{-2}^{\mathbb{R}}$
CI	1	-1	1	$Cl_{-3}^{\mathbb{R}}$

Table 2.2: The Altland-Zirnbauer Tenfold Way as given by the indicators FSI_U, FSI_A, FSI_C and Ind_P.

2.4 Projective Representations

It was mentioned at the start of Section 2.2 that there existed both the true symmetry group G of the system, which acts on the projective Hilbert space, and the extended symmetry group, which we now call G^E, which acts on the full Hilbert space; the difference between them being that $G = G^E/\mathcal{U}(1)$, and all scalar multiplication is removed going from G^E to G. Part of the reason for this is that the full group G^E is infinite, and the methods worked with in the last sections required finite groups, the other part is that working on the projective Hilbert space, where all states are physical and unique causes certain parts of the theory related to the quantum form of the system to be more intuitive. This makes the true symmetry group the right group to work with, in most cases.

There are however, situations when removing all of the scalars from G^E is too much. These situations rise predominately from the relevant system containing particles with fractional spin. In these cases, there exist elements in the group G of order n, so that $g^n = e$, but by applying physical knowledge of the system to the corepresentation R of G, it is known that $R(g^n) \neq \mathbb{I}$ against what is required for an element equal to the identity; instead $R(g^n) = k\mathbb{I}$, $k \in K$. The most well known example of this is that a rotation of the electron by 2π has the representation $R(\text{rot}(2\pi)) = -\mathbb{I}$ and it is only after a rotation of 4π that a representation of $\mathbb{I}$ is recovered. These cases where additional scalar factors are picked up are not possible when defining a standard corepresentation which for the symmetry group sits on the projective Hilbert space. There are however a couple of ways to work around this restriction, allowing these corepresentations with additional scalar factors to be built and then classified according to the Dyson Threefold and Altland-Zirnbauer Tenfold Way as described above - because these scalar factors *must* be taken into account to get the correct classification.

The first method would be to define a new group in between G and G^E which doesn't contain all of the scalars, but it does add the scalars $\{k \in \mathcal{U}(1) \mid \exists g \in G, n \in \mathbb{N} : g^n = e, \ R(g^n) = k\mathbb{I}\}$ as group elements, redefining multiplication so $g^n = k$ rather than e as necessary, along with adding all the necessary new combinations of the scalar elements and the ordinary group elements. This group can still be treated as an abstract group, ignoring the fact that the new elements are scalars and using them as abstract group elements for whom $R(k) = k\mathbb{I}$. This group can then be graded, and its corepresentations constructed and classified according to Sections 2.2 or 2.3 as appropriate. This method is known as finding the pullback extension of G by $M \subset \mathcal{U}(1)$, the set of necessary scalars to add, and it will be discussed along side the next method of projective corepresentations.

The second method is to recognise that the inclusion of the extra scalars arises from the corepresentation having been defined on a projective space and it then moving onto the full vector space. To deal with this, what are known as projective corepresentations are defined directly onto the full space, where every element is allowed to contain a phase factor in its representation, with multiplication rules between the phase factors allowed. This defines a new set of characters which can then be substituted into the Frobenius-Schur indicators used to construct the Dyson and Altland-Zirnbauer classifications. This is the method we discuss first, as it is the most flexible of the three, and will also be useful in explaining how symmetry groups which act on the projective Hilbert space can be turned into operators on the Hilbert space, linking together all the different

ways symmetries have to be considered. This method also can inform about other non-symmetry properties of the system - projective corepresentations are used to check if superconductors have energy gaps, and locate phase changes in their topological families for example, [37].

The final method can be used when there is the physical interpretation of a symmetry group acting on a Hilbert space with the very specific structure of $\mathcal{H} = \mathcal{H}_{\text{charge}} \otimes \mathcal{H}_{\text{spin}} \otimes \mathcal{H}_{\text{orbital}}$ and the global time-reversal and charge-conjugation operators obey $\hat{\mathcal{T}} = (\mathbb{I} \otimes T \otimes \mathbb{I})\mathcal{K}$, $\hat{\mathcal{C}} = (C \otimes \mathbb{I} \otimes \mathbb{I})\mathcal{K}$ while the representations of U act only on $\mathcal{H}_{\text{orbital}}$, [24]. In this case, the extra scalars come from taking either $T^2 = -\mathbb{I}$ or $C^2 = -\mathbb{I}$, however there is essentially the ability to factor out the contribution of T, C to the Frobenius-Schur indicators, and the standard true symmetry group can be taken with some modified Frobenius-Schur indicator equations. This is the easiest method to work with, and will apply to all systems considered in this thesis, so we describe this method after the most rigorously general method of projective representations.

We begin with the projective corepresentations of a graded group G. For most generality, it will be assumed throughout that G is $Z_2 \times Z_2$-graded, though all techniques will continue to hold for a Z_2-graded group, or even an ungraded group if the grading maps ξ, ϕ of G are set to the trivial map as needed. The projective representations of these groups are actually well studied - see for example [38, 169] for the construction of unitary projective representations and [37, 59, 69, 88] for the minor modifications required to deal with anti-unitary group elements and super-vector spaces.

To begin, we look closer at the structure of the spaces the homomorphisms act on, and consider how vectors can be equivalent up to scalar multiplication, [88]:

Definition 2.4.1. *Let $V = K^n$ be a vector space. Then define an equivalence relation on the vectors in V by*

$$x \sim y \Leftrightarrow \exists k \in K - \{0\} \text{ such that } x = ky.$$

Then the space of equivalence classes $(V - \{0\})/\sim$ is the projective vector space of V, $\mathbb{P}V$. It can also be considered as $\mathbb{P}V = V/K^\times$, the quotient of V under multiplication by the scalars K. If $V = K^n$ then $\mathbb{P}V \cong K^{n-1}$.

This has the set of invertible linear maps on it defining the projective linear group, [169]:

Definition 2.4.2. *Let $V = K^n$ be a vector space with the projective space $\mathbb{P}V$. Then the projective general linear group $PGL(V)$ is given by*

$$PGL(V) = GL(V)/K^\times = GL(\mathbb{P}V) = \mathbb{P}(GL(V)).$$

The grading operator on a super-vector space does not interfere with the equivalence relations, so projective super-vector spaces $\mathbb{P}V$ can be considered, and will be taken for the rest of this section. The set of graded invertible linear maps on the projective super-vector space can then be taken, remembering the equivalence between $GL(V)$ and $\text{Aut}(V)$:

Definition 2.4.3. *Let V be a super-vector space with graded automorphism group $\mathbf{Aut}(V)$ and let the projective space of V be $\mathbb{P}V$. Then the projective automorphism group $PGL(V)$ is given by*

$$\mathbb{P}\mathbf{Aut}(V) = \mathbf{Aut}(\mathbb{P}V)$$

34

Shifting from V to $\mathbb{P}V$ is equivalent to normalising each vector's length, and is represented by the projection operator ς from V to $\mathbb{P}V$,

$$\varsigma : V \to \mathbb{P}V, \qquad \varsigma : v \to \frac{v}{|v|}$$

which is a surjective map, but definitely not injective. It also defines a surjective morphism between $\mathbf{Aut}(V)$ and $\mathbb{P}\mathbf{Aut}(V)$, [117],

$$\sigma : \mathbf{Aut}(V) \to \mathbb{P}\mathbf{Aut}(V), \qquad \sigma(g)(\varsigma(v)) = \varsigma(g(v)) \qquad \forall g \in \mathbf{Aut}(V),\, v \in V.$$

It is then possible to define a lifting of $\mathbb{P}\mathbf{Aut}(V)$ into $\mathbf{Aut}(V)$ by a section, which is a map π, by choosing the image $\pi(p)$ for each $p \in \mathbb{P}\mathbf{Aut}(v)$ so that

$$\sigma(\pi(p)) = p.$$

It is normal that π is not a true inverse, and that $\pi(\sigma(g)) \neq g$, so π is not a homomorphism, [117]. This is because the axiom of choice has been used to choose a representative element of the set $s = \{g \in \mathbf{Aut}(V) \mid \sigma(g) = p\}$ as the value of $\pi(p)$, so the value of $\pi(\sigma(g))$ can only match with one element of s. That is, if $s = \{s_1, s_2\}$ and $\pi(p) = s_1$ is chosen, then $\pi(\sigma(s_1)) = \pi(\sigma(s_2)) = s_1 \neq s_2$.

The kernel of the map σ is $\{k\mathbb{I} \mid k \in K\}$, which is often just renamed K again, so that $K, \mathbf{Aut}(V)$ and $\mathbb{P}\mathbf{Aut}(V)$ form a short exact sequence using the inclusion map $K \hookrightarrow \mathbf{Aut}(V)$, [169]:

Definition 2.4.4. *Let A, B, C be groups with the homomorphisms $\alpha : A \to B$ and $\beta : B \to C$. If α is injective, $A \cong \alpha(A)$, β is surjective, so $C \cong B/A$ and $\mathrm{im}(\alpha) = \ker(\beta)$ then A, B, C and α, β form a short exact sequence, visualised as*

$$1 \longrightarrow A \xrightarrow{\alpha} B \xrightarrow{\beta} C \longrightarrow 1.$$

Given that $A \cong \alpha(A)$ it is usual to take $A = \alpha(A)$ and α the inclusion map.

This also defines what is known as the group extension of C by A to form B. In the case that there is a homomorphism $\pi : C \to B$ such that $\beta \circ \pi = \mathbb{I}$ is the identity, the group extension splits, and $B = A \rtimes C$ is a semidirect product.

From now on, it will be assumed that $B = \mathbf{Aut}(V)$, $C = \mathbb{P}\mathbf{Aut}(V)$ where V is a complex vector space, and $A = M(G, U) \subset \mathcal{U}(1)$, a subgroup of the unitary group.

Given the $Z_2 \times Z_2$-graded group G, and knowing that a corepresentation is wanted so that for some $g \in G$ of order n, $\mathcal{R}_{\mathbb{P}}(g^n) \neq \mathbb{I}$, then an ordinary corepresentation $\mathcal{R}$ can be taken, but considered to be on the projective space $\mathbb{P}\mathbf{Aut}(V)$. The desired corepresentation is then the lifting of $\mathcal{R}$ onto $\mathbf{Aut}(V)$, termed the projective corepresentation, where the standard corepresentation according to Definition 2.3.3 has been taken, and then scalar factors have been added as desired, [7, 88, 117]:

Definition 2.4.5. *Let G be a finite $Z_2 \times Z_2$-graded group, and V a complex super-vector space with the subspace $V_{\mathbb{R}}$ where multiplication has been restricted to $\mathbb{R}$. The projective corepresentation*

$\mathcal{R}_{\mathbb{P}} : G \to \mathbf{Aut}(V_{\mathbb{R}})$ *is defined from the super-homomorphism* $\mathcal{R} : G \to \mathbb{P}\mathbf{Aut}(V_{\mathbb{R}})$ *by taking*

$$\mathcal{R}_{\mathbb{P}}(g) = \omega(e, g)\mathcal{R}(g), \qquad \omega(e, g) \in \mathcal{U}(1)$$

where the map $\omega : G \times G \to U(1)$ *provides the factor system of the projective corepresentation, and obeys the rules,*

$$\mathcal{R}_{\mathbb{P}}(g_1)\mathcal{R}_{\mathbb{P}}(g_2) = \omega(g_1, g_2)\mathcal{R}(g_1 g_2) \tag{2.9}$$

$$\omega(g_1, g_2)\omega(g_1 g_2, g_3) = \omega(g_1, g_2 g_3)\omega^{g_1}(g_2, g_3) \tag{2.10}$$

$$\mathcal{R}_{\mathbb{P}}(g)z = z^g \mathcal{R}_{\mathbb{P}}(g), \qquad \mathcal{R}_{\mathbb{P}}(g) \begin{cases} \in \mathbb{P}\mathbf{Aut}(V_{\mathbb{R}})^0 \xi(g) = 1 \\ \in \mathbb{P}\mathbf{Aut}(V_{\mathbb{R}})^1 \xi(g) = -1 \end{cases} \tag{2.11}$$

where

$$z^g = \begin{cases} z & \phi(g) = 1 \\ z^* & \phi(g) = -1 \end{cases}.$$

This projective corepresentation $\mathcal{R}_{\mathbb{P}}$ can be found by taking a standard corepresentation $\mathcal{R}$ of G and interpreting it as the base corepresentation over $\mathbb{P}\mathbf{Aut}(V_{\mathbb{R}})$ and then finding a suitable set of factors ω that obey the rules above, which is equivalent to constructing $\pi(\mathcal{R})$; or by constructing the pullback extension G' of G and finding a standard corepresentation $\mathcal{R}'$ of G' on $GL(V)$, [88, 169]:

Definition 2.4.6. *Let* G *be a finite graded group, with* $\sigma : \mathbf{Aut}(V_{\mathbb{R}}) \to \mathbb{P}\mathbf{Aut}(V_{\mathbb{R}})$ *and corepresentation* $\mathcal{R} : G \to \mathbb{P}\mathrm{Aut}(V_{\mathbb{R}})$. *The pull-back extension* G' *of* G *is defined as*

$$G' = \{(g, A) \in G \times \mathbf{Aut}(V_{\mathbb{R}}) \mid \sigma(A) = \mathcal{R}(g)\}$$

The group G' is called the universal covering group of G. Furthermore, taking the maps

$$\tilde{\sigma} : G' \to G, \qquad \tilde{\sigma}(g, A) = g$$

$$\tilde{\pi} : G \to G', \qquad \tilde{\pi}(g) = (g, \pi(\mathcal{R}(g)))$$

there is then the commutative diagram

so that given any two points in the diagram, any path between them gives a sequence of maps that can be composed in the order they are traversed along, and the end function for each path will be equivalent. In this case, it implies that

$$\mathcal{R}_{\mathbb{P}} = \pi \circ \mathcal{R} = \mathcal{R}' \circ \tilde{\pi}.$$

The universal covering group G' found in the pullback extension of G is equivalent to the afore-mentioned version of finding the projective representations by allowing some scalars to remain in the group when factoring out $\mathcal{U}(1)$.

Due to the fact that π requires choosing a single element out of the sets $\{g \in \mathbf{Aut}(V_{\mathbb{R}}) \mid \sigma(g) = p\}$ for each $g \in G$, there exist multiple ways π can be constructed. This leads to there being several ways to add scalars back into the corepresentation and choose ω. This leads to the fact that the projective corepresentation $\mathcal{R}_{\mathbb{P}}$ isn't unique. In order to reduce the number of these possible projective corepresentations under consideration, we look to identify when two projective corepresentations are equivalent, so we don't double count. First, we identify that projective corepresentations which differ only by a unitary phase factor, can be identified, [88]:

Definition 2.4.7. *Let G be a finite $Z_2 \times Z_2$-graded group with projective corepresentations $\mathcal{R}_{\mathbb{P},1}$, $\mathcal{R}_{\mathbb{P},2}$ by the factor systems ω_1, ω_2. $\mathcal{R}_{\mathbb{P},1}, \mathcal{R}_{\mathbb{P},2}$ are associated projective corepresentations if and only if*

$$\omega_2(g_1, g_2) = \frac{c(g_1 g_2)}{c(g_1) c^{g_1}(g_2)} \omega_1(g_1, g_2) \ \forall g_1, g_2 \in G, \qquad \mathcal{R}_{\mathbb{P},2}(g) = c(g) \mathcal{R}_{\mathbb{P},1}(g)$$

where $c : G \to \mathcal{U}(1)$ is a map.

This allows a definition of equivalence, [163]:

Definition 2.4.8. *Let G be a finite $Z_2 \times Z_2$-graded group with associated projective corepresentations $\mathcal{R}_{\mathbb{P},2}(g) = c(g) \mathcal{R}_{\mathbb{P},1}(g)$. Then $\mathcal{R}_{\mathbb{P},1}, \mathcal{R}_{\mathbb{P},2}$ are equivalent projective corepresentations if $c(e) = 1$.*

Associativity means that given a projective corepresentation $\mathcal{R}_{\mathbb{P}}$ with factor system ω, then a gauge transformation $\omega \to \omega'$ can always be done so to remove the $\omega(e, g)$ factor prefix from un-multiplied elements, [7], that is, the factor system can always be chosen so that,

$$\omega(e, e) = \omega(e, g) = \omega(g, e) = 1 \ \forall g \in G.$$

In Theorem 2.3.12, we give a method of classifying each corepresentation of every possible $Z_2 \times Z_2$-graded group according to the Altland-Zirnbauer way, applying it to the small groups to get the tables in Appendix E. We claim that knowing about the universal covering group, it is also possible to use this technique to classify every *projective* corepresentation of G - each possible universal covering group G' of G is identified and then Theorem 2.3.12 applied to the corepresentations of the covering group to get the result for G. This makes the results of Theorem 2.3.12, and the tables in Appendix E, much more general - they can be applied to systems with any kind of fractional spin for example - the correct covering group just needs to be found and then it can be looked up in the tables if small enough, or the Frobenius-Schur indicators calculated. It is just necessary to be able to identify possible covering groups, either specifically, or systematically searching for all of them.

The problem of finding all the covering groups, is really one of finding a factor system, and then using this to define new elements and multiplication rules in G. The method of finding all factor systems is also documented for non-graded unitary projective representations, see for

example [38, 169], which will give a basis for expanding to finding all factor systems for a projective corepresentation.

We begin with considering exactly how many elements of ω need to be known in order to fully define it. The multiplication rule on the factors of different elements in Equation 2.10 means that given a generating set S of U and taking $S' = s \cup \{\alpha, \gamma, \pi\}$ as a generating set of the $Z_2 \times Z_2$-graded group G, then only the factors $\omega(s'_1, s'_2)$, $\forall s'_1, s'_2 \in S'$ actually need be chosen and the rest can be calculated through the factor multiplication rule. This result is expanded in [163], so that all that is needed to be known is the factor system ω_H where $H = U$ for a Z_2-graded group, and $H = U \cup \pi U$ for a $Z_2 \times Z_2$-graded group, so it covers the unitary elements of G.

The method defines the equivalence relation $h_1 \sim h_2 \Leftrightarrow \exists n \in \mathbb{N}$ such that $h_2 = \alpha^n h_1 \alpha^{-n}$ divides H into equivalence classes C_h which have transversal T_H in H. Taking the subset $H_0 \subset T$ of the transversal containing elements whose conjugacy classes have even order,

$$H_0 = \{t \in T_H \mid |C_t| = 2m, \ m \in \mathbb{N}\}$$

the following function $D_{\omega_H} : H \to \mathbb{C}$ can be constructed,

$$D_{\omega_H}(h) = \begin{cases} \prod_{n=0 \ n=2m}^{|C_h|-2} \omega_H^*(\alpha^{(n+1)} h \alpha^{-(n+1)}, \alpha^2) \omega_H(\alpha^2, \alpha^{(n-1)} h \alpha^{-(n-1)}) & h \in H_0 \\ 1 & h \notin H_0 \end{cases}.$$

Then ω_H can be used to construct a factor system of G, [163]:

Theorem 2.4.9. *Let G be a graded group, with the unitary subgroup H. If ω_H is a factor system of H, such that there exists an equivalent factor system ω'_H and*

$$\omega'_H(h, h') \omega'_H(\alpha^{-1} h \alpha, \alpha^{-1} h' \alpha) = D_{\omega_H}(h) D_{\omega_H}(h') D_{\omega_H}^*(hh')$$

$$\omega'(\alpha h \alpha^{-1}, \alpha^2) \omega'_H(\alpha^2, \alpha^{-1} h \alpha) = D_{\omega_H}^*(\alpha h \alpha^{-1}) D_{\omega_H}(h)$$

for all $h, h' \in H$, then a factor system ω_G of G is defined by

$$\omega_G(h, h') = \omega_H(h, h'), \qquad \omega_G(\alpha, h) = 1, \qquad \omega_G(h, \alpha) = D_{\omega_H}(h).$$

Calculating all possible factor systems of G, or even just a particular factor system, becomes a problem of knowing the values of the factor system on the ungraded group H. This is, as mentioned, a well studied problem and is related to the co-homology of the group H. For a discussion of this see for example [38, 169].

For many practical applications in physics, it will be possible to define simpler methodologies. For example, the case where the vector (Hilbert) space the problem is defined over, and thus the space the representations are defined over, splits into a 'charge' component, a 'spin' component and an 'orbital' component, [14, 24, 73],

$$V \to V_{\text{charge}} \otimes V_{\text{spin}} \otimes V_{\text{orbital}}. \tag{2.12}$$

The unitary-commuting symmetries which define U don't interact with the particles spin, and they don't flip particles into holes, so they must act entirely on the orbital space, and take the representation

$$\rho_V(u \in U) \to \mathbb{I}_{V_{\text{charge}}} \otimes \mathbb{I}_{V_{\text{spin}}} \otimes \rho_{V_{\text{orbital}}}(u \in U). \tag{2.13}$$

If this $\rho_{V_{\text{orbital}}}$ is a representation of U for $U \triangleleft G = U \cup \alpha U \cup \gamma U \cup \pi U$, which generates the corepresentation of $\mathcal{R}$ of G on V_{orbital}, then the ordinary corepresentation matrices on $\mathbb{I}_{V_{\text{charge}}} \otimes V_{\text{spin}} \otimes V_{\text{orbital}}$ are given by, [24],

$$\mathcal{R}(u \in U) \to \mathbb{I}_{V_{\text{charge}}} \otimes \mathbb{I}_{V_{\text{spin}}} \otimes \mathcal{R}(u) \tag{2.14}$$

$$\mathcal{R}(a \in \alpha U) \to \left(\mathbb{I}_{V_{\text{charge}}} \otimes \mathbb{I}_{V_{\text{spin}}} \otimes \tilde{\mathcal{R}}(a) \right) \mathcal{T} = \left(\mathbb{I}_{V_{\text{charge}}} \otimes \mathbb{I}_{V_{\text{spin}}} \otimes \tilde{\mathcal{R}}(a) \right) \mathcal{K} \tag{2.15}$$

$$\mathcal{R}(c \in \gamma U) \to \left(\mathbb{I}_{V_{\text{charge}}} \otimes \mathbb{I}_{V_{\text{spin}}} \otimes \tilde{\mathcal{R}}(c) \right) \mathcal{C}$$

$$= \left(\mathbb{I}_{V_{\text{charge}}} \otimes \mathbb{I}_{V_{\text{spin}}} \otimes \tilde{\mathcal{R}}(c) \right) \left(\begin{pmatrix} 0 & \mathbb{I} \\ \mathbb{I} & 0 \end{pmatrix} \otimes \mathbb{I}_{V_{\text{spin}}} \otimes \mathbb{I}_{V_{\text{orbital}}} \right) \mathcal{K} \tag{2.16}$$

$$\mathcal{R}(p \in \pi U) \to \left(\mathbb{I}_{V_{\text{charge}}} \otimes \mathbb{I}_{V_{\text{spin}}} \otimes \mathcal{R}(p) \right) \mathcal{P}$$

$$= \left(\mathbb{I}_{V_{\text{charge}}} \otimes \mathbb{I}_{V_{\text{spin}}} \otimes \mathcal{R}(p) \right) \left(\begin{pmatrix} 0 & \mathbb{I} \\ \mathbb{I} & 0 \end{pmatrix} \otimes \mathbb{I}_{V_{\text{spin}}} \otimes \mathbb{I}_{V_{\text{orbital}}} \right) \tag{2.17}$$

where $\mathcal{T}, \mathcal{C}$ and $\mathcal{P}$ are considered to be time-reversal, charge-conjugation and chiral operators respectively. The reason for these representations appearing the way they do is based on the physical interpretations of what each of the spaces $\mathcal{H}_{\text{charge}}, \mathcal{H}_{\text{spin}}$ and $\mathcal{H}_{\text{orbital}}$ cover, and how they interact with the operators $\hat{\mathcal{T}}, \hat{\mathcal{C}}$ and $\hat{\mathcal{P}}$. This is discussed in Appendix C and Section 3.1.

In this case, taking the projective representation is then a standing in for substituting $\mathcal{T} \to \mathcal{T} = (\mathbb{I}_{V_{\text{charge}}} \otimes T \otimes \mathbb{I}_{V_{\text{orbital}}})\mathcal{K}$, $\mathcal{C} \to \mathcal{C} = (C \otimes \mathbb{I}_{V_{\text{spin}}} \otimes \mathbb{I}_{V_{\text{orbital}}})\mathcal{K}$ and $\mathcal{P} \to \mathcal{P} = (P \otimes \mathbb{I}_{V_{\text{orbital}}})$ for a suitably chosen triple of unitary operators T, C, P which are chosen from ten options, as in Table 2.3, depending on whether $\alpha U, \gamma U$ and πU are empty or not and depending on the nature of the system they are being defined on. Generally, $T^2 = \mathbb{I}$ implies a bosonic system, $T^2 = -\mathbb{I}$ implies fermionic system, while the form of C generally relates to the spin dependence/independence of the main-diagonal components of the associated Hamiltonian when written under the BdG formalism - $C^2 = -\mathbb{I}$ when H_{11}, H_{22} are spin-dependent and $C^2 = -\mathbb{I}$ when they are spin-independent, [14].

Furthermore, because T, C, P act on the spin and charge spaces, and the representations of U on the orbital space, the Frobenius-Schur Indicators from Theorem 2.3.12 can be modified to cover this special case of projective corepresentations by including a factor of T^2, C^2, as was done for the Z_2-graded groups in [48], and now extending to the $Z_2 \times Z_2$-graded groups:

Theorem 2.4.10. *Let $G = U \cup \alpha U \cup \gamma U \cup \pi U$ be a $Z_2 \times Z_2$ graded group with an irreducible representation ρ of U on the vector space $V_{orbital}$. Let $V = V_{charge} \otimes V_{spin} \otimes V_{orbital}$ be a super vector space, and the projective corepresentations of G generated by ρ be given as*

$$\mathcal{R}(u \in U) = \mathbb{I}_{V_{charge}} \otimes \mathbb{I}_{V_{spin}} \otimes \mathcal{R}(u)$$

$$\mathcal{R}(a \in \alpha U) = \left(\mathbb{I}_{V_{charge}} \otimes \mathbb{I}_{V_{spin}} \otimes \tilde{\mathcal{R}}(a) \right) (\mathbb{I}_{V_{charge}} \otimes T \otimes \mathbb{I}_{orbital})\mathcal{K}$$

$$\mathcal{R}(c \in \gamma U) = \left(\mathbb{I}_{V_{charge}} \otimes \mathbb{I}_{V_{spin}} \otimes \tilde{\mathcal{R}}(c) \right) (C \otimes \mathbb{I}_{V_{spin}} \otimes \mathbb{I}_{V_{orbital}})\mathcal{K}$$

$$\mathcal{R}(p \in \pi U) = \left(\mathbb{I}_{V_{charge}} \otimes \mathbb{I}_{V_{spin}} \otimes \mathcal{R}(p)\right)\left(P \otimes \mathbb{I}_{V_{orbital}}\right)$$

Then the Altland-Zirnbauer class of the projective corepresentation generated by ρ is given by the modified Frobenius-Schur indicators,

$$FSI_A(\rho) = \frac{T^2}{|U|} \sum_{a \in \alpha U} \chi_\rho(a^2) \tag{2.18}$$

$$FSI_C(\rho) = \frac{C^2}{|U|} \sum_{c \in \gamma U} \chi_\rho(c^2) \tag{2.19}$$

$$FSI_P(\rho) = \frac{1}{|U|} \sum_{u \in U} \chi_\rho(u)\chi_\rho^*(\pi^{-1}u\pi) \tag{2.20}$$

with the classes given by Table 2.2.

In particular this means that if U is the trivial group, the Altland-Zirnbauer class of G is decided entirely by whether A, C, P are non-empty, and how T, C square, as seen in the rightmost columns of Table 2.3, with the existence of $\mathcal{P}$ telling apart the classes A and AIII. A more general adaptation of the Frobenius-Schur indicators can be derived using the relations in [38].

The group extensions relating to these projective corepresentations are known specifically as the Double Groups, and specific rules exist to calculate them, [7, 24, 126]. Double groups were actually the precursor to projective representations in the physics community, and in many areas are still the more studied of the pair, however they are significantly more restrictive and many have argued that projective representations are better to use, [7]. Double groups make the most sense when $V_{\text{Orbital}} = SO(3)$ so the addition of the spin space is equivalent to the lifting from $SO(3)$ to $SU(2)$, which is a very specific geometric interpretation inapplicable to more abstract groups. Furthermore, projective representations and the related co-homologies have additional benefits in studying things like energy gaps and symmetry-protected-topological phases in topological insulators [37], or they can be used to describe Majorana zero modes in topological super-conductors and they have links with quantum Monte-Carlo simulations, [177].

Class	T	C	P	$\hat{\mathcal{T}}^2$	$\hat{\mathcal{C}}^2$	$\pi \in G$
A	$-$	$-$	$-$	$-$	$-$	No
AI	$\mathbb{I}$	$-$	$-$	$\mathbb{I}$	$-$	No
AII	$\begin{pmatrix} 0 & 1 \\ -1 & 0 \end{pmatrix}$	$-$	$-$	$-\mathbb{I}$	$-$	No
$AIII$	$-$	$-$	$\begin{pmatrix} 0 & \mathbb{I} \\ \mathbb{I} & 0 \end{pmatrix}$	$-$	$-$	Yes
BDI	$\mathbb{I}$	$\begin{pmatrix} 0 & 1 \\ 1 & 0 \end{pmatrix}$	$\begin{pmatrix} 0 & \mathbb{I} \\ \mathbb{I} & 0 \end{pmatrix}$	$\mathbb{I}$	$\mathbb{I}$	Yes
CII	$\begin{pmatrix} J & 0 \\ 0 & J \end{pmatrix}$	$\begin{pmatrix} 0 & J \\ J & 0 \end{pmatrix}$	$C \otimes T$	$-\mathbb{I}$	$-\mathbb{I}$	Yes
D	$-$	$\begin{pmatrix} 0 & 1 \\ 1 & 0 \end{pmatrix}$	$-$	$-$	$\mathbb{I}$	No
C	$-$	$\begin{pmatrix} 0 & -1 \\ 1 & 0 \end{pmatrix}$	$-$	$-$	$-\mathbb{I}$	No
CI	$\mathbb{I}_2$	$\begin{pmatrix} 0 & -1 \\ 1 & 0 \end{pmatrix}$	$\begin{pmatrix} 0 & -\mathbb{I}_2 \\ \mathbb{I}_2 & 0 \end{pmatrix}$	$\mathbb{I}$	$-\mathbb{I}$	No
$DIII$	$\begin{pmatrix} J & 0 \\ 0 & J \end{pmatrix}$	$\begin{pmatrix} 0 & \mathbb{I}_2 \\ \mathbb{I}_2 & 0 \end{pmatrix}$	$C \otimes T$	$-\mathbb{I}$	$\mathbb{I}$	No

Table 2.3: Possible choices for the matrices T, C, P depending on which of the sets $\alpha U, \gamma U$ and πU are non-empty, [64]. The right hand columns can also be used to identify the Altland-Zirnbauer class of a projective corepresentation for a $Z_2 \times Z_2$-graded group where $U = \mathbb{I}$ is the trivial group. The matrix J is given by $J = \begin{pmatrix} 0 & 1 \\ -1 & 0 \end{pmatrix}$

3. *Symmetric Quantum Systems and Chaos*

We now turn to the discussion of symmetries quantum systems, having defined the basic framework of quantum theory in Appendix C. This involves discussing the invariance of Hilbert spaces and Hamiltonians under certain operators, and how these form quantum symmetries, and lead to special structure on the Hamiltonians that can be classified in Sections 3.1 and 3.1.1. Finally, the classical limit of quantum systems will be discussed, and the idea of quantum chaos introduced in Section 3.2.

3.1 Quantum Symmetries

The study of quantum symmetry is the study of the invariant transforms of the Hilbert space $\mathcal{H}$, and its projective counter-part, $\mathbb{P}\mathcal{H}$. Rigorous definitions for both are given in Appendix C with more context for the choice of their definition, but they are restated here for ease of reference. Firstly, the Hilbert space describes the state-space of a quantum system $\mathcal{Q}$, so that the vectors $|\psi\rangle$ are the possible states of the system, and it takes the form of a chosen complex inner product space, [155]:

Definition 3.1.1. *Let $\mathcal{Q}$ be a quantum system, then its Hilbert Space $\mathcal{H}$ is a complex vector space, with vectors ψ and inner product $\langle \cdot, \cdot \rangle$, such that:*

- *$\langle \cdot, g \rangle$ is a linear function for all $g \in \mathcal{H}$.*

- *$\langle f, g \rangle = \langle g, f \rangle^*$*

- *$\langle f, f \rangle \geq 0$ for all $f \in \mathcal{H}$.*

The norm shall be defined as $\|\psi\| = \sqrt{\langle \psi, \psi \rangle}$.

A common example is $L_2(\mathbb{R}^n)^m$, the set of dimension m vectors with each entry being a square integrable function over $\mathbb{R}^n$. The projective Hilbert space $\mathbb{P}\mathcal{H}$ then describes the unique physical states in $\mathcal{H}$, so that all of the copies $c|\psi\rangle$ of $|\psi\rangle$ for $c \in \mathbb{C} - \{0\}$ are removed, [117, 176]:

Definition 3.1.2. *Let $\mathcal{H}$ be the Hilbert space of the quantum system $\mathcal{Q}$. Then the projective Hilbert space $\mathbb{P}\mathcal{H}$ is defined as the space of rays,*

$$\mathbb{P}\mathcal{H} = (\mathcal{H} - \{0\})/\mathbb{C}^\times.$$

It is possible to define a projection operator σ from $\mathcal{H}$ to $\mathbb{P}\mathcal{H}$,

$$\sigma : |\psi\rangle \to |\sigma(\psi)\rangle = |\Psi\rangle \in \mathbb{P}\mathcal{H}, \qquad \sigma : |\psi\rangle \to \frac{|\psi\rangle}{\sqrt{|\langle\psi|\psi\rangle|}} \tag{3.1}$$

which also allows a representative state $|\Psi\rangle$ to be chosen for each ray.

Describing the invariant transforms of $\mathcal{H}$ and $\mathbb{P}\mathcal{H}$ then begins with defining a general transformation on the full Hilbert space, which are termed the operators on the Hilbert space, as given by Wigner, [175], and as per Definition C.1.3:

Definition 3.1.3. *Let $\mathcal{Q}$ be a quantum system with Hilbert space $\mathcal{H}$. An operator $\hat{O}$ is a map on the Hilbert space, $\hat{O} : \mathcal{H} \to \mathcal{H}$, that is either linear, $\hat{O}(a|\psi\rangle + b|\phi\rangle) = a\hat{O}|\psi\rangle + b\hat{O}|\phi\rangle$ or anti-linear, $\hat{O}(a|\psi\rangle + b|\phi\rangle) = a^*\hat{O}|\psi\rangle + b^*\hat{O}|\phi\rangle$.*

Note that in contrast to standard quantum theory, where operators must be linear, anti-linear transforms are allowed in Wigner's definition. Doing so is essential to his study of quantum time-reversal symmetries, and the later extension to charge-conjugation and chiral symmetry - it is only possible to define time-reversal, charge-conjugation and their generalised forms through anti-linear operators. When dealing with linear operators, quantum theory would identify a special subset of them as unitary; with the anti-linear operators included, we identify the special subset of operators as the set of unitary or anti-unitary operators, [175]:

Definition 3.1.4. *Let $\mathcal{H}$ be the Hilbert space for the quantum system $\mathcal{Q}$ with inner product $\langle\cdot,\cdot\rangle$. Then if, $\hat{O}$ is an operator and,*

- *$\left\langle \hat{O}\phi \middle| \hat{O}\psi \right\rangle = \langle\phi|\psi\rangle \ \forall |\phi\rangle |\psi\rangle \in \mathcal{H}$ and $\hat{O}$ is linear, then $\hat{O}$ is a unitary operator.*

- *$\left\langle \hat{O}\phi \middle| \hat{O}\psi \right\rangle = \langle\phi|\psi\rangle^* \ \forall |\phi\rangle |\psi\rangle \in \mathcal{H}$ and $\hat{O}$ is anti-linear, then $\hat{O}$ is an anti-unitary operator.*

The collection of linear unitary operators, and anti-linear anti-unitary operators define the group $\mathrm{Aut}(\mathcal{H}_\mathbb{R})$, the set of linear, invertible transformations of the subspace of the Hilbert space generated by multiplication by $\mathbb{R}$ rather than by $\mathbb{C}$. When the domain of these functions is expanded to $\mathcal{H}$, then the group $\mathrm{Aut}_{\mathrm{qtm}}(\mathcal{H})$ is formed.

Knowing from Section 2.4 that for every vector space V, given $\mathrm{Aut}(V)$, a corresponding set of transformations $\mathbb{P}\mathrm{Aut}(V)$ can be defined over $\mathbb{P}V$ allows us to define a general transform on $\mathbb{P}\mathcal{H}$, and understand the impact of operators on the projective Hilbert space. This involves taking the projection operator $\sigma : \mathcal{H} \to \mathbb{P}\mathcal{H}$ and using it to define the projection from $\mathrm{Aut}_{\mathrm{qtm}}(\mathcal{H})$ onto its projective counterpart, $\mathbb{P}\mathrm{Aut}_{\mathrm{qtm}}(\mathcal{H}) = \mathrm{Aut}_{\mathrm{qtm}}(\mathbb{P}\mathcal{H})$,

$$\Sigma : \mathrm{Aut}_{\mathrm{qtm}}(\mathcal{H}) \to \mathrm{Aut}_{\mathrm{qtm}}(\mathbb{P}\mathcal{H}) \qquad \Sigma\left(\hat{O}\right)|\Psi\rangle = \Sigma\left(\hat{O}\right)|\sigma(\psi)\rangle = \left|\sigma\left(\hat{O}\psi\right)\right\rangle \qquad \forall |\psi\rangle \in \mathcal{H}.$$

This states that applying the projected operator to a projected state is equal to applying the un-projected operator to the un-projected state and then projecting down onto the projective Hilbert space. This is to be expected, as the projection operator is only dividing out all of the scalar factors, which commutes with all other operations.

We can now begin to define symmetries, considering which subsets of $\mathrm{Aut}_{\mathrm{qtm}}(\mathcal{H})$ and $\mathrm{Aut}_{\mathrm{qtm}}(\mathbb{P}\mathcal{H})$ leave the quantum system intact. These transformations are the ones that leave characteristic

quantum features of the system the same. Beginning with the projective Hilbert space, this means preserving structure of the transmission amplitude, so the probability to move between two states remains the same, as the key physical quantity describing the relation between different states. According to Wigner, [175], this is:

Definition 3.1.5. *Let $\mathbb{P}\mathcal{H}$ be the projective Hilbert space of a quantum system. Then the subset S of $\mathrm{Aut}_{\mathrm{qtm}}(\mathbb{P}\mathcal{H})$ preserving the quantum system and forming the set of potential symmetries of the system is the set of bijective maps $s : \mathbb{P}\mathcal{H} \to \mathbb{P}\mathcal{H}$ that are linear on $\mathbb{P}\mathcal{H}_{\mathbb{R}}$ and which preserve the transition probability,*

$$P(s(\Phi) \to s(\Psi)) = P(\Phi \to \Psi).$$

It is more important in terms of defining symmetries that the quantum structure is preserved over making sure that the operators generating the symmetries are either unitary or anti-unitary. Thus we need to check whether there are any transformations of $\mathbb{P}\mathcal{H}$ in $\mathrm{Hom}(\mathbb{P}\mathcal{H}_{\mathbb{R}})$ preserving the transition probabilities that aren't in $\mathrm{Aut}_{\mathrm{qtm}}(\mathbb{P}\mathcal{H})$. However, by Wigner's Theorem, [117, 175, 176], we know that $\mathrm{Aut}_{\mathrm{qtm}}(\mathbb{P}\mathcal{H})$ contains all of the transition-probability preserving transformations:

Theorem 3.1.6 (Wigner). *Let $\mathcal{H}, \mathbb{P}\mathcal{H}$ be the Hilbert and projective Hilbert spaces of a quantum system $\mathcal{Q}$, related by the map $\sigma : \mathcal{H} \to \mathbb{P}\mathcal{H}$. Let $\mathrm{Aut}_{\mathrm{qtm}}(\mathcal{H})$ and $\mathrm{Aut}_{\mathrm{qtm}}(\mathbb{P}\mathcal{H})$ be the groups defined by Definition 3.1.4 and 3.1.5. Then the set of maps preserving the transition probability,*

$$S' = \{s \in \mathrm{Hom}(\mathbb{P}\mathcal{H}_{\mathbb{R}}) \mid P(s(\Phi) \to s(\Psi)) = P(\Phi \to \Psi) \; \forall \, |\Phi\rangle, |\Psi\rangle \in \mathbb{P}\mathcal{H}\}$$

is contained entirely in $\mathrm{Aut}_{\mathrm{qtm}}(\mathbb{P}\mathcal{H})$ and $S = S' \subset \mathrm{Aut}_{\mathrm{qtm}}(\mathbb{P}\mathcal{H})$.

Proof. See [175] or [150, 151] for several examples of proofs. $\square$

This means that general homomorphisms on $\mathbb{P}\mathcal{H}_{\mathbb{R}}$ need not be considered, and only the maps generated by the unitary and anti-unitary operators on $\mathcal{H}$. This is how Wigner's theorem is more commonly stated - every symmetry on the system corresponds to either a unitary or anti-unitary operator.

Members of this group $S \subset \mathrm{Aut}_{\mathrm{qtm}}(\mathbb{P}\mathcal{H})$ are still only described as potential symmetries of the system however, as while they are already guaranteed to leave the Hilbert space and transition probabilities invariant under transformation, to be full symmetries of the system they will have to fulfil the extra restriction of preserving the quantum structure on $\mathcal{H}$. This is the requirement that the operators which generate S either commute or anti-commute with the Hamiltonian.

The symmetry group of the system G sits in $\mathrm{Aut}_{\mathrm{qtm}}(\mathbb{P}\mathcal{H})$, thus to check whether elements of S are included in G under the commutation rule requires defining a method of finding each of the associated operators in $\mathrm{Aut}_{\mathrm{qtm}}(\mathcal{H})$ for every member of $\mathrm{Aut}_{\mathrm{qtm}}(\mathbb{P}\mathcal{H})$. We already have the projection operator $\Sigma : \mathrm{Aut}_{\mathrm{qtm}}(\mathcal{H}) \to \mathrm{Aut}_{\mathrm{qtm}}(\mathbb{P}\mathcal{H})$, so the method of doing this is by constructing the section $\Pi : \mathrm{Aut}_{\mathrm{qtm}}(\mathbb{P}\mathcal{H}) \to \mathrm{Aut}_{\mathrm{qtm}}(\mathcal{H})$ as per Section 2.4. This uses the axiom of choice to define Π by taking each element $s \in \mathrm{Aut}_{\mathrm{qtm}}(\mathbb{P}\mathcal{H})$ and picking one of the set of operators that is mapped to it by Σ, $\left\{ \hat{S} \in \mathrm{Aut}_{\mathrm{qtm}}(\mathcal{H}) \mid \Sigma(\hat{S}) = s \right\}$, to define $\Pi(s)$,

$$\Pi : \mathrm{Aut}(\mathbb{P}\mathcal{H}) \to \mathrm{Aut}(\mathcal{H}), \quad s \to \Pi(s) = \hat{S} \in \left\{ \hat{S} \in \mathrm{Aut}_{\mathrm{qtm}}(\mathcal{H}) \mid \Sigma(\hat{S}) = s \right\}.$$

Furthermore, we note that Σ is a surjective homomorphism with the kernel $\mathcal{U}(1)$ and the groups $\mathcal{U}(1)$, $\mathrm{Aut}_{\mathrm{qtm}}(\mathcal{H})$ and $\mathrm{Aut}_{\mathrm{qtm}}(\mathbb{P}\mathcal{H})$ define the short exact sequence under Σ:

$$1 \longrightarrow \mathcal{U}(1) \lhook\joinrel\longrightarrow \mathrm{Aut}_{\mathrm{qtm}}(\mathcal{H}) \mathrel{\mathop{\rightleftarrows}^{\Sigma}_{\Pi}} \mathbb{P}\mathrm{Aut}_{\mathrm{qtm}}(\mathcal{H}) \longrightarrow 1$$

As before, there will be a number of possible choices for $\Pi(s)$, which will correspond to different physical properties of the quantum system - for example the spin of the particles, and whether the Hamiltonian is spin dependent. There will be short discussions as to the correspondence between the physical nature of the quantum systems and the extensions below, mainly in the simplified setup of $\mathcal{H} = \mathcal{H}_{\mathrm{charge}} \otimes \mathcal{H}_{\mathrm{spin}} \otimes \mathcal{H}_{\mathrm{orbital}}$. Anyway, with a method of identifying the operators corresponding to a member of $\mathrm{Aut}_{\mathrm{qtm}}(\mathbb{P}\mathcal{H})$, it is now possible to identify the symmetry group of a quantum system as the elements whose lifts either commute or anti-commute with the Hamiltonian, [24, 117]:

Definition 3.1.7. *Let $\mathcal{Q}$ be a quantum system with Hilbert space $\mathcal{H}$ Hamiltonian $\hat{H}$. Then the symmetry group of the system $G \subset \mathrm{Aut}_{\mathrm{qtm}}(\mathbb{P}\mathcal{H})$ is defined as the automorphisms of $\mathbb{P}\mathcal{H}$ whose lifts $\Pi : s \to \hat{S}$ into $\mathrm{Aut}_{\mathrm{qtm}}(\mathcal{H})$ are compatible with the Hamiltonian so that either,*

- $[\hat{S}, \hat{H}] = \hat{S}\hat{H} - \hat{H}\hat{S} = 0$ *which are Symmetries of the Dynamics of the system*

- $\left\{\hat{S}, \hat{H}\right\} = \hat{S}\hat{H} + \hat{H}\hat{S} = 0$ *which are Symmetries of the Spectra*

This defines the symmetry group G as,

$$G = \left\{g \in \mathrm{Aut}_{\mathrm{qtm}}(\mathbb{P}\mathcal{H}) \mid \Pi(g)\hat{H} = \pm\hat{H}\Pi(g),\ |\langle g\Phi|g\Psi\rangle|^2 = |\langle\Phi|\Psi\rangle|^2\ \forall\ |\Psi\rangle, |\Phi\rangle \in \mathbb{P}\mathcal{H}\right\}.$$

This forms the group G, which can be seen to contain elements of four types - if an element $s \in G$ lifts to an operator $\hat{S}$, then $\hat{S}$ can either be a unitary operator that commutes with the Hamiltonian; an anti-unitary operator that commutes with the Hamiltonian; a unitary operator that anti-commutes with the Hamiltonian; or an anti-unitary operator that anti-commutes with the Hamiltonian. These classifications can be used to form a partition of G into the sets U, A, C, P according to

	$\left\langle\hat{S}^\dagger\phi\middle|\hat{S}\psi\right\rangle = \langle\phi|\psi\rangle$	$\left\langle\hat{S}^\dagger\phi\middle|\hat{S}\psi\right\rangle = \langle\phi|\psi\rangle^*$
$\hat{S}\hat{H} = \hat{H}\hat{S}$	$\hat{S} \in U$	$\hat{S} \in A$
$\hat{S}\hat{H} = -\hat{H}\hat{S}$	$\hat{S} \in P$	$\hat{S} \in C$

This means that G is a group of the form $G = U \cup A \cup C \cup P$ with $U \lhd G$ a normal subgroup of G. This is equivalent to Definition 2.3.1 of a $Z_2 \times Z_2$ graded group:

Theorem 3.1.8. *Let $\mathcal{Q}$ be a quantum system with the symmetry group G. Then $G \subset \mathrm{Aut}_{\mathrm{qtm}}(\mathbb{P}\mathcal{H})$ is $Z_2 \times Z_2$-graded with respect to the gradings*

$$\phi : G \to Z_2, \quad \phi(g) = \begin{cases} 1 & \langle g\Phi|g\Psi\rangle = \langle\Phi|\Psi\rangle\ \forall\ |\Phi\rangle, |\Psi\rangle \in \mathbb{P}\mathcal{H} \\ -1 & \langle g\Phi|g\Psi\rangle = \langle\Phi|\Psi\rangle^*\ \forall\ |\Phi\rangle, |\Psi\rangle \in \mathbb{P}\mathcal{H} \end{cases} \tag{3.2}$$

$$\xi : G \to Z_2, \quad \xi(g) = \begin{cases} 1 & \Pi(g)\hat{H} = \hat{H}\Pi(g) \\ -1 & \Pi(g)\hat{H} = -\hat{H}\Pi(g) \end{cases} \tag{3.3}$$

Then G can be partitioned into the sets U, A, C, P according to

$$U = \{s \in G \mid (\phi(g), \psi(g)) = (1,1)\} \qquad A = \{s \in G \mid (\phi(g), \psi(g)) = (-1,1)\}$$
$$C = \{s \in G \mid (\phi(g), \psi(g)) = (-1,-1)\} \qquad P = \{s \in G \mid (\phi(g), \psi(g)) = (1,-1)\}$$

so that $U \lhd G$ and choosing $\alpha \in A$, $\gamma \in C$, $\pi \in P$, $G = U \cup \alpha U \cup \gamma U \cup \pi U$.

This now means that if G is considered as an abstract $Z_2 \times Z_2$-graded group, then mapping elements of G onto their associated operators in $\mathrm{Aut}_{\mathrm{qtm}}(\mathcal{H})$ is the method of projective corepresentations discussed in Section 2.4. That is, the Hilbert space can be considered a super-vector space, or linking to the charge-spin-orbital construction of the Hilbert space, it can be split into a charge-space part, $\mathcal{H}_{\mathrm{charge}}$, and a non-charge-space, $\mathcal{H}'$, so that $\mathcal{H} = \mathcal{H}_{\mathrm{charge}} \otimes \mathcal{H}' = (|p\rangle \; |h\rangle)^T \otimes \mathcal{H}'$ with the particle states $(|p\rangle \; 0)^T \otimes |\psi\rangle$ forming the even subspace and the hole states forming the odd subspace $(0 \; |h\rangle)^T \otimes |\psi\rangle$.

The automorphism groups of $\mathcal{H}$ and $\mathbb{P}\mathcal{H}$ can then be graded with respect to the super-Hilbert space, becoming $\mathrm{Aut}_{\mathrm{qtm}}(\mathcal{H}) \to \mathbf{Aut}_{\mathrm{qtm}}(\mathcal{H})$ and $\mathrm{Aut}_{\mathrm{qtm}}(\mathbb{P}\mathcal{H}) \to \mathbf{Aut}_{\mathrm{qtm}}(\mathbb{P}\mathcal{H})$. These are then substituted in to Definition 2.4.5 with G, so that the most general map from the symmetry group to the symmetry operators is given by:

Definition 3.1.9. *Let $\mathcal{Q}$ be a quantum system with the abstract $Z_2 \times Z_2$-graded symmetry group G. Let $\mathcal{H} = \mathcal{H}_{charge} \otimes \mathcal{H}'$ be the super Hilbert space of the system with the super-vector space of unitary and anti-unitary operators $\mathbf{Aut}_{\mathrm{qtm}}(\mathcal{H})$ on $\mathcal{H}$, and its projection onto $\mathbb{P}\mathcal{H}$ as $\mathbf{Aut}_{\mathrm{qtm}}(\mathbb{P}\mathcal{H})$, the transformations of the projective Hilbert space.*

Let $\mathcal{R} : G \to \mathbf{Aut}_{\mathrm{qtm}}(\mathbb{P}\mathcal{H})$ be a corepresentation of G. Then, there exists a factor system $\omega : G \times G \to \mathcal{U}(1)$ which is chosen according to the physical properties of the system $\mathcal{Q}$, such that each element $g \in G$ can be mapped onto an operator $\mathcal{R}_{\mathbb{P}}(g)$ on $\mathcal{H}$ so that,

$$\mathcal{R}_{\mathbb{P}}(g) = \omega(e, g)\mathcal{R}(g) \tag{3.4}$$

$$\mathcal{R}_{\mathbb{P}}(g_1)\mathcal{R}_{\mathbb{P}}(g_2) = \omega(g_1, g_2)\mathcal{R}(g_1 g_2) \tag{3.5}$$

$$\omega(g_1, g_2)\omega(g_1 g_2, g_3) = \omega(g_1, g_2 g_3)\omega^{g_1}(g_2, g_3) \tag{3.6}$$

$$\mathcal{R}_{\mathbb{P}}(g)z = z^g \mathcal{R}_{\mathbb{P}}(g), \qquad \mathcal{R}_{\mathbb{P}}(g) \begin{cases} \in \mathbf{Aut}_{\mathrm{qtm}}(\mathbb{P}\mathcal{H})^0 & \xi(g) = 1 \\ \in \mathbf{Aut}_{\mathrm{qtm}}(\mathbb{P}\mathcal{H})^1 & \xi(g) = -1 \end{cases} \tag{3.7}$$

where

$$z^g = \begin{cases} z & \phi(g) = 1 \\ z^* & \phi(g) = -1 \end{cases} \qquad \forall z \in \mathbb{C}$$

Following the projective corepresentation method, there two methods of constructing the factor systems. The first, but more complicated method is to use the methods described in Section 2.3 to define the corepresentation $\mathcal{R} : G \to \mathbf{Aut}_{\mathrm{qtm}}(\mathbb{P}\mathcal{H})$, and then take the section Π

into $\mathbf{Aut}_{\mathrm{qtm}}(\mathcal{H})$. Alternatively, the pullback extension G' of G,

$$G' = \left\{ (a, \hat{S}) \in G \times \mathbf{Aut}_{\mathrm{qtm}}(\mathcal{H}) \mid \mathcal{R}(a) = \Sigma(\hat{S}) \right\} \tag{3.8}$$

can be constructed with the ordinary corepresentation $\mathcal{R}' : G' \to \mathbf{Aut}_{\mathrm{qtm}}(\mathcal{H})$ giving the operators for G. This forms another commutative diagram giving the relations between G, G', $\mathbf{Aut}_{\mathrm{qtm}}(\mathcal{H})$ and $\mathbf{Aut}_{\mathrm{qtm}}(\mathbb{P}\mathcal{H})$ as well as the relations between $\mathcal{R}$, $\mathcal{R}'$ and $\mathcal{R}_{\mathbb{P}}$, showing the many ways that the map $\mathcal{R}_{\mathbb{P}}$ between G and its associated operators can be constructed:

$$
\begin{array}{ccccccccc}
1 & \longrightarrow & M(G, U) & \longrightarrow & G' & \overset{\tilde{\sigma}}{\underset{\tilde{\pi}}{\rightleftarrows}} & G & \longrightarrow & 1 \\
 & & \downarrow & & \downarrow{\scriptstyle \mathcal{R}'} & {\scriptstyle \mathcal{R}_{\mathbb{P}}} \swarrow & \downarrow{\scriptstyle \mathcal{R}} & & \\
1 & \longrightarrow & \mathcal{U}(1) & \longrightarrow & \mathbf{Aut}_{\mathrm{qtm}}(\mathcal{H}) & \overset{\Sigma}{\underset{\Pi}{\rightleftarrows}} & \mathbf{Aut}_{\mathrm{qtm}}(\mathbb{P}\mathcal{H}) & \longrightarrow & 1
\end{array}
$$

In most cases using the pullback extension of G will be preferred, creating the universal covering group G' of G. As discussed before, constructing G' corresponds to adding back in just enough elements of $\mathcal{U}(1)$ to allow non-identity scalars as elements in G', for example allowing -1 as an element when the rotations of an electron are considered. This means that if for example, $g = \mathrm{Rot}(\pi/2)$, then $g^4 = e$ would hold in G and $\mathcal{R}(g^4) = \mathcal{R}(\mathrm{Rot}(2\pi)) = 1$ which is a contradiction to the known physical fact that on a half-spin system, rotation by 2π is not the identity operator but $-\mathbb{I}$. The universal covering group adding -1 as an element allows multiplication in this group to be re-defined so that $g^4 = -1$, sidestepping the issue of trying to represent an element equivalent to the identity element in G as something other than $\mathbb{I}$.

The reason for the preference of working with the universal covering group is that, as stated above and discussed further below, the additional elements which are added to G can be predicted by knowing the physical properties of the quantum system. This means that the formal definition of the universal covering group is often not needed, and G' can be identified out of the quantum system, before a standard corepresentation is taken to find the operators.

Furthermore, it allows matrix forms for the operators to be found using the corepresentation matrices from Equation 2.8. Taking the unitary commuting subgroup $U' \lhd G'$ and one of its representations, r, then the projective corepresentation of G can be constructed to give the

matrix forms of the operators described by the symmetry group:

$$
\mathcal{R}_{\mathbb{P}}(g \in U) = \begin{pmatrix}
r(\tilde{\pi}(g)) & 0 & 0 & 0 \\
0 & r^*(\tilde{\pi}(\alpha)^{-1}\tilde{\pi}(g)\tilde{\pi}(\alpha)) & 0 & 0 \\
0 & 0 & r(\tilde{\pi}(\pi)^{-1}\tilde{\pi}(g)\tilde{\pi}(\delta)) & 0 \\
0 & 0 & 0 & r^*(\tilde{\pi}(\gamma)^{-1}\tilde{\pi}(g)\tilde{\pi}(\gamma))
\end{pmatrix}
$$

$$
\mathcal{R}_{\mathbb{P}}(g \in \alpha U) = \begin{pmatrix}
0 & r(\tilde{\pi}(g)\tilde{\pi}(\alpha)) & 0 & 0 \\
r^*(\tilde{\pi}(\alpha)^{-1}\tilde{\pi}(g)) & 0 & 0 & 0 \\
0 & 0 & 0 & r(\tilde{\pi}(\pi)^{-1}\tilde{\pi}(g)\tilde{\pi}(\gamma)) \\
0 & 0 & r^*(\tilde{\pi}(\gamma)^{-1}\tilde{\pi}(g)\tilde{\pi}(\pi)) & 0
\end{pmatrix} \mathcal{K}
$$

$$
\mathcal{R}_{\mathbb{P}}(g \in \delta U) = \begin{pmatrix}
0 & 0 & r(\tilde{\pi}(g)\tilde{\pi}(\pi)) & 0 \\
0 & 0 & 0 & r^*(\tilde{\pi}(\alpha)^{-1}\tilde{\pi}(g)\tilde{\pi}(\gamma)) \\
r(\tilde{\pi}(\pi)^{-1}\tilde{\pi}(g)) & 0 & 0 & 0 \\
0 & r^*(\tilde{\pi}(\gamma)^{-1}\tilde{\pi}(g)\tilde{\pi}(\alpha)) & 0 & 0
\end{pmatrix}
$$

$$
\mathcal{R}_{\mathbb{P}}(g \in \gamma U) = \begin{pmatrix}
0 & 0 & 0 & r(\tilde{\pi}(g)\tilde{\pi}(\gamma)) \\
0 & 0 & r^*(\tilde{\pi}(\alpha)^{-1}\tilde{\pi}(g)\tilde{\pi}(\pi)) & 0 \\
0 & r(\tilde{\pi}(\pi)^{-1}\tilde{\pi}(g)\tilde{\pi}(\alpha)) & 0 & 0 \\
r^*(\tilde{\pi}(\gamma)^{-1}\tilde{\pi}(g)) & 0 & 0 & 0
\end{pmatrix} \mathcal{K}
$$

$$(3.9)$$

In the trivial extension, where $\tilde{\pi}(g) = g \ \forall g \in G$, $G' = G$, this reduces to the standard corepresentation matrices.

There is a lot more that can be discussed with regards to the matrix structure of the operators generated like this. For now though, we consider classifying the behaviour of the operators in each of the sets U, A, C, P when applied to the eigenstates of the Hamiltonian $\hat{H}$.

Firstly, for any element $g \in G$, the action of its operator $\mathcal{R}_{\mathbb{P}}$ on an energy eigenstate, $|\psi_n\rangle$ of $\hat{H}$, can be checked by seeing what energy eigenvalue is returned by applying $\hat{H}$ to $|\mathcal{R}_{\mathbb{P}}(g)\psi_n\rangle$. Using the fact that operators of G are required to either commute or anti-commute with the Hamiltonian according to ξ, then the relation, [24],

$$\hat{H}|\mathcal{R}_{\mathbb{P}}(g)\psi_n\rangle = \hat{H}\mathcal{R}_{\mathbb{P}}(g)|\psi_n\rangle = \xi(g)\mathcal{R}_{\mathbb{P}}(g)\hat{H}|\psi_n\rangle = \xi(g)\mathcal{R}_{\mathbb{P}}(g)E_n|\psi_n\rangle = \xi(g)E_n|\mathcal{R}_{\mathbb{P}}(g)\psi_n\rangle \quad (3.10)$$

is found.

That is, all the operators generated by G share an eigenbasis $|\psi_n\rangle \to |E_n, a\rangle$ with the Hamiltonian and preserve the absolute value of the eigenvalues associated to eigenstate. However, while the operators in U, A for which $\xi(s) = 1$ preserve the eigenvalues, $\mathcal{R}_{\mathbb{P}}(g) : |E_n, a\rangle \to |E_n, a'\rangle$; the operators in C, P for which $\xi(s) = -1$ flip the sign, $\mathcal{R}_{\mathbb{P}} : |E_n, a\rangle \to |-E_n, a'\rangle$. This means that if C, P are non-empty, and if E_n is an eigenstate, then so must be $-E_n$, which causes a mirror symmetry in the spectra about 0, which is why these operators are known as spectral mirror symmetries. The prime appears on a, as it is possible that G may also provide a re-ordering on the basis states.

We now look at the specific forms and interpretations of elements of G acting as operators. This is a lot of work to do when G is a general $Z_2 \times Z_2$-graded group, however we note that the

48

possible lifts of G into $\mathbf{Aut}_{\mathrm{qtm}}(\mathcal{H})$ are greatly simplified and heavily limited when $U = \{\mathbb{I}\}$. This might seem restrictive, however, we note that when U contains more than the identity, then by applying techniques from Section C.1.2 which will be discussed further in Section 3.1.1, the full Hilbert space decomposes into independent subspaces $\mathcal{H} = \bigoplus_a \bigoplus_{n=1}^{s_a} \mathcal{H}_a$ which can be considered independently with their own independent symmetry groups G_a acting on each $\mathcal{H}_a$ separately. It is guaranteed that these local symmetry groups have $U_a = \{\mathbb{I}\}$, [24, 79, 180]. This means that the following analysis can be done for the group elements of G_a in the simplified case, describing the operators and their interpretations before the subspaces in $\mathcal{H}$ are recombined by taking the direct sums; the operators found in the subspaces may also be combined using direct sums to get their forms on $\mathcal{H}$.

Thus, the simplest case $U = \{\mathbb{I}\}$ can always be constructed and considered.

First, we show that G has a very restricted form when $U = \{\mathbb{I}\}$. In this simplified case, G has to be generated by a subset of $\{\alpha, \gamma, \pi\}$ where α, γ and π are elements of A, C and P respectively:

Lemma 3.1.10. *Let $G = U \cup A \cup C \cup P$ be the symmetry group of a quantum system. If $U = \{\mathbb{I}\}$ then $G \subseteq \{\mathbb{I}, \alpha, \gamma, \pi\}$, $\alpha \in A$, $\gamma \in C$, $\pi \in P$, where $\alpha^2 = \gamma^2 = \pi^2 = \mathbb{I}$ and $\alpha\gamma = \gamma\alpha$, $\alpha\pi = \pi\alpha$, $\gamma\pi = \pi\gamma$, $\alpha\gamma = \pi$.*

This gives five options for the form of G: $G = \{\mathbb{I}\}$; $G = \{\mathbb{I}, \alpha\}$; $G = \{\mathbb{I}, \gamma\}$; $G = \{\mathbb{I}, \pi\}$; and $G = \{\mathbb{I}, \alpha, \gamma, \pi\}$.

Proof. We begin by showing that $G \subset \{\mathbb{I}, \alpha, \gamma, \pi\}$. Given $G = U \cup A \cup C \cup P$ has U as a normal subgroup by definition of a $Z_2 \times Z_2$-graded group, then there must be a traversal $T \subset \{\alpha, \gamma, \pi\}$ of U in G, where $\alpha \in A$ if $A \neq \emptyset$, $\gamma \in C$ if $C \neq \emptyset$, and $\pi \in P$ if $P \neq \emptyset$. As $U = \{\mathbb{I}\}$, then $gU = \{g\}$ holds for all $g \in G$, and thus $A = \alpha U = \{\alpha\}$ or $A = \emptyset$, $C = \gamma U = \{\gamma\}$ or $C = \emptyset$, and $P = \pi U = \{\pi\}$ or $P = \emptyset$. Taking the union of these sets gives $G \subset \{\mathbb{I}, \alpha, \gamma, \pi\}$.

Next we apply Lemmas 2.2.3 and 2.3.2, that the options for $|G|/|U|$ are 4, 2, and 1 to limit the forms of G to $G = \{\mathbb{I}\}$; $G = \{\mathbb{I}, \alpha\}$; $G = \{\mathbb{I}, \gamma\}$; $G = \{\mathbb{I}, \pi\}$; and $G = \{\mathbb{I}, \alpha, \gamma, \pi\}$. This proves the last statement of the theorem, and also forces the involutive nature of α, γ or π when $|G| = 2$.

Finally, it is required to check the relations on α, γ and π when $G = \{\mathbb{I}, \alpha, \gamma, \pi\}$. This can be done by noting that when all of U, A, C and P are non-empty, a $Z_2 \times Z_2$-graded group must satisfy $G/U \cong K_4$. As $U = \{\mathbb{I}\}$, then $G \cong G/U \cong K_4$, which gives all the required relations on the elements of G. $\qquad\square$

With standardised symmetry elements, we can introduce standard labels for the lifts of each of the elements of the symmetry group:

Lemma 3.1.11. *Let $\mathcal{H}$ be Hilbert space with Hamiltonian $\hat{H}$ that has symmetry group $G \subset \{\mathbb{I}, \alpha, \gamma, \pi\}$. Then the lifts of α, γ, π onto $\mathbf{Aut}_{\mathrm{qtm}}(\mathcal{H})$ are associated to the operators $\hat{\mathcal{T}}, \hat{\mathcal{C}}$ and $\hat{\mathcal{P}}$,*

$$\mathcal{R}_{\mathbb{P}}(\alpha) = \hat{\mathcal{T}}, \qquad \mathcal{R}_{\mathbb{P}}(\gamma) = \hat{\mathcal{C}}, \qquad \mathcal{R}_{\mathbb{P}}(\pi) = \hat{\mathcal{P}}$$

To understand the forms of these operators, and later their physical interpretations, it is easiest to start looking at their squares, $\hat{\mathcal{T}}^2$, $\hat{\mathcal{C}}^2$ and $\hat{\mathcal{P}}^2$. These are all unitary commuting operators, which can be checked by showing that $\hat{\mathcal{T}}^2$, $\hat{\mathcal{C}}^2$ and $\hat{\mathcal{P}}^2$ obey the unitarity, Hamiltonian

commutativity and linearity requirements,

$$\left\langle \hat{\mathcal{T}}^2\phi\middle|\hat{\mathcal{T}}^2\psi\right\rangle = \left\langle \hat{\mathcal{T}}\phi\middle|\hat{\mathcal{T}}\psi\right\rangle^* = \langle\phi|\psi\rangle \quad \hat{\mathcal{T}}^2\hat{H} = \hat{\mathcal{T}}\hat{H}\hat{\mathcal{T}} = \hat{H}\hat{\mathcal{T}}^2 \quad \hat{\mathcal{T}}^2 z = \hat{\mathcal{T}}z^*\hat{\mathcal{T}} = z\hat{\mathcal{T}}^2$$

$$\left\langle \hat{\mathcal{C}}^2\phi\middle|\hat{\mathcal{C}}^2\psi\right\rangle = \left\langle \hat{\mathcal{C}}\phi\middle|\hat{\mathcal{C}}\psi\right\rangle^* = \langle\phi|\psi\rangle \quad \hat{\mathcal{C}}^2\hat{H} = -\hat{\mathcal{C}}\hat{H}\hat{\mathcal{C}} = \hat{H}\hat{\mathcal{C}}^2 \quad \hat{\mathcal{C}}^2 z = \hat{\mathcal{C}}z^*\hat{\mathcal{C}} = z\hat{\mathcal{C}}^2$$

$$\left\langle \hat{\mathcal{P}}^2\phi\middle|\hat{\mathcal{P}}^2\psi\right\rangle = \left\langle \hat{\mathcal{P}}\phi\middle|\hat{\mathcal{P}}\psi\right\rangle = \langle\phi|\psi\rangle \quad \hat{\mathcal{P}}^2\hat{H} = \hat{\mathcal{P}}\hat{H}\hat{\mathcal{P}} = \hat{H}\hat{\mathcal{P}}^2 \quad \hat{\mathcal{P}}^2 z = \hat{\mathcal{P}}z\hat{\mathcal{P}} = z\hat{\mathcal{P}}^2$$

This will allow the application to each of them the lemma that any unitary commuting operator on a Hilbert space for which $U = \{\mathbb{I}\}$ must be multiplication by a scalar phase:

Lemma 3.1.12. *If $U = \{\mathbb{I}\}$ then any unitary commuting symmetry operator on the Hilbert space must be scalar multiplication by elements of $\mathcal{U}(1)$.*

Proof. Let $\hat{S}$ be a unitary commuting operator, then $\Sigma(\hat{S}) \in U = \mathbb{I}$ and $\hat{S} \in \ker(\Sigma) = \mathcal{U}(1)$. $\qquad\square$

This can now be used to show that each of $\hat{\mathcal{T}}$, $\hat{\mathcal{C}}$ and $\hat{\mathcal{P}}$ squares to plus or minus the identity in a suitable basis, [24]:

Theorem 3.1.13. *Let $G \subseteq \{\mathbb{I}, \alpha, \gamma, \pi\}$ such that $\alpha^2 = \gamma^2 = \pi^2 = \mathbb{I}$. Let the lifts of α, γ, π be $\hat{\mathcal{T}}, \hat{\mathcal{C}}$ and $\hat{\mathcal{P}}$ respectively. Then there exists a basis such that,*

$$\hat{\mathcal{T}}^2 = \pm\mathbb{I}, \qquad \hat{\mathcal{C}}^2 = \pm\mathbb{I}, \qquad \hat{\mathcal{P}}^2 = \mathbb{I}$$

Proof. As Σ is a homomorphism then,

$$\Sigma\left(\hat{\mathcal{T}}^2\right) = \Sigma\left(\widehat{\mathcal{T}^2}\right) = \mathbb{I} \Longleftrightarrow \mathcal{T}^2 = z_\mathcal{T}\mathbb{I} \qquad z_\mathcal{T} \in \mathcal{U}(1)$$

due to the fact that $\hat{\mathcal{T}}^2$ must be a unitary commuting operator, which must lie in the kernel of Σ, which is just scalar multiplication. This also holds respectively for $\hat{\mathcal{C}}^2 = z_\mathcal{C}\mathbb{I}$ and $\hat{\mathcal{P}}^2 = z_\mathcal{P}\mathbb{I}$ too.

The anti-linearity property of $\hat{\mathcal{T}}$ means that

$$\hat{\mathcal{T}}z_\mathcal{T} = \hat{\mathcal{T}}\hat{\mathcal{T}}^2 = \hat{\mathcal{T}}^2\hat{\mathcal{T}} = z_\mathcal{T}\hat{\mathcal{T}} = z_\mathcal{T}^*\hat{\mathcal{T}}$$

and that $z_\mathcal{T} = \pm 1$ must be real. Similarly, as $\hat{\mathcal{C}}$ is also anti-linear, $z_\mathcal{C} = \pm 1$.

In the case of $\hat{\mathcal{P}}$, the choice of $\hat{\mathcal{P}}$ can be scaled as $\hat{\mathcal{P}}' = z_\mathcal{P}^{-1}\hat{\mathcal{P}}$ as $\hat{\mathcal{P}}$ is linear, thus $\hat{\mathcal{P}}$ can be chosen to square to $\mathbb{I}$ by choice of basis. $\qquad\square$

As well as knowing that each of $\hat{\mathcal{T}}$, $\hat{\mathcal{C}}$ and $\hat{\mathcal{P}}$ square to $\pm\mathbb{I}$, their form is also restricted by the fact that they are projective corepresentations of G and when written as matrices, must have the block structure seen in Equation 3.9. These two requirements completely define the possible matrix forms for $\hat{\mathcal{T}}$, $\hat{\mathcal{C}}$ and $\hat{\mathcal{P}}$ for each possible combination of $\hat{\mathcal{T}}^2$, $\hat{\mathcal{C}}^2$, and $\hat{\mathcal{P}}$ existing - of which there are ten possible combinations. These matrices are easiest to define over the Hilbert space $\mathcal{H} \cong \mathbb{C}^m \otimes \mathbb{C}^n \otimes \mathcal{H}'$, separating out the blocks that $\hat{\mathcal{T}}$ and $\hat{\mathcal{C}}$ act on, [24, 64]:

Theorem 3.1.14. *Let $\mathcal{Q}$ be a quantum system with symmetry group $G \subset \{\mathbb{I}, \alpha, \gamma, \pi\}$ so that there are no unitary-commuting symmetries. Then the Hilbert space can be expressed as $\mathcal{H} = \mathbb{C}^m \otimes \mathbb{C}^n \otimes \mathcal{H}'$ and the operators $\hat{\mathcal{T}}$, $\hat{\mathcal{C}}$ and $\hat{\mathcal{P}}$ corresponding to the symmetry transforms α, γ and*

Class	m	n	T	C	P	$\hat{\mathcal{T}}^2$	$\hat{\mathcal{C}}^2$	$\pi \in G$
A	m	1	$-$	$-$	$-$	$-$	$-$	No
AI	m	1	$\mathbb{I}$	$-$	$-$	$\mathbb{I}$	$-$	No
AII	m	2	$\begin{pmatrix} 0 & 1 \\ -1 & 0 \end{pmatrix}$	$-$	$-$	$-\mathbb{I}$	$-$	No
$AIII$	2	n	$-$	$-$	$\begin{pmatrix} 0 & \mathbb{I}_n \\ \mathbb{I}_n & 0 \end{pmatrix}$	$-$	$-$	Yes
BDI	2	1	$\mathbb{I}$	$\begin{pmatrix} 0 & 1 \\ 1 & 0 \end{pmatrix}$	$\begin{pmatrix} 0 & 1 \\ 1 & 0 \end{pmatrix}$	$\mathbb{I}$	$\mathbb{I}$	Yes
CII	4	4	$\begin{pmatrix} J & 0 \\ 0 & J \end{pmatrix}$	$\begin{pmatrix} 0 & J \\ J & 0 \end{pmatrix}$	$C \otimes T$	$-\mathbb{I}$	$-\mathbb{I}$	Yes
D	2	n	$-$	$\begin{pmatrix} 0 & 1 \\ 1 & 0 \end{pmatrix}$	$-$	$-$	$\mathbb{I}$	No
C	2	n	$-$	$\begin{pmatrix} 0 & -1 \\ 1 & 0 \end{pmatrix}$	$-$	$-$	$-\mathbb{I}$	No
CI	2	1	$\mathbb{I}$	$\begin{pmatrix} 0 & -1 \\ 1 & 0 \end{pmatrix}$	$\begin{pmatrix} 0 & -1 \\ 1 & 0 \end{pmatrix}$	$\mathbb{I}$	$-\mathbb{I}$	No
$DIII$	2	4	$\begin{pmatrix} J & 0 \\ 0 & J \end{pmatrix}$	$\begin{pmatrix} 0 & 1 \\ 1 & 0 \end{pmatrix}$	$C \otimes T$	$-\mathbb{I}$	$\mathbb{I}$	No

Table 3.1: Possible choices for the matrices T, C, P depending on whether α, γ and π are in G, and the square of $\hat{\mathcal{T}}$ and $\hat{\mathcal{C}}$, [64, 73]. Where the size of $\mathcal{H}_{\text{charge}}$ and $\mathcal{H}_{\text{spin}}$ is restricted by the form of the operators $\hat{\mathcal{C}}$ and $\hat{\mathcal{T}}$ respectively, then values for m and n have been given. The matrix J is given by $J = \begin{pmatrix} 0 & 1 \\ -1 & 0 \end{pmatrix}$.

π respectively may be expressed as

$$\hat{\mathcal{T}} = (\mathbb{I}_m \otimes T \otimes \mathbb{I}_{\mathcal{H}'})\mathcal{K}$$
$$\hat{\mathcal{C}} = (C \otimes \mathbb{I}_n \otimes \mathbb{I}_{\mathcal{H}'})\mathcal{K}$$
$$\hat{\mathcal{P}} = (P \otimes \mathbb{I}_{\mathcal{H}'})$$

where T, C and P are taken from Table 3.1 according to how $\hat{\mathcal{T}}$ and $\hat{\mathcal{C}}$ square and if $\pi \in G$.

Note how $\mathcal{H} = \mathbb{C}^m \otimes \mathbb{C}^n \otimes \mathcal{H}' \cong \mathcal{H}_{\text{charge}} \otimes \mathcal{H}_{\text{spin}} \otimes \mathcal{H}_{\text{orbital}}$, the Hilbert space introduced at the end of Section C.1.1 and used in Theorem 2.4.10. This both justifies the use of this structure on the Hilbert space, and makes clear the link between the Altland-Zirnbauer class of a projective corepresentation of G and the form of the operators $\hat{\mathcal{T}}$, $\hat{\mathcal{C}}$ and $\hat{\mathcal{P}}$ - Theorem 3.1.14 is exactly Theorem 2.4.10, only in the language of quantum operators instead of corepresentation matrices. Note this connection would always have to exist - the operators are defined by the corepresentation and must take structure from its classification, however it is now seen, and will have further effects on the structure of the Hilbert space and Hamiltonian.

First though, having identified that the operators may be described on $\mathcal{H}_{\text{charge}} \otimes \mathcal{H}_{\text{spin}} \otimes \mathcal{H}_{\text{orbital}}$, we can use their matrix forms, and their interaction with the operators $\hat{q}_k$, $\hat{p}_k$, $\hat{J}_k$ and $\hat{c}_k$, $\hat{c}_k^\dagger$ to study the effect of $\hat{\mathcal{T}}$, $\hat{\mathcal{C}}$ and $\hat{\mathcal{P}}$ on each of these operators, giving them physical interpretations.

Firstly, $\hat{\mathcal{T}}$ conjugates everything with imaginary components so that, [176],

$$\hat{\mathcal{T}}^{-1}q_k\hat{\mathcal{T}} = \hat{q}_k, \quad \hat{\mathcal{T}}^{-1}p_k\hat{\mathcal{T}} = -\hat{p}_k, \quad \hat{\mathcal{T}}^{-1}\hat{J}_k\hat{\mathcal{T}} = -\hat{J}_k, \quad \hat{\mathcal{T}} : \begin{pmatrix} |p\rangle \\ |h\rangle \end{pmatrix} \to \begin{pmatrix} |p\rangle \\ |h\rangle \end{pmatrix} \tag{3.11}$$

This leaves particle type and position unchanged, but flips the direction of all of the momentums - this is equivalent to the operation of time-reversal. Also, when $U > \{\mathbb{I}\}$ then any symmetry operator which has the same type of interaction $\hat{\mathcal{T}}$ has with the Hamiltonian and transition amplitude will be known as a generalised time-reversal symmetry - this covers the anti-unitary, commuting operators, or those generated by elements of A.

Next, $\hat{\mathcal{C}}$ conjugates the imaginary components, but also inverts the charge space, and switches creation and annihilation operators in the second quantised basis, [14, 112],

$$\hat{\mathcal{C}} : \begin{pmatrix} |p\rangle \\ |h\rangle \end{pmatrix} \to \begin{pmatrix} |h\rangle \\ |p\rangle \end{pmatrix}, \qquad \hat{\mathcal{C}} : \hat{c}_i \to \hat{c}_i^\dagger \tag{3.12}$$

which is interpreted as transforming particles into anti-particles - this is known as charge-conjugation - or the particle-hole symmetry. This time, when $U > \{\mathbb{I}\}$, then any symmetry operator which has the same type of interaction $\hat{\mathcal{C}}$ has with the Hamiltonian and transition amplitude is known as a generalised charge-conjugation symmetry - this covers the anti-unitary, anti-commuting operators, or those generated by elements of C.

Finally, $\hat{\mathcal{P}} = \hat{\mathcal{T}}\hat{\mathcal{C}}$ combines the two operations $\hat{\mathcal{T}}$ and $\hat{\mathcal{C}}$,

$$\hat{\mathcal{P}} = \hat{\mathcal{C}} \circ \hat{\mathcal{T}} \tag{3.13}$$

This is the chiral operator, or the sub-lattice symmetry operator as it can occur due to sub-lattice symmetries, [112]. It is thus sometimes denoted as the operator $\hat{\mathcal{S}}$ as the sub-lattice symmetry, [112, 139]. When $U > \{\mathbb{I}\}$, then any symmetry operator which has the same type of interaction $\hat{\mathcal{P}}$ has with the Hamiltonian and transition amplitude is known as a generalised chiral symmetry - this covers the unitary, anti-commuting operators, or those generated by elements of P.

We note that the anti-commutation of $\hat{\mathcal{C}}$ and $\hat{\mathcal{P}}$ with the Hamiltonian as a symmetry requirement holds only with the first-quantised Hamiltonian, they commute with the second quantised Hamiltonian, [112], which is part of why they may be called symmetries despite not commuting with the first quantised Hamiltonian - the notion of symmetry normally applies to operators commuting with the Hamiltonian in the wider physics literature, which would be violated by the charge-conjugation and chiral operators.

This now also allows the discussion of the reasons for why each of the names of the cosets of U in G are chosen for the case of the $Z_2 \times Z_2$-graded group - U and A carry over from the Z_2-graded case, where they stand for the *unitary* and *anti-unitary* elements respectively. The subsets C and P are labelled after the $\hat{\mathcal{C}}$ and $\hat{\mathcal{P}}$ operators.

We can also now discuss how the factor system can be predicted from the physical properties of the system for the projective corepresentation taking G to the operators $\hat{\mathcal{T}}$, $\hat{\mathcal{C}}$ and $\hat{\mathcal{P}}$. This is because it is well known that the forms of the operators $\hat{\mathcal{T}}$, $\hat{\mathcal{C}}$ and $\hat{\mathcal{P}}$, not even necessarily as symmetries, are fixed by the physical properties of the system. This is best expressed as a method

of inferring the squares of $\hat{\mathcal{T}}$ and $\hat{\mathcal{C}}$, as from here their matrix forms can be read off from Table 3.1 by treating them as if they were symmetries, and taking $\hat{\mathcal{P}} = \hat{\mathcal{C}}\hat{\mathcal{T}}$. Of course their actual status as symmetries still remains to be checked after finding their forms.

Firstly, if the system comprises of bosons or an even number of fermions, then $\hat{\mathcal{T}}^2 = \mathbb{I}$; while an odd number of fermions requires $\hat{\mathcal{T}}^2 = -\mathbb{I}$, [30]. The form of $\hat{\mathcal{C}}^2$ requires expressing the system's Hamiltonian in the BdG formalism,

$$\hat{H}_{\mathrm{BdG}} = \begin{pmatrix} H_0 - E_F & -i\sigma_y\Delta \\ i\sigma_y\Delta^* & E_F - H_0^* \end{pmatrix}$$

and if H_0 is spin-dependent, then $\hat{\mathcal{C}}^2 = \mathbb{I}$ while if H_0 is spin-independent, then $\hat{\mathcal{C}}^2 = -\mathbb{I}$, [14]. These two simple rules are all that is needed to infer the forms of the time-reversal, charge-conjugation and chiral operators on a system, finding their forms and allowing them to be checked if they are symmetries. This can be used to describe the factor system taking G as an abstract group to the operators through a projective corepresentation, or it also allows the Altland-Zirnbauer class of the system to be checked directly by which of them are symmetries and their squares, without needing to work with the projective corepresentations when there are no non-trivial unitary symmetries.

The different forms of $\hat{\mathcal{T}}$, $\hat{\mathcal{C}}$ and $\hat{\mathcal{P}}$ also dictate the structure of the Hilbert space they sit in. This was seen in Theorem 3.1.14 and Table 3.1, where the sizes of $\mathcal{H}_{\mathrm{charge}} \cong \mathbb{C}^m$ and $\mathcal{H}_{\mathrm{spin}} \cong \mathbb{C}^n$ could be limited by the forms of the symmetries $\hat{\mathcal{T}}$ and $\hat{\mathcal{C}}$. More restrictions on $\mathcal{H}$ can be seen by comparing an eigenstate $|\psi_n\rangle$ with its image under $\hat{\mathcal{T}}, \hat{\mathcal{C}}$ and $\hat{\mathcal{P}}$, [24]:

Theorem 3.1.15. *Let $\mathcal{H}$ be the Hilbert space of a quantum system with Hamiltonian $\hat{H}$ and energy eigenstates $|\psi_n\rangle$ spanning the Hilbert space. Then, there exists a basis $|\psi_n'\rangle$ where:*

- *If $\hat{\mathcal{T}}^2 = \mathbb{I}$ then $\left|\hat{\mathcal{T}}\psi_n'\right\rangle \cong |\psi_n'\rangle$*

- *If $\hat{\mathcal{T}}^2 = -\mathbb{I}$ then $\left|\hat{\mathcal{T}}\psi_n'\right\rangle \not\cong |\psi_n'\rangle$ and all eigenvalues E_n are doubly degenerate.*

- *In all cases, $\left|\hat{\mathcal{C}}\psi_n'\right\rangle \not\cong |\psi_n'\rangle \not\cong \left|\hat{\mathcal{P}}\psi_n'\right\rangle$*

Proof. When $\hat{\mathcal{T}}^2 = -\mathbb{I}$, then the orthogonality test for $|\psi_n\rangle$ and $\left|\hat{\mathcal{T}}\psi_n\right\rangle$ is

$$\left\langle\psi_n\middle|\hat{\mathcal{T}}\psi_n\right\rangle = \left\langle\hat{\mathcal{T}}\psi_n\middle|\hat{\mathcal{T}}^2\psi_n\right\rangle^* = -\left\langle\hat{\mathcal{T}}\psi_n\middle|\psi_n\right\rangle^* = -\left\langle\psi_n\middle|\hat{\mathcal{T}}\psi_n\right\rangle = 0$$

so they are linearly independent states. As there are two linearly independent states with the eigenvalue E_n, it is doubly degenerate.

When $\hat{\mathcal{T}}^2 = \mathbb{I}$, then if the two eigenstates $|\psi_n\rangle$ and $\left|\hat{\mathcal{T}}\psi_n\right\rangle$ are not already equal, then a change of basis

$$|\psi_n'\rangle = \frac{1}{\sqrt{2}}\left(|\psi_n\rangle + \left|\hat{\mathcal{T}}\psi_n\right\rangle\right)$$

satisfies $\left|\hat{\mathcal{T}}\psi_n'\right\rangle = |\psi_n'\rangle$.

Class	$\hat{H}$	Class	$\hat{H}$
A		$AIII$	$= \begin{pmatrix} 0 & h \\ h^\dagger & 0 \end{pmatrix}$
AI	$\in \mathbb{R}$	BDI	$= \begin{pmatrix} 0 & h \\ h^T & 0 \end{pmatrix}, h = h^*$
AII	$= \begin{pmatrix} h_1 & h_2 \\ -h_2^* & h_1^* \end{pmatrix}$	CII	$= \begin{pmatrix} 0 & h \\ h^\dagger & 0 \end{pmatrix}, h = \begin{pmatrix} k_1 & k_2 \\ -k_2^* & k_1^* \end{pmatrix}$
C	$= \begin{pmatrix} h_1 & h_2 \\ -h_2^* & h_1^* \end{pmatrix}$	CI	$= \begin{pmatrix} 0 & h \\ h^* & 0 \end{pmatrix}, h^T = h$
D	$= \begin{pmatrix} h_1 & h_2 \\ -h_2^* & -h_1^T \end{pmatrix}, h_1 = h_1^\dagger, h_2 = -h_2^T$	$DIII$	$= \begin{pmatrix} 0 & h \\ -h^* & 0 \end{pmatrix}, h^T = -h$

Table 3.2: Canonical structure on the Hamiltonian of a quantum system according to the Altland-Zirnbauer class of its symmetry group $G \subseteq \{\mathbb{I}, \alpha, \gamma, \pi\}$, [1, 24, 39, 156].

In the final case, as $|\psi_n\rangle$ has eigenvalue E_n, while $\left|\hat{\mathcal{C}}\psi_n\right\rangle$ and $\left|\hat{\mathcal{P}}\psi_n\right\rangle$ have eigenvalue $-E_n$, they must be linearly independent of $|\psi_n\rangle$, $\left|\hat{\mathcal{C}}\psi_n'\right\rangle \ncong |\psi_n'\rangle \ncong \left|\hat{\mathcal{P}}\psi_n'\right\rangle$. $\qquad\square$

The degeneracy when $\hat{\mathcal{T}}^2 = -\mathbb{I}$ is known as Kramer's degeneracy, and means that whenever $\hat{\mathcal{T}}^2 = -\mathbb{I}$, the Hamiltonian is of even dimension. The structure of the Hamiltonian can be further classified when the corepresentation class of G is considered, [117]:

Theorem 3.1.16. *Let $\mathcal{Q}$ be a quantum system with Hilbert space $\mathcal{H}$, Hamiltonian $\hat{H}$ and symmetry group G with a projective corepresentation $\mathcal{R}_\mathbb{P}$ on $\mathcal{H}$. Let $Z(\mathcal{R}_\mathbb{P})$ be the super-algebra generated by the super-commutant of $\mathcal{R}_\mathbb{P}$. Then $\hat{H} \in Z$.*

Proof. $\mathcal{R}_\mathbb{P}$ forms the set of operators on $\mathcal{H}$ generated by G. By definition of a symmetric operator, $\mathcal{R}_\mathbb{P}(g)\hat{H} = \xi(g)\hat{H}\mathcal{R}_\mathbb{P}(g) \ \forall g \in G$. This is also the definition of an element being in the super-commutant. Thus, $\hat{H} \in Z(\mathcal{R}_\mathbb{P})$. $\qquad\square$

Using the matrix forms of $\hat{\mathcal{T}}$, $\hat{\mathcal{C}}$ and $\hat{\mathcal{P}}$ when $U = \mathbb{I}$ gives a more explicit form, [24, 156]:

Theorem 3.1.17. *Let $\hat{H}$ be the Hamiltonian of a system with symmetry group $G \subseteq \{\mathbb{I}, \alpha, \gamma, \pi\}$. Given the Altland-Zirnbauer class of G, then there exists a basis for the Hilbert space where $\hat{H}$ is isomorphic to a Hermitian matrix with the additional structure given by Table 3.2.*

This is an incredibly strong restriction on the different canonical forms of the Hamiltonian, and will allow for random matrix theory to be applied to the Hamiltonians by statistically sampling the super-commutant of the symmetry class of the system, this will be further discussed in Chapter 4. We note that the Altland-Zirnbauer classification is essential to this process of taking a quantum system and then doing random matrix statistics on it - it is only because we are able to take a symmetry group, then take its projective-corepresentation and its super-commutant, which is now guaranteed by the Altland-Zirnbauer classification not to be one of infinitely many different forms, but one of ten different forms which have similar and well defined statistics. The ensembles coming out of the Altland-Zirnbauer classification also explains why the random matrix behaviour is universal to all systems sharing a symmetry group - these systems all obviously share an Altland-Zirnbauer class, so their Hamiltonians sit inside the same ensembles.

3.1.1 Non-Trivial Unitary Symmetries: Spectral Splitting, Symmetry Reduced Bases And Desymmetrisation

We come now to discussing the general case where there may be non-trivial unitary symmetries. This case has already been alluded to in several places - first we stated in the introduction that the effect of non-trivial unitary symmetries was to cause spectral splitting, so that the full energy spectrum contains a number of independent spectra to which random matrix theory had to be applied separately; in the above section, we claimed it was possible to derive a 'desymmetrised' system, finding a subspace such that all unitary symmetries in it were trivial, and only in these subspaces could the ten Altland-Zirnbauer ensembles occur. Here we elaborate on the effects of non-trivial unitary symmetries on the spectral statistics of a quantum system, deriving the symmetry reduced basis for the system, and show how both of the effects of the spectrum splitting and desymmetrising the system arise out of the construction of the symmetry reduced basis. We also discus the process of restricting the time-reversal, charge-conjugation and chiral operators to the systems constructed through desymmetrisation or the symmetry reduced basis, discussing how the form of the local symmetry group in the subspace may be inferred based on the corepresentation associated to the subspace. This allows the techniques discussed in the section above for analysing the structure of the Hilbert space and Hamiltonian to be applied to the subspaces, and the random matrix ensembles appearing in them derived for each subspectrum.

We begin with describing the creation of subspaces in the Hilbert space due to the unitary symmetries, forming the independent subspectra in the full spectrum, and in the process defining the symmetry reduced basis for the system.

Let then $\mathcal{Q}$ be a quantum system with a symmetry group $G = U \cup \alpha U \cup \gamma U \cup \pi U$ and projective corepresentation $\mathcal{R}_\mathbb{P} : G \to \mathbf{Aut}_{\mathrm{qtm}}(\mathcal{H})$ taking G to a set of symmetry operators on $\mathcal{H}$. Let U contain non-trivial elements. Let G' be the universal covering group of G found with the pullback extension. We can happily work with the covering group G' and its corepresentation $\mathcal{R}'$ onto $\mathbf{Aut}_{\mathrm{qtm}}(\mathcal{H})$, and will in fact assume that we are, relabelling $G' \to G$ throughout with $\mathcal{R}' \to \mathcal{R}$ giving the symmetry operators.

First we note, that if $U \subset G$ is a set of non-trivial symmetry transformations mapped to operators $\mathcal{R}(u)$ that are unitary and commute with the Hamiltonian for all $u \in U$, then $\hat{H}$ and $\mathcal{R}(u)$ share an eigenbasis for all $u \in U$ by Theorem 3.10. Firstly, this means that if $|E_n, a\rangle$ is an eigenstate of $\hat{H}$ with energy E_n, then $\mathcal{R}(u) |E_n, a\rangle = |E_n, a'\rangle$ is also an eigenstate with energy E_n, but it is potentially linearly independent of the original eigenstate. Secondly, the operators are all simultaneously block diagonalisable.

We consider this block-diagonalised basis. To do this we note that the corepresentation $\mathcal{R}$ of G once restricted to U acts as a linear, unitary representation of U. This can be seen by taking the matrix form of the corepresentation for U on $\mathcal{H} = \mathcal{H}_U \oplus \alpha\mathcal{H}_U \oplus \pi\mathcal{H}_U \oplus \gamma\mathcal{H}_U$, as generated by the unitary representation of U on $\mathcal{H}_U$ by Equation 2.8,

$$
\mathcal{R}(u \in U) = \begin{pmatrix} R(u) & 0 & 0 & 0 \\ 0 & R^*(\alpha^{-1}u\alpha) & 0 & 0 \\ 0 & 0 & R(\pi^{-1}u\pi) & 0 \\ 0 & 0 & 0 & R^*(\gamma^{-1}u\gamma) \end{pmatrix}.
$$

The blocks $R^*(\alpha^{-1}u\alpha)$, $R(\pi^{-1}u\pi)$ and $R^*(\gamma u\gamma)$ are still unitary representations of U when R is, thus by forgetting about the information about the elements $\mathcal{R}(a \in A)$, $\mathcal{R}(c \in C)$ and $\mathcal{R}(p \in P)$, then $\mathcal{R}$ is a unitary representation of U on $\mathcal{H}$, as per the definition of the restricted representation from Definition 2.1.4. We for now ignore the decomposition of the Hilbert space into $\mathcal{H} = \mathcal{H}_U \oplus \alpha\mathcal{H}_U \oplus \pi\mathcal{H}_U \oplus \gamma\mathcal{H}_U$ however, and consider $\mathcal{R}$ as a general unitary representation of U. This means that the decomposition into irreducible representations can be taken for it, so that $\mathcal{R}(u) \cong \bigoplus_a \bigoplus_{n=1}^{s_a} \rho_a(u)$ with a dimension d_a irreducible representation ρ_a having multiplicity s_a in $\mathcal{R}$ as a representation.

In this basis, then the eigenstates may be described by three quantum numbers, $|a, i, n\rangle$, [90], where a corresponds to a unique irreducible representation of U, $1 \leq i \leq d_a$ corresponds to a component in its dimension d_a expression, and $1 \leq n \leq s_a$ corresponds to the degenerate copy of the representation. This allows the eigenstates to be written as transforming under U as,

$$u : |a, i, n\rangle \to \mathcal{R}(u)|a, i, n\rangle = \sum_{j=1}^{d_a} (\rho_a(u))_{ji} |a, j, n\rangle. \tag{3.14}$$

Note that while sharing an eigenbasis with $\mathcal{R}$ is enough to guarantee that $\hat{H}$ is block diagonal in this basis, it is not enough to assume that $\hat{H}$ decomposes into exactly the same number of blocks as $\mathcal{R}$, with the same sizes. That is, we can't assume that $\hat{H} = \bigoplus_a \bigoplus_{n=1}^{s_a} \hat{H}_a$, so that there is one block $\hat{H}_a$ in the decomposition for each copy of ρ_a. Instead we will show that one block $\hat{H}_a$ corresponds to the combination of all degenerate copies of ρ_a in the decomposition of $\mathcal{R}$, so $\hat{H} = \bigoplus_a \hat{H}_a$.

Identifying the block structure of $\hat{H}$ in this basis is a case of computing the matrix elements H_{NM} for the states $N = |a, i, n\rangle$ and $M = |b, j, m\rangle$ and identifying the conditions for $H_{NM} = 0$. The matrix elements can be computed with the standard expression,

$$\begin{aligned} H_{NM} &= \langle a, i, j|\hat{H}|b, j, m\rangle \\ &= \frac{1}{|U|} \sum_{u \in U} \langle a, i, n|\hat{H}|b, j, m\rangle, \end{aligned}$$

where by adding the sum over U, the Rearrangement Theorem from Theorem A.0.7 can be applied, inserting $\mathcal{R}(u)$ into the matrix element while leaving H_{NM} invariant. This gives,

$$\begin{aligned} H_{NM} &= \frac{1}{|U|} \sum_{u \in U} \langle a, i, n|\mathcal{R}^{-1}(u)\hat{H}\mathcal{R}(u)|b, j, m\rangle \\ &= \frac{1}{|U|} \sum_{u \in U} \sum_{1 \leq k \leq d_a} \sum_{1 \leq l \leq d_b} (\rho_a^*(u))_{ki}(\rho(b))_{lj} \langle a, i, n|\hat{H}|b, j, m\rangle. \end{aligned}$$

Note that while there is an orthogonality condition on the characters of irreducible representations, there is also one on the matrix elements of the irreducible representations, [149],

$$\frac{1}{|U|} \sum_{u \in U} (\rho_a^*(u))_{ij}(\rho_b(u))_{kl} = \frac{\delta_{ik}\delta_{jl}\delta_{ab}}{d_a}. \tag{3.15}$$

Substituting this into the matrix element equation gives,

$$H_{NM} = \sum_{1 \le k \le d_a} \sum_{1 \le l \le d_b} \frac{\delta_{kl}\delta_{ij}\delta_{ab}}{d_a} H_{NM} \tag{3.16}$$

and $H_{NM} = 0$ if either $a \neq b$ or $i \neq j$. Thus, it is not required that $\langle a, i, n | \hat{H} | a, i, m \rangle = 0$ for $n \neq m$, and $\hat{H}$ allows for crossover between different degenerate copies of the irreducible representation ρ_a. This is our required block structure - the Hamiltonian decomposes into one block for each *unique, non-equivalent* irreducible representation of U contained in $\mathcal{R}$. This block $\hat{H}_a$ contains all the degenerate copies of the irreducible representation ρ_a. This means that if ρ_a is a dimension d_a irreducible representation with multiplicity s_a in $\mathcal{R}$, then $\hat{H}_a$ is a dimension $d_a s_a$ square matrix.

This also gives the spectral splitting property of the unitary symmetries immediately - each of the sub-Hamiltonians $\hat{H}_a$ may be treated as an independent system and will have its own independent spectrum. Being able to isolate the sub-Hamiltonians as independent systems is also how the 'desymmetrised' systems appear - the promised subspace from the previous section where $U_a = \{\mathbb{I}\}$ is trivial, though discussion of why this is will be left to after this basis is formally recognised as the symmetry reduced basis, [11, 24, 90, 110]:

Theorem 3.1.18. *Let $\mathcal{Q}$ be a quantum system with the extended symmetry group $G = U \cup \alpha U \cup \gamma U \cup \pi U$. Let $U > \{\mathbb{I}\}$ contain non-trivial elements. Let the action of G on the Hilbert space be given by the corepresentation $\mathcal{R} : G \to \mathbf{Aut}_{\mathrm{qtm}}(\mathcal{H})$, expressed over the basis $|\psi_i\rangle$ by the matrix $\mathcal{R}_{ji}(u)$,*
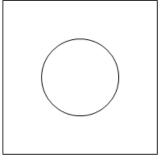
$$u : |\psi_i\rangle \to \sum_j R_{ji}(u) |\psi_j\rangle .$$

Let W be the transformation giving the decomposition of the restriction of $\mathcal{R}$ to U as a representation into irreducible components, $W : \mathcal{R} \to \bigoplus_a \bigoplus_{n=1}^{s_a} \rho_a$. Applying W to the basis $|\psi_n\rangle$ gives the basis $|a, i, n\rangle$ for $1 \le i \le d_a$ and $1 \le n \le s_a$, which transforms under U as

$$u : |a, i, n\rangle = \sum_{j=1}^{d_a} (\rho_a(u))_{ji} |a, j, n\rangle .$$

Then, the following occur:

- *The Hilbert space decomposes into subspaces, $\mathcal{H} = \bigoplus_a \mathcal{H}_a$ with $\mathcal{H}_a = \langle |a, i, n\rangle | 1 \le i \le d_a, 1 \le n \le s_a \rangle$ being the subspace spanned by the vectors associated to all equivalent copies of the unique irreducible reducible representation ρ_a of U*

- *The Hamiltonian decomposes into the block structure $\hat{H} = \bigoplus_a \hat{H}_a$ with one block for each subspace $\mathcal{H}_a$ in the Hilbert space.*

- *The energy level spectrum $\{E_i\}$ of $\mathcal{Q}$ decomposes into independent subspectra, $\{E_i\} = \bigoplus_a \{E_i\}_a$ where $\{E_i\}_a$ is the set of eigenvalues of $\hat{H}_a$.*

- *Treating $\mathcal{H}_a$ and $\hat{H}_a$ as forming an independent system, $\mathcal{Q}_a$, a local unextended symmetry group G_a can be constructed. G_a is also $Z_2 \times Z_2$-graded but has $U_a = \{\mathbb{I}\}$. The inclusion of α_a, γ_a and π_a in G_a can be predicted through the Altland-Zirnbauer class of the corep-*

(a) The full Sinai billiard.　　　　(b) The desymmetrised Sinai billiard.

Figure 3.1: The Sinai billiard and its desymmetrised form, [25]. Given the full billiard, it has geometric symmetries $U = D_8$ when there is no magnetic field imposed; by considering only an eighth of the full billiard, with particular boundary conditions on the two new edges where the rest of the billiard has been cut away, it is reduced to a subspace where $U = \{\mathbb{I}\}$.

> *resentation $\mathcal{R}_a$ generated by ρ_a, as can be the forms their operators take on $\mathcal{H}_a$ when local symmetries or alternatively the form of the universal covering group G'_a of G_a.*

The proof of the first two statements regarding the decomposition of $\mathcal{H}$ and $\hat{H}$ is the construction described prior to the theorem. We note that the decomposition and the process of identifying the necessary transform W are explored further in [11, 24, 110], while [24, 179] show that it is also possible to go further in restricting the structure of $\mathcal{H}_a$, the representation of U on $\mathcal{H}_a$, $R_a : U \to \mathrm{Aut}(\mathcal{H}_a)$, and the local sub-Hamiltonian,

$$\mathcal{H}_a = \mathbb{C}^{s_a} \otimes \mathcal{H}'_a, \qquad R_a(u) = \mathbb{I}_{s_a} \otimes \rho_a(u), \qquad \hat{H}_a = \hat{H}'_a \otimes \mathbb{I}_{s_a}.$$

Understanding the reason why it can be guaranteed that $U_a = \{\mathbb{I}\}$ is a little more complicated. The standard proof is given in [79] by Heinzner, Huckleberry and Zirnbauer, but the most intuitive reason is to understand that the symmetry reduced basis is heavily linked with the construction of both the quotient space, G/U and the fundamental domain or desymmetrised configuration space, [11, 137], and in these interpretations it is forced that $U_a = \{\mathbb{I}\}$ by their definition. That is, the definition of the quotient G/U is that $U \equiv \mathbb{I}$ are equated, while the fundamental domain or desymmetrised configuration space is the isolation of the subset of the system where every point fully in the subset is mapped out of the subset by the action of U, bar a few points on the boundary, [137]. Again, as it corresponds to the separate process of looking at the configuration space, and then removing sections of it until there are no unitary commuting symmetries, it is required that $U_a = \{\mathbb{I}\}$.

This desymmetrisation process done by modifying the geometry is well known, particularly for billiard systems. A well known example of the Sinai billiard is given in Figure 3.1, showing both the full billiard - which is square with the central circle removed and has the unitary symmetry group $U = D_8$ from its geometry - and the desymmetrised billiard which takes 1/8th of the initial billiard's area, but which has no geometric symmetries. Boundary conditions must be imposed on the new walls where the desymmetrised billiard has been 'cut' out of the full billiard, and how these are imposed allows which of the subspaces $\mathcal{H}_a$ is being considered to be controlled.

(a) A quantum graph.

$$S = \begin{pmatrix} 0 & 0 & (\frac{2}{3}-\delta_{ij})_{1\leq i,j\leq 3} & 0 \\ \mathbb{I}_3 & 0 & 0 & 0 \\ 0 & 0 & 0 & \mathbb{I}_3 \\ 0 & (\frac{2}{3}-\delta_{ij})_{1\leq i,j\leq 3} & 0 & 0 \end{pmatrix}$$

(b) Its uni-directional equivalent.

$$S' = \begin{pmatrix} 0 & (\frac{2}{3}-\delta_{ij})_{1\leq i,j\leq 3} & 0 & 0 \\ \mathbb{I}_3 & 0 & 0 & 0 \\ 0 & 0 & 0 & (\frac{2}{3}-\delta_{ij})_{1\leq i,j\leq 3} \\ 0 & 0 & -\mathbb{I}_3 & 0 \end{pmatrix}$$

(c) Its form in the symmetry reduced basis.
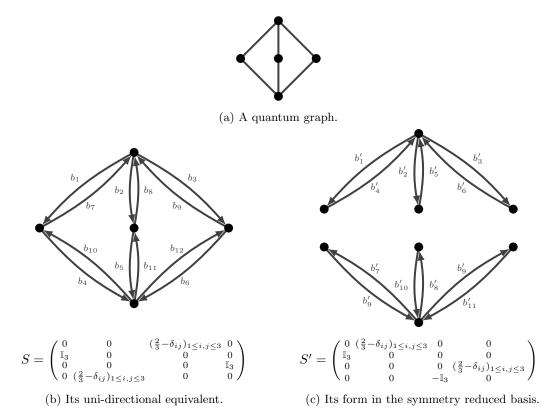
Figure 3.2: A quantum graph, having a $U = Z_2$ geometric mirror symmetry through the x-axis, and the form it takes in the symmetry reduced basis, identifying the two non-connected subgraphs within it that can be studied as separate, desymmetrised systems, [16]. Note how they correspond to cutting the graph in half along the mirror axis, and imposing a new scattering condition at the cut edges, as was the case for the Sinai billiard.

To establish the link between the symmetry reduced basis and a reduction in the geometry of the system, it is easiest to consider the quantum graph however, and understand how the symmetry reduced basis leads to the construction of the quotient graph, [11, 110]. This is a model that will be considered further in Chapters 6 and 7, so we give a brief gloss here, but further details will be covered later.

The quantum graph, an example being seen in Figure 3.2a, consists of a series of quantum wires connected together at vertices. A quantum particle then exists on one of the wires, and can travel down them and scatter between connected wires at the vertex. This behaviour can be described by two matrices - the transmission matrix, $T(E)$, describing the phases picked up by an energy E particle down the wires, and the scattering matrix, $S(E)$, where $S(E)_{b_2 b_1}$ describes the probability to scatter from the wire b_1 onto the wire b_2; the combination of them as $\Xi(E) = S(E)T(E)$ can be considered as a time-evolution operator replacing the Hamiltonian in the system. We note briefly that due to travel in the direction 'against' the direction of the wire being possible, the scattering matrix has twice the dimension of the number of physical wires if back travel is allowed. We will talk further about the exact definition and interpretations of the quantum graph and its scattering matrix in Chapter 6, but for now it will suffice to enforce instead that instead of having wires with back-travel, we replace each wire with two wires allowing only unidirectional travel, with their directions of travel in opposite direction as in Figure 3.2b. This

doesn't change the scattering matrix, and it allows us to recognise that the scattering matrix actually encodes the geometry of the system into itself - particles can only scatter between two wires b_1, b_2 if they are connected, so $S_{b_2 b_1}(E)$ is only non-zero when the start of b_2 connects to the end of b_1.

As Ξ replaces the Hamiltonian in describing the system, the symmetry reduced basis involves block diagonalising Ξ. As T is diagonal, this leads to block diagonalising S. This leads to defining a new scattering matrix $S' = \bigoplus_a S_a$, which is block diagonal. This can then be used to define a new graph geometry based on the idea that non-zero elements of S_a lead to connected bonds. The block diagonal structure means that different subgraphs end up being created, without connections between them. These subgraphs can then be studied as separate systems - and are the above defined geometrically desymmetrised systems. Figure 3.2c gives the subgraphs derived from block diagonalising the scattering matrix for the example graph in Figure 3.2b, showing how it splits into two.

Finally, we discuss how given the subspace $\mathcal{H}_a$, we can predict the form of the local unexpended symmetry group G_a and its covering group G'_a, along with the forms of any local time-reversal, charge-conjugation and chiral symmetry operators. Recall the breakdown of the Hilbert space into $\mathcal{H}_U$, and its time-reversed, charge-conjugated and chiral copies, $\mathcal{H} = \mathcal{H}_U \oplus \alpha \mathcal{H}_U \oplus \pi \mathcal{H}_U \oplus \gamma \mathcal{H}_U$, and recognise that if u acts on the state $|a, i, n\rangle$ by

$$u : |a, i, n\rangle \rightarrow \sum_{j=1}^{d_a} (\rho_a(u))_{ji} |a, j, n\rangle$$

then the matrix form of the corepresentation generated by ρ_a means that u acts on the time-reversed, charge-conjugated and chiral states found by applying the operator forms of α, γ and π in this basis - $\hat{\alpha}$, $\hat{\gamma}$ and $\hat{\pi}$ - to $|a, i, n\rangle$ as,

$$u : \hat{\alpha} |a, i, n\rangle \rightarrow \sum_{j=1}^{d_a} (\rho_a^*(\alpha^{-1} u \alpha))_{ji} \hat{\alpha} |a, i, n\rangle$$

$$u : \hat{\gamma} |a, i, n\rangle \rightarrow \sum_{j=1}^{d_a} (\rho_a^*(\gamma^{-1} u \gamma))_{ji} \hat{\gamma} |a, i, n\rangle$$

$$u : \hat{\pi} |a, i, n\rangle \rightarrow \sum_{j=1}^{d_a} (\rho_a(\pi^{-1} u \pi))_{ji} \hat{\pi} |a, i, n\rangle .$$

Asking whether a local time-reversal, charge-conjugation or chiral symmetry exists in $\mathcal{H}_a$, is then the question of whether for a basis state $|a, i, n\rangle$ its copy under either α, γ or π as appriopriate is included in $\mathcal{H}_a$. Based on $\mathcal{H}_a$ containing all basis states transforming under an irreducible representations equivalent to ρ_a, this is then the question of whether $\bar{\rho}_a = \rho_a^*(\alpha^{-1} u \alpha)$, $\hat{\rho}_a = \rho_a^*(\gamma^{-1} u \gamma)$ and $\tilde{\rho}_a = \rho_a(\pi^{-1} u \pi)$ are equivalent to ρ_a. This can be solved using the Altland-Zirnbauer class of the corepresentation generated by ρ_a, using Theorem 2.3.11, [24]:

Theorem 3.1.19. *Let $\mathcal{Q}$ be a quantum system with extended symmetry group G, and corepresentation $\mathcal{R}$ on the Hilbert space $\mathcal{H}$. Let the symmetry decomposed basis be taken for $\mathcal{Q}$, so that $\mathcal{R} = \bigoplus_a \bigoplus_{n=1}^{s_a} \rho_a$ as a representation of U on $\mathcal{H} = \bigoplus_a \mathcal{H}_a$ with basis states $|a, i, n\rangle$. Let each irreducible representation ρ_a generate a corepresentation of G as $\mathcal{R}_a$. Then a local symmetry group*

G_a can be defined on $\mathcal{H}_a$. As an unextended group, then $G_a \subseteq \{\mathbb{I}, \alpha_a, \gamma_a, \pi_a\}$ where α_a, γ_a and π_a are local time-reversal, charge-conjugation and chiral symmetries according to the inclusion rules:

- $\alpha_a \in G_a$ if and only if $\alpha \ket{a, i, n} \in \mathcal{H}_a \Leftrightarrow \bar{\rho}_a \cong \rho$ which occurs if $\mathcal{R}_a$ is of Altland-Zirnbauer class AI, AII, BDI, CII, CI or DIII.

- $\gamma_a \in G_a$ if and only if $\gamma \ket{a, i, n} \in \mathcal{H}_a \Leftrightarrow \hat{\rho}_a \cong \rho$ which occurs if $\mathcal{R}_a$ is of Altland-Zirnbauer class C, D, BDI, CII, CI or DIII.

- $\pi_a \in G_a$ if and only if $\pi \ket{a, i, n} \in \mathcal{H}_a \Leftrightarrow \tilde{\rho}_a \cong \rho$ which occurs if $\mathcal{R}_a$ is of Altland-Zirnbauer class AIII, BDI, CII, CI or DIII.

There are two things to note here. Firstly, while it is possible to 'kill' certain types of symmetry so that $A \neq \emptyset$ but $\alpha_a \notin G_a$ for example, it is not possible to create new forms of symmetry in the subsystem if a form of it didn't exist on the larger system. That is, there are the rules $A = \emptyset \Rightarrow \alpha_a \notin G_a$, $C = \emptyset \Rightarrow \gamma_a \notin G_a$ and $P = \emptyset \Rightarrow \pi_a \notin G_a$ on the form of G_a.

Secondly, if there is a generalised time-reversal, generalised charge-conjugation or generalised chiral symmetry that is killed in going to the subspace, this instead causes spectral degeneracies, [24]. That is, for a killed generalised time-reversal symmetry α, $\rho_a \not\cong \bar{\rho}_a$, so there exists a second subspace $\mathcal{H}_{\bar{a}}$ generated by $\bar{\rho}_a$ so that $\alpha : \mathcal{H}_a \to \mathcal{H}_{\bar{a}}$. As α will act as a time-reversal in $\mathcal{H}_a$, it can't change the spectrum when shifting to $\mathcal{H}_{\bar{a}}$, so there is a degeneracy created with $\{E_i\}_a = \{E_i\}_{\bar{a}}$. Similarly, a killed generalised charge-conjugation symmetry γ will have the subspace $\mathcal{H}_{\hat{a}}$ generated by $\hat{\rho}_a$, $\gamma : \mathcal{H}_a \to \mathcal{H}_{\hat{a}}$ acting as the charge-conjugation operator so that $\{E_i\}_a = \{-E_i\}_{\hat{a}}$. Finally, a killed generalised chiral symmetry π will have the subspace $\mathcal{H}_{\tilde{a}}$ generated by $\tilde{\rho}_a$, $\pi : \mathcal{H}_a \to \mathcal{H}_{\tilde{a}}$ acting as the chiral operator so that $\{E_i\}_a = \{-E_i\}_{\tilde{a}}$.

We move on to considering the forms of the lifts of the elements α_a, γ_a and π_a of G_a as operators - which, given the lack of unitary symmetries in the subspace will be the local time-reversal, charge-conjugation and chiral operators $\hat{\mathcal{T}}_a$, $\hat{\mathcal{C}}_a$ and $\hat{\mathcal{P}}_a$ in the subspace $\mathcal{H}_a$ respectively. Finding explicit expressions for their forms will require recognising $\mathcal{H}_a$ as isomorphic to the kernel space, $\mathcal{H}_a^K$, [11, 24, 110]. The kernel space is defined out of the relation in Equation 3.14 that the dimension d_a states $\ket{\psi_{a,i}} \in \mathcal{H}_a$ for $1 \leq i \leq d_a$ satisfy the action of $\mathcal{R}$ being equivalent to the action ρ_a in the basis,

$$\mathcal{R}(u) \ket{\psi_{a,i}} = \sum_{j=1}^{d_a} (\rho_a(u))_{ji} \ket{\psi_{a,j}}.$$

Forming the vector $\ket{\Psi_a}$ out of the individual $\ket{\psi_{a,i}}$ by stacking them vertically on top of each other,

$$\ket{\Psi_a} = \sum_{1 \leq j \leq d_a} \ket{e_j} \otimes \ket{\psi_{a,j}} = \left(\ket{\psi_{a,1}} \quad \dots \quad \ket{\psi_{a,d_a}} \right)^T$$

then if the dimension of $\mathcal{R}$ is d_r, the state $\ket{\Psi_a}$ must satisfy

$$\left(\mathbb{I}_{d_a} \otimes \mathcal{R}(u) - \rho_a^T(u) \otimes \mathbb{I}_{d_r} \right) \ket{\Psi_a} = 0 \qquad \forall u \in U.$$

This is equivalent to the relation that

$$|\Psi_a\rangle \in \bigcap_{u \in U} \ker \left(\mathbb{I}_{d_a} \otimes \mathcal{R}(u) - \rho_a^T(u) \otimes \mathbb{I}_{d_r} \right) = \mathcal{H}_a^K.$$

If a representation ρ_a has multiplicity s_a in $\mathcal{R}$, then $\mathcal{H}_a^K$ will then have dimension s_a, and as three quantum numbers a, i and n were needed to label a state previously, another quantum number n will need to be added here, so that $|\Psi_{a,n}\rangle$ for $1 \leq n \leq s_a$ then refers to the state related to the nth degenerate copy of ρ_a.

The kernel space is useful as it allows expressions on $\mathcal{H}$ using a map from $\mathcal{R}$ to be converted into a map on the subspace by using the relation $u : |\Psi_{a,n}\rangle \rightarrow (\mathbb{I}_{d_a} \otimes \mathcal{R}(u)) |\Psi_{a,n}\rangle = \left(\rho_a^T(u) \otimes \mathbb{I}_{d_r} \right) |\Psi_{a,n}\rangle$. In particular, there are the relations on the squares of the generalised time-reversal, generalised charge-conjugation and generalised chiral symmetries so that

$$\alpha^2 : |\Psi_{a,n}\rangle \rightarrow \left(\mathbb{I}_{d_a} \otimes \mathcal{R}(\alpha^2) \right) |\Psi_{a,n}\rangle = \left(\rho_a^T(\alpha^2) \otimes \mathbb{I}_{d_r} \right) |\Psi_{a,n}\rangle$$

$$\gamma^2 : |\Psi_{a,n}\rangle \rightarrow \left(\mathbb{I}_{d_a} \otimes \mathcal{R}(\gamma^2) \right) |\Psi_{a,n}\rangle = \left(\rho_a^T(\gamma^2) \otimes \mathbb{I}_{d_r} \right) |\Psi_{a,n}\rangle$$

$$\pi^2 : |\Psi_{a,n}\rangle \rightarrow \left(\mathbb{I}_{d_a} \otimes \mathcal{R}(\pi^2) \right) |\Psi_{a,n}\rangle = \left(\rho_a^T(\pi^2) \otimes \mathbb{I}_{d_r} \right) |\Psi_{a,n}\rangle$$

which will be essential to testing the squares of the local time-reversal and local charge-conjugation symmetries.

The local time-reversal, charge-conjugation and chiral symmetry operators can then be defined in the kernel space, [24]:

Theorem 3.1.20. *Let* $G = U \cup \alpha U \cup_\gamma U \cup \pi U$ *be a general* $Z_2 \times Z_2$*-graded group with corepresentation* $\mathcal{R}$ *on the Hilbert space* $\mathcal{H}$ *with the decomposition of* $\mathcal{R}(u) = \bigoplus_a \bigoplus_{n=1}^{s_a} \rho_a(u)$ *as a representation. Let* $\mathcal{H} = \bigoplus_a \mathcal{H}_a^K$ *be the decomposition into the kernel spaces of the Hilbert space. Let* $\hat{\alpha}$, $\hat{\gamma}$ *and* $\hat{\pi}$ *be the global generalised time-reversal, generalised charge-conjugation and generalised chiral symmetry operators. Then there are potential local time-reversal, charge-conjugation and chiral symmetries* $\hat{\mathcal{T}}_a$, $\hat{\mathcal{C}}_a$ *and* $\hat{\mathcal{P}}_a$ *in the subspace* $\mathcal{H}_a^K$ *which are given by,*

$$\hat{\mathcal{T}}_a = \begin{cases} S_{a,\alpha} \otimes \hat{\alpha} & \rho_a(u) = S_{a,\alpha} \rho^*(\alpha^{-1} u \alpha) S_{a,\alpha}^{-1} \\ \nexists \hat{\mathcal{T}}_a \text{ as a symmetry} & otherwise \end{cases}$$

$$\hat{\mathcal{C}}_a = \begin{cases} S_{a,\gamma} \otimes \hat{\gamma} & \rho_a(u) = S_{a,\gamma} \rho^*(\gamma^{-1} u \gamma) S_{a,\alpha}^{-1} \\ \nexists \hat{\mathcal{C}}_a \text{ as a symmetry} & otherwise \end{cases}$$

$$\hat{\mathcal{P}}_a = \begin{cases} S_{a,\pi} \otimes \hat{\pi} & \rho_a(u) = S_{a,\pi} \rho(\pi^{-1} u \alpha) S_{a,\pi}^{-1} \\ \nexists \hat{\mathcal{P}}_a \text{ as a symmetry} & otherwise \end{cases}$$

This also allows us to test the squares of $\hat{\mathcal{T}}_a$, $\hat{\mathcal{C}}_a$ and $\hat{\mathcal{P}}_a$, and show that the Altland-Zirnbauer class they predict in the subspace $\mathcal{H}_a^K$ is the same as the Altland-Zirnbauer class of the corepresentation generated by the irreducible representation ρ_a by any of the methods in Section 2.3.1.

This ensures that the classification of the subspaces is consistent in all methods of calculation, [24]:

Theorem 3.1.21. *Let $G = U \cup \alpha U \cup_\gamma U \cup \pi U$ be a general $Z_2 \times Z_2$-graded group with corepresentation $\mathcal{R}$ on the Hilbert space $\mathcal{H}$ with the decomposition of $\mathcal{R}(u) = \bigoplus_a \bigoplus_{n=1}^{s_a} \rho_a(u)$ as a representation. Let $\mathcal{H} = \bigoplus_a \mathcal{H}_a^K$ be the decomposition into the kernel spaces of the Hilbert space. Let $G_a \subseteq \{\mathbb{I}, \alpha_a, \gamma_a, \pi_a\}$ be the local unexteneded symmetry group on the subspace $\mathcal{H}_a^K$, whose elements give local time-reversal, charge-conjugation and chiral symmetry operators $\hat{\mathcal{T}}_a$, $\hat{\mathcal{C}}_a$ and $\hat{\mathcal{P}}_a$. Then the classification of the subspace according to the Altland-Zirnbauer Tenfold Way is the same regardless whether it is calculated using the existence of $\hat{\mathcal{T}}_a$, $\hat{\mathcal{C}}_a$ and $\hat{\mathcal{P}}_a$ as symmetry operators and the sign of the squares of $\hat{\mathcal{T}}_a$, $\hat{\mathcal{C}}_a$; or by the classification of the corepresentation $\mathcal{R}_a$ generated by the irreducible representation ρ_a generating $\mathcal{H}_a^K$. That is, the following hold:*

$$
\hat{\mathcal{T}}_a^2 = \begin{cases}
\mathbb{I} & FSI_A(\rho_a) = 1, & \begin{aligned} \rho_a(u) &= S_{a,\alpha}\rho^*(\alpha^{-1}u\alpha)S_{a,\alpha}^{-1}, \\ S_{a,\alpha}S_{a,\alpha}^* &= \rho(\alpha^2) \end{aligned} \\[2ex]
-\mathbb{I} & FSI_A(\rho_a) = -1, & \begin{aligned} \rho_a(u) &= S_{a,\alpha}\rho^*(\alpha^{-1}u\alpha)S_{a,\alpha}^{-1}, \\ S_{a,\alpha}S_{a,\alpha}^* &= -\rho(\alpha^2) \end{aligned} \\[2ex]
\hat{\mathcal{T}}_a \text{ is not a symmetry} & FSI_A(\rho_a) = 0
\end{cases}
$$

$$
\hat{\mathcal{C}}_a^2 = \begin{cases}
\mathbb{I} & FSI_C(\rho_a) = 1, & \begin{aligned} \rho_a(u) &= S_{a,\gamma}\rho^*(\gamma^{-1}u\gamma)S_{a,\gamma}^{-1}, \\ S_{a,\gamma}S_{a,\gamma}^* &= \rho(\gamma^2) \end{aligned} \\[2ex]
-\mathbb{I} & FSI_C(\rho_a) = -1, & \begin{aligned} \rho_a(u) &= S_{a,\gamma}\rho^*(\gamma^{-1}u\gamma)S_{a,\gamma}^{-1}, \\ S_{a,\gamma}S_{a,\gamma}^* &= -\rho(\gamma^2) \end{aligned} \\[2ex]
\hat{\mathcal{C}}_a \text{ is not a symmetry} & FSI_C(\rho_a) = 0
\end{cases}
$$

$$
\hat{\mathcal{P}}_a \text{ is a symmetry} \Leftrightarrow Ind_P(\rho_a) = 1 \Leftrightarrow \rho_a(u) = S_{a,\pi}\rho(\pi^{-1}u\pi)S_{a,\pi}^{-1}
$$

Proof. Having shown that $\hat{\mathcal{T}}_a$, $\hat{\mathcal{C}}_a$ and $\hat{\mathcal{P}}_a$ exist as symmetries according to the Altland-Zirnbauer corepresentation class of ρ_a in the previous theorem, it is sufficient to prove that when $\hat{\mathcal{T}}_a$ is a symmetry it squares according to $\hat{\mathcal{T}}_a^2 = \pm\mathbb{I} \Leftrightarrow S_{a,\alpha}S_{a,\alpha}^* = \pm\rho(\alpha^2)$ and that when $\hat{\mathcal{C}}_a$ is a symmetry it squares according to $\hat{\mathcal{C}}_a^2 = \pm\mathbb{I} \Leftrightarrow S_{a,\gamma}S_{a,\gamma}^* = \pm\rho(\gamma^2)$. These can be calculated directly by their action on the state $|\Psi_{a,n}\rangle$.

Firstly for $\hat{\mathcal{T}}_a$,

$$
\begin{aligned}
\hat{\mathcal{T}}_a^2 |\Psi_{a,n}\rangle &= (S_{a,\alpha}^* \otimes \hat{\alpha})(S_{a,\alpha}^* \otimes \hat{\alpha}) |\Psi_{a,n}\rangle \\
&= (S_{a,\alpha}^* S_{a,\alpha} \otimes \hat{\alpha}^2) |\Psi_{a,n}\rangle \\
&= (S_{a,\alpha}^* S_{a,\alpha} \otimes \mathbb{I}_{d_r})(\mathbb{I}_{d_a} \otimes \mathcal{R}(\alpha^2)) |\Psi_{a,n}\rangle \\
&= (S_{a,\alpha}^* S_{a,\alpha} \otimes \mathbb{I}_{d_r})(\rho_a^T(\alpha^2) \otimes \mathbb{I}_{d_r}) |\Psi_{a,n}\rangle \\
&= (S_{a,\alpha}S_{a,\alpha}^* \rho_a^{-1}(\alpha^2) \otimes \mathbb{I}_{d_r}) |\Psi_{a,n}\rangle
\end{aligned}
$$

which gives the required relation when $S_{a,\alpha}S_{a,\alpha}^* = \pm\rho_a(\alpha^2)$ is substituted in.

Equivalently for $\hat{\mathcal{C}}_a$,

$$\begin{aligned}
\hat{\mathcal{C}}_a^2 \left| \Psi_{a,n} \right\rangle &= (S_{a,\gamma}^* \otimes \hat{\gamma})(S_{a,\gamma}^* \otimes \hat{\gamma}) \left| \Psi_{a,n} \right\rangle \\
&= (S_{a,\gamma}^* S_{a,\gamma} \otimes \hat{\gamma}^2) \left| \Psi_{a,n} \right\rangle \\
&= (S_{a,\gamma}^* S_{a,\gamma} \otimes \mathbb{I}_{d_r})(\mathbb{I}_{d_a} \otimes \mathcal{R}(\gamma^2)) \left| \Psi_{a,n} \right\rangle \\
&= (S_{a,\gamma}^* S_{a,\gamma} \otimes \mathbb{I}_{d_r})(\rho_a^T(\gamma^2) \otimes \mathbb{I}_{d_r}) \left| \Psi_{a,n} \right\rangle \\
&= (S_{a,\gamma} S_{a,\gamma}^* \rho_a^{-1}(\gamma^2) \otimes \mathbb{I}_{d_r}) \left| \Psi_{a,n} \right\rangle
\end{aligned}$$

which gives the required relation when $S_{a,\gamma} S_{a,\gamma}^* = \pm \rho_a(\gamma^2)$ is substituted in. $\qquad\square$

This means that the link between the spectral statistics of a general quantum system symmetric under a $Z_2 \times Z_2$-graded group, and random matrix theory can now be given by applying the results from Theorem 3.1.17 for the case with trivial U to each of the subspaces individually, [11, 24]:

Theorem 3.1.22. *Let $\mathcal{Q}$ be a quantum system with the extended symmetry group $G = U \cup \alpha U \cup \gamma U \cup \pi U$. Let $U > \{\mathbb{I}\}$ contain non-trivial elements. Let the action of G on the Hilbert space be given by the corepresentation $\mathcal{R} : G \to \mathbf{Aut}_{\mathrm{qtm}}(\mathcal{H})$. Let $\mathcal{R}(u) = \bigoplus_a \bigoplus_{n=1}^{s_a} \rho_a(u)$ be the irreducible representation decomposition of $\mathcal{R}$ as a representation of U on $\mathcal{H}$. Then the following occur:*

- *$\mathcal{H} = \bigoplus_a \mathcal{H}_a^K$, the Hilbert space decomposes into a series of kernel spaces, with one subspace $\mathcal{H}_a^K$ for each unique irreducible representation ρ_a of U in the decomposition of $\mathcal{R}$.*

- *$\{E_i\} = \bigcup_a \{E_i\}_a$, the energy level spectrum decomposes into a series of independent subspectra, with one subspectrum $\{E_i\}_a$ for each unique irreducible representation ρ_a of U in the decomposition of $\mathcal{R}$.*

- *$\hat{H} = \bigoplus \hat{H}_a$, the Hamiltonian block diagonalises, with one block $\hat{H}_a$ for each unique irreducible representation ρ_a of U in the decomposition of $\mathcal{R}$. This sub-Hamiltonian $\hat{H}_a$ has a structure taken from Table 3.3, with the structure dictated only by the Altland-Zirnbauer class of the corepresentation $\mathcal{R}_a$ generated by ρ_a.*

Once it is known that the system fulfils the conditions to be compared with random matrix statistics, as discussed in the section below, this is what leads to the standard result that either the independent subspectra in a system with non-trivial unitary symmetries match random matrix statistics; or equating the subpectra to the spectrum of the desymmetrised system, that the spectrum of the desymmetrised system matches random matrix statistics.

We note the importance of the dependence of random matrix statistics' dependence on G_a and not G directly. Due to this, and the process of transferring the operators $\hat{\alpha}$, $\hat{\gamma}$ and $\hat{\pi}$ as $\hat{\mathcal{T}}_a$, $\hat{\mathcal{C}}_a$ and $\hat{\mathcal{P}}_a$ with the opportunity to either kill symmetries, or convert them to have the opposite sign when squared then, though a system may globally have, for example, a bosonic $\hat{\mathcal{T}}^2 = \mathbb{I}$ time-reversal symmetry, with the right choice of symmetry group G, it is possible that the subspaces could display fermionic $\hat{\mathcal{T}}_a^2 = -\mathbb{I}$ time-reversal symmetry, or even no time-reversal symmetry at all, and similarly for $\hat{\mathcal{C}}$ and $\hat{\mathcal{P}}$. This is something that has already been explored - Leyvraz, Schmit and

Class	$\hat{H}_a$	Class	$\hat{H}_a$
A		$AIII$	$= \begin{pmatrix} 0 & h \\ h^\dagger & 0 \end{pmatrix}$
AI	$\in \mathbb{R}$	BDI	$= \begin{pmatrix} 0 & h \\ h^T & 0 \end{pmatrix}, h = h^*$
AII	$= \begin{pmatrix} h_1 & h_2 \\ -h_2^* & h_1^* \end{pmatrix}$	CII	$= \begin{pmatrix} 0 & h \\ h^\dagger & 0 \end{pmatrix}, h = \begin{pmatrix} k_1 & k_2 \\ -k_2^* & k_1^* \end{pmatrix}$
C	$= \begin{pmatrix} h_1 & h_2 \\ -h_2^* & h_1^* \end{pmatrix}$	CI	$= \begin{pmatrix} 0 & h \\ h^* & 0 \end{pmatrix}, h^T = h$
D	$= \begin{pmatrix} h_1 & h_2 \\ -h_2^* & -h_1^T \end{pmatrix}, h_1 = h_1^\dagger, h_2 = -h_2^T$	$DIII$	$= \begin{pmatrix} 0 & h \\ -h^* & 0 \end{pmatrix}, h^T = -h$

Table 3.3: Canonical structure on the sub-Hamiltonian associated to the subspace $\mathcal{H}_a^K$ generated by the representation ρ_a according to the Altland-Zirnbauer class of the corepresentation $\mathcal{R}_a$ generated by ρ_a, [1, 24, 39, 156].

Seligman, [109], demonstrated that a billiard with a global $\hat{\mathcal{T}}^2 = \mathbb{I}$ symmetry and with a $U = Z_3$ geometric symmetry had a class A sub-spectrum, while Joyner, Müller and Sieber, [92], showed that a quantum graph with $U = Q_8$, $G = U \times Z_2$ system with bosonic time-reversal had a class AII sub-spectrum. However it has only been used in the context of $\hat{\mathcal{T}}$ and not $\hat{\mathcal{C}}$.

The primary aim of this work is to exploit methodology derived from [92] to demonstrate methods of algorithmically generating a system with any Altland-Zirnbauer class of sub-spectrum having been given a fixed form of $\hat{\mathcal{T}}$ and $\hat{\mathcal{C}}$ as the global time-reversal and charge-conjugation operators. Understanding how these subspaces are created out of a unitary symmetry group, and knowing how to predict the structure of $\hat{H}_a$ - and thus the random matrix statistics the subspace will conform to when this prediction is valid - this is now a question of finding specific graded groups G with the right properties to generate each subspace, which will be covered in Chapter 5, and considering when the random matrix prediction is valid to be applied, which is what is considered now.

3.2 Classical Chaos and Quantum Implications

It was discussed at the end of Appendix C how quantum mechanics can be derived by taking classical mechanics and then substituting operators for variables, and commutators for Poisson brackets. This means that each Hamiltonian quantum systems has a classical analogue, which should be recoverable in the classical limit of $\hbar \to 0$ or $E \to \infty$ per the correspondence principle; this in turn causes the natural question of whether special behaviour on the classical level carries over in any way to the quantum version, or if it doesn't, how this behaviour reappears when the classical limit is reached in the system.

One of the major behaviours under consideration is the separation on the classical side of integrable systems and chaotic systems. Integrable systems are characterised by having trajectories which are regular in the phase space; that are encased in a subset of the full phase space; and where trajectories with close initial conditions remain close throughout their path. Chaotic

systems on the other hand, have trajectories which cover the full phase space; and initially close trajectories diverge rapidly.

On the quantum side, it is not possible to accurately define a phase-space for the system or even a trajectory, [73]. This is because in the quantum setup, positions and momenta are probabilistic and the uncertainty principle excludes knowing precise information about both - which is required for defining these quantities. Furthermore, without the ability to consider trajectories in the quantum picture, any properties based on them become meaningless - including the trajectory-based definition of classical chaos. Thus a direct correspondence between classical chaos and a quantum version is not possible. However, quantitative work, [25], has seen that there are commonalities shared in the behaviour of quantum systems with classical equivalents that are chaotic, and which aren't present in the systems with integrable analogues. Here we give an overview of the types of systems which show what is known as 'quantum chaos', [157], and their universal behaviour, for more detailed discussions see [35, 70, 71, 73, 115, 157, 170].

First, we introduce some concepts necessary to define a form of classical chaos, [35, 61, 118]. Hyperbolicity is first:

Definition 3.2.1. *Let $\mathcal{C}$ be a classical system with Hamiltonian $\hat{H} = H$. Let $\mathbf{X} = (\, \mathbf{p} \ \mathbf{q} \,)^T$ be the position in the phase space $\mathcal{M}$, with the dynamical system described by the first order set of differential equations $\dot{\mathbf{X}} = \mathbf{F}(\mathbf{X})$. Trajectories in this phase space may be described by an initial condition $\mathbf{X}_0$ and the flow function, $\mathbf{\Phi}^t$, so the position in phase space at time t is $\mathbf{X}_t = \mathbf{\Phi}^t(\mathbf{X}_0)$, describing the time-evolution of the trajectory.*

Then, if $\delta\mathbf{X}_0$ describes a small deviation in the starting point of the trajectory, the time-evolution of this deviation along the trajectory may be linearly approximated by,

$$\delta\dot{\mathbf{X}} = \frac{\partial\mathbf{F}(\mathbf{X})}{\partial\mathbf{X}} \cdot \delta\mathbf{X} \;\Rightarrow\; \delta\mathbf{X}_t = \frac{\partial\mathbf{\Phi}^t(\mathbf{X}_0)}{\partial\mathbf{X}_0} \cdot \delta\mathbf{X}_0 = M(t, \mathbf{X}_0)\delta\mathbf{X}_0$$

where $M(t, \mathbf{X}_0)$ is a matrix given by the time ordered exponential,

$$M(t, \mathbf{X}_0) = \mathbb{T}\exp\int_0^t \frac{\partial\mathbf{F}}{\partial\mathbf{X}}d\tau.$$

The vectors $\delta\mathbf{X}_t$ and $\delta\mathbf{X}_0$ sit in the vector space which is tangent to the phase space at each point $\mathbf{X}$, $\mathcal{TM}(\mathbf{X})$. Furthermore, a general vector $\mathbf{v} \in \mathcal{TM}(\mathbf{X})$ in the tangent space has a Lyapnov exponent given by,

$$\lambda(\mathbf{X}, \mathbf{v}) = \lim_{t\to\infty} \frac{1}{t}\ln|M(t, \mathbf{X})\mathbf{v}|.$$

It is stable if $\lambda(\mathbf{X}, \mathbf{v}) < 0$, neutral if $\lambda(\mathbf{X}, \mathbf{v}) = 0$ and unstable if $\lambda(\mathbf{X}, \mathbf{v}) > 0$.

An invariant subset $\mathcal{I} \in \mathcal{M}$ of the phase space is then hyperbolic if:

- *For all points $\mathbf{X}$ in $\mathcal{I}$, the tangent space at $\mathbf{X}$, $\mathcal{TM}(\mathbf{X})$ decomposes into subspaces according to whether the vectors in them are stable, neutral or unstable,*

$$\mathcal{TM}(\mathbf{X}) = \mathcal{S}_S \oplus \mathcal{S}_N \oplus \mathcal{S}_U = \mathcal{S}_S \oplus ()\mathbf{F}(\mathbf{X}) \oplus \mathcal{S}_U$$

  so that the only neutral vectors lie in the direction of the flow.

- *There exists a positive constant κ and a positive function $C(\mathbf{X}, \mathbf{X}')$ such that for each $\mathbf{e}_s \in \mathcal{S}_S$ and $\mathbf{e}_u \in \mathcal{S}_U$, and for all $t \geq 0$,*

$$|M(t, \mathbf{X})\mathbf{e}_s| \leq C(\mathbf{X}\mathbf{\Phi}^t\mathbf{X})^{-1} \exp(-\kappa t)|\mathbf{e}_s|$$
$$|M(t, \mathbf{X})\mathbf{e}_u| \geq C(\mathbf{X}\mathbf{\Phi}^t\mathbf{X}) \exp(\kappa t)|\mathbf{e}_u|$$
$$\gamma(\mathbf{\Phi}^t\mathbf{X}) \geq C(\mathbf{X}\mathbf{\Phi}^t\mathbf{X})\gamma(\mathbf{X})$$

where $\gamma(\mathbf{X})$ is the angle between the stable and unstable subspaces.

The Lyaponov exponent helps describe the speed at which $\delta\mathbf{X}$ grows in time; having $\lambda > 0$ means that $\delta\mathbf{X}$ grows as $t \to \infty$. This provides the requirement for trajectories to diverge rapidly, given a small difference in their initial conditions.

Ergodicity then makes sure the phase space is covered sufficiently well:

Definition 3.2.2. *Let $\mathcal{C}$ be a classical system. It is ergodic if for all observables $F(\mathbf{q}, \mathbf{p})$ on a trajectory through the phase space, the time average of F is equal to the average of F calculated over an energy shell,*

$$\lim_{T \to \infty} \frac{1}{T} \int_0^T F(\mathbf{q}(t), \mathbf{p}(t))dt = \int \frac{d\mu(\mathbf{q}, \mathbf{p})}{\Omega} F(\mathbf{q}, \mathbf{p}),$$
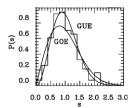
where $d\mu(\mathbf{q}, \mathbf{p})/\Omega$ is the Liouville measure; $d\mu(\mathbf{q}, \mathbf{p}) = d\mathbf{q}d\mathbf{p}\delta(H(\mathbf{q}, \mathbf{p}) - E)$ and $\Omega = \int d\mu(\mathbf{q}, \mathbf{p})$.

Definition 3.2.3. *Let $\mathcal{C}$ be a classical system. It fulfils the weakest form of chaos if it is hyperbolic and ergodic.*
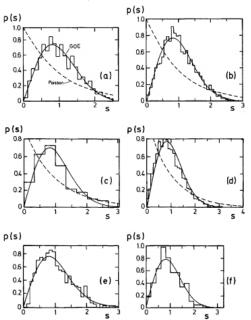
This is one definition of chaos, there are in fact many 'levels' of chaos which have different strengths of requirement, [71, 127], and there is much discussion over what level of chaos is required for the BGS-conjecture, [25, 154].

Quantitative study has considered a number of chaotic systems, either experimentally, [25, 45, 80, 107, 108, 128, 131, 134, 153, 158, 178] or numerically, [36, 92, 97, 141]. In each of these cases, when the energy level spectra for these systems is plotted a universal behaviour is found, namely that the energy levels repel each other, and the probability to find two levels close together is small when compared to that given by the Poissonian distribution which describes the energy level statistics of an integrable system according to the Berry-Tabor conjecture, [22]. This is demonstrated in Figure 3.3 by plotting the probability for two consecutive energy levels to be separated by a distance $s = E_{i+1} - E_i$, showing that once normalised to have a mean of $s = 1$, then there is a very low possibility to have $s \approx 0$.
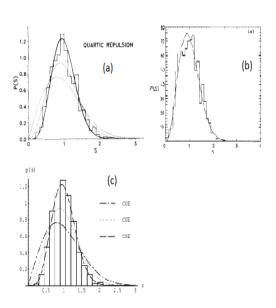
The combined work of Wigner and Dyson, and Bohigas, Giannoni and Schmidt, [25, 51, 175], posits that generic chaotic quantum systems display these universal behaviours, and they occur because over an ensemble of similar systems, the Hamiltonians are statistically distributed according to one of three random matrix ensembles - the Gaussian Unitary Ensemble or GUE; the Gaussian Orthogonal Ensemble or GOE; and the Gaussian Symplectic Ensemble or GSE. Matching the universality of the statistical behaviour, the exact ensemble a system's statistics matches can't depend on the method used in the lab to implement the system, or any of the choices of parameters such as size or material, but an over-arching property of them - this is seen to be the behaviour of the system under its time-reversal operator, $\hat{\mathcal{T}}$.

(a) Spacing distribution for a system with a broken time-reversal symmetry, demonstrating universal behaviour corresponding to the GUE ensemble. The system considered is a microwave cavity implementation of the LSS billiard, [44].

(b) Spacing distribution for systems with a $\hat{\mathcal{T}}^2 = \mathbb{I}$ symmetry, demonstrating universal behaviour corresponding to the GOE ensemble. The systems considered are the Sinai billiard, [25], (a); the Hydrogen atom in a magnetic field, [80], (b); excitations of the NO2 molecule, [178], (c); acoustic resonances of a Sinai-billiard shaped quartz block, [128], (d); chaotic microwave cavity, [45], (e); and a quarter-stadium billiard vibrating plate, [108], (f). Picture from [157].

(c) Spacing distribution for systems with a $\hat{\mathcal{T}}^2 = -\mathbb{I}$ symmetry, demonstrating universal behaviour corresponding to the GSE ensemble. The systems considered are a Hamiltonian with quartic potential, [36], (a); the spin-1/2 kicked top, [141]; and the spin-1/2 quantum cat map, [97], (c) - which is described as CSE, but is equivalent to the GSE ensemble.

Figure 3.3: The probability distribution for the distance between consecutive energy levels for several systems in either the three universality classes of GUE, GOE and GSE. Note how in each case the probability for close levels is small - this is the level repulsion that occurs in all the spectra of chaotic quantum systems.

Class	Ensemble	$\hat{\mathcal{T}}^2$	$\hat{\mathcal{C}}^2$	$\hat{\mathcal{P}} \in G$	Class	Ensemble	$\hat{\mathcal{T}}^2$	$\hat{\mathcal{C}}^2$	$\hat{\mathcal{P}} \in G$
A	GUE	$\hat{\mathcal{T}} \notin G$	$\hat{\mathcal{C}} \notin G$	No	AIII	chGUE	$\hat{\mathcal{T}} \notin G$	$\hat{\mathcal{C}} \notin G$	Yes
AI	GOE	$\mathbb{I}$	$\hat{\mathcal{C}} \notin G$	No	BDI	chGOE	$\mathbb{I}$	$\mathbb{I}$	Yes
AII	GSE	$-\mathbb{I}$	$\hat{\mathcal{C}} \notin G$	No	CII	chGSE	$-\mathbb{I}$	$-\mathbb{I}$	Yes
C	AZ-C	$\hat{\mathcal{T}} \notin G$	$-\mathbb{I}$	No	CI	AZ-CI	$\mathbb{I}$	$-\mathbb{I}$	Yes
D	AZ-D	$\hat{\mathcal{T}} \notin G$	$\mathbb{I}$	No	DIII	AZ-DIII	$-\mathbb{I}$	$\mathbb{I}$	Yes

Table 3.4: The ten random matrix ensembles a Hermitian chaotic quantum system's statistics can match according to the form of G and the squares of $\hat{\mathcal{T}}$, $\hat{\mathcal{C}}$.

Conjecture 3.2.4 (BGS-conjecture). *Let $\mathcal{Q}$ be a generic quantum system corresponding to a classical system that is chaotic. Let $\mathcal{Q}$ be symmetric under at most a time-reversal operator $\hat{\mathcal{T}}$. Then the energy level spectrum has statistics identical to the GUE random matrix ensemble if $\mathcal{Q}$ is not symmetric under $\hat{\mathcal{T}}$; the GOE ensemble if $\mathcal{Q}$ is symmetric under $\hat{\mathcal{T}}$ and $\hat{\mathcal{T}}^2 = \mathbb{I}$; and the GSE ensemble if $\mathcal{Q}$ is symmetric under $\hat{\mathcal{T}}$ and $\hat{\mathcal{T}}^2 = -\mathbb{I}$.*

There is no proof of this conjecture, however it is widely believed to hold - bar for a small set of counter examples such as the quantum star graph, [17] - and it has been supported by numerous numerical and experimental tests. Current work towards a proof is summarised in [70, 170], and a proof for the specific system of the quantum graph can be found in [62, 130, 159].

The proof that generic classically chaotic systems can be statistically modelled by a random matrix ensemble may not exist yet, but accepting that they take upon a statistical behaviour, then from the earlier parts of this chapter, it should be clear why the three ensembles are given by the behaviour of the system under time reversal - Theorem 3.1.17 describes how the Wigner-Dyson class of the Hilbert space restricts the form of the Hamiltonian to one of three types of matrices; the ensembles GUE, GOE and GSE merely consist of taking the random matrices fitting each of these restricted forms of Hamiltonian. This concept and the ensembles themselves will be discussed further in the next chapter.

With the addition of the allowance of systems to be symmetric under $\hat{\mathcal{C}}$ and $\hat{\mathcal{P}}$, [5, 6, 146, 166, 167], so the energy level spectrum is symmetric around 0, the universal behaviour of level repulsion between neighbouring energy levels remains, but an additional repulsion from a level E feeling its negative equivalent $-E$ is felt close to 0, modifying the density of states behaviour, [73, 85], and causing deviations away from the semi-circle distribution for $E \approx 0$. In this case, the BGS-conjecture is assumed to still hold, but is expanded to include an extra seven ensembles to account for the extra seven classes in Altland-Zirnbauer's classification of symmetry groups of the form $G \subseteq \left\{ \mathbb{I}, \hat{\mathcal{T}}, \hat{\mathcal{C}}, \hat{\mathcal{P}} \right\}$:

Conjecture 3.2.5. *Let $\mathcal{Q}$ be a generic quantum system corresponding to a classical system that is chaotic. Let $\mathcal{Q}$ be symmetric under a subset of operators from $\left\{ \hat{\mathcal{T}}, \hat{\mathcal{C}}, \hat{\mathcal{P}} \right\}$. Then the energy level statistics of $\mathcal{Q}$ are universal to the choice of subgroup of $G \subseteq \left\{ \mathbb{I}, \hat{\mathcal{T}}, \hat{\mathcal{C}}, \hat{\mathcal{P}} \right\}$ and the squares of $\hat{\mathcal{T}}$, $\hat{\mathcal{C}}$ if $\hat{\mathcal{T}}$, $\hat{\mathcal{C}}$ are in G, and correspond to the eigenvalue statistics of a random matrix ensemble given as in Table 3.4.*

A full description of the new ensembles will be given in the next chapter.

Again, there is strong numerical evidence for the conjecture holding, [24, 56, 64, 94], however experimental tests have been limited to only the classes AIII, BDI and CII for now, [136]. It is for this reason that we aim to find a set of systems which could be tested in the lab for each

of the remaining ensembles, to allow experimental testing of the BGS-conjecture for the rest of the Altland-Zirnbauer classes. This will not prove the conjecture, but it will provide further supporting evidence.

4. *Random Matrix Theory*

Given a quantum system and its Hamiltonian, a common question is to identify the energy level spectra $\{E_n\}$, or the set of eigenvalues of the Hamiltonian,

$$\hat{H}\,|\psi_n\rangle = E_n\,|\psi_n\rangle\,.$$

This is due to the fact that for many complicated systems, the energy level spectrum is one of the easiest measurements to make on the system, such as using neutron resonance spectroscopy to find the energy levels of heavy nuclei, [115]. However, despite the ease of the physical measurement in many of these systems, comparison to the theoretical prediction is difficult as the form of the Hamiltonian may only be approximable, or it may be entirely unknown.

This is the problem that physicists were faced with in the mid twentieth century. As discussed at the end of last chapter though, experimental data showed that for at least the set of systems whose classical analogues were chaotic, there were universal behaviours in the spectra - namely level repulsion - and it was theorized, [25], that when an ensemble of systems is taken, the statistics of $\hat{H}$ of would match the statistic of an appropriate ensemble of random matrices. Thus, while the exact spectra $\{E_n\}$ remains unknown, its statistical properties *are* derivable.

The motivation is thus: the Hamiltonian of a system must be a complex Hermitian matrix, and thus lies within the set $\mathfrak{h} = \left\{ H \in \mathbb{C}^{N \times N} \mid H = H^{\dagger} \right\}$ when expressed as a matrix. If a probability measure dH can be appropriately expressed on this set, then if the Hamiltonian isn't known, random drawing from $\mathfrak{h}$ must give a probability distribution $P(\hat{H})$ on the Hamiltonian for an ensemble of systems, the ensemble representing a collection of systems with the same structure but with randomly drawn parameters. If the statistics $P(\hat{H})$ are known, then the statistics of the energy level spectra can be derived to give a joint probability distribution $P(\{E_n\})$ for the spectra.

This is the generic case, where no further restrictions on the structure of $\hat{H}$ have been given, and by defining an entry

$$H = \begin{pmatrix} h_{11} & h_{12} & \dots & h_{1(N-1)} & h_{1N} \\ h_{12}^{*} & h_{22} & \dots & h_{2(N-1)} & h_{2N} \\ \vdots & \ddots & \ddots & \vdots & \vdots \\ h_{1N}^{*} & h_{2N}^{*} & \dots & h_{(N-1)N}^{*} & h_{NN} \end{pmatrix} \tag{4.1}$$

where h_{ij} for $j > i$ are $N^2/2 - N$ independent identically distributed complex Gaussian random variables and h_{ii} are N independent identically distributed real Gaussian random variables, [73],

and taking a suitable measure dH over the matrix space then the Gaussian Unitary Ensemble is defined, [70].

In the case where there is further structure on the system, expressed as a set $F = \{f_i\}$ of functions such that $f_i(\hat{H}) = 0$ then the set of possible Hamiltonians reduces to $\mathfrak{h}' = \left\{ H \in \mathbb{C}^{N \times N} \mid f_i(H) = 0 \; \forall f_i \in F, \; H = H^\dagger \right\} \subset \mathfrak{h}$. Given another measure dH, a new distribution $P(H)$ can be defined for the Hamiltonian and a new joint distribution $P(\{E_n\})$ for the energy level spectra.

This case is particularly applicable for systems with symmetry groups - Theorem 3.1.22 has already discussed how structure is imposed on $\hat{H}_a$ according to the Altland-Zirnbauer class of the corepresentation $\mathcal{R}_a$ generating $\mathcal{H}_a$. These ten classes now define ten ensembles of random matrices.

The first three ensembles, given by classes A,AI and AII, describe systems with at most time reversal symmetry, $\hat{\mathcal{T}} = \pm\mathbb{I}$, with the restriction set $F = \left\{ [\hat{\mathcal{T}}, \cdot] \right\}$. These were the first random matrix ensembles discovered by physicists, [50, 51, 172, 175], and are collected under the name of the Wigner-Dyson ensembles. They have been well discussed in the literature, [51, 73, 115], and will be considered in Section 4.1.

The next three ensembles are given by the classes AIII, BDI and CII which describe systems which have at either both time-reversal and charge-conjugation symmetry whose squares match, $\hat{\mathcal{T}}^2 = \hat{\mathcal{C}}^2 = \pm\mathbb{I}$ with $F = \left\{ [\hat{\mathcal{T}}, \cdot], \left\{ \hat{\mathcal{C}}, \cdot \right\} \right\}$ or who have only chiral symmetry, $F = \left\{ \left\{ \hat{\mathcal{P}}, \cdot \right\} \right\}$. These ensembles are known as the chiral ensembles and were introduced in [146, 166, 167] to explain the behaviour of the spectra of the QCD Dirac operator.

The final four ensembles were introduced by Altland and Zirnbauer to explain the spectral behaviour of particles in systems with a super-conducting region, [5, 6]. These four systems split into two types - the two ensembles generated by the classes C and D describe systems with at most charge-conjugation symmetry, $\hat{\mathcal{C}} = \pm\mathbb{I}$, $F = \left\{ \hat{\mathcal{C}}, \cdot \right\}$; while finally $DIII$ and CI generate ensembles where the restriction set is $F = \left\{ [\hat{\mathcal{T}}, \cdot], \left\{ \hat{\mathcal{C}}, \cdot \right\} \right\}$ with $\hat{\mathcal{T}}^2 = -\hat{\mathcal{C}}^2 = \pm\mathbb{I}$ so that while both time-reversal and charge-conjugation exist as symmetries, their squares have the opposite parity. Together, these four classes may be called the Andreev classes due to their applications to Andreev scattering, [64], or with the previous three ensembles are they are now collectively known as the additional seven Altland-Zirnbauer ensembles, [73], though Zirnbauer recognises that they introduced only four of the seven ensembles now commonly attributed to them, [180]. These seven ensembles are discussed in Section 4.2.

In the following sections, the properties of each random matrix ensemble will be discussed further, as well as methods of identifying which ensemble statistics an experiment's measured spectra is displaying. This will involve discussing key observable properties of the spectra including the nearest neighbour spacing of the eigenvalues, the probability distribution of the smallest eigenvalue and the local density of states around 0.

4.1 The Wigner-Dyson Ensembles

The Wigner-Dyson ensembles were introduced to describe the statistics of systems with at most time-reversal symmetry, [50, 51, 172, 175]. These are systems for which the symmetry group G

is not only Z_2-graded, $G = U \cup \alpha U$, but $G \subseteq \{\mathbb{I}, \alpha\}$. In this case, as the lift $\hat{\mathcal{T}}$ of α requires $[\hat{\mathcal{T}}, \hat{H}] = 0$ when α is a symmetry, $\hat{H}$ sits in the commutant of the corepresentation $\mathcal{R}$ of G acting on $\mathcal{H}$ by Definition 2.2.9. This was part of Theorem 3.1.16.

Knowing the allowed forms of the commutants of a Z_2-graded group from Theorem 2.2.11 and Table 2.1, this is the requirement that if the irreducible projective corepresentation $\mathcal{R}$ of G is of class A, AI or AII then $\hat{H} \in \mathbb{C}^{N \times N}, \mathbb{R}^{N \times N}$ or $\mathbb{H}^{N \times N}$ respectively; or by Theorem 3.1.17, the ensemble $\mathfrak{h}'$ is defined as the following sets:

Class of $\mathcal{R}$	$\mathfrak{h}'$	Ensemble Name
A	$\left\{ H \in \mathbb{C}^{N \times N} \mid H = H^\dagger \right\}$	Gaussian Unitary Ensemble (GUE)
AI	$\left\{ H \in \mathbb{C}^{N \times N} \mid H = H^*, H = H^T \right\}$	Gaussian Orthogonal Ensemble (GOE)
AII	$\left\{ H \in \mathbb{C}^{2M \times 2M} \middle| H = \begin{pmatrix} h_1 & h_2 \\ -h_2^* & h_1^* \end{pmatrix} \right\}$	Gaussian Symplectic Ensemble (GSE).

The ensembles themselves are named after the types of matrices which the set forming the ensemble $\mathfrak{h}'$ is invariant under conjugation by, [156],

$$GUE \quad \Rightarrow \forall U \in \mathcal{U}(N),\ H \in \mathfrak{h}' \quad U^{-1}HU \in \mathfrak{h}'$$

$$GOE \quad \Rightarrow \forall O \in \mathcal{O}(N),\ H \in \mathfrak{h}' \quad O^{-1}HO \in \mathfrak{h}'$$

$$GSE \quad \Rightarrow \forall S \in \mathrm{Sp}(N),\ H \in \mathfrak{h}' \quad S^{-1}HS \in \mathfrak{h}'$$

so that the GUE ensemble is invariant under conjugation by all unitary matrices; the GOE ensemble is invariant under conjugation by all orthogonal matrices; and the GSE ensemble is invariant under conjugation by all symplectic matrices.

The measure dH on $\mathfrak{h}'$ for each Wigner-Dyson ensemble can be derived from the decomposition $H = M^{-1}EM$ where $M \in \mathcal{U}(N)$ for the GUE ensemble; $M \in \mathcal{O}(N)$ for the GOE ensemble and $M \in Sp(N)$ for the GSE ensemble. The measure for H must then combine a measure over the eigenvalues E_i of H, and a measure over M. The measure is given by, [70],

$$dH = |\Delta(\{E_n\})|^\beta dE d\mu(U(N; \beta)), \qquad \beta = \begin{cases} 1 & GOE \\ 2 & GUE \\ 4 & GSE \end{cases}$$

where β is a parameter denoting which of the three ensembles is being considered, and which will occuer in several key places in later equations; $\Delta(\{E_n\})$ is the Vandermont determinant,

$$\Delta(\{x_n\}) = \prod_{k > l}(x_k - x_l);$$

and $d\mu(U(N; \beta))$ is the Haar measure over $SO(N)$ for $\beta = 1$; $\mathcal{U}(N)$ for $\beta = 2$; and $Sp(N)$ for $\beta = 4$. These measures are given by, [40],

$$\int_{\mathcal{U}(N)} f(M)d\mu(M) = \int_{[0,2\pi]^N} f(\theta_1, \ldots, \theta_N) \left(\prod_{1 \le j < k \le N} \left| e^{i\theta_k} - e^{i\theta_j} \right|^2 \right) \frac{\prod_{j=1}^N d\theta_j}{N!(2\pi)^N} \qquad (4.2)$$

$$\int_{SO(2N)} f(M)d\mu(M) = \frac{2^{(N-1)^2}}{\pi^N N!} \int_{[0,\pi]^N} \left(f(\theta_1, \ldots \theta_N) \prod_{1 \leq j < k \leq N} (\cos\theta_k - \cos\theta_j)^2 \right) d\theta_1 \ldots d\theta_N \tag{4.3}$$

$$\int_{SO(2N+1)} f(M)d\mu(M) = \frac{2^{N^2}}{\pi^N N!} \int_{[0,\pi]^N} \left(f(\theta_1, \ldots \theta_N) \prod_{1 \leq j < k \leq N} (\cos\theta_k - \cos\theta_j)^2 \prod_{h=1}^{N} \sin^2\left(\frac{\theta_h}{2}\right) \right) d\theta_1 \ldots d\theta_N \tag{4.4}$$

$$\int_{Sp(2N)} f(M)d\mu(M) = \frac{2^{N^2}}{\pi^N N!} \int_{[0,\pi]^N} \left(f(\theta_1, \ldots \theta_N) \prod_{1 \leq j < k \leq N} (\cos\theta_k - \cos\theta_j)^2 \prod_{h=1}^{N} \sin^2(\theta_h) \right) d\theta_1 \ldots d\theta_N \tag{4.5}$$

with θ_i being the eigenvalues of M. This then gives the Haar-contribution to dH for the GUE, even-dimension GOE, odd-dimensional GOE, and the GSE ensemble respectively.

The probability distribution for a $N \times N$ Hamiltonian H with an average distance δ_0 between each of its eigenvalues is then given by, [14],

$$P(H)dH \propto \exp\left(\frac{-\pi^2 \beta}{4N\delta_0^2} \operatorname{Tr} H^2\right) dH.$$

In most cases, the normalisation $\delta_0 \to 1$ will be taken.

The argument for the distribution being dependent only on the trace of H is based on the fact that $P(H)dH$ must be invariant under the same types of transformation that H is - that is conjugation by matrices in $\mathcal{U}(N), \mathcal{O}(N)$ or $\operatorname{Sp}(N)$ as appropriate. Combined with the requirement that each entry in the Hamiltonian drawn from the Gaussian distribution is independent, then there is the following theorem, [115],

Theorem 4.1.1. *Let $\mathfrak{h}'$ be an ensemble of matrices invariant under the transform*

$$A^{-1}HA = H \qquad \forall H \in \mathfrak{h}'$$

where $A \in \mathcal{U}(N), \mathcal{O}(N)$ or $\operatorname{Sp}(N)$. Then the probability distribution for H must be given by a function of the form

$$P(H) = \exp\left(a \operatorname{tr} H^2 + b \operatorname{tr} H + c\right) \tag{4.6}$$

for $a, b, c \in \mathbb{R}$ and $a > 0$.

The restriction to $b = 0$ for the Wigner-Dyson classes is decided by explicitly testing the 2×2 case and assuming that the result must hold for any N, [73]. The value of c can then be found as the necessary normalisation constant. This is not the only time an assumption that the results calculated for the dimension two case are universal and can be applied to any N will appear, as it will form the Wigner Surmise for calculating the nearest neighbour spacing between the eigenvalues.

From $P(H)$ the joint energy level distributions are derived as, [73, 115],

$$P(\{E_n\})d\{E_n\} = C_{N,\beta} |\Delta(\{E_n\})|^\beta \prod_k \exp\left(-\beta E_k^2/4\right) dE_k. \tag{4.7}$$

Note that due to Kramer's degeneracy energy levels will have degeneracy $d = 2$ in the GSE case; while $d = 1$ for GUE and GOE. It is only necessary to take the unique eigenvalues in the computation, so energy levels are not double counted in the GSE case. It holds generally that
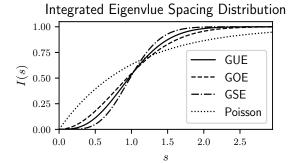
Figure 4.1: Probability distribution for the normalised spacing of the energy levels of the three Wigner-Dyson classes, compared to Poissonian statistics. Note the low probability for states to be close - this is the appearance of level repulsion. See for example [73, 115].

there are no points in the spectrum that have a degeneracy greater than d, so all eigenvalues have the same degeneracy. The reason for this will be seen when the level spacing distribution is plotted - the probability to have very close eigenvalues is vanishingly small, so degenerate eigenvalues are highly unlikely. These near impossible occurrences in a generic system are known as 'accidental' degeneracies when they happen; however there do still exist specific systems where the probability of eigenvalue degeneracies diverging from d is large. These systems must be intentionally constructed through parameter space searches, and are described as having 'diabolical' points when the degeneracy of an eigenvalue is greater than d, [23]. It will be possible to assume that we are not working in a system with diabolical points, as the probability of finding one randomly is near-zero.

The first distribution of interest is the spacing distribution. Defining the normalised distance between adjacent eigenvalues as $s_i = (E_{i+1} - E_i)/\delta_0$, the probability distribution of s can be explicitly calculated for the $N = 2$ case; and according to the Wigner Surmise, this $N = 2$ distribution serves as a sufficiently good approximation of distribution for any N for most purposes, [73]. This gives the approximated spacing distribution as,

$$P_{GOE}(s) = \frac{\pi s}{2} \exp\left(-\pi s^2/4\right)$$

$$P_{GUE}(s) = \frac{32 s^2}{\pi^2} \exp\left(-4 s^2/\pi\right)$$

$$P_{GSE}(s) = \frac{2^{18} s^4}{3^6 \pi^3} \exp\left(-64 s^2/9\pi^2\right).$$

Here δ_0 is the mean level spacing averaged over the bulk of the spectra, $\delta_0 = \langle E_{i+1} - E_i \rangle_i$ $E_i \ll \sqrt{N}$ for very large N so that the distribution $P(s)$ is normalised to have mean 1. The spacing distribution is then the first indicator used to identify which random matrix ensemble an energy level spectra corresponds to, as it gives a simple to calculate distribution, with three very characteristic forms as shown in Figure 4.1. It will be applied in this manner in Chapters 6 and 7, taking simulation data and comparing it to the analytical predictions.

The second distribution to be calculated is significantly less useful as an identifier for telling the three Wigner-Dyson classes apart - as it is identical in all three classes - but still has important application. The average density of states can be calculated by taking the average value of E_1
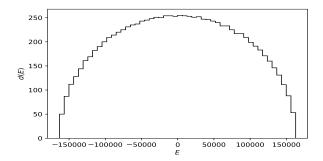
Figure 4.2: The eigenvalues of a 10000×10000 real symmetric matrix from the GOE ensemble showing the semi-circular distribution of the eigenvalues.

over an ensemble of H in $\mathfrak{h}'$,

$$\langle d(E) \rangle = \left\langle \prod_{i=2}^{N} \left(\int_0^\infty dE_i \right) P(\{E_n\}) \right\rangle_H .$$

By the Wigner Semi-circle Law this gives a semi-circular distribution, [24],

$$\langle d(E) \rangle = \begin{cases} \frac{1}{\delta_0^2} \sqrt{\delta_0^2 - \left(\frac{\pi E d}{2N} \right)^2} & |E| \leq \pm \sqrt{\frac{2N\delta_0}{\pi d}} \\ 0 & \text{otherwise} \end{cases} \tag{4.8}$$

for each of the GUE, GOE and GSE ensembles. An example of the GOE case is given in Figure 4.2. The semi-circular shape of the density of states is a global property of the random matrix ensemble, and thus won't be seen in any local densities calculated from generated simulation data. It is possible to use the data to take the two-point correlation function $R_2(x) = \delta_0^2 \langle d(E)d(E + x\delta_0) \rangle_E$ of the average density of states, and the Fourier transforms $K_1(\tau)$ and $K_2(\tau)$ of $d(E)$ and R_2 respectively as the spectral form factors; these will also have a different characteristic form for each of the Wigner-Dyson ensembles, allowing them to be used to identify the different ensembles in the data, however as we don't apply them to our numerics, we won't discuss them further. Information about them may be found in [64, 67, 73, 115].

The normalisation $\lambda_n = E_n/\delta_0$ used to calculate the nearest neighbour spacing distribution with mean one is a simplification of the procedure of unfolding the spectrum, which holds only where the average density of states is constant. Unfolding is necessary as the nearest neighbour spacing is supposed to show local fluctuations in the eigenvalue distribution, while the density of states shows global fluctuations. An accurate study of the local fluctuations thus needs the global effects removed to be accurate, which is done by unfolding the spectra, or dividing each eigenvalue by the local average density, $E_n \rightarrow \lambda_n = E_n/\bar{d}(E)$ with $\bar{d}(E) = |\{E_i \in [E - \Delta E, E + \Delta E]\}|/2\Delta E$, [73]. This will be very near to a constant $\bar{d}(E) \sim \delta_0$ when N is very large and away from the edges of the spectra, but when near to the edges of the spectra for small N, or in cases where $d(E)$ varies greatly throughout the spectrum - such for the seven Altland-Zirnbauer ensembles - the properly unfolded spectrum should be used.
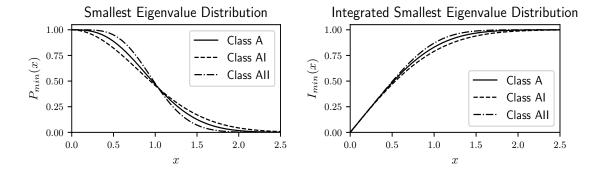
Figure 4.3: The probability distribution $P_{\min}$ of the smallest normalised eigenvalue x.

Numerically this process also changes, taking the evaluation of the counting function $N(E)$, which is the number of eigenvalues smaller than E, [67],

$$E \to N(E) = \sum_{E_j \in \{E_i\}} \theta(E - E_j), \qquad \theta(x) = \begin{cases} 1 & x > 0 \\ 0.5 & x = 0 \\ 0 & x < 0 \end{cases} \tag{4.9}$$

as the unfolding.

Finally, the distribution of the first positive normalised eigenvalue x is calculated, giving the energy gap, or the probability that there is a distance x gap between zero energy, and the lowest energy level in the system. It is found by assuming that $E_i = x$ is the smallest eigenvalue eigenvalue, and then calculating the probability all other eigenvalues lie in the range (x, ∞), [123],

$$P_{\min}(x) = \frac{1}{(N-1)!} \prod_{i=2}^{N} \left(\int_x^\infty d\lambda_i \right) P(\{\lambda_n\}).$$

By [56], the integrated smallest eigenvalue distribution $I_{\min}(x) = \int_0^x P(x')dx'$ can instead be related to the level spacing distribution by

$$I_{\min}(x) = \int_0^x sP(s)ds + x \int_x^\infty P(s)ds$$

for the Wigner-Dyson classes. Substituting in the level spacing distributions for each class, this gives the integrated distributions as,

$$I_{\min,A}(x) = 1 - \exp\left(-4x^2/\pi\right) + x\,\mathrm{erfc}(2x/\sqrt{\pi})$$
$$I_{\min,AI}(x) = \mathrm{erf}(x\sqrt{\pi}/2)$$
$$I_{\min,AII}(x) = 1 + x\,\mathrm{erfc}(8x/3\sqrt{\pi}) - (144\pi x^2 + 81\pi^2)\exp\left(-64x^2/9\pi\right)/(9\pi)^2.$$

Again, this distribution has a form highly characteristic to each ensemble, so given a set of experimental data, it is possible to compare it to the theoretical forms of $I_{\min}(x)$ and identify the corresponding ensemble which would have generated it. The distributions are plotted in Figure 4.3. The smallest eigenvalue probability distribution has also been taken, by differentiating the

integrated distributions to get,

$$P_{\min,A}(x) = \frac{8x-4}{\pi}\exp(-4x^2/\pi) + \text{erfc}(2x/\sqrt{\pi})$$

$$P_{\min,AI}(x) = \exp(-x^2\pi/4)$$

$$P_{\min,AII}(x) = \text{erfc}(8x/3\sqrt{\pi}) - \frac{16x\exp(-64^2/9\pi)}{3\pi} + \frac{32\exp(-64x^2/9\pi)x(64x^2+27x)}{81\pi^2}.$$

It will be seen in the applications to the simulation data that it is essential to plot both, as small errors in the estimated probability distribution near zero can have a serious impact on the integrated form.

4.2 The Altland-Zirnbauer Ensembles

Wigner and Dyson described systems with at most time-reversal symmetry, but as random matrix theory was extended to cover systems with charge-conjugation or chiral symmetries, it became necessary to add seven additional classes of ensembles to their original three, [5, 6, 146, 166, 167]. These seven ensembles are generally known as the seven Altland-Zirnbauer ensembles in addition to the Wigner-Dyson ensembles, as Altland and Zirnbauer were the first to consider the ten ensembles together in the context of a complete classification of the possible statistics of chaotic quantum systems with at most time-reversal, charge-conjugation and chiral symmetry, [6, 179]. The completeness was expected but not proved initially, but it has since been shown that the ten random matrix ensembles considered by Altland and Zirnbauer are indeed the only ten ensembles the statistics of a chaotic Hermitian quantum system can match, [79, 95].

The seven new ensembles arise in the case where a quantum system has a $Z_2 \times Z_2$-graded symmetry group G with $G \subseteq \{\mathbb{I}, \alpha, \gamma, \pi\}$ and and at least one of γ, π is included in G. In this case, then for the lifts of α, γ and π to $\hat{\mathcal{T}}$, $\hat{\mathcal{C}}$ and $\hat{\mathcal{P}}$ to be symmetry operators, it is necessary $[\hat{\mathcal{T}}, \hat{H}] = 0$, $\{\hat{\mathcal{C}}, \hat{H}\} = 0$ and $\{\hat{\mathcal{P}}, \hat{H}\} = 0$ respectively. This leads to Theorem 3.1.16, which states the Hamiltonian must sit inside the super-commutant $Z(\mathcal{R})$ generated by the corepresentation $\mathcal{R}$ of G on the Hilbert space $\mathcal{H}$. Applying Theorem 3.1.17 to use the matrix forms of the super-commutants, then $\mathfrak{h}'$ is defined as in Table 4.1.

Note how the matrices all have a 2×2 block matrix form $\left(\begin{smallmatrix} A & B \\ C & D \end{smallmatrix}\right)$, this is because the Hamiltonians can be expressed as occurring over the particle-hole space, so the blocks represent transformations either preserving or inverting the particle or hole space. The different ensembles then correspond to different relations between the matrices A and D, and the matrices B and C. In the classes AIII, BDI and CII, only the off-diagonal matrices are non-zero, and the entire Hamiltonian can be expressed through the choice of a single matrix C.

When it comes to ensemble names, there are no agreed upon names for the ensembles generated by the classes D, C, DIII and CI, so we will use the Altland-Zirnbauer labels for all seven classes throughout. The classes AIII, BDI and CII do have special ensemble names however, and generate ensembles known as the chiral GUE, chiral GOE and chiral GSE ensembles, as they continue to be invariant under transformation by unitary, orthogonal and symplectic matrices like for the GUE, GOE and GSE ensembles, however the transformation is no longer conjugation by a single

Class of $\mathcal{R}$	$Z(\mathcal{R})$	$\mathfrak{h}'$	Ensemble Name
$AIII$	$Cl_1^{\mathbb{C}}$	$\left\{ H \in \mathbb{C}^{2M \times 2M} \middle\vert \begin{array}{c} H = \begin{pmatrix} 0 & C \\ C^\dagger & 0 \end{pmatrix} \\ H = H^\dagger \end{array} \right\}$	Chiral GUE (chGUE)
BDI	$Cl_1^{\mathbb{R}}$	$\left\{ H \in \mathbb{C}^{2M \times 2M} \middle\vert \begin{array}{c} H = \begin{pmatrix} 0 & C \\ C^\dagger & 0 \end{pmatrix} \\ H = H^\dagger \\ H = H^* \end{array} \right\}$	Chiral GOE (chGOE)
CII	$Cl_{-1}^{\mathbb{R}}$	$\left\{ H \in \mathbb{C}^{2M \times 2M} \middle\vert \begin{array}{c} H = \begin{pmatrix} 0 & C \\ C^\dagger & 0 \end{pmatrix} \\ C = \begin{pmatrix} k_1 & k_2 \\ -k_2^* & k_1^* \end{pmatrix} \\ H = H^\dagger \end{array} \right\}$	Chiral GSE (chGSE)
C	$Cl_{-2}^{\mathbb{R}}$	$\left\{ H \in \mathbb{C}^{2M \times 2M} \middle\vert \begin{array}{c} H = \begin{pmatrix} A & B \\ B^* & -A^* \end{pmatrix} \\ H = H^\dagger \end{array} \right\}$	AZ-C
D	$Cl_2^{\mathbb{R}}$	$\left\{ H \in \mathbb{C}^{2M \times 2M} \middle\vert \begin{array}{c} H = \begin{pmatrix} A & B \\ -B^* & -A^T \end{pmatrix} \\ A = A^\dagger \\ B = -B^T \end{array} \right\}$	AZ-D
CI	$Cl_{-3}^{\mathbb{R}}$	$\left\{ H \in \mathbb{C}^{2M \times 2M} \middle\vert \begin{array}{c} H = \begin{pmatrix} 0 & B \\ B^* & 0 \end{pmatrix} \\ H = H^\dagger \end{array} \right\}$	AZ-CI
$DIII$	$Cl_3^{\mathbb{R}}$	$\left\{ H \in \mathbb{C}^{2M \times 2M} \middle\vert \begin{array}{c} H = \begin{pmatrix} 0 & B \\ -B^* & 0 \end{pmatrix} \\ H = H^\dagger \end{array} \right\}$	AZ-DIII

Table 4.1: The ensembles $\mathfrak{h}'$ for each of the seven Altland-Zirnbauer classes, [1, 24, 39, 156].

matrix and involves two matrices acting on the sub-block C in H, [156],

$$
\begin{aligned}
chGUE &\Rightarrow \forall U, V \in \mathcal{U}(N),\ C \in \mathfrak{h}' & UCV^{-1} \in \mathfrak{h}' \\
chGOE &\Rightarrow \forall O, Q \in \mathcal{O}(N),\ C \in \mathfrak{h}' & OCQ^{-1} \in \mathfrak{h}' \\
chGSE &\Rightarrow \forall R, S \in \mathrm{Sp}(N),\ C \in \mathfrak{h}' & RCS^{-1} \in \mathfrak{h}'
\end{aligned}
$$

The probability distribution on H for the Altland-Zirnbauer classes retains the same general structure as the Wigner-Dyson classes, being proportional to the exponential of $\mathrm{Tr}\, H^2$, however there is now an extra factor of $1/2$ in the exponential, so that, [14],

$$
P(H) \propto \exp\left(\frac{-\pi^2 \beta}{8N\delta_0^2} \mathrm{Tr}\, H^2\right)
$$

describes the probability distribution for an $N \times N$ Hamiltonian with mean level spacing δ_0. Clearly, β remains an important variable distinguishing the behaviour of the different ensembles, and its value for each class can be found in Table 4.2, however when the joint eigenvalue distribution is calculated, it is seen that these ensembles pick up a second indicator variable - α - which describes the repulsion of an eigenvalue from its negative copy,

$$
P(\{E_n\})d\mathbf{E} = C_{N,\beta,\alpha} \left|\Delta(\{E_n^2\})\right|^\beta \prod_k |E_k|^\alpha \exp\left(-\beta E_k^2/4\right) dE_k. \tag{4.10}
$$

It is noted that the Vandermont determinant is now dependent on E_j^2 not E_j as well. Also, the correct measure for the set is still the Haar measure.

The values of α possible for each ensemble are also plotted in Table 4.2. It is noted that for the ensembles AIII, BDI and CII, α does not have a fixed value, but depends on the parameter ν, which is the degeneracy of the zero-energy level eigenvalue. We note that while it is guaranteed that every non-zero eigenvalue has the same degeneracy d - as per the case for the Wigner-Dyson ensembles - the zero eigenstates have a special position as the only eigenstates which can be transformed into themselves under the action of $\hat{\mathcal{C}}$ and $\hat{\mathcal{P}}$. This and their triviality in terms of the eigenvalue equation allow them to take on a totally different degeneracy number than the rest of the system. The possible values of ν are also a characteristic of the ensemble - the classes C and CI can never have a zero eigenvalue, whereas the classes D and DIII may have an at most a degeneracy 1 zero eigenvalue. On the other hand, the classes AIII, BDI and CII may have any natural number of zero eigenvalue eigenstates. The number of zero-eigenvalues the system has will affect the density of states, and thus the smallest eigenvalue distribution, so it is important to track it in addition to α.

There are then four numbers describing the characteristic behaviour of an Altland-Zirnbauer ensemble - ν, d, β and α which for each ensemble can take the values in Table 4.2.

The characteristic distributions described for the Wigner-Dyson classes are again considered.

First is the level spacing distribution. The level spacing distribution must be calculated in the bulk of the spectrum, away from zero. In this area, where 0 is far way, the effects of the spectral mirror symmetry are small, as an eigenvalue is too far way from its negative counterpart to be repelled from it strongly. Due to this, the level spacing distributions for the Altland-Zirnbauer ensembles will match the distribution of the Wigner-Dyson ensemble which has a matching β value. For the classes BDI and CI this is then the GOE ensemble; the classes AIII, C and D will

	$AIII$	BDI	CII	C	D	CI	$DIII$
ν	$0,1,2,\ldots$	$0,1,2,\ldots$	$0,1,2,\ldots$	0	$0,1$	0	$0,1$
d	1	1	2	1	1	1	2
β	2	1	4	2	2	1	4
α	$1+2\nu$	ν	$3+4\nu$	2	0	1	1

Table 4.2: The four parameters which can be used to describe an Altland-Zirnbauer ensemble, given the general form, ν, ,d, β and α, [14].

match the GUE statistics; and the classes CII and DIII will match the spacing distribution of the GSE.

The mean density of states however does show significant divergence from the Wigner-Dyson ensembles as the level repulsion between the positive and negative energy levels causes large fluctuations away from the Wigner Semicircle near $E = 0$. These fluctuations can furthermore be seen in the local density of states near zero, meaning that they that they can be used as a comparison for simulated experimental data, helping to identify which of the ensembles appears. The characteristic forms for the fluctuations in the local mean density of states near 0 for each Altland-Zirnbauer ensemble are given by, [85],

$$\langle d(E)\rangle_{AIII} = \frac{\pi^2|E|}{2}\left(J_\nu^2(\pi|E|) - J_{\nu-1}(\pi|E|)J_{\nu+1}(\pi|E|)\right) + \nu\delta(|E|) \tag{4.11}$$

$$\langle d(E)\rangle_{BDI} = \frac{\pi}{2}\left(\pi|E|\left(J_\nu^2(\pi|E|) - J_{\nu-1}(\pi|E|)J_{\nu+1}(\pi|E|)\right)\right. \tag{4.12}$$

$$\left. + J_\nu(\pi|E|)R_\nu(\pi|E|)\right) + \nu\delta(|E|) \tag{4.13}$$

$$\langle d(E)\rangle_{CII} = \frac{\pi}{2}\left(2\pi|E|\left(J_{2\nu}^2(2\pi|E|) - J_{2\nu-1}(2\pi|E|)J_{2\nu+1}(2\pi|E|)\right)\right. \tag{4.14}$$

$$\left. + J_{2\nu}(2\pi|E|)R_{2\nu}(2\pi|E|)\right) + \nu\delta(|E|) \tag{4.15}$$

$$\langle d(E)\rangle_C = 1 - \frac{\sin(2\pi|E|)}{2\pi|E|} \tag{4.16}$$

$$\langle d(E)\rangle_D = 1 + \frac{\sin(2\pi|E|)}{2\pi|E|} + \nu\delta(|E|) \tag{4.17}$$

$$\langle d(E)\rangle_{CI} = \frac{\pi}{2}\left(\pi|E|(J_0^2(\pi|E|) + J_1^2(\pi|E|)) - J_0(\pi|E|)J_1(\pi|E|)\right) \tag{4.18}$$

$$\langle d(E)\rangle_{DIII} = \frac{\pi}{2}\left(2\pi|E|\left(J_0(2\pi|E|)J_1'(2\pi|E|) + J_1^2(2\pi|E|)\right)\right. \tag{4.19}$$

$$\left. + (-1)^\nu J_1(2\pi|E|)\right) + \nu\delta(|E|) \tag{4.20}$$

with

$$R_n(x) = \int_0^x J_n(x')dx'.$$

The cases for $\nu = 0$, N large are plotted in Figure 4.4. Note that in each case, the eigenvalues are repelled from 0 or attracted to it, often with oscillations continuing away from zero and gradually decreasing, and in every case the distribution is symmetric. All of this extra behaviour comes from the interaction between an energy level and its negative copy so that they repel each other, along with the change of the Vandermont determinant to use the square of the energy levels. Due to this, the oscillations fade away as $|E|$ increases, and the system begins to behave more like a Wigner-Dyson ensemble.
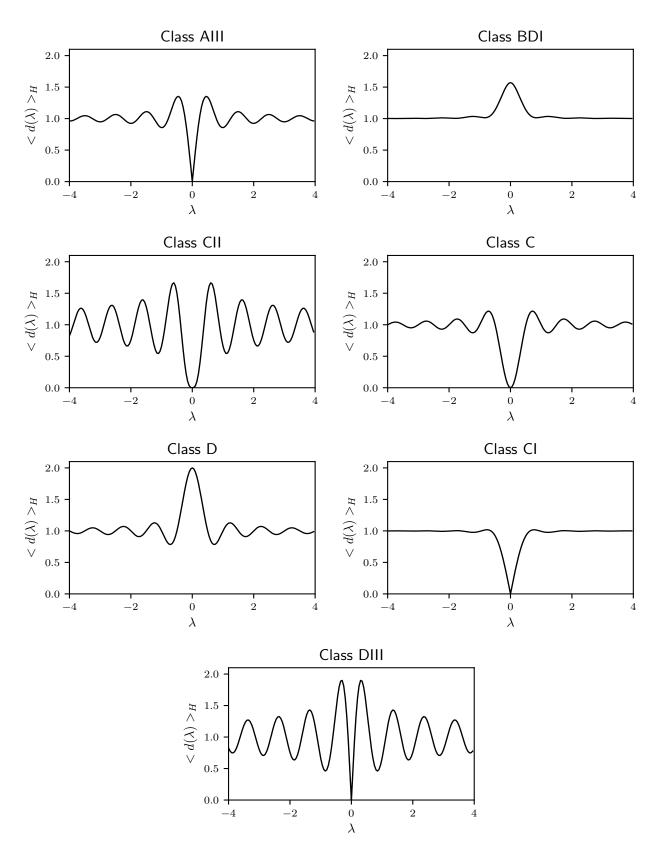
Figure 4.4: Average density of states about 0 for the normalised energy spectra λ when $\nu = N_f = 0$ and N large.

These distributions will also have characteristic forms of $R_2(x)$, the 2-point correlator of the density of states, and $K_1(\tau)$ and $K_2(\tau)$ the spectral form factors. However, without their application to the later numeric simulations, we leave discussion of these distributions to [64] and the references within. Note that K_2 is dependent only on the value of β for the ensembles, so like the level spacing distribution, it will reduce to one of the forms of the Wigner-Dyson ensembles.

The distribution of the smallest positive eigenvalue will prove to be the most useful method of identifying which of the different Altland-Zirnbauer ensembles appear in the simulated spectral data of the systems in Chapter 7. With the chosen example systems of Quantum Graphs and Dirac Graphs, where the first N eigenvalues E_i are identified by identifying all N roots of a function $\zeta(E)$ in a range $[0, \delta_0 N]$, the smallest eigenvalue distribution requires the fewest number of runs of the root finding algorithms, and is thus computationally the fastest to return results. Quantitatively, it was possible to return calculated smallest eigenvalue distributions for the example systems in Chapter 7 in under an afternoon per class, while the mean density of states required several days worth of computation for still poorer agreement between the simulations and the theoretical predictions. Use of the smallest eigenvalue distribution as an indicator for the Altland-Zirnbauer ensembles is not without precedent either - the distributions of the edges of the spectrum of random matrices has seen much dedicated study, [123, 162, 164], with its use as an indicator function for the different Altland-Zirnbauer classes in [56], and its use to identify deviations away from 'pure' Altland-Zirnbauer ensembles appearing in [125]. Away from the Altland-Zirnbauer classes, the smallest eigenvalue distribution has been applied to checking simulated data against the random matrix theory predictions for the chSE ensemble, [15], Laguarre ensembles, [123] and the β-Wishart-Laguerre ensembles, [106], this being a non-exhaustive list.

We now identify the smallest eigenvalue distributions for the Altland-Zirnbauer classes. Substituting the joint eigenvalue distribution for N unique positive eigenvalues for the Altland-Zirnbauer classes into the general form for the smallest eigenvalue distribution gives the distribution,

$$
\begin{aligned}
P_{\min}(x) &= \frac{1}{(N-1)!} \prod_{i=2}^{N} \left(\int_x^\infty dE_i \right) P(\{E_n\}) \\
&= \frac{C x^\alpha e^{-\beta x^2/4}}{(N-1)!} \left(\int_x^\infty \right)^{N-1} \prod_{2 \le i < j \le N} |E_i^2 - E_j^2|^\beta \prod_{k=2}^{N} E_k^\alpha |E_k^2 - x^2|^\beta e^{-\beta E_k^2/4} dE_k \quad (4.21)
\end{aligned}
$$

which after the change of variables $y_k = (E_{k+1}^2 - x^2)$, $dy_k = 2E_{k+1}dE_{k+1}$, $m = (\alpha - 1)/2$ and $n = N - 1$ is, [123, 164],

$$
P_{\min}(x) = \frac{C x^\alpha e^{-N\beta x^2/4}}{2^n (N-1)!} \left(\int_0^\infty \right)^n \prod_{1 \le i < j \le n} |y_i - y_j|^\beta \prod_{k=1}^{n} (y_k + x^2)^m y_k^\beta e^{-N\beta y_k/4} dy_k
$$

The integral is a constant in the cases $m = 0 \Rightarrow \alpha = 1$, giving,

$$
P_{\min}(x) = C'(N) x^\alpha e^{-A(N)\beta x^2}
$$

and thus can be dropped in favour of calculating the normalisation of $P(x)$ directly, so that the distributions for AIII, CI and DIII for $\nu = 0$, $N \to \infty$ are given by,

$$
I_{\min AIII,\, \nu=0}(x) = 1 - \exp\left(-\pi^2 x^2/4\right)
$$
$$
I_{\min CI}(x) = 1 - \exp\left(-\pi^2 x^2/8\right)
$$

$$I_{\min DIII,\,\nu=0} = 1 - \exp\big(-\pi^2 x^2/2\big)$$

where the correct values for the constants are taken from [58]. The results for the classes BDI and CII have been found through multiple methods including Vandermont determinant techniques, [167], and the QCD partition function, [42], and are given by, [125],

$$I_{\min BDI,\,\nu=0}(x) = 1 - \exp\big(-\pi^2 x^2/8 - \pi x/2\big)$$
$$I_{\min CII}(x) = 1 - \cosh(\pi x)\exp\big(-\pi^2 x^2/2\big).$$

Where these analytic expressions exist for $I_{\min}, P_{\min}$ and $\nu = 0$, it is also possible to derive the expressions for $\nu > 0$ by using the recursion relations given by [106].

There is, however, no readily available closed-form expression for the smallest eigenvalue distribution for the remaining classes C and D. To have a theoretical prediction to compare simulation data against, we then turn to their numerical approximation. In all cases of the Altland-Zirnbauer ensembles, solving Equation 4.21 for $P_{\min}(x)$ and then finding the integrated smallest eigenvalue distribution $I(x)$ is equivalent to calculating the Fredholm Determinant, [164],

$$I_{\min}(x) = \int_0^x P_{\min}(x')dx' = 1 - \mathrm{Det}(\mathbb{I} - K_m\mid_{L^2([0,x^2])})$$

where the Fredholm determinant is an integral equation defined with a kernal A on $L_2([a,b])$, [29],

$$\mathrm{Det}(\mathbb{I} - zA\mid_{[a,b]}) = \sum_{n=0}^{\infty} \frac{z^n}{n!} \prod_{i=1}^{n} \left(\int_a^b dt_i \right) \det(A(t_p, t_q))\mid_{p,q=1}^{n}. \tag{4.22}$$

The integrated smallest eigenvalue distribution $I_{\min}(x)$ then takes $z = 1$, $a = 0$, $b = x^2$ and $A = K_m$ for $m = (\alpha - 1)/2$ with, [162],

$$K_m(x,y) = \begin{cases} \frac{\sqrt{y}J_m(\sqrt{x})J_m'(\sqrt{y}) - \sqrt{x}J_m'(\sqrt{x})J_a(\sqrt{y})}{2(x-y)} & x \neq y \\ \frac{1}{4}\big(J_m^2(\sqrt{x}) - J_{m+1}(\sqrt{x})J_{m-1}(\sqrt{x})\big) & x = y. \end{cases} \tag{4.23}$$

The smallest eigenvalue distribution for the classes C and D are then given by the Fredholm determinants for the kernels $K_{1/2}$ and $K_{-1/2}$ respectively.

We here now apply the algorithm given by Bornemann in [29] to approximate any Fredholm determinant by taking the symmetrised version of Nyström's linearisation of the integral equation,

$$\mathrm{Det}(\mathbb{I} - zA) \approx \det\Big(\delta_{ij} + zw_i^{1/2}A(x_i, x_j)w_j^{1/2}\Big)\mid_{i,j=1}^{m} \tag{4.24}$$

where $\{x_i\}$ are m points chosen in the range $[a,b]$ with weights w_i by the Gauss-Legendre quadrature,

$$\int_a^b f(x)dx \approx \sum_{i=1}^m w_i f(x_i),$$

$$x_i = \frac{b-a}{2}\zeta_i + \frac{a+b}{2}, \qquad\qquad \zeta_i = i\text{th root of } L_m(x) \text{ in } [-1,1]$$
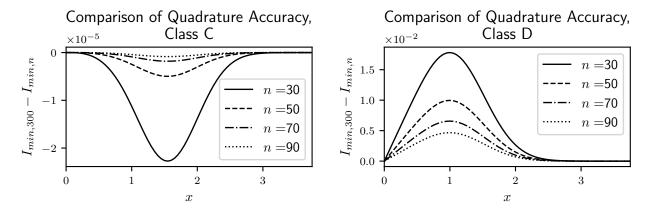
$$w_i = \frac{b-a}{2}\frac{2}{(1-x_i^2)(L_m'(x_i))^2}$$

Python has built in methods to compute the Gauss-Legendre quadrature; defining a method to build the matrix $(\delta_{ij} + zw_i^{1/2}A(x_i,x_j)w_j^{1/2})\mid_{i,j=1}^m$, so inputting the kernel from Equation 4.23 allows an approximation of the integrated distribution of the smallest eigenvalue. Using the standard two point numeric differentiation routine can then calculate the smallest eigenvalue probability distribution $P_{\min}(x)$ out of $I_{\min}(x)$.

There is still the issue of accuracy in the numerical approximations. The accuracy is dependent on the number n of quadrature points used to do the integral, returning a function $I_{\min,n}(x)$ rather than the true $I_{\min}(x)$. It is then necessary to choose an n such that $I_{\min}(x) - I_{\min,n}(x)$ is sufficiently small, but the computation time for $I_{\min,n}(x)$ is not excessive. To do this, $I_{\min,N}(x) - I_{\min,n}(x)$ is taken for several values of n, with $N \gg n$, and assuming that $I_{\min,N}(x) \sim I_{\min}(x)$ is a sufficiently good approximation. Plotting these in Figures 4.5a and 4.5b for $N = 300$ and $n = \{30, 50, 70, 90\}$, it is seen that in the case of class C, the accuracy is already of the order 2×10^{-4} for $n = 30$, so this is a good number of points to take. For class D the error is only under 1×10^{-2} when at least 50 points are taken, and it is not significantly so unless at least 90 points are taken. The requirement that the error should be no more than 1×10^{-2} is due to the fact the smallest eigenvalue distribution is a function on the scale of 10^{-1}, so this is the requirement the error be in the third significant figure rather than the second. In practise, 50 points will be enough, with the note that the approximation always underestimates the function $I_{\min}$, so a good numerical simulation will produce an estimate of $I_{\min,D}(x)$ that slightly exceeds the approximated analytic prediction.

The smallest eigenvalue distributions for the Altland-Zirnbauer classes are then plotted and compared in Figure 4.6.

Comparison of Quadrature Accuracy, Class C

Comparison of Quadrature Accuracy, Class D

(a) Error in the Fredholm determinant of $K_{1/2}$ for class C. (b) Error in the Fredholm determinant of $K_{-1/2}$ for class D.

Figure 4.5: Calculating the error in the estimate of the Fredholm determinant of the kernels $K_{\pm 1/2}$ for different numbers of quadrature points n. This gives the parameters to find the smallest eigenvalue distribution for the class C and D ensembles through numerical integration.
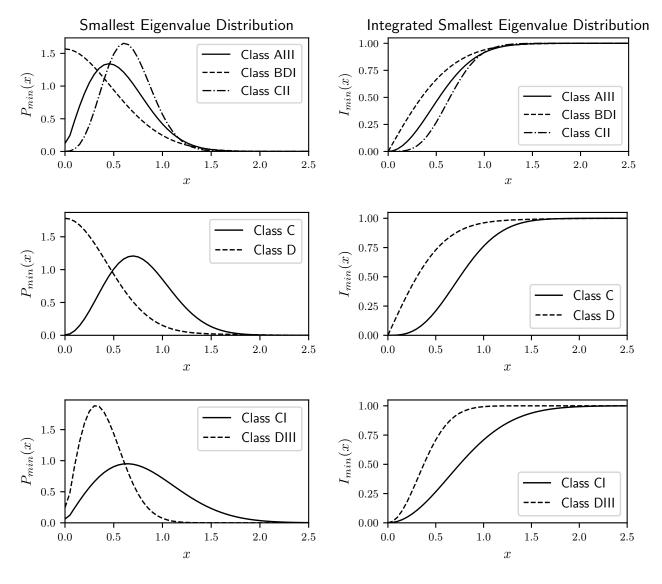
Figure 4.6: The probability distribution $P_{\min}(x)$, and integrated probability distribution $I_{\min}(x)$ of the smallest positive normalised eigenvalue x

5. *Identifying Minimal Examples of The Altland-Zirnbauer Classes*

At the end of Chapter 3 it was discussed how chaotic quantum systems show universal behaviours depending on their symmetries, and it has been theorized that the quantum analogues of chaotic classical systems display random matrix statistics, forming the BGS-conjecture. There is as yet, no general proof of the BGS-conjecture, so testing it often falls to defining quantum systems that are predicted to show a certain type of random matrix statistics and then comparing the experimental results to the predicted ensemble.

To this end, it is necessary to be able to test several systems per Altland-Zirnbauer class to see repeated agreement with the BGS-conjecture.

However, the Altland-Zirnbauer classes require particle-hole and chiral symmetries which can be hard to produce physically - despite numerous systems being simulated numerically, [13, 56, 64], experimental realisation has occurred only for the chiral classes AIII, BDI and CII, [14, 136]. The similar problem of testing the AII ensemble in the lab was solved by Joyner, Sieber and Müller in [92] which bypassed the need to work with fermions by adding an appropriate geometric symmetry to the system and using the symmetry-decomposed basis to isolate a sub-spectrum with the AII ensemble statistics as per Theorem 3.1.21. By doing so, their system could be tested in the lab using microwave wires, [113, 133, 134, 135].

It is our desire to extend this method to the Altland-Zirnbauer ensembles, showing that given any form of global time-reversal and charge-conjugation, an appropriately geometrically symmetric system can be found such that the symmetry-reduced basis produces a sub-spectrum that is locally any one desired ensemble from the ten presented in Chapter 4. This means, that if a particular form of $\hat{\mathcal{T}}$ and $\hat{\mathcal{C}}$ is found to be easy to realise experimentally, then by combining them with geometric symmetries, the BGS-conjecture can be tested on these systems for any of the ten ensembles in Chapter 4, sidestepping the difficulty of building experiments that would be required for harder forms of $\hat{\mathcal{T}}, \hat{\mathcal{C}}$. This is hoped to ease the difficulty in realising the Altland-Zirnbauer enesmbles in the lab.

To do this, we must demonstrate that for any given global time-reversal and charge-conjugation operators, $\hat{\mathcal{T}} = (\mathbb{I}_{\text{charge}} \otimes T \otimes \mathbb{I}_{\text{orbital}})\mathcal{K}$ and $\hat{\mathcal{C}} = (C \otimes \mathbb{I}_{\text{spin}} \otimes \mathbb{I}_{\text{orbital}})\mathcal{K}$ and any desired Altland-Zirnbauer class of corepresentation, X, there exists a symmetry group $G = U \cup \alpha U \cup \gamma U \cup \pi U$ such that one of the corepresentations of G generates a subspace that is of Altland-Zirnbauer class X.

This requires classifying all the corepresentations of the $Z_2 \times Z_2$-graded groups according to the Altland-Zirnbauer Tenfold Way until an example has been found for each Altland-Zirnbauer class. We do this by identifying a method of algorithmically identifying and classifying all the $Z_2 \times Z_2$-graded groups, then applying this to all the groups of order less than $|G| = 40$, the results for this being given in Appendix E. This includes an extension to the work done by Cracknell in [41] where the Z_2-graded crystallographic groups were classified according to the Wigner-Dyson classes; we give the class of all Z_2-graded groups of order less than $|G| = 30$.

In Chapters 6 and 7, methods of taking the symmetry groups we have found here and turning them into corresponding systems will be discussed, completing the desired work.

5.1 Searching For Graded Groups

In order to classify the representations of $Z_2 \times Z_2$-graded groups, it is first necessary to be able to identify if a given group G is $Z_2 \times Z_2$-graded. Only then can the set of small groups be iterated over, classifying all the applicable $Z_2 \times Z_2$ groups.

The problem of checking if a group is $Z_2 \times Z_2$ graded is the same as checking if two homomorphisms $\phi, \xi : G \to Z_2$ exist and fulfil the requirements of a $Z_2 \times Z_2$ graded group given by Definition 2.3.1. Part of this problem has already been solved by Indenbom, [84], giving a method to find all Z_2 gradings of a given group, G:

Theorem 5.1.1 (Indenbom). *Let G be a finite group such that $2 \mid |G|$. Then the group homomorphism $\phi : G \to Z_2$ is a non-trivial Z_2-grading of G if and only if ϕ is a one dimensional irreducible representation of G such that $\phi(g) = \pm 1 \ \forall g \in G$ and $|\{g \in G \mid \phi(g) = 1\}| = |\{g \in G \mid \phi(g) = -1\}| = |G|/2$.*

Proof. Let the set of Z_2-gradings of G be $\Phi = \{\phi\}$ and the set of suitable representations of G be $P = \{\rho\}$. The if and only if requirement is equivalent to showing $\Phi = P$.

Firstly, $\Phi \subseteq P$. Let $\phi \in \Phi$. Then as a homomorphism onto $Z_2 \subset \mathbb{C}$, it is a one dimensional representation and automatically irreducible. Furthermore, $\phi(g) = \pm 1$ by definition, and as $|A| = |U|$, $|\{g \in G \mid \phi(g) = 1\}| = |\{g \in G \mid \phi(g) = -1\}|$. Then $\phi \in P \ \forall \phi \in \Phi \implies \Phi \subseteq P$.

Also, $P \subseteq \Phi$. Let $\rho \in P$, then $\rho : G \to Z_2$ as a homomorphism and $G/\ker(\rho) = Z_2$ as $|\ker(\rho)| = |G|/2$ and there is only one group of order 2. So ρ is a Z_2 grading of G and $\rho \in P$ $\forall \rho \in P \implies P \subseteq \Phi$.

$$P \subseteq \Phi \text{ and } \Phi \subseteq P \implies \Phi = P.$$

$\square$

This can be used to find all Z_2 gradings of G by identifying all suitable representations of G and taking them as the gradings. There is an obvious generalisation of Indenbom's Theorem to identify the $Z_2 \times Z_2$-graded groups, by checking if *two Z_2-gradings* exist on G and whether they interact according to Definition 2.3.1:

Theorem 5.1.2. *Let G be a group such that $4 \mid |G|$. Then the group homomorphisms $\phi, \xi : G \to Z_2$ provide a $Z_2 \times Z_2$-grading of G if and only if ϕ, ξ are orthogonal one dimensional irreducible*

representations of G such that $\phi(g) = \pm1$, $\xi(g) = \pm1$ $\forall g \in G$ and

$$|G|/2 = |\{g \in G \mid \phi(g) = 1\}| = |\{g \in G \mid \xi(g) = 1\}|$$

Proof. Let P be the set of pairs of orthogonal one dimensional representations of G fulfilling the conditions,

$$P = \left\{ (\rho_1, \rho_2) \mid \rho_1 \perp \rho_2,\ \rho_1(g) = \pm1,\ \rho_2(g) = \pm1,\ \begin{array}{ll} |\{g \in G \mid \rho_1(g) = 1\}| & = |G|/2 \\ |\{g \in G \mid \rho_2(g) = 1\}| & = |G|/2 \end{array} \right\}$$

and let $\Phi = \{(\phi, \xi)\}$ be the set of $Z_2 \times Z_2$-gradings of G. The requirement to be proved is that $\Phi = P$.

Firstly, $\Phi \subseteq P$. Let $(\phi, \xi) \in \Phi$. Then individually, ϕ, ξ are Z_2-gradings of G and are thus both one dimensional representations of G according to Theorem 5.1.1, with

$$|G|/2 = |\{g \in G \mid \phi(g) = 1\}|$$
$$= |\{g \in G \mid \xi(g) = 1\}|$$

according to the definition of a graded group. Also, $\exists g \in G$ such that $\phi(g) = -\xi(g)$ so that ϕ, ξ provide orthogonal representations as there is an element for which the characters of the two representations are different. Therefore $\Phi \subseteq P$.

Conversely, every pair $(\rho_1(g), \rho_2(g)) \in P$ provides two Z_2-gradings of G by Theorem 5.1.1. Furthermore, orthogonality of ρ_1, ρ_2 requires that

$$|\{g \in G \mid \rho_1(g) = \rho_2(g)\}| = |\{g \in G \mid \rho_1(g) = -\rho_2(g)\}| = |G|/2.$$

Combined with the requirement that $|\{g \in G \mid \rho_1(g) = 1\}| = |\{g \in G \mid \rho_2(g) = 1\}| = |G|/2$ this requires that

$$|G|/4 = |\{g \in G \mid \rho_1(g) = \rho_2(g) = 1\}|$$
$$= |\{g \in G \mid \rho_1(g) = -\rho_2(g) = 1\}|$$
$$= |\{g \in G \mid -\rho_1(g) = \rho_2(g) = 1\}|$$
$$= |\{g \in G \mid -\rho_1(g) = -\rho_2(g) = 1\}|$$

and (ρ_1, ρ_2) provides a homomorphism from G to $Z_2 \times Z_2$ that is a $Z_2 \times Z_2$ grading of G and $P \subseteq \Phi$. Thus, $P = \Phi$ and all $Z_2 \times Z_2$ gradings can be found by finding the set P. $\qquad\square$

Finding all $Z_2 \times Z_2$-graded groups is then a case of iterating over all groups G whose order is divisible by four and checking their one dimensional representations. Note that this finds only the $Z_2 \times Z_2$-graded groups such that all of A, C and P are non-empty. If a $Z_2 \times Z_2$-graded group with only one of A, C and P non-empty, then Indenbom's method for the Z_2-graded groups may be used, but with the group partitioned into the sets U and whichever of A, C and P is non-empty.

Application of these methods then requires having access to databases of groups and their characters, with the ability to work with group elements and operations. This is possible due to

the existence of programs like GAP, [60], which are designed for work exactly like this and which even have lists of the small finite groups, with their own internal orderings that can be iterated over, allowing systematic searches through the small groups.

GAP identifies a group G by a tuple $(|G|, n)$ where n is a position in an internal arbitrary ordering on the groups of order $|G|$. Conversion from GAP's notation to more human-readable labels can be found for example at [49, 124], but GAP notation is now used consistently in programming, and can be useful as a universal label for groups that have many names. Small examples of GAP's naming notation are given by $(2,1) = Z_2$, $(4,1) = Z_4$, $(4,2) = Z_2 \times Z_2$, $(6,1) = D_6$, and $(6,2) = Z_6$ while larger examples include $(32,49) = (Z_2 \times D_4) \rtimes_6 Z_2$.

Where possible, standard descriptive names for groups will be used. Code-generated results will use the modified GAP notation for a group,

$$(|G|, n) \to G_{|G|}^n, \qquad (|U|, n) \to U_{|U|}^n.$$

With GAP's databases of groups and their character tables and conjugacy classes, the algorithms discussed above can be implemented. Using its methods, it is possible to take a group and then look at the databased character table to check if any of the one-dimensional representations of G form $Z_2 \times Z_2$-gradings of G. If any do, then for each grading, it sorts the elements into the sets U, A, C, P, identifies the group U, finds its character table and then computes the Altland-Zirnbauer class for each of the irreducible representations of U for the given partition of G. This can then be printed to file for later access, and will result in the tables in Appendix E after some additional formatting has been done.

What is now required is a way to efficiently describe partitions of G. In the case of the $Z_2 \times Z_2$ graded group, to label a group G and its grading, it is sufficient to list the names of the groups $G, U, U \cup \alpha U, U \cup \gamma U$ and $U \cup \pi U$. To do this efficiently we use the pair of labels $U_{|U|}^k$ describing the unitary normal subgroup, and the tuple $G_{4|U|}^m(n, p, q)$ which contains GAP's group numbers for $G, U \cup \alpha, U \cup \gamma$ and $U \cup \pi$, the pair together being read as

$$
\begin{aligned}
U &= (|U|, k) \\
G &= (4|U|, m) \\
U_{|U|}^k, \ G_{4|U|}^m(n, p, q) \longrightarrow U \cup \alpha U &= (2|U|, n) \\
U \cup \gamma U &= (2|U|, p) \\
U \cup \pi U &= (2|U|, q)
\end{aligned}
$$

An example classifying each of the possible corepresentations of the partitions of the groups groups G with normal subgroup $U = Z_2$ is given in Table 5.1 - this covers the groups $G = Z_4 \times Z_2, Z_2^3, D_8, Q_8$, while the allowed partitions are given by,

$U_2^1, \ G_8^2(2,1,1) \to G = Z_4 \times Z_2, \ U = Z_2, \ U \cup \alpha U = Z_2^2, \ U \cup \gamma U = Z_4, \ U \cup \pi U = Z_4$

$U_2^1, \ G_8^2(1,2,1) \to G = Z_4 \times Z_2, \ U = Z_2, \ U \cup \alpha U = Z_4, \ U \cup \gamma U = Z_2^2, \ U \cup \pi U = Z_4$

$U_2^1, \ G_8^3(2,1,2) \to G = Z_2^3, \ U = Z_2, \ U \cup \alpha U = Z_2^2, \ U \cup \gamma U = Z_4, \ U \cup \pi U = Z_2^2$

$U_2^1, \ G_8^3(2,2,1) \to G = D_8, \ U = Z_2, \ U \cup \alpha U = Z_2^2, \ U \cup \gamma U = Z_2^2, \ U \cup \pi U = Z_4$

U_2^1	C_0	C_1	$G_8^2(2,1,1)$	$G_8^2(1,2,1)$	$G_8^3(2,1,2)$	$G_8^3(2,2,1)$	$G_8^4(1,1,1)$	$G_8^5(2,2,2)$
ρ_0	1	1	BDI	BDI	BDI	BDI	BDI	BDI
ρ_1	1	-1	CI	$DIII$	CI	BDI	CII	BDI

Table 5.1: The Altland-Zirnbauer classes of each $Z_2 \times Z_2$-graded group with $U = Z_2$, for each irreducible representation of U. Note how the trivial representation of U always returns the class BDI.

T^2	C^2	A	AI	AII	$AIII$	BDI	CII	D	C	CI	$DIII$
$\mathbb{I}$	$-\mathbb{I}$	A	AI	AII	$AIII$	CI	$DIII$	C	D	BDI	CII
$-\mathbb{I}$	$\mathbb{I}$	A	AII	AI	$AIII$	$DIII$	CI	D	C	CII	BDI
$-\mathbb{I}$	$-\mathbb{I}$	A	AII	AI	$AIII$	CII	BDI	C	D	$DIII$	CI

Table 5.2: The necessary substitutions to get the correct Altland-Zirnbuer class in Tables 5.1, 5.4 and in Appendix E when at least one of $\hat{\mathcal{T}}, \hat{\mathcal{C}}$ squares to $-\mathbb{I}$, [24].

$$U_2^1,\ G_8^4(1,1,1) \rightarrow G = Q_8,\ U = Z_2,\ U \cup \alpha U = Z_4,\ U \cup \gamma U = Z_4,\ U \cup \pi U = Z_4$$
$$U_2^1,\ G_8^5(2,2,2) \rightarrow G = Z_2^3,\ U = Z_2,\ U \cup \alpha U = Z_2^2,\ U \cup \gamma U = Z_2^2,\ U \cup \pi U = Z_2^2$$

when translated into the standard group names.

The independence of the classification from the exact elements used to form the sets U, A, C, P is useful, as repeatedly identifying single group elements is something computers are poor at - GAP stores group elements as a randomly ordered list, which changes with every instantiation so there is no way to guarantee that a given description of a group would generate the same group when re-entered into GAP. Thus, if the exact individual elements were needed, they would need to be identified entirely by hand to get a useable labelling on them, which would significantly increase the workload. Instead, while a partition of G must still be identified by hand, the simplest partition resulting in the groups $U, U \cup \alpha U, U \cup \gamma U$ and $U \cup \pi U$ can always be taken, this normally involves identifying three of the generating elements of G as α, γ and π and taking the subgroup generated by the remaining elements as U, though exceptions where $u = \alpha^2$ or similar do occur. This does also mean there will often be multiple possible ways of forming the partition $U_{|U|}^k,\ G_{4|U|}(n, p, q)$ when it comes to building a system.

Note that these tables of group classifications are given with the assumption that the global time-reversal and charge-conjugation operators on the system in consideration are given by $\hat{\mathcal{T}} = (\mathbb{I}_{\text{charge}} \otimes T \otimes \mathbb{I}_{\text{orbital}})\mathcal{K}$ and $\hat{\mathcal{C}} = (C \otimes \mathbb{I}_{\text{spin}} \otimes \mathbb{I}_{\text{orbital}})\mathcal{K}$ with $T^2 = C^2 = \mathbb{I}$. If this is not the case and at least one of T, C squares to $-\mathbb{I}$, then tables can still be used to identify the Altland-Zirnbauer classes of the corepresentations but under the substitutions given in Table 5.2. If these factorised forms of $\hat{\mathcal{T}}$ and $\hat{\mathcal{C}}$ are not applicable, then construction of the universal covering group of G, and then checking the entries for G' will give the correct answer.

The case where it is allowed that one of A, C is empty reduces to the problem of finding the Z_2-graded groups. There is no real difference in the process as for the $Z_2 \times Z_2$ case, except it is now sufficient to label using just G and U. Having calculated the classification of the small groups under Dyson Tenfold Way, as in Section E.1, the necessary substitutions for the Altland-Zirnbauer classes are given by Table 5.3. The example for $U = Z_2$ is given in Table 5.4 for both

	$A = \emptyset$	$C = \emptyset$
$\mathbb{R}I, \mathbb{C}I, \mathbb{H}I$	D	AI
$\mathbb{R}II, \mathbb{C}II, \mathbb{H}II$	C	AII
$\mathbb{R}III, \mathbb{C}III1, \mathbb{C}III2, \mathbb{H}III$	A	A

Table 5.3: The substitutions needed to turn the classification of a corepresentation of a Z_2-graded under Dyson's Tenfold Way, as given in Section E.1, into an Altland-Zirnbauer class of a corepresentation of a $Z_2 \times Z_2$-graded group where either $A = \emptyset$ or $C = \emptyset$. The Altland-Zirnbauer class is solely given by the second half of the Dyson class.

U_2^1	C_0	C_1	G_4^1	G_4^2
ρ_0	1	1	AI/D	AI/D
ρ_1	1	-1	AII/C	AI/D

Table 5.4: The Altland-Zirnbauer classes for each corepresentation of a $Z_2 \times Z_2$-graded group with $U = Z_2$ and either $A = \emptyset$ or $C = \emptyset$.

the case $C = \emptyset$ and $A = \emptyset$. The same substitutions given in Table 5.2 may be used in the case that $T^2 = -\mathbb{I}$ or $C^2 = -\mathbb{I}$.

Finally in the case where G is $Z_2 \times Z_2$-graded but $A = C = \emptyset$, $P \neq \emptyset$, the two Altland-Zirnbauer classes that a representation of U can generate are $A, AIII$. These can all be found by studying the Dyson Tenfold Way classification of the Z_2-graded groups as given in Theorem 2.2.15, with the mappings from Dyson's ten classes as given in Theorem 2.2.15 onto the possible two classes $A, AIII$ given by,

$$\mathbb{R}I, \mathbb{R}II, \mathbb{H}I, \mathbb{H}II, \mathbb{C}III2 \rightarrow AIII$$

$$\mathbb{C}I, \mathbb{C}II, \mathbb{R}III, \mathbb{H}III, \mathbb{C}III1 \rightarrow A$$

An example of the classification of the groups $G = U \cup P$ for $U = Z_3$ is given in Table 5.5.

U_3^1	C_0	C_1	C_3	G_6^1	G_6^2
ρ_0	1	1	1	$AIII$	$AIII$
ρ_1	1	$e^{2i\pi/3}$	$e^{-2i\pi/3}$	A	$AIII$
ρ_2	1	$e^{-2i\pi/3}$	$e^{2i\pi/3}$	A	$AIII$

Table 5.5: The Altland-Zirnbauer classes for each corepresentation of a $Z_2 \times Z_2$-graded group with $U = Z_3$, $A = C = \emptyset$ and $P \neq \emptyset$.

5.2 Minimal Examples of the Altland-Zirnbauer Tenfold Way

Having a method to search for $Z_2 \times Z_2$-graded groups and identify the ensembles they generate in their symmetry-decomposed bases when used as symmetry groups, we can now identify the groups with smallest order showing each Altland-Zirnbauer class as the minimal examples of the Altland-Zirnbauer Tenfold Way:

Theorem 5.2.1. *Let $\mathcal{Q}$ be a quantum system with global time-reversal, charge-conjugation and chiral operators so that*

$$\hat{\mathcal{T}}^2 = \mathbb{I}, \qquad \hat{\mathcal{C}}^2 = \mathbb{I}, \qquad \hat{\mathcal{P}}^2 = \mathbb{I}.$$

Then, for each Altland-Zirnbauer class there exists a graded symmetry group G of minimal order such that its normal subgroup of unitary-commuting symmetries, U, has an irreducible representation generating a corepresentation of G of that class. There is also an associated subspace in the Hilbert space of the system which displays spectral statistics matching the random matrix ensemble associated to the Altland-Zirnbauer class.

The symmetry group G takes the form $G = U \cup A \cup C \cup P$, $A = \alpha U$, $C = \gamma U$, $P = \pi U$. Allowing some of A, C, P to be empty, the relevant symmetry groups and representations are given by

Class	G	U	$U \cup \alpha U$	$U \cup \gamma U$	$U \cup \pi U$	Irreducible Representation of U
A	Z_1	Z_1				Trivial
AI	Z_2	Z_1	Z_2			Trivial
AII	Z_4	Z_2	Z_4			Sign
$AIII$	Z_2	Z_1			Z_2	Trivial
BDI	Z_2^2	Z_1	Z_2	Z_2	Z_2	Trivial
CII	Q_8	Z_2	Z_4	Z_4	Z_4	Sign
C	Z_4	Z_2		Z_4		Sign
D	Z_2	Z_1		Z_2		Trivial
$DIII$	$Z_4 \times Z_2$	Z_2	Z_4	Z_2^2	Z_4	Sign
CI	$Z_4 \times Z_2$	Z_2	Z_2^2	Z_4	Z_4	Sign

In the case that at least one of T, C doesn't square to the identity, then having taken the substitutions for the classes as given in Table 5.2, the result still holds.

Proof. It can be seen in Tables 5.1, 5.4, 5.5 that these gradings and representations give the correct Altland-Zirnbauer classes according to the Frobenius-Schur indicators. Proof that these are the minimal groups requires showing that no smaller groups exist for each example. This can be seen by referencing the tables compiled in Appendix E. $\qquad\square$

In practise, the cases where the trivial representation is used returns poor numerical simulations. For this reason we used the modified theorem:

Theorem 5.2.2. *Let $\mathcal{Q}$ be a quantum system with global time-reversal, charge-conjugation and chiral operators so that*

$$\hat{\mathcal{T}}^2 = \mathbb{I}, \qquad \hat{\mathcal{C}}^2 = \mathbb{I}, \qquad \hat{\mathcal{P}}^2 = \mathbb{I}.$$

Then, for each Altland-Zirnbauer class there exists a graded symmetry group G of minimal order such that its normal subgroup of unitary-commuting symmetries, U, has an irreducible non-trivial representation generating a corepresentation of G of that class. There is also an associated subspace in the Hilbert space of the system which displays spectral statistics matching the random matrix ensemble associated to the Altland-Zirnbauer class.

The symmetry group G takes the form $G = U \cup A \cup C \cup P$, $A = \alpha U$, $C = \gamma U$, $P = \pi U$. Allowing some of A, C, P to be empty, the relevant symmetry groups and representations are given by

Class	G	U	$U \cup \alpha U$	$U \cup \gamma U$	$U \cup \pi U$	Irreducible Representation of U
A	Z_6	Z_3	Z_6			Complex
AI	D_6	Z_3	D_6			Complex
AII	Z_4	Z_2	Z_4			Sign
$AIII$	Z_6	Z_3			Z_6	Complex
BDI	D_{12}	Z_3	D_6	D_6	Z_6	Complex
CII	Q_8	Z_2	Z_4	Z_4	Z_4	Sign
C	Z_4	Z_2		Z_4		Sign
D	D_6	Z_3		D_6		Complex
$DIII$	$Z_4 \times Z_2$	Z_2	Z_4	Z_2^2	Z_4	Sign
CI	$Z_4 \times Z_2$	Z_2	Z_2^2	Z_4	Z_4	Sign

In the case that at least one of T, C doesn't square to the identity, then having taken the substitutions for the classes as given in Table 5.2, the result still holds.

This allows for some of the sets A, C, P to be empty, in the case that it is required that all of U, A, C, P are non-empty it is still possible to find symmetry groups G to cover each of the ten Altland-Zirnbauer classes:

Theorem 5.2.3. *Let $\mathcal{Q}$ be a quantum system with global time-reversal, charge-conjugation and chiral operators so that*

$$\hat{\mathcal{T}}^2 = \mathbb{I}, \qquad \hat{\mathcal{C}}^2 = \mathbb{I}, \qquad \hat{\mathcal{P}}^2 = \mathbb{I}.$$

Then, for each Altland-Zirnbauer class there exists a graded symmetry group G of minimal order such that its normal subgroup of unitary-commuting symmetries, U, has an irreducible non-trivial representation generating a corepresentation of G of that class. There is also an associated subspace in the Hilbert space of the system which displays spectral statistics matching the random matrix ensemble associated to the Altland-Zirnbauer class.

The symmetry group G takes the form $G = U \cup A \cup C \cup P$, $A = \alpha U$, $C = \gamma U$, $P = \pi U$. Requiring all of A, C, P to be non-empty, the relevant symmetry groups and representations are given by

Class	G	U	$U \cup \alpha U$	$U \cup \gamma U$	$U \cup \pi U$	Irreducible Representation
A	$Z_2 \times M_4(2)$	Z_8	$Z_8 \times Z_2$	$M_4(2)$	$M_4(2)$	$e^{i\pi/4}$ Complex
AI	D_{12}	Z_3	D_6	Z_6	D_6	Complex
AII	Q_{16}	Z_4	Q_8	Z_8	Q_8	Complex
$AIII$	$Z_6 \times Z_2$	Z_3	Z_6	Z_6	Z_6	Complex
BDI	D_{12}	Z_3	D_6	D_6	Z_6	Complex
CII	Q_8	Z_2	Z_4	Z_4	Z_4	Sign
C	D_{12}	Z_3	Z_6	D_6	D_6	Complex
D	Q_{16}	Z_4	Z_8	Q_8	Q_8	Complex
$DIII$	$Z_4 \times Z_2$	Z_2	Z_4	Z_2^2	Z_4	Sign
CI	$Z_4 \times Z_2$	Z_2	Z_2^2	Z_4	Z_4	Sign

Where $M_4(2) = \left\langle a, b \middle| a^2 = b^8 = 1, \ aba = b^5 \right\rangle$ and
$Q_{16} = \left\langle a, b \middle| a^8 = 1, \ b^2 = a^4, \ bab^{-1} = a^{-1} \right\rangle$.

In the case that at least one of T, C doesn't square to the identity, then having taken the substitutions for the classes as given in Table 5.2, the result still holds.

Proof. See the tables in Section E.2 for the classification of the $Z_2 \times Z_2$-graded groups according to the Frobenius-Schur Indicators. It can be checked that the above examples give the stated classes, and that that there are no smaller groups fulfilling the requirements. $\square$

It of course still necessary to demonstrate experimentally that systems with these symmetry groups show the spectral statistics predicted by their Altland-Zirnbauer statistics. Developing the necessary algorithm to build systems with time-reversal symmetries in Chapter 6, and charge-conjugation and chiral symmetries in Chapter 7, this experimental confirmation will come in Sections 6.2.3 and 7.3.2.

6.   *Quantum Graphs*

So far, we have demonstrated that given a fixed global form of $\hat{\mathcal{T}}, \hat{\mathcal{C}}$ and $\hat{\mathcal{P}}$, then for any Altland-Zirnbauer class X, there exists a symmetry group G with an irreducible representation ρ_a of U generating a corepresentation of class X. Furthermore, given a suitable quantum system symmetric under G and with ρ_a in the decomposition of G's action on $\mathcal{H}$ by the corepresentation $\mathcal{R}$, then the subspace $\mathcal{H}_a$ generated by ρ_a shows random matrix statistics of type X, assuming the BGS-conjecture holds, and the system is chaotic. It is now necessary to demonstrate that such a suitable quantum system can always be found.

The first part of this problem has already been solved by Joyner, Müller and Sieber, [92], where in the specific case of a symmetry group G fulfilling the requirements that $C = P = \emptyset$ and $\alpha = e$ so that $G = U \times Z_2$ they gave an algorithm to construct a quantum graph that was symmetric under G and contained all of U's irreducible representations in G's action. Separate to [92], uni-directional quantum graphs have been used to construct systems with GSE statistics by breaking time-reversal symmetry by preventing flow in one direction along the bonds, then combining differently directed sections to build new time-reversal systems, [3]. In many ways, it is unsurprising that quantum graphs would provide a suitable model for work like this - in abstract group theory, graphs are commonly used to visualise group structure, while in physics they have long been used as models for quantum chaos, [67, 101, 102, 103, 104], as they are one of the few systems where the BGS-conjecture has been proven, [130], and explicit and simple conditions exist for a graph to show the universal behaviour associated with chaos, [62, 159].

Here, we introduce quantum graphs as a model in Section 6.1, discussing the definition of symmetry on a graph and random matrix theory in the context of quantum graphs. We expand the definition of a symmetric quantum graph to allow for generalised time-reversal symmetries, and in Section 6.2.1, we then expand the algorithm given in [92] to cover generating systems with any Z_2-graded symmetry group, $G = U \cup \alpha U$ by the application of magnetic potentials. Implementing the minimal examples for showing the Wigner-Dyson statistics according to Theorem 5.2.2, we in Section 6.2.3 demonstrate their compliance with the BGS-prediction. This will serve as a stepping stone to the Dirac graphs in Chapter 7 where quantum graphs will be modified to include particle-hole symmetry and all ten Altland-Zirnbuer classes will be constructed.

6.1   Quantum Graphs

The definition of a quantum graph begins with the definition of an abstract graph, [18, 67]:

Definition 6.1.1. *The graph Γ is the tuple $(\mathcal{V}, \mathcal{E})$ such that $\mathcal{V} = \{v_1, v_2, \ldots v_N\}$ is a set of vertex labels, and $\mathcal{E} = \{(v_i, v_j), (v_m, v_n), \ldots\}$ is a set of unordered pairs of vertices (v_i, v_j) denoting an edge connecting the vertices v_i and v_j. For ease of reading, if a graph has N vertices, they will be labelled with the integers $1, 2 \ldots N$. If $N < \infty$ then Γ will be a finite graph.*

The information contained by the graph can be represented fully by listing the number of edges between two vertices i and j. Doing this as a $N \times N$ matrix forms the adjacency matrix, A_Γ,

$$(A_\Gamma)_{ij} = |\{e \in \mathcal{E} \mid e = (i, j)\}|, \ (A_\Gamma)_{ii} = 2|\{e \in \mathcal{E} \mid e = (i, i)\}|$$

with the loops (i, i) having to be double counted, as the edge is connected to the vertex twice. The number of edges connected to a single vertex gives its valency, $d_i = \sum_j A_{ij}$.

The neighbourhood Γ_i of a vertex i is the set of vertices connected directly to it, $\Gamma_i = \{j \in \mathcal{V} \mid (i, j) \in \mathcal{E}\}$.

In most cases, we will be considering only graphs without loops so that there are no edges of the form $e = (i, i)$; and graphs without repeated edges $(A_\Gamma)_{ij} \leq 1$. This will mean that (i, j) identifies a unique edge e in $\mathcal{E}$, these graphs will be called simple graphs. Any non-simple graph can be turned into a simple graph by inserting an extra vertex into the middle of the repeated edge or loop, [67]. In this case, the neighbourhood of a vertex and its valency are connected by the relation $d_i = |\Gamma_i|$. The exception to the rule of considering only simple graphs will occur when constructing the quotient graph, where loops are common, but only in an intermediate step before methods are applied to return it to being simple. From here on out, we will assume that all the considered are simple, or have been made to be simple.

Defining position based functions on a graph will require a method of locating a point on an edge. The beginning of this process is defining a direction on each of the edges, [18, 67]:

Definition 6.1.2. *Let Γ be a simple graph, a direction can be chosen on each edge, $(i, j) \to [i, j]$ so that the edge starts at the vertex i and ends at the vertex j, $i \to j$. A directed edge is a bond and the collection of them forms the set $\mathcal{B}$.*

This defines a directed graph.

Given an undirected edge (i, j), a direction could be assigned as either $[i, j] : i \to j$ or $[j, i] : j \to i$. If $b = [i, j]$ is chosen, then $\bar{b} = [j, i]$ is the reversal of b. As they have a direction, the bonds $[i, j]$ and $[j, i]$ are not equivalent, and it is possible to define a simple directed graph containing both of them; simplicity on a directed graph requires there are no repeated *bonds*. This is important, as an undirected graph can correspond to the directed graph which also contains all the bond reversal of its bonds, [18],

$$(i, j) \in \mathcal{E} \Leftrightarrow [i, j], [j, i] \in \mathcal{B}.$$

When it comes to defining quantum graphs, it will be assumed that if $b \in \mathcal{B}$ then $\bar{b} \notin \mathcal{B}$, however when working with some concepts, it will be easier to label some quantities as if $\bar{b}$ was in $\mathcal{B}$, this is a quirk of the mathematical notation however - it really refers to the act of travelling down the bond b against the direction of the bond.

The concepts of neighbourhood and valency will extend onto the directed graph once the direction of the bonds has been accounted for, [67].

Definition 6.1.3. *Let Γ be a directed graph. Then there are two directed neighbourhoods of a vertex i based on whether a bond originates at the vertex, or terminates at the vertex,*

$$\Gamma_i^+ = \{j \in \mathcal{V} \mid [i,j] \in \mathcal{B}\}, \; \Gamma_i^- = \{j \in \mathcal{V} \mid [j,i] \in \mathcal{B}\}, \; \Gamma_i = \Gamma_i^+ \cup \Gamma_i^-$$

with the undirected neighbourhood being the union of the two directed neighbourhoods. The directed valencies of i are then given by

$$d_i^+ = \left|\Gamma_i^+\right|, \; d_i^- = \left|\Gamma_i^-\right|, \; d_i = d_i^+ + d_i^-.$$

Given a directed graph, it is now possible to assign a length L_b to each bond b so that the bond can be considered the segment of the real line $[0, L_b] \subset \mathbb{R}$. Any point along this line can then be specified as a distance x_b from the originating vertex of the bond, defining metric graph, [18].

Definition 6.1.4. *Let Γ be defined as a directed graph. Associating to each bond $b = [i,j]$ a section of the real line $[0, L_b] \subset \mathbb{R}$ with euclidean metric and position function x_b on b such that $x_b \mid_i = 0$, $x_b \mid_j = L_b$ so that if $\overline{b} \in \mathcal{B}$, $L_b = L_{\overline{b}}$ and $x_{\overline{b}} = L_b - x_b$ forms a metric graph.*

By taking the union of the intervals on each of the edges on the graph, the space on the full graph can be described as

$$V = \bigcup_{b \in \mathcal{B}} [0, L_b] \subset \mathbb{R}^{|\mathcal{B}|}.$$

Taking a vector of positions on the separate edges, $\boldsymbol{x} = \begin{pmatrix} x_1 & x_2 & \dots & x_{|\mathcal{B}|} \end{pmatrix}^T$ then allows a function space on the graph, [18],

$$L_2(\Gamma) = \bigoplus_{b \in \mathcal{B}} L_2([0, L_b]),$$

and it is possible to define a function on the graph:

Definition 6.1.5. *Let $f_i(x) : \mathbb{R} \to K^n$ be a set of $|\mathcal{B}|$ functions. Then given a metric graph Γ,*

$$F(\mathbf{x}) = (f_1^T(x_1), f_2^T(x_2), \dots f_{|\mathcal{B}|}^T(x_{|\mathcal{B}|}))^T$$

is a function on Γ, when appropriate boundary conditions are defined at each vertex in $\mathcal{V}$.

The appropriate functions for defining a standard quantum graph are the solutions to Schrödinger's equation on each bond, [16, 67, 100]:

Definition 6.1.6. *Let Γ be a metric graph with Hilbert space $\mathcal{H} = \oplus_{b \in \mathcal{B}} L_2([0, L_b])$. Define a magnetic potential A_b on each bond b. Take the functions $\psi_b(x_b) = \begin{pmatrix} \psi_b^1(x_b) & \dots & \psi_b^n(x_b) \end{pmatrix}^T$ as the n-component solutions to Schrödinger's magnetic time-independent equation,*

$$-\left(\frac{\partial}{\partial x_b} + iA_b\right)^2 \psi_b(x_b) = E_b \psi_b(x_b)$$

98

on each bond. The unconstrained solution on the whole graph is then,

$$\Psi(\mathbf{x}) = \left(\psi_1^T(x_1), \psi_2^T(x_2), \dots \psi_{|\mathcal{B}|}^T(x_{|\mathcal{B}|}) \right)^T$$

A set of boundary conditions can be given by a pair of $2n|\mathcal{B}| \times 2n|\mathcal{B}|$ matrices C_1, C_2, chosen so that $\mathrm{rank}(C_1 \mid C_2) = 2n|\mathcal{B}|$ and $C_1 C_2^\dagger = C_2 C_1^\dagger$. With the vectors

$$\Psi_1 = \begin{pmatrix} \psi_1(0) \\ \vdots \\ \psi_{|\mathcal{B}|}(0) \\ \psi_1(L_1) \\ \vdots \\ \psi_{|\mathcal{B}|}(L_{|\mathcal{B}|}) \end{pmatrix}, \qquad \Psi_2 = \begin{pmatrix} \psi_1'(0) \\ \vdots \\ \psi_{|\mathcal{B}|}'(0) \\ -\psi_1'(L_1) \\ \vdots \\ -\psi_{|\mathcal{B}|}'(L_{|\mathcal{B}|}) \end{pmatrix}$$

defined, then a valid, constrained solution on the graph then fulfils the boundary condition that

$$C_1 \Psi_1 + C_2 \left(\Psi_2 + \left(\begin{pmatrix} iA_b & 0 \\ 0 & -iA_b \end{pmatrix} \otimes \mathbb{I}_n \right) \Psi_1 \right) = 0 \tag{6.1}$$

with A_b the diagonal matrix

$$A_b = \begin{pmatrix} A_1 & & \\ & \ddots & \\ & & A_{|\mathcal{B}|} \end{pmatrix}.$$

First, we note that in almost all cases, we will consider only quantum graphs with one dimensional solutions ψ_b on their bonds, and will assume that all graphs in this Chapter are as such.

Second, the term 'quantum graph' can be used in the literature, [18], to refer more generally to a metric graph with the solution of any differential equation defined on the bonds - a definition which includes the Dirac graph which is considered in Chapter 7. Technically, the system defined above should then be known as a 'Schrödinger quantum graph', however as this term isn't used in the literature, and the common name for it is still the 'quantum graph', [67], we restrict the term to cover only the above graphs.

Third, the boundary condition requirement is designed to ensure the operators on the graph are self-adjoint and that the solution and its derivative fulfil dictated conditions at each vertex - and for any self-adjoint solution, there exists an expression for C_1 and C_2 that will generate it. Due to this, it is common to consider the boundary condition at a single vertex i. The solution and modified derivative local to the vertex can be expressed by the vector and operator, [16, 102],

$$F(i) = \oplus_{b \in \mathcal{B}: i \in b} \psi_b \mid_i, \qquad \mathcal{D}_i = \iota_i(b) \left(\frac{\partial}{\partial x_b} + iA_b \right)$$

with ι_i acting to ensure that the derivative is always taken in the outwards direction, away from the vertex. This requires negating the derivatives for incoming edges to take the derivative against

the direction of the bond,

$$\iota_i(b) = \begin{cases} 1 & b = [i,j] \\ -1 & b = [j,i] \end{cases}$$

and the boundary condition problem is now given by requiring that

$$C_1 \mid_i F(i) + C_2 \mid_i \mathcal{D}F(i) = 0 \tag{6.2}$$

at each vertex, where the expression has been simplified by subtracting the magnetic potential within the derivative. The matrices $C_1 \mid_i, C_2 \mid_i$ are the restriction of C_1 and C_2 to contain only the bonds of the form $[i,j]$ and $[j,i]$.

This can be used to construct the matrices C_1, C_2 for different types of boundary conditions at each vertex. For example, the Dirichlet boundary condition $\psi_b \mid_0 = 0 \ \forall b \in \mathcal{B}$ is given by the matrices, [18],

$$C_1 \mid_i = \mathbb{I}, \qquad C_2 \mid_i = 0$$

while the Kirchhoff or Neumann-like conditions, where the solution on each of the bonds connected to the vertex must agree at the vertex, and the total flux through the vertex must be zero, [12],

$$\psi_b \mid_i = \psi_{b'} \mid_i \ \forall b, b' \in \mathcal{B} : i \in b, b' \qquad \sum_{b \in \mathcal{B}: i \in b} \iota_i(b)\psi_b' \mid_i = 0 \tag{6.3}$$

so that the function is continuous at i and there is current conservation at the vertex, is given by the matrices

$$C_1 \mid_i = \begin{pmatrix} 1 & -1 & & & \\ & 1 & -1 & & \\ & & \ddots & \ddots & \\ & & & 1 & -1 \\ 0 & 0 & 0 & 0 & 0 \end{pmatrix}, \qquad C_2 \mid_i = \begin{pmatrix} 0 & 0 & 0 & 0 & 0 \\ 0 & 0 & 0 & 0 & 0 \\ \vdots & \vdots & \vdots & \vdots & \vdots \\ 0 & 0 & 0 & 0 & 0 \\ 1 & 1 & 1 & 1 & 1 \end{pmatrix}.$$

In most cases in the study of quantum graphs, the Kirchhoff conditions are taken at each vertex, however we will continue to allow a more general set of boundary conditions. More information on the forms of $C_1 \mid_i$ and $C_2 \mid_i$ for generating different types of boundary conditions, and other methods of parametrising the boundary conditions on quantum graphs can be found in [18].

To find the solutions $\Psi(\mathbf{x})$ on the whole graph, we begin by looking at ψ_b the solution of the one dimensional Schrödinger equation on a single bond, [16, 67],

$$\psi_b(x_b) = e^{-iA_b x_b}\left(\mu_b e^{ikx_b} + \tilde{\mu}_b e^{-ikx_b}\right)$$
$$= \mu_b e^{i(k-A_b)x_b} + \hat{\mu}_b e^{i(k+A_b)(L_b - x_b)}$$

with

$$\hat{\mu}_b = e^{-i(k+A_b)L_b}\tilde{\mu}_b, \qquad k = \sqrt{E}.$$

We see that there are two possible ways of expressing the constants that arise from solving the second order differential equation. The first pair of amplitudes, $\mu_b, \tilde{\mu}_b$, are the standard constants

100

for a second order differential equation solution, and describe a single, mixed travelling wave-packet solution; the second pair $\mu_b, \hat{\mu}_b$, treats the two solutions e^{ikx} and e^{-ikx} as the amplitudes of two travelling plane waves, the first, with amplitude μ_b travelling along b with the direction of the bond, the second, with amplitude $\hat{\mu}_b$ travelling against the direction of the bond - which is the same as travelling down the reversed bond, [67]. This explains the change in sign of A_b in the solution - the effect of the magnetic potential flips sign in taking the reversal - as well as the use of $L_b - x_b = x_{\bar{b}}$ to measure the displacement of the wave packet. Due to this, we note gain that when defining a quantum graph, bond reversals are not allowed as separate bonds as they are already counted in the solution of the original bond. We also note that $\hat{\mu}_{[i,j]} \to \mu_{[j,i]}$ is a common relabelling of the back-travelling wave amplitude which will be useful for standardising the labelling.

Both expressions $\mu_b, \tilde{\mu}_b$ and $\mu_b, \hat{\mu}_b = \mu_{\bar{b}}$ have been given, as for the purposes of working with time-reversal, using the version with $\tilde{\mu}_b$ will be easier, however outside of this, it is more common to work with $\hat{\mu}_b$.

Note that by knowing E and $\mu_b, \hat{\mu}_b$ for all $b \in \mathcal{B}$, it is possible to reconstruct the full solution Ψ of the graph. This allows a change of basis to the amplitude space, [67],

$$\Psi \to \boldsymbol{\mu} = \begin{pmatrix} \mu_1 & \dots & \mu_{|\mathcal{B}|} & \hat{\mu}_1 & \dots & \hat{\mu}_{|\mathcal{B}|} \end{pmatrix}^T.$$

A solution on the graph then requires the set of constants $\mu_b, \hat{\mu}_b$ to take values consistent with the boundary conditions expressed in Equation 6.1. To test for this, we follow [78] and express the vectors Ψ_1, Ψ_2 in terms of $\boldsymbol{\mu}$,

$$\Psi_1 = \begin{pmatrix} \mathbb{I} & e^{i(k+A_b)L_b} \\ e^{i(k-A_b)L_b} & \mathbb{I} \end{pmatrix} \boldsymbol{\mu}$$

$$\Psi_2 = \begin{pmatrix} i(k\mathbb{I} - A_b) & -i(k\mathbb{I} + A_b)e^{i(k+A_b)L_b} \\ -i(k\mathbb{I} - A_b)e^{i(k-A_b)L_b} & i(k\mathbb{I} + A_b) \end{pmatrix} \boldsymbol{\mu}$$

so that Equation 6.1 becomes

$$0 = C_1 \begin{pmatrix} \mathbb{I} & e^{i(k+A_b)L_b} \\ e^{i(k-A_b)L_b} & \mathbb{I} \end{pmatrix} \boldsymbol{\mu} + ikC_2 \begin{pmatrix} \mathbb{I} & -e^{i(k+A_b)L_b} \\ -e^{i(k-A_b)L_b} & \mathbb{I} \end{pmatrix} \boldsymbol{\mu}$$

$$= (C_1 + ikC_2)\boldsymbol{\mu} + (C_1 - ikC_2) \begin{pmatrix} 0 & e^{i(k+A_b)L_b} \\ e^{i(k-A_b)L_b} & 0 \end{pmatrix} \boldsymbol{\mu}.$$

The matrix $C_1 + ikC_2$ is always invertible for real $k \neq 0$ as it is Hermitian, [100]. Multiplying by the inverse then gives

$$\boldsymbol{\mu} = -(C_1 + ikC_2)^{-1}(C_1 - ikC_2) \begin{pmatrix} 0 & \mathbb{I} \\ \mathbb{I} & 0 \end{pmatrix} \begin{pmatrix} e^{i(k+A_b)L_b} & 0 \\ 0 & e^{i(k-A_b)L_b} \end{pmatrix} \boldsymbol{\mu} \qquad (6.4)$$

which is a requirement that $\boldsymbol{\mu}$ is invariant under the action of

$$\Xi(k) = -(C_1 + ikC_2)^{-1}(C_1 - ikC_2)\begin{pmatrix} 0 & \mathbb{I} \\ \mathbb{I} & 0 \end{pmatrix}\begin{pmatrix} e^{i(k+A_b)L_b} & 0 \\ 0 & e^{i(k-A_b)L_b} \end{pmatrix}$$

and would imply that $\boldsymbol{\mu}$ is an eigenvector of $\Xi(k)$ with eigenvalue 1.

The physical interpretation of this is as a scattering-transmission problem, [67, 103, 104],

$$\boldsymbol{\mu} = S(k)\begin{pmatrix} 0 & \mathbb{I} \\ \mathbb{I} & 0 \end{pmatrix}T(k)\boldsymbol{\mu} = \Xi(k)\boldsymbol{\mu} \tag{6.5}$$

with

$$S(k) = -(C_1 + ikC_2)^{-1}(C_1 - ikC_2), \qquad T(k) = \begin{pmatrix} e^{i(k+A_b)L_b} & 0 \\ 0 & e^{i(k-A_b)L_b} \end{pmatrix} \tag{6.6}$$

the scattering and transmission matrices. The plane waves described by the amplitudes in $\boldsymbol{\mu}$ leave a vertex and are transmitted along the bonds by $T(k)$, picking up a phase as they travel from $x_b = 0 \rightarrow x_b = L_b$. They are then incident at a vertex, the appropriate reordering of the elements being done by the $\left(\begin{smallmatrix} 0 & 1 \\ 1 & 0 \end{smallmatrix}\right)$ to get the directions right, and $S(k)$ scatters them down the connected bonds, ready to restart the process. In this case, $\Xi(k)$ can be interpreted as a sort of discrete time evolution operator, and $\boldsymbol{\mu} = \Xi(k)\boldsymbol{\mu}$ becomes the time invariance requirement of the Time Independent Schrödinger operator.

Note that the right multiplication of $(C_1 + ikC_2)^{-1}(C_1 - ikC_2)$ by $\left(\begin{smallmatrix} 0 & 1 \\ 1 & 0 \end{smallmatrix}\right)$ is often absorbed into the definition of the scattering matrix to give its 'standard' form, [100],

$$S_{\text{standard}}(k) = S(k)\begin{pmatrix} 0 & \mathbb{I} \\ \mathbb{I} & 0 \end{pmatrix}.$$

Studying symmetries of the graphs will require looking at the scattering behaviour of the graph at the vertex level. Using the vertex boundary conditions from Equation 6.2, then a local vertex scattering matrix $\sigma^{(i)}$ is defined as, [18],

$$\sigma^{(i)} = -(C_1\,|_i + ikC_2\,|_i)^{-1}(C_1\,|_i - ikC_2\,|_i), \qquad \overrightarrow{\mu}_i = \sigma^{(i)}(k)\overleftarrow{\mu}_i \tag{6.7}$$

with

$$\overrightarrow{\mu}_i = \oplus_{b=[i,j]:b \text{ or } \bar{b}\in\mathcal{B}}\mu_b, \qquad \overleftarrow{\mu}_i = \oplus_{b=[j,i]:b \text{ or } \bar{b}\in\mathcal{B}}e^{i(k+A_b)L_b}\mu_b$$

where $\overrightarrow{\mu}_i$ contains the amplitudes leaving the vertex i, and $\overleftarrow{\mu}_i$ contains the amplitudes entering the vertex i - which as $\mu_{[j,i]}$ is an amplitude leaving the vertex j, must be multiplied by the appropriate part of the transmission matrix to get its form at the end of the bond and entering i. The full scattering matrix is then reconstructed from the local vertex scattering matrices as

$$S(k)_{[k,l],[i,j]} = \delta_{jk}(\sigma^{(j)})_{[k,l],[i,j]}$$

Substituting in the vertex boundary matrices for the Kirchhoff conditions from Equation 6.3, then gives the scattering matrix, [18, 67],

$$S(k)_{[k,l],[i,j]} = \delta_{jk}\left(\frac{2}{d_j} - \delta_{il}\right)$$

so that an incoming wave at a vertex is scattered equally across all connected bonds, including backscattering.

Equation 6.5 also gives a clear statement for when an energy level E exists in the spectra of a quantum graph - there must exist a solution to the eigenvalue problem $\boldsymbol{\mu} = \Xi(\sqrt{E})\boldsymbol{\mu}$. This occurs whenever the matrix $\Xi(k)$ has an eigenvalue of value 1, defining the relationship, [67],

$$E \text{ is an energy level } \iff \zeta(E) = \det\left(\mathbb{I} - S\left(\sqrt{E}\right)T\left(\sqrt{E}\right)\right) = 0$$

which is a secular equation.

The energy level spectra of the graph can theoretically then be calculated by iterating over E, calculating the function $\zeta(E)$ from the left-hand side of the secular equation, and then running a root finding program. In practise ζ is both complex and too unstable to compute numerically, and instead the real secular equation is used, [90],

$$\zeta_{\mathbb{R}}(k) = (\det(S(k)T(k)))^{-1/2}\det\left(\mathbb{I} - S(k)T(k)\right) = 0 \tag{6.8}$$

The function $\zeta_{\mathbb{R}}(k)$ is always real, and if $S(k)$ is a constant, it simplifies to

$$\zeta_{\mathbb{R}}(k) = \frac{1}{e^{ik\sum_b L_b}\sqrt{\det(S)}}\det\left(\mathbb{I} - S(k)T(k)\right) \tag{6.9}$$

Finding the energy level spectrum is then as simple as using a numerical root finding program can on $\zeta_{\mathbb{R}}(k)$ when the degeneracy of the eigenvalues is odd. If the degeneracy of the eigenvalues is even, then all roots are repeated roots and a minimisation program on $|\zeta_{\mathbb{R}}(k)|^{1/2}$ should be used instead, as traditional root finding programs mostly need a function that changes sign when passing through the root, which a repeated root doesn't. In addition to this, numerical errors mean that it is further unlikely that the root even touches the x-axis during practical evaluation, so minimisation is a much better routine to run. By taking the square root of the absolute value of $\zeta_{\mathbb{R}}$, it is guaranteed that the function is positive and minimisation is right rather than maximisation of a negative function, and the square root increases the sharpness of the troughs, improving the speed at which the minimisation routine returns good results, [91].

6.1.1 Time-Reversal on Quantum Graphs

As a one-dimensional system, time reversal on the Schrödinger equation on the line is defined by $\hat{\mathcal{T}} = u\mathcal{K}$, $u \in \mathcal{U}(1)$, [175], and it can be seen that $\psi(-t, x)$ satisfies the conjugated time-dependent Schrödinger equation, $-i\hbar\frac{\partial}{\partial t}\psi(-t, x) = \hat{H}^*\psi(-t, x)$. It is assumed here that no phase shift is included in order to take the simplest possible form of $\hat{\mathcal{T}}$, $\hat{\mathcal{T}} = \mathcal{K}$, this also keeps the form of the time-reversal consistent with the standard forms given in Table 2.3. Its action on a solution $\psi(x)$

written in the form of the wave-packet with amplitudes $\mu, \tilde{\mu}$ is then given by

$$\hat{\mathcal{T}} : e^{-iAx}\left(\mu e^{ikx} + \tilde{\mu} e^{-ikx}\right) \rightarrow e^{iAx}\left(\mu^* e^{-ikx} + \tilde{\mu}^* e^{ikx}\right) = e^{iAx}\left(\mu' e^{ikx} + \tilde{\mu}' e^{-ikx}\right) = \psi'(x),$$

which is equivalent to the solution defined on a second line with potential $-A$ and with the new constants $\mu' = \tilde{\mu}^*$, $\tilde{\mu}' = \mu^*$ when the factors of e^{ikx} and e^{-ikx} are equated. In most cases $\psi'(x)$ will not provide a solution to the original system - the magnetic potential has been negated, and $\mu', \tilde{\mu}'$ will not fulfil the boundary conditions of $\psi(x)$, and the system has broken time-reversal symmetry.

In the case that $A = 0$ and $\mu' = \tilde{\mu}^*$, $\tilde{\mu}' = \mu^*$ are again compatible with the boundary conditions of the system, then this generates a new solution of the Schrödinger equation on the same line, and $\hat{\mathcal{T}}$ is a symmetry of the system.

This carries over onto the quantum graph - if $A_b = 0 \ \forall b \in \mathcal{B}$ and if $\hat{\mathcal{T}}\Psi$ meets the now simplified boundary condition requirement

$$C_1\Psi_1 + C_2\Psi_2 = 0 \tag{6.10}$$

then $\hat{\mathcal{T}}$ provides a symmetry of the system. This means that the symmetrised time-evolution operator $\Xi(k) = T^{1/2}(k)S(k)T^{1/2}$ must be invariant under the action of $\hat{\mathcal{T}}$, in particular that $S(k)$ is invariant under $\hat{\mathcal{T}}$, [67].

Testing the scattering matrix condition invariance requirement is easiest to do at the local vertex level, which using Equation 6.7, is equivalent to requiring that, [27],

$$\hat{\mathcal{T}}\overrightarrow{\mu}_i = \hat{\mathcal{T}}\sigma_i(k)\hat{\mathcal{T}}^{-1}\hat{\mathcal{T}}\overleftarrow{\mu}_i = \sigma^{(i)}(k)\hat{\mathcal{T}}\overleftarrow{\mu}_i. \tag{6.11}$$

Checking for this requires first calculating the action of $\hat{\mathcal{T}}$ on the vectors $\overrightarrow{\mu}_i, \overleftarrow{\mu}_i$. To do this, we look at the action of $\hat{\mathcal{T}}$ on $\boldsymbol{\mu}$, which by comparing to the single wire case can be seen to be,

$$\hat{\mathcal{T}}\begin{pmatrix} \boldsymbol{\mu} \\ \tilde{\boldsymbol{\mu}} \end{pmatrix} = \begin{pmatrix} 0 & \mathbb{I} \\ \mathbb{I} & 0 \end{pmatrix}\begin{pmatrix} \boldsymbol{\mu}^* \\ \tilde{\boldsymbol{\mu}}^* \end{pmatrix}.$$

Taking then the alternative representation of the outgoing and incoming amplitudes $\overrightarrow{\mu}_i, \overleftarrow{\mu}_i$ at i written using μ_b and $\tilde{\mu}_b$ for a vertex with outgoing bonds $1, 2, \ldots d_i^+$ and incoming bonds $d_i^+ + 1, d_i^+ + 2, \ldots d_i$, [27],

$$\overrightarrow{\mu}_i = \begin{pmatrix} \mu_1 \\ \vdots \\ \mu_{d_i^+} \\ \exp\left(-i(k + A_{d_i^+ + 1})L_{d_i^+ + 1}\right)\tilde{\mu}_{d_i^+ + 1} \\ \vdots \\ \exp\left(-i(k + A_{d_i})L_{d_i}\right)\tilde{\mu}_{d_i} \end{pmatrix}, \qquad \overleftarrow{\mu}_i = \begin{pmatrix} \tilde{\mu}_1 \\ \vdots \\ \tilde{\mu}_{d_i^+} \\ \exp\left(i(k + A_{d_i^+ + 1})L_{d_i^+ + 1}\right)\mu_{d_i^+ + 1} \\ \vdots \\ \exp\left(i(k + A_{d_i})L_{d_i}\right)\mu_{d_i} \end{pmatrix}$$

where for the outgoing bonds, $\mu_b, \tilde{\mu}_b$ are the full amplitudes as the particle has originated at the vertex and hasn't yet travelled along a bond to pick up the phase shift from the transmission

matrix; whereas they have for the incoming bonds so multipliction by the exponential from the transmission matrix is necessary, as well as switching around μ_b and $\tilde{\mu}_b$ in $\overrightarrow{\mu}_i, \overleftarrow{\mu}_i$ to make sure the particles are travelling in the right direction relative to the vertex. Then, applying $\hat{\mathcal{T}}$'s transformation of $\mu, \tilde{\mu}$ to $\overrightarrow{\mu}_i, \overleftarrow{\mu}_i$ it is seen that,

$$\overleftarrow{\mu}_{\hat{\mathcal{T}},i} = \hat{\mathcal{T}}\overleftarrow{\mu}_i = \overrightarrow{\mu}_i^{*}, \qquad \overrightarrow{\mu}_{\hat{\mathcal{T}},i} = \hat{\mathcal{T}}\overrightarrow{\mu}_i = \overleftarrow{\mu}_i^{*}.$$

Substituting this into Equation 6.11 gives

$$\overleftarrow{\mu}_i^{*} = \sigma^{(i)}(k)\overrightarrow{\mu}_i^{*}$$

which under rearrangement gives the requirement for a graph to be symmetric under $\hat{\mathcal{T}} = \mathcal{K}$ as

$$\sigma^{(i)}(k) = \sigma^{(i)T}(k). \tag{6.12}$$

This is automatically satisfied by taking the Kirchhoff boundary conditions where $\sigma^{(i)}(k)$ is symmetric, [67], which are the standard boundary conditions to work with. Because of this, it is standard to assume a graph with no magnetic potentials on any of the bonds is time-reversal symmetric, but one with magnetic potentials is not, so the magnetic potentials are used to kill time-reversal symmetry, [27, 67]. However we shall show below how careful choice of positive and negative magnetic potentials can be used to build anti-unitary symmetries into quantum graphs with forms that are more general than $\hat{\mathcal{T}} = \mathcal{K}$ and $\sigma^{(i)} = \sigma^{(i)T}$.

6.1.2 General Symmetries of Quantum Graphs

For abstract graphs, symmetries are given by the action of a group on the vertices as a permutation that preserves the connectivity of the graph, [90]:

Definition 6.1.7. *Let Γ be a graph and G a group. Define the action of G on the graph as the permutation of the vertices by*

$$g : i \to gi.$$

The action on the bonds is then

$$g : [i,j] \to [gi, gj].$$

If this leaves $\mathcal{B}$ invariant,

$$[i,j] \in \mathcal{B} \iff [gi, gj] \in \mathcal{B} \quad \forall g \in G \; i, j \in \mathcal{B}$$

then Γ is symmetric under G.

Symmetries of quantum graphs must be compliant with this definition. Furthermore, they must leave the additional structure of the quantum graph alone - the bond lengths, potentials and vertex scattering matrices. For a unitary element, this is simply ensuring nothing about the graph changes, which means preserving bond lengths, $L_{ub} = L_b$; scattering matrices, $\sigma^{(ui)} = \sigma^{(i)}$; and matrix potentials, $A_{ub} = A_b \; \forall u \in U$. On the other hand, we know that the anti-unitary symmetries include the action of time-reversing the graph as part of their action on the graph. In

the last section, it was shown that for time-reversal to be a symmetry by itself, it was necessary that $A_b = -A_b = 0$ $\forall b \in B$, and $\sigma^{(i)} = \sigma^{(i)T}$ $\forall i \in \mathcal{V}$. We note that all that is needed to include a vertex permutation alongside the time-reversal operation in the symmetry check is to include the multiplication by the unitary element on the left handside of both of these relations, defining the general anti-unitary symmetry conditions as $A_{gb} = -A_b = 0$ $\forall b \in B$, $g \in \alpha U$ and $\sigma^{(gi)} = \sigma^{(i)T}$ $\forall i \in \mathcal{V}$, $g \in \alpha U$. This is of course, also allowing for permutations of the orderings of the bonds in the entries of $\sigma^{(g)}$.

This then gives the general definition of a quantum graph with a Z_2-graded symmetry group as:

Definition 6.1.8. *Let $G = U \cup \alpha U$ be a finite Z_2-graded group and Γ a quantum graph. Define the action of G on Γ as the permutation of the vertices by*

$$g : i \rightarrow gi$$

Γ is symmetric under G if and only if the following relations hold:

$$[i,j] \in \mathcal{B} \Leftrightarrow [gi, gj] \in \mathcal{B}, \qquad L_{[gi,gj]} = L_{[i,j]}$$

$$A_{[gi,gj]} = \begin{cases} A_{[i,j]} & g \in U \\ -A_{[i,j]} & g \in \alpha U \end{cases} \qquad (\sigma^{(gi)})_{[gi,gj],[gk,gl]} = \begin{cases} (\sigma^{(i)})_{[i,j],[k,l]} & g \in U \\ (\sigma^{(i)^T})_{[i,j],[k,l]} & g \in \alpha U \end{cases}$$

In the case where $A_b = 0$ $\forall b \in \mathcal{B}$ and $\sigma^{(i)} = \sigma^{(i)T} = \sigma^{(i)}_{\text{Kirchhoff}}$ $\forall i \in \mathcal{V}$ the old definition of symmetric quantum graphs used by [92] is recovered. These graphs have only unitary symmetries and time-reversal $\hat{\mathcal{T}} = \mathcal{K}$ and have symmetry groups $G = U \times Z_2$, which produces an incredibly limited subset of the symmetric graphs under the new definition - of the 59 possible Z_2-graded groups of order at most $|G| \leq 20$, only 18 are of the form $G = U \times Z_2$ - approximately 30.5% of the total, and this proportion decreases dramatically as larger groups G are considered.

Given that unitary symmetries exist on the graph, then as per Theorem 3.1.18, there will be multiple independent sub-spectra within the energy level spectrum and when looking at the random matrix predictions it will be necessary to isolate the sub-spectra by constructing the symmetry decomposed basis, taking a change of basis to split the system into independent sub-systems.

To begin this process, we require the representation of U acting on Γ. As the unitary elements of G are solely permutations of the vertices, it permits the application of the permutation representation to define the action of U on a single bond solution ψ_b as, [90],

$$u : \psi_b \rightarrow \psi_{u^{-1}b}(x_{g^{-1}b}) \qquad \forall u \in U$$

This gives a matrix representation of U on Ψ as

$$u : \Psi \rightarrow P(u)\Psi, \qquad (P(u))_{ij} = \delta_{i,u^{-1}j} \tag{6.13}$$

with $P(u)$ a matrix permutation representation as the more general version of the regular representation, Definition 2.1.11, the regular representation actually forming the smallest permutation

106

representation of a group where there aren't elements only acting trivially - it is common for a general permutation representation to have more elements in the set being permuted than group elements. The representation of U on the amplitude space is then given by

$$u : \boldsymbol{\mu} \to \begin{pmatrix} P(u) & 0 \\ 0 & P^{-1}(u) \end{pmatrix} \boldsymbol{\mu}. \tag{6.14}$$

P is reducible, being a permutation representation, and applying Theorem 3.1.18 there exists a change of basis W such that,

$$\Gamma = \cup_a \Gamma / \rho_a = \cup_a \Gamma_a, \quad W L_2(\Gamma) W^{-1} = \oplus_a L_2(\Gamma_a), \quad W \Xi(k) W^{-1} = \oplus_a \oplus_{n=1}^{s_a} \Xi_a(k) \tag{6.15}$$

$$W \begin{pmatrix} P(u) & 0 \\ 0 & P^{-1}(u) \end{pmatrix} W^{-1} = \oplus_a \begin{pmatrix} \rho_a^T(u) & 0 \\ 0 & \rho_a^{-1T}(u) \end{pmatrix} \otimes \mathbb{I}_{s_a} \tag{6.16}$$

so that Γ splits into a number of independent sub-graphs, and the secular equation then factorises,

$$\det(\mathbb{I} - \Xi(k)) = \prod_a \det(\mathbb{I} - \Xi_a(k))^{s_a}$$

so that the spectra of Γ splits into a number independent sub-spectra, one for each unique, non-equivalent irreducible representation ρ_a in P, each with eigenvalues of degeneracy s_a. This forms the symmetry decomposed basis, with the method to choose W found in [11].

As was mentioned in Section 3.1.1 in relation to the Sinai billiard, studying a symmetry decomposed subspace is equivalent to constructing a system that is only a segment of the whole system, and adding appropriate boundary conditions at the new edges. On quantum graphs, this is the process of forming the quotient of a quantum graph, going from Γ to the quotient graph $\Gamma/(U, \rho_a)$ by removing the symmetries in U using information from an irreducible representation ρ_a of U, a method introduced in [12, 129]. The most rigorous method of defining the quotient graph is given in [11, 110]; a more intuitive method is discussed in [16, 90], which is the method we will follow.

Let Γ be a graph symmetric under a unitary symmetry group U, then a minimal sub-graph Γ_U can be defined so that $U\Gamma_U$ generates all of Γ by multiplication:

Definition 6.1.9. *Let Γ be a quantum graph symmetric under the unitary symmetry group U. Then the Fundamental Domain Γ_U is the sub-graph of Γ defined by the vertex set $\mathcal{V}_U$ and bond set $\mathcal{B}_U$:*

$$\mathcal{V}_U = \min \{v \in \mathcal{V} \mid \forall w \in \mathcal{V} \; \exists v' \in \mathcal{V}_U, u \in U \; such \; that \; w = uv'\}$$
$$\mathcal{B}_U = \{b \in \mathcal{B} \mid b = [v, v'], \; v, v' \in \mathcal{V}_U\}$$
$$\quad + \min \{b \in \mathcal{B} \mid b = [v, w] \; : \; v \in \mathcal{V}_U, w \in \Gamma_v - \mathcal{V}_U \; and \; \forall b' \in \mathcal{B} \; \exists b'' \in \mathcal{B}_U,$$
$$\quad u \in U \; b' = ub''\}$$

(a) Γ (b) Γ_U
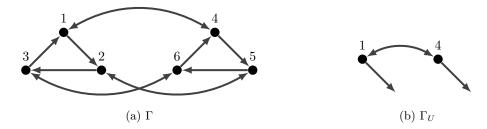
Figure 6.1: Given the graph Γ in (a) is symmetric under the group $U = Z_3$ generated by the permutation $u = (1, 2, 3)(4, 5, 6)$, the fundamental domain of U can be chosen as in (b).

Then for every point x_b on a bond b outside of Γ_U, there exists a bond $b' \in \mathcal{B}_U$ and a point $x'_{b'}$ and an element $u \in U$ such that

$$b = u^{-1}b', \qquad \psi_b(x_b) = \rho^T(u^{-1})\psi_{b'}(x'_{b'})$$

It is more common however to add dummy vertices to the centre of each of the bonds and take the fundamental domain to have its boundary on the dummy vertices, as per Figure 6.2a, in comparison to Figure 6.1. This prevents bonds existing in the graph of the fundamental domain without being connected to a vertex.

The cut bonds come in pairs $b_1 = [v_1, d_1]$, $b_2 = [d_2, v_2]$ so that $\exists u \in U$ such that $d_2 = ud_1$. Then d_2 is equated to d_1 under multiplication by u, and they can be considered the same point, merging the two cut bonds into two bonds linked at $d_2 \equiv d_1$, as per Figure 6.2b, so long as the periodic boundary condition

$$d_2 = ud_1 \equiv d_1, \qquad \psi_{[d_2, v_2]}\big|_{d_2} = \rho^T(u^{-1})\psi_{[v_1, d_1]}\big|_{d_1}$$

is taken at the vertex $d_1 \equiv d_2$. If ρ_a has dimension greater than one, this requires a multidimensional function on the bonds, where if $n = \dim(\rho_a)$, the amplitude space increases to

$$\boldsymbol{\mu} \to \begin{pmatrix} \mu_{1,1} & \cdots & \mu_{1,n} & \mu_{|\mathcal{B}|,1} & \cdots & \mu_{|\mathcal{B}|,n} & \mu_{\bar{1},1} & \cdots & \mu_{\bar{1},n} & \mu_{|\bar{\mathcal{B}}|,1} & \cdots & \mu_{|\bar{\mathcal{B}}|,n} \end{pmatrix}^T \qquad (6.17)$$

while T and S act the same on each of the components of the multi-dimensional μ_b spinor,

$$T(k) \to T(k) \otimes \mathbb{I}_n, \qquad S(k) \to S(k) \otimes \mathbb{I}_n. \qquad (6.18)$$

The periodic boundary condition can then be considered as an expression of the vertex scattering matrix,

$$\overrightarrow{\mu}_i = \sigma_i \overleftarrow{\mu}_i = \begin{pmatrix} 0 & \rho^T(u^{-1}) \\ \rho^{-T}(u^{-1}) & 0 \end{pmatrix} \overleftarrow{\mu}_i$$

or, as the dummy vertex has only two bonds connected to it, the representation matrix can instead be merged into the transmission matrix for the bond $[v_1, v_2]$,

$$T'(k)_{[v_1,v_2]} = \rho^T(u)T(k)_{[v_1,v_2]}, \qquad T'(k)_{[v_2,v_1]} = \rho^{-T}(u)T(k)_{[v_2,v_1]}$$

(a) Γ_U

(b) Fundamental domain with merged bonds

(c) Quotient Graph
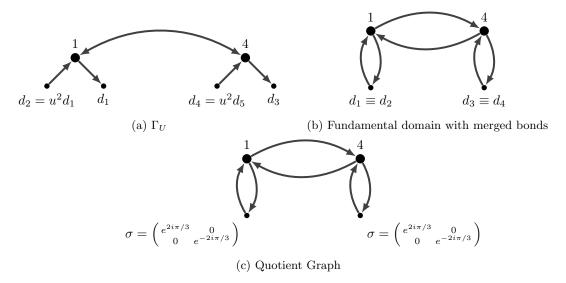
Figure 6.2: Continuing the example in Figure 6.1, the fundamental domain Γ_U is constructed using the dummy vertices (a) and then the vertices merged (b) with appropriate vertex scattering matrices taken from the boundary conditions to form the quotient graph (c) for U of the quantum graph on Γ

which if ρ is of dimension one can be interpreted as the solution picking up an additional phase while travelling on the bond; if ρ is of dimension two or more, it constitutes a mixing of the spinor states while travelling on bond.

This then defines the quotient graph:

Definition 6.1.10. *Let Γ be a quantum graph which is symmetric under a unitary group U with no fixed points. Let P be the permutation representation of U on Γ and $\rho_a \in P$ be an irreducible representation of U with $n = \dim(\rho_a)$. Let Γ_U be the fundamental domain of Γ under U with the merged dummy vertices. Then the quotient graph $\Gamma/(U, \rho_a)$ of Γ by ρ_a of U is given by Γ_U with the scattering and transmission matrices*

$$S(k) = -(C_1 \mid_{\Gamma_U} + ikC_2 \mid_{\Gamma_U})^{-1}(C_1 \mid_{\Gamma_U} - ikC_2 \mid_{\Gamma_U})$$

$$T(k)_{[i,j],[k,l]} = \delta_{ik}\delta_{jl}e^{i(k+A_{[i,j]})L_{[i,j]}} \begin{cases} 1 & inner\ bond\ on\ \Gamma_U \\ \rho^T(u) & cut\ bond\ on\ \Gamma_U\ wrt\ u \in U \end{cases}$$

6.1.3 Quantum Graphs, Quantum Chaos and Random Matrix Statistics

We consider now quantum graphs in the context of studying the correspondence between the statistics of their spectra and the statistics of random matrix ensembles. This will focus on identifying when a quantum graph can be considered a chaotic quantum system, and identifying specific expressions for the quantities $N(k)$ and $d(k)$ discussed in Chapter 4. In the process, it will be seen that quantum graphs have some highly useful properties in the context of studying quantum chaos, such as general approximations becoming exact, [67], and clear rules as to when

a graph is sufficiently chaotic to show random matrix statistics in its spectra in the semi-classical limit, [62, 159].

Historically, the correspondence of quantum graph energy levels and random matrix statistics was first seen quantitatively by Kottos and Smilansky, [101, 102], by comparing systems with and without magnetic potentials to the GUE and GOE ensembles and seeing numerical agreement in the case that the bond lengths were incommensurate, that is when

$$\nexists m \in \mathbb{Q}^{|\mathcal{B}|} \text{ such that } \sum_{i=1}^{|\mathcal{B}|} m_i L_i = 0 \tag{6.19}$$

and the graph is sufficiently connected. For symmetric graphs, the incommensurate bond lengths condition will be relaxed to requiring that the unique bond lengths are incommensurate.

A more formal approach to identifying chaotic quantum graphs requires the identification of a classical system corresponding to the quantum graph. This is in contrast to most chaotic quantum systems, where the classical system is already known as it was used to define the quantum system through quantization, [18]. However, it is possible to identify a classical system which will indicate if the quantum graph is chaotic. It will though, be probabilistic rather than deterministic - as as the clearest classical equivalent is of a ball travelling along a wire in the graph and whenever it reaches a vertex, scattering down one of the connected wires according to the Markov process, [101]:

Definition 6.1.11. *Let* Γ *be a metric graph with a quantum graph defined on it by the scattering and transition matrices* $S, T(k)$*. Then a Markov process can be defined on* Γ *for a particle on a bond* i *at one time-step moving to the bond* j *at the next time-step by the transition matrix* T,

$$T_{ji} = |S(k)_{ij}|^2 \tag{6.20}$$

With this equivalent classical system identified, the requirement for the quantum graph on Γ to show random matrix statistics in the semi-classical limit - represented on graphs as a sequence of graphs with increasing number of bonds - is then related to the eigenvalues of T, [62, 159]:

Theorem 6.1.12. *Let* T *be the transition matrix defining the Markov process on the quantum graph* Γ*. Then* T *has one eigenvalue* η_1 *such that* $\eta_1 = 1$*. Then* Γ *demonstrates quantum chaos with energy level statistics matching a random matrix ensemble if and only if*

- $|\eta_i| < 1 \ \forall i \in [2, |\mathcal{B}|]$.

- *For* $\Delta_\Gamma = \max_{i \in [2, |\mathcal{B}|]} (1 - |\eta_i|)$, *then* $\Delta_\Gamma \sim |\mathcal{B}|^{-\alpha}$ *in the limit* $|\mathcal{B}| \to \infty$ *where* $0 \leq \alpha < 1/2$.

It will not be possible to take the semi-classical limit of $|\mathcal{B}| \to \infty$ on the graphs considered later as this would require a well-defined method of taking the limit of the number of bonds to infinity, which isn't practical here, instead it will have to be assumed that the graph is sufficiently large to model the limit well. For the same reason, testing the asymptote condition for Δ_Γ in the limit $|\mathcal{B}| \to \infty$ will not be possible. However, it will be possible to test the condition that only one eigenvalue η_i lies on the unit circle, and all others lie within it, and this will be done for all the graphs which are simulated. This will at least demonstrate that the studied graphs do not fail at the first hurdle of determining whether they are chaotic or not - from there on, it will have

to be hoped that satisfying the heuristic conditions found by Kottos and Smilansky is sufficient to see good agreement with the random matrix prediction in the graph's spectrum.

The system dependent random matrix quantities can then be calculated for the quantum graphs. The counting function, [67],

$$N(k) = \sum_{n=1}^{\infty} \theta(k - k_n), \qquad \theta(k) = \begin{cases} 0 & k < 0 \\ 1/2 & k = 0 \\ 1 & k > 0 \end{cases}$$

keeps track of the number of energy levels k_n smaller than k. On quantum graphs, it can be written in terms of the secular function ζ, [67],

$$N(k) = N_0 + \frac{\sum_{b \in \mathcal{B}} L_b}{\pi d} k + \frac{1}{\pi} \operatorname{Im} \ln \zeta(\delta) - \frac{1}{\pi} \operatorname{Im} \ln \zeta(k + i\epsilon) \tag{6.21}$$

in the limit $\epsilon, \delta \to 0$, where N_0 is the value of $N(0)$. It is usual to split this into a 'smooth' or Weyl part and an 'oscillating' part,

$$N(k) = N^{Weyl}(k) + N^{osc}(k) \qquad N^{Weyl}(0) = N_0 + \frac{1}{\pi} \operatorname{Im} \ln \zeta(\delta) \tag{6.22}$$

$$N^{Weyl}(k) = \frac{\sum_{b \in \mathcal{B}} L_b}{\pi d} k + N^{Weyl}(0) \qquad N^{osc}(k) = \frac{-1}{\pi} \operatorname{Im} \ln \zeta(k + i\epsilon). \tag{6.23}$$

Further approximations of N can be taken by applying the periodic orbit approximation to $N^{\mathrm{osc}}(k)$, as discussed in Appendix D. This method of approximating $N(E)$ using a sum over periodic orbits can be applied to any generic chaotic quantum system in its semi-classical regime, however as is noted in the appendix, it becomes exact in the case of a quantum graph, [67].

With the approximation of $N(k)$, the unfolding procedure to normalise the eigenvalues from Chapter 4 - which appears as the substitution $k \to N(k)$ on the quantum graph - can be approximated as, [67],

$$k \to N(k) \to N^{\mathrm{Weyl}}(k) = \frac{\sum_{b \in \mathcal{B}} L_b}{\pi d} k + N^{Weyl}(0)$$

assuming that everything except the smooth part is highly oscillatory and averages out. In the case of calculating properties such as the level spacing distribution, where only the relative distance between eigenvalues matters, it will also be possible to drop the translation term $N^{\mathrm{Weyl}}(0)$ and use the simplified unfolding

$$k \to \frac{\sum_{b \in \mathcal{B}} L_b}{\pi d}.$$

The density of states is then the derivative of the counting function, [67],

$$d(k) = \frac{\mathrm{d}N(k)}{\mathrm{d}k} \qquad\qquad d^{Weyl}(k) = \frac{\sum_{b \in \mathcal{B}} L_b}{\pi d}$$

$$= d^{Weyl}(k) + d^{osc}(k) \qquad\qquad d^{osc}(k) = \frac{-1}{\pi} \frac{\mathrm{d}}{\mathrm{d}k} \operatorname{Im} \ln \zeta(k + i\epsilon) \tag{6.24}$$

which means the mean density of states is $\delta_0 = L/\pi d$ for $L = \sum_b L_b$. This depends only on the total length of the graph and the degeneracy of the eigenvalues, agreeing with the Wigner semi-circle law in the infinite spectrum limit.

There is of course the question of what to average over to form an ensemble. For a large graph with incommensurate bond lengths, averaging over the bulk of the spectrum for a single graph is equivalent to averaging over an ensemble of graphs and their scattering matrices $S(k)$, [67]. This will be sufficient for calculating the spacing distributions, but calculating the density of states requires information about a specific section of the spectra - in this case, averaging over an ensemble of $S(k)$ is necessary. To do this, a single graph is defined with fixed bond connectivity, length and magnetic potential, then the unique vertex scattering matrices will be drawn from the unitary matrices according to the Haar measure, then the rest of the vertex scattering matrices are derived by the symmetry rules for the vertex scattering matrices. The desired ensemble average then is found by averaging over the value calculated for a sequence of Haar distributed boundary conditions.

6.2 Minimal Examples of the Wigner-Dyson Ensembles on Quantum Graphs

6.2.1 Constructing $G = U \cup \alpha U$ Symmetric Graphs

The natural action of a symmetry group as a vertex permutation means that it will be very easy to find a graph Γ which is symmetric under a group G. Not only that, but by building the right graph, it is possible to guarantee every possible sub-spectra of the system appears. Given also that we have seen that large, well connected quantum graphs display random matrix statistics, then they are the perfect model for looking for example systems for generic symmetry groups G.

A method for building quantum graphs with symmetry groups of the form $G = U \times Z_2$ has been given in [90, 92]. As discussed above, this is a very small subset of the full range of possible Z_2-graded groups G, however the methodology can be easily updated to suit the definition of symmetry under a Z_2-graded group given by Definition 6.1.8.

Abstract group theory often applies the construction of the Cayley graph $\Gamma(G, S)$ for a given group G and generating set S:

Definition 6.2.1. *Let G be a finite group and S a generating set on G. The Cayley graph $\Gamma(G, S)$ is defined by taking the elements of the group as the vertex set, $\mathcal{V} = G$, and defining the bond set so that for each $s \in S$, there is a bond of 'colour' s between the vertices v_1, v_2 if and only if $v_2 = v_1 s$,*

$$v_1 \to_s v_2 \iff v_2 = v_1 s$$

The Cayley graph is used to display the multiplicative structure of G, and also automatically provides a graph that is symmetric under left multiplication by G.

Theorem 6.2.2. *Let G be a finite group, S a generating set of it and $\Gamma(G, S)$ its Cayley graph. Define the action of G on $\Gamma(G, S)$ as the permutation of the vertices given by matrix multiplication*

on the left,

$$g : g' \rightarrow gg'$$

Then $\Gamma(G,S)$ is symmetric under G.

Proof. As each vertex is labelled by a group element, the action of G on Γ is the action of left group multiplication within the group. The symmetry requirement is the same as the multiplication cancellation of factors rule,

$$i \rightarrow_s j \iff j = is \iff g(j = is) \iff gj = gis \iff gi \rightarrow_s gj$$

$\square$

The methodology in [92] is that given a group U, then the Cayley graph $\Gamma(U,S)$ of U can be turned into a quantum graph by taking Kirchhoff conditions at each vertex, and given lengths for the bonds $[e,s]$ $\forall s \in S$, then the quantum graph is symmetric under $G = U \times Z_2$. Their construction relies on the fact that the Cayley graph provides a base graph that fulfils the vertex permutation rule, using this graph to define the quantum graph with Kirchoff boundary conditions. With this, the only additional requirement to meet their symmetry requirements is that if two bonds can be mapped to each other by the group action, they must have the same length. The graph can be constructed to have this property, by taking a subset of bonds which are inequivalent under the group action - here this would be the bonds $[e,s]$ for $s \in S$ the generating set, as the group action cannot map bonds of one 'colour' s to bonds of a different 'colour', s' - and define the incommensurate lengths $L_{[e,s]}$ before using the symmetry rules to construct the rest of the bond lengths, rather than as a test for symmetry. This will produce a quantum graph symmetric under $G = U \times Z_2$.

To find a graph symmetric under a general $Z_2 \times Z_2$-graded group G, as per Definition 6.1.8, all that is needed is to expand the Cayley graph to be a Cayley graph of G not U, allowing the permutation part of the generalised time-reversal symmetries to exist on the elements αu; and to include the bond potentials and scattering matrices in the things that are generated for the unique bonds and vertices and then extended to the rest of the graph through the symmetry relations. This allows the following quantum graph to be constructed as a specific example of a graph symmetric under a $Z_2 \times Z_2$-graded group:

Theorem 6.2.3. *Let G be a Z_2-graded group $G = U \cup \alpha U$. Let S be a generating of G.*

The quantum graph defined by taking $\Gamma(G,S)$, choosing the quantities $L_{[e,s]}, A_{[e,s]}$ for each $s \in S$, and taking $\sigma^{(e)} \in \mathcal{U}(d_e)$, before constructing the rest of the quantities on the graph by using the relations

$$L_{[gi,gj]} = L_{[i,j]}$$

$$A_{[gi,gj]} = \begin{cases} A_{[i,j]} & g \in U \\ -A_{[i,j]} & g \in \alpha U \end{cases} \qquad (\sigma^{gi})_{[gi,gj],[gk,gi]} = \begin{cases} (\sigma_i)_{[i,j],[k,i]} & g \in U \\ (\sigma^{(i)T})_{[i,j],[k,i]} & g \in \alpha U \end{cases}$$

is symmetric under G.
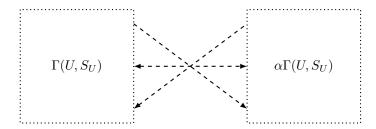
Figure 6.3: The interlinked two part structure of a quantum graph $\Gamma(G, S_U \cup \{\alpha\})$ generated by the union of the generating set S_U of the index two normal subgroup U, and α, the last remaining generator of G.

There is then the choice of how to choose the generating set S. The obvious answer is $S = S_U \cup \{\alpha\}$, where S_U is the minimal generating set of U. This, in all cases except $G = Z_{2n}$, forms the minimal generating set for G, as α provides the addition to S_U needed to take the set from generating U to generating G. Having the minimum generating set for $G \neq Z_{2n}$ is desirable as it minimises the number of bonds included in the graph, as increasing the number of bonds increases the computation time for the real secular equation, and thus all derived quantities and statistics; in the case of $G = Z_{2n}$, the minimal generating set of G is $\{\alpha\}$ which is too small to generate enough bonds on the graph with the quotient graph phases to get good numerics, so it is still better to work with $G = S_U \cup \{\alpha\}$ in this case. The other advantage of this choice is that $\Gamma(G, S_U \cup \{\alpha\})$ picks up a two part structure - it is formed by two interlinked copies of $\Gamma(U, S_U)$. One of these can be thought to be the 'original' unitary subsystem, with its image under the action of αU bolted on to preserve the symmetry under G, as seen in Figure 6.3.

This two-part structure will create a universal graph structure once quotients have been taken, and will allow for a lot of simplifications in calculating periodic orbits on the graphs.

6.2.2 Identifying and Isolating Sub-spectra

With the method given in Theorem 6.2.3 to take a group $G = U \cup \alpha U$ and find a quantum graph symmetric under it, we have fulfilled the first requirement in finding a minimal system for displaying an energy level sub-spectrum $\{E_i\}_a$ generated by the irreducible representation ρ_a. The next requirement is to show that if U acts on $\Gamma(G, S_U \cup \{\alpha\})$ as P, then ρ_a is part of the decomposition of P. By using the Cayley graph, this is guaranteed, as the permutation representation of U on $\Gamma(G, S_U \cup \{\alpha\})$ contains the regular representation which includes one copy of every irreducible representation. This is derived from the fact that a group acting on its own Cayley graph does so by its regular representation:

Lemma 6.2.4. *Let U be a group with Cayley graph $\Gamma(U, S)$. Then the permutation representation P of U acting on $\Gamma(U, S)$ is given by the regular representation.*

Proof. The definition of P in Equation 6.13 matches the Definition 2.1.11 of the regular representation when the Cayley graph is chosen. $\square$

U then acts separately on each copy of its Cayley graph in the full Cayley graph of G as its regular representation, as well as permuting the connecting bonds:

(a) When $\alpha^2 = e$ (b) When $\alpha^2 \neq e$
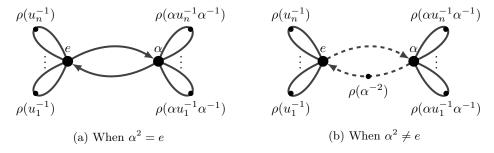
Figure 6.4: The form of the quotient graph $\Gamma(G, S_U \cup \{\alpha\})/(U, \rho)$ for Z_2-graded $G = U \cup \alpha U$ where U has n generators $u_1, \ldots u_n$ and ρ is an irreducible representation of U.

Lemma 6.2.5. *The permutation representation of U on the Cayley graph $\Gamma(G, S_U \cup \{\alpha\})$ includes a direct sum of two copies of the regular representation R_U of U,*

$$P = R_U \mid_{\Gamma(U, S_U)} \oplus R_U \mid_{\alpha \Gamma(U, S_U)} \oplus R'$$

Proof. The Cayley graph $\Gamma(G, S)$ when constructed with the generating set $S = S_U \cup \{\alpha\}$ is given by two interconnected copies of $\Gamma(U, S_U)$, $\Gamma(G, S_U \cup \{\alpha\}) = \Gamma(U, S_U) \cup \alpha \Gamma(U, S_U) \cup \Gamma'$ where Γ' forms the interlinking bonds. U acts on each sub-graph separately, and its action on each copy of $\Gamma(U, S_U)$ is its regular representation, R_U, so if R' is the permutation on Γ' under U,

$$P = R_U \mid_{\Gamma(U, S_U)} \oplus R_U \mid_{\alpha \Gamma(U, S_U)} \oplus R'$$

$\square$

Theorem 6.2.6. *Let $G = U \cup \alpha U$ be a Z_2-graded group, and $\Gamma(G, S_U \cup \{\alpha\})$ be the quantum graph generated by Theorem 6.2.3. Let U have irreducible representations $\{\rho_i\}$.*

Then $\Gamma(G, S)$ has an energy level spectrum which is composed of $|\{\rho_i\}|$ independent sub-spectra which contains a copy of the sub-spectra generated by ρ_a for every $\rho_a \in \{\rho_i\}$.

Proof. Follows directly from Lemma 6.2.5 that the action of U on $\Gamma(G, S_U \cup \{\alpha\})$ includes the regular representation of U; Theorem 2.1.12, that the regular representation contains a copy of every irreducible representation of U, so that the action of U on $\Gamma(G, S_U \cup \{\alpha\})$ includes a copy of every irreducible representation of U; and Lemma 6.2.5 to describe the splitting of the spectrum into sub-spectra with one sub-spectrum per unique irreducible representation of U in the system. $\square$

This means that for every theoretically identified sub-spectrum identified for a system, the quantum graph $\Gamma(G, S)$ includes it. This is very powerful when searching for minimal systems for the Wigner-Dyson classes, as it guarantees any identified pair of Z_2-graded group G and irreducible representation ρ of U can be found in a quantum graph.

To isolate the sub-spectra they generate, it is necessary to construct the quotient graph by U. When quotienting out U, the set $\mathcal{V}_U$ can always be taken as $\mathcal{V}_U = \{e, \alpha\}$, as every other element of G can be reached by multiplication of these two elements by members of S_U - this because G is generated by $S_U \cup \{\alpha\}$. Furthermore, the bond $[e, u_i]$ always equates to the bond $[u_i^{-1}, e]$
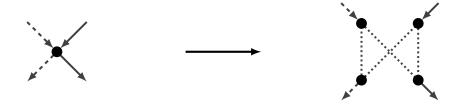
Figure 6.5: Substituting a vertex for the sub-graph given by $A_\Gamma = [[0, 1, 1, 0], [1, 0, 0, 1], [1, 0, 0, 1], [0, 1, 1, 0]]$.

$\forall u_i \in S_U$, and similarly, $[\alpha, \alpha u_i] \equiv [\alpha u_i^{-1}, \alpha]$ $\forall u_i \in S_U$ and $[\alpha, \alpha^2] \equiv [\alpha^{-1}, e]$. This generates the same universal form of quotient graph of two linked vertices with a number of self-loops coming off them for every possible $\Gamma(G, S_U \cup \{\alpha\})$, the number of loops being decided by the number of generators of U in S_U, as can be seen in Figure 6.4. Also, the phases on the cut bonds are always the same - $\rho(u_i^{-1}), \rho(\alpha u_i^{-1} \alpha^{-1})$ $\forall u_i \in S_U$ and $\rho(\alpha^2)$ for the respective bonds.

This means that if $\Gamma(G, S_U \cup \{\alpha\})/(U, \rho)$ is to be constructed to test the spectral statistics generated by the pair G, ρ, it isn't actually necessary to construct $\Gamma(G, S_U \cup \{\alpha\})$ in the first place, if $\rho(u_i^{-1}), \rho(\alpha u_i^{-1} \alpha^{-1})$ $\forall u_i \in S_U$ and $\rho(\alpha^2)$ are known, the values can just be substituted into Figure 6.4, and the correct quotient graph will be found.

There was however, the requirement of Kottos and Smilansky for seeing random matrix statistics in the spectrum that the graphs considered are simple and contain sufficiently many bonds. Both of these requirements are broken in the process of taking the quotient of the graph, however there is a method to substitute each vertex for a small sub-graph, improving the complexity, [92]. The process is demonstrated in Figure 6.5 for a single vertex with two incoming and two outgoing bonds. The single vertex is replaced with four interconnected vertices, described by the adjacency matrix $A_\Gamma = [[0, 1, 1, 0], [1, 0, 0, 1], [1, 0, 0, 1], [0, 1, 1, 0]]$. Each bond connected to the original vertex is connected to one of the four new vertices. Each one should be connected to a different vertex in the sub-graph, and if an incoming bond of type s connects to the vertex i and the corresponding outgoing bond of type s connects to j, neither $[i, j]$ or $[j, i]$ should be included in the sub-graph. This is a heuristically found rule based on experimenting with different graph structures, which is part of the requirement that the sub-graph be neither too spare or too complete to get good random matrix statistics, [91]. Furthermore, once the connecting bonds between different sub-graphs are added, no vertex should have degree less than three. For any given construction, various sub-graphs must be trialled, but it was found here that an edge density of approximately 60-75% was needed. Also, each of the original bonds should be 'doubled' so that two different copies are taken to improve the connectivity between the different sub-graphs.

There are other advantages to using the vertex sub-graphs. Firstly, taking the quotient graph introduces self-loops into the graph, when simple graphs are needed. By adding the vertex sub-graphs, the loops now start and finish at different vertices and the graph returns to being simple. Secondly, the Cayley graph relies on the directed bonds to ensure its symmetry class, however when a Cayley graph is turned into a quantum graph, the pseudo-inclusion of the bond-reversals by $\hat{\mu}_b \leftrightarrow \mu_{\bar{b}}$ can generate extra symmetries on the quantum graph. The vertex sub-graphs can then also be used to preserve the original symmetry group, firstly by having incoming bonds arrive

at one vertex and leave at a separate vertex to introduce a form of directionality on the graph, and also by being chosen to break any symmetries, [92]. It is normally sufficient to randomly choose the vertex subgraph to be used.

It should be noted that every vertex must be replaced with exactly the same vertex subgraph with the bonds entering and exiting in the same way each time to preserve the large scale symmetries of the graph.

6.2.3 Minimal Examples for the Wigner-Dyson Ensembles

The motivation for introducing Z_2-graded symmetric quantum graphs was to be able to define the smallest possible systems with each of the Wigner-Dyson ensembles describing their spectral statistics. The process for this required identifying pairs G, ρ of Z_2-graded groups and irreducible representations ρ of $U \triangleleft G$ such that ρ generated a corepresentation $\mathcal{R}$ of Wigner-Dyson type I, II or III; identifying a quantum graph generated by $\Gamma(G, S_U \cup \{\alpha\})$ and taking the quotient by ρ would then give either GOE, GUE or GSE statistics based on the class of $\mathcal{R}$. This method is now ready to test whether the groups and representations given by Theorem 5.2.2 for the classes A, AI and AII give the correct random matrix statistics.

The groups and representations identified in Theorem 5.2.2 are given in Table 6.1 - not using the examples that rely on the trivial representation, as the numerics for these are always poor when compared to the random matrix prediction. This is probably due to removing a level of complexity in the graph when the phases on the cut bonds are trivial, an example of these poor numerics is given in Figure 6.6. Implementing the groups from Table 6.1 as quantum graphs $\Gamma(G, S_U \cup \{\alpha\})$ under the algorithm given in Theorem 6.2.3, they form the graphs in Figure 6.7.

To isolate the desired subspectra and find the graph which will give the desired random matrix statistics, it is then required to take the quotients $\Gamma(G, S_U \cup \{\alpha\})/(U, \rho)$. This can be done by the procedure described in Section 6.1.2, or else the universal form of the quotient graph from Figure 6.4 can be used directly. This gives the graph in Figure 6.8, which is also presented with its expansion by a vertex subgraph. The required values of the phases $p_{1a}\rho(u^{-1})$, $p_{1b} = \rho(\alpha u^{-1}\alpha^{-1})$ and $p_{2b} = \rho(\alpha^{-2})$ needed on the cut-and-merged bonds are given in Table 6.2 for each ensemble.

Class	G	U	Irreducible Representation
A	Z_6	Z_3	Complex
AI	D_6	Z_3	Complex
AII	Z_4	Z_2	Sign

Table 6.1: The smallest Z_2-graded groups G such that there exists an irreducible representation of U generating the appropriate Altland-Zirnbauer class of corepresentation. Simpler examples of pairs G, ρ which give A and AI statistics exist, however they take ρ as the trivial representation, and simulations using the trivial representation always give poor numerics when compared to the RMT prediction, so more complicated exmples are taken here.
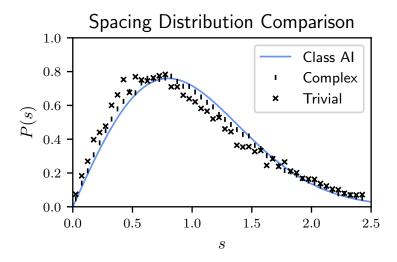
Figure 6.6: Comparing the approximation of the GOE spacing distribution for the quotient graph $\Gamma(D_6, S_U \cup \alpha)/(Z_3, \rho)$ for the trivial and complex representations of Z_3. The trivial representation shows more deviation from the true values, and this behaviour carries over to other graphs, so we avoid taking the trivial representation throughout.

(a) $\Gamma(Z_6, \{u, \alpha\})$.

(b) $\Gamma(Z_4, \{u, \alpha\})$.

(c) $\Gamma(D_6, \{u, \alpha\})$.
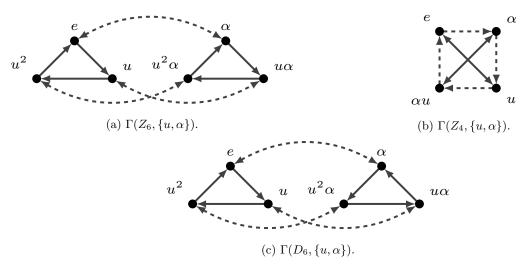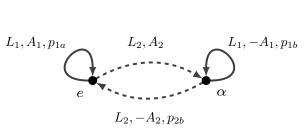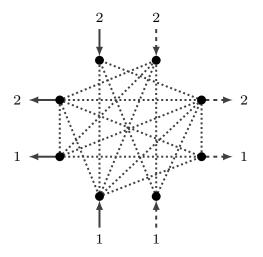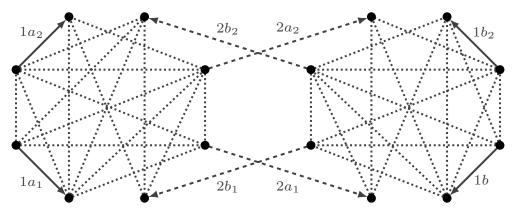
Figure 6.7: The quantum graphs generated by the algorithm of Theorem 6.2.3 as the minimal graphs with a GUE sub-spectra (a), GSE sub-spectra (b) and GOE sub-spectra (c). In each case, the solid bonds are bonds of type u; the dashed bonds are bonds of type α.

(a) Unexpanded quotient graph.

(b) Vertex Sub-graph, using 8 vertices, 19 edges and two copies of the bonds u and α.

(c) The expanded quotient graph. Each pair of bonds ia, ib have the relation $L_{ia} = L_{ib}$, $A_{ia} = -A_{ib}$. The phases $p_{ia,b}$ are chosen according to the type of quotient graph.

Figure 6.8: Deriving the example graphs for the different Wigner-Dyson classes. For the phases $p_{1a}\rho(u^{-1})$, $p_{1b} = \rho(\alpha u^{-1}\alpha^{-1})$ and $p_{2b} = \rho(\alpha^{-2})$ required to get each Wigner-Dyson class of statistics, see Table 6.2.

Class	$p_{1a} = \rho(u^{-1})$	$p_{1b} = \rho(\alpha u^{-1}\alpha^{-1})$	$p_{2b} = \rho(\alpha^{-2})$
A	$\exp(2i\pi/3)$	$\exp(2i\pi/3)$	1
AI	$\exp(2i\pi/3)$	$\exp(-2i\pi/3)$	1
AII	-1	-1	-1

Table 6.2: The values of $\rho(u^{-1})$, $\rho(\alpha u^{-1}\alpha^{-1})$ and $\rho(\alpha^{-2})$ to take on Figure 6.4 and Figure 6.8 to give each of the Wigner-Dyson ensembles as the spectral statistics.

All that is now required is to define the values required to run the numerical simulations. For each graph, the unique bond lengths and potentials are drawn uniformly from the range $[2, 5]$ which almost certainly guarantees that they are incommensurate. The unique vertex scattering matrix $\sigma^{(e)}$ is then drawn form the unitary ensemble with Haar measure. Symmetry is then used to find the values on the rest of the graph, according to Theorem 6.1.8.

This brings us to an outline of the general numerical routine used to identify energy levels or eigenvalues of the system. The general problem will be to identify all energy levels occurring in an unfolded range $k \in (k_L, k_H)$; this corresponds to finding all the roots of $\zeta(k)$ in this range when $d = 1$ or all the minima of $|\zeta(k)|^{1/2}$ when $d = 2$. The process is fairly simple in each case. First, when $d = 1$, then by calculating $\zeta(k_i)$ for $k_i = k_L + i\delta k$, a series of equally spaced points in the range $k \in (k_L, k_H)$, a grid search can be done for the roots - if $\text{sign}(\zeta(k_i)) = -\text{sign}(\zeta(k_{i+1}))$, then there is a root in the range (k_i, k_{i+1}). This bounds each of the roots, and then a root finding program can be run on each root individually to locate it more precisely. When $d = 2$, the main difference is switching to tracking the derivative of $|\zeta(k)|^{1/2}$. Using the points $k_i = k_L + i\delta k$ to do a grid search for the minima, there is a minima in the range (k_i, k_{i+1}) if $\text{sign}(d|\zeta(k_i)|^{1/2}/dk) - \text{sign}(d|\zeta(k_{i+1})|^{1/2}/dk) = -2$. This bounds the minima, and allows a bounded optimisation to be done to locate each individual minima; choosing the bounded version to make sure the local minima and not a global minima is found.

We note that when the constant average level density, δ_0 holds, and the unfolding is taken as $k \to k/\delta_0$, it is expected to find $(k_H - k_L)/\delta_0$ eigenvalues in the range $k \in (k_L, k_H)$. In the more general case when the unfolding $k \to f(k) = \lambda$ has to be used, then N eigenvalues are predicted to lie in a range $k \in [f^{-1}(\lambda_0), f^{-1}(\lambda_0 + N)]$, where the unfolded spectrum having mean level spacing 1 has been used to predict N eigenvalues in the range $\lambda \in (\lambda_0, \lambda_0 + N)$ and then the inverse unfolding procedure has been taken. These methods will allow us to define the necessary search ranges to find specific number of eigenvalues in our simulations.

We also note that there is an algorithm used in [144] that uses the rotation of the eigen-angles to find the roots that is faster than straight calculation of the real secular equation method described above, however given the number of eigenvalues computed here, the method used was sufficiently fast for our calculations.

In terms of the measures we are approximating, simulating the level spacing distribution can then be done by calculating 10,000 eigenvalues on a single graph by searching for all eigenvalues in the range $k \in (k_0, k_0 + 10,000\delta_0)$, unfolding them by using $k \to k/\delta_0 = \lambda$ and then taking the distance between consecutive levels to form their distribution. As remarked earlier, it is sufficient here to work on a single realisation of the graph rather than an ensemble of graphs as long s sufficient eigenvalues are taken.

Class	$|\eta_1|$	$|\eta_2|$
A	1.00	0.917
AI	1.00	0.874
AII	$0.999\overline{9}$	0.925

Table 6.3: Checking the values of the eigenvalues of $T_{ij} = |S(k)_{ji}|^2$ according to Theorem 6.1.11. Assuming the eigenvalues are ordered so that $|\eta_1| \geq |\eta_2| \geq \cdots \geq |\eta_N|$, then the first requirement for chaos is that $|\eta_1| = 1$ and $|\eta_2| < 1$. In each case the condition is satisfied. All numbers rounded to three significant figures and come from a single initialisation.

If the smallest eigenvalue distribution is being calculated, then an ensemble of similar graphs must be created. This is done by defining a number of graphs according to Definition 6.2.3 with the same Cayley graph, bond lengths and potentials, but for each copy of the quantum graph, the unique vertex scattering matrix $\sigma^{(e)}$ is drawn repeatedly from $\mathcal{U}(d_e)$ by the Haar measure to form an ensemble of graphs. In this case, 10,000 graphs were created in this manner. The real secular equation is then calculated for increasing k until a root is located for each graph, before its value is unfolded and being added to the distribution. The more accurate unfolding procedure is needed for this method, taking $k \to k/\delta_0 + \operatorname{Im}\ln(\zeta(\delta))/\pi = \lambda$, $\delta \approx 0$, to remove the translation of the energy spectrum by $N^{\mathrm{osc}}(k)$, which will vary for each realisation of the graph. This also allows us to identify the start of the search range for the eigenvalue as $k = -(\operatorname{Im}\ln\zeta(\delta))/\delta_0\pi$, as the value which unfolds to $\lambda = 0$.

We now come to the results of our simulations.

Firstly, the first condition for chaos required from Theorem 6.1.11 can be checked, with the results given in Table 6.3 showing compliance with the requirement that the matrix $T_{ij} = |S(k)_{ji}|^2$ has one eigenvalue of size 1, and all others lie within the unit circle. This confirms that the graphs are mixing, and do not necessarily fail to show chaos.

The results of the numerical simulations in terms of the level spacing distribution and smallest eigenvalue distribution are then presented in Figures 6.9-6.14.

The spacing distributions for the classes A, AI and AII are given in Figures 6.9, 6.11 and 6.13 respectively, with the probability distributions, and integrated probability distributions compared to the theoretical predictions, and with the errors plotted to show that the absolute error is small - of the order 10^{-2} for the probability distributions of the classes A and AI, while the class AII graph has error of order 10^{-1}. The error in the integrated distribution is in each case of the order 10^{-2}.

The smallest eigenvalue distributions for the classes A, AI and AII are given in Figures 6.10, 6.12 and 6.14 respectively, with the probability distributions, and integrated probability distributions compared to the theoretical predictions, and with the errors also given. The relative error in the probability distribution is now large, of the order 10^1, however as it is highly oscillatory, the error in the integrated distribution is significantly smaller. A large factor in this is probably the trade off between choosing to do a large number of runs on a comaparetively small graph - the graphs here feature 38 bonds, and when graphs with 136 bonds were tested for the class AI Dirac graph using 10,000 runs, as seen in Figure 7.18, the error was significantly smaller despite using fewer runs - 1/10th of the runs to be accurate. This holds true for the corresponding graphs

for the classes A and AII as well. The choice to use a small number of bonds but large ensemble was made here as the spacing distributions were also being calculated on the graphs, where the number of bonds has a large effect on the computational time required and it was chosen to prioritise good all-around statistics, particularly when it was only the probability distribution $P_{\min}(x)$ that was seeing large oscillatory errors.

Overall, in each case it can be seen that the graphs correspond well to their respective random matrix statistics, supporting the BGS-conjecture on quantum graphs.
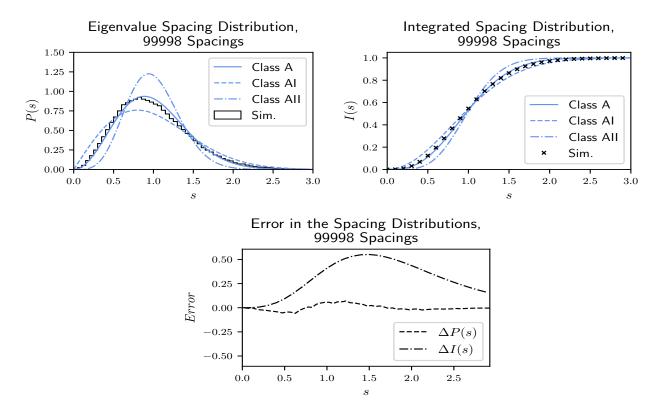
Figure 6.9: Spacing distribution results for $\Gamma(Z_6, \{u, \alpha\})/(Z_3, \rho)$ for the complex representation, demonstrating agreement with the predicted class A GUE ensemble.
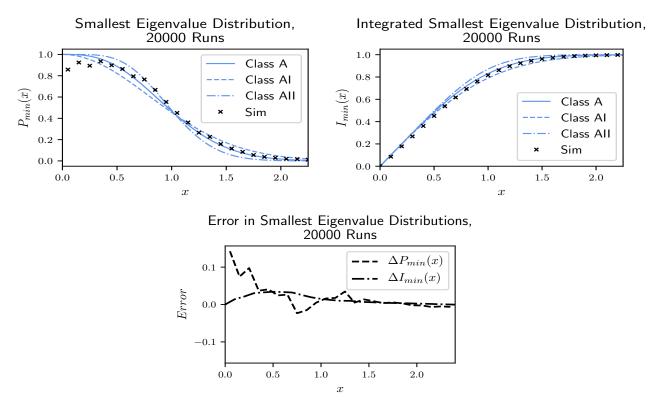
Figure 6.10: Smallest eigenvalue distribution results for $\Gamma(Z_6, \{u, \alpha\})/(Z_3, \rho)$ for the complex representation, demonstrating agreement with the predicted class A GUE ensemble.
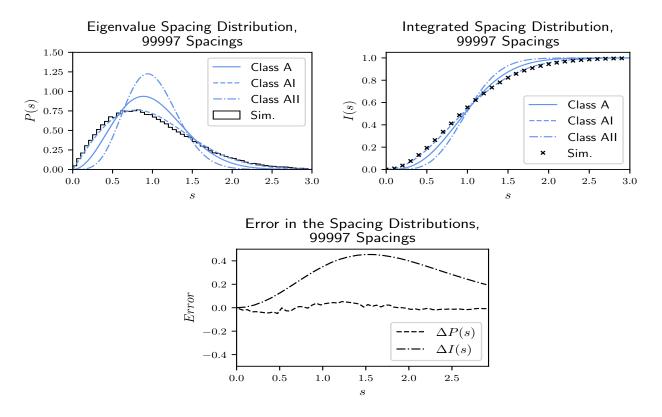
Figure 6.11: Spacing distribution results for $\Gamma(D_6, \{u, \alpha\})/(Z_3, \rho)$ for the complex representation, demonstrating agreement with the predicted class AI GOE ensemble.
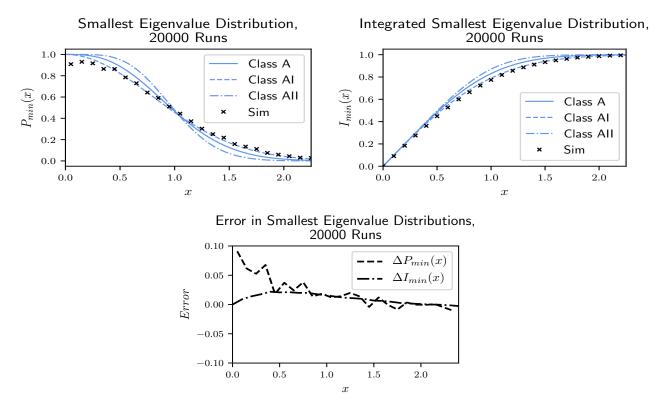
Figure 6.12: Smallest eigenvalue distribution results for $\Gamma(D_6, \{u, \alpha\})/(Z_3, \rho)$ for the complex representation, demonstrating agreement with the predicted class AI GOE ensemble.
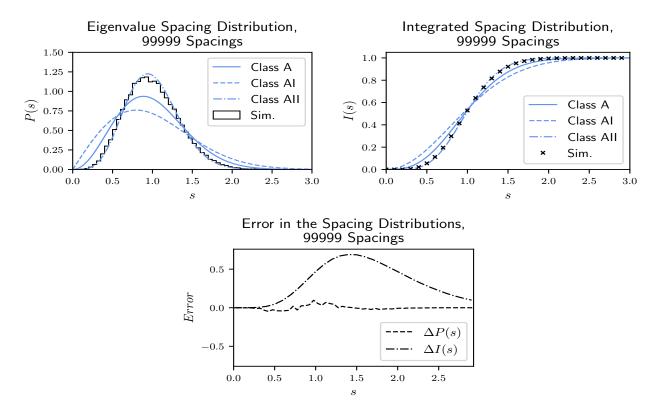
Figure 6.13: Spacing distribution results for $\Gamma(Z_4, \{u, \alpha\})/(Z_2, \rho)$ for the sign representation, demonstrating agreement with the predicted class AII GSE ensemble.
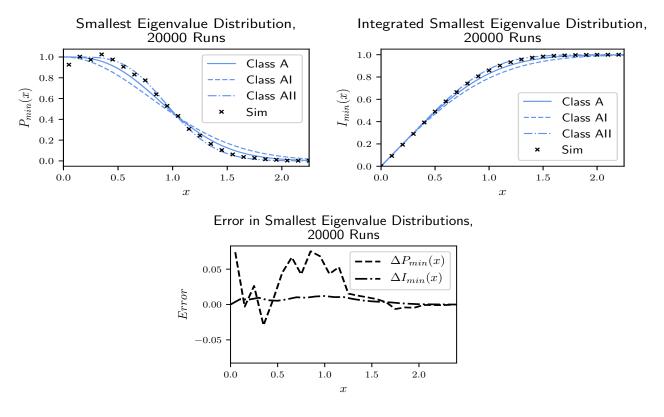
Figure 6.14: Smallest eigenvalue distribution results for $\Gamma(Z_4, \{u, \alpha\})/(Z_2, \rho)$ for the sign representation, demonstrating agreement with the predicted class AII GSE ensemble.

7. Dirac Graphs

The intent set out at the start of this thesis was to demonstrate that there was a single type of system with fixed $\hat{\mathcal{T}}$, $\hat{\mathcal{C}}$ symmetries, which under the addition of further unitary commuting symmetries, could be used to construct an example system for each type of random matrix statistics from the Altland-Zirnbauer classification through the formation of sub-spectra in the energy level spectrum. Theorem 5.2.2 has already identified for each ensemble a graded symmetry group G and a representation ρ of U generating the subspace which will show these statistics; what remains is to show that there is a type of system that can be constructed to be symmetric under G and include this subspace. We will actually go further, and demonstrate that these systems can be constructed to be symmetric under every possible symmetry group G described by Altland and Zirnbauer, and contain all of the possible subspaces and sub-spectra for the pair G, U.

Chapter 6 already covered constructing systems for the classes A, AI and AII by applying the Cayley graph geometry to the Schrödinger quntum graph. However, as the potential-less Schrödinger equation does not permit negative solutions, it is not a suitable system for any of the ensembles which involve a form of charge-conjugation or chiral symmetry - the classes AIII, BDI, CII, C, D, CI and DIII. However if a variant of the quantum graph which replaced the solutions of the Schrödinger equation on the bonds with the solutions of some quantum equation with charge-conjugation symmetry could be taken, then it would be possible to describe charge-conjugation and chiral symmetric graphs. This would allow the algorithms of Chapter 6 to be supplanted on to the the new type of graph, in particular using the Cayley graph geometry to define a system symmetric under a symmetry group G with all of the associated sub-spectra appearing in the energy level spectrum, and being able to be isolated through the quotient graph procedure.

There are several known methods of constructing these charge-conjugation symmetric quantum graphs, [77], though two are of particular interest - the Andreev graph, and the Dirac graph.

First, the Andreev graph, [144], uses the Bogolubov-de Gennes Hamiltonian from Equation C.10,

$$\hat{H} = \begin{pmatrix} \hat{h} + \hat{V} & \Delta \\ -\Delta^* & -\hat{h}^T - \hat{V}^T \end{pmatrix}, \qquad \psi(x) = \begin{pmatrix} u_\uparrow(x) \\ u_\downarrow(x) \\ v_\uparrow(x) \\ v_\downarrow(x) \end{pmatrix}$$

as an alternative to the Schrödinger equation to define the functions on the bonds. The particles and holes travel along normal-conducting quantum wires forming the graph bonds, hitting su-

perconductor boundaries at the vertices and experiencing Andreev reflection, [144], converting particles into holes that also pick up a phase factor based on an order parameter of the superconductor. The Andreev graphs have already seen use in building systems with each of the ten Altland-Zirnbauer ensembles, by drawing the exterior vertex scattering matrices of a star graph from the desired Altand-Zirnbauer ensemble, [64, 144], however they provide a poor fit for generalising the Cayley graph algorithm discussed above due to the action of a group U on a solution being given by the representation

$$\rho \to \begin{pmatrix} \rho & 0 \\ 0 & \rho^* \end{pmatrix}$$

on the particle-hole space, [24]. The complex conjugate on the action on the hole space means that the quotient can't be used to control the killing of the particle-hole symmetry in the same way it killed the time-reversal symmetries on the Schrödinger quantum graph when quotients are taken.

Thus, we turn to the Dirac graph defined by Bulla and Trenkler, [31], by putting the one dimensional Dirac operator onto the graph. These graphs behave much more similarly to the Schrödinger quantum graphs and will be able to be transplanted almost directly into the algorithms for defining symmetric quantum graphs and their quotients lifted from Chapter 6 to give methods for defining symmetric Dirac graphs and their quotients.

Therefore we will discuss the definition of a Dirac graph in Section 7.1. We will then introduce the notion of time-reversal symmetry on Dirac graphs as studied by [27, 78] and add new definitions of charge-conjugation and chiral symmetry on Dirac graphs in Section 7.2.1. From here, the general definition of a symmetric Dirac graph can now be given in Section 7.2.2. Finally, in Section 7.3.1 we extend the algorithm from Theorem 6.2.3 to take a $Z_2 \times Z_2$-graded symmetry group G and derive a compliant Dirac graph, applying it to the examples given in Theorem 5.2.2 as the minimal examples for each of the Altland-Zirnbauer ensembles. The results will be given in Section 7.3.2, demonstrating the expected random matrix agreement and completing the aims of this work.

7.1 The Dirac Graph

7.1.1 The Dirac Equation on the Line

The Dirac equation was introduced by Dirac as a model for relativistic electrons, with its standard presentation being a four-dimensional equation over three dimensional space, [161]:

Definition 7.1.1. *Let $\mathcal{H} = L_2(\mathbb{R}^3)^4$ be a Hilbert space, then the Hamiltonian describing a charge e particle in the external electromagnetic field $(\phi, \mathbf{A})$ is*

$$\hat{H}(e) = c\boldsymbol{\alpha} \cdot \left(\mathbf{p} - \frac{e}{c}\mathbf{A}(t, \mathbf{x})\right) + \beta mc^2 + e\phi(t, \mathbf{x}) \tag{7.1}$$

where $\boldsymbol{\alpha} = (\alpha_1, \alpha_2, \alpha_3)$, and α_i, β define a Dirac Algebra,

$$\alpha_i, \beta \in \mathbb{C}^{4\times 4}, \qquad \alpha_i^2 = \beta^2 = \mathbb{I}, \qquad \begin{aligned}[\alpha_i, \alpha_j] &= 2\delta_{ij}\mathbb{I}.\\ [\alpha_i, \beta] &= 0.\end{aligned} \tag{7.2}$$

The standard representation of α, β is given by taking the Pauli matrices,

$$\sigma_1 = \begin{pmatrix} 0 & 1 \\ 1 & 0 \end{pmatrix}, \qquad \sigma_2 = \begin{pmatrix} 0 & -i \\ i & 0 \end{pmatrix}, \qquad \sigma_3 = \begin{pmatrix} 1 & 0 \\ 0 & -1 \end{pmatrix}$$

with α_i and β then defined as

$$\alpha_i = \begin{pmatrix} 0 & \sigma_i \\ \sigma_i & 0 \end{pmatrix}, \qquad \beta = \begin{pmatrix} \mathbb{I}_2 & 0 \\ 0 & -\mathbb{I}_2 \end{pmatrix}. \tag{7.3}$$

The time-dependent Dirac equation is then given by

$$\hat{H}(e)\psi(e; t, \mathbf{x}) = i\hbar \frac{\partial}{\partial t} \psi(e; t, \mathbf{x}) \tag{7.4}$$

while the time-independent Dirac equation is

$$\hat{H}(e)\psi(e, E; \mathbf{x}) = E\psi(e, E; \mathbf{x}) \tag{7.5}$$

The solutions ψ include e inside the brackets as though it is not a free variable for ψ, it does affect the form of ψ by being a variable for $\hat{H}(e)$, so it will be useful to locate e in ψ as a variable for when comparisons between solutions $\psi(e), \psi(e')$ with different charges are made. This is the same reason that E appears as a variable for the time-independent equation, comparisons will be made between eigen-solutions for different values of E.

There are some simplifications which can be made to Equation 7.1. Firstly, for our purposes, it can be assumed that $\phi = 0$, $\hbar = c = 1$ and that $\mathbf{A}(t, \mathbf{x}) = \mathbf{A}$ is a constant when working on a graph. Secondly, defining the Dirac equation on a graph will require its restriction to one spacial dimension variable. This can be taken by considering only one of the α_1, α_2 or α_3 components - here taking α_2 component. In the one-dimensional case, it is also possible to satisfy the Dirac algebra requirement with 2×2 matrices found by taking a transform of α_2 and β into a block diagonal form, however, we choose to stick with the standard four-dimensional α_2 and β matrices, to be able to use the standard charge conjugation operator for the Dirac equation.

With these modifications, the Dirac equation then becomes, [27],

$$\hat{H}(e) = \alpha_2 \left(-i\frac{\partial}{\partial x} - eA \right) + \beta m \tag{7.6}$$

which in expanded form is

$$
\hat{H}(e) =
\begin{pmatrix}
0 & 0 & 0 & -1 \\
0 & 0 & 1 & 0 \\
0 & -1 & 0 & 0 \\
1 & 0 & 0 & 0
\end{pmatrix}
\frac{\partial}{\partial x} +
\begin{pmatrix}
m & 0 & 0 & eiA \\
0 & m & -eiA & 0 \\
0 & eiA & -m & 0 \\
-eiA & 0 & 0 & -m
\end{pmatrix}.
$$

The time-independent Dirac equation then takes the form

$$
\begin{pmatrix}
w' \\
x' \\
y' \\
z'
\end{pmatrix}
=
\begin{pmatrix}
eiA & 0 & 0 & E+m \\
0 & eiA & -E-m & 0 \\
0 & E-m & eiA & 0 \\
-E+m & 0 & 0 & eiA
\end{pmatrix}
\begin{pmatrix}
w \\
x \\
y \\
z
\end{pmatrix},
$$

which can be solved as a linear ordinary partial differential equation, having the plane-wave positive energy solutions, [27],

$$
\psi(e, E > 0; x) = e^{ieAx}
\left(
\mu_\alpha
\begin{pmatrix}
1 \\
0 \\
0 \\
i\gamma(k)
\end{pmatrix}
e^{ikx} + \mu_\beta
\begin{pmatrix}
0 \\
1 \\
-i\gamma(k) \\
0
\end{pmatrix}
e^{ikx}
\right.
$$
$$
\left.
+\hat{\mu}_\alpha
\begin{pmatrix}
1 \\
0 \\
0 \\
-i\gamma(k)
\end{pmatrix}
e^{-ikx} + \hat{\mu}_\beta
\begin{pmatrix}
0 \\
1 \\
i\gamma(k) \\
0
\end{pmatrix}
e^{-ikx}
\right)
$$

(7.7)

with,

$$
k = \sqrt{E^2 - m^2}, \qquad \gamma(k) = \frac{\sqrt{k^2 + m^2} - m}{k} = \frac{|E| - m}{\sqrt{E^2 - m^2}}.
$$

At this point the labelling the amplitudes $\mu_\alpha, \mu_\beta, \hat{\mu}_\alpha, \hat{\mu}_\beta$ of the component exponential solutions may seem arbitrary, but there will be useful structure and physical interpretation possible once the operation of particle-hole inversion is discussed.

Unlike the Schrödinger equation where negative energy solutions require a potential, negative energy solutions $E < 0$ are also now consistent with the definition of the potential-less Dirac

equation in Equation 7.6, and take the form,

$$\psi(e, E < 0; x) = e^{ieAx} \left(\mu_\alpha \begin{pmatrix} i\gamma(k) \\ 0 \\ 0 \\ 1 \end{pmatrix} e^{ikx} + \mu_\beta \begin{pmatrix} 0 \\ -i\gamma(k) \\ 1 \\ 0 \end{pmatrix} e^{ikx} \right.$$

$$\left. + \hat{\mu}_\alpha \begin{pmatrix} -i\gamma(k) \\ 0 \\ 0 \\ 1 \end{pmatrix} e^{-ikx} + \hat{\mu}_\beta \begin{pmatrix} 0 \\ i\gamma(k) \\ 1 \\ 0 \end{pmatrix} e^{-ikx} \right).$$

(7.8)

In the case $m = 0$ for massless particles, these equations can be combined and the solution for any energy is given by

$$\psi(e, E \neq 0; x) = e^{ieAx} \left(\mathrm{sgn}(E)\mu_\alpha \begin{pmatrix} 1 \\ 0 \\ 0 \\ i \end{pmatrix} e^{iEx} + \mu_\beta \begin{pmatrix} 0 \\ 1 \\ -i \\ 0 \end{pmatrix} e^{iEx} \right.$$

$$\left. + \hat{\mu}_\alpha \begin{pmatrix} 1 \\ 0 \\ 0 \\ -i \end{pmatrix} e^{-iEx} + \mathrm{sgn}(E)\hat{\mu}_\beta \begin{pmatrix} 0 \\ 1 \\ i \\ 0 \end{pmatrix} e^{-iEx} \right) e^{i\pi(1-\theta(E))/2}$$

$$= e^{ieAx} \left(\mu_\alpha(e, E) \begin{pmatrix} 1 \\ 0 \\ 0 \\ i \end{pmatrix} e^{iEx} + \mu_\beta(e, E) \begin{pmatrix} 0 \\ 1 \\ -i \\ 0 \end{pmatrix} e^{iEx} \right.$$

$$\left. + \hat{\mu}_\alpha(e, E) \begin{pmatrix} 1 \\ 0 \\ 0 \\ -i \end{pmatrix} e^{-iEx} + \hat{\mu}_\beta(e, E) \begin{pmatrix} 0 \\ 1 \\ i \\ 0 \end{pmatrix} e^{-iEx} \right)$$

$$\psi(e, E = 0; x) = e^{ieAx} \begin{pmatrix} \mu_\alpha \\ \mu_\beta \\ \hat{\mu}_\alpha \\ \hat{\mu}_\beta \end{pmatrix},$$

where the dependence of the amplitudes $\mu_\alpha, \mu_\beta, \hat{\mu}_\alpha$ and $\hat{\mu}_\beta$ on e, E is now explicit. It will be assumed in calculations later that $m = 0$, which is allowable, as a non-negative mass would only cause a translation of the energy level statistics along the real line. This would mean that by the

definition of k, $k = |E|$ and $\gamma(k) = 1$, however, if calculating the $m = 0$ solution directly, it would be found that the correct substitution is $k \to E$. In the following, it will be easiest to work with the generic k, and only take the limit $m \to 0$, with the replacement $k = E$ at the end.

Negative energy solutions for a particle make no physical sense, so instead anti-particles are constructed - particles with all the same physical properties as the original, except for their reversed charge. For electrons e^-, this defines the positron e^+ with charge $-e$, having taken e as negative. They have solutions to the Dirac equation given by,

$$
\psi(-e, E > 0; x) = e^{-ieAx} \left(\mu'_\alpha \begin{pmatrix} 1 \\ 0 \\ 0 \\ i\gamma(k) \end{pmatrix} e^{ikx} + \mu'_\beta \begin{pmatrix} 0 \\ 1 \\ -i\gamma(k) \\ 0 \end{pmatrix} e^{ikx} \right.
$$
$$
\left. + \hat{\mu}'_\alpha \begin{pmatrix} 1 \\ 0 \\ 0 \\ -i\gamma(k) \end{pmatrix} e^{-ikx} + \hat{\mu}'_\beta \begin{pmatrix} 0 \\ 1 \\ i\gamma(k) \\ 0 \end{pmatrix} e^{-ikx} \right)
$$

(7.9)

which are related to the negative energy electron solutions by the charge conjugation operator $\hat{\mathcal{C}}$, [161],

$$
\hat{\mathcal{C}} = i\beta\alpha_2\mathcal{K} = \begin{pmatrix} 0 & 0 & 0 & 1 \\ 0 & 0 & -1 & 0 \\ 0 & -1 & 0 & 0 \\ 1 & 0 & 0 & 0 \end{pmatrix} \mathcal{K}, \qquad \hat{\mathcal{C}}\hat{H}(e) = -\hat{H}(-e)\hat{\mathcal{C}}, \qquad \psi(e, -E; x) = \hat{\mathcal{C}}\psi(-e, E; x).
$$

(7.10)

A negative energy $-E < 0$ solution for a charge e is then considered to be a charge-conjugated positive energy solution for the anti-particle with charge $-e$. The eigenbasis of the system can then be considered not to consist of electron states of both positive and negative energy, but to consist of states describing positive energy electrons, and states describing charge-conjugated positive energy positrons, so the energy in each eigenstate is positive,

$$
\{\psi(e, E > 0)\} \cup \{\psi(e, -E < 0)\} \longrightarrow \{\psi(e, E > 0)\} \cup \left\{\hat{\mathcal{C}}\psi(-e, E > 0)\right\},
$$

keeping the system consistent with the physical interpretation where $E > 0$ must hold without negative potential. This also allows the four spinors labelled by their amplitudes $\mu_\alpha, \mu_\beta, \hat{\mu}_\alpha, \hat{\mu}_\beta$ to take the physical interpretation of a forward travelling electron wave-packet with amplitudes $\mu_\alpha, \hat{\mu}_\alpha$ and a backwards travelling positron wave packet with amplitudes $\mu_\beta, \hat{\mu}_\beta$.

There are two other details to note with regards to the symmetries of the Dirac Equation on the line $[-L, L]$. Firstly, as it takes only the first partial derivative in x, not the second, even when there is no magnetic field, a solution ψ is not symmetric under $x \to -x$. Secondly, the

time-reversal operator can be defined as, [27],

$$\hat{\mathcal{T}} = -\begin{pmatrix} \sigma_2 & 0 \\ 0 & \sigma_2 \end{pmatrix}\mathcal{K} \tag{7.11}$$

for the Dirac equation. It can be seen to provide a symmetry in the case that $A = 0$.

Given then the matrix forms of $\hat{\mathcal{T}}$ and $\hat{\mathcal{C}}$, the Dirac equation on the line can be classified according to the Altland-Zirnbauer Tenfold Way,

Theorem 7.1.2. *The Dirac Equation on the line $[0, L]$ defines a system of Altland-Zirnbauer class DIII when $A = 0$.*

Proof. The Dirac equation on the line is only symmetric under $\hat{\mathcal{C}}, \hat{\mathcal{T}}$ and $\hat{\mathcal{C}}\hat{\mathcal{T}}$, thus the Altland-Zirnbauer class can be found by checking how $\hat{\mathcal{C}}, \hat{\mathcal{T}}$ square. Given that

$$\hat{\mathcal{C}}^2 = \mathbb{I} = -\hat{\mathcal{T}}^2$$

then it has to be of class DIII. $\qquad\square$

7.1.2 The Dirac Graph

The Dirac graph can be thought of as a direct modification to the quantum graphs defined in Definition 6.1.6, by swapping out the use of Schrödinger's equation for Dirac's equation, [27, 78]:

Definition 7.1.3. *Let Γ be a metric graph with Hilbert space $\mathcal{H} = \bigoplus_{b \in \mathcal{B}} L_2([0, L_b])^4$. Define a magnetic potential A_b on each bond b. Take the functions $\psi_b(x_b)$ on each bond as the solutions to Dirac's magnetic time-independent equation,*

$$\left(\alpha_2\left(-i\frac{\partial}{\partial x} - eA\right) + \beta m\right)\psi_b(x_b) = E_b\psi_b(x_b),$$

then an unconstrained solution on the whole graph can be given by the vector

$$\Psi(\mathbf{x}) = \big(\psi_1(x_1), \psi_2(x_2), \dots, \psi_{|\mathcal{B}|}(x_{|\mathcal{B}|})\big)^T.$$

A set of boundary conditions on the bond solutions must be given by a pair of $4|\mathcal{B}| \times 4|\mathcal{B}|$ matrices C_1, C_2, chosen so that $\mathrm{rank}(C_1 \mid C_2) = 4|\mathcal{B}|$ and $C_1C_2^\dagger = C_2C_1^\dagger$. With the vectors

$$\psi^+ = \left(\psi_1^1(0), \dots, \psi_1^{|\mathcal{B}|}(0), \psi_2^1(0), \dots, \psi_2^{|\mathcal{B}|}, \psi_1^1(L_1), \dots, \psi_1^{|\mathcal{B}|}(L_{|\mathcal{B}|}), \psi_2^1(L_1), \dots, \psi_2^{|\mathcal{B}|}(L_{|\mathcal{B}|})\right)^T$$

$$\psi^- = \left(-\psi_4^1(0), \dots, -\psi_4^{|\mathcal{B}|}(0), \psi_3^1(0), \dots, \psi_3^{|\mathcal{B}|}, \psi_4^1(L_1), \dots, \psi_4^{|\mathcal{B}|}(L_{|\mathcal{B}|}), -\psi_3^1(L_1), \dots, -\psi_3^{|\mathcal{B}|}(L_{|\mathcal{B}|})\right)^T$$

defined, then a valid constrained solution Ψ on the graph satisfies the boundary condition that,

$$C_1\psi^+ + C_2\psi^- = 0. \tag{7.12}$$

The boundary conditions given here derive from the necessity of ensuring the Dirac operator on the graph is self-adjoint, a discussion on the derivation of this form appearing in [27]. Though they

appear very different to the version using the derivative for the quantum graph as per Equation 6.1, they are actually closer to those defined for the quantum graph using the derivative then they would appear - ψ^- is actually equivalent to $\frac{\partial}{\partial x}\psi^+ - ieA\psi^+$, so this is actually a useful simplification of the quantum graph version that is possible due to the forms of the vectors in the solution Ψ.

Solving the Dirac graph for a given charge e and an energy E then again requires finding a set of amplitudes $\mu_\alpha, \mu_\beta, \hat{\mu}_\alpha, \hat{\mu}_\beta$ such that they are consistent with Equation 7.12. In the method from [78], and in the same way as for quantum graphs in Section 6.1, it is possible to consider the solution in the basis defined by the amplitudes of the solution on each of the bonds,

$$\boldsymbol{\mu} = \begin{pmatrix} \mu & \hat{\mu} \end{pmatrix}^T = \begin{pmatrix} \mu_{\alpha,1} & \mu_{\beta,1} & \cdots & \mu_{\alpha,|\mathcal{B}|} & \mu_{\beta,|\mathcal{B}|} & \hat{\mu}_{\alpha,1} & \hat{\mu}_{\beta,1} & \cdots & \hat{\mu}_{\alpha,|\mathcal{B}|} & \hat{\mu}_{\beta,|\mathcal{B}|} \end{pmatrix}^T$$

and then use the boundary conditions to derive the scattering and transmission expression of the Dirac Graph. From there, a secular equation $\det(\mathbb{I} - \Xi(E)) = 0$ can then be derived to find the energy level spectrum.

The vectors ψ^+, ψ^- are related to $\boldsymbol{\mu}$ by

$$\psi^+ = \begin{pmatrix} \mathbb{I} & \mathbb{I} \\ e^{i(k+eA_i)L_i} & e^{-i(k-eA_i)L_i} \end{pmatrix} \begin{pmatrix} \mu \\ \hat{\mu} \end{pmatrix}, \quad \psi^- = i\gamma(k) \begin{pmatrix} -\mathbb{I} & \mathbb{I} \\ e^{i(k+eA_i)L_i} & -e^{-i(k-eA_i)L_i} \end{pmatrix} \begin{pmatrix} \mu \\ \hat{\mu} \end{pmatrix}$$

so the boundary condition problem expressed with $\boldsymbol{\mu}$ then becomes

$$0 = \left(C_1 \begin{pmatrix} \mathbb{I} & \mathbb{I} \\ e^{i(k+eA_i)L_i} & e^{-i(k-eA_i)L_i} \end{pmatrix} + i\gamma(k)C_2 \begin{pmatrix} -\mathbb{I} & \mathbb{I} \\ e^{i(k+eA_i)L_i} & -e^{-i(k-eA_i)L_i} \end{pmatrix} \right) \begin{pmatrix} \mu \\ \hat{\mu} \end{pmatrix}$$

$$= (C_1 - i\gamma(k)C_2) \begin{pmatrix} \mathbb{I} & 0 \\ 0 & e^{-i(k-eA_i)L_i} \end{pmatrix} \begin{pmatrix} \mu \\ \hat{\mu} \end{pmatrix} + (C_1 + i\gamma(k)C_2) \begin{pmatrix} 0 & \mathbb{I} \\ e^{i(k+eA_i)L_i} & 0 \end{pmatrix} \begin{pmatrix} \mu \\ \hat{\mu} \end{pmatrix}$$

Rescaling $\boldsymbol{\mu}$ to get rid of the factor of $\begin{pmatrix} \mathbb{I} & 0 \\ 0 & e^{-i(k-eA_i)L_i} \end{pmatrix}$,

$$\tilde{\boldsymbol{\mu}} = \begin{pmatrix} \mathbb{I} & 0 \\ 0 & e^{-i(k-eA_i)L_i} \end{pmatrix} \boldsymbol{\mu}$$

also consolidates both the exponential parts into the same matrix factor. Then taking advantage of the fact that $(C_1 - i\gamma(k)C_2)$ is always invertible as it is Hermitian, [100], scattering and transmission matrices equivalent to those given in Equation 6.6 for the Schrödinger quantum graph drop out,

$$\tilde{\boldsymbol{\mu}} = -(C_1 - i\gamma(k)C_2)^{-1}(C_1 + i\gamma(k)C_2) \begin{pmatrix} 0 & e^{i(k-eA_i)L_i} \\ e^{i(k+eA_i)L_i} & 0 \end{pmatrix} \tilde{\boldsymbol{\mu}}$$

$$= S(e,k)T(e,k)\tilde{\boldsymbol{\mu}} = \Xi(e,k)\tilde{\boldsymbol{\mu}}$$

where

$$S(e,k) = -(C_1 - i\gamma(k)C_2)^{-1}(C_1 + i\gamma(k)C_2), \qquad T(e,k) = \begin{pmatrix} 0 & e^{i(k-eA_i)L_i} \\ e^{i(k+eA_i)L_i} & 0 \end{pmatrix}.$$

As it is being assumed that $m = 0$, then $k = E$ and it is possible to relabel $k \to E$ from here on.

Note how here it is not common to factor out a copy of $\left(\begin{smallmatrix} 0 & \mathbb{I} \\ \mathbb{I} & 0 \end{smallmatrix}\right)$ from T to bring it into main diagonal form, but instead it is left in its non-main-diagonal block form. This means there is no difference between the derived scattering matrix and the 'standard' forms as there was for quantum graphs.

Again $\Xi(e, E) = S(e, E)T(e, E)$ can be considered a form of time evolution operator, transmitting and scattering a wave packet down the bonds, so that the relation $\tilde{\boldsymbol{\mu}} = \Xi(e, E)\tilde{\boldsymbol{\mu}}$ becomes a version of the time independence problem. A valid solution $\tilde{\boldsymbol{\mu}}$ then must be an eigenstate of $\Xi(e, E)$ with eigenvalue 1. Thus, there again exists an energy level in the system whenever the secular equation

$$0 = \det\big(\mathbb{I}_{4|\mathcal{B}|} - S(e, E)T(e, E)\big) \tag{7.13}$$

is consistent. The real secular equation can also be defined again, having the form

$$\zeta(e, E) = \frac{1}{e^{ik\sum_b L_b}\sqrt{\det(S(e, E))}} \det\left(\mathbb{I} - S(e, E)T(e, E)\right) \tag{7.14}$$

so that whenever $\zeta(e, E)$ has a root, there is an energy level in the spectrum of the Dirac graph. This allows exactly the same numerical program as for the quantum graph to be run to find the spectrum of Dirac graph - iterating over E and calculating $\zeta(e, E)$ and then running root finding programs to find roots with an odd degeneracy, or a minima finding routine on $|\zeta(e, E)|^{1/2}$ to find roots with an even degeneracy.

7.1.3 The Dirac Graph as a Quantum Graph

The Dirac graph is completely described by the time evolution invariance equation,

$$\tilde{\boldsymbol{\mu}} = -(C_1 - i\gamma(k)C_2)^{-1}(C_1 + i\gamma(k)C_2) \begin{pmatrix} 0 & e^{i(k-eA_i)L_i} \\ e^{i(k+eA_i)L_i} & 0 \end{pmatrix} \tilde{\boldsymbol{\mu}}$$

$$= S(e, k)T(e, k)\tilde{\boldsymbol{\mu}} = \Xi(e, k)\tilde{\boldsymbol{\mu}}$$

which is formed of the scattering matrix, $S(e, k) = -(C_1 - i\gamma(k)C_2)^{-1}(C_1 + i\gamma(k)C_2)$, where the block $S(e, k)_{b_1, b_2}$ with $b_1 = [i, j], b_2 = [m, i]$ describes the how much of the two component wave coming into the vertex along b_2 with the vector of amplitudes $(\mu_{b_2,\alpha}, \mu_{b_2,\beta})^T$ scatters onto the bond b_1 as the amplitude vector $(\mu_{b_1,\alpha}, \mu_{b_1,\beta})^T$; and the transmission matrix $T(e, k) = \left(\begin{smallmatrix} 0 & e^{i(k-eA_i)L_i} \\ e^{i(k+eA_i)L_i} & 0 \end{smallmatrix}\right)$ where $e^{i(k-eA_i)L_i}$ is the diagonal matrix $\mathrm{diag}(e^{i(k+eA_{b_1})L_{b_1}}, e^{i(k+eA_{b_1})L_{b_1}}, \ldots, e^{i(k+eA_{b_{|\mathcal{B}|}})L_{b_{|\mathcal{B}|}}}, e^{i(k+eA_{b_{|\mathcal{B}|}})L_{b_{|\mathcal{B}|}}})$, and which transforms amplitudes at the start of the bonds into amplitudes at the ends of the bonds. This equation was derived by taking the boundary condition expression and re-expressing it in terms of the amplitudes, then re-arranging the equation to get an invariance condition.

The same method was employed in the case of the quantum graph, resulting in the equations,

$$\boldsymbol{\mu} = -(C_1 + ikC_2)^{-1}(C_1 - ikC_2) \begin{pmatrix} 0 & e^{i(k+A_b)L_b} \\ e^{i(k-A_b)L_b} & 0 \end{pmatrix} \boldsymbol{\mu}$$

$$= S(k)T(k) = \Xi(k)\boldsymbol{\mu}$$

where $S(k) = -(C_1 + ikC_2)^{-1}(C_1 - ikC_2)$ and $T(k) = \begin{pmatrix} 0 & e^{i(k+A_b)L_b} \\ e^{i(k-A_b)L_b} & 0 \end{pmatrix}$ are the scattering and transmission matrices with the same interpretation as the Dirac graph case.

These basic equations have much the same form when S, T are independent of e and k or E, except for two differences - firstly, the Dirac graph method of rescaling $\boldsymbol{\mu} \to \tilde{\boldsymbol{\mu}}$ to collate the matrices with exponential parts into a single matrix that becomes the transition matrix is not necessary in the case of the quantum graph; secondly, there is a sign change within the definition of the scattering matrix - the inverse is taken of $(C_1 + ikC_2)$, not $(C_1 - i\gamma(k)C_2)$. This mathematical similarity means that when taken out of the context of the Dirac graph, the Dirac graph's scattering and transmission matrices can be re-interpreted as defining a quantum graph with a two component wave function.

That is, let $C_{1,D}, C_{2,D}$ be the boundary condition matrices for the Dirac graph with bond lengths $\{L_b\}$ and bond potentials $\{A_b\}$. Then the quantum graph with 2 component wave functions on its bonds, and with bond lengths $\{L_b\}$ and bond potentials $\{A_b\}$ taken from the Dirac case, and boundary condition matrices $C_{1,C} = C_{1,D}$ and $C_{2,C} = -C_{2,D}$ will have an energy level k in its spectra if and only if the Dirac graph it was defined from does for the same k. Note that the rescaling of $\boldsymbol{\mu} \to \tilde{\boldsymbol{\mu}}$ has no effect in going from the Dirac graph to the quantum graph, as they appear only as part of an invariance equation so their forms don't matter, only that $\Xi(e, k)$ and $\Xi(k)$ have an eigenvalue of one.

Given that a Dirac graph is mathematically equivalent to a quantum graph, then the results proved for quantum graphs also hold for Dirac graphs - including the results from Section 6.1.3 and which discuss when the graphs will be chaotic and approximations for their density of states, and the result from Appendix D that the periodic-orbit approximation for the semi-classical approximation of the density of states is exact. Thus, for the same reasons that quantum graphs proved to be a good system for testing that the random matrix predictions for the spectral statistics of bosonic-type chaotic quantum systems indeed hold; Dirac graphs will be a good model for testing that the random matrix predictions for the spectral statistics of fermionic-type chaotic quantum systems indeed hold.

Furthermore, given that quantum graphs with single component wave-functions are known to be build-able in the lab as microwave wire graphs, [83], this opens avenues to realising the Dirac graph in the lab. The issue of the microwave wires graph only taking one component wave functions but the Dirac graph requiring a two component wave function can be circumvented by considering each single bond of the Dirac graph as a *pair* of bonds on the microwave graph, with one amplitude component on each half of the pair, as per Figure 7.1.

This demonstrates a basic construction that can be used to realise magnetic-field free Dirac graphs in the lab, which is important as the desire of the thesis was to find a system which can be easily constructed in the lab and which could be used to demonstrate statistics from each of the ensembles considered by Altland and Zirnbauer. It would seem that the one issue

(a) The Dirac graph with two-component wave functions on each bond.

(b) The associated microwave network, splitting a two-component wave function over a pair of bonds.

Figure 7.1: Realising the Dirac graph as a microwave wire network.

is that the graphs discussed below rely on the use of carefully chosen magnetic potentials to kill time-reversal and charge-conjugation symmetry, while also controlling the creation of new generalised time-reversal, generalised charge-conjugation and generalised chiral symmetries; and it would seem that in not being able to build magnetic potentials into the microwave networks these graphs wouldn't be realisable. However, magnetic potentials were introduced on these graphs only as a method of breaking time-reversal or charge conjugation symmetry, and it is possible to look for other mechanisms that would do this. For the quantum graph, microwave wires which allow transmission in only one direction have been considered as a method, [2], and have already been used to control one type of generalised time-reversal symmetry, [3]. It is expected that uni-directionality would be another possible method of breaking the anti-unitary symmetries and re-constructing their generalised forms; taking the direction-reversed copies of the unitary-commuting sub-graph to construct the charge-conjugated and time-reversed copies. If so, then paired with an appropriate method of drawing the scattering matrices to fully sample the ensemble of possible graphs, the uni-directional graphs would provide an experimental method of realising the Dirac graphs discussed below in the lab.

7.2 Symmetric Dirac Graphs

7.2.1 Time-Reversal and Charge-Conjugation on Dirac Graphs

The action of $\hat{\mathcal{T}}$ and $\hat{\mathcal{C}}$ have been defined for the Dirac equation on a line, where they provide symmetries of the system. Their action can be defined on the Dirac graph by their action on each of the bonds individually, while their action on the scattering matrix $S(e, E)$ can be found by considering the expression of a general scattering matrix $S(e, E)$ as a function of the Green's functions of its associated Hamiltonian, $\hat{H}$, [64],

$$G_{\pm}(e, E) = \frac{1}{E \pm i\epsilon - \hat{H}(e)}, \quad G_{-}(e, E) = G_{+}^{\dagger}(e, E), \quad S(e, E) = G_{+}(e, E) G_{-}(e, E)^{-1}. \qquad (7.15)$$

This allows the question of finding the action of $\hat{\mathcal{T}}, \hat{\mathcal{C}}$ on $S(e, E)$ to become a question of their action on the Hamiltonian $\hat{H}(e)$, which is already known, and it can be seen that

$$\hat{\mathcal{T}} G_{\pm}(e, E) \hat{\mathcal{T}}^{-1} = G_{\mp}(e, E) \qquad \Rightarrow \hat{\mathcal{T}} S(e, E) \hat{\mathcal{T}}^{-1} = S^{\dagger}(e, E) \qquad (7.16)$$

$$\hat{\mathcal{C}} G_{\pm}(e, E) \hat{\mathcal{C}}^{-1} = -G_{\pm}(-e, -E) \qquad \Rightarrow \hat{\mathcal{C}} S(e, E) \hat{\mathcal{C}}^{-1} = S(-e, -E) \qquad (7.17)$$

136

which is in agreement with the general form given by [14].

On the unconstrained line, these operators $\hat{\mathcal{T}}, \hat{\mathcal{C}}$ provide a symmetry when $A = 0$; this extends to the Dirac graph when $A_b = 0 \ \forall b \in \mathcal{B}$ and when the boundary conditions at the vertices fulfil specific requirements. These requirements can, as in Section 6.1.1 be found by considering the action of $\hat{\mathcal{T}}, \hat{\mathcal{C}}$ on the amplitude space local to single vertex. This is the procedure in [27] used to identify the conditions for a Dirac graph to be symmetric under $\hat{\mathcal{T}}$, but it is generalised here to include symmetry under the charge-conjugation operator.

As in Section 6.1.1, the local scattering problem at a vertex i relates the amplitudes of the incoming waves $\overleftarrow{\mu}_i$ to the outgoing amplitudes $\overrightarrow{\mu}_i$,

$$\overrightarrow{\mu}_i(e, E) = \sigma^{(i)}(e, E) \overleftarrow{\mu}_i(e, E), \qquad \sigma^{(i)}(e, E) = S(e, E)\mid_i$$

where at a vertex with outgoing bonds $1, 2, \ldots d_i^+$ and incoming bonds $d_i^+ + 1, d_i^+ + 1, \ldots d_i$, $\overrightarrow{\mu}_i, \overleftarrow{\mu}_i$ are described in terms of $\mu_\alpha, \mu_\beta, \hat{\mu}_\alpha$ and $\hat{\mu}_\beta$ by

$$\overrightarrow{\mu} = \begin{pmatrix} \mu_\alpha^1 \\ \mu_\beta^1 \\ \vdots \\ \mu_\alpha^{d_i^+} \\ \mu_\beta^{d_i^+} \\ \exp\left(-i(k - eA_{d_i^+ + 1})L_{d_i^+ + 1}\right)\hat{\mu}_\alpha^{d_i^+ + 1} \\ \exp\left(-i(k - eA_{d_v^t + 1})L_{d_v^t + 1}\right)\hat{\mu}_\beta^{d_i^+ + 1} \\ \vdots \\ \exp\left(-i(k - eA_{d_v})L_{d_v}\right)\hat{\mu}_\alpha^{d_v} \\ \exp\left(-i(k - eA_{d_i})L_{d_i}\right)\hat{\mu}_\beta^{d_i} \end{pmatrix}, \quad \overleftarrow{\mu} = \begin{pmatrix} \hat{\mu}_\alpha^1 \\ \hat{\mu}_\beta^1 \\ \vdots \\ \hat{\mu}_\alpha^{d_i^+} \\ \hat{\mu}_\beta^{d_i^+} \\ \exp\left(i(k + eA_{d_+^t + 1})L_{d_+^t + 1}\right)\mu_\alpha^{d_i^+ + 1} \\ \exp\left(i(k + eA_{d_i^+ + 1})L_{d_i^+ + 1}\right)\mu_\beta^{d_i^+ + 1} \\ \vdots \\ \exp\left(i(k + eA_{d_i})L_{d_i}\right)\mu_\alpha^{d_i} \\ \exp\left(i(k + eA_{d_i})L_{d_i}\right)\mu_\beta^{d_i} \end{pmatrix}.$$

Multiplication of the phases in the lower half of the vectors by $\exp(i(k + A_b)L_b)$ occurs as these are the phases on the bonds which are incoming at i - so $b = [j, i]$ and the phases $\mu_{\alpha,\beta}^b$ and $\hat{\mu}_{\alpha,\beta}^b$ without the added phase are the values at the vertex j not i; multiplying by the phase transmits the amplitudes to i. This is also why μ^b and $\hat{\mu}^b$ are swapped in the way they appear in $\overleftarrow{\mu}$ and $\overrightarrow{\mu}$ - these vectors are about the direction of travel of the amplitudes relative to the vertex, not the bonds, and on an incoming bond, the direction travelling away from the vertex is the direction travelling against the bond, and vice versa - hence why $\hat{\mu}$ appears in $\overrightarrow{\mu}$ and μ appears in $\overleftarrow{\mu}$.

The requirement for symmetry is then that given the time-reversed vectors, $\overrightarrow{\mu}_{i,\mathcal{T}}(e, E) = \hat{\mathcal{T}} \overrightarrow{\mu}_i(e, E)$, $\overleftarrow{\mu}_{i,\mathcal{T}}(e, E) = \hat{\mathcal{T}} \overleftarrow{\mu}_i(e, E)$, or the charge-conjugated vectors, $\overrightarrow{\mu}_{i,\mathcal{C}}(-e, -E) = \hat{\mathcal{C}} \overrightarrow{\mu}_i(e, E)$, $\overleftarrow{\mu}_{i,\mathcal{C}}(-e, -E) = \hat{\mathcal{C}} \overleftarrow{\mu}_i(e, E)$, the local scattering relations continue to hold for the right choice of e, E. This is the requirement that the relations

$$\overrightarrow{\mu}_{i,\mathcal{T}}(e, E) = \sigma^{(i)}(e, E) \overleftarrow{\mu}_{i,\mathcal{T}}(e, E) \tag{7.18}$$

$$\overrightarrow{\mu}_{i,\mathcal{C}}(-e, -E) = \sigma^{(i)}(-e, -E) \overleftarrow{\mu}_{i,\mathcal{C}}(-e, -E) \tag{7.19}$$

must hold.

The explicit action of $\hat{\mathcal{T}}, \hat{\mathcal{C}}$ on the vector forms of $\overrightarrow{\mu}_i, \overleftarrow{\mu}_i$ can be found by comparing the amplitudes of each component in $\psi(e, E; x)$ and $\psi(-e, -E; x)$ to $\hat{\mathcal{T}}\psi(e, E; x)$ and $\hat{\mathcal{C}}\psi(e, E; x)$ respectively so that it is found that

$$
\begin{pmatrix} \mu_{\alpha,\mathcal{T}}(e,E) \\ \mu_{\beta,\mathcal{T}}(e,E) \\ \hat{\mu}_{\alpha,\mathcal{T}}(e,E) \\ \hat{\mu}_{\beta,\mathcal{T}}(e,E) \end{pmatrix} = \begin{pmatrix} 0 & J \\ J & 0 \end{pmatrix} \begin{pmatrix} \mu_{\alpha}(e,E) \\ \mu_{\beta}(e,E) \\ \hat{\mu}_{\alpha}(e,E) \\ \hat{\mu}_{\beta}(e,E) \end{pmatrix}^* \tag{7.20}
$$

$$
\begin{pmatrix} \mu_{\alpha,\mathcal{C}}(-e,-E) \\ \mu_{\beta,\mathcal{C}}(-e,-E) \\ \hat{\mu}_{\alpha,\mathcal{C}}(-e,-E) \\ \hat{\mu}_{\beta,\mathcal{C}}(-e,-E) \end{pmatrix} = i \begin{pmatrix} -\mathbb{I}_2 & 0 \\ 0 & \mathbb{I}_2 \end{pmatrix} \begin{pmatrix} \mu_{\alpha}(e,E) \\ \mu_{\beta}(e,E) \\ \hat{\mu}_{\alpha}(e,E) \\ \hat{\mu}_{\beta}(e,E) \end{pmatrix}^* \tag{7.21}
$$

where

$$
J = \begin{pmatrix} 0 & 1 \\ -1 & 0 \end{pmatrix}.
$$

This then gives the forms for $\overrightarrow{\mu}_{i,\mathcal{T},\mathcal{C}}, \overleftarrow{\mu}_{i,\mathcal{T},\mathcal{C}}$ as,

$$
\overrightarrow{\mu}_{i,\mathcal{T}} = i(\mathbb{I}_{d_i} \otimes J)\overleftarrow{\mu}_i^* \qquad\qquad \overleftarrow{\mu}_{i,\mathcal{T}} = i(\mathbb{I}_{d_i} \otimes J)\overrightarrow{\mu}_i^* \tag{7.22}
$$

$$
\overrightarrow{\mu}_{i,\mathcal{C}} = i \begin{pmatrix} -\mathbb{I}_{2d_i^+} & 0 \\ 0 & \mathbb{I}_{2d_i^-} \end{pmatrix}\overrightarrow{\mu}_i^* \qquad\qquad \overleftarrow{\mu}_{i,\mathcal{C}} = i \begin{pmatrix} \mathbb{I}_{2d_i^+} & 0 \\ 0 & -\mathbb{I}_{2d_i^-} \end{pmatrix}\overleftarrow{\mu}_i^* \tag{7.23}
$$

Substituting Equation 7.22 into Equation 7.18 gives the requirement on $\sigma^{(i)}$ for time-reversal symmetry,

$$
\sigma^{(i)}(e,E) = (\mathbb{I}_{d_i} \otimes J)^{-1}\sigma^{(i)T}(e,E)(\mathbb{I}_{d_i} \otimes J) \tag{7.24}
$$

while substituting Equation 7.23 into Equation 7.19 gives for charge-conjugation symmetry the requirement that

$$
\sigma^{(i)}(e,E) = \begin{pmatrix} -\mathbb{I}_{2d_i^+} & 0 \\ 0 & \mathbb{I}_{2d_i^-} \end{pmatrix} \sigma^{(i)*}(-e,-E) \begin{pmatrix} \mathbb{I}_{2d_i^+} & 0 \\ 0 & -\mathbb{I}_{2d_i^-} \end{pmatrix}. \tag{7.25}
$$

Assuming σ is independent of e and E, this means for a Dirac graph to have both time-reversal and charge-conjugation symmetry, $\sigma^{(i)}$ must satisfy both the relations

$$
\sigma^{(i)} = u^{(i)}(X^{(i)} \otimes \mathbb{I}_2)u^{(i)-1} \tag{7.26}
$$

$$
\sigma^{(i)} = \begin{pmatrix} A^{(i)} & B^{(i)} \\ B^{(i)T} & D^{(i)} \end{pmatrix} \tag{7.27}
$$

where $u^{(i)} = \text{diag}(u_1, u_2, \ldots u_{d_i})$, $u_i \in U(2)$, $A^{(i)T} = -A^{(i)}$, $D^{(i)T} = -D^{(i)}$ and $A^{(i)} \in \mathbb{C}^{2d_i^+ \times 2d_i^+}$, $B^{(i)} \in \mathbb{C}^{2d_i^+ \times 2d_i^-}$ and $D^{(i)} \in \mathbb{C}^{2d_i^- \times 2d_i^-}$, for each $i \in \mathcal{V}$. The choice in [27] is to take $X^{(i)}$ as the scattering matrix found for the Schrödinger quantum graph, however this creates a graph that

is symmetric under $\hat{\mathcal{T}}$ and $\hat{M}\hat{\mathcal{C}}$ where $\hat{M}: b \to \bar{b}$ exchanges the directions of the bonds, which is insufficient to either fully break or maintain the spectral mirror symmetry as is required here.

The action of $\hat{\mathcal{T}}, \hat{\mathcal{C}}$ can also be calculated on $\tilde{\boldsymbol{\mu}}$, and is given by the operators

$$\hat{\mathcal{T}} = i \begin{pmatrix} 0 & \mathbb{I}_{|\mathcal{B}|} \otimes J \\ \mathbb{I}_{|\mathcal{B}|} \otimes J & 0 \end{pmatrix} \mathcal{K}, \qquad \hat{\mathcal{C}} = i \begin{pmatrix} -\mathbb{I}_{2|\mathcal{B}|} & 0 \\ 0 & \mathbb{I}_{2|\mathcal{B}|} \end{pmatrix} \mathcal{K}. \tag{7.28}$$

which allows the chiral operator $\hat{\mathcal{P}} = \hat{\mathcal{C}}\hat{\mathcal{T}}$ to be inferred as

$$\hat{\mathcal{P}} = \begin{pmatrix} -\mathbb{I}_{2|\mathcal{B}|} & 0 \\ 0 & \mathbb{I}_{2|\mathcal{B}|} \end{pmatrix} \begin{pmatrix} 0 & \mathbb{I}_{|\mathcal{B}|} \otimes J \\ \mathbb{I}_{|\mathcal{B}|} \otimes J & 0 \end{pmatrix}. \tag{7.29}$$

The condition on the vertex scattering matrices for the graph to be symmetric under $\hat{\mathcal{P}}$ are also the combination of the vertex scattering matrix conditions for time-reversal and charge-conjugation symmetry:

$$\sigma^{(i)} = \begin{pmatrix} \mathbb{I}_{d_i^+} \otimes J & 0 \\ 0 & -\mathbb{I}_{d_i^-} \otimes J \end{pmatrix} \sigma^{(i)\dagger}(-e, -E) \begin{pmatrix} \mathbb{I}_{d_i^+} \otimes J & 0 \\ 0 & -\mathbb{I}_{d_i^-} \otimes J \end{pmatrix}. \tag{7.30}$$

This will be automatically satisfied if the graph is symmetric under both $\hat{\mathcal{T}}$ and $\hat{\mathcal{C}}$, as would be expected.

The Altland-Zirnbauer class of the Dirac graph with no additional symmetries can now be checked - and was the case for the Dirac equation on the line, it sits in the class $DIII$,

Lemma 7.2.1. *Let Γ be a Dirac graph that contains no unitary commuting symmetries, and no magnetic potentials on the bonds. Let the relations $\sigma^{(i)} = u^{(i)}(X^{(i)} \otimes \mathbb{I}_2)u^{(i)-1}$ with $u^{(i)} = \mathrm{diag}(u_1, u_2, \ldots u_{d_i})$, $u_i \in U(2)$ and $\sigma^{(i)} = \begin{pmatrix} A^{(i)} & B^{(i)} \\ B^{(i)T} & D^{(i)} \end{pmatrix}$ with $A^{(i)} \in \mathbb{C}^{2d_i^+ \times 2d_i^+}$, $B^{(i)} \in \mathbb{C}^{2d_i^+ \times 2d_i^-}$ and $D^{(i)} \in \mathbb{C}^{2d_i^- \times 2d_i^-}$ hold for all $i \in \mathcal{V}$. Then the graph is a member of the Altland-Zirnbauer class DIII.*

Proof. The defined graph is symmetric under $\hat{\mathcal{T}}$, $\hat{\mathcal{C}}$ and $\hat{\mathcal{T}}\hat{\mathcal{C}}$ and no other symmetries. Therefore, the Altland-Zirnbauer class of the system can be calculated by taking the squares of the time-reversal and charge-conjugation symmetries. Given their forms as

$$\hat{\mathcal{T}} = i \begin{pmatrix} 0 & \mathbb{I}_{|\mathcal{B}|} \otimes J \\ \mathbb{I}_{|\mathcal{B}|} \otimes J & 0 \end{pmatrix} \mathcal{K}, \qquad \hat{\mathcal{C}} = i \begin{pmatrix} -\mathbb{I}_{2|\mathcal{B}|} & 0 \\ 0 & \mathbb{I}_{2|\mathcal{B}|} \end{pmatrix} \mathcal{K}$$

on the whole graph, it can be seen that their squares are

$$\hat{\mathcal{C}}^2 = \mathbb{I} = -\hat{\mathcal{T}}^2$$

which means the correct class is DIII. $\qquad \square$

7.2.2 General Symmetries of Dirac Graphs

The definition of a generally symmetric quantum graph from Definition 6.1.7 carries over to the Dirac Graph with the obvious generalisation based on the action of $\hat{\mathcal{T}}$ and $\hat{\mathcal{C}}$ on the vertex scattering matrices:

Definition 7.2.2. *Let $G = U \cup \alpha U \cup \gamma U \cup \pi U$ be a finite $Z_2 \times Z_2$-graded group and Γ a Dirac graph. Define the action of G on Γ as a graph as the permutative homomorphism of the vertices by*

$$g : i \rightarrow gi.$$

Then Γ is symmetric under G as a Dirac graph if and only if the following relations hold $\forall g \in G$, $\forall i, j \in \mathcal{V}$,

$$[i,j] \in \mathcal{B} \Leftrightarrow [gi, gj] \in \mathcal{B}, \qquad L_{[gi,gj]} = L_{[i,j]}$$

$$A_{[gi,gj]} = \begin{cases} A_{[i,j]} & g \in U \cup \pi U \\ -A_{[i,j]} & g \in \alpha U \cup \gamma U \end{cases}$$

$$\sigma^{(gi)}_{[gi,gj],[gk,gi]}(e,E) = \begin{cases} \sigma^{(i)}_{[i,j],[k,i]}(e,E) & g \in U \\ (\mathbb{I}_{d_i} \otimes J)^{-1}\sigma^{(i)T}_{[i,j],[k,i]}(e,E)(\mathbb{I}_{d_i} \otimes J) & g \in \alpha U \\ \begin{pmatrix} -\mathbb{I}_{2d_i^+} & 0 \\ 0 & \mathbb{I}_{2d_i^-} \end{pmatrix} \sigma^{(i)*}_{[i,j],[k,i]}(-e,-E) \begin{pmatrix} \mathbb{I}_{2d_i^+} & 0 \\ 0 & -\mathbb{I}_{2d_i^-} \end{pmatrix} & g \in \gamma U \\ \begin{pmatrix} \mathbb{I}_{d_i^+} \otimes J & 0 \\ 0 & -\mathbb{I}_{d_i^-} \otimes J \end{pmatrix} \sigma^{(i)\dagger}_{[i,j],[k,i]}(-e,-E) \begin{pmatrix} \mathbb{I}_{d_i^+} \otimes J & 0 \\ 0 & -\mathbb{I}_{d_i^-} \otimes J \end{pmatrix} & g \in \pi U \end{cases}$$

The preservation of the connectivity and bond lengths is direct from the standard definition of a symmetric graph. The requirement on the magnetic potentials is unchanged from the definition of a symmetric quantum graph - anti-unitary group elements cause a sign flip in A_b in their action, so this is accounted for in the definition. The rules on $\sigma^{(i)}$ are found by taking Equations 7.24 and 7.25 and swapping $\sigma^{(i)}$ for $\sigma^{(gi)}$ on the left-hand side so the action of the operator includes a vertex permutation when testing for symmetry. The action under an element in πU is found by combining Equations 7.24 and 7.25 so that the action without the vertex permutation is given by $\hat{\mathcal{C}}\hat{\mathcal{T}} = \hat{\mathcal{P}}$. In this way, generalised time-reversal, charge-conjugation and chiral symmetries can be represented on a Dirac graph.

If these graphs are to be used to test random matrix predictions, it will again be necessary to construct the symmetry decomposed basis or the quotient graph in order to isolate single sub-spectra. There will be little difference in the procedure as given in Section 6.1.2 - the representation of U on Γ will be found, and then the decomposition of this representation into irreducible representations provides the necessary symmetry decomposed basis transformation, giving the correct transformation to split $\Xi(e, E)$ into block diagonal form and the spectra into independent sub-spectra.

Again, the action of U on Γ is solely a permutation of the vertices, so it can be represented as acting on the bond functions ψ_b,

$$u : \psi_b \to \psi_{u^{-1}b}(x_{u^{-1}b}) \qquad \forall u \in U$$

which gives the action of u on the graph solution Ψ as

$$u : \Psi \to (P(u) \otimes \mathbb{I}_4)\Psi, \qquad (P(u))_{ij} = \delta_{i,u^{-1}j} \tag{7.31}$$

where P is the matrix permutation representation of U acting on the bonds of Γ. The tensor product with $\mathbb{I}_4$ occurs to take into account the fact that U must act the same on each component of the spinors ψ_b.

On the amplitude space described by $\tilde{\boldsymbol{\mu}}$, taking as before the relabelling $\hat{\mu}_{\alpha,\beta,[i,j]} \to \mu_{\alpha,\beta,[j,i]}$, so that the inverse of P arises as the action on the hole space as the bond directions have been reversed, the representation of U is given by

$$u : \tilde{\boldsymbol{\mu}} \to \begin{pmatrix} P(u) \otimes \mathbb{I}_2 & 0 \\ 0 & P^{-1}(u) \otimes \mathbb{I}_2 \end{pmatrix} \tilde{\boldsymbol{\mu}}. \tag{7.32}$$

Note how the only change from the Schrödinger quantum graph of Equation 6.14 is to add a right tensor product by $\mathbb{I}_2$. This means that when calculating the subspaces in the graph by taking the transformation of basis into the symmetry decomposed basis - the basis where P is decomposed into irreducible representations - it is possible to just take the appropriate transformation W for the Schrödinger case, and then right-tensor by $\mathbb{I}_2$. That is, if $\begin{pmatrix} P(u) & 0 \\ 0 & P^{-1}(u) \end{pmatrix}$ can be decomposed into irreducible representations by W in the Schrödinger graph case as in Equation 6.16, the Dirac graph version can be decomposed by $W \otimes \mathbb{I}_2$,

$$(W \otimes \mathbb{I}_2)^{-1} \begin{pmatrix} P(u) \otimes \mathbb{I}_2 & 0 \\ 0 & P^{-1}(u) \otimes \mathbb{I}_2 \end{pmatrix} (W \otimes \mathbb{I}_2) = \begin{pmatrix} \bigoplus_i \bigoplus_{a=1}^{s_i} \rho_i(u) \otimes \mathbb{I}_2 & 0 \\ 0 & \bigoplus_i \bigoplus_{a=1}^{s_i} \rho_i^*(u) \otimes \mathbb{I}_2 \end{pmatrix}. \tag{7.33}$$

As before, the evolution operator Ξ then block diagonalises,

$$(W \otimes \mathbb{I}_2)^{-1} \Xi(e, E)(W \otimes \mathbb{I}_2) = \bigoplus_i \bigoplus_{a=1}^{s_i} \Xi_i(e, E) \tag{7.34}$$

and the secular equation factorises as

$$\det(\mathbb{I} - \Xi(e, E)) = \prod_i \det(\mathbb{I} - \Xi_i(e, E))^{s_i} \tag{7.35}$$

so that the energy spectrum splits into $|\{i\}|$ independent sub-spectra of multiplicities s_i. The exact form for W can as before, be found by applying the method of [11] - and the transformation $W \otimes \mathbb{I}_2$ can actually be computed directly with this method without resorting to the mid-way step of using the reduction to the quantum graph case if wanted. While [11] discusses the Schrödinger case exclusively, the Dirac graph can be considered as a Schrödinger graph where every bond has been doubled, or where each bond carries a two-dimensional wave function, so there is no idealogical issue with applying their method, this will be discussed further in Section 7.1.3 below.

Furthermore, going through their calculations, the new right-hand tensor product by $\mathbb{I}_2$ that appears in the Dirac graph representation of U factors out of all of their calculations, and once again returns $W \otimes \mathbb{I}_2$ as the correct quotienting transformation, confirming the easier method of relating back to the Schrödinger problem.

In terms of the heuristic derivation of the quotient graph - which if constructed with the irreducible representation ρ_i automatically has the statistics of the subspace related to the representation ρ_i - there is no change needed from the Schrödinger case described in Section 6.1.2. The method is discussed in detail there, however in summary, it is a matter of finding the fundamental domain and isolating it from the full graph, with the edges leaving the fundamental domain being cut at dummy vertices. The pairs of cut bonds $[v_1, d_1]$ and $[d_2, v_2]$ are then appropriately merged by equating the dummy vertices d_1, d_2 when there exists $u \in U$ such that $d_2 = ud_1$, the periodic boundary condition at the vertex $d_1 \equiv d_2 \equiv d$ being $\psi_{[d,v_2]} \mid_d = \rho^T(u^{-1})\psi_{[v_1,d]} \mid_d$. This can either be used to define a vertex scattering matrix

$$
\sigma^{(d)} = \begin{pmatrix} 0 & \rho^T(u^{-1}) \\ \rho^{-1T}(u^{-1}) & 0 \end{pmatrix} \otimes \mathbb{I}_2
$$

or it can be merged into the transmission matrix for the bond $[v_1, v_2]$, so the dummy vertex d is dropped. This however, completes the general definition of the quotient graph on the Dirac graph. Further discussion on the structure of the quotient graphs will be possible but require a particular type of symmetric graph to be chosen, however it can be said that universal forms very similar to those seen in Section 6.2.2 will once again appear.

7.3 Minimal Examples of the Altland-Zirnbauer Ensembles on Dirac Graphs

7.3.1 Constructing $G = U \cup \alpha U \cup \Gamma U \cup \pi U$ Symmetric Graphs and Their Quotients

We now turn to showing that any symmetry group $G = U \cup \alpha U \cup \gamma U \cup \pi U$ can be represented as a Dirac graph Γ, and that for every irreducible representation ρ of U, there is exactly one copy of ρ in the action R of U on Γ. This will allow the implementation of the systems identified by Theorem 5.2.2 and demonstrate that every Altland-Zirnbauer random matrix ensemble can be represented on a Dirac Graph.

As has been previously discussed, quantum graphs are optimal systems for identifying constructions which are symmetric under a Z_2-graded group, and which can be guaranteed to contain the representation ρ, an algorithm being given in Theorem 6.2.3 to build a graph for each symmetry group $G = U \cup \alpha U$ by identifying the Cayley graph as an example. Once an anti-commuting symmetry is required, and the symmetry group become $Z_2 \times Z_2$-graded, Dirac graphs become the system of choice, and the algorithm is updated to use the definition of symmetry from Definition 7.2.2, so that given a $Z_2 \times Z_2$-graded group G, its Cayley graph generates a specific example of a Dirac graph symmetric under G,

Theorem 7.3.1. *Let G be a $Z_2 \times Z_2$-graded group $G = U \cup A \cup C \cup P$. Let S be a generating set of G.*

The Dirac graph defined by taking the Cayley graph $\Gamma(G, S)$, choosing the quantities $L_{[e,s]}, A_{[e,s]}$ for each $s \in S$ and choosing $\sigma^{(e)} \in \mathcal{U}(d_e)$, with their values on the rest of the graph constructed by the rules

$$L_{[gi,gj]} = L_{[i,j]}, \qquad A_{[gi,gj]} = \begin{cases} A_{[i,j]} & g \in U \cup \pi U \\ -A_{[i,j]} & g \in \alpha U \cup \gamma U \end{cases}$$

$$\sigma^{(gi)}_{[gi,gj],[gk,gi]}(e, E) = \begin{cases} \sigma^{(i)}_{[i,j],[k,i]}(e, E) & g \in U \\ (\mathbb{I}_{d_i} \otimes J)^{-1} \sigma^{(i)T}_{[i,j],[k,i]}(e, E)(\mathbb{I}_{d_i} \otimes J) & g \in \alpha U \\ \begin{pmatrix} -\mathbb{I}_{2d_i^+} & 0 \\ 0 & \mathbb{I}_{2d_i^-} \end{pmatrix} \sigma^{(i)*}_{[i,j],[k,i]}(-e, -E) \begin{pmatrix} \mathbb{I}_{2d_i^+} & 0 \\ 0 & -\mathbb{I}_{2d_i^-} \end{pmatrix} & g \in \gamma U \\ \begin{pmatrix} \mathbb{I}_{d_i^+} \otimes J & 0 \\ 0 & -\mathbb{I}_{d_i^-} \otimes J \end{pmatrix} \sigma^{(i)\dagger}_{[i,j],[k,i]}(-e, -E) \begin{pmatrix} \mathbb{I}_{d_i^+} \otimes J & 0 \\ 0 & -\mathbb{I}_{d_i^-} \otimes J \end{pmatrix} & g \in \pi U \end{cases}$$

is symmetric under left multiplication by G.

There is again the the question of which generating set S should be taken for G. Following the choice of $S_U \cup \{\alpha\}$ where S_U is the generating set of U for the Z_2-graded case, the obvious choice would be to expand the set T_G taken in addition to S_U to include a representative of every present type of non unitary-commuting symmetry on the system needed to cover G. This makes the generating set $S_U \cup T_G$ where T_G is a transversal for U in G. That is, $T_G \subseteq \{\alpha, \gamma, \pi\}$, with the exact definition of T_G being given by the relations $\alpha \in T_G \Leftrightarrow A \neq \emptyset$, $\gamma \in T_G \Leftrightarrow C \neq \emptyset$ and $\pi \in T_G \Leftrightarrow P \neq \emptyset$ *and* $A = C = \emptyset$ - given that $\pi = \alpha\gamma$, then π is not needed as a generating element, and including it would mean the minimal generating set wasn't being taken, thus including π in T_G along with α and γ is unnecessary and would only generate additional bonds to slow the computations down. Thus, the options for T_G are $\{\alpha\}$, $\{\gamma\}$, $\{\pi\}$ and $\{\alpha, \gamma\}$ and $|T_G| = 1, 2$.

This maintains the very regular and universal structure on the generated graph as seen for the quantum graph in Figure 6.3, with the graph splitting into a series of copies of the sub-graph $\Gamma(U, S_U)$ interlinked by bonds generated by elements of T_G. If $T_G = \{\alpha\}$, then the structure is exactly the same as in the quantum graph case, having a copy of $\Gamma(U, S_U)$ and a copy of its time-reversed counter-part, $\alpha\Gamma(G, S_U)$ as seen by comparing Figure 7.2a with Figure 6.3. In the case that $T_G = \{\gamma\}$ or $T_G = \{\pi\}$, then the graph retains its two part structure, but now it consists of a unitary commuting original sub-graph, and either its charge-conjugated or chiral-reversed copy as in Figures 7.2b and 7.2c respectively.

When $T_G = \{\alpha, \gamma\}$, the graph now takes on a four part structure, containing the unitary-commuting sub-graph $\Gamma(U, S_U)$ and its copies $\alpha\Gamma(U, S_U)$, $\gamma\Gamma(U, S_U)$ and $\alpha\gamma\Gamma(U, S_U)$ under the action of α, γ and $\alpha\gamma$. These sub-graphs are then interlinked by the bonds generated by α and γ, giving the structure as in Figure 7.2d, and making clear the structure of the quotient $G/U = K_4$ as the Klein-4 group.

(a) $\Gamma(G, S_U \cup \{\alpha\}$

(b) $\Gamma(G, S_U \cup \{\gamma\})$

(c) $\Gamma(G, S_U \cup \{\pi\})$

(d) $\Gamma(G, S_U \cup \{\alpha, \gamma\})$
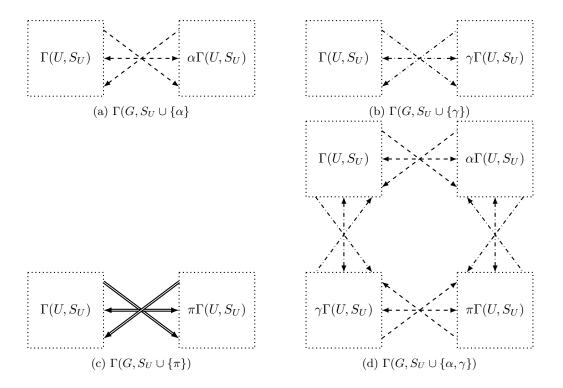
Figure 7.2: The subgraph structure of $\Gamma(G, S_U \cup T_G)$ for each of the three forms of $T_G \neq \emptyset$. In all four cases, dashed bonds are generated by α, dash-dotted bonds by γ and doubled lines by π.

The proof that the graph so constructed includes every possible energy level sub-spectrum for the graded group G needs little modification from the proof of the equivalent Theorem 6.2.5 in the case of the quantum graph. The permutation representation of U is still the independent action of U on each of its either two or four interlinked copies of its Cayley graph, thus P includes the regular representation, which has exactly one copy of each irreducible representation of U, thus there is one copy of each sub-spectrum,

Theorem 7.3.2. *Let G be a $Z_2 \times Z_2$-graded group and $\Gamma(G, S_U \cup T_G)$ be the Dirac graph defined as by Definition 7.3.1. Let $\{E_i\}_n$ be the sub-spectrum generated by an irreducible representation ρ_n of U. Then $\{E_i\}_n$ is present in the spectrum of $\Gamma(G, S_U \cup T_G)$, and has multiplicity one.*

Proof. The graph $\Gamma(G, S_U \cup T_G)$ is isomorphic to the decomposition into interconnected sub-graphs, $\Gamma(G, S_U \cup T_G) = \left(\cup_{i=1}^{2|T_G|} \Gamma(U, S_U) \right) + \Gamma'$ where Γ' describes the interconnecting bonds. The permutation representation of U on each copy of $\Gamma(U, S_U)$ is given independently by its regular representation, $\mathcal{R}$, so the permutation representation of U on $\Gamma(G, S_U \cup T_G)$ must be given by

$$P \cong \left(\bigoplus_{i=1}^{2|T_G|} \mathcal{R} \right) + R'$$

where R' describes the permutation of the interconnecting bonds. According to Theorem 2.1.12, $\mathcal{R}$ contains exactly one copy of each irreducible representation ρ_n of U. Thus, the symmetry decomposed basis of $\Gamma(G, S_U \cup T_G)$ includes one of every possible subspace, and there is a copy of every possible independent energy level sub-spectra in the full spectrum of $\Gamma(G, S_U \cup T_G)$. $\quad\square$

When isolating the sub-spectra using the quotient graph $\Gamma(G, S_U \cup T_G)/(U, \rho)$, there is again a universal structure to the graphs dependent only on which sets $A, C, P \subset G$ are non-empty - the vertices making up the fundamental domain are always $\{e, \alpha\}$ if $G = U \cup \alpha U$; $\{e, \gamma\}$ if $G = U \cup \gamma U$; $\{e, \pi\}$ if $G = U \cup \pi U$; and $\{e, \alpha, \gamma, \pi\}$ if $G = U \cup \alpha U \cup \gamma U \cup \pi U$. These are connected by bonds, and bonds generated by $u_i \in S_U$ become a number of loops coming off each vertex - these bonds can't link between different vertices, as elements of U can only permute e, α, γ and π within the sets U, A, C and P respectively, so the bond $[\alpha, \alpha u]$ is always connected to $[\alpha u^{-1}, \alpha]$ as a loop in the quotient graph, and similarly for the other vertices and bonds. This means the quotient graph always consists of either two or four interconnected vertices, with a number of self-loops at each vertex given by the number of generators of U in S_U. The four possible quotient graphs are given in Figure 7.3.

Given that the only part of the quotient graphs dependent on the chosen group G and representation ρ are the phases on the cut bonds - which are $\rho(u_i^{-1})$ on the loops coming off e; $\rho(\alpha u_i^{-1} \alpha^{-1})$ on the loops coming off α; $\rho(\gamma u_i^{-1} \gamma^{-1})$ on the loops coming off γ; $\rho(\pi u_i^{-1} \pi^{-1})$ for the loops coming off π; $\rho(\alpha^{-2})$ for $[\alpha, e]$, $\rho(\gamma^{-2})$ for $[\gamma, e]$; and either $\rho(\pi^{-2})$ for $[\pi, e]$ or $\rho(\gamma \alpha^{-1} \gamma^{-1} \alpha^{-1})$ for $[\pi, \gamma]$ and $\rho(\alpha \gamma^{-2} \alpha^{-1})$ for $[\pi, \alpha]$ - then by knowing these values for G, ρ, and each $u_i \in S_U$, it is actually possible to calculate the quotient of the Dirac Cayley graph without having to construct the full graph. All that is actually necessary once these values are known is to substitute them directly into the graphs given by Figure 7.3 - this means that graphs for the isolated sub-spectra may in fact be constructed directly without having to calculate large and complicated the Cayley graphs for groups with many generators, which is a massive simplification.

(a) $T_G = \{\alpha\}$

(b) $T_G = \{\gamma\}$

(c) $T_G = \{\pi\}$

(d) $T_G = \{\alpha, \gamma\}$
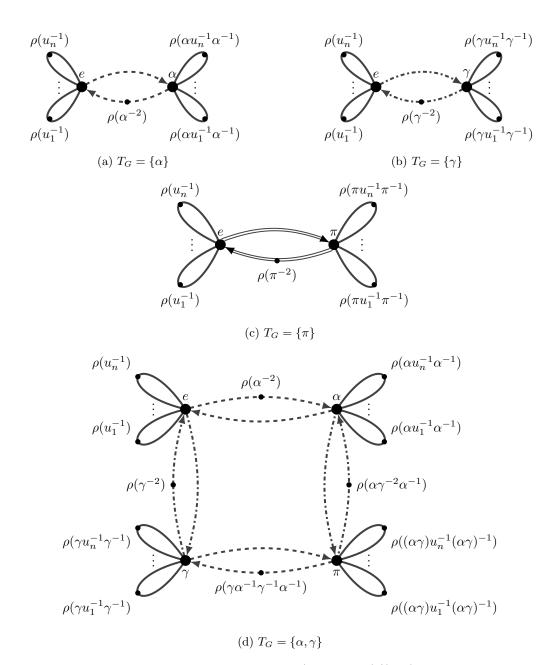
Figure 7.3: The four possible forms for a quotient graph $\Gamma(G, S_U \cup T_G)/(U, \rho)$ based on the form of T_G. Solid lines are generated by elements in U, dashed lines by elements of A, dash-dotted lines by elements of C, and doubled lines by elements of P. These quotient graph forms are universal for any Dirac graph generated from the Cayley graph of a $Z_2 \times Z_2$-graded group G when the generating set is chosen to be $S_U \cup T_G$.

146

7.3.2 Minimal Examples for the Altland-Zirnbauer Ensembles

Throughout this thesis, the final end-point has always been clear - identify a set of ten systems that are 'minimal' in size and complexity and demonstrate that they show spectral statistics matching each of the ten Altland-Zirnbauer random matrix ensembles, while all sharing the same global form of $\hat{\mathcal{T}}$ and $\hat{\mathcal{C}}$. All of the constituent parts for this have now been found - the time-reversal, $\hat{\mathcal{T}}$, charge-conjugation, $\hat{\mathcal{C}}$ and chiral, $\hat{\mathcal{P}}$, operators have been defined and their link to the Altland-Zirnbauer ensembles have been discussed. Symmetry groups have been introduced, containing unitary and anti-unitary elements, and elements which either commute or anti-commute with the Hamiltonian, their effect in splitting the Hilbert space up into independent subspaces has been described, along with how the forms of the global time-reversal and charge-conjugation operators can be different in the subspaces as local operators. Using this, appropriate groups and subspaces were identified to cover all of the ten Altland-Zirnbauer classes. Finally, an algorithm was found to generate appropriate systems and isolate the subspectra. All that is left is to apply numerical simulation to the problem, demonstrating that the theoretical predictions hold.

There is little change to the procedure discussed in Section 6.2.3 for the quantum graphs - the relevant graded groups and their unitary subgroup representations are identified and then their Cayley graphs constructed, applying the algorithm from Theorem 7.3.1 to get a Dirac graph, before quotienting out U to isolate the subspectrum and then applying the vertex-subgraph procedure to repair the graph complexity and identify the final Dirac graph to be worked with. Ensembles of graphs can then be taken by iterating over choices of $\sigma^{(e)}$ drawn from $\mathcal{U}(d_e)$ by the Haar measure, calculating the smallest eigenvalue distributions and densities of state. The one key difference is that the Dirac graph starts in a $DIII$ ensemble before additional symmetries are applied, so the substitutions of Table 5.2 must be used.

Applying this to Theorem 5.2.2 then the minimally-sized graded groups G and irreducible representations ρ needed to cover the Altland-Zirnbauer ensembles are given by the pairs in Table 7.1. Three of these classes - A, AI and AII - were covered on the quantum graphs, but we will repeat their treatment on the Dirac graphs here anyway for comparison. The Dirac graphs for the ten cases can then be generated using Theorem 7.3.1 to generate graphs of the form $\Gamma(G, S_U \cup T_G)$, where $T_G = \{\alpha\}$ for the classes A, AI and AII; $T_G = \{\gamma\}$ for the classes C and D; $T_G = \{\pi\}$ for the class AIII; and $T_G = \{\alpha, \gamma\}$ for the classes BDI, CI, CII and DIII. This gives graphs with a two-part structure when $|T_G| = 1$ and four-part structure when $|T_G| = 2$, as seen in Figure 7.2.

Taking the quotients by U of these graphs will give the minimal graphs for each ensemble. By the end of last section, this can be done by taking the universal forms of the quotient graphs for the different T_G from Figure 7.3, and substituting in the necessary phases onto the cut-and-merged bonds. Given that $|S_U| = 1$ in all ten cases considered, these are a subset of the phases $\rho(u^{-1})$, $\rho(\alpha^{-2})$, $\rho(\gamma^{-2})$, $\rho(\pi^{-2})$, $\rho(\alpha u^{-1}\alpha^{-1})$, $\rho(\gamma u^{-1}\gamma^{-1})$, $\rho(\pi u^{-1}\pi^{-1})$, $\rho(\gamma \alpha^{-1}\gamma^{-1}\alpha^{-1})$, $\rho(\alpha\gamma u^{-1}\gamma^{-1}\alpha^{-1})$ and $\rho(\alpha\gamma^{-2}\alpha^{-1})$ based on the form of T_G. The values for each of the ensembles given in Table 7.1 can be found in Tables 7.2 and 7.3.

Class	G	U	$U \cup \alpha U$	$U \cup \gamma U$	$U \cup \pi U$	Irreducible Representation of U
A	Z_6	Z_3	Z_6			Complex
AII	D_6	Z_3	D_6			Complex
AI	Z_4	Z_2	Z_4			Sign
$AIII$	Z_6	Z_3			Z_6	Complex
$DIII$	D_{12}	Z_3	D_6	D_6	Z_6	Complex
CI	Q_8	Z_2	Z_4	Z_4	Z_4	Sign
C	Z_4	Z_2		Z_4		Sign
D	D_6	Z_3		D_6		Complex
BDI	$Z_4 \times Z_2$	Z_2	Z_4	Z_2^2	Z_4	Sign
CII	$Z_4 \times Z_2$	Z_2	Z_2^2	Z_4	Z_4	Sign
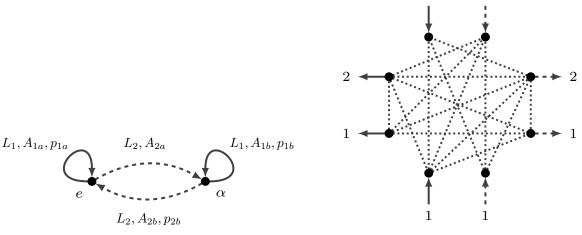
Table 7.1: The graded groups G of minimal size needed to cover each of the ten Altland-Zirnbauer ensembles when paired with appropriate non-trivial representation ρ of U. The grading is described by considering what group the sets $U, U \cup \alpha U, U \cup \gamma U$ and $U \cup \pi U$ are isomorphic to.

Class	$p_{1a} = \rho(u^{-2})$	$p_{1b} = \rho(\alpha^{-2})$	$p_{2b} = \rho(\alpha u^{-1}\alpha^{-1})$
A	$\exp(2i\pi/3)$	1	$\exp(2i\pi/3)$
AI	-1	-1	-1
AII	$\exp(2i\pi/3)$	1	$\exp(-2i\pi/3)$
		$p_{1b} = \rho(\gamma^{-2})$	$p_{2b} = \rho(\gamma u^{-1}\gamma^{-1})$
C	-1	-1	-1
D	$\exp(2i\pi/3)$	1	$\exp(-2i\pi/3)$
		$p_{1b} = \rho(\pi^{-2})$	$p_{2b} = \rho(\pi u^{-1}\pi^{-1})$
AIII	$\exp(2i\pi/3)$	1	$\exp(2i\pi/3)$

Table 7.2: The phases required on the bonds of the graph given in Figure 7.4 to get each of the classes A, AI, AII, C, D or AIII as the energy level statistics ensemble.

		DIII	CI	CII	BDI
$p_{1a} = \rho(u^{-2})$		$\exp(2i\pi/3)$	-1	-1	-1
$p_{1b} = \rho(\alpha u^{-1}\alpha^{-1})$		$\exp(-2i\pi/3)$	-1	-1	-1
$p_{1c} = \rho(\gamma u^{-1}\gamma^{-1})$		$\exp(-2i\pi/3)$	-1	-1	-1
$p_{1d} = \rho(\alpha\gamma u^{-1}\gamma^{-1}\alpha^{-1})$		$\exp(2i\pi/3)$	-1	-1	-1
$p_{2a} = \rho(\alpha^{-2})$		1	-1	1	-1
$p_{3a} = \rho(\gamma^{-2})$		1	-1	-1	1
$p_{2b} = \rho(\gamma\alpha^{-1}\gamma^{-1}\alpha^{-1})$		1	-1	1	-1
$p_{3b} = \rho(\alpha\gamma^{-2}\alpha^{-1})$		1	-1	-1	1

Table 7.3: The phases required on the bonds of the graph given in Figure 7.5 or 7.6 to get each of the classes DIII, CI, CII or BDI as the energy level statistics ensemble.

(a) Unexpanded quotient graph.

(b) Vertex Sub-graph, using 8 vertices, 19 edges and two copies of the bonds u and α or u and γ.

(c) The expanded quotient graph.
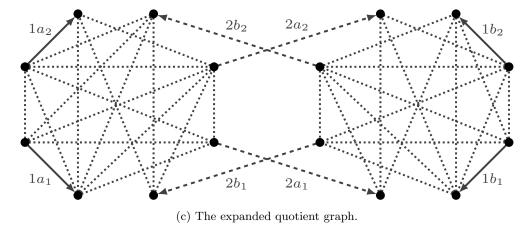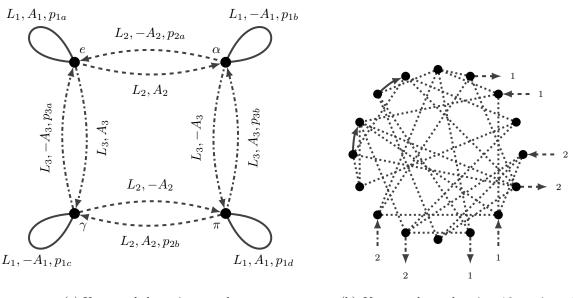
Figure 7.4: Deriving the example graphs for the classes with $|T_G| = 1$. The phases on each of the bonds required to achieve the classes A,AI,AII when the graph is interpreted as being the quotient $\Gamma(G, S_U \cup \{\alpha\})/(U, \rho)$ can be found in the top three rows of Table 7.2; while the phases required to generate the classes C and D when the graph is interpreted as being the quotient $\Gamma(G, S_U \cup \{\gamma\})/(U, \rho)$ form the center two rows; the phases required for the class AIII when the graph is interpreted as being the quotient $\Gamma(G, S_U \cup \{\pi\})/(U, \rho)$ re in the bottom row. Note that in the cases A, AI, AII, C and D, $A_{1a} = -A_{1b}$ and $A_{2a} = -A_{2b}$, while in the case of class AIII, $A_{1a} = A_{1b}$ and $A_{2a} = A_{2b}$, this because π is unitary operator.

(a) Unexpanded quotient graph.

(b) Vertex sub-graph using 16 vertices, 28 bonds and two copies of each of the bonds generated by α, γ and u.

(c) The expanded quotient graph.
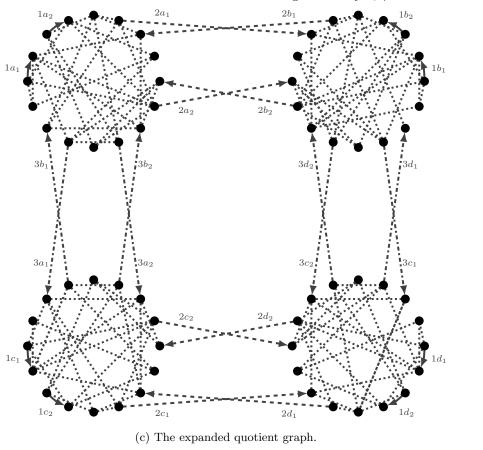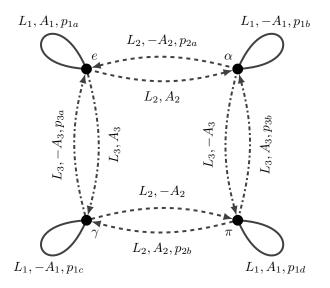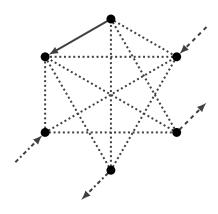
Figure 7.5: Deriving the example graphs for systems with $T_G = \{\alpha, \gamma\}$. See Table 7.3 for what phases should be chosen for each of the bonds to get the different Altland-Zirnbauer classes BDI, CII, DIII and CI.

(a) Unexpanded quotient graph.

(b) Vertex sub-graph, using 6 vertices, 11 bonds and one copy of each of the bonds generated by α, γ nd u.

(c) The expanded quotient graph.
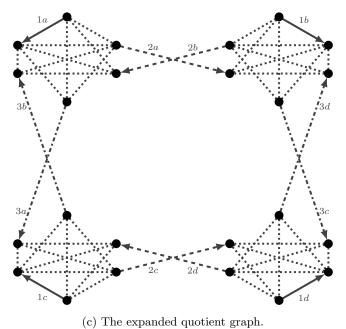
Figure 7.6: Deriving the smaller example graphs for the classes with $T_G = \{\alpha, \gamma\}$ for testing the average density of states numerically. Table 7.3 contains the phases for each of the bonds required to get each Altland-Zirnbauer class.

All that is that is then required is to substitute in the appropriate vertex sub-graphs. For the two-part graphs, the vertex sub-graph used for the quantum graph can be reused, leading to the structure in Figure 7.4. For the four part graphs, we use a new vertex sub-graph with sixteen vertices, so there are four 'spare' vertices after the main graph bonds have been added, with twenty-eight bonds in the sub-graph, leading to the structure in Figure 7.5. This size of graph is fine for calculating the smallest eigenvalue distribution, but it is too large for the much more computationally intensive average density of states. In this case, we use a smaller sub-graph of six vertices and eleven bonds, leading to the graph in Figure 7.6. This means that the connecting bonds cannot be doubled and the results for an individual graph are poorer, but this is made up for by being able to take a larger ensemble.

We now consider the practicalities of simulating the characteristic statistics of the random matrix ensembles on Dirac graphs - that is ensemble generation, solving the secular equation, the unfolding procedure, and identifying the eigenvalue search ranges for the density of states and smallest eigenvalue distributions.

Firstly, both of the measures taken here - the average level spacing distribution and the smallest eigenvalue distribution - need to be averaged over an ensemble of graphs. As in Chapter 6, this is done by fixing a graph with its bond lengths and bond potentials, and then iterating over draws of $\sigma^{(e)}$ from $\mathcal{U}(d_e)$ according to the Haar measure, computing the rest of the vertex scattering matrices from the symmetry relations.

Next, solving the Dirac graph numerically is no different to working with the Schrödinger quantum graph - the real secular equation is calculated in steps, roots or minima bounded based on the sign of the function or its derivative as necessary, and then a root finding or minimisation problem is run as required to find precisely each of the eigenvalues. This means that all code and techniques discussed in the last chapter can be carried over from the quantum graph case.

For the unfolding procedure, we first note that the semi-classical approximations for the random matrix quantities discussed for the quantum graphs in Section 6.1.3 carry over, [27], and in particular approximations of the counting function from Equation 6.22 is the same,

$$N(E) = N^{Weyl}(E) + N^{osc}(E) \qquad\qquad N^{Weyl}(0) = N_0 + \frac{1}{\pi} \operatorname{Im} \ln \zeta(\delta)$$

$$N^{Weyl}(E) = \frac{\sum_{b \in \mathcal{B}} L_b}{\pi d} E + N^{Weyl}(0) \qquad\qquad N^{osc}(E) = \frac{-1}{\pi} \operatorname{Im} \ln \zeta(E + i\epsilon)$$

so that $\delta_0 = \overline{d} = L/\pi d$ is still the average density of states in the bulk and the unfolding procedure remains

$$E \to N(E) \to N^{\text{Weyl}}(E) = \lambda$$

However, while the approximation $E \to E/\delta_0$ of the unfolding could be taken for the quantum graph's spacing distribution calculation as all that mattered were the relative spacings, for the average density of states and the smallest eigenvalue distribution, the translation term $N^{\text{Weyl}}(0)$ will be required for the unfolding. Without compensating for it, a single calculation of the spectrum will have its value of $\lambda = 0$ and mirror symmetry at $E = -N^{\text{Weyl}}(0) = \operatorname{Im} \ln \det \left(\mathbb{I} - S(e, \delta) T(e, \delta) \right) \neq 0$ in the limit $\delta \to 0$. This will be different for every initialisation of S in the ensemble, so each iteration in the average will be centred differently and lead to poor

statistics due to the results of the constituent spectra of the ensemble being out of alignment. This can be fixed by accounting for the translations in the spectra and by taking instead the unfolding

$$E \rightarrow \frac{\sum_{b \in \mathcal{B}} L_b}{\pi d} E + \frac{1}{\pi} \operatorname{Im} \ln \zeta(\delta) = \lambda,$$

using $\delta \approx 0$. This correctly centres the spectra about 0 in each case, allowing the correct averaging.

We can now turn to the question of what ranges the eigenvalues should be identified in for each of the characteristic distributions of the ensembles.

The density of states will be calculated by finding all eigenvalues in a range $E \in [N_L, N_H]$, and then averaging over these positions with the ensemble. The density of states is symmetric about zero, so having first demonstrated a symmetry in the solution for the Altland-Zirnbauer ensembles, it should be only be necessary to calculate the average density of states over the positive half of the real line to verify its agreement with the analytical results for the Altland-Zirnbauer ensembles. That would be searching for the first N eigenvalues in the unfolded range $\lambda \in [0, N]$, which can be reversed engineered into the folded range,

$$E \in \left[-\frac{d \operatorname{Im} \ln \zeta(\delta)}{\sum_{b \in \mathcal{B}} L_b}, \frac{d(N\pi - \operatorname{Im} \ln \zeta(\delta))}{\sum_{b \in \mathcal{B}} L_b} z \right] = [N_L, N_H]$$

by using the inverse of the unfolding routine. This would be a sufficient range to search in, were it not the fact that the numerical root and minimisation routines need a buffer around each root to work. This means that for roots very close to the bounds of the search range, it is actually beneficial to extend the search range slightly to allow a bigger buffer for them and improve the numerics. This makes the actual search range worked with generally $E \in [N_L - 0.5, N_H + 0.5]$ for example. Furthermore, this will catch the eigenvalues that should be inside the range but are sufficiently close to the bound that small numeric errors knock them out of the range, improving the statistics at the edges of the bounds. This is incredibly important on the zero end which sits in the centre of the spectra at the mirror symmetry and is part of the largest deviation away from the Wigner-Dyson statistics, and which is where the ensembles are best characterised in their differences. This will also occasionally find extra roots, and when they occur to the left of N_L, will show the spectral mirror symmetry in action, further validating the result.

We also note, that due to the necessity to smooth out the 'spikiness' of the density of states averaged over an ensemble of graphs, it is necessary to also do a short-range averaging over the energy range. This is as simple as using a histogram to plot the averaged density of states, but we note that depending on how the bins are arranged with relation to the range of calculated eigenvalues, this can lead to the under-representation of the average density of states in the outer two bins if they overlap areas where eigenvalues were not computed. In this case, having the buffer in the calculation means that the under-representation is less of an issue, as it lies outwith the range in consideration and can be trimmed off if required.

Finally for the average density of states, note that none of the Dirac graphs have a zero energy level when the real secular equation is calculated, so only the simplest forms of the analytical predictions for $\langle d(k) \rangle_H$ and $P_{\min}(x)$ are needed.

When calculating the smallest eigenvalue distribution, it is possible to begin calculating the real secular equation at small but negative λ, stepping forward until a root is detected. Again,

it is important that the unfolding is taken into account when giving the range to search in - the translation by $N^{\mathrm{Weyl}}(0)$ must be taken into account. Once again, inverting the unfolding relation gives the correct range, which is $E \in [-(\mathrm{Im}\ln\zeta(\delta))/\delta_0\pi, x]$.

To start the results of our numerical simulations, we note that the requirements for chaos on a quantum graph from Theorem 6.1.11 carry over onto the Dirac graph due to the Dirac graph being interpretable as a quantum graph with doubled bonds. We then first check that the first of two requirements from Theorem 6.1.11 for a graph to show chaos - that the matrix $T_{ij} = |S_{ij}|^2$ has one eigenvalue $|\eta_1| = 1$ and all other eigenvalues lie within the unit circle, $|\eta_i| < 1 \; \forall i > 1$ - is satisfied by the graphs. The tests for this are given in Table 7.4 for the graphs based on those given in Figures 7.4 and 7.5 which will be used to calculate the smallest eigenvalue distributions for all ten classes and the average density of states for the class A, AI, AII, AIII, C and D graphs; and in Table 7.5 for the graphs in Figure 7.6 which will be used to calculate the average density of states of the class BDI, CII, CI and DIII graphs. In each case, agreement with the condition can be seen.

Class	$|\eta_1|$	$|\eta_2|$	Class	$|\eta_1|$	$|\eta_2|$
A	1.0000	0.86061	AIII	1.0000	0.84591
AI	0.99999·	0.85582	BDI	0.99999·	0.92171
AII	1.0000	0.86811	CII	1.0000	0.93999
C	0.99999·	0.86602	CI	1.0000	0.93427
D	0.99999·	0.84869	DIII	1.0000	0.93032

Table 7.4: Checking the ordered eigenvalues $\eta_1 \geq \eta_2 \geq \cdots \geq \eta_N$ of the Markov process matrix $T_{ij} = |S_{ij}^2|$ derived from the scattering matrix for each of the example graphs identified in Figures 7.4 and 7.5. The first chaos requirement is that $|\eta_1| = 1$ and $|\eta_2| < 1$, which holds in each case. All numbers rounded to five significant figures and come from a single initialisation.

Class	$|\eta_1|$	$|\eta_2|$	Class	$|\eta_1|$	$|\eta_2|$
BDI	1.0000	0.90211	CI	0.99999·	0.890091
CII	0.99999·	0.88061	DIII	0.99999·	0.918761

Table 7.5: Checking the ordered eigenvalues $\eta_1 \geq \eta_2 \geq \cdots \geq \eta_N$ of the Markov process matrix $T_{ij} = |S_{ij}^2|$ derived from the scattering matrix for each of the example small graphs identified in Figure 7.6 for testing the density of states of the four-part graphs. The first chaos requirement is that $|\eta_1| = 1$ and $|\eta_2| < 1$, which holds in each case. All numbers rounded to five significant figures and come from a single initialisation.

Next, we show that the spectral mirror symmetry appears for the classes AIII, BDI, CII, C, D, DIII and CI while it is broken in the classes A, AI and AII. We calculate all the eigenvalues in the unfolded range $\lambda \in (-4, 4)$, expecting eight, and then form the pairs λ_n, λ_{-n} based on their ordering $\lambda_{-4} < \cdots < \lambda_{-1} < 0 < \lambda_1 < \cdots < \lambda_4$. Taking the differences $|\lambda_n - \lambda_{-n}|$ measures how close the two come to showing a mirror symmetry. The results of doing this for each class are given in Table 7.6 for the graphs generated from Figures 7.4 and 7.5, while Table 7.7 gives the case for the small density of state test graphs described by Figure 7.6. In each case though, the necessary behaviour is demonstrated, up to small numeric errors. That is, $|\lambda_n + \lambda_{-n}| \approx 0.1$ or bigger in the classes A, AI and AII; on the other hand, the difference is of the order 10^{-13} or smaller for most cases where the spectral mirror symmetry is expected to hold, covering the classes BDI, C, D and CII. The only classes which have larger errors are the classes CII and DIII, which have a divergence of order 10^{-3} between an energy level and its negative counterpart, but this is still small, and the spectral mirror symmetry still holds.

Class	$|\lambda_1 + \lambda_{-1}|$	$|\lambda_2 + \lambda_{-2}|$	$|\lambda_3 + \lambda_{-3}|$	$|\lambda_4 + \lambda_{-4}|$
A	0.22604	0.07873		
AI	0.37619	1.07259	0.45656	
AII	0.16970	0.16247	0.35103	0.031756
AIII	1.1291×10^{-12}	1.1326×10^{-12}	1.1133×10^{-12}	1.1120×10^{-12}
BDI	8.8818×10^{-16}	1.7764×10^{-15}	7.9936×10^{-15}	3.9968×10^{-15}
CII	2.6019×10^{-3}	4.0608×10^{-3}	4.3769×10^{-3}	3.7039×10^{-3}
C	9.1038×10^{-14}	1.1324×10^{-14}	9.3259×10^{-15}	1.8652×10^{-14}
D	1.7551×10^{-13}	1.9695×10^{-13}	1.6165×10^{-13}	1.6831×10^{-13}
CI	2.1316×10^{-14}	2.0872×10^{-14}	8.4377×10^{-15}	2.2204×10^{-15}
DIII	5.0139×10^{-3}	2.6018×10^{-3}	2.3324×10^{-3}	4.0099×10^{-3}

Table 7.6: Testing whether the calculated spectrum has a spectral mirror symmetry by taking the difference between λ_n and $-\lambda_{-n}$ for each of the ten ensembles. It can be seen that up to small numerical errors, the results agree with a spectral mirror symmetry existing in the classes AIII, BDI, CII, C, D, DIII and CI while the classes A, AI and AII don't have a spectral mirror symmetry. Missing values correspond to finding fewer than four eigenvalues in the range $(-4, 0)$, as the estimate of N eigenvalues in the range $(\lambda - 0, \lambda_0 + N)$ breaks in the negative regime without the spectral mirror symmetry. All numbers rounded to five significant figures and come from a single initialisation.

Class	$|\lambda_1 + \lambda_{-1}|$	$|\lambda_2 + \lambda_{-2}|$	$|\lambda_3 + \lambda_{-3}|$	$|\lambda_4 + \lambda_{-4}|$
BDI	4.6629×10^{-15}	3.9968×10^{-15}	2.1539×10^{-14}	2.6645×10^{-15}
CII	3.2280×10^{-3}	3.1280×10^{-3}	5.2003×10^{-3}	2.8588×10^{-3}
CI	4.7740×10^{-15}	1.3323×10^{-15}	1.7764×10^{-15}	1.3323×10^{-15}
DIII	4.8405×10^{-3}	3.1889×10^{-3}	3.6356×10^{-3}	3.1382×10^{-3}

Table 7.7: Testing whether the calculated spectrum has a spectral mirror symmetry by taking the difference between E_n and $-E_{-n}$ for each of the four small graphs given in Figure 7.6 in order to test the average density of states. It can be seen that up to small numerical errors, the results agree with a spectral mirror symmetry existing in each of the classes as predicted. All numbers rounded to five significant figures and come from a single initialisation.

The results of calculating the smallest eigenvalue distribution and the density of states through simulation of the above graphs can then be found in Figures 7.7 to 7.26.

First are the density of states simulations for the ten classes in Figures 7.7 to 7.16. It can be seen first that all three of the Wigner-Dyson classes are modelled well, with their simulated average density of states being formed of very small oscillations around the constant value of one. In all three cases, these oscillations are of the order 10^{-2}. We also note the aforementioned under-representation of the density of states in the first data point for the class AII graph, which was one of the reasons for allowing the buffer in the choice of the energy range.

Moving onto the additional seven Altland-Zirnbauer ensembles, the numerics matches the random matrix predictions well in the range $[-1, 1]$, however, way from here, the accuracy to the prediction lessons, particularly in the classes CII, D and DIII. These ensembles should show large oscillations in the density of states but the numerics have oscillations that trend to zero too quickly, or are out of phase with the analytic predictions. This would suggest in these cases the second-smallest and third-smallest eigenvalues are not being found as accurately as the smallest eigenvalue. This is likely in part due to the moderate number of runs that is being averaged over - as the class CII and DIII are the worst, but they use only 35,000 runs instead of the 150,000 runs used for the class AIII which does have good agreement between the numerics and the oscillatory analytic prediction even away from 0.

Looking at the smallest eigenvalue distributions in Figures 7.17 to 7.26, very good agreement is seen between the numerics and the random matrix predictions both for the probability distribution and the integrated probability distribution - the integrated distributions tend to have an error in the order of 10^{-2} or 10^{-3}. Larger errors occur in the probability distribution, but they are really only significant at the absolute smallest scale when $x \approx 0$ in the classes AII and AIII and the numerics strongly underestimate the true probability - which may be due numerical errors pushing positive roots falsely onto the negative side of zero, or due to the first root being on the wrong side of the first value taken in the grid search for roots before the optimisation routines are run. It should be noted that only 20,000 runs were taken for each class, yet the agreement with the random matrix predictions is excellent already, and further runs would only improve it.

With this, we can assume success in realising all of the Altland-Zirnbauer classes, and their associated ensembles on the Dirac graph, supporting the generalised BGS-Conjecture.
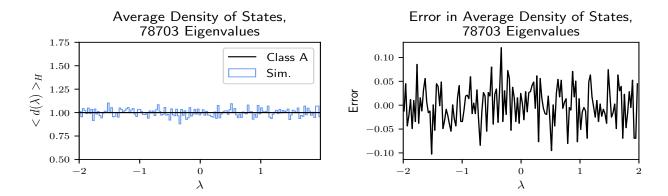
Figure 7.7: The simulated average density of states for the graph $\Gamma(Z_6, \{u, \alpha\})/Z_3$ as shown in Figure 7.4, with the phases taken from Table 7.2. Note the agreement with the predicted constant value of the statistics for the class A ensemble.
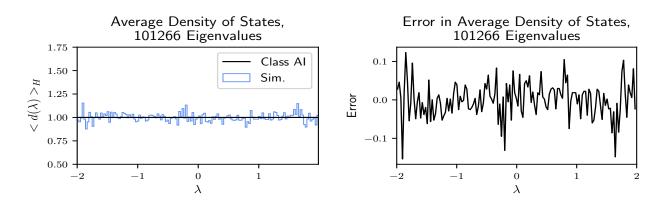
Figure 7.8: The simulated average density of states for the graph $\Gamma(Z_4, \{u, \alpha\})/Z_2$ as shown in Figure 7.4, with the phases taken from Table 7.2. Note the agreement with the predicted constant value of the statistics for the class AI ensemble.
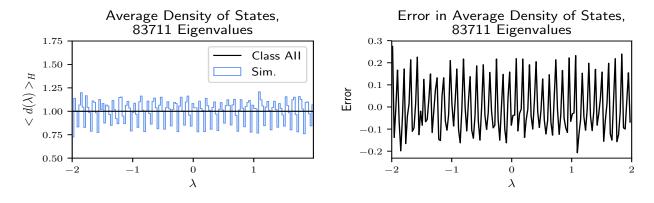
Figure 7.9: The simulated average density of states for the graph $\Gamma(D_6, \{u, \alpha\})/Z_3$ as shown in Figure 7.4, with the phases taken from Table 7.2. Note the agreement with the predicted constant value of the statistics for the class AII ensemble.
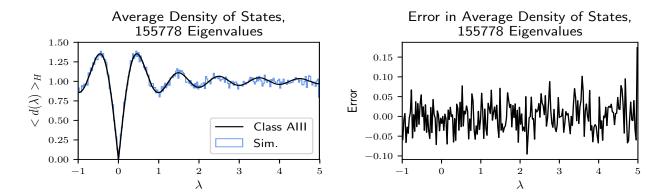
Figure 7.10: The simulated average density of states for the graph $\Gamma(Z_6, \{u, \alpha\})/Z_3$ as shown in Figure 7.4, with the phases taken from Table 7.2. Note the agreement with the chGUE statistics of the Altland-Zirnbauer class AIII.
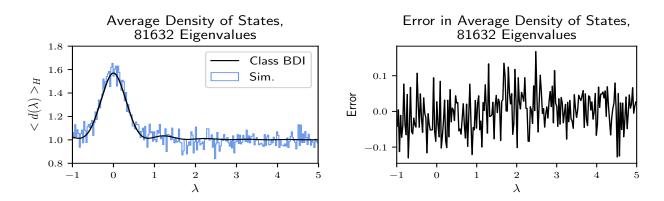
Figure 7.11: The simulated average density of states for the graph $\Gamma(Z_4 \times Z_2, \{u, \alpha, \gamma\})/Z_2$ as shown in Figure 7.6, with the phases taken from Table 7.3. Note the agreement with the chGOE statistics of the Altland-Zirnbauer class BDI.
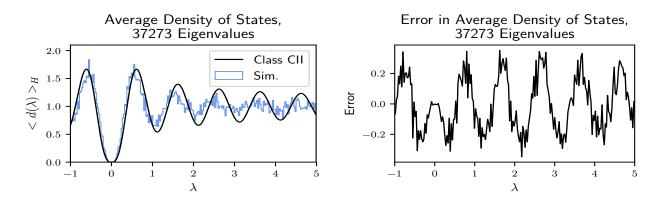
Figure 7.12: The simulated average density of states for the graph $\Gamma(Z_4 \times Z_2, \{u, \alpha, \gamma\})/Z_2$ as shown in Figure 7.6, with the phases taken from Table 7.3. Note the agreement with the chGSE statistics of the Altland-Zirnbauer class CII.
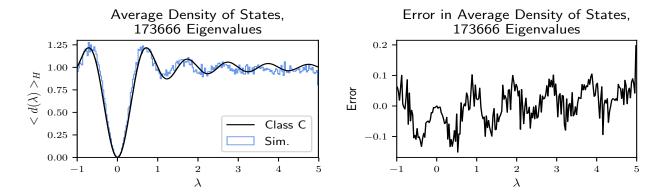
Figure 7.13: The simulated average density of states for the graph $\Gamma(Z_4, \{u, \gamma\})/Z_2$ as shown in Figure 7.4, with the phases taken from Table 7.2. Note the agreement with the random matrix statistics of the ensemble related to the Altland-Zirnbauer class C.
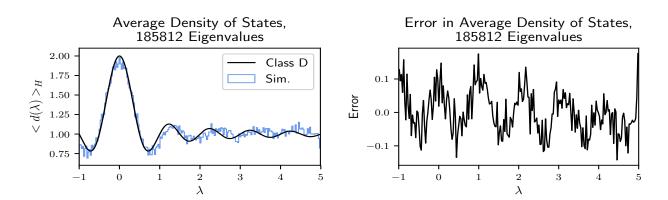
Figure 7.14: The simulated average density of states for the graph $\Gamma(Z_6, \{u, \gamma\})/Z_3$ as shown in Figure 7.4, with the phases taken from Table 7.2. Note the agreement with the random matrix statistics of the ensemble related to the Altland-Zirnbauer class D.
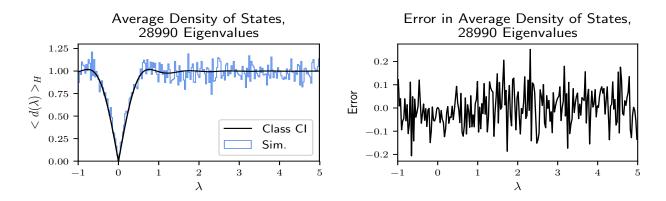
Figure 7.15: The simulated average density of states for the graph $\Gamma(Q_8, \{u, \alpha, \gamma\})/Z_2$ as shown in Figure 7.6, with the phases taken from Table 7.3. Note the agreement with the random matrix statistics of the ensemble related to the Altland-Zirnbauer class CI.
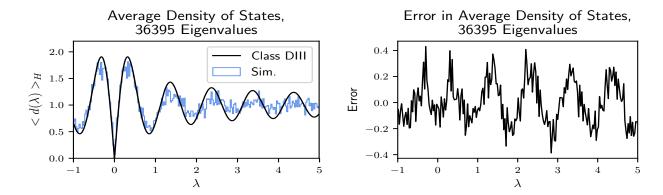
Figure 7.16: The simulated average density of states for the graph $\Gamma(D_{12}, \{u, \alpha, \gamma\})/Z_3$ as shown in Figure 7.6, with the phases taken from Table 7.3. Note the agreement with the random matrix statistics of the ensemble related to the Altland-Zirnbauer class DIII.
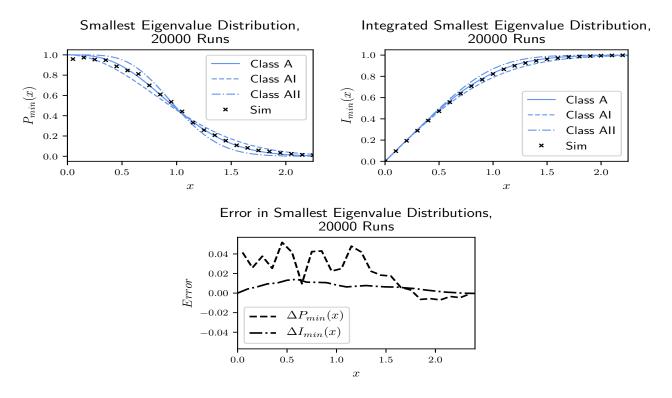
Figure 7.17: The simulated smallest eigenvalue distribution for the graph $\Gamma(Z_6, \{u, \alpha\})/Z_3$ as shown in Figure 7.4, with the phases taken from Table 7.2. Note the agreement with the GUE ensemble.
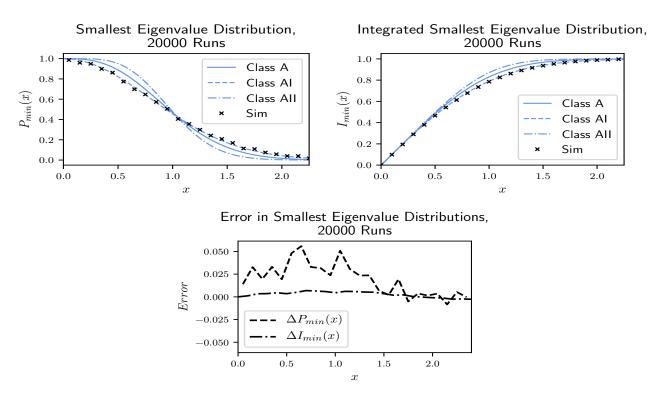
Figure 7.18: The simulated smallest eigenvalue distribution for the graph $\Gamma(Z_4, \{u, \alpha\})/Z_2$ as shown in Figure 7.4, with the phases taken from Table 7.2. Note the agreement with the GOE ensemble.
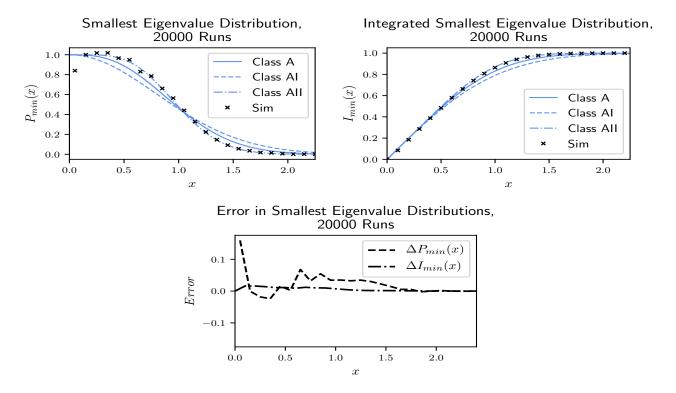
Figure 7.19: The simulated smallest eigenvalue distribution for the graph $\Gamma(D_6, \{u, \alpha\})/Z_3$ as shown in Figure 7.4, with the phases taken from Table 7.2. Note the agreement with the GSE ensemble.
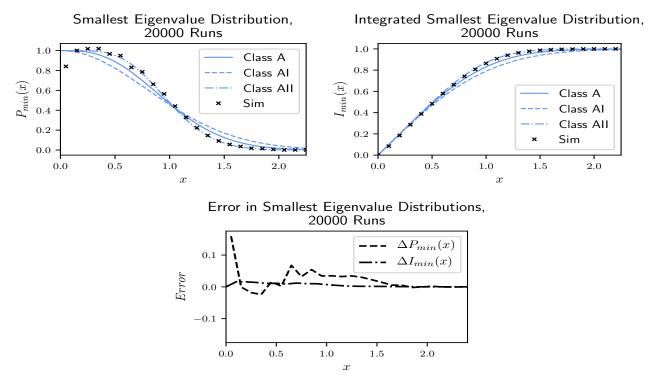
Figure 7.20: The simulated smallest eigenvalue distribution for the graph $\Gamma(Z_6, \{u, \pi\})/Z_3$ as shown in Figure 7.4, with the phases taken from Table 7.2. Note the agreement with the chGUE ensemble.
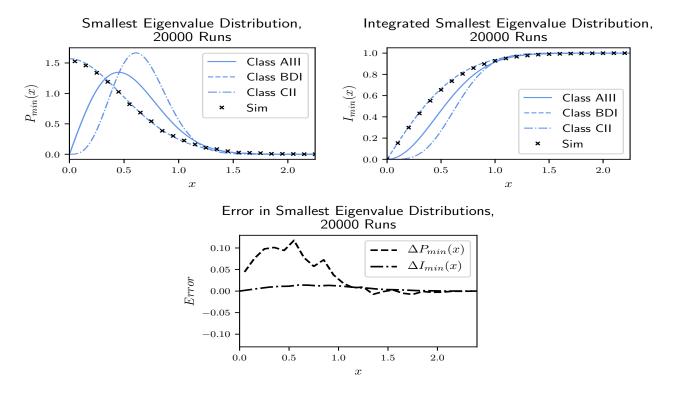
Figure 7.21: The simulated smallest eigenvalue distribution for the graph $\Gamma(Z_4 \times Z_2, \{u, \alpha, \gamma\})/Z_2$ as shown in Figure 7.5, with the phases taken from Table 7.3. Note the agreement with the chGOE ensemble.
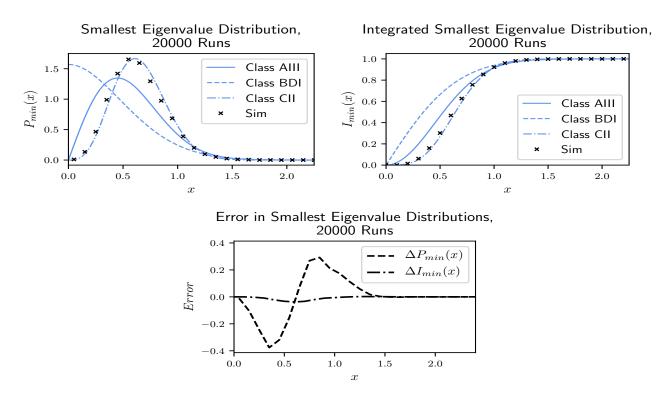
Figure 7.22: The simulated smallest eigenvalue distribution for the graph $\Gamma(Z_4 \times Z_2, \{u, \alpha, \gamma\})/Z_2$ as shown in Figure 7.5, with the phases taken from Table 7.3. Note the agreement with the chGSE ensemble.
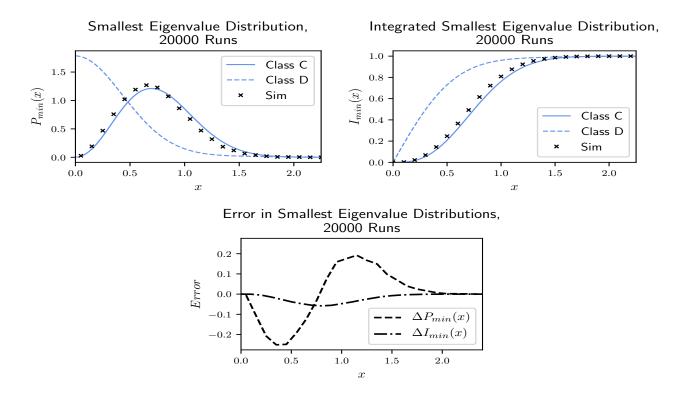
Figure 7.23: The simulated smallest eigenvalue distribution for the graph $\Gamma(Z_4, \{u, \gamma\})/Z_2$ as shown in Figure 7.4, with the phases taken from Table 7.2. Note the agreement with the random matrix statistics of the ensemble related to the Altland-Zirnbauer class C.
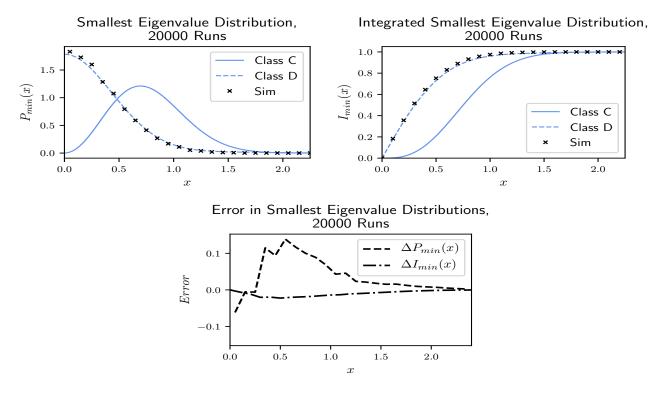
Figure 7.24: The simulated smallest eigenvalue distribution for the graph $\Gamma(D_6, \{u, \gamma\})/Z_3$ as shown in Figure 7.4, with the phases taken from Table 7.2. Note the agreement with the random matrix statistics of the ensemble related to the Altland-Zirnbauer class D.
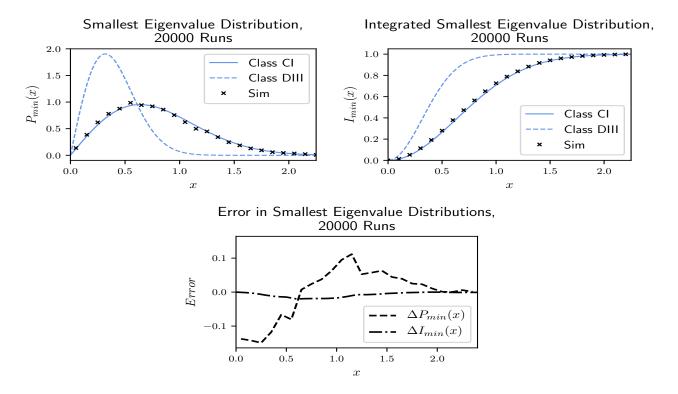
Figure 7.25: The simulated smallest eigenvalue distribution for the graph $\Gamma(Q_8, \{u, \alpha, \gamma\})/Z_2$ as shown in Figure 7.5, with the phases taken from Table 7.3. Note the agreement with the random matrix statistics of the ensemble related to the Altland-Zirnbauer class CI.
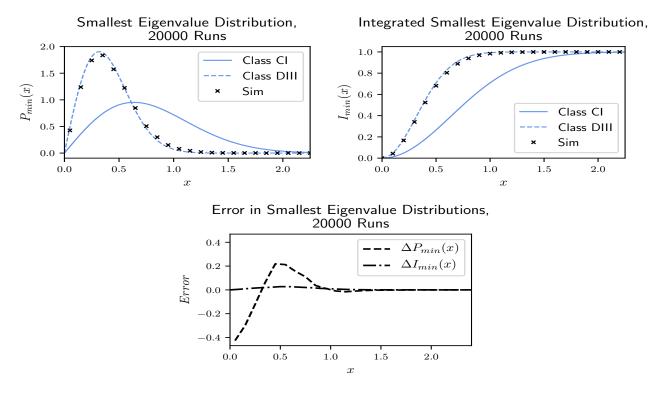
Figure 7.26: The simulated smallest eigenvalue distribution for the graph $\Gamma(D_{12}, \{u, \alpha, \gamma\})/Z_3$ as shown in Figure 7.5, with the phases taken from Table 7.3. Note the agreement with the random matrix statistics of the ensemble related to the Altland-Zirnbauer class DIII.

As an extension to finding the minimal graphs showing each of the ten Altland-Zirnbauer classes, it was stated that Dirac graphs allow all $Z_2 \times Z_2$-graded groups to be represented on them as symmetry groups. To verify this further than just with the above examples, we also look to confirm the second theorem of Section 5.2, Theorem 5.2.3, which showed that a 'full' $Z_2 \times Z_2$-graded group could always be used to generate any Altland-Zirnbauer class. The groups identified to cover this problem are now given in Table 7.8, once the substitutions for the DIII base symmetry have been taken. Of these, the classes BDI, CII ,DIII and CI have already been considered above, and can be ignored. For the remaining classes, they can be constructed as Dirac graphs by using the universal form of the quotient graph for $T_G = \{\alpha, \gamma\}$ with the phases taken from Table 7.9. This gives the quotient graph structure in Figure 7.27, which also presents the chosen subgraph to be used for the vertex expansion - which sits between the graphs in Figures 7.5 and 7.6 in terms of size to slightly speed up computation times here.
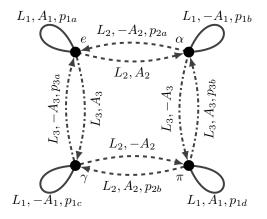
This gives the graphs which are posited to be derived from systems with all three of generalised time-reversal, generalised charge-conjugation and generalised chiral symmetries, yet have only one of them as a local symmetry.
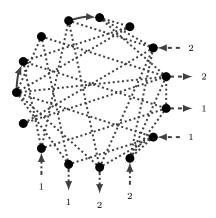
Class	G	U	$U \cup \alpha U$	$U \cup \gamma U$	$U \cup \pi U$	Irreducible Representation
A	$Z_2 \times M_4(2)$	Z_8	$Z_8 \times Z_2$	$M_4(2)$	$M_4(2)$	$e^{i\pi/4}$ Complex
AII	D_{12}	Z_3	D_6	Z_6	D_6	Complex
AI	Q_{16}	Z_4	Q_8	Z_8	Q_8	Complex
$AIII$	$Z_6 \times Z_2$	Z_3	Z_6	Z_6	Z_6	Complex
$DIII$	D_{12}	Z_3	D_6	D_6	Z_6	Complex
CI	Q_8	Z_2	Z_4	Z_4	Z_4	Sign
D	D_{12}	Z_3	Z_6	D_6	D_6	Complex
C	Q_{16}	Z_4	Z_8	Q_8	Q_8	Complex
BDI	$Z_4 \times Z_2$	Z_2	Z_4	Z_2^2	Z_4	Sign
CII	$Z_4 \times Z_2$	Z_2	Z_2^2	Z_4	Z_4	Sign

Table 7.8: Minimal examples of $Z_2 \times \mathbb{Z}_2$-graded groups and the associated representations of U to produce each of the Altland-Zirnbauer ensembles on a Dirac graph, given the requirement that $T_G = \{\alpha, \gamma\}$. The group $M_4(2)$ is described by the presentation $\langle u, \gamma | u^8 = \gamma^2 = 1, \gamma u \gamma = u^5 \rangle$.
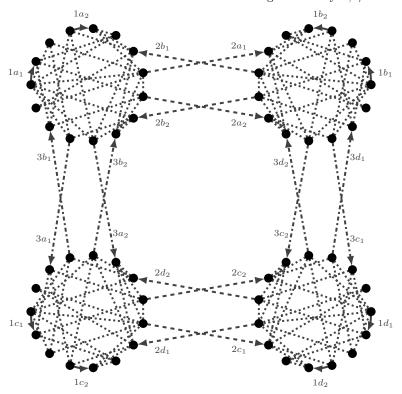
	A	AI	AII	D	C	AIII
$\rho(u^{-1})$	$\exp(-i\pi/4)$	$-i$	$\exp(2i\pi/3)$	$\exp(2i\pi/3)$	$-i$	$\exp(2i\pi/3)$
$\rho(\alpha u^{-1} \alpha^{-1})$	$\exp(-i\pi/4)$	i	$\exp(-2i\pi/3)$	$\exp(2i\pi/3)$	$-i$	$\exp(2i\pi/3)$
$\rho(\gamma u^{-1} \gamma^{-1})$	$\exp(3i\pi/4)$	$-i$	$\exp(2i\pi/3)$	$\exp(-2i\pi/3)$	i	$\exp(2i\pi/3)$
$\rho(\alpha\gamma u^{-1} \gamma^{-1} \alpha^{-1})$	$\exp(3i\pi/4)$	i	$\exp(-2i\pi/3)$	$\exp(-2i\pi/3)$	i	$\exp(2i\pi/3)$
$\rho(\alpha^{-2})$	1	-1	1	1	$-i$	1
$\rho(\gamma^{-2})$	1	$-i$	1	1	-1	1
$\rho(\gamma\alpha^{-1}\gamma^{-1}\alpha^{-1})$	1	$-i$	1	1	i	1
$\rho(\alpha\gamma^{-2}\alpha^{-1})$	1	i	1	1	$-i$	1

Table 7.9: The phases required on the bonds of the graph given in Figure 7.27 to get each of the classes A, AI, AII, C, D or AIII as the energy level statistics ensemble.

(a) Unexpanded quotient graph.

(b) Vertex sub-graph using 15 vertices, 28 bonds and two copies of each of the bonds generated by α, γ and u.

(c) Expanded quotient graph.

Figure 7.27: Deriving the example graphs for the classes A, AI, AII, AIII, C and D on graphs with a four-fold structure so that $T_G = \{\alpha, \gamma\}$. See Table 7.9 for what phases should be chosen for each of the bonds to get the different Altland-Zirnbauer classes.

The same run-down of numeric tests can be applied to these graphs as were applied to the previous graphs.

First, the first test for chaos according to Theorem 6.1.11 is shown in Table 7.5, showing that the requirement for all eigenvalues but one to lie within the unit circle is kept. The spectral mirror symmetry check for these graphs is then given in Table 7.11, and the spectral mirror symmetry is indeed broken in the classes A, AI and AII, where $|\lambda_n - \lambda_{-n}| > 0.1$ which is a significant divergence from the mirror symmetry requirement of $\lambda_{-n} = -\lambda_n$. On the other hand, this relation holds to within an at most order 10^{-12} error for the classes AIII, C and D which is well within the allowance for numerical error, and the spectral mirror symmetry exists.

Class	$|\eta_1|$	$|\eta_2|$	Class	$|\eta_1|$	$|\eta_2|$
A	1.0000	0.9253	AIII	1.0000	0.91721
AI	1.0000	0.92764	D	0.99999.	0.92028
AII	1.0000	0.91775	C	1.0000	0.91247

Table 7.10: Checking the ordered eigenvalues $\eta_1 \geq \eta_2 \geq \cdots \geq \eta_N$ of the Markov process matrix $T_{ij} = \left|S_{ij}^2\right|$ derived from the scattering matrix for each of the example four-part graphs identified in Figure 7.27 for the classes A, AI, AII, AIII, C and D. The first chaos requirement is that $|\eta_1| = 1$ and $|\eta_2| < 1$, which holds in each case. All numbers rounded to five significant figures and come from a single initialisation.

Class	$|\lambda_1 + \lambda_{-1}|$	$|\lambda_2 + \lambda_{-2}|$	$|\lambda_3 + \lambda_{-3}|$	$|\lambda_4 + \lambda_{-4}|$
A	0.60644	0.26655	0.57989	1.0458
AI	1.9616	2.2080	0.52603	0.10947
AII	0.17889	0.31438	0.318891	0.26556
AIII	2.1126×10^{-12}	2.1037×10^{-12}	2.1134×10^{-12}	2.0899×10^{-12}
C	1.4155×10^{-14}	3.9080×10^{-14}	1.6431×10^{-14}	7.9936×10^{-15}
D	3.0531×10^{-15}	1.4322×10^{-14}	3.7748×10^{-14}	1.4655×10^{-14}

Table 7.11: Testing whether the calculated spectrum has a spectral mirror symmetry by taking the difference between λ_n and $-\lambda_{-n}$ for the four-part version of the graphs for the ensembles A, AI, AII, AIII, C and D. It can be seen that up to small numerical errors, the results agree with a spectral mirror symmetry existing in the classes AIII, C and D while the classes A, AI and AII don't have a spectral mirror symmetry. All numbers rounded to five significant figures and come from a single initialisation.

It is now possible to consider the results of simulating the characteristic distributions of the random matrix ensembles through the defined graphs. In general, we only take the results of the calculations of the smallest eigenvalue distribution, as the density of states calculations on these graphs are too computationally intensive to do large quantities. These distributions can be can be seen in Figures 7.28 to 7.33, and it can be immediately noted that while very good results are found in the classes AI, AIII, C and D, the results are significantly poorer in the classes A and AII.

First, we note that there is a small underestimate of the density of states for the class A in the range $(-0.1, 0.25)$, as seen in the top left hand corner of Figure 7.28. This is possibly a fragment of the finite size of the graph, though no others have occurred in any of the other systems studied here. This underestimate in the density of states however, has the knock-on effect of underestimating the smallest eigenvalue distribution probability for the same range, and then overestimating the probability in the rest of distribution due to the normalisation. This has the effect of erroneously matching the simulation estimate with the class AII statistics for the smallest eigenvalue distribution, particularly in the integrated distribution case. This significant error can happen in the integrated case, as all that it counts is the cumulative distribution of the data, so oscillations and deviations lower down can be hidden quickly if they smooth out when summed together. This makes the importance of not relying on only the integrated distributions incredibly clear, as it is only when the probability distribution is checked that the errors near zero are seen. We note however, that plotting the level spacing distribution away from zero, good agreement with the class A prediction is seen; with the conformation that the spectral mirror symmetry has been broken in Table 7.11, there is then reasonable evidence that the system does sit in the class A as predicted.

Worse, in the class AII in Figure 7.30, there is a large over-estimate of the first eigenvalue occurring at $x \approx 0.5$, which has the knock-on effect of causing the underestimate of all other values due to the normalisation of the distribution. The poor agreement with the random matrix prediction is surprising as the structure of the graph and the cut-bond phases are exactly the same as the class D graph, except for swapping the phases between the $\alpha\Gamma$ and $\gamma\Gamma$, and the class D graph gives excellent agreement. Plotting the density of states for the graph around zero, it is seen that it is oscillatory rather than constant - this is an issue, as it is unlikely it is an artefact of the size of the graph. However, plotting the density of states far from zero, the oscillations have disappeared, and the constant density of states is well approximated by the graph - as is the level spacing distribution when that is calculated. It is possible that the issues close to zero are from including $\gamma\Gamma(G, S_U \cup \alpha, \gamma)$ and $\pi\Gamma(G, S_U \cup \alpha, \gamma)$, without sufficiently killing off the effects of the spectral mirror symmetry on the first eigenvalue distribution. However we note that the spectral mirror symmetry is provably broken given the check in Table 7.11, and the spacing distribution does still match the AII class well.

Overall though, we conclude a success in showing all the Altland-Zirnbauer classes can be realised out of 'full' $Z_2 \times Z_2$-graded groups where $A \neq \emptyset$, $C \neq \emptyset$ and $P \neq \emptyset$.
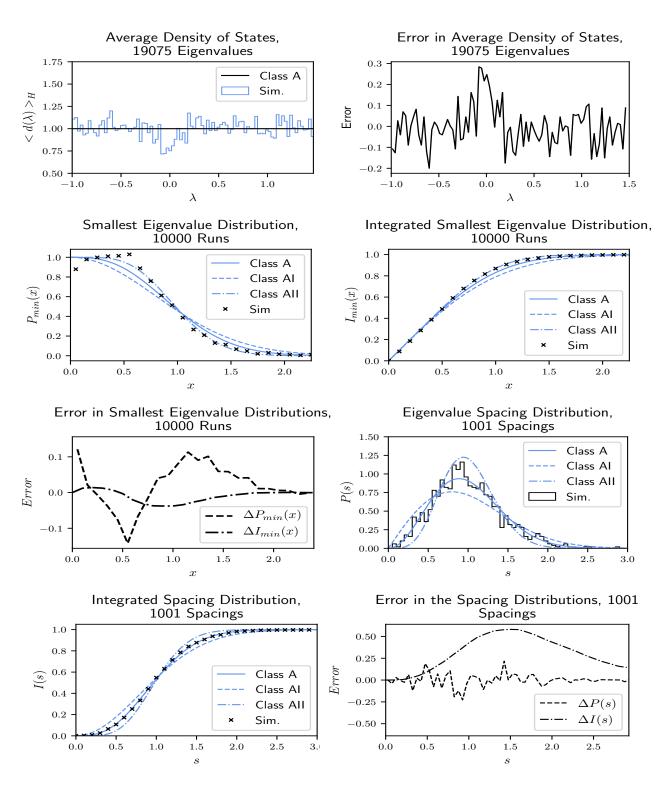
Figure 7.28: The results of the numerical simulations for the graph from Figure **??**, taking the phases from Table 7.9 for a predicted Altland-Zirnbauer class of A, and GUE statistics. The underestimate of $< d(E) >_H$ in the range $(-0.1, 0.25)$ causes a large error in the smallest eigenvalue distribution, even causing it to look like the AII class in the integrated distribution. However, the level spacing distribution clearly shows the GUE statistics.

171
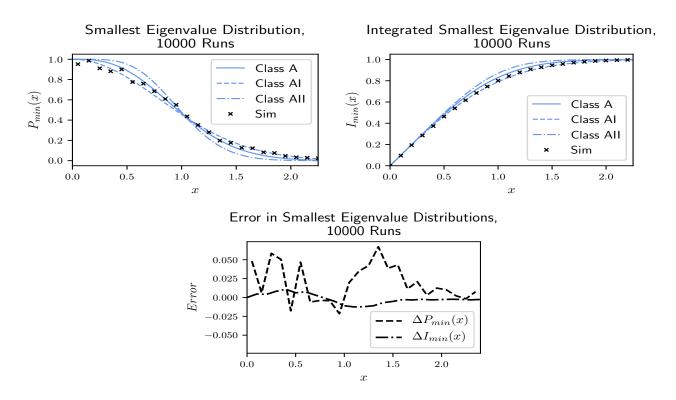
Figure 7.29: The results of the numerical simulations for the graph from Figure 7.27, taking the phases from Table 7.9 for a predicted Altland-Zirnbauer class of AI, and GOE statistics.
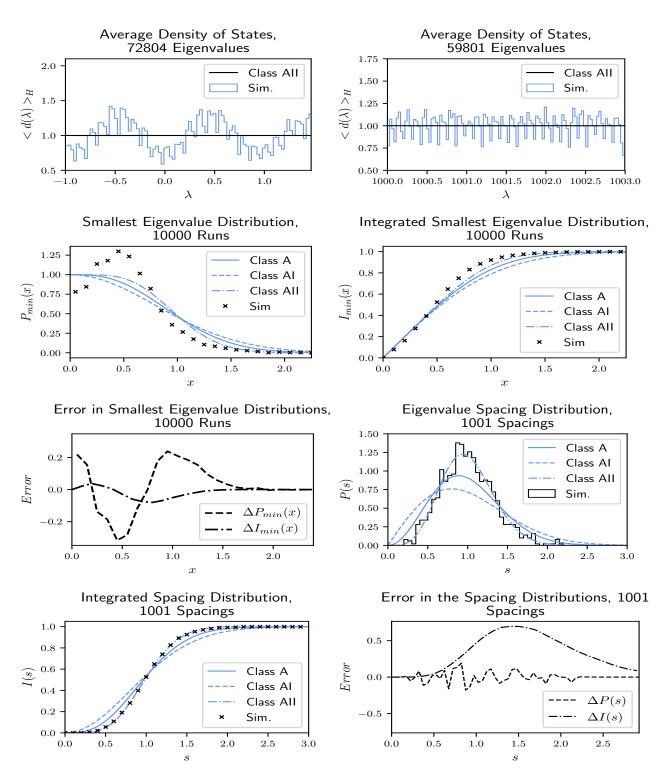
Figure 7.30: The results of the numerical simulations for the graph from Figure 7.27, taking the phases from Table 7.9 for a predicted Altland-Zirnbauer class of AII, and GSE statistics. Due to the oscillatory form of the density of states around zero, the smallest eigenvalue statistics are poor, but given this behaviour vanishes away from zero, and the constant $< d(E) >_H$ is correctly estimated, then the level spacing distribution gives a good estimate for the correct class AII. The poorness of the smallest eigenvalue distribution is surprising, as the graph is generated by taking the graph for the class D and interchanging α and γ, with the class D version giving very good statistics.
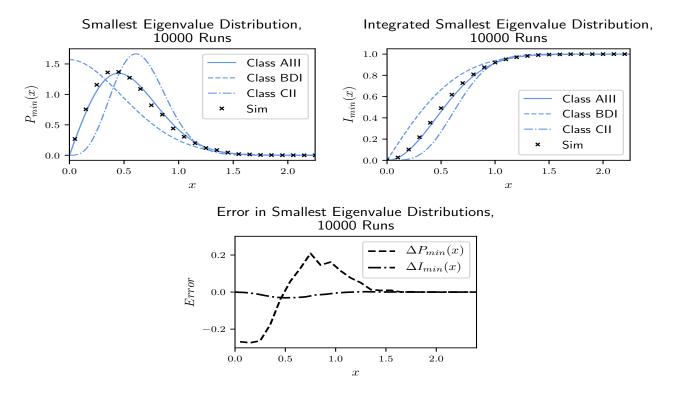
Figure 7.31: The results of the numerical simulations for the graph from Figure 7.27, taking the phases from Table 7.9 for a predicted Altland-Zirnbauer class of AIII, and chGUE statistics.
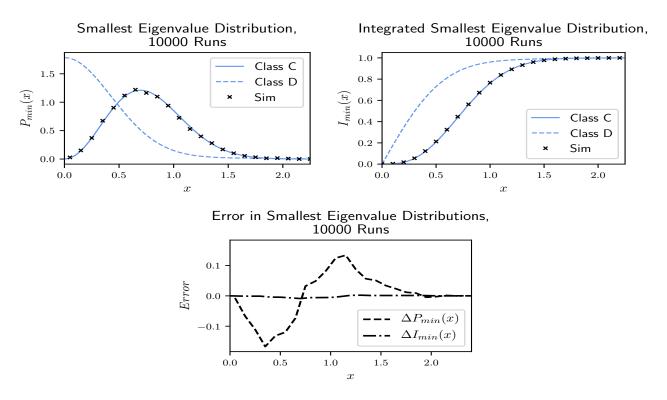
Figure 7.32: The results of the numerical simulations for the graph from Figure 7.27, taking the phases from Table 7.9 for a predicted Altland-Zirnbauer class of C, and the associated random matrix ensemble statistics.
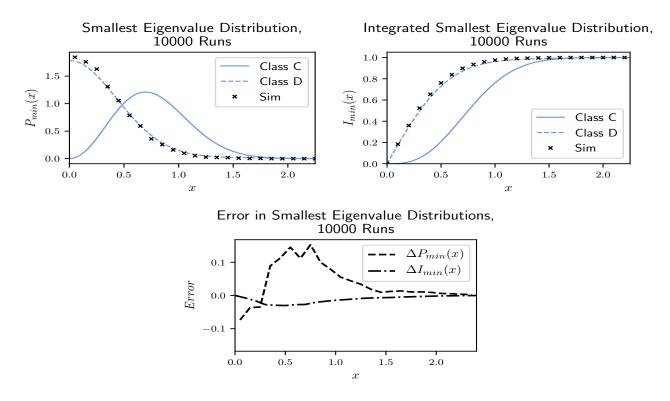
Figure 7.33: The results of the numerical simulations for the graph from Figure 7.27, taking the phases from Table 7.9 for a predicted Altland-Zirnbauer class of D, and the associated random matrix ensemble statistics.

8.   Conclusions and Outlook

The intent at the start of this thesis was to ascertain if the techniques of working with systems with unitary commuting symmetries could potentially decrease the difficulty of realising the Altland-Zirnbauer ensembles in the lab. These methods take a system without unitary commuting symmetries, and which has a fixed global form of time-reversal $\hat{\mathcal{T}}$ and charge-conjugation $\hat{\mathcal{C}}$ symmetry so that it sits in one of the Altland-Zirnbauer classes BDI, CII, CI or DIII. Application of unitary commuting symmetries to the system, and moving to generalised time-reversal and charge-conjugation symmetries, then causes the spectra to split into sub-spectra which can have a different Altland-Zirnbauer class to the base system without symmetries. It was asked that given any form of initial $\hat{\mathcal{T}}$ and $\hat{\mathcal{C}}$, so to maximise the number applicable systems which might be considered for testing, if it was possible to find a set of symmetry groups G to apply to the system such that a subspace with each ensemble of Altland and Zirnbauer statistics existed.

It can be stated, that based on the results of this thesis, that it is indeed possible to find such symmetry groups. Their existence and form were derived and proved in Chapter 5; while numeric verification that they do indeed generate systems with each of ten ensembles in their statistics was given for the specific example system of the Dirac Graph in Chapter 7.

As a review, the first three chapters covered the theory behind how quantum symmetries, quantum chaos and random matrix statistics are linked.

In Chapter 2, the definitions of graded groups and the structure of their corepresentations were discussed. The corepresentations varied from standard unitary representations in that they could contain anti-linear and anti-unitary elements. Two types of graded group were considered - the Z_2-graded groups and the $Z_2 \times Z_2$-graded groups. The corepresentations of the $Z_2 \times Z_2$-graded groups had the extra structure of being a super-vector space, so that elements could be grading-preserving or grading-inverting. This led to the definition of its super-commutant, which was identified as being one of the ten real super-division algebras by the Altland-Zirnbauer Tenfold Way. A number of methods of identifying the class of a corepresentation were discussed, including for projective corepresentations.

The notion of quantum symmetries as transforms of the projective Hilbert space preserving the characteristic properties of the quantum system was then introduced in Chapter 3. Identifying the symmetry group as a $Z_2 \times Z_2$-graded group, the symmetries could be linked to operators through a projective corepresentation. This allowed physical interpretations of the symmetry operators to be made - they were either geometric, or generalised time-reversal, generalised charge-conjugation, or generalised chiral symmetries. The existence of geometric symmetries caused the energy level spectrum to split into independent sub-spectra, and the system into independent

sub-systems. We noted that in the subspaces, the symmetry operators could only be local time-reversal, charge-conjugation and chiral operators, and that the local Hamiltonian had to be a member of the local symmetry group's super-commutant. This linked the classification of the structure of the Hamiltonian to the classification of a corepresentation according to the Altland-Zirnbauer Tenfold Way, and provides the gateway to linking quantum systems to random-matrix theory. The empirical evidence for the correspondance between the statistics of certain quantum systems and random matrix theory was then discussed, and the necessary requirement for the underlying classical system to be chaotic given according to the BGS-conjecture.

Chapter 4 then discussed the ten random matrix ensembles that a chaotic quantum system's statistics could match, describing the characteristic forms of their densities of states, spacing distributions and smallest eigenvalue distributions.

Understanding the theory behind how symmetry groups create subspaces with random matrix statistics matching the Altland-Zirnbauer class of a corepresentation, and having methods to predict which statistics will be found for which symmetry group, the main question of the thesis could begin to be answered. This started with defining a search algorithm to identify all $Z_2 \times Z_2$ graded groups in Chapter 5. By applying the classification methods to each identified $Z_2 \times Z_2$-graded group, an example of a symmetry group producing a subspace with the desired statistics was found for each Altland-Zirnbauer class. This gave theoretical proof of the central question of the thesis.

Testing the theory from Chapter 5 with numerical simulations was the aim of Chapters 6 and 7. First, the quantum graph - already having been used to build systems with limited forms of symmetry groups by Joyner, Müller and Sieber - was introduced in Chapter 6 as a model for a system with time-reversal type, but not charge-conjugation or chiral type symmetries. The previous definitions of symmetry on a quantum graph were supplanted with the most general definition of symmetry on a quantum graph, and an algorithm for identifying a quantum graph symmetric under a general Z_2-graded group given. The special structure of these graphs was described, and the predictions of finding GUE, GOE and GSE statistics on the systems identified by Chapter 5 tested. Good agreement was found, marking the first stage of numeric testing of the predictions.

To test the rest of the predictions, the Dirac graph was introduced as a model. Following work in the literature on defining their behaviour under time-reversal, their behaviour under charge-conjugation was studied. Identifying the boundary conditions for the Dirac graph to sit in the class DIII, the model was shown to be an applicable system for testing the central theorem of the thesis. The definition of a symmetric Dirac graph was found in the most general sense, and another algorithm given for taking a $Z_2 \times Z_2$-graded group and producing a matching symmetric Dirac graph. Applying this to the symmetry groups identified in Chapter 5, allowed the simulation of the characteristic distributions for the random matrix ensembles. Numerical verification of finding the seven additional Altland-Zirnbauer ensembles in these graphs was then given, completing the the goals of the thesis.

In terms of outlook, there are several obvious points. First is clearly experimental verification of these results in the lab. For the systems described in Chapter 6, it is already known that the base non-magnetic quantum graph can be built in the lab as a microwave network, [83]. This has been used to build the quantum graph identified by Joyner, Müller and Sieber, [92], in the

lab, [113, 133, 134, 135]. We note that there is the apparent issue that the graphs discussed in Chapter 6 require the use of a magnetic potential on the wires to break the time-reversal symmetry, however this is something that microwave networks have not been realised with, or with an equivalent of to date. This would be an issue if it were not for the fact that switching to a microwave network allows the time-reversal symmetry to be broken by working with microwave circulators, [107], which break the symmetry by allowing travel down the wires in only one direction. These uni-directional graphs have been used to find GUE statistics, [107], and very recent work, [3], has identified a specific construction of a $G = Z_4$, $U = Z_2$ quantum graph with GSE statistics through including multiple copies of a sub-graph with the direction of travel flipped between different copies to create and control the generalised time-reversal symmetry. We note the similarity to the structure of the quantum graphs with Z_2-graded symmetry groups discussed in Chapter 6, and posit that this is a sufficient replacement on the microwave network for the magnetic potential. That is, when constructing the microwave network, directions of travel are picked for the wires in the unitary sub-graph, and then everywhere where the magnetic potential would be flipped, the direction of travel is flipped instead. This, we note, ties into the condition on the forms of the vertex scattering matrices which can also break the time-reversal symmetry, as enforcing uni-directionality on the bonds imposes form on the vertex scattering matrices.

Having a way to build generalised time-reversal symmetries into a quantum graph, there is then the question of building Dirac graphs in the lab with generalised time-reversal and generalised charge-conjugation symmetries. We have already discussed how a Dirac graph may be re-interpreted as a quantum graph with doubled bonds, and using the idea of switching from magnetic bonds to uni-directional microwave wires gives a possible way to realise the random matrix ensembles of the Altland-Zirnbauer classes in the lab. Switching the focus from magnetic potentials to the vertex scattering matrices is also highly relevant and consistent with the generalised charge-conjugation case, as the enforcement of an element g in G being of charge-conjugation type and not time-reversal type is all through the relation between the vertex scattering matrices $\sigma^{(e)}$ and $\sigma^{(g)}$. Thus, there is promise in using microwave networks to implement the graphs discussed in Chapter 7 through the use of carefully modulated vertex scattering matrices. This will likely involve the use of a mix of circulators and methods of rotating phases within the wires - which will raise the question of how ensembles of graphs can be easily generated - but it is hopefully feasible to realise the systems described in Chapter 7 in the lab with this methodology. Even if it isn't, it is hopeful that the techniques for constructing systems with generalised time-reversal and charge-conjugation symmetries could be applied to a more suitable model to see the Altland-Zirnbauer classes in the lab.

Outside of experimental verification, there are a number of possible applications of the work done here. First is the use of the graphs described within as a verification tool for chaotic quantum systems - that is, given a system, its symmetry group can be found, and then a Dirac graph showing the same statistics can be generated. This follows from the fact that the statistics of the system are dependent only on the symmetry group, and it would allow for results checking, or if a particular property was identified in the statistics of a system with a particular symmetry group, the equivalent Dirac graph could be identified. This would be of particular use if the other system was hard to compute results for, as the numerics needed to work with Dirac graphs are fairly simple.

The other thing to do would be to complete the semi-classical analysis of magnetic quantum quotient graphs. This was started in Appendix D with the periodic orbit approximation of the density of states being found and an algorithm for the speeding up of the calculation of the periodic orbits of symmetric graphs being described. Further work would find the form factor approximations and apply them to the graphs discussed in this thesis. This links into the work done in [27, 28, 65, 102] on the spectral statistics of quantum graphs and their spin counterparts.

There is also the question of applying these results to areas of study outside of the standard field of Hermitian quantum chaos. The Altland-Zirnbauer classes are essential to studies in condensed matter, and for super-conductors and topological-insulators insulators in particular, [14, 37, 39, 143]. The symmetry class of the system defines important properties of the system - including whether the system has an energy gap, whether two systems are topologically equivalent, universal conductance frequencies, the Chern winding number and creates the periodic table of topological insulators among other things. Due to to periodic table of topological insulators, understanding the symmetry classification also means understanding the limits of what topological insulators can be built, and theoretically knowing what symmetry groups cause which symmetry classes gives more information on where examples for different classes of topological insulator can be searched for. This gives application to the tables in Appendix E in particular. It should also be noted that in many ways the field of condensed matter has pushed the study of symmetric systems further than is used in random matrix theory, and this has led to a disconnect between the areas that could need correcting. It is essential then to consider what techniques developed in condensed matter could benefit random matrix theory, and whether key questions of random matrix theory have in fact been previously answered in the condensed matter field. Examples of condensed matter work into the theory surrounding the Altland-Zirnbauer classification include studies of the interaction of the Altland-Zirnbauer classification with crystal structure, [145], and CPT symmetries, [81]; while papers which include more 'pure' or abstract theory surrounding the theory of corepresentations include [37, 69]. This also includes additional research into the experiments allowed for in condensed matter theory, and the possibilities for testing random matrix predictions on them.

Finally, we note that the classification of Altland and Zirnbauer of Hermitian systems can be considered to sit inside a classification of thirty-eight different types of non-Hermitian system, [19, 95]. This classification is still based in the classification of the system's symmetries but has an expanded number of classes due to the fact $H^* \neq H^T$ so there are more possible behaviours for the symmetries within relation to the Hamiltonian, creating extra classes. This means additional random matrix ensembles are possible in these systems. These non-Hermitian systems are seeing a large amount of current study - see the many examples cited in [95] - as they make up dissipative equivalents of Hermitian systems, [87], which are more physical than those with perfect closure of the phase space; and several models in condensed matter, [95], and the study of symmetry in these models is every bit as important as for their Hermitian counterparts as symmetry encodes information about all of the same properties as it did for the Hermitian case. There is then a question as to whether it would be possible to build a variant on quantum graphs that could be used to demonstrate the non-Hermitian random matrix ensembles - we posit that given that self-adjointness was enforced on the graph through the vertex boundary condition equations, a different choice of boundary condition equation could create non-Hermitian graphs. This would then require studying the process of sub-space creation and the symmetry decomposed basis

for the non-Hermitian case, and the effect on creating the local symmetry groups. However, if these example graphs are found, then they should allow every possible universal random matrix ensemble for chaotic quantum systems to be realised, up to some special cases. This would be very powerful, as it would give a tool for realising every random matrix ensemble with symmetry connections, massively simplifying the search for example systems.

A.   *Group Theory*

We give here a primer on the abstract field of group theory, a topic whose basics are covered in [53, 86, 99], while a broader and more detailed covering of the field can be found in [138].

In short, Group Theory studies the structure behind sets with multiplication rules. By lifting from concrete sets with multiplication defined on them - such as the *nth* roots of unity, or $n \times n$ invertible matrices - to studying the multiplication rules as abstract objects of their own, common structures can be identified, and proofs given at a general level that can then be applied to specific examples.

We begin with the formal definition of a group as a set with a multiplication rule that has an element that acts trivially, always returns elements within the set, is invertible, and is independent in the order which pairs in an expression are multiplied.

Definition A.0.1. *A group $(G, \cdot)$ is the set G of elements with a multiplication rule $\cdot : G \times G \to G$ that obeys the properties*

Identity: *$\exists e \in G$ such that $e \cdot g = g \cdot e = g \ \forall g \in G$*

Inverse: *$\forall g \in G$, $\exists g^{-1} \in G$ such that $g \cdot g^{-1} = g^{-1} \cdot g = e$*

Closure: *$\forall g_1, g_2 \in G$, $g_1 \cdot g_2 \in G$.*

Associativity: *$g_1 \cdot (g_2 \cdot g_3) = (g_1 \cdot g_2) \cdot g_3 \ \forall g_1, g_2, g_3 \in G$.*

Given some group elements, combinations of their multiples $g_1 g_2 \cdots \in G$ will be known as a word. There will always be an infinite number of words which can be constructed from the group elements, but by applying the multiplication map to turn pairs of elements into one element, it can be seen that many words are in fact equivalent - for example, if $g_1 \cdot g_2 = g_3$ and $g_3 \cdot g_3 = e$, then the words $g_1 g_2 g_1 g_2 \equiv g_3 g_3 \equiv e$ are all the same. This allows the set of unique words which can be written using elements of G without being equivalent to be created, this set is exactly the set of elements of G. In many cases, G will contain an infinite number of elements, but we will be concerned only with those groups G that contain a finite amount.

Definition A.0.2. *Let G be a group, if $|G| < \infty$ then G is a finite group.*

The fact that the set of unique words describes the element set of a group can be used to define a group from a subset of elements. Taking a subset S of G as what is known as a generating set, and defining all of the relations between them under multiplication allows all the unique words which can be written using them to be found, which then describes a unique group based on this

multiplication rule. The method of defining a group in this manner is known as taking the group presentation.

Definition A.0.3. *A generating set, is a subset $S \subset G$, such that every element of G can be written as words using only elements of S and their inverses, $\forall g \in G,\ g = a_1 a_2 \ldots a_n$ where for each a_i, either $a_i \in S$ or $a_i^{-1} \in S$.*

If $|S| = \min\left(\{|S_i| \mid S_i \text{ generates } G\}\right)$ then S is a minimal generating set, however it is possible to choose a generating set larger than the minimal.

Definition A.0.4. *Given a generating set S of G, the relations R for S is the set of words form-able from S and S^{-1} that are equal to the identity,*
$R = \left\{ a_1 a_2 \cdots \mid a_i \in S \text{ or } a_i^{-1} \in S,\ a_1 a_2 \cdots = e \right\}.$

Definition A.0.5. *Let G be a group, then given a generating set S of G and the relations R of S the group presentation of G is $\langle S|R \rangle$.*

To read a group presentation, all possible words using generators S are taken, using the relations to simplify the generated elements and then removing any duplicates from the set.

Example A.0.6. *Simple group presentations include,*

$$
\begin{array}{rcccc}
\text{Trivial Group} & = & \langle e| \rangle & = & \{e\} \\
C_2 & = & \langle u|u^2 = e \rangle & = & \{e, u\} \\
C_n & = & \langle u|u^n = e \rangle & = & \{e, u, \ldots, u^{n-1}\} \\
K & = & \langle u, v|u^2 = v^2 = e, uv = vu \rangle & = & \{e, u, v, uv\} \\
D_3 & = & \langle u, v|u^3 = v^2 = e, vu = u^2 v \rangle & = & \{e, u, u^2, v, uv, u^2 v\}
\end{array}
$$

There arises the issue that two different presentations can describe the same group, for example $\langle u|u^6 = e \rangle = C_6 = \langle a, b|a^3 = b^2 = e, ab = ba \rangle$. Group homomorphisms will map one group to another, and isomorphisms will identify identical group structures.

Group homomorphisms are functions between two groups that is compatible with each of their multiplications.

Definition A.0.7. *If $(G, \cdot), (G', \times)$ are groups, a group homomorphism $\phi : G \to G'$ is a function such that*

$$\phi(g_1) \times \phi(g_2) = \phi(g_1 \cdot g_2) \qquad \forall g_1, g_2 \in G.$$

If ϕ is both injective and surjective, it is a group isomorphism and $G \cong G'$.

More general functions $f : G \to \mathbb{C}$ can also be defined on a group that are not necessarily homomorphisms. While there are no universal properties that can be described for these f, there are universal properties for the sums of their values over all of G. That is, left multiplying the variable in f by h leaves the sum fixed.

Theorem A.0.8. *Let G be be a finite group and $f : G \to \mathbb{C}$ a function. Then,*

$$\sum_{g \in G} f(g) = \sum_{g \in G} f(hg) \qquad \forall h \in G.$$

This is a side-effect of the closure of G under multiplication combined with summing over all of G - left-multiplying the input variables by h merely rearranges the order the sum is taken, which is why this is known as the Rearrangement Theorem.

Given a group, subsets of its elements can also fulfil the group definition by themselves, and are known as subgroups.

Definition A.0.9. *A subgroup $H \subset G$ is a subset H of elements of G with the same multiplication rule as G, with $(H, \cdot)$ also meeting the Identity, Inverse and Closure requirements of being a group. If $|H| \neq 1, |G|$ then H is a proper subgroup.*

Left multiplication of H by an element $g \in G$ gives a subset of G's elements called the left coset of H in G.

Definition A.0.10. *Let G be a group and $H \subset G$ a subgroup, then the left coset of H in G for $g \in G$ is the set*

$$gH = \{g' \in G \mid \exists h \in H, \ g' = gh\}$$

The left cosets have a number of properties, including the fact that they can be used to partition G into subsets, each of which can be related back to the original subgroup by a single element.

Proposition A.0.11. *Let G be a group and $H \subset G$ a subgroup. Then the following holds for the left cosets of H,*

1. *All left cosets of H have the same size, $\forall g \in G, \ |gH| = |H|$.*

2. *Every element $g \in G$ appears in a coset of H, $\forall g \in G \ \exists g' \in G$ such that $g \in g'H$*

3. *Two cosets $g_1 H, g_2 H$ are either non-intersecting or are equal, $g_1 H \cap g_2 H \neq \emptyset \iff g_1 H = g_2 H$.*

4. *The unique cosets of H partition G, there exists a subset in G,*
   $T = \{g_i \in G \mid g_i H \cap g_j H = \emptyset, \ \cup_i g_i H = G\}$, whose union of cosets of H is G. It is usual to choose $g_0 = e$, and T is a transversal of G for H while $[G : H] = |T|$ is called the index of H in G.

Proof.

1. There is a homomorphism between H and gH given by $\phi(h) = gh$, with an inverse $\phi^{-1}(h) = g^{-1}h$ so that it is bijective. Thus $|gH| = |H| \ \forall g \in G$.

2. $e \in H \implies g \in gH$.

3. Assume that $g_1 H \cap g_2 H \neq \emptyset$ but $g_1 H \neq g_2 H$ so there $\exists y \in g_1 H, \ y \notin g_2 H$ without loss of generality.

   Then, $\exists h_1, h_2, h_1' \in H$ such that $g_1 h_1 = x = g_2 h_2$ and $y = g_1 h_1'$. As H obeys the requirement of group inverses, $\exists h_3 \in H$ such that $h_1 = h_1' h_3$ and $yh_3 = x$ or that $y = x h_3^{-1}$. Then $y = g_2 h_2 h_3^{-1} = g_2 h_4 \in g_2 H$ which is a contradiction. Thus, the original statement $g_1 H \cap g_2 H \neq \emptyset \iff g_1 H = g_2 H$ holds.

4. We prove by construction, applying parts 2 and 3.

   Order the elements of $G = \{g_0 = e, g_1, \ldots, g_{|G|}\}$, and start with $T = \{e\}$, $P = H$. Then consider each of the g_i in turn. If $g_i \in P$, move onto g_{i+1}. If $g_i \notin P$ then take $T = T \cup g_i$ and $P = P \cup g_i H$.

   Once $g_{|G|}$ has been checked, then $P = \cup_{t \in T} tH$ and P a partition of G with T as its transversal of G.

$\square$

Corollary A.0.12. *Let G be a finite group with subgroup H and transversal T, then G can be written as*

$$G = \bigcup_{t \in T} tH.$$

Element conjugation is another method to partition a group; this starts with the definition of the conjugate of one element by another.

Definition A.0.13. *For $g, x \in G$, the conjugate of g by x is $g^x = xgx^{-1}$.*

This can be used to define the equivalence relation

$$g_1 \sim g_2 \iff \exists x \in G \text{ such that } g_2 = g_1^x$$

which then creates the conjugacy classes of the group G, as all equivalence relations create equivalence classes.

Definition A.0.14. *The conjugacy class C_g for $g \in G$ is the set of elements of G conjugate to g,*

$$C_g = \{g' \in G \mid g \sim g'\}$$

and it is by definition invariant under conjugation,

$$g'^x \in C_g \qquad \forall g' \in C_g, x \in G$$

Some special subgroups of G are invariant under conjugation, and are called normal subgroups. They will be essential for defining the groups with additional structure in Chapter 2.

Definition A.0.15. *A Normal Subgroup $N \lhd G$ is a subgroup of G that is invariant under conjugation by G,*

$$\forall n \in N, g \in G, \qquad n^g \in N.$$

The cosets of N are now unions of the conjugacy classes of G.

A multiplication rule can be put onto cosets of a normal subgroup to form their own group, known as the quotient group. This group will describe the structure around N that is built into G.

Definition A.0.16. *Let G be a finite group and $N \lhd G$ a normal subgroup, giving a transversal T for the cosets of N in G, $G = \cup_{t \in T} tN$. Then the quotient group G/N is defined on the cosets*

$\{tN \mid t \in T\}$ *with the multiplication rule* $\cdot$ *so that*

$$(t_1 N) \cdot (t_2 N) = (t_1 t_2) N$$

The order is the index of N in G, $|G/N| = [G : N]$.

Normal subgroups, quotient groups and homomorphisms are all highly related in a way that is described by the First Isomorphism Theorem.

Theorem A.0.17. *Let G, G' be groups and $\phi : G \to G'$ a group homomorphism. Then,*

- $\ker(\phi) \triangleleft G$

- $\operatorname{im}(\phi) \subset G'$

- $\operatorname{im}(\phi) \cong G/\ker(\phi)$

There exist further isomorphism theorems described in [138] but they are not relevant here.

Finally, direct product and semidirect product groups give a way to combine two groups to form a bigger group. First, the direct product group is defined by taking all possible pairs (g_1, g_2) of elements with $g_1 \in G_1$ and $g_2 \in G_2$ and defining the multiplication as occuring on ech element of the pair separately.

Definition A.0.18. *Let $(G_1, \cdot), (G_2, \times)$ be two finite groups. Then their direct product group $G_1 \times G_2$ is defined as $(\{(a, b) \mid a \in G_1, b \in G_2\}, *)$ with the multiplication rule*

$$(a_1, b_1) * (a_2, b_2) = (a_1 \cdot a_2, b_1 \times b_2).$$

It has order $|G_1 \times G_2| = |G_1||G_2|$.

There are two ways of defining the semidirect product - the inner and out semidirect product. The inner semidirect product takes a group and recognises when it is a semidirect product of two subgroups; the outer semidirect product group uses two groups and a homomorphism to define a new group which is the semidirect product of the base group.

Definition A.0.19. *Let G be a group and N, K be two subgroups of G such that N is normal. Then if,*

- $N \cap K = \{e\}$, *so the only common element in the group is the identity*

- $G = \bigcup_{k \in K} kN$, *so that K provides a transversal of N in G.*

G is a semidirect product of N by K and $G = N \rtimes K$.

Examples of semidirect products include the dihedral groups, $D_n = Z_n \rtimes Z_2$, and the alternating groups on four elements, $A_4 = Z_2^2 \rtimes Z_3$. The outer semidirect product does the inverse of the inner semidirect product and starts with the subgroups and defines their supergroup through the action of K on N:

Definition A.0.20. *Let N, K be groups and let $\theta : K \to \mathrm{Aut}(N)$ be a homomorphism. Then the outer semidirect product group $G = N \rtimes_\theta K$ is defined as the set of ordered pairs $(n, k) \in N \times K$ with the bilinear operator $\cdot$ defined as*

$$(n_1, k_1) \cdot (n_2, k_2) = (n_1 \theta(k_1) n_2, k_1 k_2)$$

There are many useful properties explored for the semidirect product group in [138]. The key one in this thesis will be it application to splitting group extensions, as discussed in Section 2.4.

B. Z_2-Graded Vector Spaces and Algebras

Here we extend the concepts of linear algebra to vector spaces and algebras that have been graded to form the super vector spaces and super algebras needed to describe the corepresentations of $Z_2 \times Z_2$-graded groups for the Altland-Zirnbauer Tenfold Way as per Chapter 2. More detailed discussion is given in [93, 117, 165] which is where the material for this appendix is drawn from.

B.1 Z_2-Graded Linear Algebra

We begin with the definition of graded vector spaces and their homomorphisms. In all cases, the descriptor 'super' means that the relevant object has had a Z_2-grading put on it. For vector spaces this takes the following form:

Definition B.1.1. *Let V be a vector space over the field K. Then V permits a Z_2-grading and is a super-vector space if and only if*

$$V = V^0 \oplus V^1$$

with V^0, V^1 respectively the even and odd subspace. V comes with the parity operator,

$$P_V v = \begin{cases} v & v \in V^0 \\ -v & v \in V^1 \end{cases}$$

If V^0 and V^1 have finite dimensions m, n respectively so that $V^0 \cong K^m$ and $V^1 \cong K^n$ then V may be denoted as $K^{m|n}$.

Vectors that live entirely in one of the subspaces are then known as homogeneous vectors, and the subspace of V they sit within can be defined by their degree,

$$|v| = \begin{cases} \bar{0} & v \in V^0 \\ \bar{1} & v \in V^1 \end{cases}, \qquad P_V v = (-1)^{|v|} v$$

which as indicator form of the parity operator P_V.

When it comes to transformations between super-vector spaces, both graded and ungraded homomorphisms between super-vector spaces exist:

Definition B.1.2. *Let V, W be super-vector spaces, the space $\underline{\mathbf{Hom}}(V, W)$ of ungraded homomorphisms between V and W is the set of homomorphisms between V and W when considered*

as un-graded spaces that also commute with the parity operators of V, W,

$$\underline{\mathbf{Hom}}(V, W) = \{T \in \mathrm{Hom}(V_{ungraded}, W_{ungraded}) \mid TP_V = P_W T\}$$

Definition B.1.3. *Let V, W be super-vector spaces, the space $\mathbf{Hom}(V, W)$ of Z_2-graded homomorphisms between V and W is given by*

$$\mathbf{Hom}(V, W)^0 = \mathbf{Hom}(V^0, W^0) \oplus \mathbf{Hom}(V^1, W^1)$$

$$\mathbf{Hom}(V, W)^1 = \mathbf{Hom}(V^0, W^1) \oplus \mathbf{Hom}(V^1, W^0)$$

so that $\mathbf{Hom}(V, W)^0 \cong \underline{\mathbf{Hom}}(V, W)$ preserves the parity, and $\mathbf{Hom}(V, W)^1$ inverts it.

Usefully, if the bases for V, W are given in terms of the bases of V^0, V^1, W^0, W^1 as $\begin{pmatrix} V^0 & V^1 \end{pmatrix}^T$, $\begin{pmatrix} W^0 & W^1 \end{pmatrix}^T$ then $\mathbf{Hom}(V, W)^0$ and $\mathbf{Hom}(V, W)^1$ have the block-diagonal and block-off diagonal forms

$$T \in \mathbf{Hom}(V, W)^0 \Rightarrow T = \begin{pmatrix} A & 0 \\ 0 & B \end{pmatrix}, \qquad T \in \mathbf{Hom}(V, W)^1 \Rightarrow T = \begin{pmatrix} 0 & C \\ D & 0 \end{pmatrix}.$$

We also note that in the case $W = V$, and all the elements are invertible, then $\mathbf{Hom}(V, V)$ has the special name of the set of graded *automorphisms*, $\mathbf{Aut}(V)$.

Tensor products of super-vector spaces can be defined:

Definition B.1.4. *Let V, W be super-vector spaces, then the tensor product is*
$V \otimes W = \{(v, w) \mid v \in V, w \in W\}$ *with*

$$
\begin{array}{rcl}
(V \otimes W)^0 & = & (V^0 \otimes W^0) \oplus (V^1 \otimes W^1) \\
(V \otimes W)^1 & = & (V^0 \otimes W^1) \oplus (V^1 \otimes W^0)
\end{array}, \qquad |(v, w)| = |v| + |w|
$$

The grading on $V \otimes W$ then depends on whether the homogeneous elements v, w of V, W making up $v \otimes w$ have the same degree or not - if they do, $|v \otimes w| = 0$ and the element is even; if they don't, $|v \otimes w| = 1$ and the element is odd.

The major change from going liner algebra to super liner algebra is that commutativity in its strongest sense is lost. Instead it is necessary to define super commutation, where the relation between a set of operations and the same set of operations done in reverse depends on which of the even and odd subspaces the homogeneous elements involved sit within. The first occurrence of this is in the tensor product, where the isomorphism between $V \otimes W$ and $W \otimes V$ is not $v \otimes w \to w \otimes v$ but

$$w \otimes v = (-1)^{|v||w|} v \otimes w.$$

This is the form of expression which will be seen to replace all forms of commutation in linear algebra, with the addition of the $(-1)^{|v||w|}$ often termed the 'Koszul sign rule', which will appear commonly on super-objects.

There is now sufficient apparatus defined to introduce the super algebra, or Z_2-graded algebra,

Definition B.1.5. *Let k be a field, and A be a super-vector space over k. Then equipping A with the bilinear operator $\cdot : A \otimes A \to A$, $a_1 \cdot a_2 = a_1 a_2$ forms the super-algebra with the grading of homogeneous elements behaving under multiplication as*

$$|a_1 \cdot a_2| = |a_1| + |a_2|.$$

The behaviour of the common properties of algebras - associativity, commutativity, centers, tensoring, divisibility by non-zero elements, modules and simpleness - can be checked under the shift to super-algebras. Associativity remains a possible property of super-algebras without change:

Definition B.1.6. *Let A be a Z_2-graded algebra, if*

$$(a_1 \cdot a_2) \cdot a_3 = a_1 \cdot (a_2 \cdot a_3) \qquad \forall a_1, a_2, a_3 \in A$$

then A is an associative Z_2-graded algebra.

However, as would be expected, commutation again becomes super-commutation between elements, and the Koszul sign rule then reappears.

Definition B.1.7. *Let A be a super-algebra. Let $a, a' \in A$ be elements, if*

$$a \cdot a' = (-1)^{|a||a'|} a' \cdot a$$

then a and a' super-commute. If all pairs $a, a' \in A$ super-commute, then A is a super-commutative algebra; otherwise the center $Z(A) = \left\{ a \in A \mid a \cdot a' = (-1)^{|a||a'|} a' \cdot a \ \forall a' \in A \right\}$ of A can be considered, and is defined as the subset of elements which do super-commute with all other elements of A. If A is super-commutative, then the center equals the algebra, $Z(A) = A$.

Tensor products on super-algebras also gain contribution from the Kozul sign rule:

Definition B.1.8. *Let A, A' be super-algebras, then their graded tensor product $A \hat{\otimes} A'$ is defined as the super-algebra defined over the super-vector space $V = A \otimes A'$ with the bilinear operator $\cdot$ given by*

$$(a_1, a_1') \cdot (a_2, a_2') = (-1)^{|a_1'||a_2|}(a_1 \cdot a_2, a_1' \cdot a_2')$$

In normal linear algebra, a simple algebra A is defined as an algebra where there are no subspaces within it invariant under both left and right multiplication by all of the elements A, as long as the bilinear operator on A is not trivially 0:

Definition B.1.9. *Let A be an algebra over the field K, if $a \cdot a'$ is non-zero for $a, a' \neq 0$, and there does not exist a non-trivial two-sided ideal L, that is a subset $L < A$ such that $\forall x, y \in L$, $z \in A$ and $c \in k$ then,*

- $x + y \in L$

- $cx \in L$

- $z \cdot x \in L$ and $x \cdot z \in L$

then A is simple.

An ideal is then the algebra equivalent of the normal subgroup in group theory, and the requirement for simpleness equivalent to a group G having no normal subgroup that wasn't either the trivial group of G itself. The direct sum of a series of simple algebras is then known as a semi-simple algebra. In the terms of super-algebras, a super-algebra is simple if there are no non-trivial two-sided super-ideals:

Definition B.1.10. *Let A be a super-algebra over the super-vector space V, if $a \cdot a'$ is non-zero for $a, a' \neq 0$, and there does not exist a non-trivial two-sided super-ideal L, that is a subset $L < A$ such that $\forall x, y \in L$, $z \in A$ and $c \in k$ then,*

- $x + y \in L$

- $cx \in L$

- $z \cdot x \in L$ *and* $x \cdot z \in L$

then A is simple.

Again, if A is not simple, but can be expressed as the direct sum of simple super-algebras, then A is semi-simple.

A module M of an algebra A is a vector space where vectors in M can not only be multiplied by a scalar, but there exists a bilinear map $A \times M \to M$ that can be used to define the multiplication of elements of M by A. This is the algebra equivalent of a representation of a group.

Definition B.1.11. *Let A be an algebra, let M be a vector space. Then M is a left A-module with the definition of the bilinear map $\times : A \times M \to M$ that is consistent with the bilinear operator $\cdot$ on A,*

- $1 \times m = m$ $\forall m \in M$ *so the identity acts trivially.*

- $(x \cdot y) \times m = x \times (y \times m)$ *so the two operators are associative with respect to each other.*

On super-algebras, a super-module picks up the requirement that it exists over a super-vector space, and that it respects the multiplication rule on the degree of the gradings:

Definition B.1.12. *Let A be a super-algebra and M be a super vector space. Then M is a left super-module of A with the definition of a bilinear map $\times : A \times M \to M$ that is both consistent with the bilinear operator $\cdot$ on A and which respects the multiplication rule from A for the grading of the homogeneous vectors,*

- $1 \times m = m$ $\forall m \in M$ *so the identity acts trivially.*

- $(x \cdot y) \times m = x \times (y \times m)$ *so the two operators are associative with respect to each other.*

- $|x \times m| = |x| + |m|$.

Note that the super-algebra A when considered as the super-vector space it is defined over, can always be taken as its own super-module. The link between modules of algebras and representations of groups continues to the idea of decomposability. A representation that wasn't the

direct sum of smaller representations was called irreducible, a super-module that isn't a direct sum of sub super-modules is simple:

Definition B.1.13. *Let M be a super-module of the super-algebra A. Let $M' \subset M$ be a subset of M, if M' fulfils the requirements of being both a super-vector space, and being a super-module of A then it is a sub-super-module of M.*

If M has no non-trivial sub-super-modules, then it is a simple super-module of A; if it can be written as the direct sum of simple super-modules, then it is a semi-simple super-module of A.

A standard algebra is described as a division algebra if it is possible to define division by all elements within it except 0:

Definition B.1.14. *Let D be an algebra over the field K. If for each $a \in D$ and $b \in D - 0$, there exists a unique element $x \in D$ such that $a = b \cdot x$, and a unique element $y \in D$ such that $a = y \cdot b$, then D is a division algebra.*

On super-algebras, the requirement for all non-zero elements to be divisible is relaxed to include only the homogeneous elements:

Definition B.1.15. *Let D be a super-algebra. If for each $a \in D$ and $b \in D - 0$ such that a and b are homogeneous, then there exists a unique homogeneous element $x \in D$ such that $= b \cdot x$, and a unique homogeneous element $y \in D$ such that $a = y \cdot b$ then D is a super-division algebra.*

The associative super-division algebras over the field $\mathbb{R}$ will prove essential to understanding the reasoning behind why the Altland-Zirnbauer classification contains only ten classes.

B.2 The Super Clifford Algebras

We now introduce examples of super-algebras. The simplest are $\mathbb{R}^{n|0}, \mathbb{C}^{n|0}$ and $\mathbb{H}^{n|0}$ which are super-algebras where only the even subspace is non-trivial, and contains one of $\mathbb{R}^n, \mathbb{C}^n$ or $\mathbb{H}^n$; these behave exactly like their ungraded versions as the odd part is empty.

The other type of algebra which will need to be considered for the Altland-Zirnbauer classification are the Clifford algebras, [43]. Their ungraded form is given as:

Definition B.2.1. *Let V be a vector space over the field K with a finite orthonormal basis $\{e_i\}$ that is ordered with respect to the index i, having N elements. Let $\eta : V \times V \to V$ be defined with reference to $r \in \mathbb{N}$, $s = N - r$, as,*

$$\eta(e_i, e_j) = \begin{cases} 0 & i \neq j \\ 1 & j \leq r \\ -1 & r < j \leq s + r \end{cases} .$$

Then the Clifford algebra $Cl_{+r,-s}^K$ is defined as the algebra over V with the bilinear form $\cdot$ defined so that

$$e_i \cdot e_j + e_j \cdot e_i = (2\eta(e_i, e_j))1.$$

The simplest example of a Clifford algebra is $\mathbb{C}$ which is equivalent to $Cl^{\mathbb{R}}_{+0,-1}$, with $e_1 = i$ and $e_1^2 = -1$. Other examples include $\mathbb{R} \cong Cl^{\mathbb{R}}_{+0,-0}$ and $\mathbb{H} \cong Cl^{\mathbb{R}}_{+0,-2}$.

There are also some notational quirks to take note of. The structure of the name $Cl^K_{+r,-s}$ used here is to put the field the algebra is defined over in the superscript, and then the number r of elements which square to $+1$ and the number s of elements which square to -1 in the subscript along with the sign of their squares. There are other ways of arranging this information, including $Cl^K(r+, s-)$, [117], while sometimes instead of putting the field in the superscript, formatting the text Cl is used - mainly to denote $Cl^{\mathbb{C}}$ as $\mathbb{C}l$ - or if $K = \mathbb{R}$, the reference to K can sometimes be dropped altogether. Furthermore in the form we use, it is common to drop the prefix $+$ from $+r$ in the subscript, though the $-$ prefix is always kept in $-s$; also if one of r, s is zero, it is not referenced in the subscript. Thus, $Cl^{\mathbb{R}}_{+0,-1}$ can be written Cl_{-1}.

In order to apply the Clifford algebras as super-algebras, it is necessary to grade them. The correct grading is given by [117]:

Definition B.2.2. *Let $Cl^K_{r,-s}$ be a Clifford algebra over the field K. Then $Cl^K_{r,-s}$ may be considered a super-algebra under the grading derived from*

$$|e_{i_1} \ldots e_{i_n}| = \begin{cases} \bar{0} & n = 2m \\ \bar{1} & n = 2m+1 \end{cases}$$

which for liner combinations of elements is

$$\left| \sum_j e_{i_{j,1}} \ldots e_{i_{j,n_j}} \right| = \begin{cases} \bar{0} & n_j = 2m_j \ \forall j \\ \bar{1} & n_j = 2m_j + 1 \ \forall j \\ inhomogeneous & otherwise \end{cases}$$

This means that the elements are graded with respect to whether they are formed of an even number of basis elements, or an odd number of basis elements.

The reason we care about the Clifford algebras is that they form most of the real associative super-division algebras, which allows the corepresentations of $Z_2 \times Z_2$-graded groups to be classified according to Section 2.3.1. The identification of the ten real associative super-division algebras was done by Wall, [168], and while the proof that there are only ten of them is beyond covering here, as is the method of identifying them, once the ten are known to be the following set of Clifford algebras, each can be easily checked to be a super-division algebra relatively easily, [117].

Theorem B.2.3. *There are only ten real associative super-division algebras and these are $\mathbb{C}^{1|0}$, $\mathbb{R}^{1|0}$, $\mathbb{H}^{1|0}$ and $Cl^{\mathbb{C}}_1$, $Cl^{\mathbb{R}}_{\pm 1}$, $Cl^{\mathbb{R}}_{\pm 2}$ and $Cl^{\mathbb{R}}_{\pm 3}$.*

Proof. We only prove that each of the above real associative super-algebras is a division algebra, leaving the proof that there are only ten of them to [168]. To do this, for each algebra, we identify the inverse for each of the homogeneous elements.

- Firstly, $\mathbb{C}^{1|0}, \mathbb{R}^{1|0}, \mathbb{H}^{1|0}$ are isomorphic to their ungraded versions as the odd part is empty, and $\mathbb{C}, \mathbb{R}$ and $\mathbb{H}$ are division algebras, so their graded counterparts are super-division algebras.

- For $Cl_1^{\mathbb{C}}$, the even homogeneous elements are $c \in \mathbb{C}$, which have inverse c^{-1} due to being in $\mathbb{C}$. The odd homogeneous elements are given by ce_1 with $e_1^2 = -1$ and $c \in \mathbb{C}$, so $(ce_1)^{-1} = -c^{-1}e_1$.

- For $Cl_{\pm 1}^{\mathbb{R}}$ the even elements are $r \in \mathbb{R}$, so their inverse is $r^{-1} \in \mathbb{R}$. The odd homogeneous elements are given by re_1, $r \in \mathbb{R}$ and $e_1^2 = \pm 1$, their inverse is then $\pm r^{-1}e_1$.

- For $Cl_{\pm 2}^{\mathbb{R}}$, the even elements are $(x + ye_1e_2)$ and $e_1e_2 = \pm e_2e_1$. As $(e_1e_2)^2 = 1$, then $(x - ye_1e_2)(x + ye_1e_2) = x^2 + y^2$ with $x^2 + y^2$ being invertible as a member of $\mathbb{R}$. The inverse of $(x + ye_1e_2)$ is then $(x^2 + y^2)^{-1}(x - ye_1e_2)$.

  The odd elements are given by $(xe_1 + ye_2)$, with $(xe_1 + ye_2)^2 = \pm x^2 \pm y^2 + (x - y)e_1e_2$ which is a homogeneous even element, which by the first part has the inverse $((x^2 + y^2)^2 + (x+y)^2)^{-1}(\pm(x^2 + y^2) - (x - y)e_1e_2)$. This gives the inverse of $(xe_1 + ye_2)$ as $((x^2 + y^2)^2 + (x-y)^2)^{-1}(\pm(x^2 + y^2) - (x - y)e_1e_2)(xe_1 + ye_2)$

- For $Cl_{-3}^{\mathbb{R}}$, the even elements are given by $(w + xe_1e_2 + ye_1e_3 + ze_2e_3)$ and $e_1e_2 = -e_2e_1$, $e_1e_3 = -e_2e_3$ and $e_3e_2 = -e_2e_3$. We note that the algebra generated by elements of this form is equivalent to $\mathbb{H}$, which is a division algebra, therefore all even homogeneous elements are invertible.

  The odd elements are given by $(ae_1 + be_2 + ce_3 + de_1e_2e_3)$, multiplying this by e_1, gives the even homogeneous element $(-a + be_1e_2 + ce_1e_2 - de_2e_3)$. Given this is even and homogeneous, it must be invertible and have inverse $(-a + be_1e_2 + ce_1e_2 - de_2e_3^{-1}$. The inverse of $(ae_1 + be_2 + ce_3 + de_1e_2e_3)$ then exists and is $(-a + be_1e_2 + ce_1e_2 - de_2e_3^{-1}e_1$. All odd homogeneous elements then have inverses.

- For $Cl_{-3}^{\mathbb{R}}$, it is claimed that $Cl_{-3}^{\mathbb{R}} \cong \mathbb{H}^{1,0}\hat{\otimes}Cl_{-1}$. By the graded tensor product, the even subspace then consists of the pairs (h, x) where $h \in \mathbb{H}$ and $x \in R$. As $\mathbb{H}$ is a division algebra, there exists an inverse for h, h^{-1}, as is also the case for $x \in R$. The inverse for (h, x) is then (h^{-1}, x^{-1}).

  Odd homogeneous elements are given by (h, xe_1), which multiplying by $(1, e_1)$ gives $-(h, -x)$, which has the inverse $-(h^{-1}, -x^{-1})$. This gives the inverse of the odd homogeneous elements as $-(h^{-1}, -x^{-1})(1, e_1)$.

$\square$

Graded Clifford algebras have many other properties that have an impact on the Altland-Zirnbauer classification, and other aspects of quantum theory that are linked to symmetry classifications such as the Bott periodicity clock, and the periodic table of topological insulators, but these are outwith the scope of this thesis. Information on these aspects of the Clifford algebras my be found in [8, 43, 111, 117, 165].

C. Quantum Mechanics

Here we give formal definitions for important concepts in quantum theory - including the Hilbert space, projective Hilbert space, operators and adjoint operators. We motivate the link between classical and quantum physics that comes from deriving quantum mechanics from classical mechanics under the substitution of variables as operators, and the advantages and methods of decomposing the Hilbert space into sub-spaces, in particular into the form $\mathcal{H} = \mathcal{H}_{\text{charge}} \otimes \mathcal{H}_{\text{spin}} \otimes \mathcal{H}_{\text{orbital}}$ form which will be relied upon throughout the thesis.

There are many good introductions to quantum systems, with varying intentions of mathematical purity. More physics-leaning ones include [9, 68]; a more mathematical treatment is given in [75].

C.1 Quantum Systems

A quantum system is the name given to any problem studied under the assumption that some form of quantum mechanics applies. That is, the system cannot be described under classical mechanics as it is defined on the quantum length scale, and exhibits key quantum behaviour: wave-particle duality, non-determinism and the uncertainty principle for example. Describing quantum systems will require defining what a 'state' in the system means, how these states evolve with time, and how they can be interacted with to retrieve measurements; a pathway similar to defining classical mechanics is possible however, as quantum mechanics is derived from Hamiltonian mechanics.

Firstly, a quantum system must be defined over a space, [155]:

Definition C.1.1. *Let $\mathcal{Q}$ be a quantum system, then its Hilbert Space $\mathcal{H}$ is a complex vector space, with vectors ψ and inner product $\langle \cdot, \cdot \rangle$, such that*

- *$\langle \cdot, g \rangle$ is a linear function for all $g \in \mathcal{H}$.*

- *$\langle f, g \rangle = \langle g, f \rangle^*$*

- *$\langle f, f \rangle \geq 0$ for all $f \in \mathcal{H}$.*

The norm shall be defined as $\|\psi\| = \sqrt{\langle \psi, \psi \rangle}$.

The common choice is $\mathcal{H} = L_2(\mathbb{R}^n)$, with the standard Euclidian measure, [68, 155]. This is the space of functions $\phi : \mathbb{R}^n \to \mathbb{C}$ for a given n such that

$$\int_{\mathbb{R}^n} |\phi(\boldsymbol{x})|^2 d\boldsymbol{x} \in (-\infty, \infty)$$

is finite. Then the inner product is defined as

$$\langle \phi, \psi \rangle = \int \phi^*(\boldsymbol{x}) \psi(\boldsymbol{x}) d\boldsymbol{x}.$$

When states are multidimensional, the standard choice is $L_2^m(R^n)$, so the state is an m-dimensional vector $\boldsymbol{\phi}$, with each entry a function from $L_2(\mathbb{R}^n)$, with inner product

$$\langle \boldsymbol{\phi}, \boldsymbol{\psi} \rangle = \int_{\mathbb{R}^n} \boldsymbol{\phi}^\dagger(\boldsymbol{x}) \boldsymbol{\psi}(\boldsymbol{x}) d\boldsymbol{x}.$$

It is also useful to introduce the Dirac notation, $\psi \to |\psi\rangle$. Vectors in $\mathcal{H}^\dagger$ are now denoted $\langle\psi|$ so that the inner product is $\langle \phi, \psi \rangle = \langle \phi | \psi \rangle$.

The Hilbert space defines the space of possible states $|\psi\rangle$ that a quantum system can reside in. As each state is a function, not a scalar point, immediately comes the fact that each state defines a 'wave-function' not a particular fixed state, this 'wave-function' is generally considered to be a function which under the action of operators, as defined in Section C.1.1, can be used to generate a probability distribution over $\mathbb{R}^n$ for a measurement, by taking the absolute value squared of wave-function. This is all according to the Copenhagen Interpretation, which is the most generally accepted interpretation of quantum mechanics, [68].

Given that a absolute-value-square of a state is a probability distribution, there is a restriction that it is normalised, $\|\langle \psi | \psi \rangle\|^2 = 1$ which defines a physical or realisable state. Any non-physical state can be turned into a physical state by dividing out the square root of its magnitude,

$$|\psi'\rangle = \frac{1}{\sqrt{\|\psi\|}} |\psi\rangle . \tag{C.1}$$

Mapping states onto their physical versions creates a redundancy of states which are related by scalar multiplication, it defines the ray

$$[\psi] = \{|\psi'\rangle \in \mathcal{H} \mid |\psi'\rangle = c|\psi\rangle, \ c \in \mathbb{C} - \{0\}\} \tag{C.2}$$

where every $|\psi'\rangle \in [\psi]$ differs only by a scalar multiple and can be mapped onto the same physical state. If only the physical states are considered, then the redundant states are described by the set

$$l_\psi = \{|\psi'\rangle \in \mathcal{H} \mid |\psi'\rangle = c|\psi\rangle, \ c \in U(1)\} \qquad |\langle \psi, \psi \rangle|^2 = 1$$

where the factors c describe a change of the phase of the state; these are again 'essentially the same' state for many considerations.

To remove the redundancy, it is usual to work over the projective Hilbert space, rather than the full Hilbert space, [117, 176]:

Definition C.1.2. *Let $\mathcal{H}$ be the Hilbert space of the quantum system $\mathcal{Q}$. Then the projective Hilbert space $\mathbb{P}\mathcal{H}$ is defined as the space of rays,*

$$\mathbb{P}\mathcal{H} = (\mathcal{H} - \{0\})/\mathbb{C}^{\times}.$$

It is possible to define a projection operator σ from $\mathcal{H}$ to $\mathbb{P}\mathcal{H}$,

$$\sigma : |\psi\rangle \rightarrow |\sigma(\psi)\rangle = |\Psi\rangle \in \mathbb{P}\mathcal{H}, \qquad \sigma : |\psi\rangle \rightarrow \frac{|\psi\rangle}{\sqrt{|\langle\psi|\psi\rangle|}} \tag{C.3}$$

which also allows a representative state $|\Psi\rangle$ to be chosen for each ray.

If a system changes state, either due to time evolution, or spontaneously changing state due to measurement, the inner product of of the two states gives the transition amplitude, and its norm the transition probability to go from state Φ to state Ψ,

$$P(\Phi \rightarrow \Psi) = |\langle\Psi|\Phi\rangle|^2$$

Finally, if an orthonormal basis $|\psi_n\rangle$ exists for a Hilbert space, $\langle\psi_m|\psi_n\rangle = \delta_{mn}$, then any state can be written as a linear combination of the basis states,

$$|\phi\rangle = \sum_n c_n |\psi_n\rangle, \qquad c_n = \langle\phi|\psi_n\rangle.$$

C.1.1 Operators, Measurements and Eigenstates

Having defined quantum states, it is now necessary to define methods to interact with them, which is done through the use of operators, [175]:

Definition C.1.3. *Let $\mathcal{Q}$ be a quantum system with Hilbert space $\mathcal{H}$. An operator $\hat{O}$ is a map on the Hilbert space, $\hat{O} : \mathcal{H} \rightarrow \mathcal{H}$, that is either linear, $\hat{O}(a |\psi\rangle + b |\phi\rangle) = a\hat{O} |\psi\rangle + b\hat{O} |\phi\rangle$ or anti-linear, $\hat{O}(a |\psi\rangle + b |\phi\rangle) = a^*\hat{O} |\psi\rangle + b^*\hat{O} |\phi\rangle$.*

Note how this definition allows operators to be anti-linear unlike the standard definition, [9, 75], which allows only linear maps. This allowance of anti-linearity will be essential for defining the operations of time-reversal, charge-conjugation and the chiral operator.

Given a set of orthonormal basis states $|\psi_n\rangle$ for the Hilbert space $\mathcal{H}$, these can be used to construct a matrix form for each operator on $\mathcal{H}$. If a linear operator $\hat{O}_L$ acts on the pure state $|\psi_n\rangle$, then $\hat{O}_L |\psi_n\rangle$ must have a linear decomposition over the basis, [68],

$$\hat{O}_L |\psi_n\rangle = \sum_m O_{L,nm} |\psi_m\rangle, \qquad O_{L,nm} = \left\langle\psi_n\middle|\hat{O}_L\psi_m\right\rangle = \langle\psi_n|\hat{O}_L|\psi_m\rangle.$$

Iterating over n defines the $N \times N$ matrix O_L, where N is the dimension of the Hilbert Space, that describes the action of $\hat{O}_L$ on the basis $|\psi_n\rangle$. The expressions $\langle\psi_m|\hat{O}_L|\psi_n\rangle$ are known as the matrix elements of $\hat{O}_L$. The anti-linear operators $\hat{O}_A$ also have a construction as linear matrix operators $\hat{L}_A$ combined with the action of complex conjugation to the right, $\mathcal{K}$, $\hat{O}_A = \hat{L}_A\mathcal{K}$. The

unitary part can be expressed as a matrix with elements given by,

$$\hat{O}_A \ket{\psi_n} = \sum_m L_{A,nm} \ket{\psi_m}^*, \qquad L_{A,nm} = \left\langle \psi_n \middle| \hat{L}_A \psi_m \right\rangle = \bra{\psi_n} \hat{L}_A \left(\ket{\psi_m}^* \right).$$

It can be common in the physics literature, [30, 47, 48], to choose the orthonormal basis so that the Hilbert space splits into a subspace $\mathcal{H}_1 = \text{span}(\ket{\psi_n})$, and its copy under a chosen anti-linear operator $\hat{A}$, $\hat{A}\mathcal{H}_1 = \text{span}(\ket{\phi_n}) = \text{span}(\hat{A}\ket{\psi_n})$. A generic anti-linear operator can then be written as $\hat{O}_A = L'_A \hat{A}$. This allows the matrix elements on the basis $\left(\ket{\psi_n} \ket{\phi_n} \right)^T$ to then be written as the matrix operators,

$$O_L = \begin{pmatrix} \bra{\psi_m}\hat{O}_L\ket{\psi_n} & 0 \\ 0 & \bra{\phi_m}\hat{O}_L\ket{\phi_n} \end{pmatrix}, \quad O_A = \begin{pmatrix} 0 & \bra{\psi_m}\hat{O}_A\ket{\phi_n} \\ \bra{\phi_m}\hat{O}_A\ket{\psi_n} & 0 \end{pmatrix} \mathcal{K} \qquad \text{(C.4)}$$

Splitting up the Hilbert space into a subspace basis, and then its image under certain operators will be a common technique throughout the thesis. More details on splits like this can be found in the aforementioned citations, and in [24].

The matrix element is interpreted as having $\hat{O}$ act on the state $\ket{\psi_n}$. However, it is equally valid to consider the operator acting on $\bra{\psi_n}$. To do this, it is necessary to define the adjoint operator of $\hat{O}$, $\hat{O}^\dagger$, [75]:

Definition C.1.4. *Let $\mathcal{Q}$ be a quantum system with Hilbert space $\mathcal{H}$ and operator $\hat{O}$.*

In the case that $\hat{O}$ is bounded, so that there $\exists C$ a constant, $\left\| \hat{O}\psi \right\| \leq C \|\psi\| \ \forall \psi \in \mathcal{H}$ then there exists a unique operator $\hat{O}^\dagger : \mathcal{H}^\dagger \to \mathcal{H}^\dagger$ such that

$$\left\langle \phi, \hat{O}\psi \right\rangle = \left\langle \hat{O}^\dagger \phi, \psi \right\rangle \qquad \forall \phi, \psi \in \mathcal{H}$$

with $\hat{O}^\dagger$ being the adjoint operator for $\hat{O}$.

If $\hat{O}$ is unbounded, then it is defined only on a subspace $\text{dom}(\hat{O}) \subset \mathcal{H}$. The adjoint operator $\hat{O}^\dagger$ has domain defined by the relation

$$\phi \in \text{dom}(\hat{O}^\dagger) \iff \left\langle \phi, \hat{O}\cdot \right\rangle \text{ is bounded on } \text{dom}(\hat{O})$$

and is defined so that the action of the adjoint operator on $\phi \in \text{dom}(\hat{O}^\dagger)$ gives the state $\chi = \hat{O}^\dagger \phi$ which is the unique state where

$$\langle \chi, \psi \rangle = \left\langle \phi, \hat{O}\psi \right\rangle \qquad \forall \psi \in \text{dom}(\hat{O})$$

In Dirac notation, the action of the adjoint operator on the states $\bra{\psi}$ is thus given by

$$\left\langle \hat{O}\psi \middle| = \bra{\psi} \hat{O}^\dagger.$$

Matrix elements for the operators $\hat{O}$, $\hat{O}^\dagger$ have the relation

$$\bra{\psi_m}\hat{O}^\dagger\ket{\psi_n} = \bra{\psi_n}\hat{O}\ket{\psi_m}^* \iff \left(O^\dagger\right)_{mn} = (O_{nm})^* \qquad \text{(C.5)}$$

or the matrix representations of $\hat{O}$, $\hat{O}^\dagger$ have the obvious relation by the Hermitian Transpose, $O^\dagger = \left(O^T\right)^*$.

In certain cases, the operator and its adjoint are equal, [75],

Definition C.1.5. *Let $\mathcal{Q}$ be a quantum system with Hilbert space $\mathcal{H}$, with operator $\hat{O}$ and adjoint operator $\hat{O}^\dagger$. If $\mathrm{dom}(\hat{O}^\dagger) = \mathrm{dom}(\hat{O})$ and $\hat{O}^\dagger \phi = \hat{O}\phi \ \forall \phi \in \mathrm{dom}(\hat{O})$ then $\hat{O} = \hat{O}^\dagger$ and the operator is self-adjoint or Hermitian.*

Any measurement that can be made on a quantum system corresponds to some *linear* self-adjoint operator $\hat{O}$, with the possible values that the measurement can take being the eigenvalues λ of $\hat{O}$, $\hat{O}\ket{\psi_\lambda} = \lambda\ket{\psi_\lambda}$ with $\ket{\psi_\lambda}$ being a physical state. The necessity of being able to measure only real values - as complex measurements would be unphysical - is guaranteed as self-adjacent operators have only real eigenvalues. This is due to applying the relation $\braket{\phi|\psi} = \braket{\psi|\phi}^*$ to the states $\ket{\psi_\lambda}, \hat{O}\ket{\psi_\lambda}$,

$$\lambda = \lambda \braket{\psi_\lambda|\psi_\lambda} = \left\langle \psi_\lambda \middle| \hat{O}\psi_\lambda \right\rangle = \left\langle \hat{O}\psi_\lambda \middle| \psi_\lambda \right\rangle^* = \lambda^* \braket{\psi_\lambda|\psi_\lambda}^* = \lambda^*$$

and $\lambda = \lambda^* \Leftrightarrow \lambda \in \mathbb{R}$.

Starting with a system in the state $\ket{\phi}$, taking a measurement that returns the value λ causes the system to spontaneously transition $\ket{\psi_\lambda}$. Given that the transition probability to go from $\ket{\phi}$ to $\ket{\psi_\lambda}$ is $|\braket{\psi_\lambda|\phi}|^2$, then the probability to measure λ must be

$$P(\lambda) = |\braket{\psi_\lambda|\phi}|^2$$

which means that for this to have a non-zero probability, $\ket{\psi_\lambda}$ and $\ket{\phi}$ can't be orthogonal.

In the special case where the eigenvalues λ are discrete and countable, the eigenstates of a linear operator $\hat{O}$ are orthonormal and span the Hilbert space, and they can be used to write a generic state as a linear combination of the eigenstates,

$$\ket{\phi} = \sum_\lambda c_\lambda \ket{\psi_\lambda}$$

where $\sum_\lambda |c_\lambda|^2 = 1$. The probability to measure λ is then $P(\lambda) = |c_\lambda|^2$. In this case, a basis state will be known s a 'pure state', while linear combinations of pure states are known as 'mixed states'. This is as pure states $\ket{\psi_\lambda}$ will always measure λ, and mixed states $\ket{\phi}$ can return any measurement value whose eigenstates are part of the linear decomposition of $\ket{\phi}$.

A similar construction of the Hilbert space as being spanned by the eigenvectors of a linear operator with a continuous eigenvalue spectrum is possible, the numbered eigenstates becoming a continuous function of eigenstates $\ket{\psi_\lambda} \to \ket{\psi(\lambda)}$, and swapping out the sum for an integral in the linear decomposition. However, it will be assumed here that the eigenvalues are discrete and countable, so that they can be labelled by the natural numbers.

Note that two linear operators $\hat{O}_1$ and $\hat{O}_2$ will rarely share an eigenbasis. If they don't, then if the sequence of measurements $\hat{O}_1, \hat{O}_2, \hat{O}_1$ is taken, it is probable that the values measured by $\hat{O}_1$ in the first and second instance are different. Two operators will share an eigenbasis only if they commute, [9],

Lemma C.1.6. *Let $\mathcal{H}$ be a Hilbert space with two operators $\hat{O}, \hat{O}'$. Define the two new operators $\hat{O}\hat{O}' - \hat{O}'\hat{O} = [\hat{O}, \hat{O}']$ as the commutator of $\hat{O}$ and $\hat{O}'$, and $\hat{O}\hat{O}' + \hat{O}'\hat{O} = \left\{\hat{O}, \hat{O}'\right\}$ as the anti-commutator of $\hat{O}$ and $\hat{O}'$. Then if,*

- *$[\hat{O}, \hat{O}'] |\psi\rangle = 0$ for all $|\psi\rangle \in \mathcal{H}$, $\hat{O}, \hat{O}'$ commute.*

- *$\left\{\hat{O}, \hat{O}'\right\} |\psi\rangle = 0$ for all $|\psi\rangle \in \mathcal{H}$, $\hat{O}, \hat{O}'$ anti-commute.*

Theorem C.1.7. *Let $\hat{O}, \hat{O}'$ be linear operators on the Hilbert space $\mathcal{H}$. Then they share an eigenbasis if and only if they commute,*

$$[\hat{O}, \hat{O}'] |\psi\rangle = 0 \qquad \forall |\psi\rangle \in \mathcal{H}$$

Proof. See [9] $\qquad\qquad\qquad\qquad\qquad\qquad\qquad\qquad\qquad\qquad\qquad\qquad\qquad\qquad\qquad$ $\square$

This means that if an operator eigenbasis is being used to describe the Hilbert space, it is important to choose the right operator. For many applications, and for those applications discussed here, the correct operator is the Hamiltonian $\hat{H}$, the operator whose eigenvalues correspond to the energy levels of the system,

$$\hat{H} |\psi_n\rangle = E_n |\psi_n\rangle .$$

As would be implied by the name, the Hamiltonian $\hat{H}$ is the quantum equivalent of the classical Hamiltonian, [9],

$$H(\boldsymbol{q}, \boldsymbol{p}) = T(\boldsymbol{q}, \boldsymbol{p}) + V(\boldsymbol{q}, \boldsymbol{p}), \qquad \frac{\mathrm{d}}{\mathrm{d}t} q_k = \{q_k, H\}, \quad \frac{\mathrm{d}}{\mathrm{d}t} p_k = \{p_k, H\} \qquad \text{(C.6)}$$

with the Poisson bracket being

$$\{f, g\} = \sum_j \frac{\partial f}{\partial q_j} \frac{\partial g}{\partial p_j} - \frac{\partial f}{\partial p_j} \frac{\partial g}{\partial q_j}.$$

Thus, the classical Hamiltonian describes not only the energy of a classical system, but also the time-evolution of its variables.

The quantum Hamiltonian can be found by directly replacing classical variables with quantum operators in the classical Hamiltonian, $q_i \rightarrow \hat{q}_i$, $p_i \rightarrow \hat{p}_i$. Then for a free particle in a potential, the classical and quantum Hamiltonians are

$$H(\boldsymbol{q}, \boldsymbol{p}, t) = \frac{1}{2m} \sum_j p_j^2 + V(\boldsymbol{q}, \boldsymbol{p}, t) \rightarrow \hat{H}(\{\hat{q}_k\}, \{\hat{p}_k\}, t) = \frac{1}{2m} \sum_j \hat{p}_j^2 + V(\{\hat{q}_k\}, \{\hat{p}_k\}, t). \quad \text{(C.7)}$$

$$\hat{q}_k = q_k, \qquad \hat{p}_k = -i\hbar \frac{\partial}{\partial q_k} \qquad\qquad\qquad \text{(C.8)}$$

Note that this consideration of quantum mechanics assumes that operators outside of the Hamiltonian are time-independent, while the states they act on are time-dependent $|\psi, t\rangle$; this is known as the Schrödinger picture, [68]. A second time-dependent operator is allowed $\hat{U}(t, t_0)$, derived from the Hamiltonian which 'evolves' the states through time,

$$i\hbar \frac{\partial}{\partial t} \hat{U}(t, t_0) = \hat{H}(t) \hat{U}(t, t_0), \qquad U(t, t_0) |\psi, t_0\rangle = |\psi, t_0 + t\rangle \qquad \text{(C.9)}$$

and which has the special form when the Hamiltonian is free of explicit time-dependence,

$$\hat{U}(t, t_0) = \exp\left(-i\hat{H}t/\hbar\right).$$

Finally, there are several quantum mechanical concepts associated to angular momentum. The first is the orbital angular momentum operator, which is derived from the classical operator

$$\hat{L}_i = \epsilon_{ijk}\hat{q}_j\hat{p}_k$$

and describes the rotation of a particle's centre of mass about an axis not through its centre of mass. Classical rotation about the centre of mass axis is known as spin, and once again occurs in quantum mechanics. However, in quantum mechanics, spin is an intrinsic quality of the particle, not a factor of the dynamics of the system, and it is related to a magnetic moment of the particle, [68], and which is quantised. Spin is associated to an operator in each dimension, defined by the Dirac Algebra,

$$[\hat{S}_j, \hat{S}_k] = i\hbar\epsilon_{ijk}\hat{S}_i$$

and has the most common matrix representation in terms of the Pauli matrices,

$$\hat{S}_k = \frac{\hbar}{2}\sigma_k, \qquad \sigma_1 = \begin{pmatrix} 0 & 1 \\ 1 & 0 \end{pmatrix}, \quad \sigma_2 = \begin{pmatrix} 0 & -i \\ i & 0 \end{pmatrix}, \quad \sigma_3 = \begin{pmatrix} 1 & 0 \\ 0 & -1 \end{pmatrix}$$

From the three $\hat{S}_k$ operators, $\hat{S}^2$ can be defined,

$$\hat{S}^2 = \sum_k \hat{S}_k^2$$

which shares an eigenbasis with $\hat{S}_3$, and has eigenstates $|s, m\rangle$, $s \geq 0$ $m \in [-s, s]$, $m = -s + n$, $n \in \mathbb{N}$ so that, [68],

$$\hat{S}^2 |s, m\rangle = \hbar^2 s(s+1) |s, m\rangle, \qquad S_3 |s, m\rangle = \hbar m |s, m\rangle$$

with s representing the spin quantum number of the system, which can only take the values $s = p/2$, $p \in \mathbb{N}$, and the value of which is fixed by the type of particle in the system - particles with spin $s = (2p + 1)/2$ are known as fermions and include the spin 1/2 electron and positron and all six flavours of quarks, and the spin 3/2 Δ baryon; particles with integer spin are known as bosons and include the spin 0 photon, and the spin 1 proton and neutron. Note that the Pauli matrix forms for $\hat{S}_k$ are valid for the spin-half systems, other representations of $\hat{S}_k$ must be used for systems with other spin numbers.

With electrons, as $s = 1/2$, m can take only two values, $m = \pm 1/2$. This leads to the concept of spin-up states $|\uparrow\rangle = |1/2, 1/2\rangle$, where $m = 1/2$ and the spin is aligned with the positive z-axis, and spin-down states $|\downarrow\rangle = |1/2, -1/2\rangle$, where $m = -1/2$ and the spin is aligned with the negative z-axis. In spaces where there are additional parameters, the spin up and down states can be used to partition the Hilbert space into an 'orbital' part that sits over $\mathbb{R}^3$, a spin space which covers

the spin-up and spin-down variants of the wave-function, and a charge-space, [14, 24, 73],

$$\mathcal{H} = \mathcal{H}_{\text{charge}} \otimes \mathcal{H}_{\text{spin}} \otimes \mathcal{H}_{\text{orbital}}, \qquad |\psi\rangle = |\psi_{\text{charge}}\rangle \otimes \begin{pmatrix} |\uparrow\rangle \\ |\downarrow\rangle \end{pmatrix} \otimes |\psi_{\text{orbital}}\rangle$$

where the vector $(\,|\uparrow\rangle\ |\downarrow\rangle\,)^T$ is known as a spinor. The Hamiltonian can be expressed up on this space by writing it in its second-quantised form, see [73], which takes the form of a sum over the creation operators $\hat{c}_a^\dagger$ and annihilation operators $\hat{c}_a$, $\left\{\hat{c}_a, \hat{c}_b^\dagger\right\} = \delta_{ab}$, $\{\hat{c}_a, \hat{c}_b\} = \left\{\hat{c}_a^\dagger, \hat{c}_b^\dagger\right\} = 0$,

$$\hat{H} = \sum_{a,b} \hat{c}_a^\dagger h_{a,b} \hat{c}_b + \frac{1}{2} \hat{c}_a^\dagger \Delta_{a,b} \hat{c}_b^\dagger + \frac{1}{2} \hat{c}_b \Delta_{a,b}^* \hat{c}_b$$

and expressed on $(\psi_\uparrow, \psi_\downarrow, \psi_\uparrow^\dagger, \psi_\downarrow^\dagger)$ takes the form of the Bogoliubov-deGennes Hamiltonian, [14],

$$\hat{H}_{BdG} = \begin{pmatrix} H_0 - E_F & -i\sigma_y \Delta \\ i\sigma_y \Delta^* & E_F - H_0^* \end{pmatrix}. \tag{C.10}$$

In another interpretation $|\psi_{\updownarrow}\rangle$ forms particle solutions $|p_\uparrow\rangle$ and $|p_\downarrow\rangle$, while $\left|\psi_{\updownarrow}^\dagger\right\rangle$ forms anti-particle or hole solutions, $|h_\uparrow\rangle$ and $|h_\downarrow\rangle$. Whether the solution $|\psi^\dagger\rangle$ is interpreted as an anti-particle or a hole is entirely dependent on the physical set-up of the system - the anti-particle interpretation is preferred in most cases, such as for the free particle; while the hole interpretation occurs in conductors where all electron positions are filled except for a small number of holes, which can then act as pseudo-particles, only with the opposite charge to the electron. Mathematically however, the two interpretations are the same, and we use the pairs of terms particle/anti-particle and particle/hole interchangeably.

With this clarified however, we can identify $\mathcal{H}_{\text{charge}}$ as $\mathbb{C}^2$ when both particle and hole solutions exist, with $|p\rangle = (1\,0)^T$ and $|h\rangle = (0\,1)^T$, and $\mathbb{C}$ when only particle solutions exist. The reduction to $\mathbb{C}$ in certain situations can occur for $\mathcal{H}_{\text{spin}}$ can also occur; if the system has integer spin then $\mathcal{H}_{\text{spin}} = \mathbb{C}$; the above mentioned $\mathcal{H}_{\text{spin}} = \mathbb{C}^2$ happens when $s = 1/2$, and $|\uparrow\rangle = (1\,0)^T$, $|\downarrow\rangle = (0\,1)^T$); while fractional spin other than $s = 1/2$ will led to other spaces than $\mathcal{H}_{\text{spin}} = \mathbb{C}^2$. This leaves this breakdown of the Hilbert space incredibly flexible, and responsive to the set-up of the system while still following a general formulation. This will allow a very useful breakdown of time-reversal, charge-conjugation and chiral operators and what parts of the Hilbert space they operate on in the main section of the Thesis in Chapters 2 and 3.

The operators $\hat{q}_k, \hat{p}_k, \hat{L}_k, \hat{S}_k$ then break down into operators in the subspaces as

$$\hat{q}_k \to \mathbb{I}_{\mathcal{H}_{\text{charge}}} \otimes \mathbb{I}_{\mathcal{H}_{\text{spin}}} \otimes \hat{q}_k \tag{C.11}$$

$$\hat{p}_k \to \mathbb{I}_{\mathcal{H}_{\text{charge}}} \otimes \mathbb{I}_{\mathcal{H}_{\text{spin}}} \otimes \hat{p}_k \tag{C.12}$$

$$\hat{L}_k \to \mathbb{I}_{\mathcal{H}_{\text{charge}}} \otimes \hat{L}_k \otimes \mathbb{I}_{\mathcal{H}_{\text{orbital}}} \tag{C.13}$$

$$\hat{S}_k \to \mathbb{I}_{\mathcal{H}_{\text{charge}}} \otimes \hat{S}_k \otimes \mathbb{I}_{\mathcal{H}_{\text{orbital}}} \tag{C.14}$$

The two types of angular momentum operator can be combined, forming the total angular momentum operator,

$$\hat{J}_k = \hat{S}_k + \hat{L}_k$$

which has the form on the Hilbert space $\mathcal{H} = \mathcal{H}_{\text{charge}} \otimes \mathcal{H}_{\text{spin}} \otimes \mathcal{H}_{\text{orbital}}$,

$$\hat{J}_k \to \mathbb{I}_{\mathcal{H}_{\text{charge}}} \otimes \hat{J}_k \otimes \mathbb{I}_{\mathcal{H}_{\text{orbital}}} \tag{C.15}$$

C.1.2 Degenerate Eigenvalues and Reducible Hilbert Spaces

As seen when denoting the spin eigenstates, it is useful to use the eigenvalue as the label for the eigenstate, so if $\hat{O}|\psi_n\rangle = \lambda_n |\psi_n\rangle$, we relabel $|\psi_n\rangle \to |\lambda_n\rangle \to |n\rangle$ if there is an ordering on the eigenvalues λ_n. This is fine in the case where all eigenvalues λ_n are non-degenerate, however when there are degenerate eigenvalues, there will be multiple eigenstates $|\psi_n\rangle, |\psi'_n\rangle$ corresponding to a single eigenvalue λ_n.

Again, as done with the spin eigenstates, it is still possible to label the states according to the eigenvalue label, however an additional identifier must be used to order the different eigenstates, $|\psi_n\rangle \to |n, a\rangle$ where a runs from 1 to the multiplicity of the eigenvalue λ_n. If $\hat{O}'$ is a second operator that commutes with the operator $\hat{O}$ defining the eigenbasis, its eigenstate labels can be used to identify the different eigenstates. That is, if $|\psi_n\rangle, |\psi'_n\rangle$ share the same eigenvalue λ_n under $\hat{O}$, but have eigenvalues λ'_a, λ'_b under $\hat{O}'$ respectively, then they can be labelled $|n, a\rangle$ and $|n, b\rangle$ respectively too. If there are still degenerate labels, then sufficient additional operators can be added to the set until each eigenstate is uniquely labelled by what is known as a set of quantum numbers. The set of operators used to do this is known as complete set of operators.

Sates $|n, a\rangle$ which correspond to a eigenvalue λ_n define a subspace in the Hilbert space, [9],

Theorem C.1.8. *Let $\mathcal{H}$ be a Hilbert space with operator $\hat{O}$. Let the eigenstates $|n, a\rangle$ of $\hat{O}$ form an eigenbasis for $\mathcal{H}$. Either, there are no eigenvalues of $\hat{O}$ with multiplicity greater than one, and the Hilbert space is irreducible; or there exists an eigenvalue λ_m with multiplicity greater than one which defines the sub-Hilbert space $\mathcal{H}_m$,*

$$\mathcal{H}_m = span(\{|m, a\rangle : a \in [1, s_m]\})$$

and $\mathcal{H} = \mathcal{H}_m \oplus \mathcal{H}_m^\perp$ is a reducible Hilbert space.

This is very similar to the Theorem 2.1.8 for the reducibility of a representation. It is expected then, that there is a concept of a completely reducible Hilbert space,

Theorem C.1.9. *Let $\mathcal{H}$ be a Hilbert space with an orthonormal basis $|m, a\rangle$ given by the eigenstates of the operator $\hat{O}$. Let the eigenvalues λ_n each have multiplicity s_n. Then each eigenvalue λ_n generates a subspace $\mathcal{H}_n$ of the full Hilbert space spanned by the vectors $|n, a\rangle$ for $a = 1, \ldots s_n$, and the Hilbert space can be completely decomposed into independent orthogonal subspaces,*

$$\mathcal{H} = \oplus_n \mathcal{H}_n$$

Proof. The proof is the same as for Maschke's Theorem. Let $\mathcal{H}$ be a Hilbert space, either it is irreducible, or $\mathcal{H} = \mathcal{H}_m \oplus \mathcal{H}_m^\perp$. Then $\mathcal{H}_m, \mathcal{H}_m^\perp$ are Hilbert spaces so the same reducibility

argument applies. This continues, until all the Hilbert spaces in the decomposition of $\mathcal{H}$ are irreducible, $\mathcal{H} = \oplus_n \mathcal{H}_n$. $\qquad\square$

D. *The Periodic Orbit Expansion for Symmetric Graphs*

In this appendix we return to two of the properties introduced in Chapter 4 as characterising the ten random matrix ensembles described by Wigner, Dyson, Altland and Zirnbauer. These were first the density of states,

$$d(k) = \sum_{k' \in \{k_n\}} \delta(k - k')$$

with the ensemble average being given by Equation 4.8 for the three Wigner-Dyson classes, and Equations 4.11 to 4.20 for the Altland-Zirnbauer classes; and second, the counting function $N(k)$,

$$N(k) = \sum_{k' \in \{k_n\}} \theta(k - k'), \qquad N(k) = \int_{-\infty}^{k} d(k')dk'$$

for k the wave number, and thus, there being similar forms $d(E)$ and $N(E)$ for the energy itself.

These functions and methods of approximating them have been well studied in the general quantum chaos literature, with one of the main techniques being the semiclassical approximation. In this approximation, properties of the quantum system may be approximated by averaging their values taken over a number of classical orbits; in particular the periodic orbits, [10, 71, 72]. This leads to the approximation of $d(E)$ in a general system by a form of the Gutzwiller Trace formula, [71], which is given here in the specific case of the two dimensional quantum billiard, [119, 157],

$$d(E) = \frac{-1}{\pi} \lim_{\eta \to 0} \text{Im} \int_{\mathbb{R}^n} G(r, r, E + i\eta)d^n r$$
$$\approx \frac{mA}{2\pi\hbar^2} + \text{Im} \left(\frac{m}{\pi\hbar^2 k} \sum_p \frac{L_p(-1)^{n_p}}{r_p \sqrt{|\text{tr } M_p - 2|}} e^{ikL_p + i\pi/2} \right), \qquad k^2 = \frac{2mE}{h^2}.$$

The sum here is taken over all periodic orbits p in the billiard, the paths where there exists a minimum time t_p such that $q(nt_p + t) = q(t)$ and $v(nt_p + t) = v(t)$, $\forall n \in \mathbb{N}$ and $\forall t \leq t_p$ so that after $t = t_p$, the orbit retraces its original path without deviation. If the total time the path takes is T_p, and $t_p = T_p$, then the orbit is primitive, otherwise the number of repetitions of the primitive orbit is $r_p = T_p/t_p$. The length of the orbit is then $L_p = \oint_0^{T_p} |\dot{q}(t)|dt$, while n_p describes the number of reflections against the boundary of the billiard, M_p the stability matrix of the orbit, and A the size of the billiard.

The advantage of approximating $d(E)$ semiclassically is that it allows other measures of the spectral statistics to be approximated, universal features to be identified, and compared to the

random matrix theory predictions, and this has been used to probe the standard Wigner-Dyson BGS-Conjecture, forming one of the key techniques in attempting to justify or derive it, [70, 170]. Taking the Fourier transform of the two-point correlator of $d(E)$ to define the form factor $K(\tau)$ of the system - which has a characteristic form for each of the random matrix ensembles associated to a Wigner-Dyson class of system - then it is well understood how the periodic orbits give a leading term approximation of the expression of $K_2(\tau)$ from random matrix theory, [21]. The first correction term is also known to come from the periodic orbits - specifically from pairs of orbits where the second orbit is equal to the first orbit, except that at a self-intersection point the orbit has been cut apart and part of it reversed before the orbit is reconnected, creating a pair of orbits that traverse most of their length parallel, except for a section where they run anti-parallel. These are known as Sieber-Richter pairs of orbits, [147, 148]. Higher order corrections come from pairs of orbits where there are more 'encounters' between them, where more self-intersection points have had the splitting-reversing-reconnecting procedure applied, or else the self-intersection involves more than two instances of the orbit passing through the point; the inclusion of these gives the full form of the spectral form factor, [118, 120, 121, 122].

Despite having fully matched the spectral form factor in the Wigner-Dyson case through the periodic orbit approximation, this method is currently still insufficient as a general proof of the BGS-Conjecture as it applies only to the regime where semiclassical analysis is valid, and it does not show there are not further corrections due to unconsidered pairs of orbits, which would move the approximation away from the calculated random matrix prediction, [122]; nor does it cover the case for many-body systems, [170]. Not being able to show there are no further corrections is only a problem in the general case though, as it is known that in the specific example of the quantum graph, the periodic orbit expansion is exact, [102, 130], which is why it is known that the BGS-conjecture is true on the quantum graph.

Furthermore, to get a form factor that is characteristic for the Altland-Zirnbauer classes, it is necessary to work with $K_1(\tau) = \mathcal{FT}(\langle d(E) \rangle_H)$, there has been some limited work on identifying the periodic orbit contributions to $K_1(\tau)$, and mainly on a spin variant of the quantum graph, [64, 65, 66, 144].

Due to this, an expression for the periodic orbit expansion has been given for each variant on the quantum graph that has been discussed in the literature, [27, 64, 65, 67, 102], to facilitate either further semiclassical study of these graphs or numerically test the periodic orbit expansion against the random matrix predictions. We continue this tradition, deriving the periodic orbit approximation for the quotient graph derived from a magnetic Dirac graph. We also start the process of numerically testing the periodic orbit approximation on the sorts of graphs used in Chapters 6 and 7 by considering how periodic orbits can be identified on them - and as these graphs are large, how symmetry can be used to increase the speed of doing so.

D.1   The Trace Formulae For Quantum Graphs

In Chapter 6 and 7, expressions for the density of states and the counting function were given in terms of the secular equation,

$$N(k) = N^{\text{Weyl}}(k) - \frac{1}{\pi} \operatorname{Im} \ln \zeta(k + i\epsilon) = N^{\text{Weyl}}(k) - \frac{1}{\pi} \operatorname{Im} \ln \det \left(\mathbb{I} - S(k + i\epsilon) T(k + i\epsilon) \right)$$

$$d(k) = d^{\text{Weyl}}(k) - \frac{1}{\pi} \frac{\mathrm{d}}{\mathrm{d}k} \operatorname{Im} \ln \zeta(k + i\epsilon) = d^{\text{Weyl}} - \frac{1}{\pi} \frac{\mathrm{d}}{\mathrm{d}k} \operatorname{Im} \ln \det \left(\mathbb{I} - S(k + i\epsilon)T(k + i\epsilon) \right)$$

Using the substitution $\ln \det(A) = \operatorname{tr} \ln(A)$ and $\ln(\mathbb{I} - A) = -\sum_{n=1}^{\infty} \frac{1}{n} A^n$, [67], then the oscillating non-Weyl term of $N(k)$ simplifies to

$$N^{\text{osc}}(k) = \frac{1}{\pi} \operatorname{Im} \left(\sum_{n=1}^{\infty} \frac{1}{n} \operatorname{tr} \Xi^n(k + i\epsilon) \right) \tag{D.1}$$

where $\Xi(k) = S(k)T(k)$. In the scattering picture the effect of calculating the nth power of Ξ is that $(\Xi^n)_{ij}$ describes the Gaussian wave-packet starting on the bond j, then scattering down n bonds to finish on the bond i. The diagonal elements Ξ_{ii}^n then describe the periodic orbits of length n, starting and ending on the bond i. These periodic orbits are a sequence of bonds $p = (b_1 b_2 \ldots b_n)$ such that $b_i = [v_i, v_{i+1}]$, with $b_{n+k} \equiv b_k$ and $b_n = [v_n, v_1]$, [18]. The period T_p is defined as the minimum shift so that $(b_{T_p+1} \ldots b_n b_1 \ldots b_{T_p}) = (b_1 b_2 \ldots b_n)$ and the repetition number is $r_p = n/T_p \in \mathbb{N}$. The set of primitive periodic orbits of any length will be called $\mathcal{P}$, while $\mathcal{P}_n$ will be the primitive orbits of length n.

If the quantum graph has an m-dimensional wave-function on it, so that $\psi_b(x_b) = \left(\psi_{b,1}(x_b) \quad \ldots \quad \psi_{b,m}(x_b) \right)^T$, then the trace of Ξ is given by, [27, 67],

$$\frac{1}{n} \operatorname{tr} \Xi^n(k) = \operatorname{tr} \sum_{(b_1 \ldots b_n) \in \mathcal{P}} \sum_{r_p=1}^{\infty} \frac{1}{r_p} \left(S_{b_1 b_n}(k) T_{b_n}(k) S_{b_n b_{n-1}}(k) T_{b_{n-1}}(k) \ldots \right.$$
$$\left. \ldots S_{b_3 b_2}(k) T_{b_2}(k) S_{b_2 b_1}(k) T_{b_1}(k) \right)^{r_p}$$

where each T_{b_i}, $S_{b_{i+1} b_i}$ is a $m \times m$ matrix. Given that $T_{b_i} = p_{b_i} \exp(i(k + A_{b_i}) L_{b_i}) \mathbb{I}_m$, where p_{b_i} is the phase picked up by cutting the bond for the quotient graph, then this becomes, [67],

$$N^{\text{osc}}(k) = \lim_{\epsilon \to 0} \frac{1}{\pi} \operatorname{Im} \left(\sum_{p \in \mathcal{P}} \sum_{r_p=1}^{\infty} \frac{e^{i(k+i\epsilon)r_p L_p} \Phi_p^{r_p} \Psi_p^{r_p} \mathcal{A}_p^{r_p}(k + i\epsilon)}{r_p} \right) \tag{D.2}$$

where,

$$\Phi_p = \prod_{b \in p} e^{i A_b L_b}, \qquad \Psi_p = \prod_{b \in p} p_b,$$

$$\mathcal{A}_p(k + i\epsilon) = \operatorname{tr} \left(S_{b_1 b_n}(k + i\epsilon) S_{b_n b_{n-1}}(k + i\epsilon) \ldots S_{b_b b_1}(k + i\epsilon) \right).$$

If the scattering matrix is independent of k, then by re-summing over r_p and using the infinite sum approximation of $\ln(1 - x)$ as $\ln(1 - x) = \sum_{r=1}^{\infty} x^r / r$, this can be rewritten as, [67],

$$N(k) = -\lim_{\epsilon \to 0} \frac{1}{\pi} \operatorname{Im} \sum_{p \in \mathcal{P}} \ln \left(1 - \mathcal{A}_p \Phi_p \Psi_p e^{i(k+i\epsilon)L_p} \right). \tag{D.3}$$

Taking the derivative of this, then the Weyl part of the density of states can be written as a sum over primitive periodic orbits by,

$$d^{\text{Weyl}}(k) = \lim_{\epsilon \to 0} \frac{1}{\pi} \frac{\mathrm{d}}{\mathrm{d}k} \operatorname{Im} \left(\sum_{p \in \mathcal{P}} \sum_{r_p=1}^{\infty} \frac{e^{i(k+i\epsilon)r_p L_p} \Phi_p^{r_p} \Psi_p^{r_p} \mathcal{A}_p^{r_p}(k + i\epsilon)}{r_p} \right)$$

$$= \lim_{\epsilon \to 0} \frac{1}{\pi} \operatorname{Re} \sum_{p \in \mathcal{P}} \sum_{r_p=1}^{\infty} L_p e^{i(k+i\epsilon)r_p L_p} \Phi_p^{r_p} \Psi_p^{r_p} \mathcal{A}_p^{r_p}$$

$$= \lim_{\epsilon \to 0} \operatorname{Re} \sum_{p \in \mathcal{P}} \frac{L_p}{\pi} \frac{\Phi_p \Psi_p \mathcal{A}_p e^{i(k+i\epsilon)L_p}}{1 - \Phi_p \Psi_p \mathcal{A}_p e^{i(k+i\epsilon)L_p}}$$

using the simplifications of [67] when S is independent of k to turn $\sum_{r=1}^{\infty} x^r = x/(1-x)$ when $x < 1$. This forms the periodic orbit trace formulae on the quantum graph, equivalent in function to the Gutzwiller trace formulae, except it is now exact.

D.2   Identifying Periodic Orbits on Symmetric Graphs

We now come to consider the requirements to be able to numerically test the periodic orbit approximation on quantum graphs by computing $N(k)$, $d(k)$ or $K_1(\tau)$ using a number of periodic orbits taken from a graph. To get good approximations of these values, it will be necessary to identify all periodic orbits in the graph passing along up to $2|\mathcal{B}|$ bonds as the graph equivalent to requiring all periodic orbits up to the Heisenberg time for a general quantum system, [67]. Based on the equations above, it will however be sufficient to identify only the primitive orbits.

The difficulty in identifying all primitive periodic orbits on a quantum graph is in finding an algorithm that is both fast and memory efficient. On the complete n-graph, for example, it is possible to be very RAM efficient by generating the set of length m-orbits as generating the set of lists of vertices $\{(v_1, v_2, \ldots, v_m) \mid v_i \in [0, n-1], v_i \neq v_{i-1}\}$ with the bond paths being defined as $(b_1 b_2 \ldots b_m)$, $b_i = [v_i, v_{i+1}]$. This can be done by a series of m for loops, which iterate over $[0, n-1]$ for each entry v_i so that it stores only m values at a time, however it stores each orbit multiple times - m/r times - as it counts each rotation of the starting vertices as separate. This makes it a computationally long program that is very heavy on the storage memory.

Here we demonstrate a method that uses combinations of simple periodic orbits to build all of the non-simple orbits. We give a method of determining repeated orbits and filtering them out to save on memory and to make sure there is no double counting in the trace formulae. These algorithms will work on any graph, however they will still be slow on large graphs, specifically those discussed in Chapters 6 and 7. To that end, we show how the symmetric structure of the vertex-subgraph expanded quotient graph can be used to 'fold' the full graph into a smaller graph for calculation.

D.2.1   Identifying Periodic Orbits

We begin with a general method of identifying all unique periodic orbits on a simple graph. Firstly, we identify the bijection between representations of periodic orbits as lists of vertices and as lists of bonds:

Definition D.2.1. *Let Γ be a simple graph with vertex set $\mathcal{V}$ and bond set $\mathcal{B}$. Let $(b_1 \ldots b_n)$ be a sequence of n bonds $b_i \in \mathcal{B}$ such that $b_i = [v_i, v_{i+1}]$ for $i < n$ and $b_n = [v_n, v_1]$ for $\{v_i\} \subset \mathcal{V}$, so that $(b_1 \ldots b_n)$ describes a length n-periodic orbit on Γ. Then the same orbit is described by the vertex list $(v_1 v_2 \ldots v_n)$.*
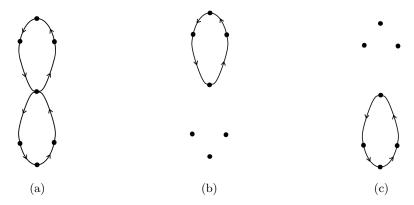
Figure D.1: The figure-of-eight orbit in (a) can be split at the middle vertex into two distinct simple orbits - the loop through the upper three vertices in (b); and the loop through the three lower vertices in (c).

Alternatively, let $(v_1 v_2 \ldots v_n)$ be a sequence of n vertices $v_i \in \mathcal{V}$ such that for each pair v_i, v_{i+1}, there exists $b_i \in \mathcal{B}$ such that $b_i = [v_i, v_{i+1}]$, with $b_n = [v_n, v_1]$. Then $(v_1 v_2 \ldots v_n)$ describes the same periodic orbit as $(b_1 \ldots b_n)$.

In terms of the algorithms developed below, it will be easier to work with the vertex representation of a periodic orbit. Note that the bijection holds only when Γ is simple, as otherwise there exists a pair of bonds $b = b' = [i, j]$ and the identification of $i, j \to b$ is not unique.

We now add a second classification of the properties of a periodic orbit, identifying it as either having a self-intersection, so it visits a vertex more than once, or having no self-intersections and being simple, [102]. These simple orbits will prove to be the building blocks for constructing all of the primitive orbits on the graph.

Definition D.2.2. *Let Γ be a simple graph with periodic orbit $p = (v_1 \ldots v_n)$. Then if there are no repeated vertices in p, $\nexists i, j$ such that $v_i = v_j$, so each vertex is visited only once then p is a simple or irreducible orbit. Otherwise, p is reducible.*

Given a reducible periodic orbit where a single vertex v is repeated once, $p = (v_1 \ldots v_i v v_{i+2} \ldots v_j v v_{j+2} \ldots v_n)$, then the graph p forms a figure-of-eight orbit. If the loops are cut apart at v where they intersect, as in Figure D.1, then p can be split into two simple circular orbits. Rigorously, if an orbit p has a self-intersection at the v, then it can be decomposed into two simple periodic orbits,

$$p = p_1 \cup p_2, \qquad p_1 = (v_1 \ldots v_i v v_{j+2} \ldots v_n), \quad p_2 = (v v_{i+2} \ldots v_j).$$

This process can be done for more complicated orbits where there are multiple repeated vertices, and vertices repeated more than once. It can be done once, creating another two reducible orbits, or it can be repeated until all orbits involved are simple - isolating a single repeated vertex in one of the orbits, using this to partition the orbit in two, and taking the interior and exterior sections of the partition as the decomposed form of this orbit in the full decomposition of p; heuristically this suggests that simple orbit decomposition of reducible orbits is always possible, though it will need defining rigorously. With the quantitative process of orbit decomposition, there are several things to note though. First, as can be seen when considering the possible splits of the orbit

(a) $p \cup_{i,j} p'$ (b) $p \cup_{i,(n-j)} \bar{p}'$

Figure D.2: A comparison of the effect of adding the orbits p, p' as $p \cup_{i,j} p'$ and $p \cup_{i,(n-j)} \bar{p}'$, forming a Sieber-Richter pair of orbits.

$(1, 2, 3, 4, 2, 5, 3, 6),$

$$p = (1, 2, 3, 4, 2, 5, 3, 6) = \begin{cases} (1, 2, 5, 3, 6) \cup (2, 3, 4) & \text{split on 2 first} \\ (1, 2, 3, 6) \cup (3, 4, 2, 5) & \text{split on 3 first} \end{cases} \tag{D.4}$$

the orbit decomposition is not unique, and highly dependent on the order in which the splits are taken; this will carry over to the simple orbit decomposition. Second, just using the $\cup$ notation may not be clear as to how the splits in the orbit have been taken, and how the full orbit should be reconstructed. Splitting the orbit $p = (1, 2, 3, 4, 1, 3, 5, 3, 6)$ on the outer pair of 3s, then the decomposition is $p = (3, 4, 1, 3, 5) \cup (3, 6, 1, 2)$ but to recombine it, it is unclear when looking at the decomposition without the information about the full orbit whether the second orbit $(3, 6, 1, 2)$ has been removed from the first occurrence of three in $(3, 4, 1, 3, 5)$ or the second.

Thus, when we rigorously define the addition of two orbits - a definition implicit in the ability to decompose orbits - we include a method to track where the insertion of the second orbit into the first occurs:

Definition D.2.3. *Let $p = (v_1 v_2 \ldots v_n)$ and $p' = (v_1' v_2' \ldots v_m')$ be two periodic orbits on the graph Γ. Let $v_i = v_j'$. Then the addition of the orbits $p \cup_{i,j} p'$ inserts the orbit p' starting at v_j into the orbit p at the point v_i,*

$$p \cup_{i,j} p' = (v_1 \ldots v_i v_{j+1}' \ldots v_m' v_1' \ldots v_j' v_{i+1} \ldots v_n) \tag{D.5}$$

As an aside, we note that if $\bar{p}' = (v_n v_{n-1} \ldots v_1)$ is the reversal of the orbit so it is traced out backwards, then $p \cup_{i,j} p'$ and $p \cup_{i,(n-j)} \bar{p}'$ is one way to form a Sieber-Richter pair of orbits, as seen in Figure D.2.

We are now in a position to start simplifying the problem of finding all the orbits of a graph. We show that every reducible orbit can indeed be constructed out of simple orbits:

Theorem D.2.4. *Let $\mathcal{P}$ be the set of primitive periodic orbits. Let $\mathcal{S}$ be the set of simple periodic orbits. Then for every $p \in \mathcal{P}$, there exists the sequences $\{s_m\} \in \mathcal{S}$, $\{i_m\}$, and $\{j_m\}$ such that*

$$p = s_1 \cup_{i_1, j_1} s_2 \cup_{i_2, j_2} \ldots$$

Proof. This is the complete decomposition of p into simple orbits. Let p be a periodic orbit. Either p is simple, or it is possible to find two vertices $v_i, v_j \in p$ such that $v_i = v_j$. Then, $p = (v_1 \ldots v_i v_{j+1} \ldots v_n) \cup_{i,1} (v_i \ldots v_{j-1}) = p_1 \cup_{i,1} p_2$. Furthermore, either p_1, p_2 are simple, or they can be decomposed as above. Applying this iteratively defines the complete eduction of p into simple orbits. □

This means that if all the simple orbits are known, then finding all orbits of length n is a case of taking all possible sequences $\{s_i\}$, such that $n = \sum_{s \in \{s_i\}} |s|$, with the set of all possible ways they can be combined and adding then them together.

This shifts the problem of calculating all periodic orbits to the problem of calculating all simple periodic orbits. The simple orbits of a graph can be calculated by a number of algorithms, here we use the *simple_cycles* algorithm from networkx in Python, [74], which implements the method of Johnson from [89]. Separating out $\mathcal{P}$ and $\mathcal{S}$ into subsets according to size, and considering $\mathcal{P}'$, the set of orbits allowing non-primitive elements,

$$\mathcal{P}'_n = \{p \in \mathcal{P}' \mid |p| = n\} \subset \mathcal{P}', \qquad \mathcal{S}_n = \{s \in \mathcal{S} \mid |s| = n\} \subset \mathcal{S}$$

then knowing $\mathcal{P}'_2 \ldots \mathcal{P}'_{n-1}$, the next set of periodic orbits, $\mathcal{P}'_n$, can be constructed as

$$\mathcal{P}'_n = \mathcal{S}_n \bigcup \left(\cup_{m=2}^{\lfloor n/2 \rfloor} \cup_{p \in \mathcal{P}'_m} \cup_{p' \in \mathcal{P}'_{n-m}} \cup_{i,j:v_i=v'_j} \cup_{i,j} p' \right).$$

This gives the algorithm for finding all orbits on G up to a specific length, while allowing repetition in the orbit so $r_p \geq 1$. It is necessary to allow for $r_p > 1$ in building the orbits, as taking the combination with a second orbit may break the non-primitive nature of the orbit, for example $(1, 2, 1, 2) \cup_{2,1} (2, 3, 4)$ uses a non primitive orbit $(1, 2, 1, 2)$ to make the primitive orbit $(1, 2, 3, 4, 2, 1, 2)$. Thus, non-primitive orbits should only be discarded at the very end of the computation once all the desired sets $\mathcal{P}'_n$ have been found by using $\mathcal{P}_n = \{p \in \mathcal{P}'_n \mid r_p = 1\}$.

What does need to be done at the end of computing each $\mathcal{P}'_n$ is discarding the non-unique orbits to save on both memory and run time. Two orbits p, p' are equivalent if $|p| = |p'| = n$ and there exists a shift of size m such that $(v_1 \ldots v_n) = (v'_m \ldots v'_n v'_1 \ldots v'_{m-1}) = p'_{m\rightarrow}$, where $p'_{m\rightarrow}$ denotes a shift of the starting point of p' m places to the right. It is possible to take every new p added to $\mathcal{P}'_n$ and check that for each possible shift m, $p_{m\rightarrow} \notin \mathcal{P}'_n$. It is however faster to agree upon a standardised presentation for an orbit - that is a way of choosing a standardised starting point in the orbit - and transforming the orbit into this presentation before potentially adding it to $\mathcal{P}'_n$ if it isn't already included. We do this by taking the alphabetically smallest version of $p_{m\rightarrow}$ under shifts m:

Definition D.2.5. *Let p, p' be two periodic orbits on a graph Γ of length n. Then, $p \leq p'$ if the sequence $(v_1, \ldots, v_n)$ comes before $(v'_1, \ldots, v'_n)$ alphabetically. That is, there $\exists i \leq n$ such that for all $j < i$, $v_j = v'_j$ and $v_i < v'_i$.*

Definition D.2.6. *Let p be a periodic orbit on Γ. Then the standard ordering of p, p_s is defined as $p_s = p_{m\rightarrow}$ with m chosen so that $p_s \leq p_{k\rightarrow}$ for all $k \in [1, n]$.*

Checking if p is already included in $\mathcal{P}'_n$ is then a case of transforming each orbit into its standard presentation before adding it to $\mathcal{P}'_n$. As p_s can be found by using built in algorithms

to identify the minimum element k in p, then all entries of p equal to k, then comparing each of the possible shifts required to get k as a starting element, this massively speeds up the checking when compared to testing each individual shift.

Finally, to complete finding the set of primitive periodic orbits, it is only necessary to filter out the non-primitive orbits. This can be done by checking whether for each $m \mid n$, $p = \cup_{i=1}^{n/m} (v_1 \dots v_m)$. Thus concludes the discussion on finding the periodic orbits of a general graph.

D.2.2 Using Symmetry to Reduce Graph Size

We note again the necessity of computing all periodic orbits up to the Heisenburg length so that $n \leq 2|\mathcal{B}|$ in order to be able to get a good estimate of the values being approximated by the periodic orbit expansion, [67]. For the sorts the sorts of graphs considered in Chapters 6 and 7, where the graphs contained between 46 and 136 bonds this is beyond prohibitively expensive though - it would require finding all orbits with maximum length 92 or 272. Even the smallest possible four-part graph consistent with the structure in Chapter 7, presented in Figure D.3a, having 24 bonds requires orbits of up to length 48, yet it can take weeks to calculate just the orbits of length 14.

The issue is that the algorithms used to generate the orbits scale poorly both in the number of bonds on the graph, and in the number of orbits they have to calculate. For a graph with N bonds, V vertices and $S = |\mathcal{S}|$ simple orbits, it takes $\mathcal{O}((N + V)(S + 1))$ time to identify all of $\mathcal{S}$; it is harder to estimate the exact scaling of the process of combining the simple orbits together to form $\mathcal{P}'_n$, however, it at a minimum scales as $\mathcal{O}(\sum_{m=2}^{\lfloor n/2 \rfloor} |\mathcal{P}'_m||\mathcal{P}'_{n-m}|)$ based on the need to loop through all pairs p, p' in $\mathcal{P}'_m \otimes \mathcal{P}'_{n-m}$ for $2 \leq m \leq \lfloor n/2 \rfloor$, and this must be done for every $n \leq 2|\mathcal{B}|$.

It is desirable then to look for a way to reduce the time these calculations take. It will not be possible to reduce the maximum length of the orbits that need to be calculated, but we will show that it is possible to find a smaller graph, Γ_{folded} based on the full graph through symmetry, and through the calculation of the orbits of Γ_{folded} find all orbits the orbits on the original graph. Due to the difference in size between Γ and Γ_{folded} and the reduced number of possible orbits however, there will be a generally approximately $(|\mathcal{V}|/|\mathcal{V}_{\text{folded}}|)^2$ factor speed-up in the computation through reducing N, V and $|\mathcal{S}|$. For the graphs considered in Chapter 6 and 7 this will work out as either fourfold, or sixteenfold depending on whether $|T_G| = 1$ or $|T_G| = 2$.

Recall the very regular structure of the vertex-expanded quotient graphs $\Gamma(G, S_U \cup T_G)/(U, \rho)$ from Chapter 7. If Γ_{sg} is the subgraph used to expand the vertices, then if $|T_G| = 1$, then $\Gamma(G, S_U \cup T_G)/(U, \rho)$ consists of two interlinked copies of Γ_{sg}; while if $|T_G| = 2$, it contains four interlinked copies of Γ_{sg}. An example where $|T_G| = 2$ is provided in Figure D.3a.

This graph $\Gamma(G, S_U \cup T_G)/(U, \rho)$ is symmetric under both α and γ as an abstract graph rather than a Dirac graph, and if the vertex labels are chosen properly then the permutations on the vertices by α and γ may be expressed by adding or subtracting kn as required to the vertex labels, where $n = |\mathcal{V}_{\text{sg}}|$ and $k \in \mathbb{N}$. In particular, if the vertex sub-graph has n vertices, then the vertices of Γ_{sg} are labelled by $0 \dots n - 1$; the vertices of $\alpha\Gamma_{\text{sg}}$ by $n \dots 2n - 1$; the vertices of $\gamma\Gamma_{\text{sg}}$ by $2n \dots 3n - 1$; and the vertices of $\alpha\gamma\Gamma_{\text{sg}}$ by $3n \dots 4n - 1$. It can then be seen that the vertex

permutations induced by α and γ are given by,

$$\alpha : v \rightarrow \begin{cases} v + n & v < 2n \text{ or } 2n \leq v < 3n \\ v - n & n \leq v < 2n \text{ or } v \geq 3n \end{cases} \tag{D.6}$$

$$\alpha^{-1} : v \rightarrow \begin{cases} v + n & v < 2n \text{ or } 2n \leq v < 3n \\ v - n & n \leq v < 2n \text{ or } v \geq 3n \end{cases}$$
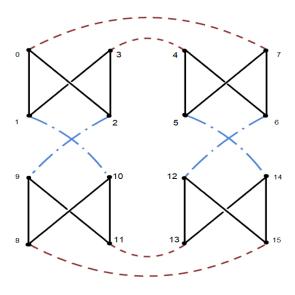
$$\gamma : v \rightarrow \begin{cases} v + 2n & v < 2n \\ v - 2n & v \geq 2n \end{cases} \tag{D.7}$$
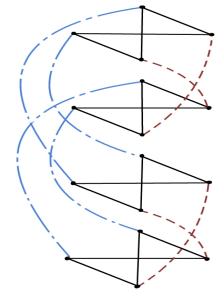
$$\gamma^{-1} : v \rightarrow \begin{cases} v + 2n & v < 2n \\ v - 2n & v \geq 2n \end{cases}$$
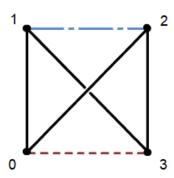
Note that because α and γ are involutions in the quotient space, as discussed in Section 3.1.1, then $\alpha^{-1} = \alpha$ and $\gamma^{-1} = \gamma$.

(a) An example of a vertex-subgraph expanded quotient graph.

(b) An alternate visualisation of the graph in (a), where each sub-graph is stacked along the z-axis.

(c) The projection of the graph in (b) onto the $x - y$ plane, so that the subgraphs merge into the complete 4 graph.

Figure D.3: A look at the method of constructing a four-part expanded quotient graph, (a), before stacking the individual sub-graphs vertically, (b) and using projection to 'fold' it into the small graph in (c). In each case, black bonds are from the vertex-subgraph, the red dashed bond are generated by α, and the blue dot-dashed bonds are generated by γ.

We consider now the process of defining Γ_{folded}. Consider a graph with structure similar to that in Figure D.3a, so it consists of interlinked copies of multiple copies of a graph Γ_{sg}. This may be drawn in the $x - y$ plane as is standard, or it may be drawn in three dimensions by stacking each copy of Γ_{sg} along the z-axis as in Figure D.3b. Taking the projection of this graph onto the $x - y$ plane forms the graph like in Figure D.3c; formally this graph is found by applying the projection operator P_{folding} to the each of the vertices and bonds of $\Gamma(G, S_U \cup T_G)/(U, \rho)$ with its action as,

$$P_{\text{folding}} : v \to v \bmod_n \qquad v \in \mathcal{V}$$
$$P_{\text{folding}} : b = [v_1, v_2] \to [v_1 \bmod_n, v_2 \bmod_n] \qquad b \in \mathcal{B}$$

so that $\Gamma_{\text{folded}} = P_{\text{folding}}\Gamma(G, S_U \cup T_G)/(U, \rho)$, $\mathcal{V}_{\text{folded}} = \{P_{\text{folded}} v \mid v \in \mathcal{V}\}$ and $\mathcal{B}_{\text{folded}} = \{P_{\text{folded}} b \mid b \in \mathcal{B}\}$ with repeated elements removed to make sure Γ_{folded} is simple.

It is now a case of showing all orbits on $\Gamma(G, S_U \cup T_G)/(U, \rho)$ can be found from the orbits on Γ_{folded}, and identifying the process of converting an orbit on Γ_{folded} into an orbit on $\Gamma(G, S_U \cup T_G)/(U, \rho)$.

Note firstly though, that there are the relations on the size of $\mathcal{V}_{\text{folded}}$, $\mathcal{B}_{\text{folded}}$ and $\mathcal{S}_{\text{folded}}$ with respect to $\mathcal{V}$, $\mathcal{B}$ and $\mathcal{S}$ - $|\mathcal{V}_{\text{folded}}| = |\mathcal{V}|/2|T_G|$, $|\mathcal{B}_{\text{folded}}| = |\mathcal{B}|/2|T_G|$ and $|\mathcal{S}_{\text{folded}}| < |\mathcal{S}|/2|T_G|$ as a simple orbit on the full graph $\Gamma(G, S_U \cup T_G)/(U, \rho)$ will not be simple on Γ_{folded} if it passes through both v and at least one of αv, γv or $\alpha\gamma v$ on the full graph. This means that taking the formula for the time scaling of the algorithm to find all the simple orbits, if time T is taken for the full graph, time $T_{\text{folded}} < T/4|T_G|^2$ is taken on the folded graph. This will lead to the promised fourfold or sixteenfold speed up for calculating the simple orbits.

It is easy to show that every orbit on $\Gamma(G, S_U \cup T_G)/(U, \rho)$ appears as an orbit of Γ_{folded}. All that is needed is to apply the projection operator to each element of $p(v_1, \ldots, v_n)$, $p_{\text{folded}} = P_{\text{folding}} p = (P_{\text{folding}}(v_1), \ldots, P_{\text{folding}}(v_n))$. This means that if a way to invert the projection operator, then orbits on Γ_{folded} can be converted into orbits on $\Gamma(G, S_U \cup T_G)/(U, \rho)$, finding all of the possible orbits.

Take an orbit p on the unfolded graph, in the three dimensional picture. It can move about on a single copy of the subgraph, but if b_{α_i} and b_{γ_i} are the bonds interlinking the different subgraphs, then every time the orbit crosses one of these bonds, it will move up or down the stack of subgraphs. We can use this to invert P_{folding}.

Let $b_{\alpha,f} = [v_{a1}, v_{a2}] = P_{\text{folding}} b_{\alpha_i}$ $\forall i$ be the bond in Γ_{folded} associated to α, and $b_{\gamma,f} = [v_{c1}, v_{c2}] = P_{\text{folding}} b_{\gamma_i}$ $\forall i$ be the bond associated to γ. Then recalling the definition of α and γ in terms of the vertex permutations from Equations D.6 and D.7, P_{folding} can be inverted by taking an orbit p_{folded} and searching from the left of the orbit for the consecutive pairs of vertices v_{a1}, v_{a2}, v_{a2}, v_{a1}, v_{c1}, v_{c2} and v_{c2}, v_{c1} and then each time one appears adding the appropriate following transform,

$$p_{\text{folded}} = (v_1, \ldots, v_{i-1}, v_{a1}, v_{a2}, \ldots, v_n) \Rightarrow \alpha_i : p_{\text{folded}} \to (v_1, \ldots, v_{i-1}, v_{a1}, \alpha(v_{a2}), \ldots, \alpha(v_n))$$
$$p_{\text{folded}} = (v_1, \ldots, v_{i-1}, v_{a2}, v_{a1}, \ldots, v_n) \Rightarrow \alpha_i^{-1} : p_{\text{folded}} \to (v_1, \ldots, v_{i-1}, v_{a2}, \alpha^{-1}(v_{a1}), \ldots, \alpha^{-1}(v_n))$$
$$p_{\text{folded}} = (v_1, \ldots, v_{i-1}, v_{c1}, v_{c2}, \ldots, v_n) \Rightarrow \gamma_i : p_{\text{folded}} \to (v_1, \ldots, v_{i-1}, v_{c1}, \gamma(v_{c2}), \ldots, \alpha(v_n))$$
$$p_{\text{folded}} = (v_1, \ldots, v_{i-1}, v_{c2}, v_{c1}, \ldots, v_n) \Rightarrow \gamma_i^{-1} : p_{\text{folded}} \to (v_1, \ldots, v_{i-1}, v_{c2}, \gamma^{-1}(v_{c1}), \ldots, \gamma^{-1}(v_n)),$$

to the inverse function of P_{folding} for this specific orbit. This is equivalent to watching for the orbit to cross the bond that would shift it up or down in the stack, and then using the vertex permutation forms of α and γ to perform these shifts.

As an example for the graphs presented in Figure D.3, where $b_{\alpha,f} = [0,3]$ and $b_{\gamma,f} = [1,2]$, the orbit $p_{\text{folded}} = (0,3,2,1,3,0,2,1)$ may be transformed onto the full graph by $\gamma_7^{-1} \circ \alpha_5^{-1} \circ \gamma_3^{-1} \circ \alpha_1$, giving

$$
\begin{aligned}
p &= \gamma_7^{-1} \circ \alpha_5^{-1} \circ \gamma_3^{-1} \circ \alpha_1(0,3,2,1,3,0,2,1) \\
&= \gamma_7^{-1} \circ \alpha_5^{-1} \circ \gamma_3^{-1}(0,7,6,5,7,4,6,5) \\
&= \gamma_7^{-1} \circ \alpha_5^{-1}(0,7,6,13,15,12,14,13) \\
&= \gamma_7^{-1}(0,7,6,13,15,8,10,9) \\
&= (0,7,6,13,15,8,10,1)
\end{aligned}
$$

This allows the conversion of orbits on Γ_{folded} into paths on the full graph - it is not yet guaranteed that the unfolded orbit will end up as an orbit on the full graph, as the start and end points of the unfolded path may end up on different copies of the subgraph and not link back up. This is why a final check that for the unfolded path $p = (v_1, \ldots v_n)$ there exists $b = [v_n, v_1] \in \mathcal{B}$. If there does, then p provides an orbit, if it doesn't then it can be discarded. We also note that a non-primitive orbit on Γ_{folded} may be primitive on $\Gamma(G, S_U \cup T_G)/(U, \rho)$ if it passes through multiple copies of the subgraph - $p_{\text{folded}} = (0,2,3,0,2,3)$ which unfolds to $p = (0,2,3,4,6,7)$ is an example. This gives another reason to not discard calculated repeated orbits when finding the periodic orbits of Γ_{sg} before the end; discarding of the non-primitive orbits should only be done after the unfolding.

The process of generating the orbits on Γ_{folded} using the techniques in the section above and unfolding them then gives all periodic orbits on $\Gamma(G, S_U \cup T_G)/(U, \rho)$ starting on the copy of Γ_{sg} corresponding to the unitary subgraph. To finally get all orbits on $\Gamma(G, S_U \cup T_G)/(U, \rho)$, it is necessary to apply each of the transformations α, γ and $\alpha \circ \gamma$ to each calculated orbit, shifting the starting points to $\alpha \Gamma_{\text{sg}}$, $\gamma \Gamma_{\text{sg}}$ and $\alpha\gamma \Gamma_{\text{sg}}$ respectively, removing any repeated orbits. This will finally give all periodic orbits on $\Gamma(G, S_U \cup T_G)/(U, \rho)$. The fact that this increases the number of orbits by approximately a factor of $2|T_G|$ - ignoring the double counting of orbits which sit over more than one copy of the subgraph - is why there is again an approximately fourfold or sixteenfold speedup of the orbit-combination-process building the primitive orbits on Γ_{folded} instead of $\Gamma(G, S_U \cup T_G)/(U, \rho)$ by reducing the length of the lists $\mathcal{P}'_n$.

We can now summarise the process of identifying all primitive orbits on a symmetric graph:

- Take the graph $\Gamma(G, S_U \cup T_G)/(U, \rho)$ and identify its image Γ_{folded} under the projection P_{folding}.

- Identify the simple orbits $\mathcal{S}_{\text{folded}}$ on Γ_{folded}.

- Combine the simple orbits into the non-simple orbits on Γ_{folded} to form the set of periodic orbits $\mathcal{P}'$ which includes non-primitive orbits.

- Identify the unfolded path on $\Gamma(G, S_U \cup T_G)/(U, \rho)$ for each orbit in $\mathcal{P}'$. Discard any paths which aren't orbits.

- Discard any non-primitive orbits on $\Gamma(G, S_U \cup T_G)/(U, \rho)$.

- For each orbit p, construct αp, γp and $\alpha \gamma p$, discarding any repeated orbits.

This process will be generalisable to other symmetric graphs, and not just the two-part and four-part graphs generated by the vertex-expanded quotients of Cayley graphs for the Z_2 and $Z_2 \times Z_2$-graded groups. This can be done by identifying the appropriate vertex permutation transformations in line with the method used to define α and γ, forming the projection operator P_{folding} and its inverse out of the vertex permutation transformations.

E. *Classification of the Small Groups by the Dyson and Altland-Zirnbauer Tenfold Ways*

We give here the classification of the Z_2-graded groups of size $|G| \leq 30$ according to Dyson's Tenfold Way from Theorem 2.2.15; and the classification of the $Z_2 \times Z_2$-graded groups of size $|G| \leq 40$ according to the Altland-Zirnbauer Tenfold Way from Theorem 2.3.12. This is where the data required for the proofs in Chapter 5 to identify the minimal graded groups and irreducible representations generating each Altland-Zirnbauer class comes from.

The tables are organised by the unitary commuting subgroups U - each table consists of the character table of U on the left hand, and on the right, the possible graded groups G having $U \lhd G$, with the details of the partition. In the column below, corresponding to each irreducible representation of U, is given the class of the corepresentation of G generated by the representation of U and this particular choice of G and its partition. Note that for certain pairs of G and U, multiple partitions of G are possible, and each have been given.

As a reminder, a modified version of the GAP notation is used, so that $U_{|U|}^n = (|U|, n)$ and $G_{|G|}^m = (|G|, n)$, while the partition for a $Z_2 \times Z_2$-graded group is described by,

$$
\begin{aligned}
U &= (|U|, k) \\
G &= (4|U|, m) \\
U_{|U|}^k, \ G_{4|U|}^m(n, p, q) \longrightarrow U \cup \alpha U &= (2|U|, n) \\
U \cup \gamma U &= (2|U|, p) \\
U \cup \pi U &= (2|U|, q).
\end{aligned}
$$

It is possible to translate from GAP notation to more descriptive group names by the application of [49] or [124], which are databases of the small groups. They also provide presentations for each of the groups which can be used to calculate the structure of G as a graded group, and to identify what sorts of symmetries they involve.

GAP notation is also in use in the character tables, where $E(n)$ denotes the nth root of unity, $E(n) = \exp(2\pi i/n)$.

Finally, these classifications are given with the assumption that the system they apply to has global time-reversal and charge-conjugation operators that are involutions. If at least one of $\hat{\mathcal{T}}$, $\hat{\mathcal{C}}$ squares to $-\mathbb{I}$ then either the method of projective representations and universal covering groups has to be used from Section 2.4, constructing G' and then looking up G' in the tables; or else if

the corepresentations can be expressed over charge-spin-orbital space per Theorem 2.4.10, then the tables below can still be applied to G, but after using the following substitutions, [24]:

T^2	C^2	A	AI	AII	$AIII$	BDI	CII	D	C	CI	$DIII$
$\mathbb{I}$	$-\mathbb{I}$	A	AI	AII	$AIII$	CI	$DIII$	C	D	BDI	CII
$-\mathbb{I}$	$\mathbb{I}$	A	AII	AI	$AIII$	$DIII$	CI	D	C	CII	BDI
$-\mathbb{I}$	$-\mathbb{I}$	A	AII	AI	$AIII$	CII	BDI	C	D	$DIII$	CI

Now begins the classification of the small groups under the Dyson Tenfold, and Altland-Zirnbauer Tenfold Ways.

E.1 Classification of the Small Z_2-Graded Groups by the Dyson Tenfold Way

U_1^1	C_0	G_2^1
Γ_0	1	$\mathbb{R}I$

U_2^1	C_0	C_1	G_4^1	G_4^2
Γ_0	1	1	$\mathbb{R}I$	$\mathbb{R}I$
Γ_1	1	-1	$\mathbb{R}II$	$\mathbb{R}I$

U_3^1	C_0	C_1	C_2	G_6^1	G_6^2
Γ_0	1	1	1	$\mathbb{R}I$	$\mathbb{R}I$
Γ_1	1	$E(3)$	$E(3)^2$	$\mathbb{C}I$	$\mathbb{C}III2$
Γ_2	1	$E(3)^2$	$E(3)$	$\mathbb{C}I$	$\mathbb{C}III2$

U_4^1	C_0	C_1	C_2	C_3	G_8^1	G_8^2
Γ_0	1	1	1	1	$\mathbb{R}I$	$\mathbb{R}I$
Γ_1	1	-1	1	-1	$\mathbb{R}II$	$\mathbb{R}I$
Γ_2	1	i	-1	$-i$	$\mathbb{C}III2$	$\mathbb{C}III2$
Γ_3	1	$-i$	-1	i	$\mathbb{C}III2$	$\mathbb{C}III2$

U_4^1	G_8^3	G_8^4
Γ_0	$\mathbb{R}I$	$\mathbb{R}I$
Γ_1	$\mathbb{R}I$	$\mathbb{R}I$
Γ_2	$\mathbb{C}I$	$\mathbb{C}II$
Γ_3	$\mathbb{C}I$	$\mathbb{C}II$

U_4^2	C_0	C_1	C_2	C_3	G_8^2	G_8^3
Γ_0	1	1	1	1	$\mathbb{R}I$	$\mathbb{R}I$
Γ_1	1	-1	1	-1	$\mathbb{R}I$	$\mathbb{R}I$
Γ_2	1	1	-1	-1	$\mathbb{R}II$	$\mathbb{R}III$
Γ_3	1	-1	-1	1	$\mathbb{R}II$	$\mathbb{R}III$

U_4^2	G_8^5
Γ_0	$\mathbb{R}I$
Γ_1	$\mathbb{R}I$
Γ_2	$\mathbb{R}I$
Γ_3	$\mathbb{R}I$

U_5^1	C_0	C_1	C_2	C_3	C_4	G_{10}^1
Γ_0	1	1	1	1	1	$\mathbb{R}I$
Γ_1	1	$E(5)$	$E(5)^2$	$E(5)^3$	$E(5)^4$	$\mathbb{C}I$
Γ_2	1	$E(5)^2$	$E(5)^4$	$E(5)$	$E(5)^3$	$\mathbb{C}I$
Γ_3	1	$E(5)^3$	$E(5)$	$E(5)^4$	$E(5)^2$	$\mathbb{C}I$
Γ_4	1	$E(5)^4$	$E(5)^3$	$E(5)^2$	$E(5)$	$\mathbb{C}I$

U_5^1	G_{10}^2
Γ_0	$\mathbb{R}I$
Γ_1	$\mathbb{C}III2$
Γ_2	$\mathbb{C}III2$
Γ_3	$\mathbb{C}III2$
Γ_4	$\mathbb{C}III2$

U_6^1	C_0	C_1	C_2	G_{12}^4
Γ_0	1	1	1	$\mathbb{R}I$
Γ_1	1	-1	1	$\mathbb{R}I$
Γ_2	2	0	-1	$\mathbb{R}I$

U_6^2	C_0	C_1	C_2	C_3	C_4	C_5
Γ_0	1	1	1	1	1	1
Γ_1	1	-1	1	-1	1	-1
Γ_2	1	-1	$E(3)^2$	$-E(3)^2$	$E(3)$	$-E(3)$
Γ_3	1	-1	$E(3)$	$-E(3)$	$E(3)^2$	$-E(3)^2$
Γ_4	1	1	$E(3)^2$	$E(3)^2$	$E(3)$	$E(3)$
Γ_5	1	1	$E(3)$	$E(3)$	$E(3)^2$	$E(3)^2$

U_6^2	G_{12}^1	G_{12}^2	G_{12}^4	G_{12}^5
Γ_0	$\mathbb{R}I$	$\mathbb{R}I$	$\mathbb{R}I$	$\mathbb{R}I$
Γ_1	$\mathbb{R}II$	$\mathbb{R}II$	$\mathbb{R}I$	$\mathbb{R}I$
Γ_2	$\mathbb{C}II$	$\mathbb{C}III2$	$\mathbb{C}I$	$\mathbb{C}III2$
Γ_3	$\mathbb{C}II$	$\mathbb{C}III2$	$\mathbb{C}I$	$\mathbb{C}III2$
Γ_4	$\mathbb{C}I$	$\mathbb{C}III2$	$\mathbb{C}I$	$\mathbb{C}III2$
Γ_5	$\mathbb{C}I$	$\mathbb{C}III2$	$\mathbb{C}I$	$\mathbb{C}III2$

U_7^1	C_0	C_1	C_2	C_3	C_4	C_5
Γ_0	1	1	1	1	1	1
Γ_1	1	$E(7)$	$E(7)^2$	$E(7)^3$	$E(7)^4$	$E(7)^5$
Γ_2	1	$E(7)^2$	$E(7)^4$	$E(7)^6$	$E(7)$	$E(7)^3$
Γ_3	1	$E(7)^3$	$E(7)^6$	$E(7)^2$	$E(7)^5$	$E(7)$
Γ_4	1	$E(7)^4$	$E(7)$	$E(7)^5$	$E(7)^2$	$E(7)^6$
Γ_5	1	$E(7)^5$	$E(7)^3$	$E(7)$	$E(7)^6$	$E(7)^4$
Γ_6	1	$E(7)^6$	$E(7)^5$	$E(7)^4$	$E(7)^3$	$E(7)^2$

U_7^1	C_6	G_{14}^1	G_{14}^2
Γ_0	1	$\mathbb{R}I$	$\mathbb{R}I$
Γ_1	$E(7)^6$	$\mathbb{C}I$	$\mathbb{C}III2$
Γ_2	$E(7)^5$	$\mathbb{C}I$	$\mathbb{C}III2$
Γ_3	$E(7)^4$	$\mathbb{C}I$	$\mathbb{C}III2$
Γ_4	$E(7)^3$	$\mathbb{C}I$	$\mathbb{C}III2$
Γ_5	$E(7)^2$	$\mathbb{C}I$	$\mathbb{C}III2$
Γ_6	$E(7)$	$\mathbb{C}I$	$\mathbb{C}III2$

U_8^1	C_0	C_1	C_2	C_3	C_4	C_5
Γ_0	1	1	1	1	1	1
Γ_1	1	-1	1	1	-1	-1
Γ_2	1	i	-1	1	$-i$	i
Γ_3	1	$-i$	-1	1	i	$-i$
Γ_4	1	$E(8)$	i	-1	$E(8)^3$	$-E(8)$
Γ_5	1	$-E(8)$	i	-1	$-E(8)^3$	$E(8)$
Γ_6	1	$E(8)^3$	$-i$	-1	$E(8)$	$-E(8)^3$
Γ_7	1	$-E(8)^3$	$-i$	-1	$-E(8)$	$E(8)^3$

U_8^1	C_6	C_7	G_{16}^1	G_{16}^5	G_{16}^6	G_{16}^7
Γ_0	1	1	$\mathbb{R}I$	$\mathbb{R}I$	$\mathbb{R}I$	$\mathbb{R}I$
Γ_1	1	-1	$\mathbb{R}II$	$\mathbb{R}I$	$\mathbb{R}I$	$\mathbb{R}I$
Γ_2	-1	$-i$	$\mathbb{C}III2$	$\mathbb{C}III2$	$\mathbb{C}III2$	$\mathbb{C}I$
Γ_3	-1	i	$\mathbb{C}III2$	$\mathbb{C}III2$	$\mathbb{C}III2$	$\mathbb{C}I$
Γ_4	$-i$	$-E(8)^3$	$\mathbb{C}III2$	$\mathbb{C}III2$	$\mathbb{C}III1$	$\mathbb{C}I$
Γ_5	$-i$	$E(8)^3$	$\mathbb{C}III2$	$\mathbb{C}III2$	$\mathbb{C}III1$	$\mathbb{C}I$
Γ_6	i	$-E(8)$	$\mathbb{C}III2$	$\mathbb{C}III2$	$\mathbb{C}III1$	$\mathbb{C}I$
Γ_7	i	$E(8)$	$\mathbb{C}III2$	$\mathbb{C}III2$	$\mathbb{C}III1$	$\mathbb{C}I$

U_8^1	G_{16}^8	G_{16}^9
Γ_0	$\mathbb{R}I$	$\mathbb{R}I$
Γ_1	$\mathbb{R}I$	$\mathbb{R}I$
Γ_2	$\mathbb{C}I$	$\mathbb{C}I$
Γ_3	$\mathbb{C}I$	$\mathbb{C}I$
Γ_4	$\mathbb{C}III1$	$\mathbb{C}II$
Γ_5	$\mathbb{C}III1$	$\mathbb{C}II$
Γ_6	$\mathbb{C}III1$	$\mathbb{C}II$
Γ_7	$\mathbb{C}III1$	$\mathbb{C}II$

U_8^2	C_0	C_1	C_2	C_3	C_4	C_5
Γ_0	1	1	1	1	1	1
Γ_1	1	-1	1	1	-1	-1
Γ_2	1	1	-1	1	-1	1
Γ_3	1	-1	-1	1	1	-1
Γ_4	1	i	1	-1	i	$-i$
Γ_5	1	$-i$	1	-1	$-i$	i
Γ_6	1	i	-1	-1	$-i$	$-i$
Γ_7	1	$-i$	-1	-1	i	i

U_8^2	C_6	C_7	G_{16}^2	G_{16}^3	G_{16}^4	G_{16}^5
Γ_0	1	1	$\mathbb{R}I$	$\mathbb{R}I$	$\mathbb{R}I$	$\mathbb{R}I$
Γ_1	1	-1	$\mathbb{R}I$	$\mathbb{R}I$	$\mathbb{R}I$	$\mathbb{R}II$
Γ_2	-1	-1	$\mathbb{R}II$	$\mathbb{R}III$	$\mathbb{R}II$	$\mathbb{R}I$
Γ_3	-1	1	$\mathbb{R}II$	$\mathbb{R}III$	$\mathbb{R}II$	$\mathbb{R}II$
Γ_4	-1	$-i$	$\mathbb{C}III2$	$\mathbb{C}III2$	$\mathbb{C}I$	$\mathbb{C}III2$
Γ_5	-1	i	$\mathbb{C}III2$	$\mathbb{C}III2$	$\mathbb{C}I$	$\mathbb{C}III2$
Γ_6	1	i	$\mathbb{C}III2$	$\mathbb{C}I$	$\mathbb{C}II$	$\mathbb{C}III2$
Γ_7	1	$-i$	$\mathbb{C}III2$	$\mathbb{C}I$	$\mathbb{C}II$	$\mathbb{C}III2$

U_8^2	G_{16}^6	G_{16}^{10}	G_{16}^{11}	G_{16}^{12}	G_{16}^{13}
Γ_0	$\mathbb{R}I$	$\mathbb{R}I$	$\mathbb{R}I$	$\mathbb{R}I$	$\mathbb{R}I$
Γ_1	$\mathbb{R}II$	$\mathbb{R}I$	$\mathbb{R}I$	$\mathbb{R}I$	$\mathbb{R}I$
Γ_2	$\mathbb{R}I$	$\mathbb{R}I$	$\mathbb{R}I$	$\mathbb{R}I$	$\mathbb{R}I$
Γ_3	$\mathbb{R}II$	$\mathbb{R}I$	$\mathbb{R}I$	$\mathbb{R}I$	$\mathbb{R}I$
Γ_4	$\mathbb{C}III1$	$\mathbb{C}III2$	$\mathbb{C}I$	$\mathbb{C}II$	$\mathbb{C}III1$
Γ_5	$\mathbb{C}III1$	$\mathbb{C}III2$	$\mathbb{C}I$	$\mathbb{C}II$	$\mathbb{C}III1$
Γ_6	$\mathbb{C}III1$	$\mathbb{C}III2$	$\mathbb{C}I$	$\mathbb{C}II$	$\mathbb{C}III1$
Γ_7	$\mathbb{C}III1$	$\mathbb{C}III2$	$\mathbb{C}I$	$\mathbb{C}II$	$\mathbb{C}III1$

U_8^3	C_0	C_1	C_2	C_3	C_4	G_{16}^7
Γ_0	1	1	1	1	1	$\mathbb{R}I$
Γ_1	1	-1	1	1	-1	$\mathbb{R}III$
Γ_2	1	1	-1	1	-1	$\mathbb{R}III$
Γ_3	1	-1	-1	1	1	$\mathbb{R}I$
Γ_4	2	0	0	-2	0	$\mathbb{R}I$

U_8^3	G_{16}^8	G_{16}^{11}	G_{16}^{13}
Γ_0	$\mathbb{R}I$	$\mathbb{R}I$	$\mathbb{R}I$
Γ_1	$\mathbb{R}III$	$\mathbb{R}I$	$\mathbb{R}I$
Γ_2	$\mathbb{R}III$	$\mathbb{R}I$	$\mathbb{R}I$
Γ_3	$\mathbb{R}I$	$\mathbb{R}I$	$\mathbb{R}I$
Γ_4	$\mathbb{R}II$	$\mathbb{R}I$	$\mathbb{R}II$

U_8^4	C_0	C_1	C_2	C_3	C_4	G_{16}^8
Γ_0	1	1	1	1	1	$\mathbb{R}I$
Γ_1	1	-1	1	1	-1	$\mathbb{R}I$
Γ_2	1	1	-1	1	-1	$\mathbb{R}III$
Γ_3	1	-1	-1	1	1	$\mathbb{R}III$
Γ_4	2	0	0	-2	0	$\mathbb{H}I$

U_8^4	G_{16}^9	G_{16}^{12}	G_{16}^{13}
Γ_0	$\mathbb{R}I$	$\mathbb{R}I$	$\mathbb{R}I$
Γ_1	$\mathbb{R}I$	$\mathbb{R}I$	$\mathbb{R}I$
Γ_2	$\mathbb{R}III$	$\mathbb{R}I$	$\mathbb{R}I$
Γ_3	$\mathbb{R}III$	$\mathbb{R}I$	$\mathbb{R}I$
Γ_4	$\mathbb{H}II$	$\mathbb{H}II$	$\mathbb{H}I$

U_8^5	C_0	C_1	C_2	C_3	C_4	C_5
Γ_0	1	1	1	1	1	1
Γ_1	1	-1	1	1	-1	-1
Γ_2	1	1	-1	1	-1	1
Γ_3	1	-1	-1	1	1	-1
Γ_4	1	1	1	-1	1	-1
Γ_5	1	-1	1	-1	-1	1
Γ_6	1	1	-1	-1	-1	-1
Γ_7	1	-1	-1	-1	1	1

U_8^5	C_6	C_7	G_{16}^3	G_{16}^{10}	G_{16}^{11}	G_{16}^{14}
Γ_0	1	1	$\mathbb{R}I$	$\mathbb{R}I$	$\mathbb{R}I$	$\mathbb{R}I$
Γ_1	1	-1	$\mathbb{R}I$	$\mathbb{R}I$	$\mathbb{R}I$	$\mathbb{R}I$
Γ_2	-1	-1	$\mathbb{R}III$	$\mathbb{R}I$	$\mathbb{R}I$	$\mathbb{R}I$
Γ_3	-1	1	$\mathbb{R}III$	$\mathbb{R}I$	$\mathbb{R}I$	$\mathbb{R}I$
Γ_4	-1	-1	$\mathbb{R}II$	$\mathbb{R}II$	$\mathbb{R}III$	$\mathbb{R}I$
Γ_5	-1	1	$\mathbb{R}II$	$\mathbb{R}II$	$\mathbb{R}III$	$\mathbb{R}I$
Γ_6	1	1	$\mathbb{R}III$	$\mathbb{R}II$	$\mathbb{R}III$	$\mathbb{R}I$
Γ_7	1	-1	$\mathbb{R}III$	$\mathbb{R}II$	$\mathbb{R}III$	$\mathbb{R}I$

U_9^1	C_0	C_1	C_2	C_3	C_4	C_5
Γ_0	1	1	1	1	1	1
Γ_1	1	$E(3)$	1	$E(3)^2$	$E(3)$	1
Γ_2	1	$E(3)^2$	1	$E(3)$	$E(3)^2$	1
Γ_3	1	$-E(9)^4 - E(9)^7$	$E(3)$	$E(9)^2$	$E(9)^4$	$E(3)^2$
Γ_4	1	$E(9)^4$	$E(3)$	$-E(9)^2 - E(9)^5$	$E(9)^7$	$E(3)^2$
Γ_5	1	$E(9)^7$	$E(3)$	$E(9)^5$	$-E(9)^4 - E(9)^7$	$E(3)^2$
Γ_6	1	$E(9)^2$	$E(3)^2$	$E(9)^4$	$-E(9)^2 - E(9)^5$	$E(3)$
Γ_7	1	$E(9)^5$	$E(3)^2$	$-E(9)^4 - E(9)^7$	$E(9)^2$	$E(3)$
Γ_8	1	$-E(9)^2 - E(9)^5$	$E(3)^2$	$E(9)^7$	$E(9)^5$	$E(3)$

U_9^1	C_6	C_7	C_8	G_{18}^1	G_{18}^2
Γ_0	1	1	1	$\mathbb{R}I$	$\mathbb{R}I$
Γ_1	$E(3)^2$	$E(3)$	$E(3)^2$	$\mathbb{C}I$	$\mathbb{C}III2$
Γ_2	$E(3)$	$E(3)^2$	$E(3)$	$\mathbb{C}I$	$\mathbb{C}III2$
Γ_3	$E(9)^5$	$E(9)^7$	$-E(9)^2 - E(9)^5$	$\mathbb{C}I$	$\mathbb{C}III2$
Γ_4	$E(9)^2$	$-E(9)^4 - E(9)^7$	$E(9)^5$	$\mathbb{C}I$	$\mathbb{C}III2$
Γ_5	$-E(9)^2 - E(9)^5$	$E(9)^4$	$E(9)^2$	$\mathbb{C}I$	$\mathbb{C}III2$
Γ_6	$-E(9)^4 - E(9)^7$	$E(9)^5$	$E(9)^7$	$\mathbb{C}I$	$\mathbb{C}III2$
Γ_7	$E(9)^7$	$-E(9)^2 - E(9)^5$	$E(9)^4$	$\mathbb{C}I$	$\mathbb{C}III2$
Γ_8	$E(9)^4$	$E(9)^2$	$-E(9)^4 - E(9)^7$	$\mathbb{C}I$	$\mathbb{C}III2$

U_9^2	C_0	C_1	C_2	C_3	C_4	C_5
Γ_0	1	1	1	1	1	1
Γ_1	1	$E(3)$	1	$E(3)^2$	$E(3)$	1
Γ_2	1	$E(3)^2$	1	$E(3)$	$E(3)^2$	1
Γ_3	1	1	$E(3)$	1	$E(3)$	$E(3)^2$
Γ_4	1	$E(3)$	$E(3)$	$E(3)^2$	$E(3)^2$	$E(3)^2$
Γ_5	1	$E(3)^2$	$E(3)$	$E(3)$	1	$E(3)^2$
Γ_6	1	1	$E(3)^2$	1	$E(3)^2$	$E(3)$
Γ_7	1	$E(3)$	$E(3)^2$	$E(3)^2$	1	$E(3)$
Γ_8	1	$E(3)^2$	$E(3)^2$	$E(3)$	$E(3)$	$E(3)$

U_9^2	C_6	C_7	C_8	G_{18}^3	G_{18}^4	G_{18}^5
Γ_0	1	1	1	$\mathbb{R}I$	$\mathbb{R}I$	$\mathbb{R}I$
Γ_1	$E(3)^2$	$E(3)$	$E(3)^2$	$\mathbb{C}III2$	$\mathbb{C}I$	$\mathbb{C}III2$
Γ_2	$E(3)$	$E(3)^2$	$E(3)$	$\mathbb{C}III2$	$\mathbb{C}I$	$\mathbb{C}III2$
Γ_3	$E(3)$	$E(3)^2$	$E(3)^2$	$\mathbb{C}I$	$\mathbb{C}I$	$\mathbb{C}III2$
Γ_4	1	1	$E(3)$	$\mathbb{C}III1$	$\mathbb{C}I$	$\mathbb{C}III2$
Γ_5	$E(3)^2$	$E(3)$	1	$\mathbb{C}III1$	$\mathbb{C}I$	$\mathbb{C}III2$
Γ_6	$E(3)^2$	$E(3)$	$E(3)$	$\mathbb{C}I$	$\mathbb{C}I$	$\mathbb{C}III2$
Γ_7	$E(3)$	$E(3)^2$	1	$\mathbb{C}III1$	$\mathbb{C}I$	$\mathbb{C}III2$
Γ_8	1	1	$E(3)^2$	$\mathbb{C}III1$	$\mathbb{C}I$	$\mathbb{C}III2$

U_{10}^1	C_0	C_1	C_2	C_3	G_{20}^3	G_{20}^4
Γ_0	1	1	1	1	$\mathbb{R}I$	$\mathbb{R}I$
Γ_1	1	-1	1	1	$\mathbb{R}II$	$\mathbb{R}I$
Γ_2	2	0	$E(5)^2 + E(5)^3$	$E(5) + E(5)^4$	$\mathbb{R}III$	$\mathbb{R}I$
Γ_3	2	0	$E(5) + E(5)^4$	$E(5)^2 + E(5)^3$	$\mathbb{R}III$	$\mathbb{R}I$

U_{10}^2	C_0	C_1	C_2	C_3	C_4	C_5
Γ_0	1	1	1	1	1	1
Γ_1	1	-1	1	-1	1	-1
Γ_2	1	-1	$E(5)^4$	$-E(5)^4$	$E(5)^3$	$-E(5)^3$
Γ_3	1	-1	$E(5)^3$	$-E(5)^3$	$E(5)$	$-E(5)$
Γ_4	1	-1	$E(5)^2$	$-E(5)^2$	$E(5)^4$	$-E(5)^4$
Γ_5	1	-1	$E(5)$	$-E(5)$	$E(5)^2$	$-E(5)^2$
Γ_6	1	1	$E(5)^4$	$E(5)^4$	$E(5)^3$	$E(5)^3$
Γ_7	1	1	$E(5)^3$	$E(5)^3$	$E(5)$	$E(5)$
Γ_8	1	1	$E(5)^2$	$E(5)^2$	$E(5)^4$	$E(5)^4$
Γ_9	1	1	$E(5)$	$E(5)$	$E(5)^2$	$E(5)^2$

U_{10}^2	C_6	C_7	C_8	C_9	G_{20}^1	G_{20}^2
Γ_0	1	1	1	1	$\mathbb{R}I$	$\mathbb{R}I$
Γ_1	1	-1	1	-1	$\mathbb{R}II$	$\mathbb{R}II$
Γ_2	$E(5)^2$	$-E(5)^2$	$E(5)$	$-E(5)$	$\mathbb{C}II$	$\mathbb{C}III2$
Γ_3	$E(5)^4$	$-E(5)^4$	$E(5)^2$	$-E(5)^2$	$\mathbb{C}II$	$\mathbb{C}III2$
Γ_4	$E(5)$	$-E(5)$	$E(5)^3$	$-E(5)^3$	$\mathbb{C}II$	$\mathbb{C}III2$
Γ_5	$E(5)^3$	$-E(5)^3$	$E(5)^4$	$-E(5)^4$	$\mathbb{C}II$	$\mathbb{C}III2$
Γ_6	$E(5)^2$	$E(5)^2$	$E(5)$	$E(5)$	$\mathbb{C}I$	$\mathbb{C}III2$
Γ_7	$E(5)^4$	$E(5)^4$	$E(5)^2$	$E(5)^2$	$\mathbb{C}I$	$\mathbb{C}III2$
Γ_8	$E(5)$	$E(5)$	$E(5)^3$	$E(5)^3$	$\mathbb{C}I$	$\mathbb{C}III2$
Γ_9	$E(5)^3$	$E(5)^3$	$E(5)^4$	$E(5)^4$	$\mathbb{C}I$	$\mathbb{C}III2$

U_{10}^2	G_{20}^4	G_{20}^5
Γ_0	$\mathbb{R}I$	$\mathbb{R}I$
Γ_1	$\mathbb{R}I$	$\mathbb{R}I$
Γ_2	$\mathbb{C}I$	$\mathbb{C}III2$
Γ_3	$\mathbb{C}I$	$\mathbb{C}III2$
Γ_4	$\mathbb{C}I$	$\mathbb{C}III2$
Γ_5	$\mathbb{C}I$	$\mathbb{C}III2$
Γ_6	$\mathbb{C}I$	$\mathbb{C}III2$
Γ_7	$\mathbb{C}I$	$\mathbb{C}III2$
Γ_8	$\mathbb{C}I$	$\mathbb{C}III2$
Γ_9	$\mathbb{C}I$	$\mathbb{C}III2$

U_{11}^1	C_0	C_1	C_2	C_3	C_4	C_5
Γ_0	1	1	1	1	1	1
Γ_1	1	$E(11)$	$E(11)^2$	$E(11)^3$	$E(11)^4$	$E(11)^5$
Γ_2	1	$E(11)^2$	$E(11)^4$	$E(11)^6$	$E(11)^8$	$E(11)^{10}$
Γ_3	1	$E(11)^3$	$E(11)^6$	$E(11)^9$	$E(11)$	$E(11)^4$
Γ_4	1	$E(11)^4$	$E(11)^8$	$E(11)$	$E(11)^5$	$E(11)^9$
Γ_5	1	$E(11)^5$	$E(11)^{10}$	$E(11)^4$	$E(11)^9$	$E(11)^3$
Γ_6	1	$E(11)^6$	$E(11)$	$E(11)^7$	$E(11)^2$	$E(11)^8$
Γ_7	1	$E(11)^7$	$E(11)^3$	$E(11)^{10}$	$E(11)^6$	$E(11)^2$
Γ_8	1	$E(11)^8$	$E(11)^5$	$E(11)^2$	$E(11)^{10}$	$E(11)^7$
Γ_9	1	$E(11)^9$	$E(11)^7$	$E(11)^5$	$E(11)^3$	$E(11)$
Γ_{10}	1	$E(11)^{10}$	$E(11)^9$	$E(11)^8$	$E(11)^7$	$E(11)^6$

U_{11}^1	C_6	C_7	C_8	C_9	C_{10}	G_{22}^1
Γ_0	1	1	1	1	1	$\mathbb{R}I$
Γ_1	$E(11)^6$	$E(11)^7$	$E(11)^8$	$E(11)^9$	$E(11)^{10}$	$\mathbb{C}I$
Γ_2	$E(11)$	$E(11)^3$	$E(11)^5$	$E(11)^7$	$E(11)^9$	$\mathbb{C}I$
Γ_3	$E(11)^7$	$E(11)^{10}$	$E(11)^2$	$E(11)^5$	$E(11)^8$	$\mathbb{C}I$
Γ_4	$E(11)^2$	$E(11)^6$	$E(11)^{10}$	$E(11)^3$	$E(11)^7$	$\mathbb{C}I$
Γ_5	$E(11)^8$	$E(11)^2$	$E(11)^7$	$E(11)$	$E(11)^6$	$\mathbb{C}I$
Γ_6	$E(11)^3$	$E(11)^9$	$E(11)^4$	$E(11)^{10}$	$E(11)^5$	$\mathbb{C}I$
Γ_7	$E(11)^9$	$E(11)^5$	$E(11)$	$E(11)^8$	$E(11)^4$	$\mathbb{C}I$
Γ_8	$E(11)^4$	$E(11)$	$E(11)^9$	$E(11)^6$	$E(11)^3$	$\mathbb{C}I$
Γ_9	$E(11)^{10}$	$E(11)^8$	$E(11)^6$	$E(11)^4$	$E(11)^2$	$\mathbb{C}I$
Γ_{10}	$E(11)^5$	$E(11)^4$	$E(11)^3$	$E(11)^2$	$E(11)$	$\mathbb{C}I$

U_{11}^1	G_{22}^2
Γ_0	$\mathbb{R}I$
Γ_1	$\mathbb{C}III2$
Γ_2	$\mathbb{C}III2$
Γ_3	$\mathbb{C}III2$
Γ_4	$\mathbb{C}III2$
Γ_5	$\mathbb{C}III2$
Γ_6	$\mathbb{C}III2$
Γ_7	$\mathbb{C}III2$
Γ_8	$\mathbb{C}III2$
Γ_9	$\mathbb{C}III2$
Γ_{10}	$\mathbb{C}III2$

U_{12}^1	C_0	C_1	C_2	C_3	C_4	C_5
Γ_0	1	1	1	1	1	1
Γ_1	1	-1	1	1	-1	1
Γ_2	1	$-i$	-1	1	i	-1
Γ_3	1	i	-1	1	$-i$	-1
Γ_4	2	0	-2	-1	0	1
Γ_5	2	0	2	-1	0	-1

U_{12}^1	G_{24}^4	G_{24}^5	G_{24}^7	G_{24}^8
Γ_0	$\mathbb{R}I$	$\mathbb{R}I$	$\mathbb{R}I$	$\mathbb{R}I$
Γ_1	$\mathbb{R}I$	$\mathbb{R}I$	$\mathbb{R}I$	$\mathbb{R}I$
Γ_2	$\mathbb{C}II$	$\mathbb{C}III2$	$\mathbb{C}III2$	$\mathbb{C}I$
Γ_3	$\mathbb{C}II$	$\mathbb{C}III2$	$\mathbb{C}III2$	$\mathbb{C}I$
Γ_4	$\mathbb{H}II$	$\mathbb{H}I$	$\mathbb{H}II$	$\mathbb{H}I$
Γ_5	$\mathbb{R}I$	$\mathbb{R}I$	$\mathbb{R}I$	$\mathbb{R}I$

U_{12}^2	C_0	C_1	C_2	C_3	C_4	C_5
Γ_0	1	1	1	1	1	1
Γ_1	1	-1	1	1	-1	-1
Γ_2	1	-1	$E(3)^2$	1	$-E(3)^2$	-1
Γ_3	1	-1	$E(3)$	1	$-E(3)$	-1
Γ_4	1	1	$E(3)^2$	1	$E(3)^2$	1
Γ_5	1	1	$E(3)$	1	$E(3)$	1
Γ_6	1	$-i$	1	-1	$-i$	i
Γ_7	1	i	1	-1	i	$-i$
Γ_8	1	$-i$	$E(3)^2$	-1	$-E(12)^{11}$	i
Γ_9	1	$-i$	$E(3)$	-1	$-E(12)^7$	i
Γ_{10}	1	i	$E(3)^2$	-1	$E(12)^{11}$	$-i$
Γ_{11}	1	i	$E(3)$	-1	$E(12)^7$	$-i$

U_{12}^2	C_6	C_7	C_8	C_9	C_{10}	C_{11}
Γ_0	1	1	1	1	1	1
Γ_1	1	1	-1	-1	1	-1
Γ_2	$E(3)$	$E(3)^2$	$-E(3)$	$-E(3)^2$	$E(3)$	$-E(3)$
Γ_3	$E(3)^2$	$E(3)$	$-E(3)^2$	$-E(3)$	$E(3)^2$	$-E(3)^2$
Γ_4	$E(3)$	$E(3)^2$	$E(3)$	$E(3)^2$	$E(3)$	$E(3)$
Γ_5	$E(3)^2$	$E(3)$	$E(3)^2$	$E(3)$	$E(3)^2$	$E(3)^2$
Γ_6	1	-1	$-i$	i	-1	i
Γ_7	1	-1	i	$-i$	-1	$-i$
Γ_8	$E(3)$	$-E(3)^2$	$-E(12)^7$	$E(12)^{11}$	$-E(3)$	$E(12)^7$
Γ_9	$E(3)^2$	$-E(3)$	$-E(12)^{11}$	$E(12)^7$	$-E(3)^2$	$E(12)^{11}$
Γ_{10}	$E(3)$	$-E(3)^2$	$E(12)^7$	$-E(12)^{11}$	$-E(3)$	$-E(12)^7$
Γ_{11}	$E(3)^2$	$-E(3)$	$E(12)^{11}$	$-E(12)^7$	$-E(3)^2$	$-E(12)^{11}$

U_{12}^2	G_{24}^1	G_{24}^2	G_{24}^4	G_{24}^5	G_{24}^6	G_{24}^9
Γ_0	$\mathbb{R}I$	$\mathbb{R}I$	$\mathbb{R}I$	$\mathbb{R}I$	$\mathbb{R}I$	$\mathbb{R}I$
Γ_1	$\mathbb{R}II$	$\mathbb{R}II$	$\mathbb{R}I$	$\mathbb{R}I$	$\mathbb{R}I$	$\mathbb{R}I$
Γ_2	$\mathbb{C}II$	$\mathbb{C}III2$	$\mathbb{C}I$	$\mathbb{C}I$	$\mathbb{C}I$	$\mathbb{C}III2$
Γ_3	$\mathbb{C}II$	$\mathbb{C}III2$	$\mathbb{C}I$	$\mathbb{C}I$	$\mathbb{C}I$	$\mathbb{C}III2$
Γ_4	$\mathbb{C}I$	$\mathbb{C}III2$	$\mathbb{C}I$	$\mathbb{C}I$	$\mathbb{C}I$	$\mathbb{C}III2$
Γ_5	$\mathbb{C}I$	$\mathbb{C}III2$	$\mathbb{C}I$	$\mathbb{C}I$	$\mathbb{C}I$	$\mathbb{C}III2$
Γ_6	$\mathbb{C}III2$	$\mathbb{C}III2$	$\mathbb{C}II$	$\mathbb{C}III2$	$\mathbb{C}I$	$\mathbb{C}III2$
Γ_7	$\mathbb{C}III2$	$\mathbb{C}III2$	$\mathbb{C}II$	$\mathbb{C}III2$	$\mathbb{C}I$	$\mathbb{C}III2$
Γ_8	$\mathbb{C}III1$	$\mathbb{C}III2$	$\mathbb{C}II$	$\mathbb{C}III1$	$\mathbb{C}I$	$\mathbb{C}III2$
Γ_9	$\mathbb{C}III1$	$\mathbb{C}III2$	$\mathbb{C}II$	$\mathbb{C}III1$	$\mathbb{C}I$	$\mathbb{C}III2$
Γ_{10}	$\mathbb{C}III1$	$\mathbb{C}III2$	$\mathbb{C}II$	$\mathbb{C}III1$	$\mathbb{C}I$	$\mathbb{C}III2$
Γ_{11}	$\mathbb{C}III1$	$\mathbb{C}III2$	$\mathbb{C}II$	$\mathbb{C}III1$	$\mathbb{C}I$	$\mathbb{C}III2$

U_{12}^2	G_{24}^{10}	G_{24}^{11}
Γ_0	$\mathbb{R}I$	$\mathbb{R}I$
Γ_1	$\mathbb{R}I$	$\mathbb{R}I$
Γ_2	$\mathbb{C}III2$	$\mathbb{C}III2$
Γ_3	$\mathbb{C}III2$	$\mathbb{C}III2$
Γ_4	$\mathbb{C}III2$	$\mathbb{C}III2$
Γ_5	$\mathbb{C}III2$	$\mathbb{C}III2$
Γ_6	$\mathbb{C}I$	$\mathbb{C}II$
Γ_7	$\mathbb{C}I$	$\mathbb{C}II$
Γ_8	$\mathbb{C}III1$	$\mathbb{C}III1$
Γ_9	$\mathbb{C}III1$	$\mathbb{C}III1$
Γ_{10}	$\mathbb{C}III1$	$\mathbb{C}III1$
Γ_{11}	$\mathbb{C}III1$	$\mathbb{C}III1$

U_{12}^3	C_0	C_1	C_2	C_3	G_{24}^{12}	G_{24}^{13}
Γ_0	1	1	1	1	$\mathbb{R}I$	$\mathbb{R}I$
Γ_1	1	$E(3)^2$	1	$E(3)$	$\mathbb{C}I$	$\mathbb{C}III2$
Γ_2	1	$E(3)$	1	$E(3)^2$	$\mathbb{C}I$	$\mathbb{C}III2$
Γ_3	3	0	-1	0	$\mathbb{R}I$	$\mathbb{R}I$

U_{12}^4	C_0	C_1	C_2	C_3	C_4	C_5
Γ_0	1	1	1	1	1	1
Γ_1	1	-1	-1	1	1	-1
Γ_2	1	-1	1	1	-1	1
Γ_3	1	1	-1	1	-1	-1
Γ_4	2	0	-2	-1	0	1
Γ_5	2	0	2	-1	0	-1

U_{12}^4	G_{24}^5	G_{24}^6	G_{24}^8	G_{24}^{14}
Γ_0	$\mathbb{R}I$	$\mathbb{R}I$	$\mathbb{R}I$	$\mathbb{R}I$
Γ_1	$\mathbb{R}II$	$\mathbb{R}III$	$\mathbb{R}III$	$\mathbb{R}I$
Γ_2	$\mathbb{R}I$	$\mathbb{R}I$	$\mathbb{R}I$	$\mathbb{R}I$
Γ_3	$\mathbb{R}II$	$\mathbb{R}III$	$\mathbb{R}III$	$\mathbb{R}I$
Γ_4	$\mathbb{R}II$	$\mathbb{R}I$	$\mathbb{R}II$	$\mathbb{R}I$
Γ_5	$\mathbb{R}I$	$\mathbb{R}I$	$\mathbb{R}I$	$\mathbb{R}I$

U_{12}^5	C_0	C_1	C_2	C_3	C_4	C_5
Γ_0	1	1	1	1	1	1
Γ_1	1	-1	-1	1	1	-1
Γ_2	1	-1	1	1	-1	-1
Γ_3	1	1	-1	1	-1	1
Γ_4	1	-1	-1	$E(3)^2$	1	$-E(3)^2$
Γ_5	1	-1	-1	$E(3)$	1	$-E(3)$
Γ_6	1	-1	1	$E(3)^2$	-1	$-E(3)^2$
Γ_7	1	-1	1	$E(3)$	-1	$-E(3)$
Γ_8	1	1	-1	$E(3)^2$	-1	$E(3)^2$
Γ_9	1	1	-1	$E(3)$	-1	$E(3)$
Γ_{10}	1	1	1	$E(3)^2$	1	$E(3)^2$
Γ_{11}	1	1	1	$E(3)$	1	$E(3)$

U_{12}^5	C_6	C_7	C_8	C_9	C_{10}	C_{11}
Γ_0	1	1	1	1	1	1
Γ_1	-1	1	1	-1	-1	1
Γ_2	1	1	-1	-1	1	-1
Γ_3	-1	1	-1	1	-1	-1
Γ_4	$-E(3)^2$	$E(3)$	$E(3)^2$	$-E(3)$	$-E(3)$	$E(3)$
Γ_5	$-E(3)$	$E(3)^2$	$E(3)$	$-E(3)^2$	$-E(3)^2$	$E(3)^2$
Γ_6	$E(3)^2$	$E(3)$	$-E(3)^2$	$-E(3)$	$E(3)$	$-E(3)$
Γ_7	$E(3)$	$E(3)^2$	$-E(3)$	$-E(3)^2$	$E(3)^2$	$-E(3)^2$
Γ_8	$-E(3)^2$	$E(3)$	$-E(3)^2$	$E(3)$	$-E(3)$	$-E(3)$
Γ_9	$-E(3)$	$E(3)^2$	$-E(3)$	$E(3)^2$	$-E(3)^2$	$-E(3)^2$
Γ_{10}	$E(3)^2$	$E(3)$	$E(3)^2$	$E(3)$	$E(3)$	$E(3)$
Γ_{11}	$E(3)$	$E(3)^2$	$E(3)$	$E(3)^2$	$E(3)^2$	$E(3)^2$

U_{12}^5	G_{24}^7	G_{24}^8	G_{24}^9	G_{24}^{10}	G_{24}^{14}	G_{24}^{15}
Γ_0	$\mathbb{R}I$	$\mathbb{R}I$	$\mathbb{R}I$	$\mathbb{R}I$	$\mathbb{R}I$	$\mathbb{R}I$
Γ_1	$\mathbb{R}II$	$\mathbb{R}III$	$\mathbb{R}II$	$\mathbb{R}III$	$\mathbb{R}I$	$\mathbb{R}I$
Γ_2	$\mathbb{R}I$	$\mathbb{R}I$	$\mathbb{R}I$	$\mathbb{R}I$	$\mathbb{R}I$	$\mathbb{R}I$
Γ_3	$\mathbb{R}II$	$\mathbb{R}III$	$\mathbb{R}II$	$\mathbb{R}III$	$\mathbb{R}I$	$\mathbb{R}I$
Γ_4	$\mathbb{C}II$	$\mathbb{C}III1$	$\mathbb{C}III2$	$\mathbb{C}III1$	$\mathbb{C}I$	$\mathbb{C}III2$
Γ_5	$\mathbb{C}II$	$\mathbb{C}III1$	$\mathbb{C}III2$	$\mathbb{C}III1$	$\mathbb{C}I$	$\mathbb{C}III2$
Γ_6	$\mathbb{C}I$	$\mathbb{C}I$	$\mathbb{C}III2$	$\mathbb{C}III2$	$\mathbb{C}I$	$\mathbb{C}III2$
Γ_7	$\mathbb{C}I$	$\mathbb{C}I$	$\mathbb{C}III2$	$\mathbb{C}III2$	$\mathbb{C}I$	$\mathbb{C}III2$
Γ_8	$\mathbb{C}II$	$\mathbb{C}III1$	$\mathbb{C}III2$	$\mathbb{C}III1$	$\mathbb{C}I$	$\mathbb{C}III2$
Γ_9	$\mathbb{C}II$	$\mathbb{C}III1$	$\mathbb{C}III2$	$\mathbb{C}III1$	$\mathbb{C}I$	$\mathbb{C}III2$
Γ_{10}	$\mathbb{C}I$	$\mathbb{C}I$	$\mathbb{C}III2$	$\mathbb{C}III2$	$\mathbb{C}I$	$\mathbb{C}III2$
Γ_{11}	$\mathbb{C}I$	$\mathbb{C}I$	$\mathbb{C}III2$	$\mathbb{C}III2$	$\mathbb{C}I$	$\mathbb{C}III2$

U_{13}^1	C_0	C_1	C_2	C_3	C_4	C_5
Γ_0	1	1	1	1	1	1
Γ_1	1	$E(13)$	$E(13)^2$	$E(13)^3$	$E(13)^4$	$E(13)^5$
Γ_2	1	$E(13)^2$	$E(13)^4$	$E(13)^6$	$E(13)^8$	$E(13)^{10}$
Γ_3	1	$E(13)^3$	$E(13)^6$	$E(13)^9$	$E(13)^{12}$	$E(13)^2$
Γ_4	1	$E(13)^4$	$E(13)^8$	$E(13)^{12}$	$E(13)^3$	$E(13)^7$
Γ_5	1	$E(13)^5$	$E(13)^{10}$	$E(13)^2$	$E(13)^7$	$E(13)^{12}$
Γ_6	1	$E(13)^6$	$E(13)^{12}$	$E(13)^5$	$E(13)^{11}$	$E(13)^4$
Γ_7	1	$E(13)^7$	$E(13)$	$E(13)^8$	$E(13)^2$	$E(13)^9$
Γ_8	1	$E(13)^8$	$E(13)^3$	$E(13)^{11}$	$E(13)^6$	$E(13)$
Γ_9	1	$E(13)^9$	$E(13)^5$	$E(13)$	$E(13)^{10}$	$E(13)^6$
Γ_{10}	1	$E(13)^{10}$	$E(13)^7$	$E(13)^4$	$E(13)$	$E(13)^{11}$
Γ_{11}	1	$E(13)^{11}$	$E(13)^9$	$E(13)^7$	$E(13)^5$	$E(13)^3$
Γ_{12}	1	$E(13)^{12}$	$E(13)^{11}$	$E(13)^{10}$	$E(13)^9$	$E(13)^8$

U_{13}^1	C_6	C_7	C_8	C_9	C_{10}	C_{11}
Γ_0	1	1	1	1	1	1
Γ_1	$E(13)^6$	$E(13)^7$	$E(13)^8$	$E(13)^9$	$E(13)^{10}$	$E(13)^{11}$
Γ_2	$E(13)^{12}$	$E(13)$	$E(13)^3$	$E(13)^5$	$E(13)^7$	$E(13)^9$
Γ_3	$E(13)^5$	$E(13)^8$	$E(13)^{11}$	$E(13)$	$E(13)^4$	$E(13)^7$
Γ_4	$E(13)^{11}$	$E(13)^2$	$E(13)^6$	$E(13)^{10}$	$E(13)$	$E(13)^5$
Γ_5	$E(13)^4$	$E(13)^9$	$E(13)$	$E(13)^6$	$E(13)^{11}$	$E(13)^3$
Γ_6	$E(13)^{10}$	$E(13)^3$	$E(13)^9$	$E(13)^2$	$E(13)^8$	$E(13)$
Γ_7	$E(13)^3$	$E(13)^{10}$	$E(13)^4$	$E(13)^{11}$	$E(13)^5$	$E(13)^{12}$
Γ_8	$E(13)^9$	$E(13)^4$	$E(13)^{12}$	$E(13)^7$	$E(13)^2$	$E(13)^{10}$
Γ_9	$E(13)^2$	$E(13)^{11}$	$E(13)^7$	$E(13)^3$	$E(13)^{12}$	$E(13)^8$
Γ_{10}	$E(13)^8$	$E(13)^5$	$E(13)^2$	$E(13)^{12}$	$E(13)^9$	$E(13)^6$
Γ_{11}	$E(13)$	$E(13)^{12}$	$E(13)^{10}$	$E(13)^8$	$E(13)^6$	$E(13)^4$
Γ_{12}	$E(13)^7$	$E(13)^6$	$E(13)^5$	$E(13)^4$	$E(13)^3$	$E(13)^2$

U_{13}^1	C_{12}	G_{26}^1	G_{26}^2
Γ_0	1	$\mathbb{R}I$	$\mathbb{R}I$
Γ_1	$E(13)^{12}$	$\mathbb{C}I$	$\mathbb{C}III2$
Γ_2	$E(13)^{11}$	$\mathbb{C}I$	$\mathbb{C}III2$
Γ_3	$E(13)^{10}$	$\mathbb{C}I$	$\mathbb{C}III2$
Γ_4	$E(13)^{9}$	$\mathbb{C}I$	$\mathbb{C}III2$
Γ_5	$E(13)^{8}$	$\mathbb{C}I$	$\mathbb{C}III2$
Γ_6	$E(13)^{7}$	$\mathbb{C}I$	$\mathbb{C}III2$
Γ_7	$E(13)^{6}$	$\mathbb{C}I$	$\mathbb{C}III2$
Γ_8	$E(13)^{5}$	$\mathbb{C}I$	$\mathbb{C}III2$
Γ_9	$E(13)^{4}$	$\mathbb{C}I$	$\mathbb{C}III2$
Γ_{10}	$E(13)^{3}$	$\mathbb{C}I$	$\mathbb{C}III2$
Γ_{11}	$E(13)^{2}$	$\mathbb{C}I$	$\mathbb{C}III2$
Γ_{12}	$E(13)$	$\mathbb{C}I$	$\mathbb{C}III2$

U_{14}^1	C_0	C_1	C_2	C_3	C_4	G_{28}^3
Γ_0	1	1	1	1	1	$\mathbb{R}I$
Γ_1	1	-1	1	1	1	$\mathbb{R}I$
Γ_2	2	0	$E(7)+E(7)^6$	$E(7)^2+E(7)^5$	$E(7)^3+E(7)^4$	$\mathbb{R}I$
Γ_3	2	0	$E(7)^2+E(7)^5$	$E(7)^3+E(7)^4$	$E(7)+E(7)^6$	$\mathbb{R}I$
Γ_4	2	0	$E(7)^3+E(7)^4$	$E(7)+E(7)^6$	$E(7)^2+E(7)^5$	$\mathbb{R}I$

U_{14}^2	C_0	C_1	C_2	C_3	C_4	C_5
Γ_0	1	1	1	1	1	1
Γ_1	1	-1	1	-1	1	-1
Γ_2	1	-1	$E(7)^6$	$-E(7)^6$	$E(7)^5$	$-E(7)^5$
Γ_3	1	-1	$E(7)^5$	$-E(7)^5$	$E(7)^3$	$-E(7)^3$
Γ_4	1	-1	$E(7)^4$	$-E(7)^4$	$E(7)$	$-E(7)$
Γ_5	1	-1	$E(7)^3$	$-E(7)^3$	$E(7)^6$	$-E(7)^6$
Γ_6	1	-1	$E(7)^2$	$-E(7)^2$	$E(7)^4$	$-E(7)^4$
Γ_7	1	-1	$E(7)$	$-E(7)$	$E(7)^2$	$-E(7)^2$
Γ_8	1	1	$E(7)^6$	$E(7)^6$	$E(7)^5$	$E(7)^5$
Γ_9	1	1	$E(7)^5$	$E(7)^5$	$E(7)^3$	$E(7)^3$
Γ_{10}	1	1	$E(7)^4$	$E(7)^4$	$E(7)$	$E(7)$
Γ_{11}	1	1	$E(7)^3$	$E(7)^3$	$E(7)^6$	$E(7)^6$
Γ_{12}	1	1	$E(7)^2$	$E(7)^2$	$E(7)^4$	$E(7)^4$
Γ_{13}	1	1	$E(7)$	$E(7)$	$E(7)^2$	$E(7)^2$

U_{14}^2	C_6	C_7	C_8	C_9	C_{10}	C_{11}
Γ_0	1	1	1	1	1	1
Γ_1	1	-1	1	-1	1	-1
Γ_2	$E(7)^4$	$-E(7)^4$	$E(7)^3$	$-E(7)^3$	$E(7)^2$	$-E(7)^2$
Γ_3	$E(7)$	$-E(7)$	$E(7)^6$	$-E(7)^6$	$E(7)^4$	$-E(7)^4$
Γ_4	$E(7)^5$	$-E(7)^5$	$E(7)^2$	$-E(7)^2$	$E(7)^6$	$-E(7)^6$
Γ_5	$E(7)^2$	$-E(7)^2$	$E(7)^5$	$-E(7)^5$	$E(7)$	$-E(7)$
Γ_6	$E(7)^6$	$-E(7)^6$	$E(7)$	$-E(7)$	$E(7)^3$	$-E(7)^3$
Γ_7	$E(7)^3$	$-E(7)^3$	$E(7)^4$	$-E(7)^4$	$E(7)^5$	$-E(7)^5$
Γ_8	$E(7)^4$	$E(7)^4$	$E(7)^3$	$E(7)^3$	$E(7)^2$	$E(7)^2$
Γ_9	$E(7)$	$E(7)$	$E(7)^6$	$E(7)^6$	$E(7)^4$	$E(7)^4$
Γ_{10}	$E(7)^5$	$E(7)^5$	$E(7)^2$	$E(7)^2$	$E(7)^6$	$E(7)^6$
Γ_{11}	$E(7)^2$	$E(7)^2$	$E(7)^5$	$E(7)^5$	$E(7)$	$E(7)$
Γ_{12}	$E(7)^6$	$E(7)^6$	$E(7)$	$E(7)$	$E(7)^3$	$E(7)^3$
Γ_{13}	$E(7)^3$	$E(7)^3$	$E(7)^4$	$E(7)^4$	$E(7)^5$	$E(7)^5$

U_{14}^2	C_{12}	C_{13}	G_{28}^1	G_{28}^2	G_{28}^3	G_{28}^4
Γ_0	1	1	$\mathbb{R}I$	$\mathbb{R}I$	$\mathbb{R}I$	$\mathbb{R}I$
Γ_1	1	-1	$\mathbb{R}II$	$\mathbb{R}II$	$\mathbb{R}I$	$\mathbb{R}I$
Γ_2	$E(7)$	$-E(7)$	$\mathbb{C}II$	$\mathbb{C}III2$	$\mathbb{C}I$	$\mathbb{C}III2$
Γ_3	$E(7)^2$	$-E(7)^2$	$\mathbb{C}II$	$\mathbb{C}III2$	$\mathbb{C}I$	$\mathbb{C}III2$
Γ_4	$E(7)^3$	$-E(7)^3$	$\mathbb{C}II$	$\mathbb{C}III2$	$\mathbb{C}I$	$\mathbb{C}III2$
Γ_5	$E(7)^4$	$-E(7)^4$	$\mathbb{C}II$	$\mathbb{C}III2$	$\mathbb{C}I$	$\mathbb{C}III2$
Γ_6	$E(7)^5$	$-E(7)^5$	$\mathbb{C}II$	$\mathbb{C}III2$	$\mathbb{C}I$	$\mathbb{C}III2$
Γ_7	$E(7)^6$	$-E(7)^6$	$\mathbb{C}II$	$\mathbb{C}III2$	$\mathbb{C}I$	$\mathbb{C}III2$
Γ_8	$E(7)$	$E(7)$	$\mathbb{C}I$	$\mathbb{C}III2$	$\mathbb{C}I$	$\mathbb{C}III2$
Γ_9	$E(7)^2$	$E(7)^2$	$\mathbb{C}I$	$\mathbb{C}III2$	$\mathbb{C}I$	$\mathbb{C}III2$
Γ_{10}	$E(7)^3$	$E(7)^3$	$\mathbb{C}I$	$\mathbb{C}III2$	$\mathbb{C}I$	$\mathbb{C}III2$
Γ_{11}	$E(7)^4$	$E(7)^4$	$\mathbb{C}I$	$\mathbb{C}III2$	$\mathbb{C}I$	$\mathbb{C}III2$
Γ_{12}	$E(7)^5$	$E(7)^5$	$\mathbb{C}I$	$\mathbb{C}III2$	$\mathbb{C}I$	$\mathbb{C}III2$
Γ_{13}	$E(7)^6$	$E(7)^6$	$\mathbb{C}I$	$\mathbb{C}III2$	$\mathbb{C}I$	$\mathbb{C}III2$

U_{15}^1	C_0	C_1	C_2	C_3	C_4	C_5
Γ_0	1	1	1	1	1	1
Γ_1	1	1	$E(5)^4$	1	$E(5)^4$	$E(5)^3$
Γ_2	1	1	$E(5)^3$	1	$E(5)^3$	$E(5)$
Γ_3	1	1	$E(5)^2$	1	$E(5)^2$	$E(5)^4$
Γ_4	1	1	$E(5)$	1	$E(5)$	$E(5)^2$
Γ_5	1	$E(3)^2$	1	$E(3)$	$E(3)^2$	1
Γ_6	1	$E(3)$	1	$E(3)^2$	$E(3)$	1
Γ_7	1	$E(3)^2$	$E(5)^4$	$E(3)$	$E(15)^7$	$E(5)^3$
Γ_8	1	$E(3)^2$	$E(5)^3$	$E(3)$	$E(15)^4$	$E(5)$
Γ_9	1	$E(3)^2$	$E(5)^2$	$E(3)$	$E(15)$	$E(5)^4$
Γ_{10}	1	$E(3)^2$	$E(5)$	$E(3)$	$E(15)^{13}$	$E(5)^2$
Γ_{11}	1	$E(3)$	$E(5)^4$	$E(3)^2$	$E(15)^2$	$E(5)^3$
Γ_{12}	1	$E(3)$	$E(5)^3$	$E(3)^2$	$E(15)^{14}$	$E(5)$
Γ_{13}	1	$E(3)$	$E(5)^2$	$E(3)^2$	$E(15)^{11}$	$E(5)^4$
Γ_{14}	1	$E(3)$	$E(5)$	$E(3)^2$	$E(15)^8$	$E(5)^2$

U_{15}^1	C_6	C_7	C_8	C_9	C_{10}	C_{11}
Γ_0	1	1	1	1	1	1
Γ_1	$E(5)^4$	$E(5)^3$	$E(5)^2$	$E(5)^3$	$E(5)^2$	$E(5)$
Γ_2	$E(5)^3$	$E(5)$	$E(5)^4$	$E(5)$	$E(5)^4$	$E(5)^2$
Γ_3	$E(5)^2$	$E(5)^4$	$E(5)$	$E(5)^4$	$E(5)$	$E(5)^3$
Γ_4	$E(5)$	$E(5)^2$	$E(5)^3$	$E(5)^2$	$E(5)^3$	$E(5)^4$
Γ_5	$E(3)$	$E(3)^2$	1	$E(3)$	$E(3)^2$	1
Γ_6	$E(3)^2$	$E(3)$	1	$E(3)^2$	$E(3)$	1
Γ_7	$E(15)^2$	$E(15)^4$	$E(5)^2$	$E(15)^{14}$	$E(15)$	$E(5)$
Γ_8	$E(15)^{14}$	$E(15)^{13}$	$E(5)^4$	$E(15)^8$	$E(15)^7$	$E(5)^2$
Γ_9	$E(15)^{11}$	$E(15)^7$	$E(5)$	$E(15)^2$	$E(15)^{13}$	$E(5)^3$
Γ_{10}	$E(15)^8$	$E(15)$	$E(5)^3$	$E(15)^{11}$	$E(15)^4$	$E(5)^4$
Γ_{11}	$E(15)^7$	$E(15)^{14}$	$E(5)^2$	$E(15)^4$	$E(15)^{11}$	$E(5)$
Γ_{12}	$E(15)^4$	$E(15)^8$	$E(5)^4$	$E(15)^{13}$	$E(15)^2$	$E(5)^2$
Γ_{13}	$E(15)$	$E(15)^2$	$E(5)$	$E(15)^7$	$E(15)^8$	$E(5)^3$
Γ_{14}	$E(15)^{13}$	$E(15)^{11}$	$E(5)^3$	$E(15)$	$E(15)^{14}$	$E(5)^4$

U_{15}^1	C_{12}	C_{13}	C_{14}	G_{30}^1	G_{30}^2	G_{30}^3
Γ_0	1	1	1	$\mathbb{R}I$	$\mathbb{R}I$	$\mathbb{R}I$
Γ_1	$E(5)^2$	$E(5)$	$E(5)$	$\mathbb{C}III2$	$\mathbb{C}I$	$\mathbb{C}I$
Γ_2	$E(5)^4$	$E(5)^2$	$E(5)^2$	$\mathbb{C}III2$	$\mathbb{C}I$	$\mathbb{C}I$
Γ_3	$E(5)$	$E(5)^3$	$E(5)^3$	$\mathbb{C}III2$	$\mathbb{C}I$	$\mathbb{C}I$
Γ_4	$E(5)^3$	$E(5)^4$	$E(5)^4$	$\mathbb{C}III2$	$\mathbb{C}I$	$\mathbb{C}I$
Γ_5	$E(3)$	$E(3)^2$	$E(3)$	$\mathbb{C}I$	$\mathbb{C}III2$	$\mathbb{C}I$
Γ_6	$E(3)^2$	$E(3)$	$E(3)^2$	$\mathbb{C}I$	$\mathbb{C}III2$	$\mathbb{C}I$
Γ_7	$E(15)^{11}$	$E(15)^{13}$	$E(15)^8$	$\mathbb{C}III1$	$\mathbb{C}III1$	$\mathbb{C}I$
Γ_8	$E(15)^2$	$E(15)$	$E(15)^{11}$	$\mathbb{C}III1$	$\mathbb{C}III1$	$\mathbb{C}I$
Γ_9	$E(15)^8$	$E(15)^4$	$E(15)^{14}$	$\mathbb{C}III1$	$\mathbb{C}III1$	$\mathbb{C}I$
Γ_{10}	$E(15)^{14}$	$E(15)^7$	$E(15)^2$	$\mathbb{C}III1$	$\mathbb{C}III1$	$\mathbb{C}I$
Γ_{11}	$E(15)$	$E(15)^8$	$E(15)^{13}$	$\mathbb{C}III1$	$\mathbb{C}III1$	$\mathbb{C}I$
Γ_{12}	$E(15)^7$	$E(15)^{11}$	$E(15)$	$\mathbb{C}III1$	$\mathbb{C}III1$	$\mathbb{C}I$
Γ_{13}	$E(15)^{13}$	$E(15)^{14}$	$E(15)^4$	$\mathbb{C}III1$	$\mathbb{C}III1$	$\mathbb{C}I$
Γ_{14}	$E(15)^4$	$E(15)^2$	$E(15)^7$	$\mathbb{C}III1$	$\mathbb{C}III1$	$\mathbb{C}I$

U_{15}^1	G_{30}^4
Γ_0	$\mathbb{R}I$
Γ_1	$\mathbb{C}III2$
Γ_2	$\mathbb{C}III2$
Γ_3	$\mathbb{C}III2$
Γ_4	$\mathbb{C}III2$
Γ_5	$\mathbb{C}III2$
Γ_6	$\mathbb{C}III2$
Γ_7	$\mathbb{C}III2$
Γ_8	$\mathbb{C}III2$
Γ_9	$\mathbb{C}III2$
Γ_{10}	$\mathbb{C}III2$
Γ_{11}	$\mathbb{C}III2$
Γ_{12}	$\mathbb{C}III2$
Γ_{13}	$\mathbb{C}III2$
Γ_{14}	$\mathbb{C}III2$

E.2 Classification of the Small $Z_2 \times Z_2$-Graded Groups by the Altland-Zirnbauer Tenfold Way

U_1^1	C_0	$G_4^2(1,1,1)$
Γ_0	1	BDI

U_2^1	C_0	C_1	$G_8^2(2,1,1)$	$G_8^2(1,2,1)$	$G_8^3(2,1,2)$	$G_8^3(2,2,1)$
Γ_0	1	1	BDI	BDI	BDI	BDI
Γ_1	1	-1	CI	DIII	CI	BDI

U_2^1	$G_8^4(1,1,1)$	$G_8^5(2,2,2)$
Γ_0	BDI	BDI
Γ_1	CII	BDI

U_3^1	C_0	C_1	C_2	$G_{12}^4(1,1,2)$	$G_{12}^4(1,2,1)$	$G_{12}^4(2,1,1)$
Γ_0	1	1	1	BDI	BDI	BDI
Γ_1	1	$E(3)$	$E(3)^2$	BDI	AI	D
Γ_2	1	$E(3)^2$	$E(3)$	BDI	AI	D

U_3^1	$G_{12}^5(2,2,2)$
Γ_0	BDI
Γ_1	AIII
Γ_2	AIII

U_4^1	C_0	C_1	C_2	C_3	$G_{16}^5(2,1,1)$	$G_{16}^5(1,2,1)$
Γ_0	1	1	1	1	BDI	BDI
Γ_1	1	-1	1	-1	CI	DIII
Γ_2	1	i	-1	$-i$	AIII	AIII
Γ_3	1	$-i$	-1	i	AIII	AIII

U_4^1	$G_{16}^6(2,1,1)$	$G_{16}^6(1,2,1)$	$G_{16}^7(3,1,3)$	$G_{16}^7(3,3,1)$	$G_{16}^8(3,1,4)$	$G_{16}^8(3,4,1)$
Γ_0	BDI	BDI	BDI	BDI	BDI	BDI
Γ_1	CI	DIII	CI	BDI	CI	BDI
Γ_2	AIII	AIII	AI	BDI	AI	CI
Γ_3	AIII	AIII	AI	BDI	AI	CI

U_4^1	$G_{16}^8(4,3,1)$	$G_{16}^9(4,1,4)$	$G_{16}^9(4,4,1)$	$G_{16}^{10}(2,2,2)$	$G_{16}^{11}(2,3,3)$	$G_{16}^{11}(3,2,3)$
Γ_0	BDI	BDI	BDI	BDI	BDI	BDI
Γ_1	BDI	CI	BDI	BDI	BDI	BDI
Γ_2	DIII	AII	CII	AIII	D	AI
Γ_3	DIII	AII	CII	AIII	D	AI

U_4^1	$G_{16}^{12}(2,4,4)$	$G_{16}^{12}(4,2,4)$	$G_{16}^{13}(2,2,2)$	$G_{16}^{13}(2,4,3)$	$G_{16}^{13}(2,3,4)$	$G_{16}^{13}(3,2,4)$
Γ_0	BDI	BDI	BDI	BDI	BDI	BDI
Γ_1	BDI	BDI	BDI	BDI	BDI	BDI
Γ_2	C	AII	AIII	C	D	AI
Γ_3	C	AII	AIII	C	D	AI

U_4^2	C_0	C_1	C_2	C_3	$G_{16}^2(2,2,2)$	$G_{16}^3(5,2,2)$
Γ_0	1	1	1	1	BDI	BDI
Γ_1	1	-1	1	-1	CI	CI
Γ_2	1	1	-1	-1	CII	CI
Γ_3	1	-1	-1	1	$DIII$	BDI

U_4^2	$G_{16}^3(2,5,2)$	$G_{16}^4(2,2,2)$	$G_{16}^{10}(5,2,2)$	$G_{16}^{10}(2,5,2)$	$G_{16}^{11}(5,2,5)$	$G_{16}^{11}(5,5,2)$
Γ_0	BDI	BDI	BDI	BDI	BDI	BDI
Γ_1	BDI	$DIII$	BDI	BDI	BDI	BDI
Γ_2	$DIII$	CI	CI	$DIII$	CI	BDI
Γ_3	$DIII$	CII	CI	$DIII$	CI	BDI

U_4^2	$G_{16}^{11}(5,3,3)$	$G_{16}^{11}(3,5,3)$	$G_{16}^{12}(2,2,2)$	$G_{16}^{13}(2,3,3)$	$G_{16}^{13}(3,2,3)$	$G_{16}^{14}(5,5,5)$
Γ_0	BDI	BDI	BDI	BDI	BDI	BDI
Γ_1	BDI	BDI	BDI	BDI	BDI	BDI
Γ_2	AI	D	CII	AII	C	BDI
Γ_3	AI	D	CII	AII	C	BDI

U_5^1	C_0	C_1	C_2	C_3	C_4	$G_{20}^4(1,1,2)$
Γ_0	1	1	1	1	1	BDI
Γ_1	1	$E(5)$	$E(5)^2$	$E(5)^3$	$E(5)^4$	BDI
Γ_2	1	$E(5)^2$	$E(5)^4$	$E(5)$	$E(5)^3$	BDI
Γ_3	1	$E(5)^3$	$E(5)$	$E(5)^4$	$E(5)^2$	BDI
Γ_4	1	$E(5)^4$	$E(5)^3$	$E(5)^2$	$E(5)$	BDI

U_5^1	$G_{20}^4(1,2,1)$	$G_{20}^4(2,1,1)$	$G_{20}^5(2,2,2)$
Γ_0	BDI	BDI	BDI
Γ_1	AI	D	$AIII$
Γ_2	AI	D	$AIII$
Γ_3	AI	D	$AIII$
Γ_4	AI	D	$AIII$

U_6^1	C_0	C_1	C_2	$G_{24}^{14}(4,4,4)$
Γ_0	1	1	1	BDI
Γ_1	1	-1	1	BDI
Γ_2	2	0	-1	BDI

U_6^2	C_0	C_1	C_2	C_3	C_4	C_5
Γ_0	1	1	1	1	1	1
Γ_1	1	-1	1	-1	1	-1
Γ_2	1	-1	$E(3)^2$	$-E(3)^2$	$E(3)$	$-E(3)$
Γ_3	1	-1	$E(3)$	$-E(3)$	$E(3)^2$	$-E(3)^2$
Γ_4	1	1	$E(3)^2$	$E(3)^2$	$E(3)$	$E(3)$
Γ_5	1	1	$E(3)$	$E(3)$	$E(3)^2$	$E(3)^2$

236

U_6^2	$G_{24}^4(1,1,2)$	$G_{24}^4(1,2,1)$	$G_{24}^4(2,1,1)$	$G_{24}^5(1,4,2)$	$G_{24}^5(1,2,4)$	$G_{24}^5(2,1,4)$
Γ_0	BDI	BDI	BDI	BDI	BDI	BDI
Γ_1	CII	CII	CII	$DIII$	CII	CII
Γ_2	CII	AII	C	$DIII$	AII	C
Γ_3	CII	AII	C	$DIII$	AII	C
Γ_4	BDI	AI	D	BDI	AI	D
Γ_5	BDI	AI	D	BDI	AI	D

U_6^2	$G_{24}^6(4,4,2)$	$G_{24}^6(4,2,4)$	$G_{24}^6(2,4,4)$	$G_{24}^7(1,1,5)$	$G_{24}^7(1,5,1)$	$G_{24}^7(5,1,1)$
Γ_0	BDI	BDI	BDI	BDI	BDI	BDI
Γ_1	BDI	CI	$DIII$	CII	$DIII$	CI
Γ_2	BDI	AI	D	CII	AII	C
Γ_3	BDI	AI	D	CII	AII	C
Γ_4	BDI	AI	D	BDI	AI	D
Γ_5	BDI	AI	D	BDI	AI	D

U_6^2	$G_{24}^8(1,4,5)$	$G_{24}^8(1,5,4)$	$G_{24}^8(5,1,4)$	$G_{24}^9(2,2,5)$	$G_{24}^9(2,5,2)$	$G_{24}^9(5,2,2)$
Γ_0	BDI	BDI	BDI	BDI	BDI	BDI
Γ_1	$DIII$	$DIII$	CI	CII	$DIII$	CI
Γ_2	$DIII$	AII	C	$AIII$	$AIII$	$AIII$
Γ_3	$DIII$	AII	C	$AIII$	$AIII$	$AIII$
Γ_4	BDI	AI	D	$AIII$	$AIII$	$AIII$
Γ_5	BDI	AI	D	$AIII$	$AIII$	$AIII$

U_6^2	$G_{24}^{10}(2,5,5)$	$G_{24}^{10}(5,2,5)$	$G_{24}^{11}(2,2,2)$	$G_{24}^{14}(4,4,5)$	$G_{24}^{14}(4,5,4)$	$G_{24}^{14}(5,4,4)$
Γ_0	BDI	BDI	BDI	BDI	BDI	BDI
Γ_1	$DIII$	CI	CII	BDI	BDI	BDI
Γ_2	$AIII$	$AIII$	$AIII$	BDI	AI	D
Γ_3	$AIII$	$AIII$	$AIII$	BDI	AI	D
Γ_4	$AIII$	$AIII$	$AIII$	BDI	AI	D
Γ_5	$AIII$	$AIII$	$AIII$	BDI	AI	D

U_6^2	$G_{24}^{15}(5,5,5)$
Γ_0	BDI
Γ_1	BDI
Γ_2	$AIII$
Γ_3	$AIII$
Γ_4	$AIII$
Γ_5	$AIII$

U_7^1	C_0	C_1	C_2	C_3	C_4	C_5
Γ_0	1	1	1	1	1	1
Γ_1	1	$E(7)$	$E(7)^2$	$E(7)^3$	$E(7)^4$	$E(7)^5$
Γ_2	1	$E(7)^2$	$E(7)^4$	$E(7)^6$	$E(7)$	$E(7)^3$
Γ_3	1	$E(7)^3$	$E(7)^6$	$E(7)^2$	$E(7)^5$	$E(7)$
Γ_4	1	$E(7)^4$	$E(7)$	$E(7)^5$	$E(7)^2$	$E(7)^6$
Γ_5	1	$E(7)^5$	$E(7)^3$	$E(7)$	$E(7)^6$	$E(7)^4$
Γ_6	1	$E(7)^6$	$E(7)^5$	$E(7)^4$	$E(7)^3$	$E(7)^2$

U_7^1	C_6	$G_{28}^3(1,1,2)$	$G_{28}^3(1,2,1)$	$G_{28}^3(2,1,1)$	$G_{28}^4(2,2,2)$
Γ_0	1	BDI	BDI	BDI	BDI
Γ_1	$E(7)^6$	BDI	AI	D	$AIII$
Γ_2	$E(7)^5$	BDI	AI	D	$AIII$
Γ_3	$E(7)^4$	BDI	AI	D	$AIII$
Γ_4	$E(7)^3$	BDI	AI	D	$AIII$
Γ_5	$E(7)^2$	BDI	AI	D	$AIII$
Γ_6	$E(7)$	BDI	AI	D	$AIII$

U_8^1	C_0	C_1	C_2	C_3	C_4	C_5
Γ_0	1	1	1	1	1	1
Γ_1	1	-1	1	1	-1	-1
Γ_2	1	i	-1	1	$-i$	i
Γ_3	1	$-i$	-1	1	i	$-i$
Γ_4	1	$E(8)$	i	-1	$E(8)^3$	$-E(8)$
Γ_5	1	$-E(8)$	i	-1	$-E(8)^3$	$E(8)$
Γ_6	1	$E(8)^3$	$-i$	-1	$E(8)$	$-E(8)^3$
Γ_7	1	$-E(8)^3$	$-i$	-1	$-E(8)$	$E(8)^3$

U_8^1	C_6	C_7	$G_{32}^{16}(5,1,1)$	$G_{32}^{16}(1,5,1)$	$G_{32}^{17}(5,1,1)$	$G_{32}^{17}(1,5,1)$
Γ_0	1	1	BDI	BDI	BDI	BDI
Γ_1	1	-1	CI	$DIII$	CI	$DIII$
Γ_2	-1	$-i$	$AIII$	$AIII$	$AIII$	$AIII$
Γ_3	-1	i	$AIII$	$AIII$	$AIII$	$AIII$
Γ_4	$-i$	$-E(8)^3$	$AIII$	$AIII$	$AIII$	$AIII$
Γ_5	$-i$	$E(8)^3$	$AIII$	$AIII$	$AIII$	$AIII$
Γ_6	i	$-E(8)$	$AIII$	$AIII$	$AIII$	$AIII$
Γ_7	i	$E(8)$	$AIII$	$AIII$	$AIII$	$AIII$

U_8^1	$G_{32}^{18}(7,1,7)$	$G_{32}^{18}(7,7,1)$	$G_{32}^{19}(7,1,9)$	$G_{32}^{19}(7,9,1)$	$G_{32}^{19}(9,7,1)$	$G_{32}^{20}(9,1,9)$
Γ_0	BDI	BDI	BDI	BDI	BDI	BDI
Γ_1	CI	BDI	CI	BDI	BDI	CI
Γ_2	AI	BDI	AI	BDI	BDI	AI
Γ_3	AI	BDI	AI	BDI	BDI	AI
Γ_4	AI	BDI	AI	CI	$DIII$	AII
Γ_5	AI	BDI	AI	CI	$DIII$	AII
Γ_6	AI	BDI	AI	CI	$DIII$	AII
Γ_7	AI	BDI	AI	CI	$DIII$	AII

U_8^1	$G_{32}^{20}(9,9,1)$	$G_{32}^{36}(5,5,5)$	$G_{32}^{37}(5,6,6)$	$G_{32}^{37}(6,5,6)$	$G_{32}^{38}(5,5,5)$	$G_{32}^{38}(5,6,6)$
Γ_0	BDI	BDI	BDI	BDI	BDI	BDI
Γ_1	BDI	BDI	BDI	BDI	BDI	BDI
Γ_2	BDI	$AIII$	$AIII$	$AIII$	$AIII$	$AIII$
Γ_3	BDI	$AIII$	$AIII$	$AIII$	$AIII$	$AIII$
Γ_4	CII	$AIII$	A	A	$AIII$	A
Γ_5	CII	$AIII$	A	A	$AIII$	A
Γ_6	CII	$AIII$	A	A	$AIII$	A
Γ_7	CII	$AIII$	A	A	$AIII$	A

U_8^1	$G_{32}^{38}(6,6,5)$	$G_{32}^{38}(6,5,6)$	$G_{32}^{39}(5,7,7)$	$G_{32}^{39}(7,5,7)$	$G_{32}^{40}(5,8,8)$	$G_{32}^{40}(8,5,8)$
Γ_0	BDI	BDI	BDI	BDI	BDI	BDI
Γ_1	BDI	BDI	BDI	BDI	BDI	BDI
Γ_2	$AIII$	$AIII$	D	AI	D	AI
Γ_3	$AIII$	$AIII$	D	AI	D	AI
Γ_4	$AIII$	A	D	AI	A	A
Γ_5	$AIII$	A	D	AI	A	A
Γ_6	$AIII$	A	D	AI	A	A
Γ_7	$AIII$	A	D	AI	A	A

U_8^1	$G_{32}^{41}(5,9,9)$	$G_{32}^{41}(9,5,9)$	$G_{32}^{42}(5,9,7)$	$G_{32}^{42}(5,8,8)$	$G_{32}^{42}(5,7,9)$	$G_{32}^{42}(7,5,9)$
Γ_0	BDI	BDI	BDI	BDI	BDI	BDI
Γ_1	BDI	BDI	BDI	BDI	BDI	BDI
Γ_2	D	AI	D	D	D	AI
Γ_3	D	AI	D	D	D	AI
Γ_4	C	AII	C	A	D	AI
Γ_5	C	AII	C	A	D	AI
Γ_6	C	AII	C	A	D	AI
Γ_7	C	AII	C	A	D	AI

U_8^1	$G_{32}^{42}(8,5,8)$	$G_{32}^{43}(6,8,7)$	$G_{32}^{43}(6,7,8)$	$G_{32}^{43}(7,6,8)$	$G_{32}^{43}(8,6,7)$	$G_{32}^{44}(6,9,8)$
Γ_0	BDI	BDI	BDI	BDI	BDI	BDI
Γ_1	BDI	BDI	BDI	BDI	BDI	BDI
Γ_2	AI	D	D	AI	AI	D
Γ_3	AI	D	D	AI	AI	D
Γ_4	A	A	D	AI	A	C
Γ_5	A	A	D	AI	A	C
Γ_6	A	A	D	AI	A	C
Γ_7	A	A	D	AI	A	C

U_8^1	$G_{32}^{44}(6,8,9)$	$G_{32}^{44}(8,6,9)$	$G_{32}^{44}(9,6,8)$
Γ_0	BDI	BDI	BDI
Γ_1	BDI	BDI	BDI
Γ_2	D	AI	AI
Γ_3	D	AI	AI
Γ_4	A	A	AII
Γ_5	A	A	AII
Γ_6	A	A	AII
Γ_7	A	A	AII

U_8^2	C_0	C_1	C_2	C_3	C_4	C_5
Γ_0	1	1	1	1	1	1
Γ_1	1	-1	1	1	-1	-1
Γ_2	1	1	-1	1	-1	1
Γ_3	1	-1	-1	1	1	-1
Γ_4	1	i	1	-1	i	$-i$
Γ_5	1	$-i$	1	-1	$-i$	i
Γ_6	1	i	-1	-1	$-i$	$-i$
Γ_7	1	$-i$	-1	-1	i	i

U_8^2	C_6	C_7	$G_{32}^3(2,5,5)$	$G_{32}^3(5,2,5)$	$G_{32}^4(2,5,5)$	$G_{32}^4(5,2,5)$
Γ_0	1	1	BDI	BDI	BDI	BDI
Γ_1	1	-1	CI	$DIII$	CI	$DIII$
Γ_2	-1	-1	CII	CI	CII	CI
Γ_3	-1	1	$DIII$	CII	$DIII$	CII
Γ_4	-1	$-i$	$AIII$	$AIII$	$AIII$	$AIII$
Γ_5	-1	i	$AIII$	$AIII$	$AIII$	$AIII$
Γ_6	1	i	$AIII$	$AIII$	$AIII$	$AIII$
Γ_7	1	$-i$	$AIII$	$AIII$	$AIII$	$AIII$

U_8^2	$G_{32}^5(10,5,5)$	$G_{32}^5(5,10,5)$	$G_{32}^7(11,6,6)$	$G_{32}^7(6,11,6)$	$G_{32}^8(12,6,6)$	$G_{32}^8(6,12,6)$
Γ_0	BDI	BDI	BDI	BDI	BDI	BDI
Γ_1	CI	$DIII$	CI	$DIII$	CI	$DIII$
Γ_2	CI	BDI	CI	BDI	CI	BDI
Γ_3	BDI	$DIII$	BDI	$DIII$	BDI	$DIII$
Γ_4	$AIII$	$AIII$	AI	D	AII	C
Γ_5	$AIII$	$AIII$	AI	D	AII	C
Γ_6	$AIII$	$AIII$	AI	D	AII	C
Γ_7	$AIII$	$AIII$	AI	D	AII	C

U_8^2	$G_{32}^9(11,5,4)$	$G_{32}^9(11,4,5)$	$G_{32}^9(4,11,5)$	$G_{32}^{10}(12,5,4)$	$G_{32}^{10}(12,4,5)$	$G_{32}^{10}(4,12,5)$
Γ_0	BDI	BDI	BDI	BDI	BDI	BDI
Γ_1	CI	BDI	BDI	CI	BDI	BDI
Γ_2	CI	CI	$DIII$	CI	CI	$DIII$
Γ_3	BDI	CI	$DIII$	BDI	CI	$DIII$
Γ_4	AI	BDI	BDI	AII	$DIII$	CI
Γ_5	AI	BDI	BDI	AII	$DIII$	CI
Γ_6	AI	CI	$DIII$	AII	CII	CII
Γ_7	AI	CI	$DIII$	AII	CII	CII

U_8^2	$G_{32}^{11}(13,2,6)$	$G_{32}^{11}(13,6,2)$	$G_{32}^{11}(6,13,2)$	$G_{32}^{12}(2,5,5)$	$G_{32}^{12}(5,2,5)$	$G_{32}^{13}(5,4,4)$
Γ_0	BDI	BDI	BDI	BDI	BDI	BDI
Γ_1	BDI	CI	$DIII$	CI	$DIII$	$DIII$
Γ_2	CI	CI	$DIII$	$DIII$	CI	CI
Γ_3	CI	BDI	BDI	CII	CII	CII
Γ_4	A	$AIII$	$AIII$	$AIII$	$AIII$	C
Γ_5	A	$AIII$	$AIII$	$AIII$	$AIII$	C
Γ_6	A	$AIII$	$AIII$	$AIII$	$AIII$	D
Γ_7	A	$AIII$	$AIII$	$AIII$	$AIII$	D

U_8^2	$G_{32}^{13}(4,5,4)$	$G_{32}^{14}(5,4,4)$	$G_{32}^{14}(4,5,4)$	$G_{32}^{15}(5,6,6)$	$G_{32}^{15}(6,5,6)$	$G_{32}^{21}(10,2,2)$
Γ_0	BDI	BDI	BDI	BDI	BDI	BDI
Γ_1	CI	$DIII$	CI	CII	CII	BDI
Γ_2	$DIII$	CI	$DIII$	CI	$DIII$	CI
Γ_3	CII	CII	CII	$DIII$	CI	CI
Γ_4	AI	D	AI	A	A	$AIII$
Γ_5	AI	D	AI	A	A	$AIII$
Γ_6	AII	C	AII	A	A	$AIII$
Γ_7	AII	C	AII	A	A	$AIII$

U_8^2	$G_{32}^{21}(2,10,2)$	$G_{32}^{22}(10,3,3)$	$G_{32}^{22}(3,10,3)$	$G_{32}^{23}(10,4,4)$	$G_{32}^{23}(4,10,4)$	$G_{32}^{24}(10,2,2)$
Γ_0	BDI	BDI	BDI	BDI	BDI	BDI
Γ_1	BDI	BDI	BDI	BDI	BDI	BDI
Γ_2	$DIII$	AI	D	CI	$DIII$	CI
Γ_3	$DIII$	AI	D	CI	$DIII$	CI
Γ_4	$AIII$	$AIII$	$AIII$	D	AI	$AIII$
Γ_5	$AIII$	$AIII$	$AIII$	D	AI	$AIII$
Γ_6	$AIII$	D	AI	C	AII	$AIII$
Γ_7	$AIII$	D	AI	C	AII	$AIII$

U_8^2	$G_{32}^{24}(10,4,4)$	$G_{32}^{24}(2,10,2)$	$G_{32}^{24}(2,4,3)$	$G_{32}^{24}(2,3,4)$	$G_{32}^{24}(3,2,4)$	$G_{32}^{24}(4,10,4)$
Γ_0	BDI	BDI	BDI	BDI	BDI	BDI
Γ_1	BDI	BDI	BDI	BDI	BDI	BDI
Γ_2	CI	$DIII$	AII	AII	C	$DIII$
Γ_3	CI	$DIII$	AII	AII	C	$DIII$
Γ_4	C	$AIII$	$AIII$	$AIII$	$AIII$	AI
Γ_5	C	$AIII$	$AIII$	$AIII$	$AIII$	AI
Γ_6	D	$AIII$	C	D	AI	AII
Γ_7	D	$AIII$	C	D	AI	AII

U_8^2	$G_{32}^{25}(10,2,10)$	$G_{32}^{25}(10,10,2)$	$G_{32}^{25}(10,3,4)$	$G_{32}^{25}(10,4,3)$	$G_{32}^{25}(2,3,3)$	$G_{32}^{25}(2,4,11)$
Γ_0	BDI	BDI	BDI	BDI	BDI	BDI
Γ_1	BDI	BDI	BDI	BDI	BDI	BDI
Γ_2	CI	BDI	AI	AI	AII	CII
Γ_3	CI	BDI	AI	AI	AII	CII
Γ_4	$AIII$	$AIII$	$AIII$	$AIII$	$AIII$	D
Γ_5	$AIII$	$AIII$	$AIII$	$AIII$	$AIII$	D
Γ_6	$AIII$	$AIII$	D	C	D	C
Γ_7	$AIII$	$AIII$	D	C	D	C

U_8^2	$G_{32}^{25}(2,11,4)$	$G_{32}^{25}(3,10,4)$	$G_{32}^{25}(3,2,3)$	$G_{32}^{25}(11,2,4)$	$G_{32}^{25}(4,10,3)$	$G_{32}^{26}(2,2,2)$
Γ_0	BDI	BDI	BDI	BDI	BDI	BDI
Γ_1	BDI	BDI	BDI	BDI	BDI	BDI
Γ_2	$DIII$	D	C	CI	D	CII
Γ_3	$DIII$	D	C	CI	D	CII
Γ_4	D	$AIII$	$AIII$	AI	$AIII$	$AIII$
Γ_5	D	$AIII$	$AIII$	AI	$AIII$	$AIII$
Γ_6	D	AI	AI	AI	AII	$AIII$
Γ_7	D	AI	AI	AI	AII	$AIII$

U_8^2	$G_{32}^{26}(2,12,4)$	$G_{32}^{26}(2,4,12)$	$G_{32}^{26}(2,4,4)$	$G_{32}^{26}(4,2,12)$	$G_{32}^{26}(4,2,4)$	$G_{32}^{26}(12,2,4)$
Γ_0	BDI	BDI	BDI	BDI	BDI	BDI
Γ_1	BDI	BDI	BDI	BDI	BDI	BDI
Γ_2	$DIII$	CII	AII	CII	C	CI
Γ_3	$DIII$	CII	AII	CII	C	CI
Γ_4	C	D	$AIII$	AI	$AIII$	AII
Γ_5	C	D	$AIII$	AI	$AIII$	AII
Γ_6	C	C	C	AII	AII	AII
Γ_7	C	C	C	AII	AII	AII

U_8^2	$G_{32}^{27}(11,3,3)$	$G_{32}^{27}(3,3,11)$	$G_{32}^{27}(3,11,3)$	$G_{32}^{28}(10,4,11)$	$G_{32}^{28}(10,11,4)$	$G_{32}^{28}(10,3,3)$
Γ_0	BDI	BDI	BDI	BDI	BDI	BDI
Γ_1	BDI	BDI	BDI	BDI	BDI	BDI
Γ_2	AI	$AIII$	D	CI	BDI	AI
Γ_3	AI	$AIII$	D	CI	BDI	AI
Γ_4	BDI	D	BDI	D	D	D
Γ_5	BDI	D	BDI	D	D	D
Γ_6	AI	AI	D	C	D	$AIII$
Γ_7	AI	AI	D	C	D	$AIII$

U_8^2	$G_{32}^{28}(11,3,4)$	$G_{32}^{28}(11,4,3)$	$G_{32}^{28}(11,10,4)$	$G_{32}^{28}(4,11,3)$	$G_{32}^{28}(3,10,3)$	$G_{32}^{29}(10,4,12)$
Γ_0	BDI	BDI	BDI	BDI	BDI	BDI
Γ_1	BDI	BDI	BDI	BDI	BDI	BDI
Γ_2	AI	AI	BDI	D	D	CI
Γ_3	AI	AI	BDI	D	D	CI
Γ_4	BDI	AI	AI	D	AI	C
Γ_5	BDI	AI	AI	D	AI	C
Γ_6	AI	CI	AI	$DIII$	$AIII$	D
Γ_7	AI	CI	AI	$DIII$	$AIII$	D

U_8^2	$G_{32}^{29}(10,12,4)$	$G_{32}^{29}(10,4,4)$	$G_{32}^{29}(3,4,12)$	$G_{32}^{29}(3,4,4)$	$G_{32}^{29}(3,12,4)$	$G_{32}^{29}(12,10,4)$
Γ_0	BDI	BDI	BDI	BDI	BDI	BDI
Γ_1	BDI	BDI	BDI	BDI	BDI	BDI
Γ_2	BDI	AI	$AIII$	C	D	BDI
Γ_3	BDI	AI	$AIII$	C	D	BDI
Γ_4	C	C	C	BDI	C	AII
Γ_5	C	C	C	BDI	C	AII
Γ_6	C	$AIII$	AI	C	CI	AII
Γ_7	C	$AIII$	AI	C	CI	AII

U_8^2	$G_{32}^{29}(12,3,4)$	$G_{32}^{29}(4,3,4)$	$G_{32}^{29}(4,10,4)$	$G_{32}^{30}(10,4,3)$	$G_{32}^{30}(10,3,4)$	$G_{32}^{30}(3,10,4)$
Γ_0	BDI	BDI	BDI	BDI	BDI	BDI
Γ_1	BDI	BDI	BDI	BDI	BDI	BDI
Γ_2	AI	$AIII$	D	AI	AI	D
Γ_3	AI	$AIII$	D	AI	AI	D
Γ_4	AII	D	AII	$AIII$	$AIII$	$AIII$
Γ_5	AII	D	AII	$AIII$	$AIII$	$AIII$
Γ_6	$DIII$	AII	$AIII$	C	D	AI
Γ_7	$DIII$	AII	$AIII$	C	D	AI

U_8^2	$G_{32}^{30}(3,4,3)$	$G_{32}^{30}(3,3,4)$	$G_{32}^{30}(4,4,11)$	$G_{32}^{30}(4,3,3)$	$G_{32}^{30}(4,11,4)$	$G_{32}^{30}(11,4,4)$
Γ_0	BDI	BDI	BDI	BDI	BDI	BDI
Γ_1	BDI	BDI	BDI	BDI	BDI	BDI
Γ_2	C	AIII	AIII	AII	D	AI
Γ_3	C	AIII	AIII	AII	D	AI
Γ_4	BDI	AI	C	BDI	D	AI
Γ_5	BDI	AI	C	BDI	D	AI
Γ_6	C	D	AII	AII	DIII	CI
Γ_7	C	D	AII	AII	DIII	CI

U_8^2	$G_{32}^{31}(2,3,3)$	$G_{32}^{31}(2,12,11)$	$G_{32}^{31}(2,11,12)$	$G_{32}^{31}(3,2,3)$	$G_{32}^{31}(3,12,3)$	$G_{32}^{31}(3,3,12)$
Γ_0	BDI	BDI	BDI	BDI	BDI	BDI
Γ_1	BDI	BDI	BDI	BDI	BDI	BDI
Γ_2	AII	DIII	DIII	C	D	AIII
Γ_3	AII	DIII	DIII	C	D	AIII
Γ_4	AIII	C	D	AIII	CI	AI
Γ_5	AIII	C	D	AIII	CI	AI
Γ_6	D	C	D	AI	C	D
Γ_7	D	C	D	AI	C	D

U_8^2	$G_{32}^{31}(11,2,12)$	$G_{32}^{32}(2,4,4)$	$G_{32}^{32}(4,2,4)$	$G_{32}^{32}(4,4,4)$	$G_{32}^{33}(2,4,3)$	$G_{32}^{33}(2,3,4)$
Γ_0	BDI	BDI	BDI	BDI	BDI	BDI
Γ_1	BDI	BDI	BDI	BDI	BDI	BDI
Γ_2	CI	AII	C	AIII	AII	AII
Γ_3	CI	AII	C	AIII	AII	AII
Γ_4	AI	AIII	AIII	C	AIII	AIII
Γ_5	AI	AIII	AIII	C	AIII	AIII
Γ_6	AI	C	AII	AII	C	D
Γ_7	AI	C	AII	AII	C	D

U_8^2	$G_{32}^{33}(3,2,4)$	$G_{32}^{33}(3,4,4)$	$G_{32}^{33}(4,4,3)$	$G_{32}^{33}(4,3,4)$	$G_{32}^{34}(2,11,11)$	$G_{32}^{34}(11,2,11)$
Γ_0	BDI	BDI	BDI	BDI	BDI	BDI
Γ_1	BDI	BDI	BDI	BDI	BDI	BDI
Γ_2	C	C	AII	AIII	DIII	CI
Γ_3	C	C	AII	AIII	DIII	CI
Γ_4	AIII	CI	CI	D	D	AI
Γ_5	AIII	CI	CI	D	D	AI
Γ_6	AI	D	AII	AII	D	AI
Γ_7	AI	D	AII	AII	D	AI

U_8^2	$G_{32}^{35}(2,4,4)$	$G_{32}^{35}(2,12,12)$	$G_{32}^{35}(4,2,4)$	$G_{32}^{35}(4,4,12)$	$G_{32}^{35}(4,12,4)$	$G_{32}^{35}(12,2,12)$
Γ_0	BDI	BDI	BDI	BDI	BDI	BDI
Γ_1	BDI	BDI	BDI	BDI	BDI	BDI
Γ_2	CII	DIII	CII	AIII	D	CI
Γ_3	CII	DIII	CII	AIII	D	CI
Γ_4	D	C	AI	C	C	AII
Γ_5	D	C	AI	C	C	AII
Γ_6	C	C	AII	AII	CII	AII
Γ_7	C	C	AII	AII	CII	AII

U_8^2	$G_{32}^{35}(12,4,4)$	$G_{32}^{36}(10,5,5)$	$G_{32}^{36}(5,10,5)$	$G_{32}^{37}(10,5,5)$	$G_{32}^{37}(10,6,6)$	$G_{32}^{37}(5,10,5)$
Γ_0	BDI	BDI	BDI	BDI	BDI	BDI
Γ_1	BDI	CI	$DIII$	CI	CI	$DIII$
Γ_2	AI	BDI	BDI	BDI	BDI	BDI
Γ_3	AI	CI	$DIII$	CI	CI	$DIII$
Γ_4	AII	$AIII$	$AIII$	$AIII$	A	$AIII$
Γ_5	AII	$AIII$	$AIII$	$AIII$	A	$AIII$
Γ_6	CII	$AIII$	$AIII$	$AIII$	A	$AIII$
Γ_7	CII	$AIII$	$AIII$	$AIII$	A	$AIII$

U_8^2	$G_{32}^{37}(6,10,6)$	$G_{32}^{38}(13,6,5)$	$G_{32}^{38}(13,5,6)$	$G_{32}^{38}(5,13,6)$	$G_{32}^{39}(11,5,11)$	$G_{32}^{39}(11,11,5)$
Γ_0	BDI	BDI	BDI	BDI	BDI	BDI
Γ_1	$DIII$	CI	CI	$DIII$	CI	BDI
Γ_2	BDI	BDI	BDI	BDI	BDI	BDI
Γ_3	$DIII$	CI	CI	$DIII$	CI	BDI
Γ_4	A	$AIII$	A	A	AI	BDI
Γ_5	A	$AIII$	A	A	AI	BDI
Γ_6	A	$AIII$	A	A	AI	BDI
Γ_7	A	$AIII$	A	A	AI	BDI

U_8^2	$G_{32}^{40}(11,5,12)$	$G_{32}^{40}(11,12,5)$	$G_{32}^{40}(12,11,5)$	$G_{32}^{41}(12,5,12)$	$G_{32}^{41}(12,12,5)$	$G_{32}^{42}(13,5,13)$
Γ_0	BDI	BDI	BDI	BDI	BDI	BDI
Γ_1	CI	BDI	BDI	CI	BDI	CI
Γ_2	BDI	BDI	BDI	BDI	BDI	CI
Γ_3	CI	BDI	BDI	CI	BDI	BDI
Γ_4	AI	CI	$DIII$	AII	CII	A
Γ_5	AI	CI	$DIII$	AII	CII	A
Γ_6	AI	CI	$DIII$	AII	CII	A
Γ_7	AI	CI	$DIII$	AII	CII	A

U_8^2	$G_{32}^{42}(13,13,5)$	$G_{32}^{43}(11,6,13)$	$G_{32}^{43}(11,13,6)$	$G_{32}^{43}(13,11,6)$	$G_{32}^{44}(12,6,13)$	$G_{32}^{44}(12,13,6)$
Γ_0	BDI	BDI	BDI	BDI	BDI	BDI
Γ_1	BDI	CI	BDI	BDI	CI	BDI
Γ_2	BDI	BDI	BDI	BDI	BDI	BDI
Γ_3	BDI	CI	BDI	BDI	CI	BDI
Γ_4	$AIII$	AI	AI	D	AII	AII
Γ_5	$AIII$	AI	AI	D	AII	AII
Γ_6	$AIII$	AI	AI	D	AII	AII
Γ_7	$AIII$	AI	AI	D	AII	AII

U_8^2	$G_{32}^{44}(13,12,6)$	$G_{32}^{45}(10,10,10)$	$G_{32}^{46}(10,11,11)$	$G_{32}^{46}(11,10,11)$	$G_{32}^{47}(10,12,12)$	$G_{32}^{47}(12,10,12)$
Γ_0	BDI	BDI	BDI	BDI	BDI	BDI
Γ_1	BDI	BDI	BDI	BDI	BDI	BDI
Γ_2	BDI	BDI	BDI	BDI	BDI	BDI
Γ_3	BDI	BDI	BDI	BDI	BDI	BDI
Γ_4	C	$AIII$	D	AI	C	AII
Γ_5	C	$AIII$	D	AI	C	AII
Γ_6	C	$AIII$	D	AI	C	AII
Γ_7	C	$AIII$	D	AI	C	AII

U_8^2	$G_{32}^{48}(10,10,10)$	$G_{32}^{48}(10,12,11)$	$G_{32}^{48}(10,11,12)$	$G_{32}^{48}(10,13,13)$	$G_{32}^{48}(11,10,12)$	$G_{32}^{48}(13,10,13)$
Γ_0	BDI	BDI	BDI	BDI	BDI	BDI
Γ_1	BDI	BDI	BDI	BDI	BDI	BDI
Γ_2	BDI	BDI	BDI	BDI	BDI	BDI
Γ_3	BDI	BDI	BDI	BDI	BDI	BDI
Γ_4	$AIII$	C	D	A	AI	A
Γ_5	$AIII$	C	D	A	AI	A
Γ_6	$AIII$	C	D	A	AI	A
Γ_7	$AIII$	C	D	A	AI	A

U_8^2	$G_{32}^{49}(11,13,13)$	$G_{32}^{49}(13,11,13)$	$G_{32}^{49}(13,13,11)$	$G_{32}^{50}(12,13,13)$	$G_{32}^{50}(13,12,13)$	$G_{32}^{50}(13,13,12)$
Γ_0	BDI	BDI	BDI	BDI	BDI	BDI
Γ_1	BDI	BDI	BDI	BDI	BDI	BDI
Γ_2	BDI	BDI	BDI	BDI	BDI	BDI
Γ_3	BDI	BDI	BDI	BDI	BDI	BDI
Γ_4	AI	D	A	AII	C	A
Γ_5	AI	D	A	AII	C	A
Γ_6	AI	D	A	AII	C	A
Γ_7	AI	D	A	AII	C	A

U_8^3	C_0	C_1	C_2	C_3	C_4	$G_{32}^{39}(11,7,7)$
Γ_0	1	1	1	1	1	BDI
Γ_1	1	-1	1	1	-1	AI
Γ_2	1	1	-1	1	-1	AI
Γ_3	1	-1	-1	1	1	BDI
Γ_4	2	0	0	-2	0	BDI

U_8^3	$G_{32}^{39}(7,11,7)$	$G_{32}^{40}(11,8,8)$	$G_{32}^{40}(8,11,8)$	$G_{32}^{42}(13,8,7)$	$G_{32}^{42}(13,7,8)$	$G_{32}^{42}(7,13,8)$
Γ_0	BDI	BDI	BDI	BDI	BDI	BDI
Γ_1	D	AI	D	AI	AI	D
Γ_2	D	AI	D	AI	AI	D
Γ_3	BDI	BDI	BDI	BDI	BDI	BDI
Γ_4	BDI	CI	$DIII$	CII	$DIII$	CI

U_8^3	$G_{32}^{43}(11,8,7)$	$G_{32}^{43}(11,7,8)$	$G_{32}^{43}(13,7,7)$	$G_{32}^{43}(7,11,8)$	$G_{32}^{43}(7,13,7)$	$G_{32}^{44}(13,8,8)$
Γ_0	BDI	BDI	BDI	BDI	BDI	BDI
Γ_1	AI	AI	AI	D	D	AI
Γ_2	AI	AI	AI	D	D	AI
Γ_3	BDI	BDI	BDI	BDI	BDI	BDI
Γ_4	CI	BDI	$DIII$	BDI	CI	CII

U_8^3	$G_{32}^{44}(8,13,8)$	$G_{32}^{46}(11,11,11)$	$G_{32}^{48}(11,13,13)$	$G_{32}^{48}(13,11,13)$	$G_{32}^{49}(11,13,11)$	$G_{32}^{49}(11,11,13)$
Γ_0	BDI	BDI	BDI	BDI	BDI	BDI
Γ_1	D	BDI	BDI	BDI	BDI	BDI
Γ_2	D	BDI	BDI	BDI	BDI	BDI
Γ_3	BDI	BDI	BDI	BDI	BDI	BDI
Γ_4	CII	BDI	CI	$DIII$	CI	BDI

U_8^3	$G_{32}^{49}(13,11,11)$	$G_{32}^{50}(13,13,13)$
Γ_0	BDI	BDI
Γ_1	BDI	BDI
Γ_2	BDI	BDI
Γ_3	BDI	BDI
Γ_4	$DIII$	CII

U_8^4	C_0	C_1	C_2	C_3	C_4	$G_{32}^{40}(12,8,8)$
Γ_0	1	1	1	1	1	BDI
Γ_1	1	-1	1	1	-1	BDI
Γ_2	1	1	-1	1	-1	AI
Γ_3	1	-1	-1	1	1	AI
Γ_4	2	0	0	-2	0	$DIII$

U_8^4	$G_{32}^{40}(8,12,8)$	$G_{32}^{41}(12,9,9)$	$G_{32}^{41}(9,12,9)$	$G_{32}^{42}(13,9,8)$	$G_{32}^{42}(13,8,9)$	$G_{32}^{42}(8,13,9)$
Γ_0	BDI	BDI	BDI	BDI	BDI	BDI
Γ_1	BDI	BDI	BDI	AI	AI	D
Γ_2	D	AI	D	BDI	BDI	BDI
Γ_3	D	AI	D	AI	AI	D
Γ_4	CI	CII	CII	CI	BDI	BDI

U_8^4	$G_{32}^{43}(13,8,8)$	$G_{32}^{43}(8,13,8)$	$G_{32}^{44}(12,9,8)$	$G_{32}^{44}(12,8,9)$	$G_{32}^{44}(13,9,9)$	$G_{32}^{44}(8,12,9)$
Γ_0	BDI	BDI	BDI	BDI	BDI	BDI
Γ_1	AI	D	BDI	BDI	AI	BDI
Γ_2	BDI	BDI	AI	AI	BDI	D
Γ_3	AI	D	AI	AI	AI	D
Γ_4	BDI	BDI	CII	$DIII$	CI	CI

U_8^4	$G_{32}^{44}(9,13,9)$	$G_{32}^{47}(12,12,12)$	$G_{32}^{48}(12,13,13)$	$G_{32}^{48}(13,12,13)$	$G_{32}^{49}(13,13,13)$	$G_{32}^{50}(12,12,13)$
Γ_0	BDI	BDI	BDI	BDI	BDI	BDI
Γ_1	D	BDI	BDI	BDI	BDI	BDI
Γ_2	BDI	BDI	BDI	BDI	BDI	BDI
Γ_3	D	BDI	BDI	BDI	BDI	BDI
Γ_4	$DIII$	CII	$DIII$	CI	BDI	CII

U_8^4	$G_{32}^{50}(12,13,12)$	$G_{32}^{50}(13,12,12)$
Γ_0	BDI	BDI
Γ_1	BDI	BDI
Γ_2	BDI	BDI
Γ_3	BDI	BDI
Γ_4	$DIII$	CI

U_8^5	C_0	C_1	C_2	C_3	C_4	C_5
Γ_0	1	1	1	1	1	1
Γ_1	1	-1	1	1	-1	-1
Γ_2	1	1	-1	1	-1	1
Γ_3	1	-1	-1	1	1	-1
Γ_4	1	1	1	-1	1	-1
Γ_5	1	-1	1	-1	-1	1
Γ_6	1	1	-1	-1	-1	-1
Γ_7	1	-1	-1	-1	1	1

U_8^5	C_6	C_7	$G_{32}^2(10,10,10)$	$G_{32}^6(11,3,3)$	$G_{32}^6(3,11,3)$	$G_{32}^{21}(10,10,10)$
Γ_0	1	1	BDI	BDI	BDI	BDI
Γ_1	1	-1	CI	CI	BDI	BDI
Γ_2	-1	-1	CI	CI	$DIII$	CI
Γ_3	-1	1	BDI	BDI	$DIII$	CI
Γ_4	-1	-1	CII	A	A	CII
Γ_5	-1	1	$DIII$	A	A	CII
Γ_6	1	1	$DIII$	A	A	$DIII$
Γ_7	1	-1	CII	A	A	$DIII$

U_8^5	$G_{32}^{22}(14,10,10)$	$G_{32}^{22}(14,3,3)$	$G_{32}^{22}(10,14,10)$	$G_{32}^{22}(3,14,3)$	$G_{32}^{23}(10,10,10)$	$G_{32}^{24}(10,3,3)$
Γ_0	BDI	BDI	BDI	BDI	BDI	BDI
Γ_1	BDI	BDI	BDI	BDI	BDI	BDI
Γ_2	CI	AI	BDI	D	$DIII$	AII
Γ_3	CI	AI	BDI	D	$DIII$	AII
Γ_4	CI	CI	$DIII$	$DIII$	CI	CI
Γ_5	CI	CI	$DIII$	$DIII$	CI	CI
Γ_6	BDI	AI	$DIII$	D	CII	AII
Γ_7	BDI	AI	$DIII$	D	CII	AII

U_8^5	$G_{32}^{24}(3,10,3)$	$G_{32}^{25}(10,11,3)$	$G_{32}^{25}(10,3,11)$	$G_{32}^{25}(3,10,11)$	$G_{32}^{25}(11,10,3)$	$G_{32}^{27}(14,3,11)$
Γ_0	BDI	BDI	BDI	BDI	BDI	BDI
Γ_1	BDI	BDI	BDI	BDI	D	BDI
Γ_2	C	AI	AI	D	CI	CI
Γ_3	C	AI	AI	D	C	CI
Γ_4	$DIII$	$DIII$	CII	CII	BDI	AI
Γ_5	$DIII$	$DIII$	CII	CII	D	AI
Γ_6	C	AII	AII	C	CI	AI
Γ_7	C	AII	AII	C	C	AI

U_8^5	$G_{32}^{27}(14,11,3)$	$G_{32}^{27}(11,14,3)$	$G_{32}^{27}(11,11,11)$	$G_{32}^{28}(10,11,11)$	$G_{32}^{28}(11,10,11)$	$G_{32}^{28}(11,3,11)$
Γ_0	BDI	BDI	BDI	BDI	BDI	BDI
Γ_1	BDI	BDI	BDI	BDI	BDI	BDI
Γ_2	BDI	BDI	AI	$DIII$	CI	AI
Γ_3	BDI	BDI	AI	$DIII$	CI	AI
Γ_4	AI	D	$AIII$	AI	D	$AIII$
Γ_5	AI	D	$AIII$	AI	D	$AIII$
Γ_6	AI	D	D	AII	C	C
Γ_7	AI	D	D	AII	C	C

U_8^5	$G_{32}^{28}(11,11,3)$	$G_{32}^{29}(10,3,3)$	$G_{32}^{29}(3,10,3)$	$G_{32}^{30}(10,3,11)$	$G_{32}^{30}(10,11,3)$	$G_{32}^{30}(3,3,11)$
Γ_0	BDI	BDI	BDI	BDI	BDI	BDI
Γ_1	BDI	BDI	BDI	BDI	BDI	BDI
Γ_2	AI	CII	CII	AII	AII	AII
Γ_3	AI	CII	CII	AII	AII	AII
Γ_4	D	AI	D	CI	BDI	$AIII$
Γ_5	D	AI	D	CI	BDI	$AIII$
Γ_6	$AIII$	AII	C	AII	AII	C
Γ_7	$AIII$	AII	C	AII	AII	C

U_8^5	$G_{32}^{30}(3,11,3)$	$G_{32}^{30}(11,10,3)$	$G_{32}^{30}(11,3,3)$	$G_{32}^{31}(3,11,3)$	$G_{32}^{31}(3,3,11)$	$G_{32}^{33}(3,3,3)$
Γ_0	BDI	BDI	BDI	BDI	BDI	BDI
Γ_1	BDI	BDI	BDI	BDI	BDI	BDI
Γ_2	AII	C	C	AII	AII	AII
Γ_3	AII	C	C	AII	AII	AII
Γ_4	D	BDI	AI	$AIII$	C	$AIII$
Γ_5	D	BDI	AI	$AIII$	C	$AIII$
Γ_6	$AIII$	C	$AIII$	D	$AIII$	C
Γ_7	$AIII$	C	$AIII$	D	$AIII$	C

U_8^5	$G_{32}^{34}(11,11,11)$	$G_{32}^{45}(14,10,10)$	$G_{32}^{45}(10,14,10)$	$G_{32}^{46}(14,10,14)$	$G_{32}^{46}(14,14,10)$	$G_{32}^{46}(14,11,11)$
Γ_0	BDI	BDI	BDI	BDI	BDI	BDI
Γ_1	BDI	BDI	BDI	BDI	BDI	BDI
Γ_2	AI	BDI	BDI	BDI	BDI	BDI
Γ_3	AI	BDI	BDI	BDI	BDI	BDI
Γ_4	$AIII$	CI	$DIII$	CI	BDI	AI
Γ_5	$AIII$	CI	$DIII$	CI	BDI	AI
Γ_6	D	CI	$DIII$	CI	BDI	AI
Γ_7	D	CI	$DIII$	CI	BDI	AI

U_8^5	$G_{32}^{46}(11,14,11)$	$G_{32}^{47}(10,10,10)$	$G_{32}^{48}(10,11,11)$	$G_{32}^{48}(11,10,11)$	$G_{32}^{49}(11,11,11)$	$G_{32}^{51}(14,14,14)$
Γ_0	BDI	BDI	BDI	BDI	BDI	BDI
Γ_1	BDI	BDI	BDI	BDI	BDI	BDI
Γ_2	BDI	BDI	BDI	BDI	BDI	BDI
Γ_3	BDI	BDI	BDI	BDI	BDI	BDI
Γ_4	D	CII	AII	C	A	BDI
Γ_5	D	CII	AII	C	A	BDI
Γ_6	D	CII	AII	C	A	BDI
Γ_7	D	CII	AII	C	A	BDI

U_9^1	C_0	C_1	C_2	C_3	C_4	C_5
Γ_0	1	1	1	1	1	1
Γ_1	1	$E(3)$	1	$E(3)^2$	$E(3)$	1
Γ_2	1	$E(3)^2$	1	$E(3)$	$E(3)^2$	1
Γ_3	1	$-E(9)^4-E(9)^7$	$E(3)$	$E(9)^2$	$E(9)^4$	$E(3)^2$
Γ_4	1	$E(9)^4$	$E(3)$	$-E(9)^2-E(9)^5$	$E(9)^7$	$E(3)^2$
Γ_5	1	$E(9)^7$	$E(3)$	$E(9)^5$	$-E(9)^4-E(9)^7$	$E(3)^2$
Γ_6	1	$E(9)^2$	$E(3)^2$	$E(9)^4$	$-E(9)^2-E(9)^5$	$E(3)$
Γ_7	1	$E(9)^5$	$E(3)^2$	$-E(9)^4-E(9)^7$	$E(9)^2$	$E(3)$
Γ_8	1	$-E(9)^2-E(9)^5$	$E(3)^2$	$E(9)^7$	$E(9)^5$	$E(3)$

U_9^1	C_6	C_7	C_8	$G_{36}^4(1,1,2)$	$G_{36}^4(1,2,1)$	$G_{36}^4(2,1,1)$
Γ_0	1	1	1	BDI	BDI	BDI
Γ_1	$E(3)^2$	$E(3)$	$E(3)^2$	BDI	AI	D
Γ_2	$E(3)$	$E(3)^2$	$E(3)$	BDI	AI	D
Γ_3	$E(9)^5$	$E(9)^7$	$-E(9)^2-E(9)^5$	BDI	AI	D
Γ_4	$E(9)^2$	$-E(9)^4-E(9)^7$	$E(9)^5$	BDI	AI	D
Γ_5	$-E(9)^2-E(9)^5$	$E(9)^4$	$E(9)^2$	BDI	AI	D
Γ_6	$-E(9)^4-E(9)^7$	$E(9)^5$	$E(9)^7$	BDI	AI	D
Γ_7	$E(9)^7$	$-E(9)^2-E(9)^5$	$E(9)^4$	BDI	AI	D
Γ_8	$E(9)^4$	$E(9)^2$	$-E(9)^4-E(9)^7$	BDI	AI	D

U_9^1	$G_{36}^5(2,2,2)$
Γ_0	BDI
Γ_1	$AIII$
Γ_2	$AIII$
Γ_3	$AIII$
Γ_4	$AIII$
Γ_5	$AIII$
Γ_6	$AIII$
Γ_7	$AIII$
Γ_8	$AIII$

U_9^2	C_0	C_1	C_2	C_3	C_4	C_5
Γ_0	1	1	1	1	1	1
Γ_1	1	$E(3)$	1	$E(3)^2$	$E(3)$	1
Γ_2	1	$E(3)^2$	1	$E(3)$	$E(3)^2$	1
Γ_3	1	1	$E(3)$	1	$E(3)$	$E(3)^2$
Γ_4	1	$E(3)$	$E(3)$	$E(3)^2$	$E(3)^2$	$E(3)^2$
Γ_5	1	$E(3)^2$	$E(3)$	$E(3)$	1	$E(3)^2$
Γ_6	1	1	$E(3)^2$	1	$E(3)^2$	$E(3)$
Γ_7	1	$E(3)$	$E(3)^2$	$E(3)^2$	1	$E(3)$
Γ_8	1	$E(3)^2$	$E(3)^2$	$E(3)$	$E(3)$	$E(3)$

U_9^2	C_6	C_7	C_8	$G_{36}^{10}(4,3,3)$	$G_{36}^{10}(3,4,3)$	$G_{36}^{12}(3,3,5)$
Γ_0	1	1	1	BDI	BDI	BDI
Γ_1	$E(3)^2$	$E(3)$	$E(3)^2$	AI	BDI	$AIII$
Γ_2	$E(3)$	$E(3)^2$	$E(3)$	AI	BDI	$AIII$
Γ_3	$E(3)$	$E(3)^2$	$E(3)^2$	BDI	D	BDI
Γ_4	1	1	$E(3)$	AI	D	$AIII$
Γ_5	$E(3)^2$	$E(3)$	1	AI	D	$AIII$
Γ_6	$E(3)^2$	$E(3)$	$E(3)$	BDI	D	BDI
Γ_7	$E(3)$	$E(3)^2$	1	AI	D	$AIII$
Γ_8	1	1	$E(3)^2$	AI	D	$AIII$

U_9^2	$G_{36}^{12}(3,5,3)$	$G_{36}^{12}(5,3,3)$	$G_{36}^{13}(4,4,5)$	$G_{36}^{13}(4,5,4)$	$G_{36}^{13}(5,4,4)$	$G_{36}^{14}(5,5,5)$
Γ_0	BDI	BDI	BDI	BDI	BDI	BDI
Γ_1	$AIII$	$AIII$	BDI	AI	D	$AIII$
Γ_2	$AIII$	$AIII$	BDI	AI	D	$AIII$
Γ_3	AI	D	BDI	AI	D	$AIII$
Γ_4	A	A	BDI	AI	D	$AIII$
Γ_5	A	A	BDI	AI	D	$AIII$
Γ_6	AI	D	BDI	AI	D	$AIII$
Γ_7	A	A	BDI	AI	D	$AIII$
Γ_8	A	A	BDI	AI	D	$AIII$

U_{10}^1	C_0	C_1	C_2	C_3	$G_{40}^{12}(3,3,4)$	$G_{40}^{12}(3,4,3)$
Γ_0	1	1	1	1	BDI	BDI
Γ_1	1	-1	1	1	CII	$DIII$
Γ_2	2	0	$E(5)^2 + E(5)^3$	$E(5) + E(5)^4$	$AIII$	D
Γ_3	2	0	$E(5) + E(5)^4$	$E(5)^2 + E(5)^3$	$AIII$	D

U_{10}^1	$G_{40}^{12}(4,3,3)$	$G_{40}^{13}(4,4,4)$
Γ_0	BDI	BDI
Γ_1	CI	BDI
Γ_2	AI	BDI
Γ_3	AI	BDI

U_{10}^2	C_0	C_1	C_2	C_3	C_4	C_5
Γ_0	1	1	1	1	1	1
Γ_1	1	-1	1	-1	1	-1
Γ_2	1	-1	$E(5)^4$	$-E(5)^4$	$E(5)^3$	$-E(5)^3$
Γ_3	1	-1	$E(5)^3$	$-E(5)^3$	$E(5)$	$-E(5)$
Γ_4	1	-1	$E(5)^2$	$-E(5)^2$	$E(5)^4$	$-E(5)^4$
Γ_5	1	-1	$E(5)$	$-E(5)$	$E(5)^2$	$-E(5)^2$
Γ_6	1	1	$E(5)^4$	$E(5)^4$	$E(5)^3$	$E(5)^3$
Γ_7	1	1	$E(5)^3$	$E(5)^3$	$E(5)$	$E(5)$
Γ_8	1	1	$E(5)^2$	$E(5)^2$	$E(5)^4$	$E(5)^4$
Γ_9	1	1	$E(5)$	$E(5)$	$E(5)^2$	$E(5)^2$

U_{10}^2	C_6	C_7	C_8	C_9	$G_{40}^4(1,1,2)$	$G_{40}^4(1,2,1)$
Γ_0	1	1	1	1	BDI	BDI
Γ_1	1	-1	1	-1	CII	CII
Γ_2	$E(5)^2$	$-E(5)^2$	$E(5)$	$-E(5)$	CII	AII
Γ_3	$E(5)^4$	$-E(5)^4$	$E(5)^2$	$-E(5)^2$	CII	AII
Γ_4	$E(5)$	$-E(5)$	$E(5)^3$	$-E(5)^3$	CII	AII
Γ_5	$E(5)^3$	$-E(5)^3$	$E(5)^4$	$-E(5)^4$	CII	AII
Γ_6	$E(5)^2$	$E(5)^2$	$E(5)$	$E(5)$	BDI	AI
Γ_7	$E(5)^4$	$E(5)^4$	$E(5)^2$	$E(5)^2$	BDI	AI
Γ_8	$E(5)$	$E(5)$	$E(5)^3$	$E(5)^3$	BDI	AI
Γ_9	$E(5)^3$	$E(5)^3$	$E(5)^4$	$E(5)^4$	BDI	AI

U_{10}^2	$G_{40}^4(2,1,1)$	$G_{40}^5(1,4,2)$	$G_{40}^5(1,2,4)$	$G_{40}^5(2,1,4)$	$G_{40}^6(4,4,2)$	$G_{40}^6(4,2,4)$
Γ_0	BDI	BDI	BDI	BDI	BDI	BDI
Γ_1	CII	$DIII$	CII	CII	BDI	CI
Γ_2	C	$DIII$	AII	C	BDI	AI
Γ_3	C	$DIII$	AII	C	BDI	AI
Γ_4	C	$DIII$	AII	C	BDI	AI
Γ_5	C	$DIII$	AII	C	BDI	AI
Γ_6	D	BDI	AI	D	BDI	AI
Γ_7	D	BDI	AI	D	BDI	AI
Γ_8	D	BDI	AI	D	BDI	AI
Γ_9	D	BDI	AI	D	BDI	AI

U_{10}^2	$G_{40}^6(2,4,4)$	$G_{40}^7(1,1,5)$	$G_{40}^7(1,5,1)$	$G_{40}^7(5,1,1)$	$G_{40}^8(1,4,5)$	$G_{40}^8(1,5,4)$
Γ_0	BDI	BDI	BDI	BDI	BDI	BDI
Γ_1	$DIII$	CII	$DIII$	CI	$DIII$	$DIII$
Γ_2	D	CII	AII	C	$DIII$	AII
Γ_3	D	CII	AII	C	$DIII$	AII
Γ_4	D	CII	AII	C	$DIII$	AII
Γ_5	D	CII	AII	C	$DIII$	AII
Γ_6	D	BDI	AI	D	BDI	AI
Γ_7	D	BDI	AI	D	BDI	AI
Γ_8	D	BDI	AI	D	BDI	AI
Γ_9	D	BDI	AI	D	BDI	AI

U_{10}^2	$G_{40}^8(5,1,4)$	$G_{40}^9(2,2,5)$	$G_{40}^9(2,5,2)$	$G_{40}^9(5,2,2)$	$G_{40}^{10}(2,5,5)$	$G_{40}^{10}(5,2,5)$
Γ_0	BDI	BDI	BDI	BDI	BDI	BDI
Γ_1	CI	CII	$DIII$	CI	$DIII$	CI
Γ_2	C	$AIII$	$AIII$	$AIII$	$AIII$	$AIII$
Γ_3	C	$AIII$	$AIII$	$AIII$	$AIII$	$AIII$
Γ_4	C	$AIII$	$AIII$	$AIII$	$AIII$	$AIII$
Γ_5	C	$AIII$	$AIII$	$AIII$	$AIII$	$AIII$
Γ_6	D	$AIII$	$AIII$	$AIII$	$AIII$	$AIII$
Γ_7	D	$AIII$	$AIII$	$AIII$	$AIII$	$AIII$
Γ_8	D	$AIII$	$AIII$	$AIII$	$AIII$	$AIII$
Γ_9	D	$AIII$	$AIII$	$AIII$	$AIII$	$AIII$

U_{10}^2	$G_{40}^{11}(2,2,2)$	$G_{40}^{13}(4,4,5)$	$G_{40}^{13}(4,5,4)$	$G_{40}^{13}(5,4,4)$	$G_{40}^{14}(5,5,5)$
Γ_0	BDI	BDI	BDI	BDI	BDI
Γ_1	CII	BDI	BDI	BDI	BDI
Γ_2	$AIII$	BDI	AI	D	$AIII$
Γ_3	$AIII$	BDI	AI	D	$AIII$
Γ_4	$AIII$	BDI	AI	D	$AIII$
Γ_5	$AIII$	BDI	AI	D	$AIII$
Γ_6	$AIII$	BDI	AI	D	$AIII$
Γ_7	$AIII$	BDI	AI	D	$AIII$
Γ_8	$AIII$	BDI	AI	D	$AIII$
Γ_9	$AIII$	BDI	AI	D	$AIII$

U_{10}^2	$G_{40}^{11}(2,2,2)$	$G_{40}^{13}(4,4,5)$	$G_{40}^{13}(4,5,4)$	$G_{40}^{13}(5,4,4)$	$G_{40}^{14}(5,5,5)$

Bibliography

[1] A Agarwala, A Haldar, and VB Shenoy. The tenfold way redux: Fermionic systems with n-body interactions. *Annals of Physics*, 385:469–511, 2017.

[2] M Akila and B Gutkin. Spectral statistics of nearly unidirectional quantum graphs. *Journal of Physics A: Mathematical and Theoretical*, 48(34):345101, 2015.

[3] M Akila and B Gutkin. Gse spectra in uni-directional quantum systems. *Journal of Physics A: Mathematical and Theoretical*, 52(23):235201, 2019.

[4] H Alt, H-D Gräf, T Guhr, HL Harney, R Hofferbert, H Rehfeld, A Richter, and P Schardt. Correlation-hole method for the spectra of superconducting microwave billiards. *Physical Review E*, 55(6):6674, 1997.

[5] A Altland and MR Zirnbauer. Random matrix theory of a chaotic andreev quantum dot. *Physical Review Letters*, 76(18):3420, 1996.

[6] A Altland and MR Zirnbauer. Nonstandard symmetry classes in mesoscopic normal-superconducting hybrid structures. *Physical Review B*, 55:1142–1161, 1997.

[7] SL Altmann. Double groups and projective representations: I. general theory. *Molecular Physics*, 38(2):489–511, 1979.

[8] MF Atiyah, R Bott, and A Shapiro. Clifford modules. *Topology*, 3:3–38, 1964.

[9] G Auletta, M Fortunato, and G Parisi. *Quantum Mechanics*. Cambridge University Press, 2009.

[10] R Balian and C Bloch. Solution of the schrödinger equation in terms of classical paths. *Annals of Physics*, 85(2):514–545, 1974.

[11] R Band, G Berkolaiko, CH Joyner, and W Liu. Quotients of finite-dimensional operators by symmetry representations. *arXiv preprint arXiv:1711.00918*, 2017.

[12] R Band, O Parzanchevski, and G Ben-Shach. The isospectral fruits of representation theory: quantum graphs and drums. *Journal of Physics A: Mathematical and Theoretical*, 42(17):175202, 2009.

[13] CWJ Beenakker. Andreev billiards. In *Quantum Dots: a Doorway to Nanoscale Physics*, pages 131–174. Springer, 2005.

[14] CWJ Beenakker. Random-matrix theory of majorana fermions and topological superconductors. *Reviews of Modern Physics*, 87(3):1037, 2015.

[15] ME Berbenni-Bitsch, S Meyer, and T Wettig. Microscopic universality with dynamical fermions. *Physical Review D*, 58(7):071502, 1998.

[16] G Berkolaiko. An elementary introduction to quantum graphs. *Geometric and Computational Spectral Theory*, 700:41–72, 2017.

[17] G Berkolaiko, JP Keating, and B Winn. No quantum ergodicity for star graphs. *Communications in mathematical physics*, 250(2):259–285, 2004.

[18] G Berkolaiko and P Kuchment. *Introduction to quantum graphs*. Number 186 in Mathematics Surveys and Monographs. American Mathematical Society, 2013.

[19] D Bernard and A LeClair. A classification of non-hermitian random matrices. In *Statistical Field Theories*, pages 207–214. Springer, 2002.

[20] MV Berry. Quantizing a classically ergodic system: Sinai's billiard and the kkr method. *Annals of Physics*, 131(1):163–216, 1981.

[21] MV Berry. Semiclassical theory of spectral rigidity. *Proceedings of the Royal Society of London. A. Mathematical and Physical Sciences*, 400(1819):229–251, 1985.

[22] MV Berry and M Tabor. Level clustering in the regular spectrum. *Proceedings of the Royal Society of London. A. Mathematical and Physical Sciences*, 356(1686):375–394, 1977.

[23] MV Berry and M Wilkinson. Diabolical points in the spectra of triangles. *Proceedings of the Royal Society of London. A. Mathematical and Physical Sciences*, 392(1802):15–43, 1984.

[24] V Blatzios. *Discrete Symmetries in the Ten-fold Way and Quantum Chaos*. PhD thesis, University of Bristol, October 2017.

[25] O Bohigas, M Giannoni, and C Schmit. Characterization of chaotic quantum spectra and universality of level fluctuation laws. *Physical Review Letters*, 52(1):1, 1984.

[26] O Bohigas, RU Haq, and A Pandey. Fluctuation properties of nuclear energy levels and widths: comparison of theory with experiment. In *Nuclear data for science and technology*, pages 809–813. Springer, 1983.

[27] J Bolte and J Harrison. Spectral statistics for the dirac operator on graphs. *Journal of Physics A: Mathematical and General*, 36(11):2747, 2003.

[28] J Bolte and J Harrison. The spin contribution to the form factor of quantum graphs. *Journal of Physics A: Mathematical and General*, 36(27):L433, 2003.

[29] F Bornemann. On the numerical evaluation of fredholm determinants. *Mathematics of Computation*, 79(270):871–915, 2010.

[30] CJ Bradley and BL Davies. Magnetic groups and their corepresentations. *Reviews of Modern Physics*, 40(2):359, 1968.

[31] W Bulla and T Trenkler. The free dirac operator on compact and noncompact graphs. *Journal of Mathematical Physics*, 31(5):1157–1163, 1990.

[32] W Burnside. On groups of order $p^\alpha q^\beta$. *Proceedings of the London Mathematical Society*, 2(1):388–392, 1904.

[33] M Burrow. *Representation theory of finite groups*. Courier Corporation, 2014.

[34] G Casati, F Valz-Gris, and I Guarnieri. On the connection between quantization of nonintegrable systems and statistical theory of spectra. *Lettere al Nuovo Cimento (1971-1985)*, 28(8):279–282, 1980.

[35] G Casti and B Chirikov. *Quantum Chaos: Between Order and Disorder*. Cambridge University Press, 2006.

[36] E Caurier and B Grammaticos. Extreme level repulsion for chaotic quantum hamiltonians. *Physics Letters A*, 136(7-8):387–390, 1989.

[37] X Chen, Z-C Gu, Z-X Liu, and X-G Wen. Symmetry protected topological orders and the group cohomology of their symmetry group. *Physical Review B*, 87(15):155114, 2013.

[38] C Cheng. A character theory for projective representations of finite groups. *Linear Algebra and its Applications*, 469:230–242, 2015.

[39] C Chiu, JCY Teo, AP Schnyder, and S Ryu. Classification of topological quantum matter with symmetries. *Reviews of Modern Physics*, 88(3):035005, 2016.

[40] B Conrey. Notes on eigenvalue distributions for the classical compact groups. In F Mezzadri and Snaith NC, editors, *Recent Perspectives in Random Matrix Theory and Number Theory*, London Mathematical Society Lecture Note Series. Cambridge University Press, 2005.

[41] AP Cracknell. Corepresentations of magnetic point groups. *Progress of Theoretical Physics*, 35(2):196–213, 1966.

[42] PH Damgaard and SM Nishigaki. Distribution of the k th smallest dirac operator eigenvalue. *Physical Review D*, 63(4):045012, 2001.

[43] MR De Traubenberg. Clifford algebras in physics. `https://arxiv.org/pdf/hep-th/0506011.pdf`. Talk given at the Preparatory Lectures of the 7th International Conference on Clifford Algebras and their Applications, Toulouse, France, May 19-29, 2005.

[44] C Dembowski, H-D Gräf, A Heine, H Rehfeld, A Richter, and C Schmit. Gaussian unitary ensemble statistics in a time-reversal invariant microwave triangular billiard. *Physical Review E*, 62(4):R4516, 2000.

[45] S Deus, PM Koch, and L Sirko. Statistical properties of the eigenfrequency distribution of three-dimensional microwave cavities. *Physical Review E*, 52(1):1146, 1995.

[46] B Dietz and A Richter. Quantum and wave dynamical chaos in superconducting microwave billiards. *Chaos: An Interdisciplinary Journal of Nonlinear Science*, 25(9):097601, 2015.

[47] JO Dimmock. Representation theory for nonunitary groups. *Journal of Mathematical Physics*, 4(10):1307–1311, 1963.

[48] JO Dimmock and RG Wheeler. Irreducible representations of magnetic groups. *Journal of Physics and Chemistry of Solids*, 23(6):729–741, 1962.

[49] T Dokchister. Groupnames website. `https://people.maths.bris.ac.uk/~matyd/GroupNames/index.html`. Accessed: 12-02-2020.

[50] FJ Dyson. Statistical theory of the energy levels of complex systems. i. *Journal of Mathematical Physics*, 3(1):140–156, 1962.

[51] FJ Dyson. The threefold way. algebraic structure of symmetry groups and ensembles in quantum mechanics. *Journal of Mathematical Physics*, 3(6):1199–1215, 1962.

[52] M El-Batanouny and F Wooten. *Symmetry and condensed matter physics: a computational approach*. Cambridge University Press, 2008.

[53] JP Elliott and PG Dawber. *Symmetry in Physics, Volume 1*. Macmillan, 1979.

[54] K Erdmann and T Holm. *The Structure of Semisimple Algebras: The Artin–Wedderburn Theorem*, pages 103–116. Springer International Publishing, Cham, 2018.

[55] F Evers and AD Mirlin. Anderson transitions. *Reviews of Modern Physics*, 80(4):1355, 2008.

[56] Y Fan, S Gnutzmann, and Y Liang. Quantum chaos for nonstandard symmetry classes in the feingold-peres model of coupled tops. *Physical Review E*, 96(6):062207, 2017.

[57] FWK Firk and SJ Miller. Nuclei, primes and the random matrix connection. *Symmetry*, 1(1):64–105, 2009.

[58] PJ Forrester. The spectrum edge of random matrix ensembles. *Nuclear Physics B*, 402(3):709–728, 1993.

[59] DS Freed and GW Moore. Twisted equivariant matter. *Annales Henri Poincaré*, 14(8):1927–2023, 2013.

[60] The GAP Group. *GAP – Groups, Algorithms, and Programming, Version 4.10.2*, 2019.

[61] P Gaspard. *Chaos, scattering and statistical mechanics*, volume 9. Cambridge University Press, 2005.

[62] S Gnutzmann and A Altland. Universal spectral statistics in quantum graphs. *Physical Review Letters*, 93(19):194101, 2004.

[63] S Gnutzmann and A Altland. Spectral correlations of individual quantum graphs. *Physical Review E*, 72(5):056215, 2005.

[64] S Gnutzmann and B Seif. Universal spectral statistics in wigner-dyson, chiral, and andreev star graphs. i. construction and numerical results. *Physical Review E*, 69(5):056219, 2004.

[65] S Gnutzmann and B Seif. Universal spectral statistics in wigner-dyson, chiral, and andreev star graphs. ii. semiclassical approach. *Physical Review E*, 69(5):056220, 2004.

[66] S Gnutzmann, B Seif, and F von Oppen. Universal spectral statistics in andreev graphs: The self-dual approximation. *Proceedings TH2002 Supplement*, 101:115, 2003.

[67] S Gnutzmann and U Smilansky. Quantum graphs: Applications to quantum chaos and universal spectral statistics. *Advances in Physics*, 55(5-6):527–625, 2006.

[68] DJ Griffiths and DF Schroeter. *Introduction to Quantum Mechanics*. Cambridge University Press, 3 edition, 2018.

[69] Z-C Gu and X-G Wen. Symmetry-protected topological orders for interacting fermions: Fermionic topological nonlinear sigma models and a special group supercohomology theory. *Physical Review B*, 90(11):115141, 2014.

[70] T Guhr, A Müller-Groeling, and HA Weidenmüller. Random-matrix theories in quantum physics: common concepts. *Physics Reports*, 299(4-6):189–425, 1998.

[71] M Gutzwiller. *Chaos in Classical and Quantum Mechanics*, volume 1 of *Interdisiplinary Applied Mathemtics*. Springer, 1990.

[72] MC Gutzwiller. Periodic orbits and classical quantization conditions. *Journal of Mathematical Physics*, 12(3):343–358, 1971.

[73] F Haake. *Quantum Signatures of Chaos*. Springer, 3 edition, 2010.

[74] A Hagberg, P Swart, and D S Chult. Exploring network structure, dynamics, and function using networkx. Technical report, Los Alamos National Lab.(LANL), Los Alamos, NM (United States), 2008.

[75] BC Hall. *Quantum theory for mathematicians*, volume 267. Springer, 2013.

[76] RU Haq, A Pandey, and O Bohigas. Fluctuation properties of nuclear energy levels: Do theory and experiment agree? *Physical Review Letters*, 48(16):1086, 1982.

[77] JM Harrison. Quantum graphs with spin hamiltonians. In P Exner, JP Keating, P Kuchment, T Sunada, and A Teplyaev, editors, *Analysis on Graphs and Its Applications*, volume 77 of *Proceedings of Symposia in Pure Mathematics*. AMS, 2008.

[78] JM Harrison, T Weyand, and K Kirsten. Zeta functions of the dirac operator on quantum graphs. *Journal of Mathematical Physics*, 57(10):102301, 2016.

[79] P Heinzner, A Huckleberry, and MR Zirnbauer. Symmetry classes of disordered fermions. *Communications in mathematical physics*, 257(3):725–771, 2005.

[80] A Hönig and D Wintgen. Spectral properties of strongly perturbed coulomb systems: fluctuation properties. *Physical Review A*, 39(11):5642, 1989.

[81] C-T Hsieh, T Morimoto, and S Ryu. Cpt theorem and classification of topological insulators and superconductors. *Physical Review B*, 90(24):245111, 2014.

[82] DJ Hughes. Contributions of neutron time-of-flight experimenttion to low-energy neutron physics. In *Conference on Neutron Physics By Time-of-Flight; Gatlinburg, Tennessee; November 1956*, 1957. Talk Transcript.

[83] O Hul, S Bauch, P Pakoński, N Savytskyy, K Życzkowski, and L Sirko. Experimental simulation of quantum graphs by microwave networks. *Physical Review E*, 69(5):056205, 2004.

[84] VL Indenbom. Relation of the antisymmetry and color symmetry groups to one-dimensional representations of the ordinary symmetry groups. isomorphism of the shubnikov and space groups. *Soviet Phys Cryst.(English Translation)*, 4:578, 1959.

[85] DA Ivanov. The supersymmetric technique for random-matrix ensembles with zero eigenvalues. *Journal of Mathematical Physics*, 43(1):126–153, 2002.

[86] G James and M Liebeck. *Representations and Characters of Groups*. Cambridge University Press, 2 edition, 2004.

[87] RA Janik, MA Nowak, G Papp, and I Zahed. Non-hermitian random matrix models. *Nuclear Physics B*, 501(3):603–642, 1997.

[88] T Janssen. On projective unitary-antiunitary representations of finite groups. *Journal of Mathematical Physics*, 13(3):342–351, 1972.

[89] DB Johnson. Finding all the elementary circuits of a directed graph. *SIAM Journal on Computing*, 4(1):77–84, 1975.

[90] C Joyner. *Semiclassical Approach to Discrete Symmetries in Quantum Chaos*. PhD thesis, University of Bristol, December 2012.

[91] CH Joyner. Personal Communication, 2018.

[92] CH Joyner, S Müller, and M Sieber. Gse statistics without spin. *EPL (Europhysics Letters)*, 107(5):50004, 2014.

[93] T Józefiak. Semisimple superalgebras. In *Algebra: Some Current Trends*, pages 96–113. Springer, 1988.

[94] T Kanazawa and T Wettig. Complete random matrix classification of syk models with n= 0, 1 and 2 supersymmetry. *Journal of High Energy Physics*, 2017(9):50, 2017.

[95] K Kawabata, K Shiozaki, M Ueda, and M Sato. Symmetry and topology in non-hermitian physics. *Physical Review X*, 9(4):041015, 2019.

[96] S Keown. *An introduction to group representation theory*, volume 116 of *Mathematics in science and engineering*. Academic Press, 1975.

[97] S Keppeler, J Marklof, and F Mezzadri. Quantum cat maps with spin 1/2. *Nonlinearity*, 14(4):719, 2001.

[98] JL Kinsey and RD Levine. The application of spectral measures to the stimulated emission pumping of acetylene. In *The Structure of Small Molecules and Ions*, pages 29–37. Springer, 1988.

[99] Y Kosmann-Schwarzbach. *Groups and symmetries; from finite groups to lie groups*. Springer, 2010.

[100] V Kostrykin and R Schrader. Kirchhoff's rule for quantum wires. *Journal of Physics A: Mathematical and General*, 32(4):595, 1999.

[101] T Kottos and U Smilansky. Quantum chaos on graphs. *Physical Review Letters*, 79(24):4794, 1997.

[102] T Kottos and U Smilansky. Periodic orbit theory and spectral statistics for quantum graphs. *Annals of Physics*, 274(1):76–124, 1999.

[103] T Kottos and U Smilansky. Chaotic scattering on graphs. *Physical Review Letters*, 85(5):968, 2000.

[104] T Kottos and U Smilansky. Quantum graphs: a simple model for chaotic scattering. *Journal of Physics A: Mathematical and General*, 36(12):3501, 2003.

[105] F Kuemmeth, KI Bolotin, S-F Shi, and DC Ralph. Measurement of discrete energy-level spectra in individual chemically synthesized gold nanoparticles. *Nano letters*, 8(12):4506–4512, 2008.

[106] S Kumar. Recursion for the smallest eigenvalue density of beta-wishart-laguerre ensemble. *Journal of Statistical Physics*, 175(1):126–149, 2019.

[107] M Ławniczak, S Bauch, O Hul, and L Sirko. Experimental investigation of the enhancement factor for microwave irregular networks with preserved and broken time reversal symmetry in the presence of absorption. *Physical Review E*, 81(4):046204, 2010.

[108] O Legrand, C Schmit, and D Sornette. Quantum chaos methods applied to high-frequency plate vibrations. *EPL (Europhysics Letters)*, 18(2):101, 1992.

[109] F Leyvraz, C Schmit, and TH Seligman. Anomalous spectral statistics in a symmetrical billiard. *Journal of Physics A: Mathematical and General*, 29(22):L575, 1996.

[110] W Liu. *Degeneracies in the Eigenvalue Spectrum of Quantum Graphs*. PhD thesis, Texas A&M University, June 2016.

[111] P Lounesto. *Clifford algebras and spinors*, volume 286. Cambridge university press, 2001.

[112] AWW Ludwig. Topological phases: classification of topological insulators and superconductors of non-interacting fermions, and beyond. *Physica Scripta*, 2016(T168):014001, 2015.

[113] AM Martínez-Argüello, A Rehemanjiang, M Martínez-Mares, JA Méndez-Bermúdez, H-J Stöckmann, and U Kuhl. Transport studies in three-terminal microwave graphs with orthogonal, unitary, and symplectic symmetry. *Physical Review B*, 98(7):075311, 2018.

[114] SW McDonald and AN Kaufman. Spectrum and eigenfunctions for a hamiltonian with stochastic trajectories. *Physical Review Letters*, 42(18):1189, 1979.

[115] M Mehta. *Random Matrices*. Elsevier, 3 edition, 2004.

[116] O Millo, SJ Klepper, MW Keller, DE Prober, S Xiong, AD Stone, and RN Sacks. Reduction of the mesoscopic conductance-fluctuation amplitude in gaas/algaas heterojunctions due to spin-orbit scattering. *Physical Review Letters*, 65(12):1494, 1990.

[117] GW Moore. Lecture notes on quantum symmetries and compatible hamiltonians. Rutgers University, 2014. Available at `http://www.physics.rutgers.edu/gmoore/QuantumSymmetryBook.pdf`.

[118] S Müller. *Periodic-Orbit Approach to Universailtiy in Quantum Chaos*. PhD thesis, University of Duisburg-Essen, 2006.

[119] S Müller. Lecture notes on quantum chaos. University of Bristol, 2016.

[120] S Müller, S Heusler, A Altland, P Braun, and F Haake. Periodic-orbit theory of universal level correlations in quantum chaos. *New Journal of Physics*, 11(10):103025, 2009.

[121] S Müller, S Heusler, P Braun, F Haake, and A Altland. Semiclassical foundation of universality in quantum chaos. *Physical Review Letters*, 93(1):014103, 2004.

[122] S Müller, S Heusler, P Braun, F Haake, and A Altland. Periodic-orbit theory of universality in quantum chaos. *Physical Review E*, 72(4):046207, 2005.

[123] T Nagao and PJ Forrester. The smallest eigenvalue distribution at the spectrum edge of random matrices. *Nuclear Physics B*, 509(3):561–598, 1998.

[124] V Naik. Groupprops website. `https://groupprops.subwiki.org/wiki/Main_Page`. Accessed: 19-09-2019.

[125] SM Nishigaki. Universality crossover between chiral random matrix ensembles and twisted su (2) lattice dirac spectra. *Physical Review D*, 86(11):114505, 2012.

[126] W Opechowski. Sur les groupes cristallographiques "doubles". *Physica*, 7(6):552–562, 1940.

[127] E Ott. *Chaos in dynamical systems*. Cambridge university press, 2002.

[128] M Oxborrow and C Ellegaard. Quantum chaology in quartz. In *Proceedings of the 3rd Experimental Chaos Conference, Edinburgh*. World Scientific, 1995.

[129] O Parzanchevski and R Band. Linear representations and isospectrality with boundary conditions. *Journal of Geometric Analysis*, 20(2):439–471, 2010.

[130] Z Pluhař and HA Weidenmüller. Quantum graphs and random-matrix theory. *Journal of Physics A: Mathematical and Theoretical*, 48(27):275102, 2015.

[131] C Porter, editor. *Statistical Theories of Spectra: Fluctuations*. Number 1 in Perspectives in Physics. Academic Press, 1965.

[132] CE Porter and Rosenzweig N. Statistical properties of atomic and nuclear spectra. In Porter, editor, *Statistical Theories of Spectra: Fluctuations*, number 1 in Perspectives in Physics. Academic Press, 1965. Origionally published in Suomalasen Tiedeakatemian Toimituksia AVI, No. 44 (1960).

[133] A Rehemanjiang. *Microwave Experiments on Graphs Simulating Spin-1/2 System*. PhD thesis, University of Marburg, August 2018.

[134] A Rehemanjiang, M Allgaier, CH Joyner, S Müller, M Sieber, U Kuhl, and H-J Stöckmann. Microwave realization of the gaussian symplectic ensemble. *Physical Review Letters*, 117(6):064101, 2016.

[135] A Rehemanjiang, M Richter, U Kuhl, and H-J Stöckmann. Spectra and spectral correlations of microwave graphs with symplectic symmetry. *Physical Review E*, 97(2):022204, 2018.

[136] A Rehemanjiang, M Richter, U Kuhl, and H-J Stöckmann. Microwave realization of the chiral orthogonal, unitary, and symplectic ensembles. *Physical Review Letters*, 124(11):116801, 2020.

[137] JM Robbins. Discrete symmetries in periodic-orbit theory. *Physical Review A*, 40(4):2128, 1989.

[138] JJ Rotman. *An introduction to the theory of groups*, volume 148 of *Graduate Texts in Mathematics*. Springer Science & Business Media, 4 edition, 2012.

[139] S Ryu, AP Schnyder, A Furusaki, and AWW Ludwig. Topological insulators and superconductors: tenfold way and dimensional hierarchy. *New Journal of Physics*, 12(6):065010, 2010.

[140] K Schaadt. The quantum chaology of acoustic resonators. Master's thesis, University of Copenhagen, 1997.

[141] R Scharf. Kicked rotator for a spin-1/2 particle. *Journal of Physics A: Mathematical and General*, 22(19):4223, 1989.

[142] R Scharf, B Dietz, M Kuś, F Haake, and MV Berry. Kramers' degeneracy and quartic level repulsion. *EPL (Europhysics Letters)*, 5(5):383, 1988.

[143] AP Schnyder, S Ryu, A Furusaki, and AWW Ludwig. Classification of topological insulators and superconductors in three spatial dimensions. *Physical Review B*, 78(19):195125, 2008.

[144] BER Seif. *Chaos on quantum graphs with Andreev scattering*. PhD thesis, Universität zu Köln, 2003.

[145] K Shiozaki, M Sato, and K Gomi. Atiyah-hirzebruch spectral sequence in band topology: General formalism and topological invariants for 230 space groups. *arXiv preprint arXiv:1802.06694*, 2018.

[146] EV Shuryak and JJM Verbaarschot. Random matrix theory and spectral sum rules for the dirac operator in qcd. *Nuclear Physics A*, 560(1):306–320, 1993.

[147] M Sieber. Leading off-diagonal approximation for the spectral form factor for uniformly hyperbolic systems. *Journal of Physics A: Mathematical and General*, 35(42):L613, 2002.

[148] M Sieber and K Richter. Correlations between periodic orbits and their rôle in spectral statistics. *Physica Scripta*, 2001(T90):128, 2001.

[149] B Simon. *Representations of finite and compact groups*. Number 10 in Graduate Studies in Mathematics. American Mathematical Soc., 1996.

[150] R Simon, N Mukunda, S Chaturvedi, and V Srinivasan. Two elementary proofs of the wigner theorem on symmetry in quantum mechanics. *Physics Letters A*, 372(46):6847–6852, 2008.

[151] R Simon, N Mukunda, S Chaturvedi, V Srinivasan, and J Hamhalter. Comment on:"two elementary proofs of the wigner theorem on symmetry in quantum mechanics"[phys. lett. a 372 (2008) 6847]. *Physics Letters A*, 378(30-31):2332–2335, 2014.

[152] CH Skiadas and C Skiadas, editors. *Application of Microwave Networks to Simulation of Quantum Graphs*. CRC Press, 2017.

[153] P So, SM Anlage, E Ott, and RN Oerter. Wave chaos experiments with and without time reversal symmetry: Gue and goe statistics. *Physical Review Letters*, 74(14):2662, 1995.

[154] D Spehner. Spectral form factor of hyperbolic systems: leading off-diagonal approximation. *Journal of Physics A: Mathematical and General*, 36(26):7269, 2003.

[155] EM Stein and R Shakarchi. *Real Analysis: Measure Theory, Integration and Hilbert Spaces*. Number 3 in Princeton Lectures in Analysis. Princeton University Press, 2005.

[156] MA Stephanov, JJM Verbaarschot, and T Wettig. Random matrices. *arXiv preprint hep-ph/0509286*, 2005. As Appeared in the Wiley Encyclopedia of Electrical and Electronics Engineering.

[157] H-J Stöckmann. *Quantum Chaos: An Introduction*. Cambridge University Press, 2006.

[158] U Stoffregen, J Stein, H-J Stöckmann, M Kuś, and F Haake. Microwave billiards with broken time reversal symmetry. *Physical Review Letters*, 74(14):2666, 1995.

[159] G Tanner. Unitary-stochastic matrix ensembles and spectral statistics. *Journal of Physics A: Mathematical and Theoretical*, 34(41):8485, 2001.

[160] M Thaha, R Blümel, and U Smilansky. Symmetry breaking and localization in quantum chaotic systems. *Physical Review E*, 48(3):1764, 1993.

[161] B Thaller. *The dirac equation*. Springer Science & Business Media, 2013.

[162] CA Tracy and H Widom. Level spacing distributions and the bessel kernel. *Communications in Mathematical Physics*, 161(2):289–309, 1994.

[163] PM Van Den Broek. On the determination of factor systems of pua—representations. In *Group Theoretical Methods in Physics*, pages 435–440. Springer, 1976.

[164] M Vanlessen. Strong asymptotics of laguerre-type orthogonal polynomials and applications in random matrix theory. *Constructive Approximation*, 25(2):125–175, 2007.

[165] VS Varadarajan. *Supersymmetry for Mathematicians: An Introduction*, volume 11. American Mathematical Soc., 2004.

[166] J Verbaarschot. Spectrum of the qcd dirac operator and chiral random matrix theory. *Physical Review Letters*, 72(16):2531, 1994.

[167] JJM Verbaarschot and I Zahed. Spectral density of the qcd dirac operator near zero virtuality. *Physical Review Letters*, 70(25):3852, 1993.

[168] CTC Wall. Graded brauer groups. *Journal für die reine und angewandte Mathematik*, 1964(213):187–199, 1964.

[169] CA Weibel. *An Introduction to Homological Algebra*. Number 38 in Cambridge Studies in Advanced Mathematics. Cambridge university press, 1995.

[170] HA Weidenmüller and GE Mitchell. Random matrices and chaos in nuclear physics: Nuclear structure. *Reviews of Modern Physics*, 81(2):539, 2009.

[171] H Weyl. *The classical groups: their invariants and representations*, volume 1. Princeton university press, 1946.

[172] E Wigner. On the statistical distribution of the widths and spacings of nuclear resonance levels. *Mathematical Proceedings of the Cambridge Philosophical Society*, 47(4):790–798, 1951.

[173] E Wigner. Characteristic vectors of bordered matrices with infinite dimensions. *Annals of Mathematics*, 62(3), 1955.

[174] E Wigner. Results and theory of resonance absorbtion. In *Conference on Neutron Physics By Time-of-Flight; Gatlinburg, Tennessee; November 1956*, 1957. Talk Transcript.

[175] E Wigner. *Group theory: and its application to the quantum mechanics of atomic spectra*, volume 5. Elsevier, 2012.

[176] A Winter. *Spectral Universality and the Three-fold Way in Quantum Chaos*. PhD thesis, University of Bristol, April 2017.

[177] J Yang and Z-X Liu. Irreducible projective representations and their physical applications. *Journal of Physics A: Mathematical and Theoretical*, 51(2):025207, 2017.

[178] T Zimmermann, H Köppel, LS Cederbaum, G Persch, and W Demtröder. Confirmation of random-matrix fluctuations in molecular spectra. *Physical Review Letters*, 61(1):3, 1988.

[179] MR Zirnbauer. Symmetry classes in random matrix theory. *arXiv preprint math-ph/0404058*, 2004.

[180] MR Zirnbauer. Symmetry classes. In G Akemann, J Baik, and P Di Francesco, editors, *The Oxford Handbook of Random Matrix Theory*, chapter 3. Oxford university press, 2015.